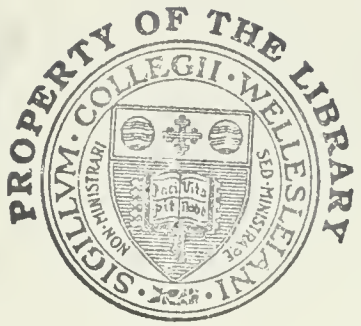
NASA Conference Publication 10152

Analysis of Returned Comet Nucleus Samples

Compiled by Sherwood Chang, Ames Research Center, Moffett Field, California

Proceedings of a workshop held at
Milpitas, California
January 16–18, 1989




PROPERTY OF THE LIBRARY
SIGILLVM · COLLEGII · WELLESLEIANI
NON · HVIVS · TRARI
SED · HVIVS · RE

NASA Conference Publication 10152

Analysis of Returned Comet Nucleus Samples

Compiled by Sherwood Chang

Proceedings of a workshop held at
Milpitas, California
January 16–18, 1989



National Aeronautics and
Space Administration

Ames Research Center
Moffett Field, California 94035-1000

1997

Go Within Observatory

ASTRO
QB
7-721
.A52
1997

TABLE OF CONTENTS

Page

PREFACE vi

WORKSHOP AGENDA vii

ORGANIZING COMMITTEE xiii

Nucleosynthesis and the Isotopic Composition of Stardust* 1
A. G. M. Tielens

Interstellar and Cometary Dust* 29
J. S. Mathis

Refractory Solids in Chondrites and Comets: How Similar?* 59
J. A. Wood

Disequilibrium Chemistry in the Solar Nebula and Early Solar System: Implications for the Chemistry of Comets* 73
B. Fegley

Sulfur Compounds in Comets 93
S. J. Kim and M. F. A'Hearn

Spectrophotometric Observations of Comet P/Giacobini-Zinner 103
I. Konno, S. Wyckoff and P. A. Wehinger

Physical Processing of Cometary Nuclei* 119
P. R. Weissman and S. A. Stern

The Organic Matter of Comet P/Halley as Inferred by Joint Gas and Solid Phase Analysis* 167
J. Kissel , F. R. Krueger and A. Korth

On the Measurement of Cosmogenic Radionuclides in Cometary Materials 183
G. F. Herzog, P. A. J. Englert, R. C. Reedy, K. Nishiizumi, C. P. Kohland and J. R. Arnold

Morphology and Compositional Differentiation of the Surface of Comets 199
W. F. Huebner and D. C. Boice

The In-Situ Particulate Size Distribution Measured for One Comet: P/Halley 205
J. A. M. McDonnell, G. S. Pankiewicz, P. N. W. Birchley, S. F. Green and C. H. Perry

Organic Chemistry in Interstellar Ices: Connection to the Comet Halley Results 217
W. A. Schutte, V. K. Agarwal, M. S. de Groot, J. M. Greenberg, P. McCain, J. P. Ferris and R. Briggs

Evolution of Carbonaceous Chondrite Parent Bodies: Insights into Cometary Nuclei?* 225
H. Y. McSween, Jr.

* Indicates invited papers

Interplanetary Dust Particles Optical Properties: A Clue to Cometary Dust Structure?....239
A. C. Levasseur-Regourd

Cometary Evolution: Clues on Physical Properties from Chondritic Interplanetary Dust Particles....247
F. J. M. Rietmeijer

Laboratory Simulations: The Primordial Comet Mantle*....255
R. E. Johnson

Metamorphism of Cosmic Dust: Processing from Circumstellar Outflows to the Cometary Regolith*....277
J. A. Nuth III

Experimental Studies of Gas Trapping in Amorphous Ice and Thermal Modelling of Comets—Implications for Rosetta....293
A. Bar-Nun, D. Prialnik, I. Kleinfeld and D. Laufer

Modifications of Comet Materials by the Sublimation Process: Results from Simulation Experiments*....315
E. Grün, J. Benkhoff, A. Bischoff, H. Düren, H. Hellmann, P. Hesselbarth, P. Hsiung, H.U. Keller, J. Klinger, J. Knölker, H. Kochan, G. Neukum, A. Oehler, K. Roessler , T. Spohn, D. Stöffler and K. Theil

The Nature of Comet Materials and Attachment to Them....333
J. Stephens

Mechanical and SEM Analysis of Artificial Comet Nucleus Samples....341
K. Thiel, H. Kochan, K. Roessler, E. Grün, G. Schwehm, H. Hellmann, P. Hsiung and G. Kölzer

Ion Bombardment Experiments Suggesting an Origin for Organic Particles in Pre-Cometary and Cometary Ices....353
T. J. Wdowiak, E. L. Robinson, G. C. Flickinger and D. A. Boyd

On the Isotope Analysis of Cometary Dust*....365
F. Begemann

Analysis of Organic Compounds in Returned Comet Nucleus Samples....377
J. R. Cronin

Concepts for the Curation, Primary Examination, and Petrographic Analysis of Comet Nucleus Samples Returned to Earth*....399
D. Stöffler, H. Düren and J. Knölker

Candidate Sample Acquisition Systems for the Rosetta Mission....417
P. G. Magnani, C. Gerli, G. Colombina and P. Vielmo

Description and Analysis of Core Samples: The Lunar Experience*....433
David S. McKay and Judith H. Allton

* Indicates invited papers

The Origin, Composition and History of Comets from Spectroscopic Studies* 455
L. J. Allamandola

Laboratory Analyses of Micron-Sized Solid Grains: Experimental Techniques and Recent Results* 473
L. Colangeli, and E. Bussoletti

Handling and Analysis of Ices in Cryostats and Glove Boxes in View of Cometary Samples 491
K. Roessler, P. Hsiung, M. Heyl, G. Neukum, A. Oehler and H. Kochan

Electron Spin Resonance (ESR) Studies of Returned Comet Nucleus Samples 505
F. D. Tsay, S. S. Kim and R. H. Liang

* Indicates invited papers

PREFACE

This conference publication contains many of the invited and contributed papers presented at the workshop on Analysis of Returned Comet Nucleus Samples. The workshop was held on January 16–18, 1989, in Milpitas, California, under the sponsorship of the Lunar and Planetary Institute and NASA Ames Research Center. After the fly-by missions to comet Halley in 1986, the prospect of launching the joint ESA/NASA Rosetta/Comet-Nucleus-Sample-Return (CNSR) mission in 2002 with a sample return from a comet in 2010 raised considerable scientific interest and provided the stimulus for the meeting. The papers assembled here provide a partial historical record of the scientific issues and measurement objectives articulated in 1989 for the analysis of returned comet nucleus samples. My plan for a timely publication of these papers after the workshop was frustrated by a lengthy illness, and by the time I returned to active work, the momentum had been lost. To colleagues whose papers did not get into print until now, I offer my deep apologies.

During the intervening years, comet missions suffered setbacks and advances. In the early 1990's the Comet Rendezvous Asteroid Fly-by Mission (CRAF, work on which was formally begun in November, 1989) was canceled by NASA, and the Rosetta/CNSR mission underwent a substantial transformation, becoming a comet rendezvous mission like CRAF and including an instrumented soft lander, but no longer a sample return. Rosetta will be launched in 2003 with arrival at comet Wirtanen in 2011 and landing in 2012. In the mid-1990's interest in samples returned from comets was stimulated by the success of the Stardust proposal in competing for a place in the Discovery Program. Stardust—a mission to fly through a cometary coma and capture dust particles intact in aerogel, and then return them to Earth—will be launched in 1999 to a fly-by of Comet Wild 2, with sample return anticipated in 2006. As these missions developed, astronomical detection of Kuiper Belt comets and the extraordinary apparitions of comets Hyakutake and Hale-Bopp continue to fuel comet science. In the same timeframe, the technical challenge of a CNSR mission was taken up by NASA in the form of the Deep Space 4/Champollion mission now taking shape as part of NASA's New Millennium Program, and including participation by the French space agency, CNES. DS-4/Champollion will be launched in 2003 to a rendezvous with periodic comet Tempel 1 in late 2005, with a landing in 2006, and cryogenic, sub-surface sample return to Earth in 2010. Another anticipated comet mission is Contour which was selected through the Discovery Program and which will fly by at least 3 short-period comets. After some substantial setbacks, the fortunes of cometary missions are once again on the upswing, though future implementation is never a sure thing.

Certainly, scientific interest in comets will persist. Astronomical observations alone leave wide gaps in our knowledge of the nature and origin of cometary volatiles and dust. Continuing studies of interplanetary dust particles will reveal more about the connections between their components and their possible origins from comets, asteroids or interstellar dust. Instrumental methods of analyses will continue to advance across a broad front toward applicability to smaller and smaller sample sizes. Synergies will arise in the advancement of analytical techniques as the prospects for return of samples from Mars in 2006 develop in parallel with those for comet nucleus sample return. Samples of comet dust will be returned from the Stardust mission in 2006, and samples of cometary ices and dust will be returned by DS-4/Champollion in 2010. Therefore, laboratory studies will be conducted on samples of known comets. It is only a matter of time.

My belated thanks go to workshop organizers and participants and to authors who supplied manuscripts. I am grateful to Paul Weissman for providing an update on comet missions.

Sherwood Chang
NASA Ames Research Center

WORKSHOP ON:
ANALYSIS OF RETURNED COMET NUCLEUS SAMPLES
AGENDA

Monday, January 16th.

7:00–8:00 a.m. **Registration**

8:00 a.m. *Welcome and Introduction to Workshop*
Sherwood Chang, NASA, Ames Research Center

8:10 a.m. *Rosetta—Comet Nucleus Sample Return Mission: Status Report*
Geoffrey Briggs, NASA Headquarters
Mr. Marcelo Coradini, European Space Agency

SESSION IA
Chairman: Sherwood Chang
8:30 a.m.–12:00 noon

SOURCES AND NATURE OF COMETARY COMPONENTS

Invited Speaker Presentations

Nucleosynthesis and the Isotopic Composition of Stardust
Alexander Tielens

Interstellar and Cometary Dust
John Mathis

Refractory Solids in Chondrite and Comets: How Similar?
John Wood

10:30 a.m. BREAK

Solar Nebular Condensates and the Composition of Comets
Jonathan Lunine

Dis-equilibrium Chemistry in the Solar Nebula and Early Solar System: Implications for the Chemistry of Comets
Bruce Fegley

Poster Presentations

Thermal and Chemical Processing of the Outermost Layer of Cometary Nuclei
Campins H. Krider E.P.

Sulfur Compounds in Comets
Kim S. A'Hearn M.

Spectrophotometric Observations of Comet P/Giacobini-Zinner
Konno I. Wyckoff S. Wehinger P.A.

Computer Simulation of Dust Grain Evolution
Liffman K.

12 Noon–1:30 p.m. GROUP LUNCH AND POSTER REVIEW

SESSION IB
Chairman: Thomas Ahrens
1:30–5:30 p.m.

FORMATION AND PHYSICAL PROCESSING OF COMETS

Invited Speaker Presentations

Comments on Comet Shapes and Aggregation Processes
William Hartmann

Physical Processing of Cometary Nuclei
Paul R. Weissman S. Alan Stern

COMPOSITION OF COMETS FROM SPACECRAFT OBSERVATION

Gas and Ice Composition of Comet P/Halley
Peter Eberhardt

3:30 p.m. BREAK

Composition of Dust from Comet P/Halley: The Mineral Fraction
Yves Langevin

The Organic Matter of Comet P/Halley as Inferred by Joint Gas and Solid Phase Analysis
J. Kissel F.R. Krueger A. Korth

Poster Presentations

On the Measurement of Cosmogenic Radionuclides in Cometary Materials
Herzog G.F. Englert P.A.J. Reedy R.C. et al.

Measurements of Long-Lived Cosmogenic Nuclides in Returned Comet Nucleus Samples
Nishiizumi K. Kohl C.P. Arnold J.R.

Morphology and Compositional Differentiation of the Surface of Comets
Huebner W.F. Boice D.C.

Role of Dust to Gas Production Rate Ratio in Cometary Physics
Ibadov S.

The In-Situ Particulate Size Distribution Measured for One Comet: P/Halley
McDonnell J.A.M. Pankiewicz G.S. et al.

Organic Chemistry in Interstellar Ices: Connection to the Comet Halley Results
Schutte W.A. Agarwal V.K. et al.

5:30–7:30 p.m. **POSTER REVIEW AND SOCIAL**
(cocktails and hors d'oeuvres buffet)

PANEL DISCUSSION
COMET SAMPLE, HANDLING, CURATION AND ALLOCATION
7:30–9:30 p.m.

Chairmen: Douglas Blanchard, NASA Johnson Space Center
Dieter Stöffler, Inst. für Planetologie, Universität Münster

Panel Members: Benton Clark, Martin Marietta
Peter Eberhardt, Physikalisches Inst., University of Bern
John Oró, University of Houston
Edward Whalley, National Research Council of Canada

Tuesday, January 17th.

SESSION IIA
Chairman: Yves Langevin
8:30–12:15 p.m.

INSIGHTS INTO COMETS OBTAINED FROM ANALYSES OF PRIMITIVE SOLAR SYSTEM MATERIALS

Invited Speaker Presentations

The Comet Rendezvous Asteroid Flyby Mission
David Morrison Marcia Neugebauer Paul Weissman

Electron Beam Analysis of Particulate Cometary Material
John Bradley

Evolution of Carbonaceous Chondrite Parent Bodies: Insights into Cometary Nuclei?
Harry Y. McSween, Jr.

10:20 a.m. BREAK

Isotopic Microanalysis of Returned Comet Nuclei Samples
Ernst Zinner

The Carbon Chemistry of Meteorites: Relationships to Comets
Sherwood Chang

Poster Presentation

Interplanetary Dust Particles Optical Properties: A Clue to Cometary Dust Structure?
A.C. Levasseur-Regourd

Identification of Solar Nebula Condensates in Interplanetary Dust Particles and Unequilibrated Ordinary Chondrites
Klöck W. Thomas K.L. McKay D.S.

Cometary Evolution: Clues on Physical Properties from Chondritic Interplanetary Dust Particles
F.J.M. Rietmeijer

Trajectory-Capture Cell Instrumentation for Measurement of Dust Particle Mass, Velocity and Trajectory, and Particle Capture
Simpson J.A. Tuzzolino A.J.

The Measurement of Trace Elements in Interplanetary Dust and Cometary Particles by Ultra-high Sensitivity INAA
Zolensky M.E. Lindstrom D.J. Lindstrom R.M. Lindstrom M.M.

SESSION IIB
Chairman: Ezio Bussoletti
1:45–5:00 p.m.

EFFECTS OF ASTRO-PHYSICAL/CHEMICAL PROCESSES ON COMETARY MATERIALS

Invited Speaker Presentations

Laboratory Simulations: The Primordial Comet Mantle
R.E. Johnson

Metamorphism of Cosmic Dust: Processing from Circumstellar Outflows to the Cometary Regolith
Joseph A. Nuth III

From Interstellar Dust to Comets
J. Mayo Greenberg

3:25 p.m. BREAK

Experimental Studies of Gas Trapping in Amorphous Ice and Thermal Modelling of Comets—Implications for Rosetta
Akiva Bar-Nun

Modifications of Comet Materials by the Sublimation Process: Results from Simulation Experiments
Eberhardt Grün and KOSI team

4:45 p.m.

The Return of Comet Samples and the Issues of Planetary Protection
John Rummel, NASA Planetary Protection Officer

PREVIEW OF POSTER PRESENTATIONS–SESSIONS IIB, IIIA & IIIB
Chairman: Larry Nyquist
5:00–5:30 p.m.

Poster Presentations–IIB

Direct Determination of the Morphology, Structure and Composition of Cometary and Interstellar Ice Analogs in the Laboratory
Blake D.F. Allamandola L.J.

Thermal Histories of the Samples of Two KOSI Comet Nucleus Simulation Experiments
Spohn T. Benkhoff J. Klinger J. Grün E. Kochan H.

The Nature of Cometary Materials and Attachment to Them
Stephens J.

Mechanical and SEM Analysis of Artificial Comet Nucleus Samples
Thiel K. Kochan H. Roessler K. Grün E. Schwehm G.
Hellmann H. Hsiung P. Kölzer G.

Ion Bombardment Experiments Suggesting an Origin for Organic Particles in Pre-Cometary and Cometary Ices
Wdowiak T.J. Robinson E.L. Flickinger G.C. Boyd D.A.

5:30–7:30 p.m. **POSTER REVIEW AND SOCIAL**
(cocktails and hors d'oeuvres buffet)

7:30 p.m. **SPECIAL ADDRESS**
by
Professor Linus Pauling

Inorganic Analogs to Biological Specificity

Dr. Linus Pauling was awarded the Nobel Prize in Chemistry in 1954 and the Nobel Peace Prize in 1963. He has received 30 honorary degrees from United States and foreign universities. In addition, he has received the following awards and honors: the Langmuir Prize, American Chemical Society, 1931; the Nichols Medal, 1941; the Linus Pauling Medal, 1966; the Davy Medal, Royal Society, 1947; Medal for Merit, 1948; Pasteur Medal, Biochemistry Society, France, 1952; Addis Medal, National Nephrosis Federation, 1955; Phillips Memorial Award, American College of Physicians, 1956; Avogardro Medal, Italian Academy of Science, 1956; Fermat Medal, Sabatier Medal and International Grotius Medal, 11957; Order of Merit, Republic of Italy; Medal, Academy Rumanian People's Republic, 1965; President of Honor, International Society of Research Nutrition and Vital Substances, 1965; Silver Model, Institute France, 1966; and, the Supreme Peace Sponsor, World Fellowship of Religions, 1966. His work includes: determination of structure of crystals and molecules; application of quantum mechanics to chemistry; rotation of molecules in crystals; sizes of ions; theory of stability of complex crystals; chemical bond; line spectra; immunochemistry; structure of proteins; molecular abnormality in relation to disease; sickle cell anemia; orthomolecular medicine, vitamin C and cancer; metals and alloys; and ferromagnetism. Dr. Pauling now leads the Linus Pauling Institute of Science and Medicine in Palo Alto, California.

Wednesday, January 18

SESSION IIIA
Chairman: Kurt Marti
8:30–12:00 noon

ANALYTICAL METHODS FOR STUDY OF COMET NUCLEUS SAMPLES

Invited Speaker Presentations

Rosetta Mission Description
Gerhard Schwehm

On The Isotope Analysis Of Cometary Dust
F. Begemann

Isotopic Compositions Of Hydrogen, Carbon, Nitrogen and Oxygen
Robert Clayton

10:20–10:40 BREAK

Analysis of Organic Compounds in Returned Comet Nucleus Samples
John R. Cronin

Concepts for the Curation, Primary Examination and Petrographic Analysis of Comet Nucleus Samples Returned to Earth
Dieter Stöffler H. Düren J. Knölker

Poster Presentations

Trace Element Abundance Determination by Synchrotron X-ray Fluorescence (SXRF) on Returned Comet Nucleus Mineral Grains
Flynn G.J. Sutton S.R.

Prompt Gamma Activation Analysis (PGAA): Technique of Choice for Nondestructive Bulk Analysis of Returned Comet Samples?
Lindstrom D.J. Lindstrom R.M.

Candidate Sample Acquisition System for the Rosetta Mission
Magnani P.G. Gerli C. Colombina G. Vielmo P.

Nondestructive Trace Element Microanalysis of As-Received Cometary Nucleus Samples Using Synchrotron X-ray Fluorescence
Sutton S.R.

12:00–1:30 p.m. LUNCH

SESSION IIIB
Chairman: Dave Stevenson
1:30–5:00 p.m.

ANALYTICAL METHODS FOR STUDY OF COMET NUCLEUS SAMPLES—CONTINUED

Invited Speaker Presentations

Analytical Study of Comet Nucleus Samples
Arden Albee

Description and Analysis of Core Samples: The Lunar Experience
David McKay

2:50 p.m. BREAK

The Origin, Composition and History of Comets from Spectroscopic Studies
Louis J. Allamandola

Laboratory Analyses of Micron-sized Solid Grains: Experimental Techniques and Recent Results
L. Colangeli **Ezio Bussoletti** A. Blanco A. Borghesi S. Fonti V. Orofino G. Schwehm

CLOSING REMARKS—Sherwood Chang

Poster Presentations

Microanalytical Characterization of Biogenic Components of Interplanetary Dust
di Brozolo F.R. Meeker G.P. Fleming R.H.

Handling and Analysis of Ices in Cryostats and Glove Boxes in View of Cometary Samples
Roessler K. Hsiung P.. Hey M. Neukum G. Oehler A. Kochan H.

Analysis of Particulates of Comet Nucleus Samples: Possible Use of Olivine as Indicator Phase
Steele I.M.

Electron Spin Resonance (ESR) Studies of Returned Comet Nucleus Samples
Tsay F.D.

END OF WORKSHOP

ORGANIZING COMMITTEE

Thomas Ahrens
California Institute of Technology

Lou Allamandola
NASA Ames Research Center

David Blake
NASA Ames Research Center

Donald Brownlee
University of Washington

Theodore E. Bunch
NASA Ames Research Center

Humberto Campins
Planetary Science Institute

Sherwood Chang, **Convener**
NASA Ames Research Center

Jeff Cuzzi
NASA Ames Research Center

Eberhard Grün
Max-Planck-Institut für Kernphysik

Martha Hanner
Jet Propulsion Laboratory

Alan Harris (Ex Officio)
Jet Propulsion Laboratory

John Kerridge
University of California, Los Angeles

Yves Langevin
Universite de Paris, Sud

Larry Nyquist, **Convener**
NASA Johnson Space Center

Gerhard Schwehm
European Space Agency, ESTEC

Paul Weissman
Jet Propulsion Laboratory

NUCLEOSYNTHESIS AND THE ISOTOPIC COMPOSITION OF STARDUST

A. G. M. Tielens
Space Sciences Division
Ames Research Center

Nucleosynthesis and the Isotopic Composition of Stardust

A.G.G.M. Tielens
Space Sciences Division
MS 245-3, Moffett Field
CA 94035

Abstract

Various components have been isolated from carbonaceous meteorites with an isotopically anomalous elemental composition. Several of these are generally thought to represent stardust containing a nucleosynthetic record of their birthsites. This paper discusses the expected isotopic composition of stardust based upon astronomical observations and theoretical studies of their birthsites: red giants and supergiants, planetary nebulae, C-rich Wolf-Rayet stars, novae and supernovae. Analyzing the stardust budget, it is concluded that about 15% of the elements will be locked up in stardust components in the interstellar medium. This stardust will be isotopically heterogenous on an individual grain basis by factors ranging from 2 to several orders of magnitude. Since comets may have preserved a relatively unprocessed record of the stardust entering the solar nebula, isotopic studies of returned comet samples may provide valuable information on the nucleosynthetic processes taking place in the interiors of stars and the elemental evolution of the Milky Way.

I Introduction

One of the most interesting developments within the field of interstellar dust in recent years is the realization that some interstellar and circumstellar grains have been incorporated into meteorites and interplanetary dust particles without totally losing their identity (see the reviews by Kerridge 1986 and by Anders et al. 1989). Evidence for this rest on the measurement of isotopic composition of such materials. Although the meteoritic composition is in gross sense remarkedly homogeneous, non-mass-dependent isotopic anomalies do exist in many elements. These include the noble gasses, the light elements (H, C, N, and

O), and the heavy elements (e.g., Ca, Ti, Cr, Ni, Nd, Sm and others). Although some unusual process in the solar nebula might have produced non-mass-dependent isotopic fractionation in some elements, it is unlikely that it could account for all of them. Moreover, the measured isotopic anomalies are very characteristic for a presolar origin of the material. In particular, some Xe and Kr isotopic anomalies associated with a carbon phase carry the signature of the nucleosynthetic s-process in red giants, suggesting the presence of largely unmodified carbon stardust in meteorites (Kerridge and Chang 1985). Other components isolated from meteorites seem to carry the nucleosynthetic record of novae and supernovae (Anders et al. 1989). The best stardust characterizations have been made for C-dust. To a large extent this reflects merely the importance of vaporization and recondensation processes in the solar nebula for the mineral component of meteorites leading to a large degree of dilution of stardust oxides. Since the solar nebula was O-rich, contamination of the C-stardust record by solar nebula condensates is probably much less severe.

Comets are among the most pristine objects in the solar system and their study may reveal much about starformation and solar nebulae processes. One popular model of comets envisions them as dirty snowbals formed by the aglomoration of ices and interstellar dust in the outer reaches of the protoplanetary disk (Greenberg 1989). In that case, processes in the solar nebula as well as on the parent body are unimportant and a large fraction of refractory stardust, including the oxides, may be readily identifiable. Thus even more than for meteorites and interplanetary dust particles, analysis of the isotopic composition of comet samples may reveal important information on the nuclear processes taking place in stardust birthsites. Such knowledge is expected to revolutionize our understanding of the composition and evolution of stars and the Milky Way.

This paper considers the isotopic composition of stardust inferred from observational and theoretical studies of their birthsites. Section II discusses the galactic stardust budget for the three main dust components identified in stellar ejecta, C-dust, silicates and SiC. The ecological impact of stardust on the total interstellar dust budget is also briefly discussed. There are several processes that can lead to the incorporation of (isotopic) trace species in a condensing solid. These are reviewed in section III. Section IV summarizes the nuclear processes taking place in the interiors of stars and their resulting evolution. The emphasis is on known or suspected sources of stardust: O-rich and C-rich red giants, red supergiants, planetary nebulae, C-rich Wolf-Rayet stars, novae and supernovae. Astronomical observations of the isotopic composition of their ejecta is discussed. Section V briefly discusses the isotopic composition of various suspected carbon-stardust components isolated from carbonaceous meteorites, their likely birthsites and the processes by which these anomalies were included

in the condensing grains. Finally, the implications for the Rosetta mission are briefly discussed in section VI.

II Stardust Characteristics

Many stars go through a pronounced phase of mass loss at the end of their life. Upon expansion, the ejected material cools down and conditions often become favorable for dust nucleation and condensation. This socalled stardust manifests itself then by extincting the stellar light and reradiating the absorbed energy at infrared wavelengths. Among the stellar objects known to be associated with newly formed dust are red giants and supergiants, novae, planetary nebulae, and WC Wolf Rayet stars. Infrared observations show evidence for the presence of amorphous silicates, hydrogenated amorphous carbon (ie., soot), polycyclic aromatic hydrocarbon molecules (ie., PAHs), silicon carbide, and magnesium sulfide grains around these objects (cf., Tielens and Allamandola 1987a). Until recently there was no direct astronomical evidence for dust formation in supernova ejecta. However, various independent lines of evidence have revealed that dust has formed in the ejecta of SN 1987A in the Large Magelanic Cloud (Wooden 1989). Moreover, small diamonds have been isolated from carbonaceous meteorites with an isotopic composition suggesting an origin in SN ejecta (Anders et al. 1989). Thus, it is likely that all SNe are important sources of stardust as well. The chemical make-up of these supernova condensates is, however, unknown.

A) The Stardust Budget

Table 1 summarizes the carbon, silicate, and SiC stardust budget of the galaxy (see Gehrz 1989; Tielens 1989). Carbon stardust predominantly, but not exclusively, forms in C-rich ejecta (ie., C/O > 1). C-giants dominate the carbon stardust budget, with a small contribution from WC stars (for detail see Tielens 1989). The novae contribution is somewhat uncertain since the composition of the ejecta is sensitive to the specific conditions and is observed to vary (Truran 1985; Wiescher et al. 1986). The value quoted in table 1 assumes a factor ten enrichment in elemental C compared to solar, which increases it slightly from the previous study (Tielens 1989). We have included the contribution from the central stars of planetary nebulae (PN), based on a typical C-mass loss rate of 10^{-9} $M_\odot$ yr^{-1} and a surface density of 40 kpc^{-2} PN in the galaxy (Pottasch 1984). Although there is no direct evidence for dust formation in these high velocity winds (≈1000 km/s), the UV/visual line spectrum of some PN nuclei resemble those of late type WC stars

which are known to condense C-dust. Note that PNe are surrounded by extensive dust shells resulting from mass loss in the preceding red giant phase, which is seperately listed and not included in the PN value given in table 1. Since the ashes from the He-burning zone are C-rich (Woosley and Weaver 1986a), type II supernovae might be an important source of C-dust (Clayton 1981). However, various observations of SN 1987a in the LMC suggest that turbulence is very important in a supernova explosion (Arnett et al. 1989). This will mix the He ashes with products of the more fiercely burned core and, for completely mixed ejecta, C is only a minor elemental component (e.g., C/O≈0.1 for a $25M_{\odot}$ progenitor; Woosley and Weaver 1986a). Little if any C-dust formation is then expected. This also holds for type Ia supernovae, but their overall contribution to the C-budget of the galaxy is never expected to be large (Thielemann et al. 1986; Woosley and Weaver 1986a). The supernova values given in table 1 correspond to the maximum amount possible and the actual contribution might be much less. The H-rich conditions in C-giant ejecta will lead to the formation of highly hydrogenated amorphous carbon dust (i.e., soot). In contrast, C-dust formed from He-ashes (eg., WC stars, SNe) will not be hydrogenated and, based on extensive laboratory studies (Curl and Smalley 1989), might have a disordered, fullerene structure (Tielens 1989)

When the elemental C/O ratio is less than unity, silicate or metal grains are expected to condense out (Salpeter 1977). M-giants and supergiants show 10 and 20μm emission or absorption features generally ascribed to the SiO stretching and bending vibrations in amorphous silicates. They are important contributors to the silicate stardust budget. The estimate for giants in table 1 is based upon solar Si abundances, an estimated H mass loss rate of 5×10^{-4} $M_{\odot}$ kpc^{-2} yr^{-1} for M-giants (Jura 1987), and assumes that all Si condense out as $(Mg,Fe)SiO_4$. Supergiants typically have a mass loss rate of 10^{-5} $M_{\odot}$ yr^{-1}. With a galactic supergiant surface density of 5 kpc^{-2}, this results in 2×10^{-7} $M_{\odot}$ kpc^{-2} yr^{-1}. Supernovae (type II as well as type Ia) are the dominant source of newly synthesized silicon and can thus be important silicate producers as well. The estimates quoted in table 1 are based on nucleosynthesis SN calculations (0.2 and 1.2 $M_{\odot}$ per type Ia and type II SN respectively; Thielemann et al. 1986; Woosley and Weaver 1986a) and a SN rate of 10^{-5} kpc^{-2} yr^{-1} for each (Tammann 1982). Since these numbers assume that all the Si condenses as silicates, they should be considered as upper limits. Some novae show evidence for silicate dust condensation, besides the more abundant C-dust (Gehrz 1988). The estimate in table 1 is based on a mass ejection of 10^{-4} $M_{\odot}$, a nova rate of 40 yr^{-1}, and a solar Si abundance (Truran 1985). Note that the composition of the condensing silicates is not well known. Observations suggest a highly disordered structure, probably the result of the low condensation temperature (Tielens and Allamandola 1987b).

Table 1: The stardust budget of the galaxy

Source	contribution (10^{-6} $M_\odot$ kpc^{-2} yr^{-1})[a]		
	carbon-dust	silicates	SiC
C-giants	2	- -	0.07
M-giant	- -	3	- -
novae	0.3	0.03	[0.007][d]
planetary nebulae	0.04[b]	- -	- -
Red Supergiants	- -	0.2	- -
WC stars	0.06	- -	- -
type II supernovae	[2][c]	[12][c]	- -
type Ia supernovae	[0.3][c]	[2][c]	- -

notes: a) Uncertainties are typically a factor 3. b) Mass loss during the red giant phase is not included (see text for details. c) Stardust formation has been observed in supernovae 1987a, but the composition of the dust is not known. d) No astronomical evidence for SiC formation in novae (see §II).

The 11.3μm feature due to SiC grains is observed in circumstellar shells around C-rich giants (and planetary nebulae) whenever the elemental C/O ratio is in the range 1 to 1.5 (Roche 1989). Assuming that all the Si condenses out, this corresponds to a production rate of 7×10^{-7} $M_\odot$ kpc^{-2} yr^{-1}. However, analysis of IR observations suggests that only 10% of the Si has condensed out in SiC in the "prototypical" C-giant IRC 10216 (Martin and Rogers 1987) and we have adopted this conservative value in table 1. Isotopic anomalous SiC grains isolated from carbonaceous meteorites probably result from nova ejection (Anders et al. 1989) but, since Si is not greatly enhanced in novae explosions, their contribution is small. Moreover, the astronomical evidence for SiC formation in nova is controversial. A 10μm feature, resembling those observed in O-rich giants and attributed to silicates, has been observed in nova V1370 Aql. However, the absence of the corresponding 20μm silicate emission feature in this nova has led to the suggestion that the carrier is a diatomic grain material, presumably SiC, despite the poor spectral match (Gehrz 1988). But, in contrast to dust shells around O-rich

giants which have dust at a range of temperatures, nova shells contain dust at a single (high) temperature and the 20μm silicate feature might be much weaker than normally expected (Roche, private comm.). Thus, the absence of this feature might not be decisive. Formation of SiC grains is not expected in SN ejecta, since either the C and Si zone are mutually exclusive or mixing produces O-rich ejecta and probably leads to oxide dust.

B) Stardust and Interstellar Dust

Studies of interstellar extinction and polarization have shown that about half of the availlable, condensible elements (i.e., heavier than He) has to be in the form of interstellar dust (Tielens and Allamandola 1987b). The ubiquity of the 10μm silicate feature, corresponding to ≈30% of the total dust mass (Cohen et al. 1989), attests to the importance of silicates in the interstellar dust budget. In general, it is assumed that this refractory grain component is formed in stellar ejecta. However, recent laboratory studies have shown that under some conditions silicate formation may also occur in the interstellar medium itself (Nuth and Moore 1988). Because of abundance constraints, the remainder of the interstellar dust mass is probably in the form of a carbonaceous dust component. Both models based upon graphite (or perhaps amorphous carbon) formed in C-rich stellar ejecta (Mathis 1989) as well as on hydrocarbon grains formed by accretion and UV photolysis in the interstellar medium (Greenberg 1989) have been proposed. Either of these models can provide excellent fits to the observed interstellar extinction and polarization given an appropriate grain size distribution. In fact, the derived grain size distributions are exceedingly similar and little additional information can be gleaned from such observations. The total elemental Si injection rate is about 4×10^{-6} $M_\odot$ kpc^{-2} yr^{-1} and, thus, about 2% of all Si is ejected in the form of SiC, of which at most ≈0.1% originates in novae. Thus, SiC stardust seems unimportant on a galactic scale and models based on it (Gilra 1972) have been largely abandoned. Observationally, a conservative upper limit on the ratio of the 11.3 μm SiC band to the 10 μm silicate band of 0.1 in the ISM translates to at least 10 times more Si in silicates than in SiC.

Studies of elemental depletion patterns in the interstellar medium also indicate that silicates and carbonaceous grains are important components of the interstellar dust (Jenkins 1989). The gas phase abundance of Si, as well as the metals, Fe, Ca, Al, and Ti, is observed to be highly depleted (by a factor 10 or more) compared to the cosmic abundance value. Presumably, the missing fraction is locked up in silicate (or metal) grains (Field 1974). Although quite uncertain, C seems to be quite depleted in the interstellar medium (by about 50%). However, elements such as O and N, which predominantly form volatile condensates (ie., H_2O

and NH_3), are much less depleted (<20%). Such elemental abundance studies have also revealed that high velocity clouds have nearly solar abundances of elements such Fe and Si (Jenkins 1989). These clouds have probably recently been shocked - hence the high velocity - which has presumably lead to destruction of most of the dust mass. Based upon expected shock frequencies in the ISM, the dust destruction rate in the ecology budget of the galaxy is then estimated to be about 1.4×10^{-4} $M_\odot$ kpc^{-2} yr^{-1}, corresponding to a stardust lifetime of about 4×10^8 yr, a number uncertain by perhaps a factor two (McKee 1989). A further 5×10^{-5} $M_\odot$ kpc^{-2} yr^{-1} of dust and its associated gas is lost due to starformation.

These numbers can be directly compared to the stardust injection rates in table 1. The maximum total dust injection rate, including SN, is 2×10^{-5} $M_\odot$ kpc^{-2} yr^{-1}. For a total ISM gas mass of 5×10^9 $M_\odot$ (Scoville and Sanders 1987) and a dust abundance of 1% by mass, this corresponds to an injection timescale of about 2.5×10^9 yr. Therefore, in equilibrium only about 15% of the stardust survives in an average patch of the ISM. If we exclude SN for which the dust fraction is not well known, the average fraction of the elements locked up in stardust is only 3%. Thus, interstellar dust models based on stardust alone, which require 70 and 90% of the C and Si in the form of stardust in the interstellar medium (Mathis 1989), face serious problems. In fact, it is difficult to explain elemental depletions of more than 75% by stardust formation alone, since that would correspond to a dust destruction rate of less than 7×10^{-6} $M_\odot$ kpc^{-2} yr^{-1} - a factor 20 lower than the theoretical expected value (McKee 1989). This problem is further compounded for the most heavily depleted elements, Fe (>90%) and Ca (>99%), which require dust destruction rates of less than 2×10^{-6} and 2×10^{-7} $M_\odot$ kpc^{-2} yr^{-1}. This is even more so since mass loss from O and B stars is known to contribute about 10% of the elements exclusively in gaseous form (Jura 1987). Obviously, accretion processes in the interstellar medium have to be very important in determining the gas phase abundance of these heavily depleted metals (Snow 1975). Given this conclusion, models based upon a dust component formed by accretion (and photolysis) processes in the interstellar medium, containing perhaps 25% of the condensible elements (Greenberg 1989), have to be taken very serious. Indeed, observations along three different lines of sight show the presence of hydrocarbon grains containing between 5 and 25% of the elemental C (Tielens and Allamandola 1987b; Cohen et al. 1989). Such hydrocarbon grains have not been observed in circumstellar dust sources and presumably reflect a dust component formed by local interstellar medium processes.

III Impurities in Stardust

Several distinctly different processes can lead to the incorporation of impurities in stardust. First, during condensation chemical substitution may take place. This is particularly true for isotopes such as ^{13}C. Second, stardust formation generally occurs under highly supercooled conditions and, even though thermochemistry might indicate the condensation of one (or more) well defined mineral (ie., Mg_2SiO_4; Grossman and Larimer 1974), dust formation may be expected to be highly heterogeneous leading to a highly mixed elemental composition. Thus, metal cations such as Ca and Al are expected to be readily substituted for Mg in circumstellar silicates, despite the difference in coordination and binding. Likewise, metals such as Fe and Ti can replace Si in SiC and N can replace C in diamond grains. The presence of such impurities at the few percent level or higher is well known for terrestrial specimens. Indeed, the colors produced by dissolved metal ions were already well appreciated by glass artisans in 14th century Venice.

Third, impurities can form chemical bonds with dangling bonds at internal or external grain surfaces during the grain condensation process. Peripheral groups such as OH are well known both for silicate as well as for carbonaceous grains. Highly disordered carbon soot with its many internal "surfaces" and edges contains in general a large complement of peripheral groups. The planar aromatic structure of soot also lends itself well to intercalation of impurities. The π electron system can accept as well as donate electrons with a typical binding energies of 0.5-1 eV and thus a variety of species can be incorporated, including metals such as Na and K. In contrast, noble gasses such as Ar and Xe have only a binding energy of 0.1-0.15 eV on a graphitic (or silicate) surface (Jaycock and Parfitt 1986), which corresponds to a residence time of $\approx 10^{-11}$ sec at a dust condensation temperature of 800 K. Thus, noble gasses are not expected to be easily incorporated into condensing grains. Nevertheless, experimental studies of Xe adsorption on carbon black samples have revealed an unexpected, tightly bound Xe component which remains up to temperatures of 1300 K (Wacker et al. 1985). Note that most of the Xe was bound on external surfaces and readily evaporated upon warm up. At the low dust temperatures of the ISM ($\approx$15K) evaporation of such a noble gas component will be of little importance, but in view of the low binding energy and the importance of gas-grain interactions in the ISM, it is unlikely that they will be preserved into the solar nebula. The tightly bound component may represents a long random walk in the extensive pore network of carbon black with release possibly inhibited by bottleneck pores. Alternatively, it is known that He implanted into graphite remains trapped at much higher temperatures ($\approx$450K) than expected from simple physisorption (E$\approx$0.02eV; Möller et al. 1982). Presumably, this involves

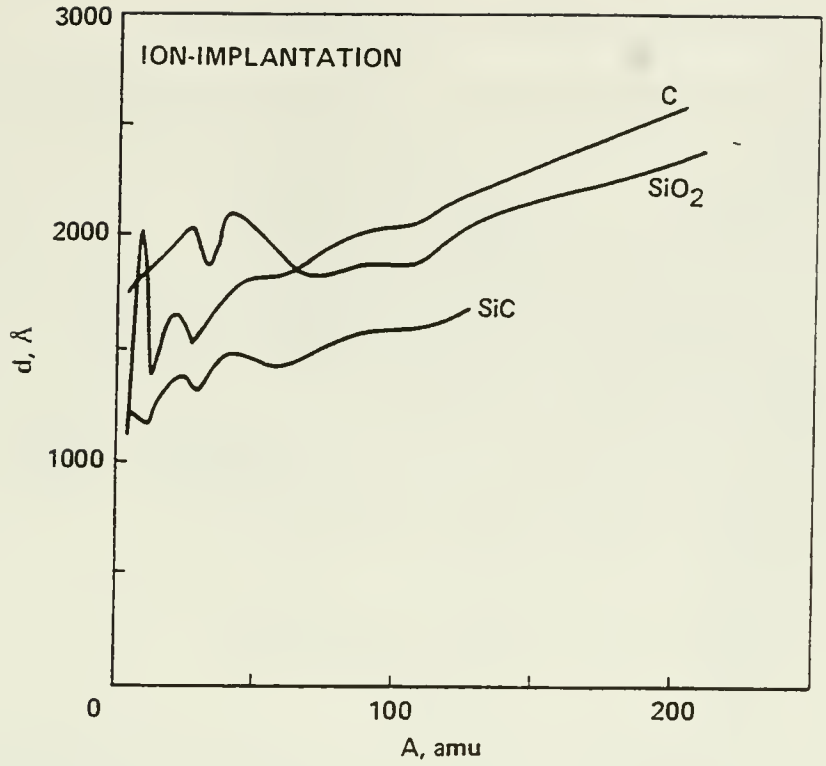


Fig. 1: The mean projected range for implantation of ions with an energy of 5 keV/amu, corresponding to a grain-gas drift velocity of 1000 km/s.

vacancies, a well known effect for metals where binding energies of a few eV have been measured (Scherzer 1983). Although the literature is much sparser, heavier noble gasses seem also to be trapped at such vacancies. Thus, stardust could contain traces of tightly bound noble gasses.

Fourth, high velocity ion implantation can lead to a large concentration of impurities, but the high velocities required limit this process to supernova and nova ejecta and the fast winds of the central stars of planetary nebulae. Figure 1 shows the mean projected range for ion-implantation in various solids (Burenkov et al. 1986). A gas-grain drift velocity of 1000 km/sec has been assumed, corresponding to ≈5 keV/amu. This picture is appropriate for (super)nova ejecta overtaking previously ejected material (Clayton 1981). In this case, the typical depth of implantation is about 1500 Å fairly independent of grain material. Since this is a physical process, all elements can be retained and this process may be in particularly important for the noble gasses which are difficult to adsorb otherwise. The penetration depth is insensitive to the mass of the impacting ion

(i.e., energy). For example, from Ar (40 amu) to Xe (130 amu) the penetration depth in graphite increases only from ≈1750 to 2200 Å. Thus, only minor fractionation will occur. Larger differences in the retention of ions of different mass may occur on a timescale associated with the diffusion of the lightest ion, but at ISM dust temperatures (≈15 K) this will be unimportant, except perhaps for H and He. When the dynamics of the outflow are dominated by radiation pressure on dust balanced by gas drag (i.e., red giants), the typical gas-grain drift velocities are quite small (<20 km/sec; Tielens 1983). Since penetration depends strongly on the ion energy, much smaller implantation depths are obtained. For example, a Kr atom impacting at 20 km/sec (≈0.2 keV) will only penetrate 5 Å (< two graphite layers). Such shallowly implanted ions are probably lost by subsequent interstellar medium processing (i.e., sputtering in low velocity shocks) and this is unlikely to be important for the isotopic composition of stardust.

I V Nucleosynthesis and Stellar Evolution

Following the seminal work by Burbride et al. (1957) and Cameron (1957), it is now generally accepted that almost all elements heavier than He have been synthesized in the interiors of stars by nuclear reactions. This transmutation of the elements plays a key role in the evolution of stars. Also the energy released stabilizes stars against gravitational collapse and, of course, provide the photons observed by us. The text books by Clayton (1968) and Rolfs and Rodney (1988) provide a thorough discussion of stellar nucleosynthesis. A recent review of the state of the art in nucleosynthesis is provided by the volume edited by Arnett and Truran (1985).

The key nuclear processes that play a role in the synthesis of the elements include the major energy burning cycles: H- burning into He; He-burning into C and O; and C-, O-, and Si-burning producing the intermediate peak (or silicon peak) and iron peak elements ($16 \leq A \leq 60$). Since the binding energy per nucleon decreases for high ($A \geq 60$) mass number, the elements more massive than Fe have to be produced by other means than static nuclear burning. Essentially, these elements are thought to result from the combined effects of capture of neutrons onto Si-peak and Fe-peak elements and β-decay. Depending on whether neutron capture is slower (s-process) or more rapid (r-process) than β-decay different elements are synthesized. The s-process will occur under neutron-rich, "static" conditions and red giants are considered the likely origin of most of the solar system s-process elements with some contribution from type II SN. The r-process characteristically occurs under "explosive" conditions, when a large number of neutrons are rapidly

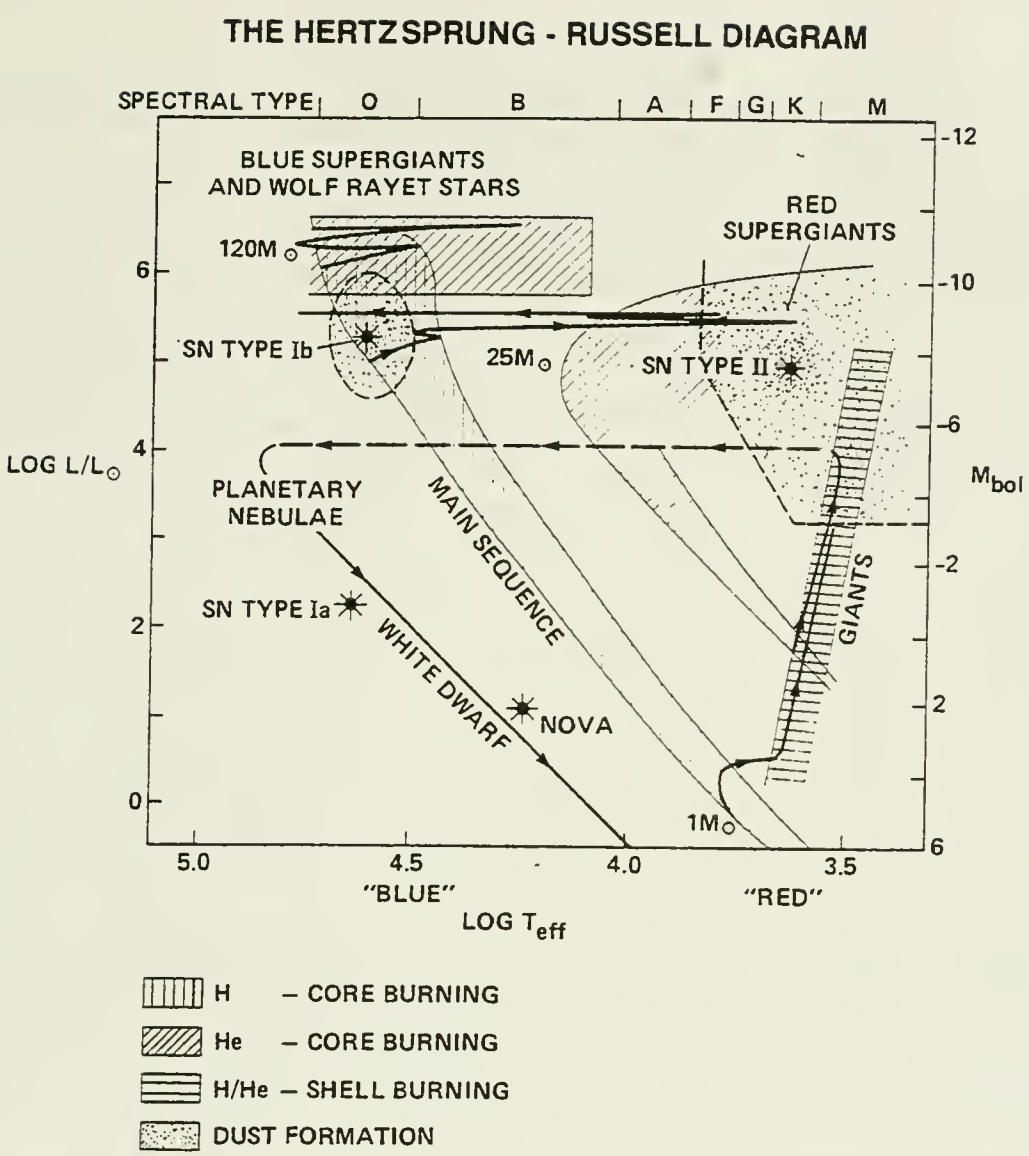


Fig. 2: A schematic Hertzsprung-Russell Diagram indicating the location of various types of stars and their internal nuclear energy source. Theoretical evolutionary tracks for three different mass stars (1, 25, and 120 $M_{\odot}$) are indicated by solid and dashed lines. Dust formation has been observed in red giants and supergiants, planetary nebulae, WC Wolf-Rayet stars, and novae. The recent type II supernova, SN1987A, also shows evidence for dust formation. See text for details.

in the released. Generally, the solar system r-process elements are attributed to supernova explosions. The origin of a few heavy elements is not well understood,

but might involve proton capture (p-process). Their abundance is however low. Finally, for completeness spallation due to the cosmic ray bombardment in the ISM should be mentioned. This process is, however, only expected to be of importance for the synthesis of the lighter elements.

Traditionally, a discussion of stellar evolution starts with the Hertzsprung-Russell diagram (HR diagram), in which a star's luminosity, L, is plotted versus its effective (ie., surface) temperature, T_{eff}, or equivalently its color (Fig 2). The overwhelming majority of the stars fall into a few well defined regions (ie., main sequence, giants, supergiants) in such a diagram. To a large extent the position of a star in this diagram is determined by its internal nuclear energy source and its mass. Due to the nucleosynthesis in their interiors, stars will (slowly) evolve. In particular, when a particular energy source is exhausted and a new one is turned on, completely different internal conditions (ie., higher density and temperature) are required. Often, the photosphere will "rapidly" adjust itself to these changed conditions and move to a new location in the HR diagram. Figure 2 shows schematically where H-, He-core burning and H/He shell burning is of importance in the HR diagram. Thus, stars on the main sequence burn H into He in their core, while red supergiants burn He into C. Giants on the other hand have exhausted their central energy supply and burn H and/or He in a shell surrounding the core.

The evolution of stars is different for different stellar masses. Stellar evolution can also be influenced by the mass loss associated with a strong stellar wind (i.e., Wolf Rayet stars). Several theoretical evolution tracks are superimposed upon the Hertzsprung-Russell diagram in figure 2 (Iben and Renzini 1983; Maeder and Meynet 1987). During several distinct evolutionary phases material can be ejected by the star either in the form of a steady wind (ie., giants, supergiants, Wolf Rayet stars) or explosively (ie., novae, supernovae). Dust nucleation and condensation has been observed to take place in the outflows from red giants, supergiants and C-rich Wolf Rayet stars (WC stars). Boundaries for dust formation in these phases are schematically indicated in fig. 2. Dust formation is also observed in some novae and, recently, in supernova 1987a.

Mixing of freshly synthesized material from the core or regions surrounding it to the surface is a common phenomena in late stages of stellar evolution. This is in particular true for the stardust forming objects: giants, supergiants and WC stars. As a result the surface composition of such objects can change drastically. Indeed, such systematic variations have been observed and form one of the most important tests of stellar evolution theory (Lambert 1988; Willis 1982; Maeder 1987). Likewise, material ejected by novae and supernovae has a distinctly non-solar composition (Truran 1985; Woosley and Weaver 1986a). Table 2 summarizes some of these variations for phases of stellar evolution associated with stardust formation. The emphasis is on the isotopes of C and O, which because of their

Table 2: Isotopic Anomalies

Object	Abundance ratios[a]					dust[b]
	$^{12}C/^{13}C$	$^{16}O/^{17}O$	$^{16}O/^{18}O$	s-process	other	
M-giants	0.1	0.25	1	- -	- -	silicates
S-giants	0.3	0.2	1.4	≈10	^{12}C	silicates
C-giants	0.3-1	- -	- -	≈20	^{12}C	SiC, C-dust
Novae	10^{-3}	10^{-3}	- -	- -	^{26}Al (^{26}Mg)	silicates
					^{22}Na (^{22}Ne)	C-dust, PAHs
red-supergiants	0.1	0.2	1	- -	- -	silicates
WC stars	[∞][c]	[∞][c]	[∞][c]	[5][c]	^{12}C, ^{22}Ne ^{23}Na	C-dust

notes: a) Observed abundance ratios relative to solar ratios in various stardust forming objects. b) Observed dust materials (see section II for details). c) Predicted theoretical values.

abundance have been the easiest to measure in astronomical spectra. Observed enhancements in the abundance of s-process elements, as well as some other relevant elements, are also indicated. The type of solid materials observed to condens out around these objects are also summarized in table 2. These have been discussed in more detail in §II and in Tielens and Allamandola (1987a). In the remainder of this section, these isotopic abundances and their nucleosynthetic origin will be discussed.

A) Evolution of low mass stars

Low mass stars ($M \leq 8\ M_\odot$) like the Sun spend most of their lifetime ($\approx 6 \times 10^9$ yr for the Sun) on the main sequence burning H into He (fig. 2). After H in the core is exhausted, H-burning in a shell surrounding the He core takes over as the energy source and the star moves over onto the giant branch. The star moves slowly up on the giant branch (ie., higher L) until the core is massive enough to ignite He burning into C and O. At this point the star will rapidly move down the giant branch to the core-He burning region of the HR diagram (fig. 2). For stars somewhat more

massive than the sun (i.e., >2.3 $M_\odot$) core He-burning occurs in a region distinct from the giant branch (at higher T_{eff}). When the He fuel is exhausted in the core, the C-O core will contract until it is supported by electron degeneracy against further gravitational collapse. In these low mass stars, central pressures and temperatures never get high enough to iginite further stable burning. The star is now in essence a C-O white dwarf surrounded by an extensive envelope in which alternating H- and He-shell burning occurs. This adds mass to the core and again the star moves up in luminosity on the (asymptotic) giant branch. When the envelope mass becomes very small mainly due to the strong stellar wind, the white dwarf core becomes visible and ionizes the previously ejected material forming a planetary nebula. At this point, nuclear energy generation has ceased and the white dwarf will slowly darken into oblivion. For the most massive stars in this regime ($\approx 8\ M_\odot$) static nuclear burning may proceed slightly further producing an O-Ne-Mg white dwarf (Nomoto 1984).

M-, S-, and C-Giants: During its evolution on the giant branch, the chemical composition of a low mass star will change. First, starting out as an O-rich M-giant, material is dredged up from the H-burning shell surrounding the He-core, resulting in an enrichment of ^{13}C, ^{14}N and ^{17}O and a small depletion in ^{12}C and possibly ^{18}O (ie., CNO cycle). Once He burning is ignited, convective instabilities may mix He ashes to the surface. As a result the star may change from an O-rich M-giant to a C-rich C-giant, possibly passing through the S-giant phase in which $C/O \approx 1$. Due to the pronounced effect of the C/O ratio on the molecular composition of these cool stars, this enrichment in C can readily be observed in the molecular composition of the stellar photosphere. During the He shell burning phases (socalled thermal pulses) conditions are favorable for the formation of s-process elements. Thus, simultaneously with the increase in ^{12}C, the abundance of s-process elements in the photosphere will increase relative to that of Fe. Observations are in good agreement with these expectations (Lambert 1988; Smith 1989). Note that this change in photospheric composition also has a pronounced influence on the chemical make up of the stardust: silicates in M-giants versus hydrogenated amorphous carbon and SiC in C-giants. This merely reflects the high stability of the CO molecule, which locks up either all of the C or all of the O, depending on which has the lesser abundance. The excess O or C is then available for oxide or carbonaceous dust formation (Salpeter 1977).

B) Low mass binaries

For members of close binary system, the last stages of evolution can be slightly different due to accretion of material from a companion on to the white dwarf surface. Slow accretion of H-rich material may reignite nuclear burning at

the white dwarfs surface in a thermal nuclear runaway, leading to a nova explosion and the ejection of about 10^{-4} $M_\odot$ (cf., Truran 1985). Such a system may experience many nova "puffs". In contrast, when accretion is rapid, the white dwarf is compressed and heats up. When enough material has accreted, nuclear burning is ignited again. A subsonic C-deflagration wave propagates outwards and the released nuclear energy completely disrupts the white dwarf in a type Ia supernova explosion (Nomoto 1985).

Novae outburst are thought to result from a thermonuclear runaway on the surface of an accreting white dwarf in a close binary system. Nuclear burning probably proceeds through the CNO cycle and enhancements in ^{14}N, ^{15}N, ^{13}C and ^{17}O and depletion of H are expected. Indeed, significant enhancements in ^{13}C and N have been observed for many novae ejecta (Truran 1985; Wiescher et al. 1986). However, enhancements in the total C, N, and O abundances as well as unexpected enhancements of Ne, Na, Mg, and Al have also been observed. It seems that hot explosive H-burning and/or mixing of white dwarf material into the ejecta can be very important. Finally, explosive H burning in novae may also lead to the formation of the radioactive elements ^{22}Na and ^{26}Al, which decay to ^{22}Ne and ^{26}Mg respectively.

The white dwarf material in type Ia supernova explosions undergoes explosive C, Ne, O and Si burning at the passage of the C deflagration wave, ultimately resulting in the production of iron-peak elements (Nomoto 1985). The outer layers burn only partially or not at all and significant amounts of intermediate mass elements such as ^{12}C, ^{16}O, ^{24}Mg, ^{28}Si, ^{32}S, ^{36}Ar, ^{40}Ca are ejected as well. The presence of such elements in the ejecta has been well established observationally (Branch et al. 1982; Branch 1984) and forms one of the major points in favor of C deflagration explosions over the C detonation models for type Ia SN explosions. If such a SN result from the accretion of material on to a white dwarf surface, rather than from the merging of two white dwarfs, than He flashes may produce some s-process elements. The conditions during the SN explosion (ie., in the precursor shock wave) may then favorable for the production of r-process elements through neutron capture on these s-process elements (Nomoto 1985).

C) Evolution of massive stars

After H is exhausted in their cores, a massive star will evolve to the right in the HR diagram and will burn He in its core as a red supergiant (Fig. 2). In contrast to low mass stars, the resulting C, O core of massive stars never becomes degenerate and, after He is exhausted, further "quiet" nuclear burning can occur, transforming C and O through a number of intermediate steps into the Fe peak

elements. Since the Fe peak elements are the most tightly bound nuclei, further burning will not release energy and the iron core will rapidly contract to nuclear densities. This core may bounce like a rubber ball driving an outward propagating shockwave. This, coupled with energy transfer between the core and the envelope through neutrinos, may lead to violent ejection of most of the star - a socalled type II supernova explosion - leaving a compact remnant behind (ie., neutron star or black hole; Woosley and Weaver 1986a). Initially, the temperature behind the outward propagating shock is high enough for further (explosive) nucleosynthesis, but a large fraction of the ejecta contains the ashes of previous burning cycles (ie., the elements C through Al). For example, detailed numerical calculations show that a 25 $M_\odot$ star leaves a 2 $M_\odot$ compact remnant behind and ejects about 4.3 $M_\odot$ of freshly synthesized heavy elements, resulting in a typical elemental enrichment of a factor 10 over solar (Woosley and Weaver 1986a). Since the later stages of evolution are very rapid, the stellar photosphere does not have time to readjust itself and they will all occur in the same part of the HR diagram, the red supergiant regime (Fig. 2).

The detailed evolution of very massive stars is heavily influenced by their mass loss rate and these stars spend only a small fraction of their (He-core burning) life as red supergiants. Instead, they mainly burn He in their core as blue or yellow supergiants (Chiosi and Maeder 1986). As a result of the mass loss, the H envelope is progressively lost. Moreover, convection will carry freshly synthesized material to the surface and the surface composition will evolve, showing progressively the H-burning (CNO cycle) and He-burning products. Thus these massive stars will evolve through the WN (N-rich) and WC (C-rich) Wolf Rayet phases. Finally, these stars will explode as supernovae, but because by that time they are H-poor, their spectrum differs from that of typical type II supernovae. Presumably, this is the origin of the type Ib supernovae (Woosley and Weaver 1986b).

Red Supergiants: Mixing during this phase will bring the products of H-burning via the CNO cycle to the photosphere. Enhancements in the ^{14}N and ^{13}C abundance are expected and have been observed (Maeder 1987). Changes in the O isotope ratios are also expected, but a detailed comparison is somewhat hampered by uncertainties in the relevant reaction rates. Such (anomalous) O isotope ratios have been observed for the M supergiants α Sco and α Ori (Lambert et al 1984; Harris and Lambert 1984) and these are summarized in table 2. These anomalous isotopic ratios will be preserved in the silicate dust observed to condens around these objects.

C-rich Wolf-Rayet stars: Due to extensive mass loss, very massive stars go through a Wolf Rayet phase in which the photospheric composition has changed drastically. In the C-rich phases (ie., WC stars), the photosphere consist of He

burning products (ie., ^{12}C, ^{22}Ne) and H, ^{13}C, ^{17}O and ^{18}O essentially disappear. WC stars will also show overabundances of ^{23}Na, $^{25,26}Mg$ and $^{29,30}Si$ (Prantzos et al. 1986). The overabundance of ^{26}Al, produced during the preceding N-rich Wolf-Rayet phase, will however disappear on a short timescale ($\approx 10^5$ yr). The dust observed to condense out around WC stars has an amorphous carbon character, but will obviously not contain H.

Type II SN explosions will eject C-, O-, Si-burning products into the ISM. This includes the iron peak elements, as well as intermediate mass elements associated with the Si peak (Woosley and Weaver 1986a). Supernovae are probably the origin of the r- and p-process elements and may also contribute to the solar abundance of some s-process elements (Woosley and Weaver 1986a). An enhancement of ^{26}Al is produced and may be incorporated into any condensing dust grains.

Only a very limited study of supernova explosions of Wolf Rayet stars (type Ib SN) have been performed, mainly concentrating on the explosion mechanism and the (possible) black hole remnant (Woosley and Weaver 1986b). It is likely that some of the iron core and the surrounding partially burned envelope will be ejected. If, as is likely, the Filipenko-Sargent object represents a type Ib SN, then O, Na and Mg are ejected by the SN explosion of such a massive star (Filipenko and Sargent 1985).

V The measured isotopic composition of stardust

In recent years various components have been isolated from carbonaceous meteorites which because of their anomalous isotopic composition are generally identified with stardust which has been incorporated into the meteorite parent body without major modification in the ISM or solar nebula (ie., melting, vaporization). Since these studies provide some clues to the stardust components that may expected in cometary bodies, it is of some relevance to briefly summarize the results on these components and their origin. Excelent reviews of this field can be found elsewhere (Anders 1988; Anders et al. 1989). We will concentrate on some of the carbonaceous components, $C\alpha$, β, δ, and ε, which correspond to amorphous carbon, diamond, and two types of SiC grains.

$C\beta$: This component consist of SiC grains with Xe isotopic abundances characteristic for the s-process. This anomaly is accompagnied by a similar enrichment in s-process Kr isotopes as well as by the presence of a substantial

enrichment in ^{13}C ($^{12}C/^{13}C \approx 40$; Anders 1988). These isotopic anomalies point towards C-rich red giants as the birth site of this stardust component (see table 2). The low $^{12}C/^{13}C$ reflects the interplay of first dredge up during the O-rich red giant phase, leading to $^{12}C/^{13}C \approx 10$, and the dredge up of pure ^{12}C during He flashes in the asymptotic red giant phase which transform the O-rich giant into a C-rich one. Further astronomical support for this identification results from the presence of the 11.3μm SiC stretching vibration in the IR spectra of many C-rich giants. Since such stars also produce copious amounts of amorphous carbon, a similar isotopic anomaly in the amorphous carbon phase of carbonaceous meteorites might also be expected. Its isolation might, however, be more difficult.

The nature of the process that lead to the trapping of the noble gas impurities is unclear. Ion-implantation is, a priori, the most likely origin for trapped noble gasses. However, the gas-grain drift velocities expected in the outflows from red giants are less than 20 km/sec (Tielens 1983), resulting in an implantation depth of less than 5Å. It is unlikely that this outermost layer would survive the frequent shocks in the ISM. The central stars of planetary nebulae, the descendant of red giants, do have high velocity winds (≈1000 km/sec) which could lead to deeper implantation, but they will interact with only a small fraction of the dust ejected in the red-giant phase. This holds even more for a possible type Ia supernova explosion, which can occur in the white dwarf descendant if it is part of a double system. Furthermore whether these ejecta would contain s-process elements remains to be seen.

The alternative explanation for the origin of the trapped noble gasses, adsorption during condensation, has its share of problems. The high release temperatures (>1400K) and high noble gas content ($Xe \approx 10^{-7}$ cm^{-3} STP /g) are hard to reconcile with adsorption. Although amorphous carbon when exposed to Xe at a partial pressure of $\approx 10^{-7}$ atm, does lead to "tightly bound" Xe ($\approx 10^{-9}$ cm^{-3} STP /g) which is released only at high temperatures (≈1000K), this probably is a particular property of the disordered structure of amorphous carbon with its large porous network (Wacker et al. 1985) and may not apply to SiC grains. Moreover, although the Xe partial pressure in these experiments was 10 orders of magnitude larger than expected for C-rich giants, the tightly bound Xe content was two orders of magnitude less than in Cβ. Further experimental studies particularly on highly disordered samples are required to address this quantitative aspect.

Surprisingly, only 4×10^{-5} of the Si in carbonaceous meteorites is contained within SiC (Anders et al. 1988). The SiC stardust budget analysis in section IIA concluded that about 2% of all the silicon is injected in into the ISM in the form of SiC. Taking into account destruction of stardust by strong SN shocks, the average volume of the ISM should contain about 0.3% of all the Si in the form of SiC stardust - about two orders of magnitude more than measured. Tang and Anders

(1988) have measured the ^{21}Ne content of SiC grains, presumably a cosmic ray spallation product, and concluded that their average ISM lifetime was only 50 Myr. This is decidedly less than the theoretical estimate ($4x10^8$ yr; McKee 1989) and may imply that the sun formed in an non-average region of the galaxy (i.e., OB association) which has been heavily affected by SN shocks. Assuming this lifetime, results in an average fraction of Si contained in SiC of $4x10^{-4}$, still an order of magnitude more than measured. Of course, such an average will not mean much if the local ISM was not in a steady state situation. An alternative explanation for the low abundance of SiC grains may be that most of the stardust (≈99%) was destroyed upon entering the solar nebula. Recent theoretical studies of the early solar nebula predict mid-plane temperatures of 1500K at the asteroid belt (Boss 1988), close to the evaporation temperature of SiC grains (≈1600K; Larimer and Bartholomay 1979). Chrondules and Ca-Al rich inclusions show abundant evidence for such high temperatures in the asteroid belt, although this might be related to transient heating events (i.e., lightning; see, Grossman et al. 1988; Hewins 1988; MacPherson et al. 1988). Likewise, the coarser matrix material, which is abundant in carbonaceous meteorites, may result from nebular and/or parent body processes (Scott et al. 1988). The stardust components identified in carbonaceous meteorites may then refer to a relatively late addition just prior to the formation of the meteoritic parent body, possibly when most of the dust has settled and temperatures are lower (i.e., reduced opacity).

Cε: This is another SiC dust component, often associated with spinel and thus separable from Cβ. It is highly enriched in ^{22}Ne and ^{13}C ($^{12}C/^{13}C \leq 10$) and shows small enrichments in the heavy isotopes of Si (Anders et al. 1989). Although most of the ^{22}Ne in the galaxy may result from He burning (in WC stars; Maeder 1983), the high isotopic fractionation suggests an origin in ^{22}Na which decays to ^{22}Ne with a half time of 2.5 yr (Clayton and Hoyle 1976). Since, in contrast to Ne, Na binds strongly, large fractionations are possible for this radioactive daugther product. The high ^{13}C enrichments are also characteristic for novae (Truran 1985). Finally, the variable enrichment in the Si isotopes may also be consistent with a novae origin, particularly if the progenitor is an Ne-O-Mg white dwarf (Wiescher et al. 1986).

Surprisingly, there is no evidence for SiC grains in the IR spectra of novae (see section II). This is somewhat discomforting since it should be detectable if all the available Si condenses out as SiC. This might imply that most of the Si forms silicates and only a minute fraction SiC. However, this poses a second problem with the nova interpretation. The meteoritic abundance of SiC containing ^{22}Ne relative to that containing s-process is about unity (Anders et al. 1989). This

should reflect the relative importance of these two sources of SiC dust. However, assuming very conservatively that all the Si in nova ejecta and only 10% in C-giant ejecta forms SiC we estimate that C-rich giants produce ten times more SiC (table 1). Of course, as for Cβ, the measured absolute amount of Si in SiC from novae is lower than predicted (see above). Another puzzling aspect is the close association of Cε, but not Cβ, with spinel. It suggests perhaps an interrelationship dating back to the nova ejecta. Now, novae are the only stardust source suspected to condens oxides (silicates) as well as C-dust (see section II), so a mixed bag of dust is perhaps feasible. It would suggest, though, that this spinel phase has to be heavily enriched in ^{17}O as well as in the daugther product of ^{26}Al, ^{26}Mg (table 2).

Here it is worth noting that another carbonaceous component (Cα) with a high ^{22}Ne content has been isolated from carbonaceous meteorites. Its structure is poorly defined but is probably some form of amorphous carbon (Anders 1988). The ^{22}Ne and ^{15}N again point towards an origin in novae. Since amorphous carbon is a suspected nova condensate, this seems entirely reasonable. The ^{22}Ne was probably trapped as intercalated ^{22}Na, while N substituted for C. The measured C and N isotopes are somewhat different from those of Cβ and might suggest a slightly different set of novae contributed to these two carbonaceous components in meteorites or a slight contamination by stardust with a different origin (i.e., C-giants ?).

Cδ: This is the most abundant form of elemental C in carbonaceous meteorites (≈0.1% of elemental C). It consists of small (25Å) diamond microcrystals containing a Xe anomaly known as Xe H-L, which is enriched in the light as well as the heavy Xe isotopes (Anders et al. 1989). Curiously, the C isotopes are solar but ^{15}N is anomalous (depleted). The measured Xe anomalies resemble the results of the p- and r-process in various zones of type II SNe (Anders 1988). The r-process might actually be driven by neutrons generated by the interaction of neutrinos (released by the central neutron star) with He atoms in the He/^{12}C-rich zone in the ejecta (Epstein et al. 1988).

The carbonaceous carrier of the Xe anomaly may have condensed in this C-rich zone of the supernova ejecta, or may represent grains formed during an earlier mass-loss phase of the SN progenitor (Clayton 1981). In either case, the trapping of the noble gasses is probably due to ion implantation. The ejected material, coasting at 1000-5000 km/sec, will drive a strong shock wave into the surrounding gas, sweeping it up, while a reverse shock will propagate backwards (in mass coordinates) slowing the ejecta down. Initially, the ejecta and swept up circumstellar material will interact only over a thickness comparable to the

stopping length ($\approx 10^{15}$ cm). Thus, only a very minor fraction of the previously ejected dust would be bombarded by the ejecta. However, the contact discontinuity "separating" the ejecta and swept up matter will be Rayleigh-Taylor unstable, driving global mixing at a (subsonic) velocity of ≈1000 km/sec. Because of their inertia, large grains in this turbulent velocity field will develop drift velocities of this same order. Thus, both dust formed in the ejecta as well as "old" dust will be bombarded by ions with energies of ≈5keV/amu and implantation to a depth of ≈1500Å will occur. Note that very small grains (<100Å) will not stop very many impacting ions (<0.1%). Moreover, they would show very large fractionation effects between for example Kr and Xe. Thus, in such a model the small microcrystals observed in carbonaceous meteorites initially had to be part of a much larger polycrystalline grain (≈1500Å; Blake et al. 1988).

Some implantation of isotopically anomalous species can also result from the thermal bombardment in the non-radiative (post) shocked gas. A shock velocity of 1000 km/sec corresponds to a thermal energy of ≈5 keV/ion and will lead to implantation at a depth of about 75 Å. Again the smallest grains (now < 25 Å) will stop only few (< 1%) impacting ions. Of course, this bombarment will also lead to sputtering from the surface and irrespective of size the outer ≈300 Å of a grain will be removed over the expansion timescale of the shock (Seab 1987). Thus, again, an initial grain size much larger (>300Å) than measured for the carrier of the Xe anomaly is implied.

Clayton (1981) has suggested that implantation occurred when the fast SN ejecta swept up C-dust ejected in a previous evolutionary phase. Since C-dust is required, a C-giant progenitor is implicated but such stars will not explode as type II SN. They can explode as a type Ia SN, if a member of a binary system, and a variant based on this premisses has been developed by Jorgensen (1988). However, it is unclear whether such SN will indeed lead to a large enrichment in r-process elements (Nomoto 1985). Moreover, the SN explosion may occur much later than the red-giant phase and little of the latters grains may be affected by the high velocity SN ejecta. Thus, it would be difficult to explain the large trapping efficiency and the large fraction of elemental C in Cδ in carbonaceous meteorites. Finally, the C isotope ratio measured in the diamonds is unlike that for C-giants and in fact, unlike any single source of C-dust (table 2). The almost solar C isotope ratio is indeed very curious, since ^{12}C and ^{13}C are made by quite different nucleosynthetic reactions (He burning versus CNO cycle) and their galactic budget is dominated by different types objects (C-giants and WC stars versus novae, and C- and O-giants). It seems unavoidable that multiple birth sites for the Cδ phase are involved, which represent an average cross section of the injection of all elemental C. Since the dominant elemental carbon sources show C-stardust formation, such a model is perhaps possible. The decreased $^{15}N/^{14}N$ ratio in Cδ

may then just reflect the imortance of C-giants in the C-stardust budget, since such stars will have been enriched in ^{14}N via the CNO cycle.

Two distinct models for the formation of interstellar diamond dust have been advocated, metastable chemical vapor deposition in stellar ejecta (Anders et al. 1989), and high pressure transformation of amorphous carbon dust due to grain-grain collisions in interstellar shocks (Tielens et al. 1987). Some laboratory techniques have been very succesful in depositing C-films with properties very similar to diamond. In general, however, amorphous carbon with a predominantly aromatic bonding character is formed. For example, burning a hydrocarbon flame will result in copious amounts of soot and (unfortunately) not diamonds. This merely reflects the thermodynamic preference for graphite at low temperatures and pressures. Although soot contains tetrahedrally bonded C, its structure - aromatic platelets connected by diamond like hydrocarbon chains - is quite unlike that of the Cδ phase (Blake et al. 1988). The conditions in the outflow from C-giants is quite similar to those in hydrocarbon flames and soot formation is expected (Tielens 1989). Indeed, C-rich PN - the descendants of C-rich giants - show abundant evidence for aromatic hydrocarbon molecules, the building blocks of soot. Likewise, red fluorescence observed in the ISM indicates a considerable amount of hydrogenated amorphous carbon (α:C-H) grains which has a structure similar to soot (Duley 1985). The IR spectra of WC stars also show evidence for aromatic rather than diamond binding of the condensing grains (Cohen et al. 1989). Nevertheless, it is perhaps possible that the very specific conditions required for diamond formation by CVD techniques are satisfied in some celestial objects. However, in the eyes of this (perhaps biased) reviewer, whether such an object can actually provide sufficient amounts of diamond and particularly a solar C isotope ratio is doubtful.

Grain-grain collisions ($v \geq 10$ km/sec) behind strong shocks can provide the high pressures (≥400 kbar) required to convert graphitic C into diamond (Tielens et al. 1987). Numerous laboratory studies have shown that this process is very efficient (Bundy et al. 1973). Several of the measured properties of the meteoritic diamond phase are readily explained by this high pressure process. These include the microcrystalline grain size (very similar to those measured in laboratory experiments), the structure (small crystals surrounded by an amorphous rim), and the quite normal $^{12}C/^{13}C$ ratio (many C-stardust birthsites of which only one contributed Xe H-L; Tielens 1989; Blake et al. 1988). The high pressure method has one major drawback: the expected leftover amorphous carbon stardust component with a similar isotopic composition has not been detected in carbonaceous meteorites to an upper limit of perhaps 10% of that of Cδ (Anders et al. 1989). Theoretical models of shock processing of interstellar dust imply that about 15% of the C-stardust survives into the solar nebula (§ II), about 10% is transformed

into diamond (Tielens et al. 1987), and the remainder is destroyed. If, however, the stardust lifetime of 50 Myr derived from SiC measurements is adopted (Tang and Anders 1988; see above), then only 3% of the C-stardust survived into the solar nebula. The fraction converted into diamonds (10%) is, however, not very affected by the absolute shock frequency since they are formed as well as destroyed by shocks (Tielens et al. 1987). Nevertheless, the predicted surviving stardust component is still somewat uncormfortably large. Of course, if dust sources and sinks in the local neighbourhood from which the sun formed were not in equilibrium (ie., nearby SNe destroyed most of the local dust; Anders et al. 1988), then essentially all of the surviving C-stardust could have been transformed into diamonds. Thus, at this point, it seems that this is not lethal argument against a shock origin for these diamonds.

Summary

As table 2 demonstrates the isotopic composition of the major elements, C and O, varies by factors two to several orders of magnitude from one class of sources to another and even within classes. Similar variations have been observed for s-process elements such as Yttrium, Zirconium, and Neodymium. The stardust condensates are expected to preserve this nucleosynthetic record on an individual grain basis. Conversely, this implies that any bulk[1] sample will contain a mixture of stardust from many different birthsites and with a very heterogeneous isotopic composition. Since the stardust birthsites also dominate the return of all elements to the ISM, the average of such a bulk sample might not differ much from solar. Indeed, the almost solar $^{12}C/^{13}C$ ratio of Cδ, despite the Xe signature indicating a SN origin, may be a good example of such a mixture. For a proper assesment of the nucleosynthetic record contained within comets, analysis on an (interstellar) grain by grain basis is therefore almost imperative.

Theoretical studies indicate that about 15% of the stardust originally ejected will survive the rigors of the ISM. Yet, meteorites seem to contain only about 0.1% of the cosmic elemental C in the form of stardust components. In fact, while about 50% of the interstellar dust must be made up of carbonaceous material. the abundance of carbonaceous solids in meteorites is much more limited (≈2% by mass). Likewise SiC stardust is much less abundant in meteorites than expected from stardust budget considerations (§V). There are two possible explanations for this discrepancy (Anders et al. 1989): 1) Solar nebula processes

[1] bulk relative to stardust masses ($\approx 10^{-14}$ g)

have lead to the vaporization of most of the interstellar dust mass in the asteroid belt. 2) The sun formed out of an anomalous region of interstellar space (e.g., an OB association) where most of the preexisting dust was destroyed by nearby SNe. Since the refractory component of cometary materials is expected to be much less affected by solar nebula and parent body processes, a comet sample return mission is expected to be very valuable for the study of particularly the more fragile stardust components. In particularly, since the oxide stardust preserved by meteorites has been heavily diluted by solar nebula condensates - probably only 0.1% of the Si is in surviving stardust and 99.9% in solar nebula condensates - such a mission is indispensable for an analysis of silicate stardust.

Since present day techniques require sample sizes larger than a micron, new powerful analytical techniques have to be developed to investigate samples on an individual interstellar/circumstellar grain basis. Given that a typical stardust grain contains only 10^9 atoms and that the accurate determination of, for example, the C isotope ratio requires "counting" to an accuracy of 10^5 atoms, the challenge is clear. In meteoritic studies this challenge has been circumvented by sorting on chemical and physical properties. This has resulted in larger samples, but some information may be lost by this averaging process. This can be particularly misleading if different birthsites lead to stardust with similar properties (ie., M-giants and supergiants) or if an isotopic ratio varies from source to source (ie., O-isotopes in M giants). Moreover, presently such sorting is primarily based on chemical properties (i.e., resistance against acid treatment, pyrolysis, combustion) and other sorting techniques - perhaps based on structural or mineralogical characteristics, may lead to hitherto unsuspected (fragile) stardust components. Now, some data can only be obtained on "bulk" samples. The anomalous isotopic composition of the noble gasses is a case in point. With a Xe abundance of $\approx 10^{-8}$ per C atom in Cδ, an individual 1000 Å grain would contain only 10 ^{136}Xe atoms and only about one in every 10^5 individual 25Å diamond microcrystallites would contain such an atom. Clearly "bulk" analysis has proven its value already. Of course, both approaches will be valuable and to some extent complimentary.

Despite these difficulties associated with the analysis of returned samples, it is expected that the Rosetta mission will provide an important testing ground for theories of nucleosynthetic origin of the elements, as well as the formation and evolution of interstellar dust, and the formation of solid bodies in the solar nebula.

References

Anders, E., 1988, in *Meteorites and the Early Solar System*, eds. J. Kerridge and M. Mathews, (Univ. Arizona Press, Tucson), p. 927.

Anders, E., Lewis, R.S., Tang, M., and Zinner, E., 1989, in *Interstellar Dust*, eds. L.J. Allamandola and A.G.G.M. Tielens, (Dordrecht, Reidel), p.389.

Arnett, D., Fryxell, B., and Müller, E., 1989, *Ap. J. Letters*, **341**, L63.

Arnett, W. D., and Truran, J.W., 1985, *Nucleosynthesis: Challenges and New Developments*, (Univ. Chicago Press, Chicago).

Blake, D.F., Freund, F., Krishnan, K.F.M., Echer, C.J., Shipp, R., Bunch, T.E., Tielens, A.G., Lipari, R.J., Hetherington, C.J.D., and Shang, S., 1988, *Nature*, **332**, 611.

Boss, A.P., 1988, *Science*, **241**, 565.

Branch, D., 1984, *Ann. N.Y. Acad. Sci.*, **422**, 186.

Branch, D., et al., 1982, *Ap. J. Letters*, **252**, L61.

Burenkov, A.F., Komarov, F.F., Kumakhov, and Temkin, M.M., 1986, *Tables of Ion Implantation Spatial Distributions*, (Gordon&Breach, New York).

Burbridge, E.M., Burbridge, G.R., Fowler, W.A., and Hoyle, F., 1957, *Rev. Mod. Phys.*, 29, 547.

Cameron, A.G.W., 1957, Chalk River Report, (Atomic Energy Canada, Ltd), CRL-41.

Chiosi, C. and Maeder, A., 1986, *Ann. Rev. Astr. Ap.*, **24**, 329.

Clayton, D.D., 1981, *Proc. Lunar Planet. Sci.*, **12B**, 1781.

Clayton, D.D., 1968, *Principles of Stellar Evolution and Nucleosynthesis*, (McGraw Hill, New York).

Clayton, D.D., and Hoyle, F., 1976, *Ap. J.*, **203**, 390.

Cohen, M., Tielens, A.G.G.M., and Bregman, J.D., 1989, *Ap. J. Letters*, **344**, in press.

Curl, R.F., and Smalley, R.E., 1988, *Science*, **242**, 1017.

Duley, W.W., 1985, *M.N.R.A.S.*, **215**, 259.

Field, G.B., 1974, *Ap. J.*, **187**, 453.

Filipenko, A.V., and Sargent, W.L.W., 1985, *Nature*, **316**, 407.

Gehrz, R.D., 1989, in *Interstellar Dust*, eds. L.J. Allamandola and A.G.G.M. Tielens, (Dordrecht, Reidel), p.445.

Gehrz, R.D., 1988 *Ann. Rev. Astr. Ap.*, **26**, 377.

Gilra, D.P., ????

Greenberg, J.M., 1989, in *Interstellar Dust*, eds. L.J. Allamandola and A.G.G.M. Tielens, (Dordrecht, Reidel), p.345.

Grossman, L., and Larimer, J.W., 1974, *Rev. Geophys. Space Phys.*, 12, 71.

Grossman, J.N., Rubin, A.E., Nagahara, H., and King, E.A., 1988, in *Meteorites and the Early Solar System*, eds. J. Kerridge and M. Mathews, (Univ. Arizona Press, Tucson), p. 619.

Harris, M.J., and Lambert, D.L., 1984, *Ap. J.*, **281**, 739.

Hewins, R.H.,1988, in *Meteorites and the Early Solar System*, eds. J. Kerridge and M. Mathews, (Univ. Arizona Press, Tucson), p. 660.

Iben, I., and Renzini, A., 1983, *Ann. Rev. Astr. Ap.*, **21**, 271.

Jaycock, M.J., and Parfitt, G.D., 1986, *Chemistry of Interfaces*, (Wiley and Sons, New York).

Jenkins, E.B., 1989 in *Interstellar Dust*, eds. L.J. Allamandola and A.G.G.M. Tielens, (Dordrecht, Reidel), p. 23.

Jura, M., 1987, in *Interstellar Processes*, eds. D. Hollenbach and H. Thronson, (Reidel, Dordrecht), p. 3.

Kerridge, J.F., 1986, in *Interrelationships among Circumstellar, Interstellar and Interplanetary Dust*, eds. J. Nuth and R. Stencel, NASA CP 2403, p.71.

Kerridge, J.F., and Chang, S., 1985, in *Protostars and Planets II*, eds. J. Black and M. Mathews, (Univ. Arizona Press, Tucson), p. 738.

Lambert, D.L., Brown, J.A., Hinkle, K.H., and Johnson, H.R., 1984, *Ap. J.*, **284**, 223.

Lambert, D.L., 1988, in *The evolution of Peculiar Red Giants*, (Reidel, Dordrecht), in press.

Larimer, J. W., and Bartholomay, M., 1979, *Geochim. Cosmochim. Acta*, **43**, 1455.

Iben, I., and Renzini, A., 1983, *Ann. Rev. Astr. Ap.*, **21**, 271.

Jorgenson, U.G., 1988, *Nature*, **332**, 702.
MacPherson, G.J., Wark, D.A., and Armstrong, J.T.,1988, in *Meteorites and the Early Solar System*, eds. J. Kerridge and M. Mathews, (Univ. Arizona Press, Tucson), p. 746.
Maeder, A., 1983, *Astr. Ap.*, **120**, 130.
Maeder, A., 1987, *Astr. Ap.*, **173**, 247.
Maeder, A., and Meynet, G., 1987,*Astr. Ap.*, **182**, 243.
Martin, P.G., and Rogers, C., 1987, *Ap. J.*, **322**, 374.
Mathis, J. S., 1989, in *Interstellar Dust*, eds. L.J. Allamandola and A.G.G.M. Tielens, (Dordrecht, Reidel), p.357.
McKee, C.F., 1989, in *Interstellar Dust*, eds. L.J. Allamandola and A.G.G.M. Tielens, (Dordrecht, Reidel), p.431.
Möller, W., Scherzer, B.M.U., and Ehrenberg, J., 1982, *J. Nucl. Mat.*, **111&112**, 669.
Nomoto, K., 1984, *Ap. J.*, **277**, 791.
Nomoto, K., 1985, in *Nucleosynthesis: Challenges and New Developments*, (Univ. Chicago Press, Chicago), p. 202.
Nuth, J.A., and Moore, M.H., 1988, *Ap. J. Letters*, **329**, L113.
Pottasch, R.N., 1984, *Planetary Nebulae*, (Reidel, Dordrecht).
Prantzos, N., Doom, C., Arnould, M., and de Loore, C., 1986, *Ap. J.*, **304**, 695.
Roche, P.F., 1989, in *Planetary Nebulae*, eds. S. Torres-Peimbert, (Kluwer, Dordrecht), p.117.
Rolfs, C.E., and Rodney,W.S., 1988, *Cauldrons in the Cosmos, nuclear Astrophysics*, (Univ. Chicago Press, Chicago).
Salpeter, E.E., 1979, *Ann. Rev. Astr. Ap.*, **15**, 267.
Scherzer, B.M.U., 1983, in *Sputtering by Particle Bombardment II*, ed. R. Behrisch, (Springer Verlag, Berlin), p.271.
Scott, E.D.R., Barber, D.J., Alexander, C.M., Hutchison, R., and Peck, J.A., 1988, in *Meteorites and the Early Solar System*, eds. J. Kerridge and M. Mathews, (Univ. Arizona Press, Tucson), p. 718.
Scoville, N.Z., and Sanders, D.B.,1987, in *Interstellar Processes*, eds. D. Hollenbach and H. Thronson, (Reidel, Dordrecht), p. 21.
Seab, G., 1987, in *Interstellar Processes*, eds. D. Hollenbach and H. Thronson, (Reidel, Dordrecht), p. 491.
Smith, V.V., 1989, in *Cosmic Abundances of Matter*, ed. C.J. Waddington, A.I.P. Conference Publication 113.
Snow, T.P., 1975, *Ap. J. Letters*, **202**, L87.
Tammann, G.A., 1982, in *Supernovae: A Survey of Current Research*, eds. M.J. Rees and R.J. Stoneham, (Reidel, Dordrecht), p. 371.
Tang, M., and Anders, E., 1988, *Ap. J. Letters*, **335**, L31.
Thielemann, F.K., Nomoto, K., and Yokoi, K., 1986, in *Nucleosynthesis and its Implications on Nuclear and Particle Physics*, eds. J. Audouze and N. Mathieu, (Reidel, Dordrecht), p. 131.
Tielens, A.G.G.M., 1983, *Ap. J.*, **271**, 702.
Tielens, A.G.G.M., 1989, in *Carbon in the Galaxy: Studies from Earth and Space*, ed. J. Tarter, NASA CP, in press.
Tielens, A.G.G.M., and Allamandola, L.J., 1987a, in *Physical Processes in Interstellar Clouds*, eds. G.Morfil and M. Scholer, (Dordrecht, Reidel), p.333.
Tielens, A.G.G.M., and Allamandola, L.J., 1987b, in *Interstellar Processes*, eds. D. Hollenbach and H. Thronson, (Reidel, Dordrecht), p. 397.
Tielens, A.G.G.M., Seab, C.G., Hollenbach, D.J., McKee, C.F., 1987, *Ap. J. Letters*, **319**, L103.
Truran, J.W., 1985, in *Nucleosynthesis: Challenges and New Developments*, (Univ. Chicago Press, Chicago), p. 292.
Wacker, J. F., Zadnik, and Anders, E., 1985, *Geochim. Cosmochim. Acta*, **49**, 1035.
Wiescher, M., Görres, J., Thielemann, F.-K., Ritter, H., 1986, *Astr. Ap.*, **160**, 56.
Willis, A.J., 1982, in *Wolf-Rayet Stars: Observations, Physics, Evolution*, eds. C.W.H. de Loore and A.J. Willis, (Dordrecht, Reidel), p.87.
Wooden, D., 1989, Ph. D. Thesis, UCSC, in preparation.
Woosley, S.E., and Weaver, T.A., 1986a, *Ann. Rev. Astr. Ap.*, **24**, 205.
Woosley, S.E., and Weaver, T.A., 1986b, in *Radiation Hydrodynamics in Stars and Compact Objects*, eds. D. Mihalas and K.H. Winkler, (Dordrecht, Reidel), p.91.

INTERSTELLAR AND COMETARY DUST

John S. Mathis
Washburn Observatory
University of Wisconsin-Madison

INTERSTELLAR AND COMETARY DUST

John S. Mathis
Washburn Observatory, University of Wisconsin-Madison

ABSTRACT

"Interstellar dust" forms a continuum of materials with differing properties which I divide into three classes on the basis of observations: (a) Diffuse dust, in the low-density interstellar medium; (b) outer-cloud dust, observed in stars close enough to the outer edges of molecular clouds to be observed in the optical and ultraviolet regions of the spectrum, and (c) inner-cloud dust, deep within the cores of molecular clouds, and observed only in the infrared by means of absorption bands of C-H, C=O, O-H, C≡N, etc.

There is a surprising regularity of the extinction laws between diffuse- and outer-cloud dust. The entire mean extinction law from infrared through the observable ultraviolet spectrum can be characterized by a single parameter. There are real deviations from this mean law, larger than observational uncertainties, but they are much smaller than differences of the mean laws in diffuse- and outer-cloud dust. This fact shows that there are processes which operate over the entire distribution of grain sizes, and which change size distributions extremely efficiently.

There is no evidence for mantles on grains in local diffuse and outer-cloud dust. The only published spectra of the star VI Cyg 12, the best candidate for showing mantles, does not show the 3.4 μm band which appreciable mantles would produce. Grains are larger in outer-cloud dust than diffuse dust because of coagulation, not accretion of extensive mantles.

Various theories of grains are included in Table 1. Core-mantle grains favored by J. M. Greenberg and collaborators, and composite grains of Mathis and Whiffen (1989), are discussed more extensively (naturally, I prefer the latter). The composite grains are fluffy and consist of silicates, amorphous carbon, ans some graphite in the same grain.

Grains deep within molecular clouds but before any processing within the solar system are presumably formed from the accretion of icy mantles on and within the coagulated outer-cloud grains. They should contain a mineral/carbonaceous matrix, without organic refractory mantles, in between the ices. Unfortunately, they may be significantly processed by chemical processes accompanying the warming (over the 10 K of the dark cloud cores) which occurs in the outer solar system. Evidence of this processing is the chemical anomalies present in interplanetary dust particles collected in the stratosphere, which may be the most primitive materials we have obtained to date. The comet return mission would greatly clarify the situation, and probably provide samples of genuine interstellar grains.

INTERSTELLAR AND COMETARY DUST

Mathis, John S.

I. INTRODUCTION AND OVERVIEW

One of the most interesting results of a comet-return mission will be the recovery of relatively pristine grains which will, hopefully, tell us a great deal about the nature of interstellar dust. The main problems in interpreting the results will be in determining the amount of processing which has taken place at two separate stages in the evolution of the returned grains: (a) since the grains left the low-density ("diffuse") interstellar medium (ISM) entered the inner regions of a relatively dense, cold, and dark molecular cloud, and formed the protocometary grains which later clumped together to become the comet's nucleus, and (b) modifications in the nature of the originally interstellar grains after they were clumped together into the comet nucleus. The chemical species present in the returned material will provide information about the reactions which took place as the nucleus was accreting.

In this paper I will try to explain what we know about interstellar grains from observations, what theories have been suggested to explain these observations, and speculate upon the evolution of the grains throughout their histories. The very term "interstellar grain" encompasses a variety of materials.

A. VARIOUS TYPES OF INTERSTELLAR DUST

It is misleading for us to refer to the solid materials seen along various lines of sight as "interstellar dust," unless we keep clearly in mind that these materials vary considerably from place to place within interstellar space. We are not dealing with any homogeneous, well-defined substance, but rather a collection of particles whose composition and size distribution surely changes considerably from the diffuse ISM to deep within the cold, dark, dense clouds in which comets are formed. The physical conditions from these two regions of space are vastly different. In parts of the diffuse ISM, the density of atomic H is about 0.1 cm^{-3} and the temperature about 10^4 K, while in the diffuse "clouds," the density is about 30 cm^{-3} and the temperature 100 K. The radiation density from starlight is about 0.5 eV cm^{-3}. In contrast, within the deepest parts of molecular clouds the density is 10^5 cm^{-3} and the temperature about 10 K, with a sky which shows no visible stars. It is small wonder that the grains are also very different in the two regions. We shall have to keep the various regions firmly in mind as we discuss the dust.

As the Galaxy rotates, its interstellar matter passes through the spiral arms, through shocks from supernovae or the violent winds of OB stars, and changes its form back-and-forth from the diffuse ISM to molecular clouds. Roughly half of the mass of the gas is in clouds or in the diffuse ISM at any given time, but the volume of the diffuse ISM is vastly larger because of its very low density.

Our knowledge of grains comes from observations, and we can conveniently divide the whole continuum of possible sites into just three different principal regions on the basis of these observations. These three kinds of dust will be called (a) the "diffuse" dust, meaning the grains in the low-density ISM which occupies most of the volume near the plane in our Galaxy; (b) the "outer-cloud dust," close enough of the edge of the cloud for us to observe the dust in the optical and even ultraviolet parts of the spectrum; and (c) the "inner-cloud dust," which is located within the inner regions of very cold, dark, and dense molecular clouds. All of these observations are made by comparing a star of a known spectral type seen through the dust to one of the same spectral type which is relatively unobscured. In practice, hot stars are far better than cool because their intrinsic spectrum in not so sensitive to their precise temperature (or, equivalently, spectral type).

Observationally, inner-cloud dust is distinguished by showing absorption bands of molecular ice (starting with water and ammonia, but in some cases including CO, methanol, and many others). The column density of dust is so large that at present observations can only be made in the near-infrared (NIR) region of the spectrum, and we have no information regarding the extinction law for wavelengths shorter than 1 μm or so. Outer-cloud and diffuse dust are studied down to wavelengths as short as 0.10 μm (with the *Copernicus* satellite) and commonly to 0.12 μm (with the *International Ultraviolet Explorer*).

It is convenient, although not ideal, to describe the wavelength dependence of the extinction by the ratio relative to the visual extinction, $A(\lambda)/A(V)$. The extinction laws of diffuse and outer-cloud dust form a continuous progression which can be characterized by a single parameter. Because of tradition, this parameter is taken to be the so-called "total-to-selective extinction ratio," R_V [$\equiv A(V)/E(B-V)$]. The average value of R_V in the diffuse ISM is 3.1. The largest values of R_V are about 5.5, found in the outer parts of the Orion and Ophiucus molecular clouds. I will rather arbitrarily define diffuse dust as having $R_V \leq 3.4$, and outer-cloud dust as $R_V > 3.4$.

B. Summary of Observations of Interstellar Dust

The observational properties of interstellar dust are well summarized by papers at the IAU Symposium 135, "*Interstellar Dust,*" held at Santa Clara University in August, 1988 (Allamandola and Tielens, 1989). There are many papers discussing various aspects of the ISM in general in the volume *Interstellar Processes* (Hollenbach and Thronson 1987). In particular, there is an excellent summary of the composition and forms of interstellar dust by Tielens and Allamandola (1987).

Continuous extinction. The continuous extinction, observed from about 5 μm to 0.1 μm, is the most valuable information available regarding the properties of interstellar dust. The extinction is

remarkably free from spectral features, which is one of the largest problems in determining the nature of the constituents and size distributions. As we will see, the extinction laws for outer-cloud and diffuse dust form a regular progression, and those of inner-cloud dust are presently unknown because of the large extinction of the starlight in those clouds.

Spectral features in extinction: There are spectral absorption features which provide insight to the nature of grains. For outer-cloud and diffuse dust, the strongest feature in the entire spectrum (in the sense of requiring the largest oscillator strength for a given column density of carriers) is the $\lambda 2175$ Å "bump," which reaches an equivalent width of 50 times Lyman-α.

Some 29 other "diffuse interstellar bands," all in the optical part of the spectrum (Herbig 1988), are quite variable in strength relative to A(V). They can be placed in at least three groups, among which there is a good correlation (Krelowski and Walker 1987, Chlewicki et al. 1987, Josafatsson and Snow 1987). Apparently the bands at 4430, 5780, and 6284 Å are not produced by coatings on the surface of aligned grains, since there is no polarization in these bands in the spectra of two polarized stars (Martin and Angel 1975). They fall in two of the three groups into which the bands have been placed. This exclusion is important, since the strength of the polarization is so great in some cases that most or all large grains must be aligned.

There are strong bands at 9.7 μm and 20 μm, both ascribed to the Si=O stretch in silicates. This feature is found in comets as well, with a somewhat different profile which indicates that cometary silicates have been partially annealed. There is a weak feature at 3.4 μm ascribed to aliphatic hydrocarbons in the spectrum of the supergiant IRS 7 near the galactic center (Butchart et al. 1986). It might arise from mantles on grains, as we shall discuss at some length later.

For inner-cloud dust, there are many spectral features of molecular ices. These have been recently reviewed by Teilens and Allamandola (1989). The lack of these features in diffuse and outer-cloud dust suggests that there is a fundamental difference in the properties we expect of the grains for the respective regions.

Emission spectral features: Much of research on dust in the past few years has been concerned with the "Unidentified Infrared Bands" (UIBs) which occur at 3.3, 3.4, 6.2, 7.7, and 11.4 μm, with weaker ones at several other wavelengths. In the diffuse ISM they account for 10 - 20% of the energy radiated by warm dust. They are found in a wide variety of objects, with the common feature that all such objects have carbon-rich or ordinary interstellar dust present, as opposed to the circumstellar dust surrounding oxygen-rich stars. Their origin is not completely clear, but both their spectra, relative strengths, and to some extent their variations from place to place are well explained by the hypothesis that they are produced by polycyclic aromatic hydrocarbons (PAHs) (Léger and Puget 1984, Allamandola, Tielens, and Barker 1985), probably ionized in the diffuse ISM.

Polarization: Interstellar polarization provides another integral of cross-sections of grains over the size distribution (see Hildebrand 1988). Unfortunately, the integral also involves the degree of alignment of grains of various sizes as well as their cross-sections, and there is no very definitive theory of alignment (Hildebrand 1987). The principal features pertaining to interstellar polarization are: (a) Only the larger grains are aligned. Ground-based observations of interstellar polarization reach a maximum at a mean wavelength of 0.55 μm, while the extinction law is much larger in the ultraviolet (especially at 0.22 μm and for $\lambda < 0.17$ μm). (b) All present theories of interstellar grains can explain the observed polarization law, if large grains are aligned but small ones are not, because the polarization cross-sections for cylinders, believed to pertain to elongated grains, mimic the observed polarization law (Mathis 1986). (c) The polarization of the 9.7 and 19 μm silicate bands in the heavily obscured object "BN" in the Orion molecular cloud might provide a powerful diagnostic for grains (Hildebrand 1988); see below in § IV. (d) Grains are aligned quite efficiently, even within dense molecular clouds. The polarization of the emitted radiation from deep within the Orion molecular cloud or near the galactic center (Dragovan 1986; Werner et al. 1988; Hildebrand 1989, Hildebrand et al. 1989) shows that the grains are very well aligned, but the physical conditions in these regions should strongly militate against alignment.

Depletions of the elements in the ISM: Observations show that several elements (Fe, Mg, Si, Al, and others) are heavily depleted in the gas phase of the ISM (see Jenkins 1987, 1988 for reviews). Roughly 90% of these elements are depleted in the diffuse ISM and 99% in the very dense regions (see Joseph 1988 for a discussion of correlations). Unfortunately, the depletions of the abundant elements C, N, and O are especially difficult to determine because their abundant ions do not happen to have resonance lines with oscillator strengths suitable for abundance analyses, and are consistent with the mean depletion of these elements ranging all of the way from almost none up to 90%. Carbon is an especially important element for interstellar dust, and there is only one determination of the column density of C^+, its most important ion within regions where hydrogen is mainly atomic. Towards the star δ Sco, Hobbs, York, and Oegerle (1982) found that about 30% of the cosmic carbon is in the gas phase. This number is probably consistent with the uncertain abundance of gaseous CO/H_2 in molecular clouds (Watson et al. 1985). Models of grains are, therefore, constrained to use no more than about 70% of the cosmic C.

Other diagnostics: The far-infrared emission from warm grains serves as some diagnostic of grains, but not as a very direct one because it also involves the heating of the grains and temperature excursions of small grains heated by a single photon. The recent theory of Chlewicki and Laureijs (1988) has used the IRAS measurements of clouds to make the very interesting suggestion that metallic Fe might be present in grains. There are also measurements of the X-ray haloes around grains (Mauche and Gorenstein 1986, and ref. therein) which provide some information regarding the spatial distribution of heavy elements in the grains.

We next consider at some length the information provided by the best-determined of these diagnostics, the interstellar extinction law.

II. Interstellar Extinction and Its Relevance to Cometary Dust

We must recall that, by definition, we can only observe the interstellar extinction law for diffuse and outer-cloud dust, while comets are undoubtedly formed deep within molecular clouds. However, the observed extinction laws have direct relevance to the processes by which dust is modified within dense regions.

A. Systematics of Observed Extinction Laws

Very recently, it has recently become clear that there is a very surprising degree of regularity among the extinction laws in various lines of sight [Cardelli, Clayton, and Mathis 1988, 1989 (CCM)]. Figure 1 shows the observed extinction laws of many lines of sight, expressed as $A(\lambda)/A(V)$, plotted against $1/R_V$, for several values of λ ranging from the red to almost the limit of the *IUE* spacecraft (1200 Å). There are good linear relationships in each case, so that clearly there is an excellent relation between the optical extinction law (as expressed by R_V) and the other wavelengths (including ultraviolet). The "mean" interstellar extinction laws of Savage and Mathis (1979) or of Seaton (1979) refer to the diffuse ISM, where $R_V \approx 3.1$, but Fig. 1 shows that they are not very appropriate for values of R_V which differ greatly from that value.

CCM has fitted the slopes of the various $A(\lambda)/A(V)$ - R_V^{-1} relations, examples of which are shown in Figure 1, by an analytic formula which represents the mean extinction law as a function

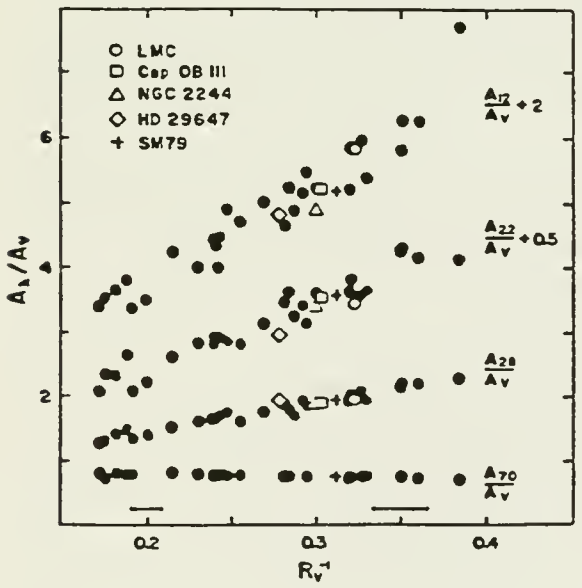


Fig. 1.—The observations of $A(\lambda)/A(V)$, plotted against $1/R_V$, where $R_V \equiv A(V)/E(B-V)$ (from Cardelli, Clayton, and Mathis 1989). A_{12} refers to 1200 Å, A_{22} to 2175 Å, A28 to 2800 Å, and A_{70} to 7000 Å (the standard R filter). The observational values of black dots are from Fitzpatrick and Massa (1988). The regularity of the observations, and the scatter about the mean relationship, is shown. The scatter is greater than the observational errors, and is therefore real.

of R_V. Fig. 2, from CCM, shows the results for three values of R_V: (a) from using the formula, and (b) observations of actual stars with those values. The central panel is about as discrepant as actual observations are from the mean relationship. The dispersion of individual extinction laws around that mean law is shown in Fig. 1 (from the spread in the individual observed points) and in Fig. 2 (as error bars). The lowest set of curves plotted in Fig. 2 are for Herschel 36, an exciting star of M8 and considered to have very "peculiar" extinction. Rather, it has a rather peculiar value of R_V (≈ 5.3), but a "normal" extinction law for that value of R_V. Note, however, that there are real deviations from the mean extinction law for any particular values of R_V. These deviations are especially large at 1200 Å, where the mean deviation of $A(\lambda)/A(V)$ from the mean extinction law is about 0.3.

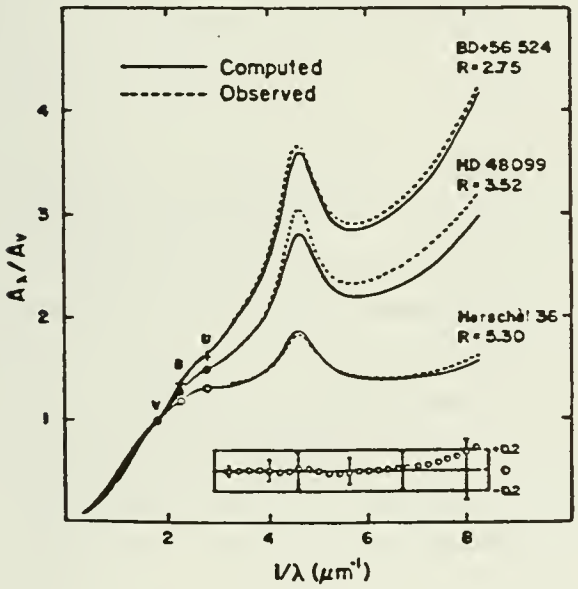


Fig. 2.—Three cases of a mean extinction law, obtained by fitting the slopes of the $A(\lambda)/A(V) - R_V^{-1}$ relationship (see Fig. 1) by an analytic formula, and actual extinction laws of stars with the appropriate values of R_V. The middle panel shows about as large of a discrepancy as exists in the data of Fitzpatrick and Massa (1988).

The implications of the information contained in Figures 1 and 2, as regards the nature and evolution of grains, are considerable. It seems that the processes which modify the size distributions and possibly the compositions of interstellar grains operate on all sizes simultaneously. It is very conceivable that some lines of sight the small grains would be heavily modified, while the larger grains, and therefore the optical extinction, were relatively untouched. However, in practice such is not the case (at least among the lines of sight we have investigated); if the short-wavelength extinction law is rising relatively steeply with λ^{-1}, the value of R_V is always relatively small, and so on. How can this fact be understood? Apparently the processes which modify the grains act over the entire size range. These processes must be quite efficient as well in order to produce such regular extinction laws for diverse regions and conditions (the stars plotted in Figures 1 and 2 are found in various directions all over the Galaxy). The overall

regularity of the extinction laws is that correlations of one extinction or color ratio with another are probably not indicative of any causal relation between the quantities; they are probably both responding to general processes.

The most efficient ways of changing grain distributions are by grain-grain collisions (shattering and coagulation) or by shocks (which can destroy grains in a variety of ways: see Seab 1987 for a review). It is "easy" to show that such processes as grain-grain interactions are quite inefficient in the rather low densities ($n_H \approx 10^3$ cm^{-3}?) in these outer regions of clouds, but the regularity of extinction laws suggests otherwise. The implications for cometary grains are that these interactions will probably continue to be efficient at even higher densities than can be observed directly, so that there might well be an unexpected uniformity of conditions of cometary grains. The grains seem to be modified quite efficiently as they progress from the outer to the inner parts of the clouds.

B. The λ2175 Bump

One of the most mysterious features of interstellar dust is the bump (see Draine 1989 for a review). It has recently been discussed in some detail (Fitzpatrick and Massa 1986; Cardelli and Savage 1988, and refs. therein). Its puzzling properties are that its central wavelength, λ_0, is almost the same for various lines of sight, but there definitely is some variation (see especially Cardelli and Savage 1988). Its width varies considerably, in a seemingly random pattern. Its strength is rather well correlated with R_V^{-1} (CCM). It is so strong that its carrier must be very abundant, almost surely C, N, or O (in my opinion, but see Duley and Williams 1988). It is one feature that most theories of grains do not try to model in great detail, although Hecht (1987) has a rather plausible explanation for many of the observed phenomena.

III. Present Theories of Grains

There are at present several theories of dust which attempt to explain the observational facts outlined above (plus a great deal which are not mention there). Several which have been recently discussed are: (a) the silicate-core/organic refractory mantle theory of Greenberg (Hong and Greenberg 1980; Greenberg 1989); (b) the bare (no mantles) silicate/graphite theory of Mathis, Rumpl, and Nordsieck (1977), often called "MRN," but considerably improved by Draine and Lee (1984; DL); (c) a recent theory of Mathis and Whiffen (1989; MW) of composite grains, in which bare grains containing silicates, amorphous carbon, and graphite are proposed; (d) silicate core grains, with hydrogenated amorphous carbon clusters upon their surfaces (Duley and Williams 1988, Duley, Williams, and Jones 1989); and (e) a mixture of silicate-core/organic- refractory-mantle particles, similar to Greenberg/Hong, but with metallic iron to provide the observed IRAS intensities (Chlewicki and Laureijs 1988). In addition, there are other theories similar to the

above, but not derived from them. A theory quite different from the others is that of biota (Hoyle and Wickramasinghe 1984; see Jabbir et al 1986 for refs. and a late version of the theory).

Table 1 summarizes some of the salient features of most of the "complete" models of grains, meaning that the entire spectral range is addressed by the model. There are models specific for the bump which I have not included. I note that the most popular explanation of the bump, graphite (shown by Table 1 to be almost unanimous), was originated by Hoyle and Wickramasinghe (1962) in the form of a prediction.

Common features of grain theories: All of the theories listed in Table 1 claim to be able to fit the observed extinction and polarization laws for the diffuse ISM. This fact illustrates the fundamental problem of understanding grains: a lack of uniqueness, imposed by the fact that only integral properties of the size distributions are observed. At some level we have to be content to judge theories on the basis of their plausibilities rather than from completely objective criteria, such as predictions which are absolutely incompatible with the observations. However, *detailed* predictions of the extinction law, ranging from 1000 μm to 0.1 μm, might also be good discriminants of grain theories, but have only been applied to DL, MW, and Duley/Williams. While the theories in general can explain the mean extinction law for the diffuse ISM, some of them might have difficulty making the differences in the extinction laws between diffuse- and outer-cloud dust plausible. There are rather powerful constraints imposed upon the models if one requires both extinction laws to be fitted by similar amounts of materials, including carbon in the various specific forms (graphitic and amorphous). There are possibly other tests (see § IV C below) which will discriminate among the various models, or even eliminate all of them.

One reason I am not emphasizing the biological theory of grains is that it requires more phosphorus than the solar abundance (Whittet 1984, Duley 1984), although Hoyle and Wickramasinghe (1984) claim that their theory can accommodate the P abundance within a factor of 1.5 if favorable assumptions are made. Observations of depletions show that phosphorus is about half in the gas phase in the diffuse ISM (Jenkins, Savage, and Spitzer 1986), making the problem even more acute.

Fitting the entire range of interstellar extinction requires a very broad distribution of sizes, which is one property shared by all theories. The observations of the silicate bands at both 9.7 μm and 20 μm almost require the presence of silicates. The breadth and lack of structure in these bands in both the Orion Nebula emission and the absorption in various objects, as well as emission from cool, oxygen-rich stars producing and ejecting circumstellar dust, indicate that the silicates are amorphous in nature. It is widely assumed that amorphous silicates present in grains contain essentially all of the silicon. Tielens and Allamandola (1987) have pointed out that

TABLE 1.

FEATURES OF SOME CURRENT GRAIN THEORIES

Brief title of theory (and authors)	Composition of Grains	Size distr. of Grains	Carrier of Bump	Refs.[a]
Core/mantle (Greenberg)	Silicate cores/organic refractory mantles; also small silicates, graphite	"Flat"[b]	Small graphite[c]	1,2
Core-mantle + iron (Chlewicki, Laureijs)	Similar as Greenberg, with small metallic iron particles, PAHs	"Flat"[b]	Small graphite[c]	3
Draine-Lee (or MRN)	Bare silicate, graphite	$a^{-3.5}$	Graphite	4,5
Duley/Williams/Jones	Silicate cores, hydrogenated amor. C clusters, small silicates	$a^{-3.5}$	OH^- ions near Si	6
Composite grains (Mathis, Whiffen)	Silicates, amor. C, small graphite in the same grains (with free small graphite, possibly silicates)	$a^{-3.5}$	Small graphite[c]	7
Fractals (Wright)	Grains with fractional dimensions (from growth)	--	--	8
IRAS-compatible dust (Rowan-Robinson)	Silicates, amorphous C	Discrete sizes	Small graphite[c]	9
Biota (Hoyle, Wickramasinghe)	Graphite, bacteria, diatoms	Discrete sizes	Small graphite[c]	10

Notes:

[a] References: 1, Hong and Greenberg (1980); 2, Chlewicki and Greenberg (1989); 3, Chlewicki and Laureijs (1988); 4, Mathis, Rumpl, and Nordsieck (1977; MRN); 5, Draine and Lee (1984; DL); 6, Duley and Williams (1988), Duley, Williams, and Jones (1989); 7, Mathis and Whiffen (1989); 8, Wright (1987); 9, Rowan-Robinson (1986); 10, Hoyle and Wickramasinghe (1984), Jabbir et al. (1986).

[b] "Flat" is really an exponential-type distribution which is plotted in Fig. 3 of this paper.

[c] "Small" graphite means that the radii of all graphite particles are $< 0.22/(2\pi)$ μm, or ≤ 0.005 μm. Below this size, the extinction properties do not change with size.

the strength of the 9.7 μm feature is such that 1.5 times the solar silicon abundance is required to produce the 9.7 μm feature from amorphous silicates alone. However, crystalline silicates have band strengths over twice as large, and it is perhaps plausible that the silicates in grains are somewhat ordered. Theories assume that all of the silicon is contained in the silicates.

Another feature which all present grain theories share is leaving at least some observations unexplained, partly because the authors feel that our present knowledge of optical constants or other physical properties does now warrant detailed modelling. These observations include the bump, which is likely to be produced by a material something like graphite or hydrogenated amorphous carbon (Hecht 1987), but which has not been positively identified. The origin of the UIBs is by no means settled; although PAHs seem to be very plausible candidates, the bands have other possible origins, and have been referred to as the "overidentified infrared bands." Except for Chlewicki/Laureijs, the theories in Table 1 do not try to make detailed predictions of the origins of the carrier(s) of these emission bands.

There are also surely small amounts of other minerals, such as silicon carbide, present in grains, since carbon stars show an emission feature which arises from this material and it is quite refractory. Other unexplained observations include the origin of the "diffuse interstellar bands," which may (or may not) have interesting implications as to the nature of grains.

Differences among the grain models: Obviously, there are differences among each of the models. Possibly the broadest difference, as regards the prediction of the nature of cometary grains, is whether or not the silicates in diffuse and outer-cloud dust are coated with tough organic refractory mantles, as envisioned in theories of Greenberg and Chlewicki/Laureijs, but not the others. The size distributions are also quite different, as shown by Figure 3. I shall discuss these differences in § IV below.

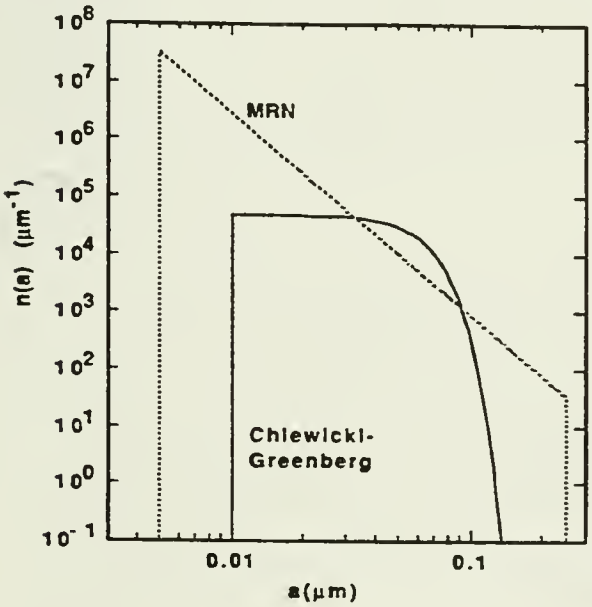


Fig. 3.—The size distributions in the theories of core/mantle grains (Hong and Greenberg 1980; the actual size distribution shown here was taken from a preprint by Chlewicki and Greenberg) and the MRN-Draine and Lee (1984) theories. Small graphite and silicate particles, of unspecified size distributions except that the sizes are < 0.05 μm or so have been omitted from the core/mantle theory.

Another apparent difference between the core/mantle theory and bare-grain theories might be the presence of elemental carbon in forms other than the small graphite needed for providing the bump, which is only about 25% of the solar abundance. There have been small diamonds found in meteorites (Lewis et al. 1987), but theories do not include them explicitly because their abundance is too low. Besides the graphite needed to produce the bump, the MW theory has most of the carbon in amorphous solid phase and Greenberg's theory has it is the organic refractory mantles. However, the situation is not so clear, since there may have been enough processing of the organic refractory mantles by cosmic rays and ultraviolet radiation to convert them essentially to amorphous carbon.

IV. MANTLES AND SIZE DISTRIBUTIONS

A. Are there mantles on diffuse- and outer-cloud dust grains?

Should we expect interstellar silicate grains in a cometary nucleus to have mantles of organic refractory materials? In this section I examine the evidence for those mantles on grains outside of the dense cores of molecular clouds. It is clear that the cometary grains will acquire mantles of molecular ices deep within the molecular cloud, and it is not those mantles we are debating.

The extinction law for the outer-cloud dust strongly indicates that the grains there are larger than the average for the diffuse ISM. There are two aspects of the mantle question I would like to address in turn: (a) Do the grains in outer-cloud dust have their increased sizes because of having acquired mantles? (b) Is there spectroscopic evidence for mantles in the diffuse ISM?

Do the grains in outer-cloud dust have their increased sizes because of having acquired mantles? If grains in the diffuse ISM have mantles, one might expect any increases in the mean grain sizes to come from accretion of more mantles. However, there is good evidence (it seems to me) that grains are larger in the outer-cloud regions mainly because of coagulation rather than accretion of mantles. The extra depletion of the refractory elements which is observed in dense regions (the gas-phase Fe going from 90% depleted to 99% in comparing diffuse ISM dust with outer-cloud dust) will increase the grain volume by only about 5%. Any *substantial* increase in grain volume must come from accretion of the abundant and relatively undepleted elements N or O, in combination with others, since C is already mostly depleted in the diffuse ISM.

The answer to the question comes from considering the absolute amount of extinction, $A(\lambda)/N(H)$, rather than the extinction law. If the grains in the outer regions of dense clouds are large, relative to those in the diffuse ISM, because they accrete materials, the extinction *per H nucleus* [i.e., $N(H\ I)+2N(H_2)$] must increase. If the grains grow by coagulation, $A(\lambda)/N(H)$ can either increase (because there is an increase of extinction efficiency by increasing the sizes of certain grains because of collective effects, mainly with the increase of scattering) or decrease (because the material in the center of the grain is somewhat shielded from absorbing the radiation).

The results of observations are discussed briefly in CCM. There are two steps in the reasoning:

(a) Lines of sight with a large value of R_V have a smaller total value of the extinction, integrated over the wavenumber x (= $1/\lambda$). One can see from Figure 2 that there will be a considerably smaller value for $\int A(\lambda)/A(V)\, dx$ for large R_V (the lower curves) than for small R_V. In CCM we found that

$$\int A(\lambda)/A(V)\, dx = (-4.3 + 79.1\, R_V^{-1})\ \mu m^{-1}\ , \qquad (1)$$

where the integral extends from the infrared (0.3 μm^{-1}) out to the largest wavenumbers observable with the *Copernicus* satellite, x = 10 μm^{-1}. The second term is dominant, and the total integral is roughly inversely proportional to R_V^{-1}.

(b) To determine the total integrated extinction, we must relate the visual extinction in equation (1), to the total H column density, which is not easily determined observationally. The problem is that the N(H I) must be found from the highly saturated Ly-α profile, and the $N(H_2)$ from the *Copernicus* observations of the Lyman and Werner bands. However, for two well-observed lines of sight (towards NU Ori and ρ Oph) in the outer regions of dense clouds, the results are unambiguous: the quantity A(V)/N(H) is *smaller* than in the diffuse ISM. There is no measurement of the H_2 column density towards NU Ori, so its value of A(V)/N(H) is an upper limit. These stars have large values of R_V. The total integrated extinction values of ρ Oph and NU Ori are 0.73 and $\leq$ 0.43 of the value in the diffuse ISM (Bohlin, Savage, and Drake 1978), respectively.

There are other stars for which estimates of N(H I) and $N(H_2)$ are available, but not so accurately determined as for ρ Oph (de Boer et al. 1986), or so extreme an A(V)/N(H I) value as for NU Ori (Shull and van Steenberg 1985). We reserve judgement on the other stars.

From this data on extinction per H nucleus one concludes that grains are larger in outer-cloud dust because of coagulation rather than accretion. Similar results were derived by Jura (1980) and Mathis and Wallenhorst (1981) on the basis of A(V)/N(H) alone. The integrated value of the extinction makes the case stronger. It is difficult to have even coagulation produce enough decrease in extinction cross-section per H (see MW), and any accretion of mantles makes this task even worse. It is very difficult to imagine that there is extensive accretion onto grains until they are deeper in clouds than can be observed at present in the ultraviolet part of the spectrum.

Is there spectroscopic evidence for mantles in the diffuse ISM? If there are mantles on grains in the diffuse ISM, one would expect to find some spectroscopic evidence for them. In fact, there is such evidence: the 3.4 μm absorption feature about 30% deep seen in the spectrum of IRS 7, a supergiant seen near the galactic center (Butchart et al. 1986) with an extinction, A(V), of $\approx$ 25

mag. The presence of that feature has been used as a justification for the existence of organic refractory mantles, since the 3.4 μm feature is an indication of an aliphatic C-H stretch absorption and the 3.4 μm feature is found in the spectrum of organic refractory mantles (Schutte 1988). Figure 4 (from Schutte 1988) shows the 2.8 - 3.8 μm spectrum of IRS 7 from Butchart et al. (1986). It also shows a spectrum of photolyzed ice, which fits the 3.1 μm portion of the IRS 7 spectrum well, and some "char," or a mixed mixture of paraffins, olefins, and other carbonaceous materials, which fit the 3.4 μm spectrum well. These might be present as mantles on grains, although their presence along the line of sight is no indication that they are coated onto grains, and the 3.0 μm "ice" band found in the spectrum is surely not present in even outer-cloud dust. Let us examine the evidence for materials of this type, mantles or not, in *local* dust.

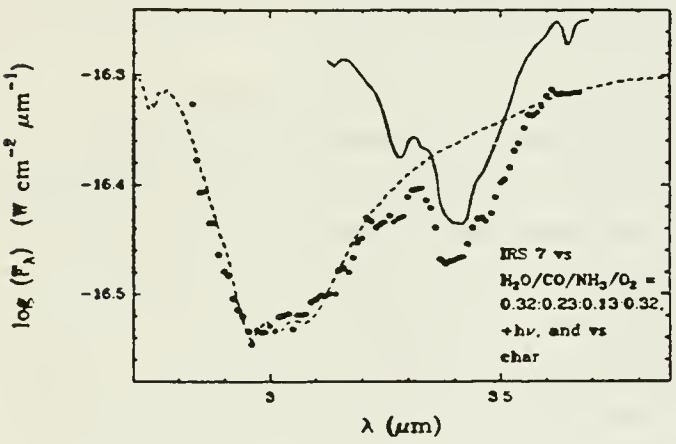


Fig. 4.—The spectrum of IRS 7 near the galactic center (spectrum from Butchart et al. 1986; figure reproduced from Schutte 1988). The 3 μm band is compared to the ultraviolet-irradiated ice sample H2O/CO/NH3/O2 = 0.32/0.23/0.13/0.32. The solid line is the spectrum of "charred" carbonaceous residue. Compare with the spectrum of absorptions through "local" dust, towards Vi Cyg 12 (Fig. 5, below).

The most likely local candidate for having the 3.4 μm feature is VI Cyg 12, a B5 Ia+ star with E(B-V) = 3.31 (Humphreys 1978; Serkowski 1965). It is the best object for studying local extinction because it is relatively nearby, is about as luminous as any other star in the Galaxy ($M_V \approx -10$!), and is very heavily reddened. Its spectrum in the 3-μm region (Gillett et al. 1975) is shown in Figure 5. The A(V) of VI Cyg 12 is 10 mag; that of IRS 7 is 25 mag. Figure 5 indicates the strengths of the absorptions at 3.1 and 3.4 μm which one would expect in VI Cyg 12, if the dust were of the same nature as towards IRS 7. To the resolution of the Gillett et al. spectrum, there is no trace of the 3.4 μm absorption feature in VI Cyg 12. However, at the discussion following a presentation at the IAU Symposium 135, *Interstellar Dust*, Dr. D. C. M. Whittet stated that VI Cyg 12 has τ(3.4 μm)/A(V) of about 1/4 that of IRS 7. Thus, it seems that the absorption by any organic refractory mantles are locally considerably less, per A(V), than towards the galactic center.

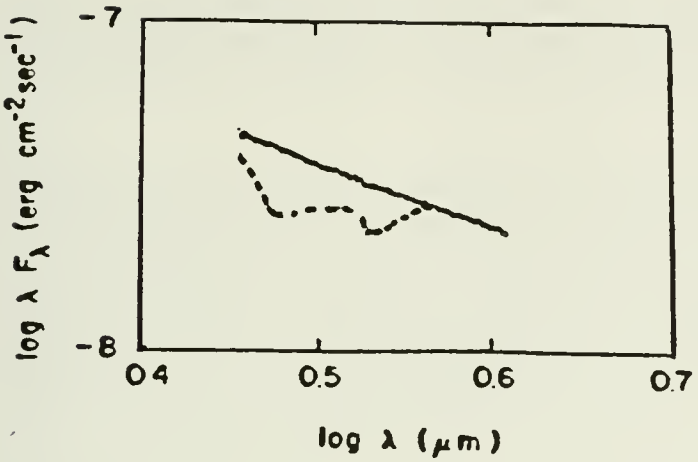


Fig. 5. — The observed spectrum of the local star VI Cyg No. 12 (Gillett et al. 1975). This is a blow-up of the portion 2.9 - 3.5 μm, with the wavelength and intensity scales superimposed. The slanted, irregular solid line shows the observations. The expected depth of the absorption is shown as the dashed line, on the assumption that the absorption per A(V) is the same as towards IRS 7 near the galactic center (Fig. 4).

But, how typical is the line of sight towards VI Cyg 12 as regards the diffuse ISM? According to one criterion, that of R_V, the answer is "very typical"; $R_V = 2.99 \pm 0.15$ (Rieke 1974), as compared to the mean of 3.1 for the diffuse ISM. But according to another criterion, that of A(V) per kpc, the answer is "very atypical." The distance of the VI Cyg association is 1.5 kpc (Schulte 1958), and the other stars in the association are reddened considerably less than No. 12. Stars No. 5 and 12 have E(B-V) = 2.00 and 3.31, respectively, which represents a difference of A(V) of 4 mag. The two stars are separated by an angle of 4.5'. This corresponds to a projected linear distance of 2 pc if d = 1.5 kpc, or an actual separation of perhaps 4 pc. The excess extinction of No. 12, relative to the other stars in the same association, is presumably caused by dust in the vicinity of the cluster, so $A(V)/d \geq 1$ mag pc^{-1} (!). Thus, the local density of the dust seen to No. 12 must be ≈ 500 times the typical value for the diffuse ISM (about 2 visual mag per kpc). It would seem reasonable that such an extreme value of density would promote mantle growth, so I would suspect that the mean absorption strength of the 3.4 μm band in the diffuse ISM is considerably below even the low value found in VI Cyg 12. Such a low value makes the volume of the organic refractory mantles rather unimportant as regards the extinction properties of the grains. There might be enough mantle on grains to influence their *surface* properties considerably, in particular how well they stick together during collisions or how well they form molecules on their surface.

It is perhaps not too surprising that dust along the entire path length to the galactic center would be somewhat different, perhaps very different, from local dust. There is a definite composition gradient in the Galaxy (Shaver et al. 1983) which indicates an increase in N(O)/N(H) of about a factor of two. Probably the abundance of other elements is higher by similar factors. Furthermore, the mean density of the ISM also increases by about a factor of four (Güsten and

Mezger 1982). Both factors favor the growth of mantles. The peculiarity of the dust towards IRC 7 is emphasized by the 3.1 μm absorption, which is not of the same shape as the usual 3.07 μm ice band, but is somewhat stronger than the 3.4 μm band which might show the existence of mantles.

Perhaps it is merely semantics to discuss whether or not there are "organic refractory" mantles in space, meaning materials similar to those which have been produced in the laboratory. As organic refractory material is processed by radiation in the laboratory (Schutte 1988), it steadily loses O and N relative to C. If the processing by the cosmic rays and ultraviolet radiation is severe enough, the mantles might become amorphous carbon for all practical purposes, and just about all of the authors listed in Table 1 can declare a victory to their respective funding agencies.

The size distribution of grains: Another major difference in the present core/mantle theories and most bare-grain theories is the size distribution, at least the grains responsible for the visual extinction. This distribution is almost a truncated step-function for the core/mantle theory, with a rather indefinite number of very small grains to provide the ultraviolet extinction, and a power-law for most others. It seems to me that the power-law size distribution is the most plausible part of the MRN theory, for both theoretical and observational reasons. Biermann and Harwit (1979) showed that collisional processes should establish a power law with the exponent in the range considered by MRN and DL (n(a) proportional to $a^{-3.5}$). Radar studies of particles in Saturn's rings (Cuzzi et al. 1984), shattered terrestrial rocks and gravel beds (Hartmann 1969), and of cometary dust (MacDonnell et al., this volume) are all heavily peaked in numbers towards small sizes, but with much or most of the mass in the larger grains. These distributions are all produced by collisional processes among the particles. Thus, if there are collisional processes among the grains, it would seem difficult to avoid an approximate power-law distribution.

The fact that grains in outer-cloud dust have apparently grown from those in the diffuse ISM by coagulation rather than by accretion implies to me that they have, in fact, grown by collisional processes. While I doubt that it is precisely a power-law size distribution which is established, I would find it difficult to believe that the size distribution is very flat.

The coagulation of grains in outer-cloud dust is a strong motivation for the composite-grain theory of MW. Grains are originally ejected from stellar atmospheres, novae, or supernovae with a certain specific composition which small particles can retain (and do, as shown by isotopic anomalies in meteorites). However, there are "large" ($a \approx 0.1$ μm) grains which provide the extinction in the optical part of the spectrum, and which observations suggest are rather heavily modified by shattering and coagulation as they go into and out of dense clouds. It is difficult to imagine that the component small particles fit together without voids or holes within them. The interplanetary dust particles (IDPs) collected by Brownlee and his coworkers (see Brownlee 1987 for a review of the solar system-interstellar dust connection) show the kind of open structure

which partially suggested these ideas. However, there has also been chemical processing of the IDPs, as shown by their occasionally homogeneous chemical compositions within grains, but varying compositions from grain to grain (Brownlee, this workshop; Mackinnon and Reitmeijer 1987).

In fact, I strongly suspect that the composite theory is too simple. There is a constant transfer of refractory elements back-and-forth from grains to the gas phase. Grains are destroyed in shocks, as shown by the low depletions in high-velocity gas (see Jenkins 1987 for several references) relative to the diffuse ISM, and there is a more severe depletion of refractory elements in dense clouds. For computational purposes, it was assumed in the composite model that the individual particles in a grain are either silicates or elemental carbon. Although this assumption is necessary to compute indices of refraction, it really seems dubious: the refractory elements, carbon as well as silicon, etc., are deposited onto grains together. The individual particles in the composite model should probably consist of a core of perhaps pure material, produced in a star, and a mantle of refractory elements (not organic refractories) surrounding the core. There might well be a coating of organic refractory on the surfaces of grains, but (it seems to me) much less than envisioned by Greenberg. The existence of the "stardust" core to grains– very refractory minerals which have survived from their formation in stellar atmospheres or supernova explosions throughout their entire lifetime in the ISM– is heavily supported by the isotopic anomalies which are found in meteorites (e.g., Clayton 1988, Tang and Anders 1988). However, I believe that most of the grain volume must have been heavily processed by processes in the diffuse ISM.

If there are few grain-grain collisions within space, after the grains are formed in cool stellar atmospheres, then the Greenberg core/mantle theory size distribution becomes much more plausible, although Biermann and Harwit (1979) considered collisions within a stellar atmosphere to be the dominant mechanism for grain evolution. If grain-grain collisions are negligible, chemically homogeneous grains are plausible if the organic refractory mantles produced in dense clouds are cleaned off by shocks, as theory (e.g., Draine and Salpeter 1979a,b) suggests. Bare grains of homogeneous compositions, as DL (or a similar silicate/amorphous-carbon theory, to avoid the problem of making large graphite grains) become plausible as well.

A good test of the various theories: While there is too much ambiguity in explaining the observations of extinction and polarization alone to discriminate among the various theories, there is an excellent test which has not yet been applied to the extent that it should be: explaining the observations of the 3.1 μm ice band, the 9.7 μm and 19 μm silicate features in the Becklin-Neugebauer (BN) object in the Orion molecular cloud (Lee and Draine 1985; Hildebrand 1988), not only as regards the relative extinctions and polarizations, but also the contrast in the polarization within and between the bands. Weak absorption features show polarization with the same wavelength dependence as extinction. As a resonance becomes stronger, the polarization

reaches a maximum at longer wavelengths than extinction, with a shift which is dependent upon grain shapes and coatings. The silicates features are strong enough to provide such a diagnostic for the environment of the silicates, and such the shift is actually observed in BN. Predictions are quite different on the various theories (coated on the core/mantle theory; juxtaposed with carbon on the MW theory; bare and alone on the DL theory). Lee and Draine (1985) found a fair fit of MRN with the observations, provided that oblate (pancake) grains of about 2:1 size ratio were assumed. Martin (1989) showed that his calculations with core/mantle grains produced a negative polarization which is not observed. I doubt that the composite grains of MW will be able to pass this test either, but one must be confident of the indices of refraction, which are more difficult to estimate in the case of composite grains than for homogeneous materials. It has a poorer chance than DL, in which case the silicates are bare, but probably a better chance than any theory in which the silicates are coated with mantles. There is one potential problem with this test: there is evidence for scattering in the surrounding K-L nebula (Werner, Dinerstein, and Capps 1983, and refs therein) in the 2 - 5 μm spectral region, with the scattered light being reflected from both BN and from IRc 2 nearby. However, the polarization of BN itself is dominated by the aligned grains rather than scattering; the total polarized intensity of the 2 - 5 μm radiation on BN itself is very much larger than that from the polarization from scattering of the surrounding KL nebula.

V. The Evolution and the Nature of Interstellar Dust

In this section I shall summarize my views regarding the evolution of interstellar dust, starting with its formation and ending with it being incorporated into a cometary nucleus.

The formation of grains, and the fact that stellar ejecta are not much like interstellar grains: There are many sources of grains: planetary nebulae, novae, supernovae, and, especially, cool giant and supergiant stars (see Gehrz 1989 for a review). Just which of these processes are the dominant ones need not concern us here— we just need to recognize that in each particular source, the grains are formed with a composition which reflects the local gaseous chemical composition, and, especially, whether C > O, or the reverse. The reason, of course, is that the element which has the lesser abundance by number is almost completely converted into the very stable molecule CO, which cannot participate in grain formation. Observations (Merrill 1977) show that O-rich stars form grains of a silicate nature, as shown by the spectra in the 10 and 20 μm region. Grains formed in a carbon-rich environment show a rather featureless optical spectrum, except for a band at 11.2 μm which is attributed to SiC. Most carbon stars are too cool and dusty to be observed in the ultraviolet part of the spectrum, but a feature resembling the bump, but displaced to 2300 Å, has been found in very carbon-rich, H-poor objects (Greenstein 1981;

Hecht et al. 1984). This bump is similar to that expected from amorphous carbon, so it is widely assumed that carbon stars produce grains of this form (see also Martin and Rogers 1987).

Roughly half of the grains come from each type of source (C- or O-rich). The materials that are injected into the diffuse ISM from the primary sources of grains, then, are not mostly grains themselves. Rather, all of the lesser of the elements carbon and oxygen is tied up in gaseous CO, which in turn is photodissociated and then photoionized into C^+ and O in most of the ISM (and in more highly ionized forms in the H^+ regions found in some 10% of the mass of the diffuse ISM). Some or most of the remaining C or O is in the form of amorphous C or silicates, respectively. Some of the silicon, but apparently not a large fraction (Martin and Rogers 1987), is tied up in the refractory SiC from the carbon-star ejecta.

Processing of the materials within the ISM: Within the ISM, grains must be processed extensively by grain-grain collisions, shocks from supernovae and stellar winds, sputtering by the hot phase of the ISM, and accretion of atoms and molecules from the gas phase. The lifetime of a particular parcel of gas in the Galaxy, as regards being incorporated into a star, is $M_{gas}/\dot{M}_{gas}$ = 5E9 $M_\odot$ /(3 $M_\odot$ yr^{-1}) > 1 Gyr. The mass contained in the very hot ISM, or in H II regions, is quite small as compared to the atomic or molecular phases, each of which contains about half of the mass. Since molecular clouds are preferentially found in the spiral arms encountered twice each galactic rotation period, or about every 10^8 yr, a typical parcel of gas should have been and out of a molecular cloud several times during its lifetime.

Present theories of the effectiveness of various processes, especially of grain destruction rates, seem to me to be in conflict with observations (see also Seab 1987). According to theory (Draine and Salpeter 1979a,b; Snow and Seab 1983), shocks from supernovae are quite destructive of grains, and it is not easy to understand why grains have not been rather completely destroyed by these shocks in times of the order of 10^8 yr. Observations provide a rather different view: except for high-velocity gas (see refs. in Jenkins 1987, p. 550), presumably being affected by one or more shocks at the present time, the refractory elements are always highly depleted. Near the galactic plane, the mass of the high-velocity gas at any instant is very small in comparison to the bulk of the ISM. The almost ubiquitous depletion of refractory elements is especially significant in view of the fact that there is a continuous return of *gaseous* refractory elements into the diffuse ISM from stars, especially those of early type and planetary nebulae. Grains are so far apart in the diffuse ISM that it is difficult to have the gaseous refractory elements condensed onto grains efficiently. One finds by integrating the theoretical size distributions, or just by the fact that the mean free path of radiation is about 1 kpc, that the area of grains is roughly 10^{-21} cm^2 $(H\ atom)^{-1}$. For the diffuse ISM clouds ($n(H) \approx 30\ cm^{-3}$) and relative speeds of refractory atoms and grains of 100 m/sec (which represents a nonthermal grain-gas relative speed), the time for a grain to collide with a grain is > 10^8 yr. Within this time, current theories of grain destruction

suggest that the grains should be destroyed, and their refractory elements returned to the gas phase. Unless we imagine that each individual parcel of gas becomes part of a *dense* molecular cloud several times within this 10^8 yr, a significant portion of the refractory elements should be in the gas phase. There is an apparent conflict between theory and observation.

The easiest way for me to understand the observed high depletions is by assuming that grains survive the rigors of the ISM far better than the theory would suggest, so they do not readily lose the Fe, Al, and other refractory elements into the gas phase. I am not only considering the survival of the silicates, but also of the carbon which is invoked to explain the bump and the total amount of extinction per H. Having carbonaceous mantles around silicate cores would not help this situation; if the mantles were destroyed, they would have to re-form in the diffuse ISM to provide enough extinction to match observations even if they protected the silicate core.

There may not be a significant error in theory of destruction of the grains after they are hit by a shock of a given speed. The estimate of the mean lifetime of the grains also depends upon the frequency with which a parcel of gas is hit by the shock. That time, in turn, is dependent upon the interstellar magnetic field and supernova frequency. A larger interstellar magnetic field than is commonly assumed (about 5 μG instead of 2 μG) greatly reduces the volume of space over which a hard shock from a supernova propagates (Cox 1988).

Even if grains are not destroyed by shocks as efficiently as theories suggest, the regularity of the observed extinction law is surprising. Draine (1985; see also Volk et al. 1980) has discussed the evolution of grains within clouds. The time required for a moderate-sized grain (0.1 μm) to increase its mass significantly is $\approx 7E10\ (n_H)^{-1}\ v_3^{-1}$ yr, where v_3 is the relative speed of grains, in units of 10^3 cm sec^{-1}. For grains in clouds of $n_H = 10^3$ cm^{-3} and v = 10 - 100 m sec^{-1}, the time is about 10^7 - 10^8 yr. However, there is a high degree of uniformity of the extinction laws in outer-cloud dust (CCM). Some of these clouds, such as near the Orion Nebula, presumably have the grains emerging from the dense regions. One would expect that in other regions the molecular cloud is growing, and the grains near the cloud reflect the nature of the diffuse ISM. If the processes by which grains are modified by interstellar processes were not surprisingly efficient, there would be a large dispersion in the relative numbers of the small to the large particles.

It is also surprising that the interstellar polarization near dense molecular clouds is fairly strong and very regular in outer-cloud dust, so the grains are clearly very well aligned. For instance, the polarization around the Cor Aus cloud (Vrba, Coyne, and Tapia 1981) is very regular and follows the contours very closely, so either the cloud is quite old or the alignment is very efficient. The extinction in the cloud shows the expected large values of R_V, so the grains have presumably coagulated while spinning. These considerations show that either my theoretical notions, or interpretation of the observations, or both, are wrong. I suspect that it is the theoretical notions.

Possibly there is surprisingly good circulation between the outer and inner parts of the cloud. If so, either the motions do not carry the grains to the mantle-forming regions (since mantles are counterindicated by the extinction/N(H) ratio in the Orion and Ophicius clouds) or the mantles are cleaned off very efficiently in the outer parts of the clouds. The circulation might be deep enough to reach local densities of 10^5 - 10^6 H_2 molecules cm^{-3}, with a correspondingly large grain density, so that grain-grain collisions occur rapidly. Such a circulation would suggest that the relative speeds of the grains relative to the gas, and to each other, is nonthermal, but instead is governed by hydromagnetic waves, in which the relative speeds depend on the charge/mass ratios of the various constituents. In this case, the grains and gas will all move rather gently with respect to each other, and the coagulation can occur with a drastically reduced time scale over estimates for the outer regions of the clouds. Since the ISM is never allowed to come very close to mechanical equilibrium because of supernovae and violent winds from early-type stars, the presence of hydromagnetic waves seems plausible. These conditions will lead to the observed reduced extinction cross-section per H nucleus.

At some point, grains penetrate the regions of the molecular clouds where molecular mantles form, and the icy coatings change the grains' properties considerably. Mantles of water, ammonia, methanol, formaldehyde, and several other molecules appear in the spectra of stars embedded within the clouds. Tielens and Allamandola (1987) give an excellent discussion and summary of this aspect of the ISM, with references to many of the claims I make below.

In the cores of dense molecular clouds, the time scale for molecules to stick to the cold grains becomes very short, and on timescales of 10^5 yr or less the heavy molecules should freeze out. It is obvious that the many microwave observations of all sorts of gas-phase molecules from molecular clouds show that this theoretical idea is quite wrong. I believe that the correct explanation is that of Greenberg and his co-workers— that explosions of the free-radical-rich icy mantles, triggered by cosmic ray heating events or grain-grain collisions, return much of the frozen ices back into the gas phase, with molecular reactions that contribute to a complex chemistry. The free radicals in the mantles must be produced by damage by ultraviolet photolysis or by cosmic rays to the otherwise amorphous stable ices. The radiation might arise from the excitation of H_2 by cosmic rays. The icy reactive mantles may well form the "yellow stuff" which is observed in the laboratory, although the efficiency of its formation is low enough so that it may not be important even within these dense cloulds.

Formation of pre-cometary dust: In the inner parts of molecular clouds, there are apparently enough "turbulent" motions (the hydromagnetic waves required to maintain relative grain motions in the outer parts of the molecular clouds?) to usually prevent the self-gravitation of the cloud to produce a collapse. Occasionally such a collapse occurs, possibly triggered by the winds or supernova explosions of previously formed early-type stars. There are no measurements of any H

column densities deep within molecular clouds, so it is pure speculation to guess that the grains continue to coalesce as they accrete icy mantles. The coalescence would imply that there are voids or spaces within the grains, since the particles cannot fit together very well. The organic cometary material found in P/Halley, such as "CHON," is condensed out of the cloud at this stage. The refractory solids, the former interstellar grains, would form a loose, weak matrix spread throughout the ices, and the evaporation of the ices when the cometary dust is warmed by sunlight would disrupt the weak grains rather efficiently.

There would have to be some additional processing of the frozen grains and ices before they accumulated into a full-fledged comet. The energy released in the impacts of the protocometary lumps as they coagulated into larger and larger groupings would probably cause some of the ices to evaporate or change into crystalline phases, and reactions between the chemically active ices would produce organic molecules as well as heat. These reactions would probably convert a considerable fraction of the elementary carbon into organic compounds which are observed in P/Halley as "CHONS" (including sulfur).

Processing of the grains would continue in the outer solar nebulae, where the temperature is far higher (> 100 K) than in the cores of dense clouds (≈ 10 K). The returned cometary materail will, of curse, reflect this processing. however, it would be far better at providing insight into the nature of the original interstellar grains than any other material in the solar system.

VI. SUMMARY

1. Observations show rather clearly that whatever processes modify the size distributions of grains operate efficiently on all sizes. Extinction laws follow a rather regular pattern over the entire wavelength range which can be observed (down to $\lambda = 0.1$ μm). There are deviations of individual extinction laws from the mean shape, but those deviations are smaller than the deviations of the mean shapes of the extinction laws from dust in the diffuse ISM as compared to that in the outer parts of dense clouds (the densest regions in which we can observe the extinction law).

2. The solid materials ejected by stars are heavily modified, but not completely destroyed, by processing in the ISM. Isotopic anomalies in meteorites show that at least some grains survive intact ("stardust"). The size distributions of interstellar grains are changed many times, though, by coagulation within the outer regions of dense clouds.

3. There are several theories (see Table 1 for references) which can explain at least the gross features of the mean extinction and polarization law for the diffuse ISM. Some have been applied to the details of the extinction law with fairly good success. None can explain the λ2175 "bump" completely well. Not many have tested as regards differences in the extinction law from the

diffuse ISM to outer-cloud dust. It seems likely to me (Mathis and Whiffen 1989) that grains in the observable outer parts of dense clouds are probably fluffy and composed of both carbon and silicates within the same grain. They should contain voids or vacuum as they coalesce.

4. Grains grow in the outer parts of dense clouds mainly by coalescing rather than accreting. The small extra fraction of refractory elements (Fe, Mg, etc.) which they accrete is not a large fraction of their volume in the diffuse ISM. The evidence for coalescence rather than accretion is that their total extinction cross-section per H atom *decreases* for the well-observed stars in the outer parts of dense clouds. Accretion adds to the grain volume, contrary to observations. The decrease in extinction arises from the reduced extinction of the inner parts of the grains.

5. It seems to me (but not to others!) that there is rather good evidence against the presence of considerable amounts of organic refractory mantles on diffuse and outer-cloud dust, mainly because of the weakness of the 3.4 μm absorption feature in VI Cyg 12, the most heavily reddened nearby star. The dust cloud seen in front of it is much denser than average (by a factor of ≈ 500), so grain mantles would be much more likely to form and survive than in the diffuse ISM. Evidently organic refractory mantles, if they are formed deep within molecular clouds, are destroyed by the processes which operate in the outer parts of those clouds. The line of sight towards IRS 7 near the galactic center, where organic refractory mantles along with ices seem to be present, differs from local dust in having a much larger fraction of heavy elements (at least oxygen) and gas density, both of which favor the formation of mantles.

6. Deep within molecular clouds, icy mantles form. I feel the scenario espoused by Prof Greenberg is correct in this case— there is probably processing by cosmic rays, both directly and by the ultraviolet radiation they produce. This processing forms the free radicals in the icy mantles. Explosions in the chemically reactive mantles release heavy molecules into the dense, cold gas in the cloud cores.

7. When the cloud cores collapse into stars, planets, and comets, the grains, with rather thick icy mantles, form icy lumps which in turn coalesce into cometary nuclei.

This work has been partially supported by Contract K 957996 from the Jet Propulsion Laboratory, for the space Astrophysics Data Analysis Program and by the Graduate School of the University of Wisconsin and the Lunar and Planetary Institute, for which I am grateful. I have benefitted from preprints and conversations with J. A. Cardelli, B. T. Draine, R. H. Hildebrand, P. G. Martin, B. D. Savage, and many others.

REFERENCES

Allamandola, L. J., and Tielens, A. G. G. M. (eds.) 1989, *Interstellar Dust*, proceedings of Symposium 135 of the International Astronomical Union, held at Santa Clara University, July 26-30, 1988 (Reidel: Dordrecht).

Allamandola, L. J., Tielens, A.G.G.M., and Barker, J. R. 1985, *Ap. J. (Lett.)*, **290**, L25.

Biermann, P., and Harwit, M. 1979, *Ap. J.(Lett.)*, **241**, L33.

Bohlin, R. C., Savage, B. D., and Drake, J. F. 1978, *Ap. J.*, **224**, 132.

Bregman, J. D., Campins, H., Witeborn, F. C., Wooden, D. H., Rank, D. M., Allamandola, L. J., Cohen, M., and Tielens, A. G. G. M. 1987, *Astr. Ap.*, **187**, 616.

Brownlee, D. E. 1987, in in *Interstellar Processes*, D. J. Hollenbach and H. A. Thronson, eds. (Reidel: Dordrecht), p. 513.

Butchart, I., McFadzean, A. D., Whittet, D. C. B., Geballe, T. R., and Greenberg, J.M. 1986, *Astr. Ap.*, **154**, L5.

Campins, H., and Ryan, E. V. 1989. *Ap. J.*, June 15, in press.

Cardelli, J. A., and Savage, B. D. 1988, *Ap. J.*, **325**, 864.

Cardelli, J. A., Clayton, G. C., and Mathis, J. S. 1988, *Ap. J. (Lett.)*, **329**, L33 .

Cardelli, J. A., Clayton, G. C., and Mathis, J. S. 1989, *Ap. J.*, submitted.

Chlewicki, G., and Greenberg, J. M. 1989, *Ap. J.*, in press.

Chlewicki, G., and Laureijs, R. J. 1988, *Astr. Ap.*, **207**, L11.

Chlewicki, G., de Groot, M. S., van der Zwet, G. P., Greenberg, J. M., Alvarez, P.P., and Mampaso, A. 1987, *Astr. Ap.*, **173**, 131.

Clayton, D. D. 1988, *Ap. J.*, **334**, 191.

Cox, D. P. 1988, in *Supernova Remnants and the Interstellar Medium*, R. S. Roger and T. L. Landecker, eds. (Cambridge University Press: Cambridge), p. 73.

Cuzzi, J. N., Lissauer, J.J., Esposito, L.W., Holberg, J. B., Marouf, E. A., Tyler, G. L., and Boischot, A. 1984, in *Planetary Rings*, ed. R. G. Greenberg and A. Brahic (Univ. of Arizona Press; Tucson), p. 73.

de Boer, K. S., Lenhart, H., van der Hucht, K. A., Kamperman, T. M., Kondo, Y., and Bruhweiler, F. C. 1986, *Astr. Ap.*, **157**, 119.

Dragovan, M. 1986, *Ap. J.*, **308**, 270.

Draine, B. D. 1985, in *Protostars and Planets II,* D. C. Black and M.S. Matthews, eds., (Univ. of Arizona Press: Tucson), p. 621.

Draine, B. T. 1989, in *Interstellar Dust*, proceedings of Symposium 135 of the International Astronomical Union, held at Santa Clara University, July 26-30, 1988 (Reidel: Dordrecht).

Draine, B. T., and Lee, H. M. 1984, *Ap. J.*, **285**, 89 (DL).

Draine, B. T., and Salpeter, E. E. 1979a, *Ap. J.*, **231**, 77.

Draine, B. T., and Salpeter, E.E. 1979b, *Ap. J.*, **231**, 438.

Duley, W. W. 1984, *Quar. J. Roy. Astr. Soc.*, **25**, 109.

Duley, W. W., and Williams, D. A. 1988, *M. N. R. A. S.*, **231**, 969.

Duley, W. W., Williams, D. A., and Jones, A. P. 1989, *M. N. R. A. S.*, in press.

Fitzpatrick, E. L., and Massa, D. 1986, *Ap. J.*, **307**, 286.

Fitzpatrick, E. L., and Massa, D. 1988, *Ap. J.*, **328**, 734.

Gehrz, R. D. 1989, in *Interstellar Dust*, proceedings of Symposium 135 of the International Astronomical Union, held at Santa Clara University, July 26-30, 1988 (Reidel: Dordrecht).

Gillett, F. C., Jones, T. W., Merrill, K. M., and Stein, W. A. 1975, *Astr. Ap.*, **45**, 77.

Greenberg, J. M. 1989, in *Interstellar Dust*, proceedings of Symposium 135 of the International Astronomical Union, held at Santa Clara University, July 26-30, 1988 (Reidel: Drodrecht).

Greenstein, J. L. 1981, *Ap. J.*, **245**, 124.

Güsten, R., and and Mezger, P. G. 1982, *Vistas in Astronomy*, **26**, 159.

Hartmann, W. K. 1969, *Icarus*, **10**, 201.

Hecht, J. H. 1987, *Ap. J.*, **314**, 429.

Hecht, J. H., Holm, A. V., Donn, B., and Wu, C.-C. 1984, *Ap. J.*, **280**, 228.

Herbig, G. H. 1988, *Ap. J.*, **331**, 999.

Hildebrand, R. H. 1987, *Ap. Lett. and Comm.*, **26**, 263.

Hildebrand, R. H. 1988, *Q. J. Roy. Astr. Soc.*, **29**, 327.

Hildebrand, R. H., Davidson, J. A., Gonatas, D., Novak, G., Platt, S. R., and Wu, X. 1989, *Ap. J.*, in press.

Hobbs, L. M., York, D. G., and Oegerle, W. 1982, *Ap. J. (Lett.)*, **252**, L21.

Hong, S. S., and Greenberg, J. M. 1980, *Astr. Ap.*, **88**, 194.

Hoyle, F., and Wickramasinghe, N. C. 1962, *M. N. R. A. S.*, **124**, 417.

Hoyle, F., and Wickramasinghe, N. C. 1984, *From Grains to Bacteria* (University College Cardiff Press).

Humphreys, R. M. 1978, *Ap. J. Suppl.*, **38**, 309.

Jabbir, N. L., Jabbar, S. R., Salih, S. A. H., and Majeed, Q. S. 1986, *Ap. Sp. Sci.*, **123**, 351.

Jenkins, E. B. 1987, in *Interstellar Processes*, D. J. Hollenbach and H. A. Thronson, eds. (Reidel: Dordrecht), p. 533.

Jenkins, E. B. 1989, in *Interstellar Dust*, proc. of IAU Symposium 135, held at Santa Clara University, July 26-30, 1988 (Reidel: Drodrecht).

Jenkins, E. B., Savage, B. D., and Spitzer, L., Jr. 1986, *Ap. J.*, **301**, 355.

Josafatsson, K., and Snow, T. P., Jr. 1987, *Ap. J.*, **319**, 436.

Joseph, C. L. 1988, *Ap. J.*, **335**, 157.

Jura, M. 1980, *Ap. J.*, **235**, 63.

Krelowski, J., and Walker, G. A. H., *Ap. J.*, **312**, 860.

Lee, H. M., and Draine, B. T. 1985, *Ap. J.*, **290**, 85.

Lewis, R. S., Tang, M., Wacker, J. F., Anders, E., and Steel, E. 1987, *Nature*, **326**, 160.

Léger, A., and Puget, J. L. 1984, *Astr. Ap.*, **137**, L5.

Mackinnon, I. D.R., and Reitmeijer, F. J. M. 1987, *Rev. of Geophy.*, **25**, 1527.

Martin, P. G. 1989, in *Interstellar Dust*, proc. of IAU Symposium 135, held at Santa Clara University, July 26-30, 1988 (Reidel: Drodrecht).

Martin, P. G., and Angel, J. R. P. 1974, *Ap. J.*, **188**, 517.

Martin, P. G., and Angel, J. R. P. 1975, *Ap. J.*, **195**, 379.

Martin, P. G., and Rogers, C. 1987, *Ap. J.*, **322**, 374.

Mathis, J. S. 1986, *Ap. J.*, **308**, 281.

Mathis, J. S., and Wallenhorst, S. G. 1981, *Ap. J.*, **244**, 483.

Mathis, J. S., and Whiffen, G. 1989, *Ap. J.*, **341**, in press (MW).

Mathis, J. S., Rumpl. W., and Nordsieck, K.H. 1977, *Ap. J.*, **217**, 425 (MRN).

Mauche, C. W., and Gorenstein, P. 1986, *Ap. J.*, **302**, 371.

Merrill, K. M. 1977, in *The Interaction of Variable Stars with Their Environment*, IAU Colloq. 42, ed. R. Kippenhahn, J. Rahe, and W. Strohmeier (Bamberg: Remeis-Sternwarte), p. 446.

Nuth, J. A. 1985, *Nature*, **318**, 166.

Rieke, G. H. 1974, *Ap. J.(Lett.)*, **193**, L81.

Rowan-Robinson, M. 1986, *M. N. R. A. S.*, **219**, 737.

Savage, B. D., and Mathis, J S. 1979, *Ann. Rev. Astron. Astrophys.*, **17**, 73.

Savage, B. D., Bohlin, R. C., Drake, J. F., and Budich, W. 1977, *Ap. J.*, **216**, 291.

Schulte, D. H. 1959, *Ap. J.*, **124**, 41.

Schutte, W. 1988, PhD. Thesis, University of Leiden.

Seab, C. G. 1987, in *Interstellar Processes*, ed. D. J. Hollenbach and H. A. Thronson (Reidel: Dordrecht), p. 491.

Seab, C. G., and Shull, J. M. 1983,*Ap. J.*, **275**, 652.

Seaton, M. J. 1979, *M. N. R. A. S.* **187**, 73p.

Serkowski, K. 1965, *Ap. J.*, **141**, 1340.

Shaver, P. A., McGee, R. X., Newton, L. M., Danks, A. C., and Pottasch,, S. R. 1983, *M. N. R. A. S.*, **204**, 53.

Shull, J. M., and van Steenberg, M. E. 1985, *Ap. J.*, **294**, 599.

Tang, M., and Anders, E. 1988, *Ap. J. (Lett.)*, **335**, L31.

Tielens, A. G. G. M., and Allamandola, L. J. 1987, in *Interstellar Processes*, ed. D. J. Hollenback and H. A. Thronson (Reidel: Dordrecht), p. 397.

Vrba, F. J., Coyne, G. V., and Tapia, S. 1981, *Ap. J.*, **243**, 489.

Volk, H. J., Jones, F. C., Morfill, G.E., and Röser, S. 1980, *Astr. Ap.*, **85**, 316.

Watson, D. L., Genzel, R., Townes, C. H., and Storey, J. W. V. 1985, *Ap. J.*, **298**, 316.

Werner, M. W., Davidson, J. A., Hildebrand, R. H., Morris, M. R., Novak, G., and Platt, W. R. 1988, *Ap. J.*, **333**, 729.

Whittet, D. C. B. 1984, *M. N. R. A. S.*, **210**, 479.

Wright, E. L. 1987, *Ap. J.*, **320**, 818.

REFRACTORY SOLIDS IN CHONDRITES AND COMETS: HOW SIMILAR?

John A. Wood
Harvard-Smithsonian Center for Astrophysics

Refractory solids in chondrites and comets: how similar?

John A. Wood

Harvard-Smithsonian Center for Astrophysics

The raw materials of the solar system were interstellar gas, grains of ice, refractory dust, and organic material. Gravitational collapse caused these ingredients to fall together into a protosun and accretion disk (the solar nebula), out of which the planetary system grew. The raw materials have been preserved to differing degrees in the most primitive solar system bodies, asteroids and comets.

The present paper deals mostly with the state of preservation of one of the primordial ingredients, the refractory dust. The study of samples of asteroids, in the form of chondritic meteorites, reveals that the dust component in the inner solar system was extensively altered by high-temperature events and processes before it was aggregated into chondritic planetesimals. The chondritic material was further altered by metamorphic heating in its parent planetesimals after accretion.

REFRACTORY SOLIDS IN CHONDRITES

The nature of these high-temperature events and processes is not known, but the evidence of their operation is pervasive and unequivocal. Chondritic meteorites are aggregations of particulate matter. There are three principal categories of particles: Ca,Al-rich inclusions, chondrules, and matrix dust grains. All were transformed by high temperatures prior to their aggregation, presumably while dispersed in the solar nebula.

Ca,Al-Rich Inclusions

Ca,Al-rich inclusions (CAI's) are objects ranging is size from several cm (very rare) down to the limit of visibility. They make up as much as 10% of the volume of some chondrites, but are absent from others. Some show clear textural evidence of having been melted; others have textures that are harder to interpret. The clearest evidence for high-temperature processing of CAI's lies in their chemical compositions: they are systematically depleted in the more volatile elements. Mg, Si, and Fe (cosmically abundant elements of intermediate volatility) are depleted by a factor of ten or more relative to the most refractory major elements (Ca, Al, Ti), compared with the cosmic abundances. The resulting enhancement of Ca, Al, and Ti in these objects explains their name; they are also referred to as *refractory inclusions*. The minerals in them tend to be rich in Ca and Al, and relatively poor in Si. They include spinel, $MgAl_2O_4$; melilite, $Ca_2(Al_2,MgSi)SiO_7$; perovskite,

$CaTiO_3$; and hibonite, $CaAl_{12}O_{19}$. CAI's also contain elevated abundances of involatile trace elements (Ba, Sr, Sc, Y, rare earth elements, Zr, Hf, Th, V, Nb, Ta, Mo, W, U, Re, Ru, Os, Rh, Ir, Pt).

The significance of these element-abundance patterns is that CAI's must have become depleted in relatively volatile elements by high-temperature events that either incompletely vaporized precursor material; or totally vaporized it, after which the system cooled and recondensed selectively, such that the CAI's incorporated early-condensing high-temperature minerals, but not later, less-refractory compounds. Isotopic mass-fractionation effects measured in Mg, Si, Ca, and Ti in CAI's indicate that the latter experienced a complex history of both partial vaporization and condensation (Fig. 1; Clayton *et al.*, 1985).

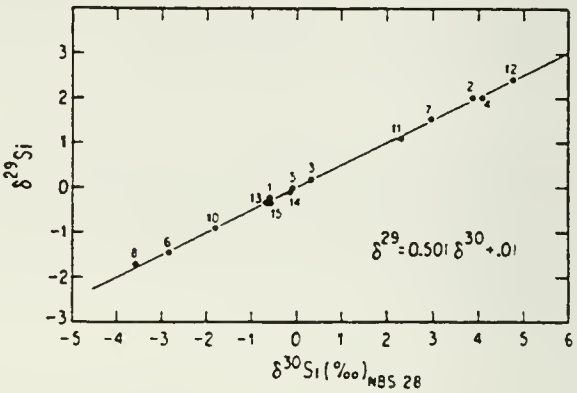


Figure 1. Isotopic compositions of Si in individual CAI's from the Allende chondrite. Mass fractionation of isotopes between the CAI's and their environment has dispersed compositions of the former along a line of slope 1:2. Points at the heavy end of the line are chiefly coarse-grained CAI's; evaporation residues tend to be isotopically heavy. Points at the light end of the line, where condensates should plot, are mostly fine-grained CAI's. Figure from Clayton *et al.* (1985), who point out that processes more complex than simple evaporation or condensation are required to explain the data.

On the other hand, some CAI's contain O, Mg, Si, Ca, Sr, Ba, Nd, and Sm with anomalous isotopic compositions not attributable to mass fractionation or radioactive decay, which are interpreted to be the surviving signatures of particular presolar nucleosynthetic sources (Fig. 2; see, *e.g.*, Lee, 1988). These show that their host CAI's must contain a *component* that was never vaporized and mixed with other solar system material. (If all the interstellar dust had been totally vaporized in the nebula, its nuclides would have mingled in the nebular gas and these anomalous isotopic signatures would have been lost.)

Chondrules

Members of the most abundant category of particles in chondrites are called chondrules. These are the order of a millimeter in diameter, tend to be spheroidal in shape, and make up as much as 75% of the volume of some chondrites. Most of them show clear textural evidence of having been melted. There is no chemical evidence for vaporization or condensation, however; the major element abundances in chondrules are close to the cosmic abundance pattern. Since the dominant metallic elements in the cosmic abundance table are Si, Mg, and Fe, the most abundant minerals in chondrules are olivine, $(Mg,Fe)_2SiO_4$, and low-Ca pyroxene, $(Mg,Fe)SiO_3$.

Many chondrules contain *relic grains* of an earlier generation of mineral matter, which was melted to form the dispersed chondrules (Nagahara, 1983; Kracher *et al*, 1984). These grains have

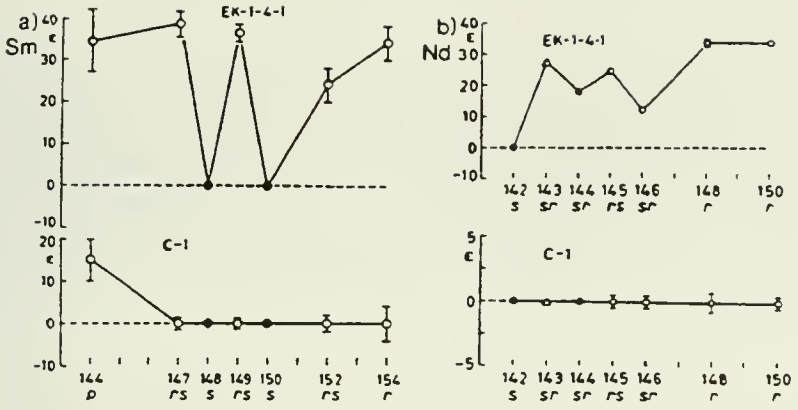


Figure 2. Isotopic anomalies in two CAI's (EK-1-4-1 and C-1) that cannot be explained by mass fractionation or any other solar system process. Mass numbers appear on the abscissa; deviations of isotopic abundances from a solar system standard (dashed line), in parts per 10^4 (epsilon units), on the ordinate. These anomalies must be presolar in origin: *r* and *s* along the ordinate denote the r- and s- nucleosynthetic processes in stellar interiors, which give rise to these nuclides. Figure from Lee (1988).

resorbed margins (*i.e.*, shapes reminiscent of partly-melted ice cubes), and compositions that differ from those of minerals surrounding them, which crystallized from the chondrule melt. The relic grains are often quite large (tens or even hundreds of microns), so they are unlikely to be surviving presolar interstellar grains; they appear to have been formed in earlier cycles of nebular activity, either by crystallization from a melt or by condensation.

Laboratory measurements in the last decade have established the time scale on which chondrules cooled (Hewins, 1988). The morphologies of crystals growing from melts, and also the degree to which chemical zonation in the forming crystals is preserved, is a function of the rate at which the melts cooled. Melt-droplets having the compositions of chondrules have been cooled at various rates under carefully controlled laboratory conditions, and it has been found that cooling rates of 100-2000 K/hr are needed to reproduce the properties of real chondrules.

The isotopic compositions of chondrules have not been studied as extensively as those of CAI's. Chondrules have been found to show the same kinds of isotopic mass fractionation effects as CAI's (Clayton *et al.*, 1985; Fig. 3), but the degree of fractionation-- the range of isotopic

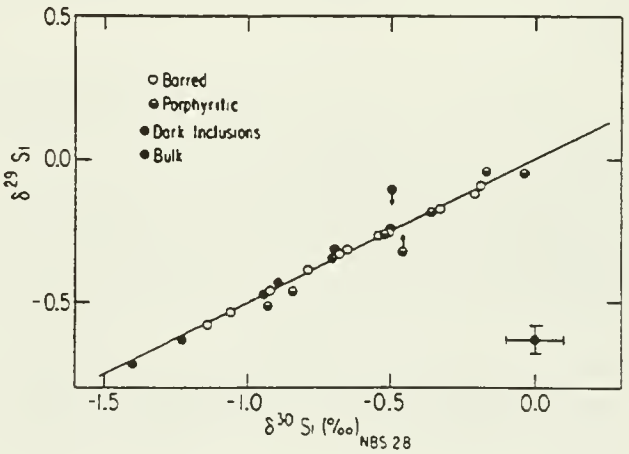


Figure 3. Isotopic composition of Si in chondrules from the Allende chondrite. Like the CAI's in Fig. 1, these display mass fractionation. Figure from Clayton *et al.* (1985).

compositions observed-- is only about 1/6 that displayed by CAI's. It is not known whether this fractionation occurred when the chondrules were melted, or if it already existed in the chondrule precursor material.

Few studies of chondrules have been made that were capable of revealing nucleosynthetic isotopic anomalies of the type observed in the Mg, Si, Ca, etc. of CAI's. The isotopic composition of O in chondrules has been found to vary in a way that is not attributable to mass fractionation (Fig. 4; Clayton *et al.*, 1985), and this has been widely ascribed to the incomplete mixing of two reservoirs (dust and nebular gas) in which presolar differences in O isotope composition were preserved, but it is also possible that a non-mass-dependent fractionation process operated in the nebula that could have produced the effect from an initially well-homogenized system (Thiemens and Heidenreich, 1983).

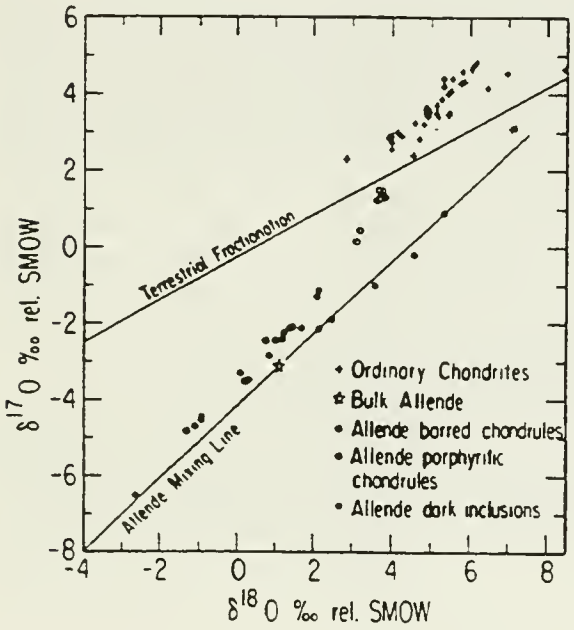


Figure 4. Isotopic composition of oxygen in chondrules from the Allende chondrite. The trend cannot be attributed to mass fractionation, or it would parallel the "Terrestrial fractionation" (slope 1:2) curve. It must reflect mixing in the chondrules of O from two (or more) reservoirs, one of which is richer in ^{16}O than the other. Figure from Clayton *et al.* (1985).

Matrix

The chondrules and CAI's in chondrites are embedded in a *matrix* of fine mineral grains, mostly in the 1-10 μm size range. In some chondrites the matrix consists of hydrated clay minerals, and it is clear that this material is secondary, having been formed in the parent meteorite planet by aqueous alteration of an earlier generation of matrix grains of unknown character (Zolensky and McSween, 1988; see McSween's paper in this volume). Where the microscopically visible grains are not obviously alteration products, they have been variously interpreted as nebular condensates and as comminuted debris from the collisions of larger objects (Scott *et al.*, 1988).

The only known *bona fide* presolar interstellar grains in chondrites occur in the matrix. These are submicron grains of carbonaceous matter: organic carbon, diamond, graphitic or amorphous carbon, and SiC (Anders *et al.*, 1988; see the contribution by Chang to this volume). These exist

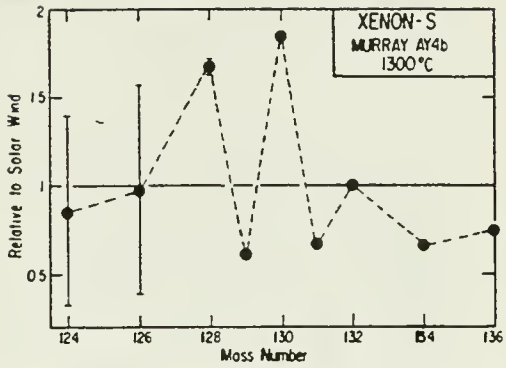


Figure 5. Isotopically anomalous Xe released upon heating a C-rich residue which was obtained by dissolving a sample of the Murray chondrite in acids. This pattern is characteristic of the Xe isotopic abundances produced by the s-process in stellar interiors. Figure from Tang *et al.* (1988).

between the larger grains described above, and make up <1% of the matrix. They exhibit distinctive anomalous isotopic signatures for C, included noble gases (*e.g.*, Fig. 5), and Si (where present), presumably impressed upon them in their different nucleosynthetic sites.

The matrix may also contain a minor component of other interstellar phases, such as silicates, but these have not been identified.

Postaccretional Metamorphism

Mineralogical and textural evidence show that after this particulate matter accumulated into chondritic planetesimals, internal temperatures in the planetesimals increased, and the chondritic material was metamorphically altered. Some of the chondrites we study today have been metamorphosed less severely than others, but none are completely unmetamorphosed. C1 and C2 carbonaceous chondrites were metamorphosed in a watery environment (Zolensky and McSween, 1988); other chondrite subtypes experienced anhydrous metamorphism (McSween *et al.*, 1988). The source of planetary heat is not known. Conjectural possibilities that are often discussed are the decay of short-lived ^{26}Al (half-life, 0.73 my), and electromagnetic induction driven by a dense solar wind emitted by the pre-main-sequence sun (Wood and Pellas, 1989).

REFRACTORY PARTICLES IN COMETS

Are the refractory particles in comets likely to be similar to these chondrite components? We have had two glimpses of the nature of cometary particles, in the form of stratospheric interplanetary dust particles and the interception of Halley's Comet dust particles by the VEGA and GIOTTO spacecraft in 1986. Interplanetary dust particles of the *chondritic porous* variety, which are distinctly different in character from the matrix or any other component of meteorites, are presumed to be of cometary origin (*e.g.*, Brownlee, 1985); certainly, some component of the interplanetary dust must be. These particles can be studied in exquisite detail using microbeam analytical techniques, but many types of study are precluded by the minuscule aggregate amount of material that has been or ever can be collected by this method. Further, stratospheric collection

techniques cannot provide samples of larger (order of 1g) refractory objects like those that were found in the Halley coma by GIOTTO. Chemical compositions and the size distribution of Halley particles were measured by the flyby spacecraft, but the latter were not equipped to study the many other properties of cometary refractory particles.

It is widely believed that chondritic and cometary refractory grains had very different histories in the solar nebula, so they must have ended up having dissimilar physical properties. Temperatures were high in the inner solar nebula, and there (as noted above) the interstellar grains that joined the disk were thermally processed into chondrules, CAI's, and matrix. The temperature in solar nebula models decreases with radial distance, however, and the outer nebula (where the giant planets formed, and presumably also the comets) was probably never hot enough to melt or vaporize silicates. There interstellar grains would have survived unchanged. Some became incorporated in accumulating comet nuclei, and today, after long residence in the Oort cloud, representatives of these particles are being released by subliming comets.

According to this picture, which is probably correct in broad outline, chondritic and cometary particles have nothing in common except their ancestry. Yet the picture rests on three oversimplified assumptions, which may not be as solidly founded as they are commonly thought to be: (1) nebular temperatures decreased outward in the nebula, (2) comets formed much farther out in the nebula (and lower on the thermal gradient) than chondrites, and (3) there was no opportunity for diffusive mixing of particles between these two widely-separated zones. These assumptions are examined in the following sections.

TEMPERATURES IN THE NEBULA

The simplistic concept that "temperature decreased outward in the nebula" dates back to Cameron's (1962) model of the nebula, which formed by the simultaneous adiabatic compression of all the mass of a rotating, gravitationally-collapsing volume of interstellar gas and dust when it fell together. Gas arriving near the center of gravity of the system fell faster, was compressed to higher pressures, and grew hotter than gas that joined the periphery of the disk. Cameron's 1962 model was abandoned when it was found that gas in a collapsing system of this type would not all fall together simultaneously; the nebula came to be seen to be an example of a protostellar accretion disk, in which gas falls onto the disk and is redistributed within it by viscous processes over a period of time (Wood and Morfill, 1988). Viscous dissipation of energy in the disk would have heated it, and the profile of temperature in it would have decreased outward, but in most nebula models the gas temperature achieved by this mechanism at 3 AU (representative of the position of the asteroid belt, the source of chondritic meteorites, in the present solar system) is only a few hundred K, far too low to melt or vaporize refractory dust.

It has also been realized that the time scale of cooling of the chondrules in meteorites (100-2000K/hr, noted above) is too rapid to be consistent with the behavior of a hot nebula. If immersion in a hot nebula had been what melted the chondrules, there is no way such a vast structure could have lost heat fast enough, nor could the chondrules have been moved from a hot zone to a cooler one fast enough, to produce this cooling rate. The thermal processing of chondrules and other refractory components must be attributed to transient, localized energy releases in the nebula, not to high ambient nebular temperatures. The nature of these transient energetic events is not known. Many proposals have been put forward, but all made to date have serious weaknesses.

[Hypotheses have included nebular lightning (Whipple, 1966), impacts (*e.g.*, Fredriksson, 1963), reconnection of magnetic field lines (Sonett, 1979), drag heating of solids falling into the nebula (Wood, 1984), and magnetic flares above the nebular surface (Levy, 1988)].

The idea that refractory particles were thermally processed in the inner solar system has to be looked at in the context of transient high-energy events rather than that of a hot nebular environment. It might seem that the effect of radial distance would be the same in both cases, since the frequency and/or intensity of all the mechanisms listed above increase with nearness to the sun and the center of gravity of the solar nebula. However, it is probably unwise to make this generalization, since the particular mechanism that melted chondrules has yet to be identified. Even if the generalization is correct, the fact that discrete events seem to have been responsible is crucial: a falling-off of effectiveness of the mechanism with radial distance might mean that the energetic events occurred less frequently, but not necessarily with less intensity. In this case, some fraction of the refractory grains far out in the nebula might have been processed in the same way the chondrite components were.

THE SOURCE OF COMET NUCLEI IN THE SOLAR SYSTEM

Oort's (1950) concept that the comet nuclei accreted in the solar system, after which gravitational encounters with the giant planets flung them out of the planetary system (some becoming gravitationally unbound, others left coasting slowly in huge Oort-cloud orbits), has gained wide acceptance. Few remember that in Oort's (1950) classic paper the comets accreted in the asteroid belt (relatively near the zone where the refractory particles in chondrites were thermally processed) and were ejected by Jupiter. It has been recognized since that Jupiter is not an efficient supplier for the Oort cloud: Jupiter's throw is too powerful, and the great majority of objects it ejected would have left at greater than the escape velocity. Only a small fraction would remain in the Oort cloud. Neptune and Uranus are gentler ejectors; most of the comets in the Oort cloud probably formed in the Neptune-Uranus zone of the nebula. From this fact the generalization has taken hold that comets formed at much greater radial distances than chondrites, where conditions were far colder.

However, while in the current picture *most* of the comets reentering the solar system from the Oort cloud formed in the Neptune-Uranus zone of the nebula, *all* of them did not. According to Safronov's (1972) analysis, approximately 8% of comets in the Oort cloud were ejected by Jupiter. Though Jupiter does waste comets by ejecting them too powerfully, this is partly offset by the fact that nuclei probably formed much more abundantly in the Jupiter zone than farther out. Once more, it is important to recognize that we are dealing with discrete entities (in this case comets rather than transient heating events), not generalized qualities or populations. A mission sent to sample the nucleus of a single comet and return material to Earth would have an 8% chance (if Safronov is right) of collecting refractory grains that experienced the nebular environment close to the asteroid belt rather than in the Neptune-Uranus zone.

But surely all the comet nuclei must have formed at much greater radial distances than asteroids, since the former incorporated ices and the latter did not? This is another generalization that cannot be made with confidence. It has become increasingly apparent that there is no sharp line of demarcation between comets and asteroids (Hartmann *et al.*, 1987). The asteroids parental to the carbonaceous chondrites may have incorporated ice when they accreted, which subsequently melted

and altered accompanying refractory dust to the assemblage of clay minerals observed today in C1 and C2 chondrites [*e.g.*, Grimm and McSween (1988); see the article by McSween in this volume]. Some asteroids may still contain subsurface ice at the present time (Lebofsky *et al.*, 1981). It is likely that planetesimals containing the whole spectrum of possible ice contents accreted in the solar nebula. Objects that formed inside the present orbit of Jupiter, close to the zone where the carbonaceous chondrite parent bodies accumulated, might have incorporated less ice and a different blend of ices than objects accreting in the Neptune zone, yet the Jupiter objects would display *bona fide* cometary activity if orbital changes brought them closer to the sun; they are comet nuclei.

If there is a sharp dichotomy that can be drawn among early solar system planetesimals, it is based on whether they grew warm enough internally to melt any water ice that was present. If not-- if because of their small size, large orbital mean distance, or some other factor, they were not heated to the extent that the parent meteorite planetesimals were-- then presolar interstellar grains can have survived in them. The porous interplanetary dust particles captured in the stratosphere have been spared hydrothermal alteration in their parent bodies. In planetesimals where the ice did melt, primordial presolar grains will have been destroyed, altered into clay minerals and other secondary products of the type found now in C1 and C2 carbonaceous chondrites. (Some of the stratospheric dust particles also have this character.)

The previous section discussed the likelihood that the amount of preaccretionary thermal processing experienced by refractory grains in the nebula diminished with radial distance. There is no assurance that the curve of degree of thermal processing (tapering outward) and the curve of condensation and accretion of ices (tapering inward) did not overlap. C2 chondrites, which were altered by planetary fluids that may have come from melting ices, also contain once-molten chondrules (though relatively few of them).

RADIAL DIFFUSION OF REFRACTORY GRAINS IN THE NEBULA

Would refractory particles necessarily accrete at the same radial distance in the nebula where they were thermally processed? Morfill (1985) has put forward a model of chondrite formation in which CAI's were thermally processed at a much smaller distance (where the nebular gas is hotter) than chondrules, after which radial diffusive transport of the two ingredients mixed them before they accreted. Such an effect, if it operated, also could have diffused chondrules outward to the zone where the giant planets formed. Stevenson (1989) has examined the tendency of refractory particles to diffuse in the nebula as a result of turbulent mixing; he finds the effect to be small, but not zero. In the steady state, particulate matter at radial distance R will contain a component of grains derived from R_p (<R) whose fractional abundance is ~R_p/R.

The steady state presupposes, however, that particles remain unaccreted for a long time, long enough for turbulent motions of the gas to diffuse them for distances of many AU. Little is known about the mechanics of accretion in the nebula or its time scale. The petrographic properties of chondrites suggest to me that accretion occurred relatively rapidly. Some chondrite subtypes differ in little more than their petrographic textures. CV3 and CO3 chondrites, for example, have almost identical major element compositions, but the chondrules in CV3 chondrites are conspicuously larger and more irregular in shape than those in CO3 chondrites (see Fig. 4 of Wood, 1985). The chondrule-forming process, whatever it was, must have operated differently on the same type of raw material at two different times and/or places in the solar nebula, producing the dissimilar popula-

tions of chondrules in these two chondrite subtypes. I have argued that a corollary conclusion can be drawn, that accretion of chondrules into chondrites must have occurred promptly, before the dispersed chondrules had a chance to diffuse into other zones of the nebula and become mixed with the products of other transient thermal events; or else these textural differences could not have been retained (Wood, 1985). Once the chondrite planetesimals achieved some size, motions of the thin nebular gas would be ineffective in diffusing them to greater radial distances. Even if this qualification Morfill's and Stevenson's conclusion is correct, however, it is unlikely that rapid accretion in the early nebula could sweep up 100% of the chondrules, CAI's, and matrix dust immediately after thermal processing created them. Some fraction of this material would remain available for dispersal to other zones of the nebula.

CONCLUSIONS

All of the refractory grains in comets may not be totally dissimilar to the refractory grains in chondritic meteorites. The great bulk of cometary grains is likely to consist of more or less well-preserved interstellar grains, probably analogous to the porous interplanetary dust particles collected in the terrestrial stratosphere. However, there may also be a component of solids that is related to particulate ingredients of chondrites, because (1) the thermal events that processed chondritic particles may also have occurred (though less frequently) in the zone of the giant planets; (2) some comets probably formed in the Jupiter zone, maybe even inside the present orbit of Jupiter, in or near the same region where chondrites formed; and (3) mechanical mixing in the turbulent nebula may have contaminated the particulate matter at large radial distances with a small component of refractory particles that were thermally processed at much smaller radial distances in the nebula.

Such a chondritic ingredient would not be without scientific interest, even though we already have access to copious amounts of these particles in the chondritic meteorites. If the chondrule- and CAI-forming events operated less energetically at the greater radial distances where comets formed, they might yield only-partly-transformed products, the study of which could shed light on the nature of the nebular high-energy events that so profoundly affected refractory material in the inner solar system. Our efforts to infer the nature of these events from the study of chondrites have been singularly unproductive to date.

References

Anders, E., Lewis, R. S., and Tang, M. (1988) Interstellar grains in meteorites: diamond and silicon carbide. In *Interstellar Dust*, Proc. of IAU Symposium 135, Santa Clara CA, in press.

Brownlee, D. E. (1985) Cosmic dust: collection and research. *Ann. Rev. Earth Planet. Sci.* **13**, 147-173.

Cameron, A. G. W. (1962) The formation of the sun and planets. *Icarus* **1**, 13-69.

Clayton, R. N., Mayeda, T. K., and Molini-Velsko (1985) Isotopic variations in solar system material: evaporation and condensation of silicates. In *Protostars and Planets II* (Eds. D. C. Black and M. S. Matthews). Univ. Arizona Press, Tucson, pp. 755-771.

Fredriksson, K. (1963) Chondrules and the meteorite parent bodies. *Trans. N. Y. Acad. Sci.* **25**, 756-769.

Grimm, R. E. and McSween, H. Y., Jr. (1988) Water and the thermal history of the CM carbonaceous chondrite parent body. *Lunar Planet. Sci. XIX*, 427-428.

Hartmann, W. K., Tholen, D. J., and Cruikshank, D. P. (1987) The relationship of active comets, "extinct" comets, and dark asteroids. *Icarus* **69**, 33-50.

Hewins, R. H. (1988) Experimental studies of chondrules. In *Meteorites and the Early Solar System* (Eds. J. F. Kerridge and M. S. Matthews). Univ. Arizona Press, Tucson, pp. 660-679.

Kracher, A., Scott, E. R. D., and Keil, K. (1984) Relict and other anomalous grains in chondrules: implications for chondrule formation. *Proc. Lunar Planet. Sci. Conf. 14th*, B559-B566.

Lebofsky, L., Feierberg, M., Tokunaga, A., Larson, H., and Johnson, J. (1981). The 1.7- to 4.2-μm spectrum of Asteroid 1 Ceres: evidence for structural water in clay minerals. *Icarus* **48**, 453-459.

Lee, T. (1988) Implications of isotopic anomalies for nucleosynthesis. In *Meteorites and the Early Solar System* (Eds. J. F. Kerridge and M. S. Matthews). Univ. Arizona Press, Tucson, pp. 1063-1089.

Levy, E. H. (1988) Energetics of chondrule formation. *Meteorites and the Early Solar System* (Eds. J. F. Kerridge and M. S. Matthews). Univ. Arizona Press, Tucson, pp. 697-711.

McSween, H. Y. Jr., Sears, D. W. G., and Dodd, R. T. (1988) Thermal metamorphism. In *Meteorites and the Early Solar System* (Eds. J. F. Kerridge and M. S. Matthews). Univ. Arizona Press, Tucson, pp. 102-113.

Morfill, G. E. (1985) Physics and chemistry in the primitive solar nebula. In *Birth and Infancy of Stars* (Eds. R. A. Lucas, A. Omont, and R. Stora). North-Holland, Amsterdam, pp. 693-792.

Nagahara, H. (1983) Chondrules formed through incomplete melting of the pre-existing mineral clusters and the origin of chondrules. In *Chondrules and their Origins* (Ed. E. A. King). Lunar Planet. Inst., Houston, pp. 211-222.

Safronov, V. S. (1972) Ejection of bodies from the solar system in the course of the accumulation of the giant planets and the formation of the cometary cloud. In *The Motion, Evolution of Orbits, and Origin of Comets*, IAU Symp. No. 45 (Eds. G. A. Chebotarev and E. I. Kazimirchak-Polonskaya). D. Reidel, Dordrecht, pp. 329-334.

Scott, E. R. D., Barber, D. J., Alexander, C. M., Hutchison, R., and Peck, J. A. (1988) Primitive material surviving in chondrites: matrix. In *Meteorites and the Early Solar System* (Eds. J. F. Kerridge and M. S. Matthews). Univ. Arizona Press, Tucson, pp. 718-745.

Sonett, C. P. (1979) On the origin of chondrules. *Geophys. Res. Lett.* **6**, 677-680.

Stevenson, D. J. (1989) Chemical heterogeneity and imperfect mixing in the solar nebula. *Astrophys. J.*, in press.

Tang, M., Lewis, R. S., Anders, E., Grady, M. M., Wright, I. P., and Pillinger, C. T. (1988) Isotopic anomalies of Ne, Xe, and C in meteorites. I. Separation of carriers by density and chemical resistance. *Geochim. Cosmochim. Acta* **52**, 1221-1234.

Thiemens, M. H. and Heidenreich, J. E. (1983) The mass independent fractionation of oxygen: a novel isotope effect and its possible cosmochemical implications. *Science* **219**, 1073-1075.

Whipple, F. L. (1966) Chondrules: suggestion concerning the origin. *Science* **153**, 54-56.

Wood, J. A. (1984) On the formation of meteoritic chondrules by aerodynamic drag heating in the solar nebula. *Earth Planet. Sci. Lett.* **70**, 11-26.

Wood, J. A. (1985) Meteoritic constraints on processes in the solar nebula. In *Protostars and Planets II* (Eds. D. C. Black and M. S. Matthews). Univ. Arizona Press, Tucson, 687-702.

Wood, J. A. and Morfill, G. E. (1988) A review of solar nebula models. In *Meteorites and the Early Solar System* (Eds. J. F. Kerridge and M. S. Matthews). Univ. Arizona Press, Tucson, pp. 329-347.

Wood, J. A. and Pellas, P. (1989) What heated the parent meteorite planetesimals? In *The Sun in Time* (Eds. C. P. Sonett, M. S. Giampapa, and M. S. Matthews). Univ. Arizona Press, Tucson, in press.

Zolensky, M. and McSween, H. Y., Jr. (1988) Aqueous alteration. In *Meteorites and the Early Solar System* (Eds. J. F. Kerridge and M. S. Matthews). Univ. Arizona Press, Tucson, pp. 114-143.

DISEQUILIBRIUM CHEMISTRY IN THE SOLAR NEBULA AND EARLY SOLAR SYSTEM: IMPLICATIONS FOR THE CHEMISTRY OF COMETS

Bruce Fegley, Jr.

Abteilung Kosmochemie
Max-Planck-Institut für Chemie
F.R. Germany

DISEQUILIBRIUM CHEMISTRY IN THE SOLAR NEBULA AND EARLY SOLAR SYSTEM: IMPLICATIONS FOR THE CHEMISTRY OF COMETS

Bruce Fegley, Jr., Abteilung Kosmochemie, Max-Planck-Institut für Chemie, Saarstrasse 23, D6500 Mainz, F.R. Germany

INTRODUCTION

A growing body of observations demonstrates that comets, like the chondritic meteorites, are disequilibrium assemblages, whose chemistry and molecular composition cannot be explained solely on the basis of models of equilibrium condensation in the solar nebula. These observations include:

1. The coexistence of reduced (e.g., CH_4 and organics) and oxidized (e.g., CO, CO_2, and H_2CO) carbon compounds observed in the gas and dust emitted by comet P/Halley (Allen *et al.* 1987;Combes *et al.* 1988; Eberhardt *et al.* 1987a; Kawara *et al.* 1988; Kissel and Krueger 1987; Krankowsky *et al.* 1986; Woods *et al.* 1986).

2. The coexistence of reduced (e.g., NH_3) and oxidized (e.g., N_2) nitrogen compounds in the gas emitted by comet P/Halley (Allen *et al.* 1987; Tegler and Wyckoff 1989; Wyckoff and Theobald 1989).

3. The observation of large amounts of formaldehyde in the gas emitted by comet P/Halley ($H_2CO/H_2O \sim 1.5 - 4$ %) and by comet Machholz (1988j) (Combes *et al.* 1988; de Pater *et al.* 1990; Mumma and Reuter 1989). Formaldehyde would be rapidly destroyed by thermal processing in the solar nebula and must be formed by some disequilibrating process either in the solar nebula or in some presolar environment.

4. The observation of large amounts of the oxidized carbon gases CO and CO_2 in comet P/Halley at levels far exceeding those predicted by chemical equilibrium models of solar nebula carbon chemistry. In fact, oxidized carbon gases ($CO + CO_2 + H_2CO$) are the most abundant volatile (after water vapor) emitted by comet P/Halley.

5. The observation of HCN, which is not a predicted low temperature condensate in the solar nebula (e.g., Lewis 1972), in comet P/Halley (e.g., Schloerb *et al.* 1987) and in comet Kohoutek (Huebner *et al.* 1974).

6. The observation of S_2, which is argued to be a parent molecule vaporized from the nucleus, in comet IRAS-Araki-Alcock (1983d) by A'Hearn *et al.* (1983) and Feldman *et al.* (1984). This molecule is not an equilibrium condensate in the solar nebula and must result from disequilibrium chemistry.

7. The deduction that organic grains (C-H-O-N particles) comprise about 30% of the dust emitted by comet P/Halley and that about 75% of the total carbon inventory of Halley is in these grains (Delsemme 1988; Jessberger *et al.* 1989) also implies substantial disequilibrium chemistry.

8. The deductions that polyoxymethylene (polymerized formaldehyde or POM) is a constituent of the C-H-O-N particles emitted from comet P/Halley (e.g., Huebner 1987; Huebner *et al.* 1987; Mitchell *et al.* 1987). If actually present in the C-H-O-N particles, POM is also a product of disequilibrating processes which took place in the solar nebula and/or in a presolar environment.

Taken together, the observations listed above indicate that a variety of disequilibrating processes such as the kinetic inhibition of thermochemical reactions, grain catalyzed chemistry, lightning induced shock chemistry, and photochemistry played an important role in establishing the chemistry and molecular composition of comet P/Halley in particular and presumably cometary material in general. However, the observational data do not by themselves constrain the timing and/or location of these various processes.

This paper reviews the relevant observational data and attempts to quantify as far as possible by using

current theoretical models and experimental data the relative importance of equilibrium and disequilibrium processes for the chemistry of comets. "Key" experimental and observational measurements which are important for better constraints on cometary origins are proposed. Finally, important measurements to be made by a comet nucleus sample return mission such as *Rosetta* are also suggested.

ABUNDANCES OF C-H-O-N-S COMPOUNDS IN COMET P/HALLEY

Although observations of other comets are rapidly increasing our knowledge of their chemistry and molecular composition, the data for comet P/Halley are the most extensive and will form the basis for most of the discussion in this paper.

Water Vapor

As Weaver (1989) has noted, prior to the return of Halley observers had constructed a strong circumstantial case for the dominance of water vapor in the volatiles emitted by comets (e.g., see Delsemme 1982). However, water vapor was first observed directly in comet P/Halley using the Fourier Transform Infrared Spectrometer (FTIR) on the Kuiper Airborne Observatory (Mumma *et al.* 1986) and was later observed in comet Wilson (1986l) with the same apparatus (Larson *et al.* 1989). Subsequent measurements by the Neutral Mass Spectrometer (NMS) on Giotto showed that H_2O comprised $\geq$ 80% of the volatiles emitted by Halley (Krankowsky *et al.* 1986) and that the water vapor has a D/H ratio in the range of $0.6 - 4.8 \times 10^{-4}$ (Eberhardt *et al.* 1987b). For reference, the terrestrial D/H ratio is about 1.6×10^{-4} and the primordial cosmic value is estimated to be 0.3×10^{-4} (Anders and Grevesse, 1989). Finally, more recent measurements by Mumma et al. (1987, 1988) have provided data on the ortho-to-para ratio of water vapor emitted by Halley and by Wilson(1986l). For Halley, the derived ortho/para ratio is 2.3 ± 0.2 while for Wilson(1986l) the derived ortho/para ratio is 3.2 ± 0.2. The Halley ortho/para ratio implies a nuclear spin temperature of 25 K while the Wilson(1986l) ortho/para ratio implies statistical equilibrium (T $\geq$ 50 K).

Carbon Compounds

As pointed out in the introduction, the second most abundant group of volatiles (after water vapor) emitted from Halley are the oxidized carbon gases CO, CO_2, and H_2CO. Five different measurements provide information on the abundance and distribution of CO emitted from Halley. The Giotto NMS data for mass 28, which is probably dominated by CO (see the discussion for N_2 below), has been interpreted as indicating a comet nucleus source for CO having $CO/H_2O \leq 0.07$ and an extended source in the inner coma for CO having $CO/H_2O \leq 0.15$ (Eberhardt *et al.* 1987a). Infrared measurements from the IKS experiment on the Vega space probes yield $CO/H_2O \sim 0.05$ for a comet nucleus source (Combes *et al.* 1988). Pioneer Venus Orbiter Ultraviolet Spectrometer (PVOUS) measurements of resonance UV emission from atomic hydrogen, oxygen, and carbon in the coma of Halley yield nominal H:O:C atomic ratios of 1 : 0.7 : 0.07, which are consistent with $CO/H_2O \sim 0.25$ or with $CO_2/H_2O \sim 0.14$ (Stewart 1987). Rocket-borne ultraviolet spectrometer measurements of resonance UV emission from atomic oxygen and carbon in the coma of Halley also yield similar CO/H_2O ratios of 0.20 ± 0.05 for the one flight and 0.17 ± 0.04 for a second flight (Woods *et al.* 1986). Finally, measurements from the International Ultraviolet Explorer (IUE) satellite also yield a rough estimate for the CO/H_2O ratio of $0.1 - 0.2$ for Halley (Festou *et al.* 1986). This set of observations is generally interpreted as indicating a nucleus source for CO having $CO/H_2O \sim 0.02 - 0.07$ (by number) and a dispersed source which accounts for the balance of the observed CO (e.g., see Eberhardt *et al.* 1987a; Weaver 1989).

Carbon monoxide has also been detected in comet West (1976 VI) with $CO/H_2O \sim 0.3$ and in comet Bradfield (1979 X) with $CO/H_2O \sim 0.02$ (see Weaver 1989, and references therein). As Weaver notes, the "high" CO abundance in Halley, the "high" CO abundance in comet West (1976 VI), and the "low" CO abundance in comet Bradfield (1979 X) are consistent and are plausibly explained by differences in the types of observations made and in the cometary dust production rates. Thus observations made with large fields of view of comets with large dust production rates (e.g., the UV observations of Halley and West) yield larger apparent CO abundances because CO production from the nucleus and also from evaporating organic grains is being observed, while the observations made with smaller fields of view (e.g., the IKS experiment) or observations made of comets with low dust production rates yield smaller apparent CO abundances because

only CO production from the nucleus is being observed.

Carbon dioxide was observed with both the NMS experiment on Giotto and the IKS experiment on Vega. The NMS data yield $CO_2/H_2O \sim 0.04$ (Krankowsky *et al.* 1986) while the IKS data yield a ratio of about 0.03 (Combes *et al.* 1988). Both ratios are appropriate for CO_2 emitted from the nucleus and together with the adopted values of $\sim 0.02-0.07$ for CO/H_2O from the nucleus yield $CO/CO_2 \sim 0.50-2.3$. In other words, roughly equal amounts of CO and CO_2 are being emitted from the nucleus of Halley. As discussed below, this rough equality has important implications for the origin of carbon-bearing gases and grains in Halley.

Interestingly, the amount of formaldehyde H_2CO emitted by Halley is of the same magnitude. The H_2CO/H_2O ratio obtained from the IKS measurements is ~ 0.04 (Combes *et al.* 1988; Mumma and Reuter 1989) while a slightly lower value of ~ 0.02 was derived from radio wavelength observations by Snyder (*et al.* 1988). Both the radio wavelength observations and the Giotto NMS data apparently indicate a distributed source for at least some of the H_2CO (Weaver *et al.* 1990). However, the IKS measurements supposedly refer to a nucleus source of H_2CO and not to formaldehyde released from the decomposition of POM in dust grains (Combes *et al.* 1988). Formaldehyde has also been observed at radio wavelengths in comet Machholz (1988j) with a production rate an order of magnitude larger than that in Halley (de Pater *et al.* 1990).

The CH_4/H_2O ratio in the volatiles emitted by Halley is also in the range of a few percent. Modeling of the Ion Mass Spectrometer data of Balsiger *et al.* (1986) by Allen *et al.* (1987) yields a $CH_4/\ H_2O$ ratio of ~ 0.02. Infrared observations from the Kuiper Airborne Observatory by Drapatz *et al.* (1987) gave an upper limit for $CH_4/\ H_2O \leq 0.04$ while IR observations at Cerro Tololo by Kawara *et al.* (1988) gave $CH_4/H_2O \sim 0.002-0.01$ for assumed rotational temperatures of 50 to 200 K. The value adopted here for the CH_4/H_2O ratio is $\sim 0.01-0.05$ from the review by Weaver (1989). Together with the adopted CO/H_2O ratio of $\sim 0.02-0.07$ and the adopted $CO_2/\ H_2O$ ratio of $\sim 0.03-0.04$, this leads to $CO/CH_4 \sim 0.4-7.0$ and $CO_2/CH_4 \sim 0.6-4.0$.

Finally, semiquantitative estimates indicate that $\sim$ 30% (by mass) of the dust emitted by Halley is organic material (e.g., see Jessberger *et al.* 1989) and that $\sim$ 2% (by mass) of the dust is polymerized formaldehyde $(H_2CO)_n$ (Mitchell *et al.* 1987). Kissel and Krueger (1987) have inferred that highly unsaturated organic compounds are abundant in the organic grains, but analysis of the dust particle mass spectra is still continuing and further information on the composition of the organic fraction may become available in the future.

Nitrogen Compounds

In contrast to the carbon compounds discussed above, neither N_2 nor NH_3 has been observed in Halley. In both cases the inferred abundances of the parent molecules are deduced from observations of daughter molecules presumably produced by photolysis of the parents.

Allen *et al.* (1987) originally derived a NH_3/H_2O ratio of $\sim 0.01-0.02$ from their analysis of the Giotto IMS data. However, a subsequent reanalysis of the same data by Marconi and Mendis (1988), who unlike Allen *et al.* (1987) assumed a highly elevated solar UV flux at the time of the Halley spacecraft encounters, led to the conclusion that $NH_3/H_2O < 0.01$ and indeed may even be zero. However, the total absence of NH_3 in Halley is extremely unlikely given the Earth-based observations of NH_2 (Tegler and Wyckoff 1989; Wyckoff *et al.* 1988, 1989a) which is most plausibly produced by the photodissociation of NH_3. In fact Tegler and Wyckoff (1989) have derived $NH_3/H_2O = 0.005 \pm 0.002$ in comet P/Halley. In the absence of any compelling evidence for favoring either the analysis of the Giotto IMS data by Allen *et al.* (1987) or the Earth-based observations of Tegler and Wyckoff (1989), the value adopted here for the NH_3/H_2O ratio is $\sim 0.005-0.02$. A similar range of values has also been adopted by Weaver (1989). Wyckoff *et al.* (1989a) have also observed NH_2 emission from comet P/Borrelly, comet Hartley-Good, and comet Thiele and derived NH_3/H_2O ratios of ~ 0.002 for Borrelly, ~ 0.0002 for Hartley-Good, and ~ 0.001 for Thiele. However, as Weaver *et al.* (1990) note, the only *direct* observation of NH_3 in a comet is a marginal detection of a radio line in comet IRAS-Araki-Alcock (1983 VII) by Altenhoff *et al.* (1983).

Until recently only upper limits were available for the N_2/H_2O ratio in Halley. However, Wyckoff and

Theobald (1989) observed N_2^+ in Halley and calculated a N_2/CO ratio $\sim 2 \times 10^{-3}$. Using the adopted value of $\sim 0.02 - 0.07$ for the CO/H_2O ratio leads to $N_2/H_2O \sim 4 \times 10^{-5}$ to 1×10^{-4}. A higher N_2/H_2O ratio of $\sim 4 \times 10^{-4}$ was derived by Wyckoff and Theobald (1989), but their calculation assumed $CO/H_2O \sim 0.2$. In any case, the low N_2/CO ratio derived by Wyckoff and Theobald (1989) indicates that most of the mass 28 peak observed in the Giotto NMS is due to CO rather than to N_2. The adopted values for the N_2/H_2O and NH_3/H_2O ratios correspond to $N_2/NH_3 \sim 0.002 - 0.025$ while the value for N_2/NH_3 calculated by Wyckoff and colleagues on the basis of their own observational data is ~ 0.1.

Finally, HCN has also been detected at radio wavelengths in comet Kohoutek (Huebner *et al.* 1974) and in Halley (Schloerb *et al.* 1987; Despois *et al.* 1986). The derived HCN/H_2O ratio is ~ 0.001 in Halley. Wyckoff *et al.* (1989b) used high resolution spectra of CN emitted from Halley to derive a $^{12}C/^{13}C$ ratio of 65 ± 9, which is significantly lower than the terrestrial value of 89.

Sulfur Compounds

Although CS and S have been observed frequently in comets (e.g., see Weaver *et al.* 1981), including Halley (Feldman *et al.* 1986a; Opal *et al.* 1986), the only "parent" sulfur-bearing molecule observed in comets to-date is S_2 (A'Hearn *et al.* 1983; Feldman *et al.* 1984). Weaver (1989) and Weaver *et al.* (1990) reviewed obserrvations of sulfur-bearing molecules in comets and noted that if all the observed CS in comets comes from CS_2, then $CS_2/H_2O \sim 0.001$ is implied. Similarly, the S_2 abundance in comet IRAS-Araki-Alcock (1983d) corresponds to $S_2/H_2O \sim 0.001$. For reference, the solar abundance of sulfur (Anders and Grevesse, 1989) corresponds to $S/O \sim 0.02$, which implies that neither CS_2 nor S_2 is the dominant reservoir of sulfur in comets. Finally, Weaver *et al.* (1990) note that there is marginal evidence for OCS in the IKS spectra of Halley and give a conservative upper limit for OCS in comets corresponding to $OCS/H_2O \sim 0.01$, or about 50% of the sulfur solar abundance.

INTERPRETATION OF THE OBSERVED ABUNDANCES

In principle, the observed molecular abundances and isotopic ratios in Halley can be used to constrain the origin of this comet in particular and by inference comets in general. However, in practice, the observational data lend themselves to a variety of interpretations which preclude any unambiguous conclusions from being reached regarding the origin of Halley. For example, Fegley and Prinn (1989) recently interpreted the abundances of CO, CH_4, N_2, and NH_3 in Halley in terms of a two component mixing model involving both "oxidized" material from the solar nebula and or the interstellar medium plus smaller amounts of "reduced" material from outer planet subnebulae. The rationale for this model is as follows. Kinetic inhibition of the $CO \rightarrow CH_4$ and the $N_2 \rightarrow NH_3$ conversions in the solar nebula leads to a CO, N_2 bearing solar nebula. However in the higher pressure environments of the giant planet subnebulae (e.g., around Jupiter, Saturn, Neptune, etc.) these conversions are both kinetically and thermodynamically favorable so CH_4 and NH_3 are the dominant carbon and nitrogen bearing gases. The early analyses of spacecraft observations of volatiles emanating from Halley indicated intermediate CO/CH_4 and N_2/NH_3 ratios which are *not* representative of either the solar nebula or of giant planet subnebulae (or in fact of pristine interstellar material). However the intermediate ratios can be obtained by the physical mixing of condensate grains formed in the two environments. This mixing could occur during the accretion of cometary nuclei and is analogous to the extensive mixing that has occurred among the different chondrite types (e.g., see Wilkening 1977).

On the other hand, Lunine (1989) and Engel *et al.* (1989) interpreted the same data solely in terms of a solar nebula origin, except for NH_3. In this model, the intermediate CO/CH_4 ratio is ascribed to the conversion of CO to CH_4 on the surfaces of Fe metal grains in the solar nebula. However, not enough NH_3 can be made to explain the intermediate N_2/NH_3 ratio by the same process and a giant molecular cloud source is postulated for NH_3. It should also be noted that the efficiency of the grain catalyzed $CO \rightarrow CH_4$ conversion is controversial (Fegley 1988; Fegley and Prinn 1989) and in fact may not be possible to any significant extent in the solar nebula. Finally, Stevenson (1990) has recently interpreted cometary chemistry solely in terms of an interstellar origin "except possibly for a small contamination which is due to catalyzed hydrogenation of CO to CH_4 and other hydrocarbons".

Rather than simply recapitulating these diverse proposals, the remainder of this paper will instead

attempt to quantify as far as possible, by using the observational data base reviewed above, in concert with current theoretical models and experimental data, several "key" issues relevant to the origin of comet Halley and of comets in general. In particular, the relative importance of equilibrium and disequilibrium processes in presolar and solar nebula environments for cometary chemistry will be addressed. "Key" experimental and observational measurements which are important for better constraints on cometary origins, including important measurements to be made by a comet nucleus sample return mission such as *Rosetta*, are also suggested.

Mechanisms for Trapping Cometary Volatiles

One important issue in cometary chemistry is the mechanism for retaining volatiles such as CO, CO_2, CH_4, N_2, NH_3, etc. in cometary nuclei. These volatiles could have been retained as ices such as CO (solid), CO_2(solid), etc. which would have formed if the nebular temperature was low enough, or they could have been retained by absorption/adsorption on the surfaces of water ice grains, or they could have been trapped in the water ice crystal structure (clathration). It is important to understand the mechanism for trapping volatiles in cometary nuclei because it provides constraints on the formation conditions of comets and also has important implications for spacecraft analyses of cometary nuclei.

For example, condensation of CO and N_2 ices, requires temperatures of $\sim 20 - 25$ K at the typical pressures (P $\sim 10^{-7}$ bars) expected in the outer solar nebula (e.g., see Yamamoto 1985). Although some investigators have argued against such low temperatures in the comet formation region, it is important to note that the observed ortho-to-para ratio in water in Halley was frozen in (or quenched) at a similar temperature of about 25 K. On the other hand, trapping of CO and N_2 by absorption/adsorption on water ice or by clathration in water ice does not require as low a temperature (e.g., see Lunine 1989). Thus identifying the form of trapped volatiles in cometary nuclei will provide information about the temperatures in the outer solar nebula during cometary formation.

Similarly, if volatiles were retained as pure ices, the different condensation temperatures of these phases may span a considerable range. Again, referring to Yamamoto's (1985) condensation calculations, water ice will condense at 152 K, HCN ice at 95 K, NH_3 ice at 78 K, CO_2 ice at 72 K, H_2CO ice at 64 K, CH_4 ice at 31 K, CO ice at 25 K, and N_2 ice at 22 K for a typical outer solar nebula gas density of $\sim 10^{13}$ molecules cm^{-3}. One consequence of volatile trapping as pure ices may be considerable heterogeneity (both radial and spatial) in the cometary nucleus. This could result simply from clumps of more or less volatile ice grains accreting together so that one portion of the comet nucleus is then composed of more volatile material than another portion or from accretion proceeding more rapidly than nebular cooling so that an onion-skin structure with concentric layers of successively more volatile ices results. The observation of outbursts and increased emissions of CO_2^+ from Halley (Feldman *et al.* 1986b) is circumstantial evidence for heterogeneity in the nucleus of this comet. On the other hand, volatile retention by sorption on or clathration in water ice grains implies a more homogeneous cometary nucleus (both radially and spatially). Circumstantial evidence reviewed by Delsemme (1982) indicates that many (but not all) cometary nuclei are homogeneous.

Unfortunately the data from the spacecraft encounters with Halley do not provide firm constraints on the volatile retention mechanisms. Again, the circumstantial evidence can be interpreted in several ways. For example, the total abundance of $CO + CO_2 + CH_4$ apparently emitted from the nucleus of Halley is $\sim 0.06 - 0.16$ relative to water. This is consistent with volatile retention as a clathrate which would yield a trapped gas/water ratio of ~ 0.17 for the ideal formula of $G \bullet 6H_2O$. (Formaldehyde was excluded from this comparison because Davidson (1973) does not list it as forming a clathrate with water ice. However if it were included, the abundance ratio relative to water would increase to $\sim 0.08 - 0.20$, which is still partially consistent with volatile retention as a clathrate.) But as mentioned above, the CO/CH_4 and N_2/NH_3 ratios observed for Halley are *not* representative of the solar nebula and argue against a simple clathrate condensation model. Also, the observed outbursts (Feldman *et al.* 1986b) argue for a heterogeneous nucleus, which is not expected from a clathrate condensation model, but which *is* expected from a two component mixing model involving both ice and clathrate components.

Since the observational evidence for volatile trapping mechanisms is circumstantial and ambiguous, it is instructive to examine volatile trapping from the perspective of the constraints imposed by physical

chemistry. What can this tell us about the possibility of volatile retention by clathrate formation?

Constraints on Clathrate Formation

Delsemme and Swings (1952) originally proposed that volatiles were retained as clathrates such as $CH_4 \bullet 6H_2O$ in order to resolve the problem of the large differences in the vapor pressures of H_2O, CH_4, etc. and the more or less simultaneous appearance of bands of OH, CH, etc. in cometary spectra. During the past 4 decades, several other investigators have reiterated the proposal that clathrates are present in cometary nuclei (e.g., Miller 1961; Delsemme and Miller 1970; Delsemme and Wenger 1970; Delsemme 1976; Sill and Wilkening 1978; and most recently Lunine 1989). However as noted by Lunine and Stevenson (1985) "there are no compelling observational data strongly for or against a primordial clathrate component to cometary volatiles and (2) no physical cometary phenomena require (or rule out) the presence of clathrates in comets."

The presence of clathrates in comets depends both on the thermodynamic stability of the relevant clathrate molecules *and* on the kinetic favorability of the clathrate formation process. The net thermochemical reaction responsible for clathrate formation can be schematically represented by:

$$G(\text{gas}) + 6H_2O(\text{ice}) = G \bullet 6H_2O(\text{solid}) \tag{1}$$

where G is a gas such as CO, CO_2, CH_4, N_2, H_2S, but not NH_3 which can form several different hydrates (e.g., $NH_3 \bullet H_2O$) with water. Assuming that both the starting water ice and the final clathrate are pure crystalline solids, their thermodynamic activities will be unity and the equilibrium constant expression for reaction (1) is given by:

$$K_1 = \frac{1}{f_G} \sim \frac{1}{P_G} \tag{2}$$

where the fugacity (f_G) can be taken as the partial pressure (P_G) for sufficiently low pressures such that the gas behaves ideally. Measured (or estimated) dissociation pressures for different clathrates can then be used to calculate their condensation curves as a function of the total assumed nebular pressure and of the partial pressures of the enclathrated gas molecules. An example of such a calculation is given in Figure 1 of Fegley (1988).

Although similar calculations have been presented repeatedly in the literature (e.g., see Lewis 1972; Sill and Wilkening 1978; Lunine and Stevenson 1985), have been used to argue for the presence of clathrates in comets, and to constrain details such as the CO/CH_4 ratio of the solar nebula gas assumed to be in equilibrium with an assumed cometary clathrate (e.g., Lunine 1989), there has been very little (if any) discussion of the reliability of the thermodynamic data used to make the calculations. However, the conclusions drawn from these calculations, especially detailed inferences about the CO/CH_4 ratio of solar nebula gas, are dependent on the accuracy and precision of the available thermodynamic data. Just how reliable are the clathrate thermodynamic data in the literature?

The main clathrates of interest for discussions of cometary chemistry are the clathrates of carbon gases such as CO, CO_2, CH_4, and N_2 clathrate. (As previously mentioned, NH_3 forms hydrates with water instead of clathrate compounds.) For discussions of sulfur chemistry, clathrates formed by H_2S and OCS would also be of interest. However, the present discussion will focus on clathrates of carbon gases and N_2.

A review of the literature shows that the available data for these clathrates are very limited and are of uncertain reliability. Most of the published data for CH_4 clathrate are for the reaction

$$CH_4(\text{gas}) + 6H_2O(\text{liquid}) = CH_4 \bullet 6H_2O(\text{solid}) \tag{3}$$

and were obtained $40 - 50$ years ago when clathrate formation in natural gas pipelines was being studied (e.g., Deaton and Frost 1946). Although these data can in fact be used to calculate the thermodynamic properties of CH_4 clathrate, this has not yet been done. Instead, literature calculations have relied on the dissociation pressure measurements of Miller (1961) and Delsemme and Wenger (1970) which are stated to be for reaction (1)-formation of CH_4 clathrate from CH_4 gas and water ice. However, neither the existence

of a clathrate having the composition $CH_4 \bullet 6H_2O$ nor the establishment of equilibrium was demonstrated in either set of measurements. Thus it is uncertain if the measured dissociation pressures are for a clathrate or for adsorption/absorption of gas on ice/clathrate mixtures and it is also uncertain if the data obtained are relevant to a clathrate having the composition $CH_4 \bullet 6H_2O$ or some other composition. Furthermore, no attempt was made to show that the low temperature data are thermodynamically consistent with the high temperature data obtained by other groups (i.e., for clathrate formation from liquid water). In the case of CO clathrate, no data were available until the dissociation pressure for the three phase equilibrium (clathrate-liquid water-gas) at $0°C$ was reported by Davidson *et al.* (1987). No data are available on the temperature dependence of the dissociation pressure for temperatures of interest for CO clathrate formation in the solar nebula ($\sim 40 - 80K$). Although dissociation pressures as a function of temperature have been reported for CO_2 clathrate (e.g., Miller 1961; Miller and Smythe 1970), the composition of the clathrate prepared was not determined and the attainment of equilibrium was not demonstrated in these studies. Finally, two different vapor pressure equations (Miller 1961, 1969) have been reported for N_2 clathrate and *neither* is based on dissociation pressure measurements at temperatures relevant for N_2 clathrate formation in the solar nebula ($\sim 40 - 80K$).

A critical assessment of the available data base, including attempts to determine the consistency of the low temperature and high temperature dissociation pressure data for several clathrates is underway and will quantify the uncertainties in the clathrate condensation calculations. However, laboratory measurements of the thermodynamic properties of the cosmochemically important CO, CH_4, CO_2, and N_2 clathrates at temperatures relevant to their formation in the solar nebula and in giant planet subnebulae are required not only to assess the applicability of solar nebula condensation calculations but also to interpret data from the CRAF mission and from a planned comet nucleus sample return mission. The thermodynamic properties of interest include the dissociation pressure, enthalpy of formation, and the heat capacity of the clathrates. Furthermore, these measurements should (1) adequately characterize the clathrate produced, (2) demonstrate the attainment of equilibrium, and (3) consider mixed clathrates as well as one component clathrates in order to determine the thermodynamic solid solution properties. In addition to thermodynamic measurements, rheological and transport properties such as the viscosity and thermal conductivity should also be measured in order to help interpret data from CRAF and a comet nucleus sample return mission.

However, as noted above, the presence of clathrates in comets also depends on the kinetic favorability of clathrate formation. Several groups have expressed concerns about the kinetic feasibility of clathrate formation in the low temperature, low pressure environment of the outer solar nebula where comets are generally believed to have been formed. For example, Lunine and Stevenson (1985) noted that their "work adds a theoretical argument against primordial clathrate being a primary component of cometary nuclei, if indeed the formation region of these bodies was in the outer (trans-Neptunian) solar nebula: kinetic inhibition of clathrate formation would be expected under conditions in the outer solar nebula." (However, it is interesting to note that despite this cautionary statement, Lunine (1989) and Engel *et al.* (1989) argue for clathrate formation in the solar nebula and the presence of solar nebula clathrates in comet P/Halley.)

The most recent study (Fegley, 1988) of the kinetics of clathrate formation clearly demonstrates the inherent difficulties. As Figure 1 in Fegley (1988) illustrates, CO clathrate $CO \bullet 6H_2O$ does not become stable until the temperature in the solar nebula drops to $\sim 60K$. At this temperature, Fegley (1988) found that the time for 6% of all CO (which is the maximum amount of CO that can be clathrated before exhausting the supply of H_2O ice) to collide with $r = 1\mu m$ spherical ice grains is $\sim 4 \times 10^4$ seconds for the solar nebula (P,T) profile used in his calculations. If every collision of a CO molecule with an ice grain led to the formation of CO clathrate, this collision time would also be the time required for CO clathrate formation in the solar nebula. However, only a small fraction of collisions that possess the necessary activation energy E_a lead to chemical reaction. Following the treatment for gas-grain reactions given by Fegley (1988), this fraction is given by

$$f_i = \nu_i \exp(-E_a/RT) \tag{4}$$

where ν_i is the total number of collisions of CO molecules with all ice grains in each cm^3 of the nebula and is given by the equation

$$\nu_i = 2.635 \times 10^{25}[P_i/(M_iT)^{1/2}]A \quad (5)$$

where P_i is the CO partial pressure in this case, M_i is the CO molecular weight, T is the temperature (Kelvins), and A is the total surface area of all ice grains per each cm^3 of the solar nebula.

Now in order for the CO clathrate formation time to be $\leq 10^{13}$ seconds, which is the estimated lifetime of the solar nebula (e.g., see Cameron 1985), the corresponding activation energy for clathrate formation E_a must be ≤ 8 kJ mole $^{-1}$. Higher activation energies will lead to longer clathrate formation times and thus to the kinetic inhibition of clathrate formation in the solar nebula. Fegley (1988) pointed out that 8 kJ mole $^{-1}$ is a low activation energy even by comparison with a facile process such as HF diffusion through ice, which has an activation energy of $\sim$ 19 kJ mole^{-1} (Haltenorth and Klinger 1969). For reference, if CO clathrate formation has a similar activation energy, the corresponding formation time for clathration of $r = 1\mu m$ spherical, monodisperse ice grains would be $\sim 10^{21}$ seconds, or about 10^4 times longer than the age of the solar system. In fact, Miller and Smythe (1970) have derived $E_a \sim 24.7$ kJ mole $^{-1}$ for formation of CO_2 clathrate; if a similar activation energy is required for CO clathrate formation it will certainly be kinetically inhibited in the solar nebula. Similar conclusions hold for the formation of N_2 clathrate, which becomes thermodynamically feasible at similar temperatures. Thus, unless the formation of CO and N_2 clathrates is dissimilar to the formation of CO_2 clathrate and is a process with essentially *no* E_a barrier, it will probably be kinetically inhibited at the low solar nebula temperatures and pressures where clathrate formation is thermodynamically feasible.

However, as pointed out by Fegley and Prinn (1989), clathrate formation is predicted to be kinetically favorable in the higher pressure environments of giant planet subnebulae. In this case, CH_4 is the dominant carbon gas and CH_4 clathrate formation becomes thermodynamically feasible at higher temperatures. For the specific giant planet subnebula (P,T) profile considered by Fegley and Prinn (1989), $CH_4 \bullet 6H_2O$ becomes stable at T $\sim$ 95 K and P $\sim 10^{-2}$ bars. This pressure is approximately 5 orders of magnitude higher than the corresponding solar nebula pressure at the $CO \bullet 6H_2O$ formation temperature of $\sim$ 60 K and thus leads to higher CH_4 gas collision rates with water ice grains. For example, the time for 22% of all CH_4 (which is the maximum amount that can be clathrated before using up all the available water ice) to collide with $r = 1\mu m$ spherical, monodisperse ice grains is only $\sim 10^{-1}$ seconds. In this case, the activation energy for formation of $CH_4 \bullet 6H_2O$ can be as large as 25 kJ mole $^{-1}$ to have the process take $\leq 10^{13}$ seconds. This activation energy is virtually identical to that derived by Miller and Smythe (1970) for CO_2 clathrate formation. Therefore, the results of these first order calculations predict (in accord with intuition) that CO and N_2 clathrate formation will be kinetically inhibited in the solar nebula but that CH_4 clathrate formation will be kinetically feasible in giant planet subnebulae. However, as previously stressed by Fegley (1988, 1990) and Fegley and Prinn (1989), experimental studies of the kinetics of clathrate formation are required for a comprehensive understanding of the kinetic constraints on clathrate formation in the solar nebula and in giant planet subnebulae. These experiments should focus on CH_4, CO, and N_2 clathrates and should be suitably designed so that the dependence of the rate on gas partial pressures, ice particle sizes, and temperature can be quantitatively measured.

Origins of Cometary C-H-O-N-S Compounds

A closely related issue to the trapping of cometary volatiles is the origin of the different $C-H-O-N-S$ compounds – both volatiles such as CO, CO_2, H_2CO, CH_4, N_2, NH_3, HCN, and S_2 as well as less volatile compounds such as polyoxymethylene POM and the $CHON$ particles. However, once again the available observational data can be interpreted in several different ways depending on one's preconceptions and basic assumptions. For example, a carbon budget for Halley which takes into account the volatile carbon-bearing gases and the carbon contained in the $CHON$ particles indicates that carbon is probably present at its solar abundance with the majority of the carbon being in the $CHON$ particles (Delsemme, 1988). This carbon mass balance could be interpreted as indicating that both the volatile carbon molecules and the less volatile $CHON$ particles originated from the same reservoir which was fractionated into volatile carbon gases and involatile organic compounds. Alternatively, the carbon mass balance could be regarded as merely a coincidence and the volatile species and the $CHON$ particles could be regarded as having separate and decoupled origins (e.g., Lunine 1989).

Prior work in this area (e.g., Fegley and Prinn 1989; Lunine 1989) has focused more on volatile carbon and nitrogen gases such as CO, CH_4, N_2, and NH_3 than on other $C-H-O-N-S$ compounds. A major result of this work is the conclusion that volatile species in comet Halley have undergone at least some chemical reprocessing in environments such as the solar nebula and the subnebulae of the giant planets and are not pristine interstellar molecules. The focus in the remainder of this section will be on the important $C-H-O-N-S$ compounds not considered in detail by these investigators and how models for their origin and abundance help to constrain the formation conditions for Halley. An underlying assumption in this work is that an interstellar origin for different species should not be proposed simply on the basis of insufficient knowledge about the diversity and complexity of chemical processes which could have operated in nebular environments (solar nebula and giant planet subnebulae) and in the early solar system.

Abundances of Carbon Compounds

The observational data reviewed earlier indicate that $CO/CO_2 \sim 0.5-2.3$, $CO/CH_4 \sim 0.4-7.0$, and $CO_2/CH_4 \sim 0.6-4.0$, or in other words roughly equal abundances of these three carbon gases within the uncertainties of the observational data. Furthermore, these gases combined account for $\sim 25-30\%$ of the total carbon in Halley with the remaining $\sim 70-75\%$ being found in the $CHON$ particles (Delsemme 1988). In this regard it is interesting to note that calculations by Lewis *et al.* (1979) predict that at chemical equilibrium in a solar composition gas $P_{CO} \sim P_{CO_2} \sim P_{CH_4} \sim \frac{1}{3}A_{gr}$, ($A_{gr}$ is the graphite abundance) at T $\sim$ 400 K and P $\sim 10^{-9}$ bars. While it is easy to show that gas phase thermochemistry cannot possibly proceed at these low temperatures and pressures, the possibility remains that grain catalyzed reactions may allow reactions to proceed at sufficiently rapid rates to approach chemical equilibrium. If one regards the graphite predicted by the calculations of Lewis *et al.* (1979) as a proxy for organic matter, then grain catalyzed thermochemistry is a possible explanation for the observed abundances of carbon gases and involatile carbon compounds in Halley. Indeed, on the basis of calculations by Fegley (1988), Lunine (1989) and Engel *et al.* (1989) have suggested that the abundances of CO, CO_2, and CH_4 in Halley are the result of grain catalyzed thermochemical reactions, although they regard the involatile organic material as having a separate and decoupled origin from the carbon gases and have not discussed its origin in the light of the work by Lewis *et al.* (1979).

Several different experimental and observational results are in favor of a grain catalyzed origin for *both* the carbon gases and the involatile organic material in Halley. Extensive industrial experience with the production of synthetic fuels from $CO + H_2$ via Fischer-Tropsch reactions (e.g., see Dry 1981; Biloen and Sachtler 1981) indicates that Fe-based materials are good catalysts for these reactions. Since Fe is the third most abundant rock-forming element (after Mg and Si) in solar composition material (Anders and Grevesse 1989) Fe-bearing grains are expected to be the most abundant and active catalyst present in the solar nebula. Also, depending on the exact experimental conditions, CO_2 and CH_4 may also be produced in addition to more complex organic compounds as a result of Fe-catalyzed Fischer-Tropsch reactions (Vannice 1982; Krebs *et al.* 1979; Dry *et al.* 1972). Furthermore, laboratory studies of Fischer-Tropsch-type reactions by Anders and coworkers (e.g., see Studier *et al.* 1968; Hayatsu and Anders 1981) have produced organic compounds similar to those observed in meteorites. Finally, involatile organic matter has been observed in association with Fe-bearing phases such as $Fe-Ni$ alloy, carbides, and oxides in chondritic interplanetary dust particles (Bradley *et al.* 1984,1989), at least some of which are believed to be samples of cometary dust (Bradley *et al.* 1989, and references therein).

On the other hand, there are also significant arguments against efficient Fe-grain catalysis of carbon gas interconversions and organic compound synthesis at low temperatures in the solar nebula. As Fegley (1988) has pointed out, the temperature range over which Fe-grain catalysis is possible is limited at high temperatures by evaporation to Fe(gas) and at low temperatures either by the formation of FeS coatings at $\sim$ 680 K or by "rusting" to form magnetite Fe_3O_4 at $\sim 370-400$ K. In fact, petrographic studies of the unequilibrated ordinary chondrites, which are generally believed to preserve a record of nebular processes, reveal FeS-rimmed metal grains, which may be nebular condensates (e.g., Rambaldi *et al.* 1980; Rambaldi and Wasson 1981,1984). Also, as Fegley (1988) and Fegley and Prinn (1989) have noted, the available kinetic data for the Fe-catalyzed $CO \rightarrow CH_4$ conversion are for ultra-clean, high-purity Fe grains which very probably do not apply to Fe grains in the solar nebula which will be contaminated by several elements

such as phosphorus, sulfur, carbon, hydrogen, nitrogen, and oxygen at T > 1000 K in the solar nebula (Kozasa and Hasegawa 1988; Fegley and Lewis 1980). Furthermore, the studies of Fischer-Tropsch reactions which have indicated similarities between the laboratory products and the organic compounds found in meteorites have generally been done under conditions such as high CO/H_2 ratios which may not be relevant to the solar nebula where the CO/H_2 ratio is $\sim 7 \times 10^{-4}$ if all carbon is present as CO.

In other words, the situation is ambiguous and again experimental work is needed to resolve the uncertainties. Of particular interest are quantitative experiments in which well characterized Fe catalysts and near solar CO/H_2 ratios are used to study the product yields, distribution, and formation rate as a function of parameters such as temperature, total pressure, CO/H_2 ratio, catalyst type and treatment, etc. As Fegley (1990) has noted, these studies have potential applications in many areas of planetary science such as the origin of the dark material, presumably organic matter on some outer planet satellites and asteroids.

Hydrogen Cyanide

As mentioned earlier, HCN has been detected in comet Kohoutek (Huebner *et al.* 1974) and in Halley (Schloerb *et al.* 1987; Despois *et al.* 1986) where the derived HCN/H_2O ratio is ~ 0.001. This ratio is many orders of magnitude larger than the predicted HCN/H_2O ratio at chemical equilibrium in the outer solar nebula ($HCN/H_2O \sim 10^{-55}$ at T $\sim$ 100 K) and is direct evidence for a potent disequilibrating mechanism in the outer solar nebula. Hydrogen cyanide is an important precursor for the abiotic synthesis of complex organic molecules (Oró and Kimball 1961; Abelson 1966) and it is of interest to determine how this much HCN could have been produced.

One possibility is the quenching of thermochemical reactions involving HCN in the inner solar nebula and the outward radial mixing of this HCN-bearing gas to the comet formation region. Calculations by Fegley presented in Prinn and Fegley (1989) predict quenching of the homogeneous gas-phase $HCN \rightarrow N_2$ conversion in the inner solar nebula at T $\sim$ 1460 K where $HCN/N_2 \sim 10^{-6}$. This corresponds to a HCN/H_2O ratio of $\sim 10^{-6.8}$, or about a factor of 6300 too low to explain the Halley observations. Grain catalysis of the $HCN \rightarrow N_2$ conversion may lead to a lower quench temperature, however; because the HCN abundance is decreasing rapidly with temperature an even lower HCN/H_2O ratio would then result. Another possibility is the quenching of the $HCN \rightarrow NH_3$ conversion in the giant planet subnebulae followed by HCN condensation onto grains and the mixing of these grains into the comet formation region after the nebular gas has dissipated. Again, calculations by Fegley presented in Prinn and Fegley (1989) predict quenching of the $HCN \rightarrow NH_3$ conversion at T $\sim$ 1220 K where $HCN/NH_3 \sim 10^{-5}$ for a model Jovian subnebula (P,T) profile. However, the corresponding HCN/H_2O ratio of $\sim 10^{-6.4}$ is also about a factor of 2500 too low. Again, grain catalysis of the $HCN \rightarrow NH_3$ conversion will result in a lower quench temperature and a lower HCN abundance. Therefore, the results of thermochemical kinetic calculations show that the HCN abundance in Halley cannot be produced by quenching either the $HCN \rightarrow N_2$ conversion in the inner solar nebula or the $HCN \rightarrow NH_3$ conversion in a giant planet subnebula.

Another possibility for explaining the HCN abundance is to look at the effect of lightning induced shock chemistry in the solar nebula. Nebular lightning has been suggested as a mechanism for chondrule formation (e.g., Cameron 1966; Whipple 1966) but may also have distinctive chemical consequences. As Fegley has noted in Prinn and Fegley (1989), the high temperatures (several times 10^3 K) reached in lightning discharges lead to increasing degrees of molecular dissociation, atomization, and ionization with increasing temperatures. The recombination of these simple fragments during the rapid cooling of the shocked gas leads initially to the production of more complex fragments, then to thermally stable molecules such as HCN. Sufficiently rapid cooling quenches these stable molecules at their high temperature abundances, which are generally enhanced over their equilibrium abundances at much lower temperatures. Thus, lightning is a potentially significant source of disequilibrium products, especially in the cool, thermochemically inactive regions of the nebula near and beyond the water ice condensation point (T $\sim$ 150 – 200 K).

Calculations by Fegley in Prinn and Fegley (1989) model lightning induced shock chemistry in the solar nebula and in giant planet subnebulae as adiabatic shock heating and predict that the maximum HCN concentrations in these two different environments occur near temperatures of 3000 – 4000 K where $\sim (0.2 - 6) \times 10^{18} HCN$ molecules are formed per mole of shocked gas. This corresponds to maximum

conversions of $\sim$ 0.3% (for the solar nebula) and $\sim$ 6.5% (for the Jovian subnebula) of the total nitrogen abundance into HCN. This compares favorably with Halley where the adopted NH_3/H_2O ratio of $\sim 0.005 - 0.02$ and the HCN/H_2O ratio of ~ 0.001 correspond to a HCN/NH_3 ratio of $\sim 0.05 - 0.2$. Thus, the HCN observed in Halley can be explained on the basis of lightning induced shock chemistry in *either* the solar nebula or in a giant planet subnebula, but only a small dilution of the shocked gas by unshocked gas (by < a factor of 20 for a solar nebula source and by < a factor of 70 for a subnebula source) is implied.

A potential problem with a lightning induced shock chemistry source for the HCN in Halley is the $^{12}C/^{13}C$ isotopic ratio of 65 ± 9 derived for CN observed in Halley (Wyckoff *et al.* 1989b). A similarly low ratio is implied for HCN which is the probable, although possibly not the only, parent for the observed CN. At the high temperatures where the HCN abundance will be quenched in the rapidly cooling shocked gas, isotopic exchange with the major carbon-bearing gases via reactions exemplified by

$$^{13}CH_4 + H^{12}CN = {}^{12}CH_4 + H^{13}CN \tag{6}$$

in giant planet subnebulae and via reactions exemplified by

$$^{13}CO + H^{12}CN = {}^{12}CO + H^{13}CN \tag{7}$$

in the solar nebula will lead to isotopic equilibration because the thermochemical isotopic fractionation factors are unity at high temperatures (e.g., see the tabulation by Richet *et al.* 1977). However, the $^{12}C/^{13}C$ ratio implied for the HCN in Halley is significantly lower than the terrestrial value of 89. But, is it also different from outer solar system values?

Unfortunately, this question can only be partially answered. A $^{12}C/^{13}C$ ratio of 89^{+25}_{-18} was derived for CH_4 on Saturn from Earth-based observations by Combes *et al.* (1977) but three different carbon isotopic ratios have been reported for Jupiter. Voyager 1 infrared observations of CH_4 gave a $^{12}C/^{13}C$ ratio of 160^{+40}_{-55} (Courtin *et al.* (1983), Earth-based observations of CH_4 gave 110 ± 35 (Fox *et al.* 1972), 70^{+35}_{-15} (DeBergh *et al.* 1976), and 89^{+12}_{-10} (Combes *et al.* 1977), and finally Earth-based observations of C_2H_2 gave 20^{+20}_{-10} (Drossart *et al.* 1985). No carbon isotopic ratios are presently available for either Uranus or Neptune.

The only data available for "icy" bodies in the outer solar system are values for four other comets because no carbon isotopic ratios are available for Titan or other outer planet satellites. As summarized by Wyckoff *et al.* (1989b), the cometary values are 70 ± 15 for Ikeya 1963 I (Stawikowski and Greenstein 1964), 100 ± 20 for Tago-Sato-Kosaka 1969 IX from Owen (1973), 115^{+30}_{-20} and 135^{+65}_{-45} for Kohoutek 1973 XII from Danks *et al.* (1974), and 100^{+20}_{-30} for Kobayashi-Berger-Milon 1975 IX from Vanýsek (1977). All of these other cometary carbon isotopic ratios are derived from observations of C_2.

Taken at face value, the reported $^{12}C/^{13}C$ ratios for outer solar system bodies range from $\sim$ 20 to $\sim$ 160 and the value for Halley is not inconsistent with this wide range. Although Wyckoff *et al.* (1989b) conclude that the low carbon isotopic ratio of $\sim$ 65 for CN from Halley appears to exclude the Uranus-Neptune region as a condensation site for this comet, the limited data which are available–none of which are in fact for Uranus or Neptune themselves–do not strongly support this conclusion. Indeed, the observation of Jovian C_2H_2 having a $^{12}C/^{13}C$ ratio of $\sim$ 20 (Drossart *et al.* 1985) illustrates the danger of using an apparently anomalous isotopic ratio as the *only* basis for assigning an interstellar origin to a molecule.

Deuterium

The D/H ratio of $0.6 - 4.8 \times 10^{-4}$ determined for water vapor in Halley (Eberhardt *et al.* 1987b) is also of interest for several reasons. First, this range is comparable to several other solar system D/H ratios including the terrestrial value of $\sim 1.6 \times 10^{-4}$, the value of $1.5^{+1.4}_{-0.5} \times 10^{-4}$ for Titan (Coustenis *et al.* 1989), the value of $9.0^{+9.0}_{-4.5} \times 10^{-5}$ for Uranus (DeBergh *et al.* 1986), and the value of $\sim 1.5 \times 10^{-4}$ for Neptune (Lutz *et al.* 1990). Second, the Halley value is at least twice as large as the estimated primordial value of $(0.3 \pm 0.1) \times 10^{-4}$ (Anders and Grevesse 1989). Last, the D/H value, like the ortho-to-para ratio in the water, is a potential cosmothermometer. However, in this case the thermometer applies to the temperature where isotopic exchange last occured rather than the temperature where nuclear spins last equilibrated.

This isotopic exchange temperature can be calculated by assuming exchange with H_2 having the primordial D/H ratio via the net reaction

$$H_2 + HDO = HD + H_2O \tag{8}$$

and using the thermochemical isotopic fractionation factors tabulated by Richet *et al.* (1977). The lower end of the range of D/H values derived for Halley ($D/H \sim 0.6 \times 10^{-4}$) corresponds to a temperature of $\sim$ 465 K, while the upper end of the range of values ($D/H \sim 4.8 \times 10^{-4}$) corresponds to a temperature of $\sim$ 148 K. Although the classical picture of isotopic exchange envisions increasing deuterium enrichment in hydrides such as H_2O, CH_4, etc. with decreasing temperature, the rates of both gas-phase and grain catalyzed D/H exchange reactions are so slow that they take longer than the estimated lifetime of the solar nebula and are therfore kinetically inhibited(e.g., see Grinspoon and Lewis 1987). Instead it is better to regard these isotopic exchange temperatures as the *maximum* temperatures at which the water in Halley last exchanged deuterium with nebular H_2. If this view is taken, then the exchange process is viewed as a back-reaction in which D-rich water is losing deuterium to the surrounding nebular H_2. This process may occur as a consequence of reactions driven by thermochemistry (e.g., in the subnebulae surrounding the giant planets) or as a consequence of reactions driven by the interstellar radiation field impinging on the outer layers of the primitive solar nebula. The latter possibility is essentially the reverse of the scheme proposed by Yung *et al.* (1988). However, if the Halley D/H and ortho-to para data are taken at face value, the isotopic exchange process either cannot affect nuclear spin exchange *or* must occur prior to nuclear spin equilibration at a significantly lower temperature. Again, this is an area where both further theoretical work and experimental studies are required to resolve the existing uncertainties.

Nebular Photochemistry and H_2CO and S_2

Finally, the presence of H_2CO in Halley and other comets and the presence of S_2 in comet IRAS-Araki-Alcock (1983d) may also provide evidence for nebular photochemistry driven by the interstellar radiation field. Several authors (e.g., Wood and Chang 1985; Prinn and Fegley 1989; Yung *et al.* 1988) have speculated on the importance of solar nebula photochemical processes, but aside from the deuterium enrichment model of Yung *et al.* (1988), no quantitative photochemical calculations are available. However Grim and Greenberg (1986) have shown that S_2 can be produced from the ultraviolet irradiation of sulfur containing ices and it is interesting to ask if this process–which they suggest took place in the interstellar medium–could also have occurred in the outer regions of the solar nebula where the only important gaseous opacity sources are H_2 and CO (because all other gases are frozen out, absorb at shorter wavelengths, or have smaller abundances). Although H_2CO may be produced by the grain catalyzed Fischer-Tropsch-type reactions discussed earlier, it is also a photochemical product of $CO + H_2O$ ice irradiation (e.g., Tielens, 1983). Both theoretical models of nebular photochemistry and experimental studies of ultraviolet irradiation of appropriate "icy" grains would appear to be fruitful areas for further research.

SUMMARY

The data obtained from the recent Earth-based, Earth-orbital, and spacecraft studies of comet P/Halley have expanded greatly our knowledge of the chemistry of comets. However, many of the observational data which have been obtained lend themselves to a variety of interpretations which preclude any unambiguous conclusions from being reached regarding the origin of Halley in particular and of comets in general. Prior work (e.g., Fegley and Prinn 1989; Lunine 1989) which has focused on more volatile carbon and nitrogen gases such as CO, CH_4, N_2, and NH_3 has led to the conclusion that volatile species in Halley have undergone at least some chemcial reprocessing in environments such as the solar nebula and the subnebulae of the giant planets and are not pristine interstellar molecules. However, a comprehensive overview of both these volatiles as well as the other species observed in Halley indicates that the picture may not be as simple as initially believed and the experimental and theoretical investigations suggested in this paper will probably contribute to a more complete understanding of the chemical processes involved in cometary formation.

ACKNOWLEDGMENTS

My cosmochemistry research is presently supported by the Max-Planck-Institut für Chemie. I want to thank the students and staff of the MPI for their help and support.

REFERENCES

Abelson, P.H., Chemical events on the primitive Earth. *Proc. Natl. Acad. Sci. (USA)* **55**, 1365–1372 (1966).

A'Hearn, M.F., Feldman, P.D., and Schleicher, D.G., The discovery of S_2 in comet IRAS-Araki-Alcock 1983d. *Astrophys. J. Lett.* **274**, L99–L103 (1983).

Anders, E. and Grevesse, N., Abundances of the elements: Meteoritic and solar. *Geochim. Cosmochim. Acta* **53**, 197–214. (1989).

Allen, M., Delitsky, M., Huntress, W., Yung, Y., Ip, W.-H., Schwenn, R., Rosenbauer, H., Shelley, E., Balsiger, H., and Geiss, J., Evidence for methane and ammonia in the coma of comet P/Halley. *Astron. Astrophys.* **187**, 502–512 (1987).

Altenhoff, W.J. *et al.*, Radio observations of comet 1983d. *Astron. Astrophys.* **187**, 502–512 (1987).

Balsiger, H. *et al.*, Ion composition and dynamics at comet Halley. *Nature* **321**, 330–334 (1986).

Biloen, P. and Sachtler, W.M.H., Mechanism of hydrocarbon synthesis over Fischer-Tropsch catalysts. in *Advances in Catalysis*, ed. D.D. Eley, H. Pines, and P.B. Weisz, Academic Press, NY, pp. 165–216 (1981).

Bradley, J.P., Brownlee, D.E., and Fraundorf, P., Carbon compounds in interplanetary dust: evidence for formation by heterogeneous catalysis. *Science* **233**, 56–58 (1984).

Bradley, J.P., Sandford, S.A., and Walker, R.M., Interplanetary dust particles. in *Meteorites and the Early Solar System*, ed. J.F. Kerridge and M.S. Matthews, University of Arizona Press, Tucson, AZ, pp. 861–895 (1989).

Cameron, A.G.W., The accumulation of chondritic material. *Earth Planet. Sci. Lett.* **1**, 93–96 (1966).

Cameron, A.G.W., Formation and evolution of the primitive solar nebula. in *Protostars and Planets II*, ed. D.C. Black and M.S. Matthews, University of Arizona Press, Tucson, AZ, pp. 1073-1099 (1985).

Combes, M., Maillard, J.P., and DeBergh, C., Evidence for a telluric value of the $^{12}C/^{13}C$ ratio in the atmosphere of Jupiter and Saturn. *Astron. Astrophys.* **61**, 531–537 (1977).

Combes, M. *et al.*, The $2.5 - 12$ μm spectrum of comet Halley from the IKS–Vega experiment. *Icarus* **76**, 404–436 (1988).

Courtin, R., Gautier, D., Marten, A., and Kunde, V., The $^{12}C/^{13}C$ ratio in Jupiter from the Voyager infrared investigation. *Icarus* **53**, 121–132 (1983).

Coustenis, A., Bézard, B., and Gautier, D., Titan's atmosphere from Voyager infrared observations. II. The CH_3D abundance and the D/H ratio from the $900 - 1200$ cm^{-1} spectral region. *Icarus* **82**, 67–80 (1989).

Danks, A.C., Lambert, D.L., and Arpigny, C., The $^{12}C/^{13}C$ ratio in comet Kohoutek (1973f). *Astrophys. J.* **194**, 745–751 (1974).

Davidson, D.W., Clathrate hydrates. in *Water: A Comprehensive Treatise*, ed. F. Franks, Plenum Press, NY, vol.2, pp. 115–234 (1973).

Davidson, D.W. *et al.*, A clathrate hydrate of carbon monoxide. *Nature* **328**, 418–419 (1987).

Deaton, W.M. and Frost, E.M., Jr., *Gas Hydrates and Their Relation to the Operation of Natural-Gas Pipe Lines*, U.S. Bureau Mines Monograph 8 (1946).

DeBergh, C., Maillard, J.P., Lecacheux, J., and Combes, M., A study of the $3\nu_3 - CH_4$ region in a high resolution spectrum of Jupiter recorded by Fourier transform spectroscopy. *Icarus* **29**, 307–310 (1976).

DeBergh, C., Lutz, B.L., Owen, T., Brault, J., and Chauville, J., Monodeuterated methane in the outer solar system. II. Its detection on Uranus at 1.6μm. *Astrophys. J.* **311**, 501–510 (1986).

Delsemme, A.H., Chemical nature of the cometary snows. *Mém. Soc. Roy. Sci. Liège* **IX**, 135–145 (1976).

Delsemme, A.H., Chemical composition of cometary nuclei. in *Comets*, ed. L. L. Wilkening, University of Arizona Press, Tucson, AZ, pp. 85–130 (1982).

Delsemme, A.H., The chemistry of comets. *Phil. Trans. R. Soc. Lond.* **325 A**, 509–523 (1988).

Delsemme, A.H. and Miller, D.C., Physico-chemical phenomena in comets–II. Gas adsorption in the snows of the nucleus. *Planet. Space Sci.* **18**, 717–730 (1970).

Delsemme, A.H. and Wenger, A., Physico-chemical phenomena in comets–I. Experimental study of snows in a cometary environment. *Planet. Space Sci.* **18**, 709–715 (1970).

Delsemme, A.H. and Swings, P., Hydrates de gaz dans les Noyaux Comètaires et les Grains Interstellaires. *Annales d'Astrophys.* **15**, 1–6 (1952).

dePater, I., Palmer, P., and Snyder, L.E., A review of radio interfermetric imaging of comets. preprint (1990).

Despois, D. *et al.*, Observations of hydrogen cyanide in comet Halley. *Astron. Astrophys.* **160**, L11–L12 (1986).

Drapatz, S., Larson, H.P., and Davis, D.S., Search for methane in comet P/Halley. *Astron. Astrophys.* **187**, 497–501 (1987).

Drossart, P., Lacy, J., Serabyn, E., Tokunaga, A., Bézard, B., and Encrenaz, T., Detection of $^{13}C^{12}CH_2$ on Jupiter at 13μm. *Astron. Astrophys.* **149**, L10–L12 (1985).

Dry. M.E., The Fischer-Tropsch synthesis. in *Catalysis Science and Technology*, ed. J.R. Anderson and M. Boudart, Springer-Verlag, Berlin, pp. 159–255 (1981).

Dry. M.E., Shingles, T., and Boshoff, L.J., Rate of the Fischer-Tropsch reaction over iron catalysts. *J. Catalysis* **25**, 99–104 (1972).

Eberhardt, P. *et al.*, The CO and N_2 abundance in comet P/Halley. *Astron. Astrophys.* **187**, 481–484 (1987a).

Eberhardt, P. *et al.*, The D/H ratio in water from comet P/Halley. *Astron. Astrophys.* **187**, 435–437 (1987b).

Engel, S., Lunine, J.I., and Lewis, J.S., Solar nebula origin for volatile gases in Halley's comet. *Icarus*, in press (1989).

Fegley, B., Jr., Cosmochemical trends of volatile elements in the solar system. in *Workshop on the Origins of Solar Systems*, ed. J.A. Nuth and P. Sylvester, LPI Technical Report No. 88-04, pp. 51-60 (1988).

Fegley, B., Jr., The applications of chemical thermodynamics and chemical kinetics to planetary atmospheres research. in *Proceedings of the First International Conference on Laboratory Research for Planetary Atmospheres*, NASA CP, in press (1990).

Fegley, B., Jr. and Lewis, J.S., Volatile element chemistry in the solar nebula: Na, K, F, Cl, Br, and P. *Icarus* **41** 439–455 (1980).

Fegley, B., Jr. and Prinn, R.G., Solar nebula chemistry: Implications for volatiles in the solar system. in *The Formation and Evolution of Planetary Systems* ed. H.A. Weaver and L. Danly, Cambridge University Press, Cambridge, England, pp. 171–211 (1989).

Feldman, P.D., A'Hearn, M.F., and Millis, R.L., Temporal and spatial behavior of the ultraviolet emissions of comet IRAS-Araki-Alcock 1983d. *Astrophys. J.* **282**, 799–802 (1984).

Feldman, P.D. *et al.*, IUE observations of comet Halley: Evolution of the UV spectrum between September 1985 and July 1986. in *Proc. 20th ESLAB Symposium on the Exploration of Halley's Comet*, ESA SP-250, pp. 325–328 (1986a).

Feldman, P.D. *et al.*, Is CO_2 responsible for the outbursts of comet Halley? *Nature* **324**, 433–436 (1986b).

Festou, M.C. *et al.*, IUE observations of comet Halley during the Vega and Giotto encounters. *Nature* **321**, 361–363 (1986).

Fox, K., Owen, T., Mantz, A.W., and Rao, K., A tentative identification of $^{13}CH_4$ and an estimate of $^{12}C/^{13}C$ in the atmosphere of Jupiter. *Astrophys. J.* **176**, L81–L84 (1972).

Grim, R.J.A. and Greenberg, J.M., Photochemical studies of S_2 formation and their implications on the source and evolution of comets. in *The Comet Nucleus Sample Return Mission Proc. Workshop Canterbury UK*, ESA SP-249, pp. 143–151 (1986).

Grinspoon, D.H. and Lewis, J.S., Deuterium fractionation in the presolar nebula: Kinetic limitations on surface catalysis. *Icarus* **72**, 430–436 (1987).

Haltenorth, H. and Klinger, J., Diffusion of hydrogen fluoride in ice. in *Physics of Ice*, ed. N. Riehl, B. Bullemer, and H. Engelhardt, Plenum Press, NY, pp. 579-584 (1969).

Hayatsu, R. and Anders, E., Organic compounds in meteorites and their origins. *Topics in Current Chemistry* **99**, 1–39 (1981).

Huebner, W.F., First polymer in space identified in comet Halley. *Science* **237**, 628–630 (1987).

Huebner, W.F., Boice, D.C., and Sharp, C.M., Polyoxymethylene in comet Halley. *Astrophys. J. Lett.* **320**, L149–L152 (1987).

Huebner, W.F., Snyder, L.E., and Buhl, D., HCN radio emission from comet Kohoutek (1973f). *Icarus* **23**, 580–584 (1974).

Jessberger, E.K., Kissel, J., and Rahe, J., The composition of comets. in *Origin and Evolution of Planetary and Satellite Atmospheres* ed. S.K. Atreya, J.B. Pollack, and M.S. Matthews, University of Arizona Press, Tucson, AZ, pp. 167–191 (1989).

Kawara, K., Gregory, B., Yamamoto, T., and Shibai, H., Infrared spectroscopic observation of methane in comet Halley. *Astron. Astrophys.* **207**, 174–181 (1988).

Kissel, J. and Krueger, F.R., The organic component in dust from comet Halley as measured by the PUMA mass spectrometer on board Vega 1. *Nature* **326**, 755–760 (1987).

Kozasa, T. and Hasegawa, H., Formation of iron-bearing materials in a cooling gas of solar composition. *Icarus* **73**, 180–190 (1988).

Krankowsky, D. *et al.*, *In situ* gas and ion measurements at comet Halley. *Nature* **321**, 326–329 (1986).

Krebs, H.J., Bonzel, H.P., and Gafner, G., A model study of the hydrogenation of *CO* over polycrystalline iron. *Surface Sci.* **88**, 269–283 (1979).

Larson, H.P., Weaver, H.A., Mumma, M.J., and Drapatz, S., Airborne infrared spectroscopy of comet Wilson (1986l) and comparisons with comet Halley. *Astrophys. J.* **338**, 1106–1114 (1989).

Lewis, J.S., Low temperature condensation from the solar nebula. *Icarus* **16**, 241–252 (1972).

Lewis, J.S., Barshay, S.S., and Noyes, B., Primordial retention of carbon by the terrestrial planets. *Icarus* **37**, 190–206 (1979).

Lunine, J.I., Primitive bodies: Molecular abundances in comet Halley as probes of cometary formation environments. in *The Formation and Evolution of Planetary Systems* ed. H.A. Weaver and L. Danly, Cambridge University Press, Cambridge, England, pp. 213–242 (1989).

Lunine, J.I. and Stevenson, D.J., Thermodynamics of clathrate hydrate at low and high pressures with application to the outer solar system. *Astrophys. J. Suppl* **58**, 493–531 (1985).

Lutz, B.L., Owen, T., and DeBergh, C., Deuterium enrichment in the primitive ices of the protosolar nebula. *Icarus*, in press (1990).

Marconi, M.L. and Mendis, D.A., On the ammonia abundance in the coma of Halley's comet. *Astrophys. J.* **330**, 513–517 (1988).

Miller, S.L., The occurrence of gas hydrates in the solar system. *Proc. Nat. Acad. Sci. USA* **47**, 1798–1808 (1961).

Miller, S.L., Clathrate hydrates of air in antarctic ice. *Science* **165**, 489–490 (1969).

Miller, S.L. and Smythe, W.D., Carbon dioxide clathrate in the Martian ice cap. *Science* **170**, 531–533 (1970).

Mitchell, D.L. *et al.*, Evidence for chain molecules enriched in carbon, hydrogen, and oxygen in comet Halley. *Science* **237**, 626–628 (1987).

Mumma, M.J. and Reuter, D., On the identification of formaldehyde in Halley's comet. *Astrophys. J.*, in press (1989).

Mumma, M.J., Blass, W.E., Weaver, H.A., and Larson, H.P., Measurements of the ortho-para ratio and nuclear spin temperature of water vapor in comets Halley and Wilson (1986l) and implications for their origin and evolution. in *The Formation and Evolution of Planetary Systems: A Collection of Poster Papers*, ed. H.A. Weaver, F. Paresce, and L. Danly, STScI publication, pp. 157–168 (1988).

Mumma, M.J., Weaver, H.A., and Larson, H.P., The ortho-para ratio of water vapor in comet P/Halley. *Astron. Astrophys.* **187**, 419–424 (1987).

Mumma, M.J., Weaver, H.A., Larson, H.P., Davis, D.S., and Williams, M., Detection of water vapor in Halley's comet. *Science* **232**, 1523–1528 (1986).

Opal, C.B., McCoy, R.P., and Carruthers, G.R., Far ultraviolet objective spectra of comet P/Halley from sounding rockets. in *Proc. 20th ESLAB Symposium on the Exploration of Halley's Comet* ESA SP-250, pp. 425–430 (1986).

Oró, J. and Kimball, A.P., Synthesis of purines under possible primitive Earth conditions. I. Adenine from hydrogen cyanide. *Arch. Biochem. Biophys.* **94**, 217–227 (1961).

Owen, T., The isotope ratio $^{12}C/^{13}C$ in comet Tago-Sato-Kosaka 1969g. *Astrophys. J.* **184**, 33–43 (1973).

Prinn, R.G. and Fegley, B., Jr., Solar nebula chemistry: Origin of planetary, satellite, and cometary volatiles. in *Origin and Evolution of Planetary and Satellite Atmospheres*, ed. S.K. Atreya, J.B. Pollack, and M.S. Matthews, University of Arizona Press, Tucson, AZ, pp. 78–136 (1989).

Rambaldi, E.R. and Wasson, J.T., Metal and associated phases in Bishunpur, a highly unequilibrated ordinary chondrite. *Geochim. Cosmochim. Acta* **45**, 1001–1015 (1981).

Rambaldi, E.R. and Wasson, J.T., Metal and associated phases in Krymka and Chainpur: Nebular formational processes. *Geochim. Cosmochim. Acta* **48**, 1885–1897 (1984).

Rambaldi, E.R., Sears, D.W., and Wasson, J.T., *Si*-rich $Fe - Ni$ grains in highly unequilibrated chondrites. *Nature* **287**, 817–820 (1980).

Richet, P., Bottinga, Y., and Javoy, M., A review of hydrogen, carbon, nitrogen, oxygen, sulphur, and chlorine stable isotope fractionation among gaseous molecules. *Ann. Rev. Earth Planet. Sci.* **5**, 65–110 (1977).

Schloerb, F.P., Kinzel, W.M., Swade, D.A., and Irvine, W.M., Observations of HCN in comet P/Halley. *Astron. Astrophys.* **187**, 475–480 (1987).

Sill, G.T. and Wilkening, L.L., Ice clathrate as a possible source of the atmospheres of the terrestrial planets. *Icarus* **33**, 13–22 (1978).

Stawikowski, A. and Greenstein, J.L., The isotope ratio C^{12}/C^{13} in a comet. *Astrophys. J.* **140**, 1280–1291 (1964).

Stevenson, D.J., Chemical heterogeneity and imperfect mixing in the solar nebula. *Astrophys. J.* **348**, 730–737 (1990).

Stewart, A.I.F., Pioneer Venus measurements of H, O, and C production in comet P/Halley near perihelion. *Astron. Astrophys.* **187**, 369–374 (1987).

Studier, M.H., Hayatsu, R., and Anders, E., Origins of organic matter in early solar system–I. Hydrocarbons. *Geochim. Cosmochim. Acta* **32**, 151–173 (1968).

Tegler, S. and Wyckoff, S., NH_2 fluorescence efficiencies and the NH_3 abundance in comet Halley. *Astrophys. J.* **343**, 445–449 (1989).

Tielens, A.G.G.M., Surface chemistry of deuterated molecules. *Astron. Astrophys.* **119**, 177–184 (1983).

Vannice, M.A., Catalytic activation of carbon monoxide on metal surfaces. in *Catalysis Science and Technology*, ed. J.R. Anderson and M. Boudart, Springer-Verlag, Berlin, pp. 139–198 (1982).

Vanýsek, V., Carbon isotope ratio in comets and interstellar medium. in *Comets, Asteroids, and Meteorites: Interrelations, Evolution, and Origins*, ed. A.H. Delsemme, University of Toledo Press, Toledo, OH, pp. 499–503 (1977).

Weaver, H.A., The volatile composition of comets. in *Highlights of Astronomy* **8**, 387–393 (1989).

Weaver, H.A., Feldman, P.D., Festou, M.C., A'Hearn, M.F., and Keller, H.U., IUE observations of faint comets. *Icarus* **47**, 449–463 (1981).

Weaver, H.A., Mumma, M.J., and Larson, H.P., Infrared spectroscopy of cometary parent molecules. in *Comets in the Post-Halley Era* ed. R. Newburn and J. Rahe, Kluwer Academic Publishers, in press (1990).

Whipple, F.L., Chondrules: suggestions concerning their origin. *Science* **153**, 54–56 (1966).

Wilkening, L.L., Meteorites in meteorites: evidence for mixing among the asteroids. in *Comets, Asteroids, Meteorites: Interrelations, Evolution, and Origins*, ed. A.H. Delsemme, University of Toledo Press, Toledo, OH, pp. 389–396 (1977).

Wood, J.A. and Chang, S. eds., *The Cosmic History of the Biogenic Elements and Compounds*, NASA SP-476 (1985).

Woods, T.N., Feldman, P.D., Dymond, K.F., and Sahnow, D.J., Rocket ultraviolet spectroscopy of comet Halley and abundance of carbon monoxide and carbon. *Nature* **324**, 436–438 (1986).

Wyckoff, S., Lindholm, E., Wehinger, P.A., Peterson, B.A., Zucconi, J.M., and Festou, M.C., The $^{12}C/^{13}C$ abundance ratio in comet Halley. *Astrophys. J.* **339**, 488–500 (1989b).

Wyckoff, S. and Theobald, J., Molecular ions in comets. *Adv. Space Res.* 9(3), 157–161 (1989).

Wyckoff, S., Tegler, S., and Engel, L., Ammonia abundances in comets. *Adv. Space Res.* 9(3), 169–176 (1989a).

Wyckoff, S., Tegler, S., Wehinger, P.A., Spinrad, H., and Belton, M.J.S., Abundances in comet Halley at the time of the spacecraft encounters. *Astrophys. J.* **325**, 927–938 (1988).

Yamamoto, T., Formation environment of cometary nuclei in the primordial solar nebula. *Astron. Astrophys.* **142**, 31–36 (1985).

Yung, Y.L., Friedl, R.R., Pinto, J.P., Bayes, K.D., and Wen, J.S., Kinetic isotopic fractionation and the origin of HDO and CH_3D in the solar system. *Icarus* 74, 121–132 (1988).

SULFUR COMPOUNDS IN COMETS

Sang J. Kim
Michael F. A'Hearn
University of Maryland

SULFUR COMPOUNDS IN COMETS

Sang J. Kim and Michael F. A'Hearn (University of Maryland)

Cometary comae exhibit abundant sulfur and sulfur compounds, most of which are absent in planetary atmospheres. Sulfur compounds have also been detected in the interstellar medium, including SO, SO_2, CS, etc., but excluding S_2 which was identified only in comet IRAS-Araki-Alcock (IAA) 1983d. The study of the origin and parent molecules of these compounds, therefore, may yield a clue to the question of the formation and evolution of comets from the interstellar medium. Our work is aimed at determining abundances of the various sulfur compounds in comets.

We have found new evidence of S_2 in the ground-based spectra of comet IAA (Fig. 1) observed by Stephen Larson (Univ. of Arizona); there was at least one S_2 outburst before the one detected by A'Hearn, Feldman and Schleicher (1). The observations indicate that S_2 is often present in comet IAA. We undertook fluorescence calculations to analyze the B-X system of S_2 which appeared both in IUE spectra (Fig. 2) and in the ground-based spectra of comet IAA. Single- (Fig. 3) and multiple-cycle (Fig. 4) fluorescence calculations indicate that fluorescent equilibrium accounts for the observed spectra despite the fact that the S_2 lifetime against solar ultraviolet radiation is relatively short. This analysis confirms unambiguously that emission peaks in the 3000 - 4000 Å spectral range of the ground-based data are due to the B-X bands of S_2 (Fig. 1) implying that S_2 should be sought in archival ground-based spectra of comets. The fluorescence calculation indicates that the previous S_2 production rates should be reduced at least a factor of two.

Most models of comets suggest that SO and/or SO_2 should be abundant in the coma both because of reactions between the observed species S and OH and because of irradiation of other sulfur compounds in icy grains prior to accretion. If the S_2 in IAA was produced by irradiation of other sulfur compounds in icy-mantles of grains as proposed by A'Hearn and Feldman (2), then SO under most circumstances should be much more abundant than S_2. A tentative identification of SO has been proposed by Wallis and Krishna-Swamy (3). We have calculated synthetic spectra of SO and compared them with spectra of various comets observed with the IUE (Fig. 5). We find no evidence for the presence of SO and set upper limits on the relative production rate of SO in comets (Table 1) assuming that the SO is a parent.

Since the abundance of S_2 in IAA was of order 10^{-4} that of water, it appears that only the upper limit of SO in IAA is approaching interesting values. Although observations with HST will be more sensitive than with IUE, it appears that *in situ* measurements may be required to detect SO and test the irradiation hypothesis for formation of S_2.

It has been difficult to explain the high resolution IUE spectra of the 0-0 band of CS at 2577 Å, because CS radicals are formed near the nucleus where collisions may affect the rotational structure of this band. Since calculation of abundances requires an accurate knowledge of the emission process, we were motivated by the imcomplete analysis by

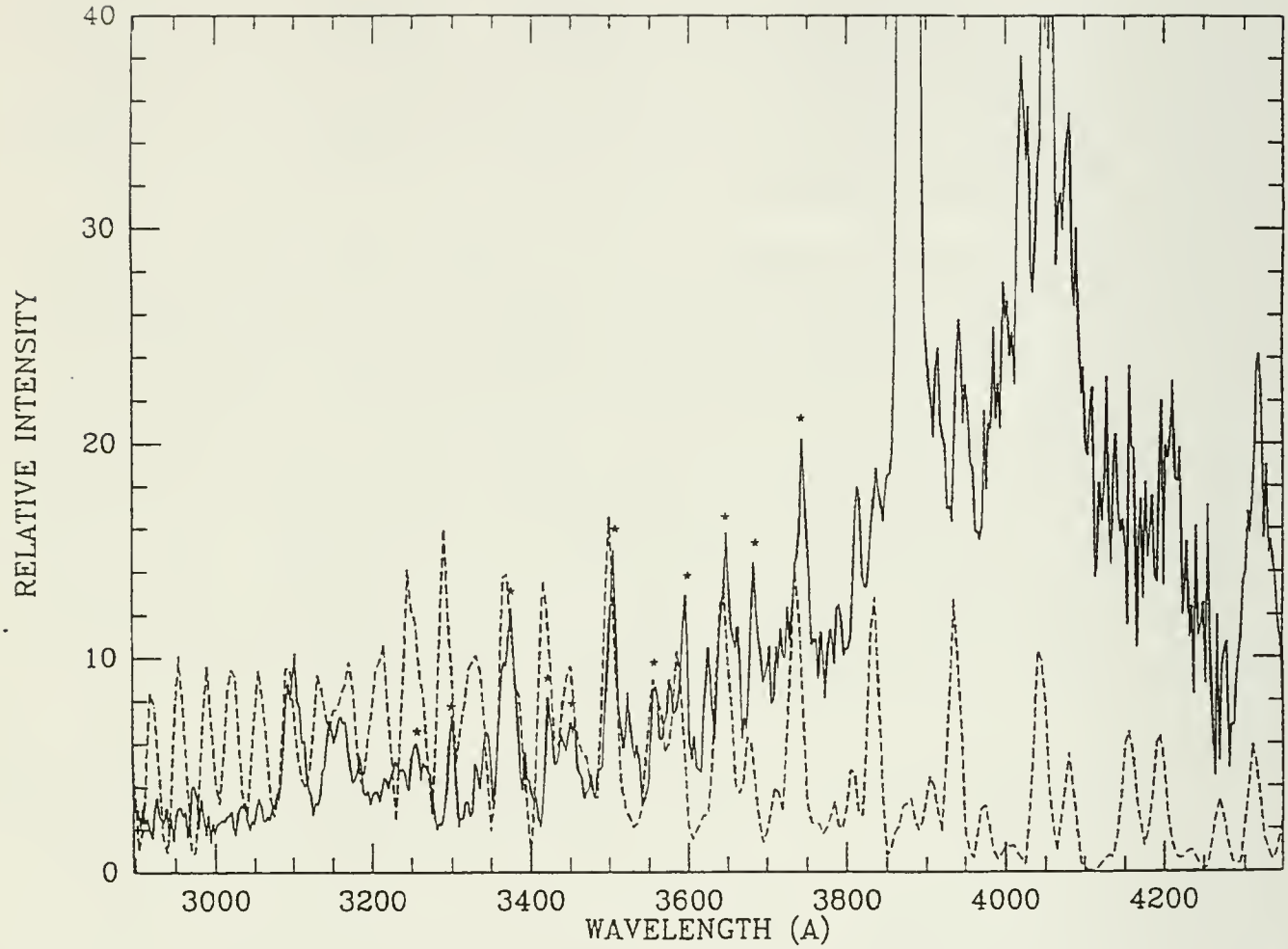


Figure 1. Comparison between a ground-based spectrum (solid line) obtained with the Catalina telescope and the B-X model of S_2 (dashed line). The identified bands of the B-X system are marked by *.

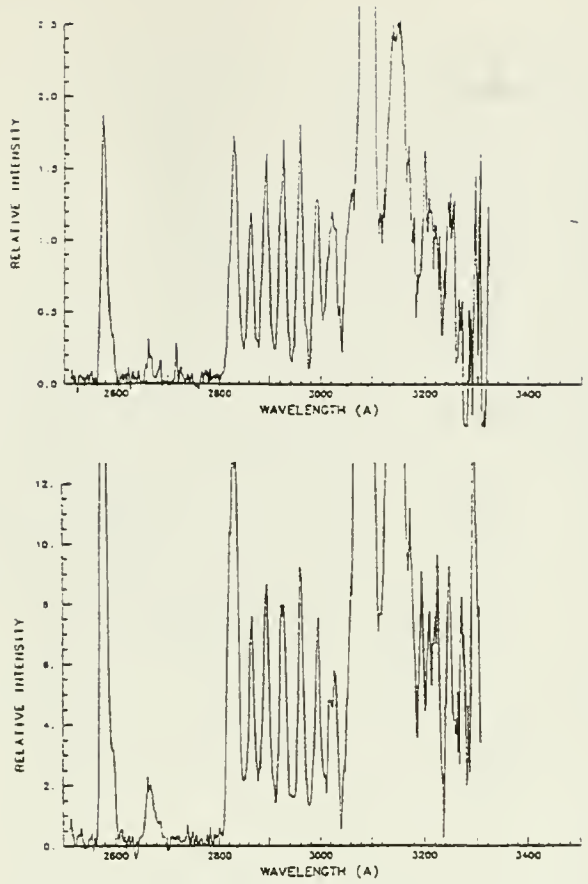


Figure 2. The B-X system of S_2 appeared in IUE spectra of comet IRAS-Araki-Alcock 1983d.

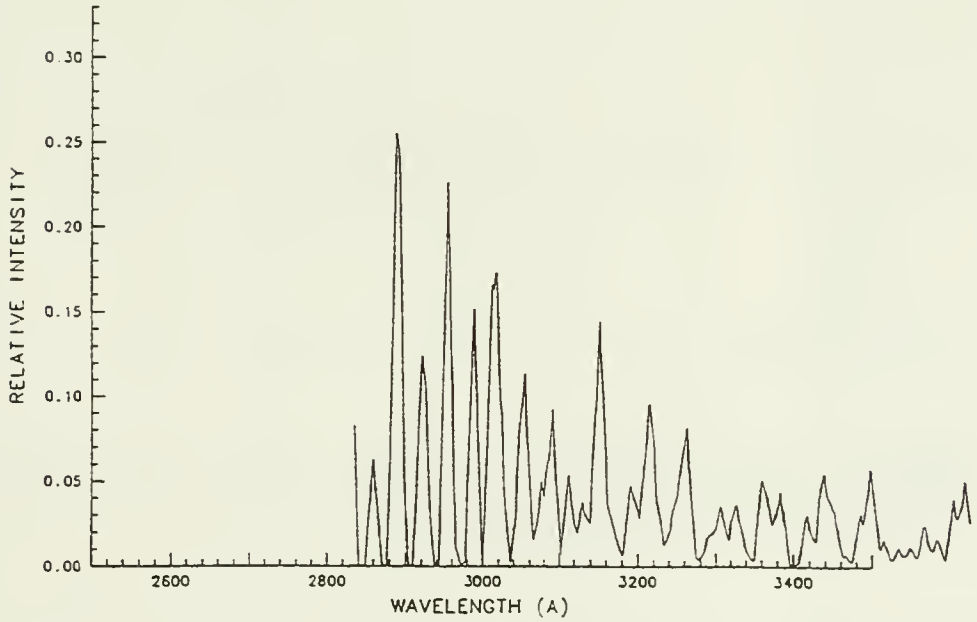


Figure 3. Single-cycle fluorescence model for the B-X system of S_2.

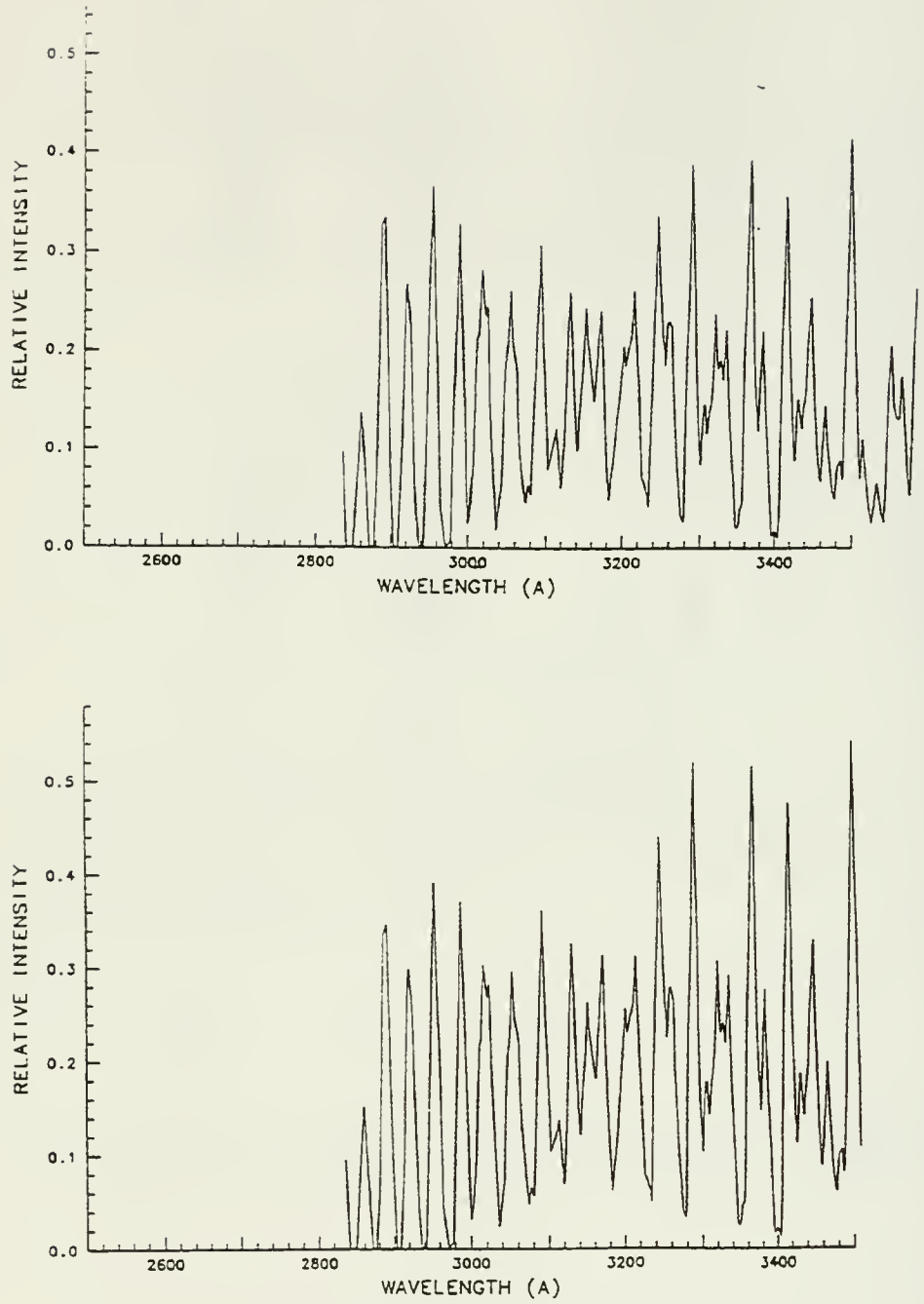


Figure 4. Fourth- and fifth-cycle fluorescence models for the B-X system of S_2. The fifth-cycle model is very similar to the fluorescent equilibrium model.

Table 1: SO in Comets

Comet	r [AU]	Date	Q(SO) [sec^{-1}]	$Q(SO)/Q(H_2O)$
I-A-A	1.0	1983 May 11	$<4\times10^{25}$	$<10^{-3}$
P/Halley	0.9	1986 Mar 13	$<6\times10^{27}$	$<10^{-2}$
P/Encke	0.8	1980 Nov 5	$<4\times10^{26}$	$<4\times10^{-2}$
Bradfield (1979l)	0.9	1980 Jan 24	$<2\times10^{26}$	$<2\times10^{-2}$
Bowell	3.4	1982 Apr 27	$<2\times10^{27}$	$<10^{-1}$
Cernis	3.4	1983 Sep 7	$<2\times10^{27}$	$<10^{-1}$

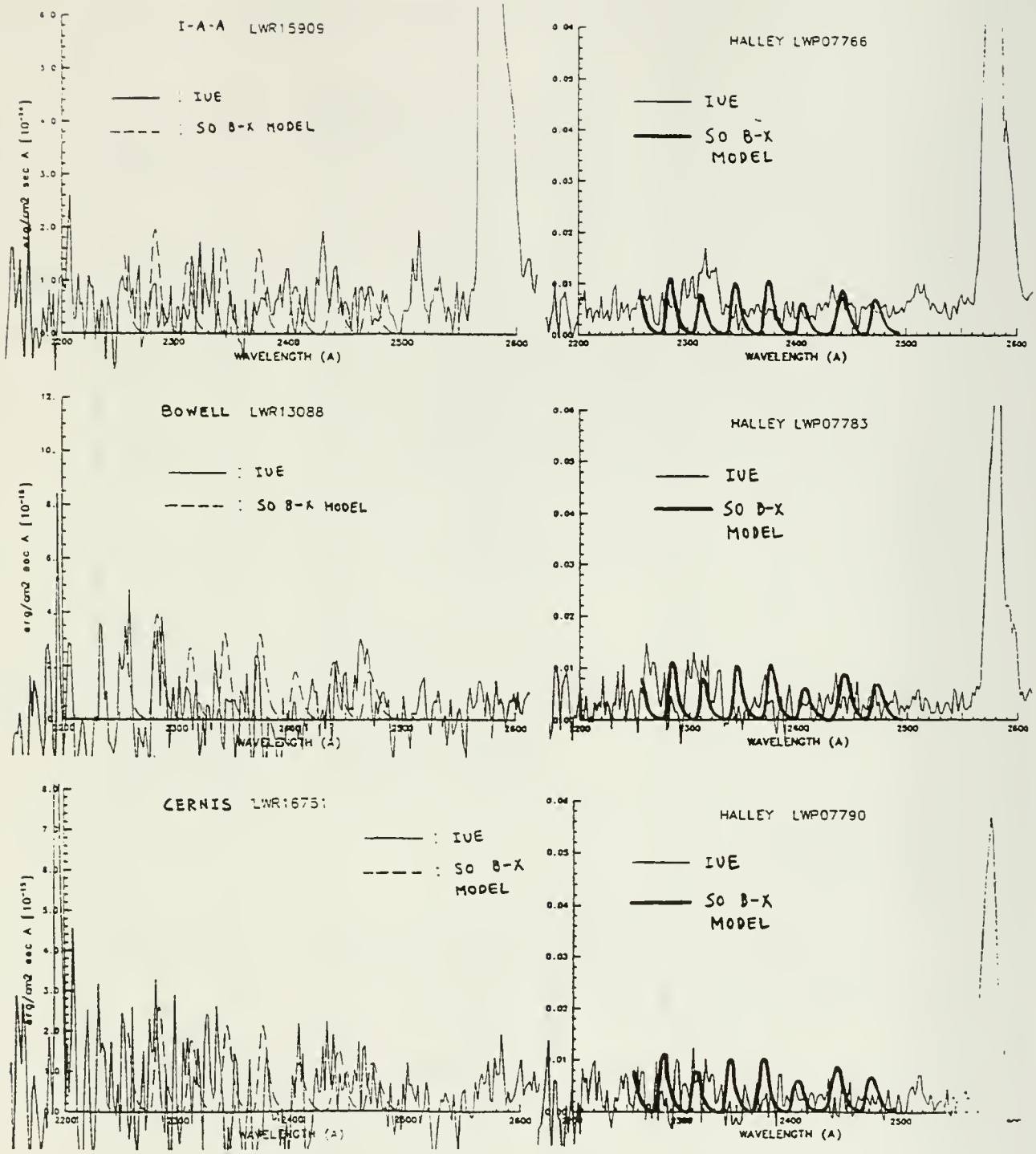


Figure 5. Comparison between SO models and IUE spectra of various comets.

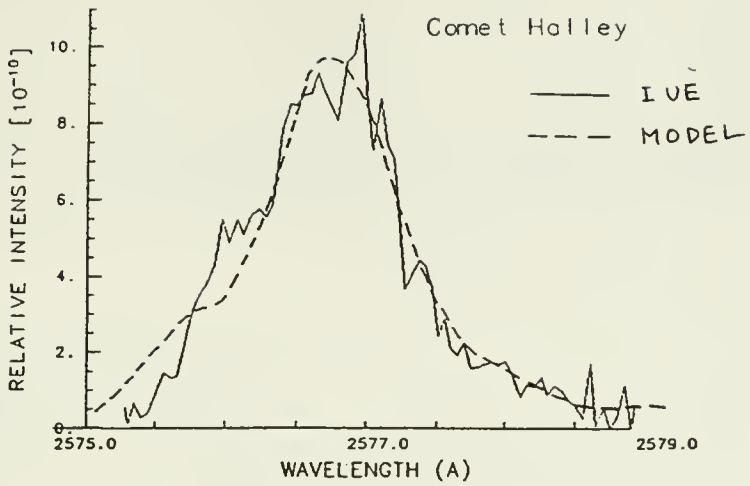


Figure 6. Comparison between the 0-0 band model of CS and an IUE spectrum of comet Halley.

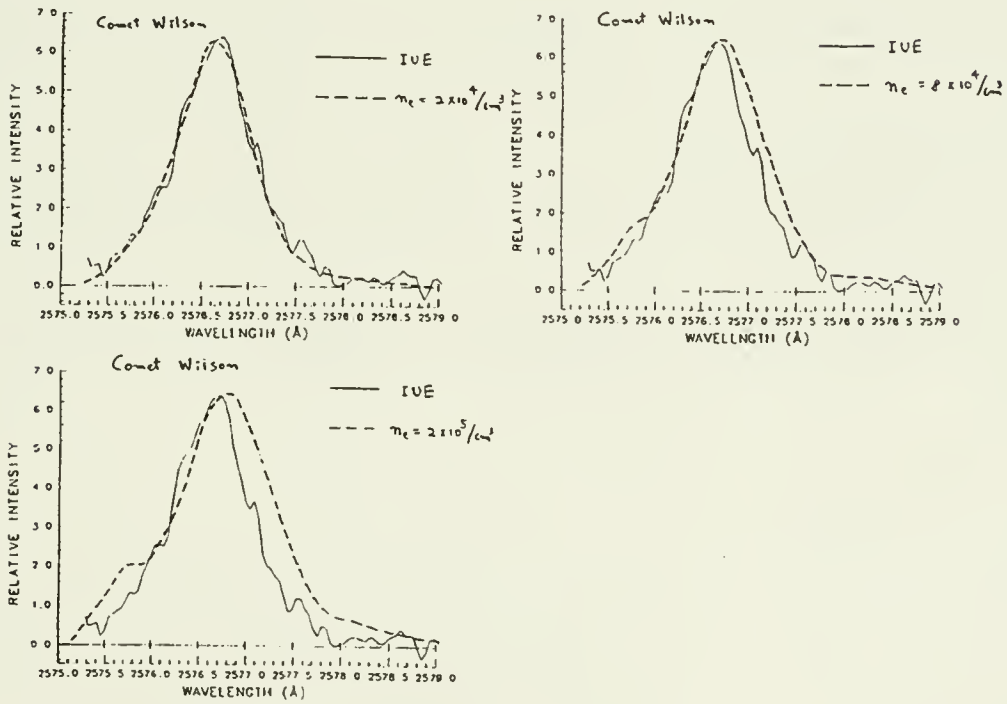


Figure 7. Comparison between an IUE spectrum of comet Wilson and the CS band models with various electron densities. The best fit indicates that the electron density is about 2×10^4 cm^3 in the region where CS forms.

Prisant and Jackson (4) to construct a band model which includes fluorescence processes initiated by solar ultraviolet radiation, and collisional excitation by electrons and neutrals. In Fig. 6 and 7, we present models of the 0-0 band, which give satisfactory fits to the high resolution IUE spectra of comets Halley and Wilson, respectively. We found that the rotational excitation by electrons is a dominant process in determining the ground state rotational population. We derived an electron density of 2×10^4 cm^3 in the region several thousand kilometers from comet Wilson's nucleus. In our future works, CS abundance will be calculated using the new g-factor and be compared with data from the interstellar medium.

Ultimately the abundances of the sulfur bearing molecules must be compared to assess the complete sulfure chemistry in comets. The atomic sulfur, also observed from IUE, is curerntly being studied by Feldman and collaborators since there are indications (5) that the g-factors for some lines of this species may be incorrect.

REFERENCES

1. A'Hearn, M.F., Feldman, P.D., and Schleicher D.G. (1983) Astrophys. J. v. 274, pp. L99-L103.

2. A'Hearn, M.F. and Feldman, P.D. (1985) in Ices in the Solar System, ed. J. Klinger et al., 463-471.

3. Wallis, M.K. and Krishna-Swamy, K.S. (1987) Astron. & Astrophys. v. 197, pp. 329-332.

4. Prisant, M.G. and Jackson, M.W. (1987) Astron. & Astrophys. v. 187, pp. 487-496.

5. Roettger, E.E., Feldman, P.D., A'Hearn, M.F., Festou, M.C., McFadden, L.A., and Gilmozzi, R., (1989) Icarus, in press.

SPECTROPHOTOMETRIC OBSERVATIONS OF COMET P/GIACOBINI-ZINNER

Ichishiro Konno
Southwest Research Institute

Susan Wyckoff
Peter A. Wehinger
Arizona State University

SPECTROPHOTOMETRIC OBSERVATIONS OF COMET P/GIACOBINI-ZINNER

Ichishiro Konno[1], Susan Wyckoff[2], and Peter A. Wehinger[2]

[1]Southwest Research Institute, [2]Arizona State University

ABSTRACT

Spectrophotometric observations of Comet P/Giacobini-Zinner were obtained in March, June, September, and October 1985. The September observations were obtained at perihelion, *exactly* at the time of the International Cometary Explorer (ICE) encounter with the comet. Spatial profiles extracted from the long-slit spectra were analyzed by using a Monte Carlo method to determine scale lengths and lifetimes for the observed radicals, C_2 and NH_2, and their respective parent molecules. The scale length for the parent of C_2 was found to be $(7.5 \pm 1.5) \times 10^4$ km and for the parent of NH_2 $(2.4 \pm 0.4) \times 10^4$ km. The brightness profile of C_2 and the lifetime of the parent of C_2 indicate that C_2 probably comes from many different sources which may include C_2H_4, C_2H_2, and dust particles. C_2 and NH_2 were found to be depleted in Giacobini-Zinner relative to an average comet by factors of 10 and 5, respectively. The water production rate was obtained for June, September, and October observations from the measurements of the [O I] 6300 Å line. The water production rate at the time of the ICE encounter was found to be 2.4×10^{28} molecules s^{-1}, in good agreement with spacecraft results.

INTRODUCTION

The primary goals of the observations of Comet Giacobini-Zinner were to 1) identify the emission lines in the spectra, 2) obtain spatial distributions of various species to identify the possible parent molecules of observed species, and 3) obtain the production rates and abundances of observed species and water. A summary of the telescopes and instruments used for observations of Comet Giacobini-Zinner are shown in Table 1. All the observations were made at the National Optical Astronomical Observatory (NOAO) at Kitt Peak. The comet was observed from March to October 1985, covering the heliocentric distances of 2.29 AU to 1.03 AU including the precise time of the ICE encounter, 11 September 1985 at 11:00 UT, giving direct comparisons of ground-based and spacecraft observations.

SPECTRA AND MEASUREMENTS

Observations on 20 March

In the spectrum obtained on 19 March 1985 only CN($\Delta v = 0$) emission was marginally present with a strength $\sim 1\sigma$ above the noise level (which was determined by measurements of the continuum). No NH_2 bands were found at the 1 σ significance level. The results of the measurement of the emission band flux and the column density are presented in Table 2. The g-factors which were used to calculate column densities for various species are shown in Table 3.

Observations on 20 and 21 June

Figures 1 and 2 show the spectra of Giacobini-Zinner at and off the nucleus on the night of 20 June 1985. The aperture was set at the nucleus and at 10″ from the nucleus along the plasma tail on 20 June and was set at the nucleus and 8″ from the nucleus along the plasma tail on 21 June. Since the nuclear spectra on the nights of 20 and 21 June are almost identical in terms of emission features and intensities, only the spectra on 20 June are shown. The emission band fluxes and the column densities are shown in Tables 4 and 5.

TABLE 1. – OBSERVATIONS OF COMET P/GIACOBINI-ZINNER

Date 1985	r (AU)	Δ (AU)	PA	Spectral resol.(Å)	Spatial resol.(km)	Telescope Kitt Peak	Detector
20 Mar	2.29	2.28	90°	20	14,000	2.1-m	IIDS
20 Jun	1.47	0.96	90°	20	5,900	2.1-m	IIDS
21 Jun	1.46	0.95	90°	20	5,800	2.1-m	IIDS
11 Sep	1.03	0.47	91°	5	400	4-m	CCD
19 Oct	1.20	0.65	91°	5	480	4-m	CCD

r: heliocentric distance; Δ: geocentric distance; PA: position angle; IIDS: intensified image dissector scanner; CC charge-coupled device

TABLE 2. – OBSERVED FLUXES AND COLUMN DENSITIES AT NUCLEUS ON 20 March 1985
r=2.29 AU Δ = 2.28 AU $\dot{r} = -14.98$ km s^{-1}

Species	Wavelength Å	Integrated flux (erg cm^{-2} s^{-1})	Column density (cm^{-2})
CN(Δv=0)	3910	$(1.8\pm0.8)\times10^{-15}$	$(2.8\pm1.2)\times10^{8}$

$\dot{r}$: heliocentric velocity

TABLE 3. – g-FACTORS

Species	g-factor at 1 AU (erg s^{-1})	Source
OH(3085)	1.995×10^{-15}	Feldman and Brune (1976)
NH(3360)	3.1×10^{-13}	Schleicher (1987b)
CN(Δv=+1)	4.684×10^{-15}*	Schleicher (1983)
CN(Δv=0)	3.33×10^{-13}**	Schleicher (1983)
C_3(4050)	1.03×10^{-12}	Cooper and Jones (1979)
CN(Δv=-1)	2.641×10^{-14}*	Schleicher (1983)
CH(Δv=0)	9.2×10^{-14}	A'Hearn et al.. (1980)
CO^+(1-0)	1.03×10^{-14}*	Magnani and A'Hearn (1986)
CO^+(1-1)	1.27×10^{-14}*	Magnani and A'Hearn (1986)
C_2(Δv=+1)	2.266×10^{-13}	A'Hearn et al.. (1985)
C_2(Δv=0)	4.533×10^{-13}	A'Hearn et al.. (1985)
NH_2(10-0)	2.99×10^{-14}	A'Hearn (1982)
NH_2(9-0)	3.13×10^{-14}	A'Hearn (1982)
H_2O^+(8-0)	1.4×10^{-14}	Lutz (1987)
[O I](6300)	1.63×10^{-14}	Festou and Feldman (1981)
NH_2(8-0)	5.34×10^{-14}	A'Hearn (1982)

*: value for $\dot{r}$(heliocentric velocity)=0. **: value for $\dot{r} = -15$ km s^{-1}

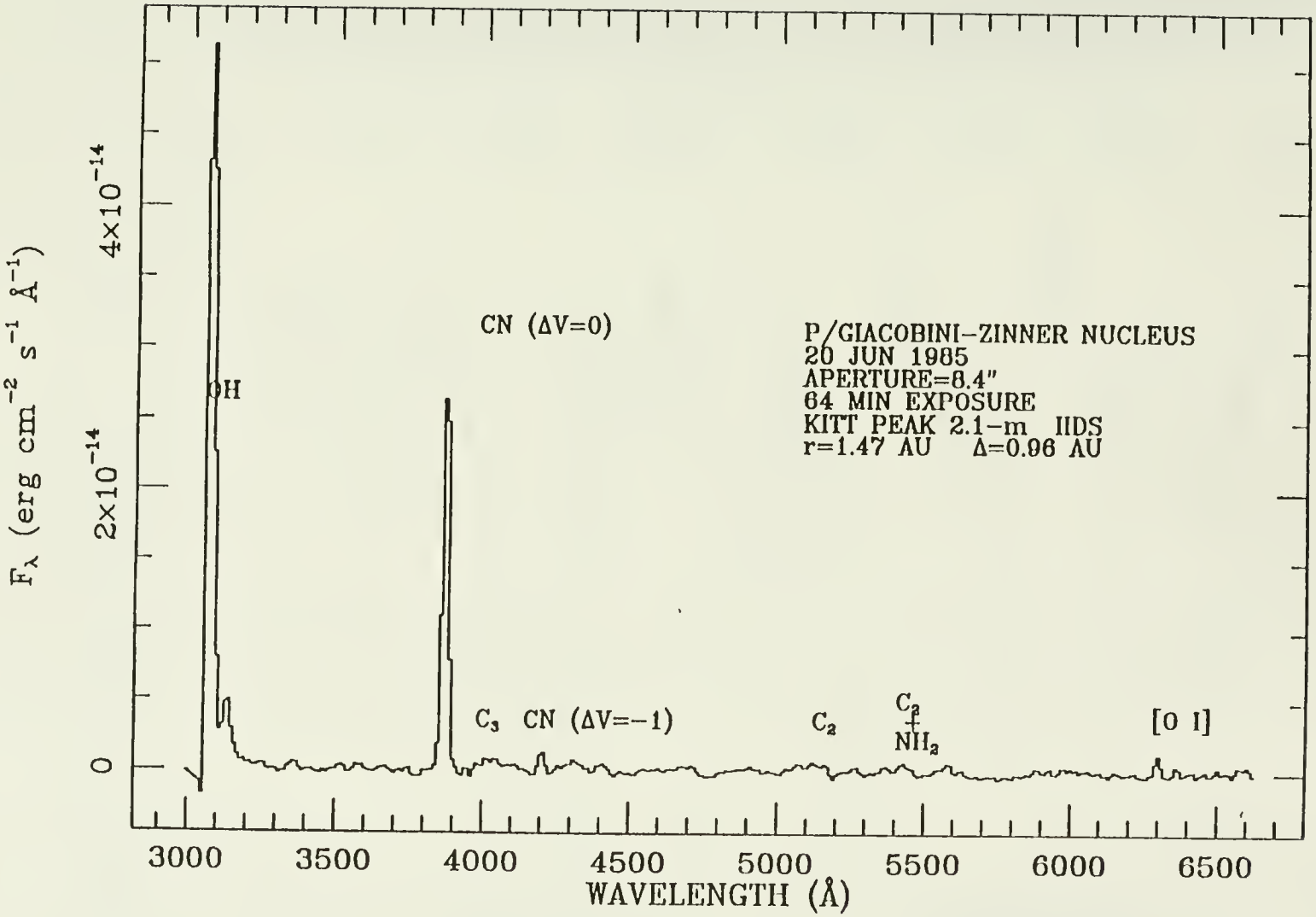


Figure 1. – Spectrum of comet P/Giacobini-Zinner at the nucleus on 20 June 1985.

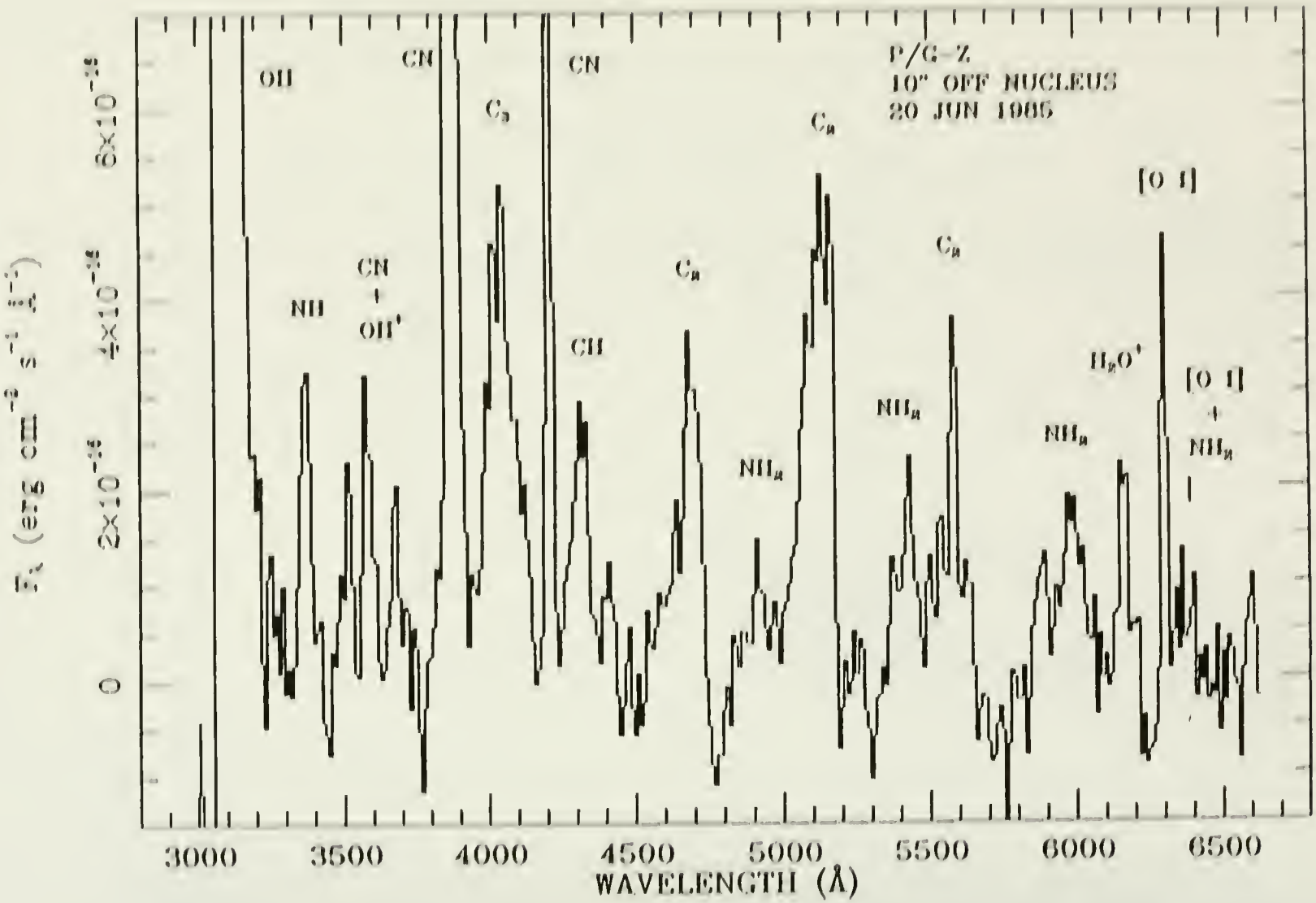


Figure 2. Spectrum of comet P/Giacobini Zinner 40 arcsec off the nucleus in the tail on 20 June 1985. H_2O^+ is more pronounced than in the nucleus spectrum, and OH^+ probably contributes to the feature at 3680 Å

TABLE 4. – OBSERVED FLUXES AND COLUMN DENSITIES AT NUCLEUS ON 20 JUNE 1985
r=1.47 AU Δ=0.96 AU ṙ = −15.27 km s^{-1}

Species	Wavelength (Å)	Integrated flux (erg cm^{-2} s^{-1})	Column density (cm^{-2})
OH	3065	(1.6±0.1)×10^{-12}	(1.7±0.1)×10^{13}
NH(0-0)	3360	(1.8±0.4)×10^{-14}	(1.9±0.3)×10^{8}
CN(Δv=−1)	3591	(9.0±4.6)×10^{-15}	(4.0±2.1)×10^{11}
CN(Δv=0)	3883	(7.3±1.07)×10^{-13}	(3.0±0.09)×10^{13}
C_3(0-0)	4050	(5.7±1.6)×10^{-14}	(1.8±0.3)×10^{8}
CN(Δv=−1)	4216	(3.1±1.1)×10^{-14}	(2.4±0.8)×10^{11}
CH(Δv=0)	4300	(3.1±1.2)×10^{-14}	(3.6±1.6)×10^{8}
C_2(Δv=0)	5070	(3.2±1.5)×10^{-14}	(2.3±1.2)×10^{8}
NH_2(9-0)	5993	(1.1±0.6)×10^{-14}	(7.1±3.7)×10^{8}
[O I]	6300	(2.7±0.6)×10^{-14}	(3.6±0.7)×10^{11}

TABLE 5. – OBSERVED FLUXES AND COLUMN DENSITIES AT
10″ TAILWARD FROM THE NUCLEUS ON 20 JUNE 1985
r=1.47 AU Δ=0.96 AU ṙ = −15.27 km s^{-1}

Species	Wavelength (Å)	Integrated flux (erg cm^{-2} s^{-1})	Column density (cm^{-2})
OH	3065	(1.5±0.06)×10^{-12}	(5.0±0.3)×10^{13}
NH(0-0)	3360	(1.2±0.2)×10^{-14}	(7.8±0.4)×10^{8}
CN(Δv=−1)	3590	(5.0±0.9)×10^{-14}	(3.6±0.4)×10^{11}
CN(Δv=0)	3883	(4.4±0.02)×10^{-13}	(1.8±0.01)×10^{13}
C_3(0-0)	4050	(4.8±0.4)×10^{-14}	(1.0±0.05)×10^{8}
CN(Δv=−1)	4216	(3.3±0.3)×10^{-14}	(1.3±0.2)×10^{11}
CH(Δv=0)	4300	(1.0±0.3)×10^{-14}	(1.8±0.5)×10^{8}
C_2(Δv=−1)	4730	(2.6±1.0)×10^{-14}	(2.1±0.9)×10^{8}
C_2(Δv=0)	5070	(7.0±0.5)×10^{-14}	(8.2±0.2)×10^{8}
NH_2(9-0)	6003	(3.9±1.4)×10^{-15}	(2.6±1.0)×10^{8}
H_2O^+(8-0)	6200	(1.2±0.1)×10^{-14}	(1.8±0.1)×10^{11}
[O I]	6300	(3.8±1.0)×10^{-15}	(1.1±0.1)×10^{11}
NH_2(8-0)	6320	(2.5±1.0)×10^{-15}	(3.6±4.0)×10^{8}

Bands of OH and CN are strikingly dominant in these spectra. These band sequences of CN Δv = 0 and Δv = −1, are seen. The C_2 Swan bands are the next strongest bands in the spectra, but as has been pointed out by several observers, these bands were not as strong in Giacobini-Zinner as in most other comets. A'Hearn and Millis (1980), Cochran and Barker (1987) and Schleicher et al. (1987) have found that Giacobini-Zinner is depleted in C_2 and C_3 relative to CN. They have independently found that the production rates of C_2 and C_3 are down by a factor of about 5 relative to CN compared with averages of other comets. Our spectra show that NH, OH and NH_2 have intensities comparable to C_2.

In the spectra obtained with the slit off the nucleus, H_2O^+ features are more prominent than on the nucleus especially on 20 June. The relative intensities of the H_2O^+ bands become stronger with the distance from the nucleus. This behavior is due to the accelerations of ions caused by the interaction of the solar wind with the comet which forms the plasma tail. A weak contribution by OH^+ to the feature at 3600 Å is probably present in the 21 June off-nucleus spectrum.

Observations on 11 September

In Figure 3 a spectral cut covering a spatial extent 2.0×10^3 km at a projected distance 8,000 km tailward from the nucleus is shown. This spectrum obtained at 11:00 UT on 11 September represents the column containing the ICE spacecraft at mid-encounter. Various ion and neutral species have been identified and are labeld in the figure. The solar continuum reflected from the cometary dust has been subtracted from the spectrum. In Tables 6 and 7 the integrated fluxes of the observed features at the nucleus and in the tail (Figure 4) are given together with the column densities. We searched for CO^+ features, expecially the (1-0) and (1-1) bands at 4555 Å and 5055 Å but no CO^+ features were seen at the 3σ significance level. Thus, we can set only an upper limit on the CO^+/H_2O^+ ratio from the flux measurements.

TABLE 6. – OBSERVED FLUXES AND COLUMN DENSITIES AT NUCLEUS ON 11 SEPTEMBER 1985
r=1.03 AU Δ=0.47 AU $\dot{r}$ = 1.96 km s^{-1}

Species	Wavelength (Å)	Integrated flux (erg cm^{-2} s^{-1})	Column density (cm^{-2})
$C_2(\Delta v=0)$	5101	$(6.6\pm1.8)\times10^{-14}$	$(1.1\pm0.3)\times10^{9}$
NH_2(10-0)	5732	$(3.7\pm2.4)\times10^{-15}$	$(9.0\pm5.9)\times10^{9}$
NH_2(9-0)	5996	$(8.9\pm3.3)\times10^{-15}$	$(2.1\pm0.8)\times10^{10}$
[O I]	6300	$(3.5\pm0.2)\times10^{-14}$	$(1.5\pm0.07)\times10^{10}$

TABLE 7. – FLUXES AND COLUMN DENSITIES AT 8,000 KM TAILWARD ON 11 SEPTEMBER 1985

Species	Wavelength (Å)	Integrated flux (erg cm^{-2} s^{-1})	Column density (cm^{-2})
CO^+(1-0)	4550	$<1.2\times10^{-15}$	$<9.2\times10^{9}$
CO^+(1-1)	5050	$<1.1\times10^{-15}$	$<7.4\times10^{9}$
$C_2(\Delta v=0)$	5078	$(4.5\pm0.4)\times10^{-14}$	$(8.5\pm0.5)\times10^{8}$
NH_2(10-0)	5720	$(3.3\pm1.2)\times10^{-15}$	$(8.8\pm3.4)\times10^{9}$
NH_2(9-0)	5994	$(2.3\pm0.8)\times10^{-15}$	$(6.0\pm2.2)\times10^{9}$
H_2O^+(8-0)	6189	$(5.3\pm2.2)\times10^{-15}$	$(3.0\pm1.2)\times10^{10}$
[O I]	6300	$(4.0\pm0.7)\times10^{-15}$	$(2.0\pm0.4)\times10^{10}$

Observations on 19 October

Figure 4 shows the spectrum of the nucleus with an extraction sum of 10 pixels which gives 8″ (5,000 km) onto the comet in the tail-axis direction. The main differences with the June and September spectra are the weaker C_2 band features. The results of measurements of fluxes and column densities are shown in Table 8.

TABLE 8. – OBSERVED FLUXES AND COLUMN DENSITIES AT NUCLEUS ON 19 OCTOBER 1985
r=1.20 AU Δ=0.65 AU $\dot{r}$ = 11.94 km s^{-1}

Species	Wavelength (Å)	Integrated flux (erg cm^{-2} s^{-1})	Column density (cm^{-2})
NH_2(9-0)	5995	$(6.4\pm4.9)\times10^{-15}$	$(1.2\pm0.9)\times10^{10}$
[O I]	6300	$(2.7\pm0.4)\times10^{-14}$	$(9.5\pm1.2)\times10^{10}$
[O I]	6364	$(8.9\pm1.3)\times10^{-15}$	$(9.3\pm1.3)\times10^{10}$

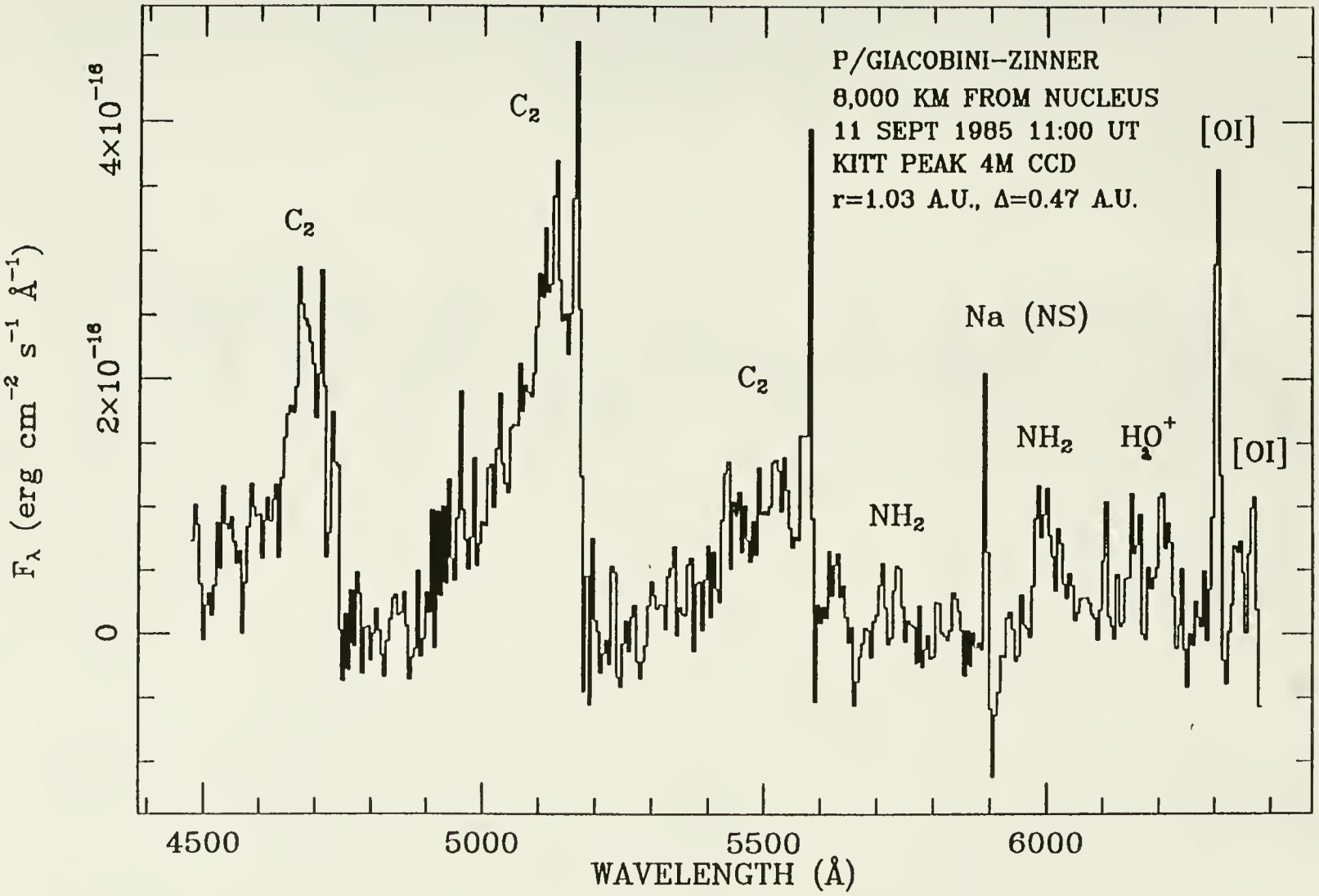


Figure 3. – Spectral extraction from a long-slit CCD spectrum of comet P/Giacobini-Zinner obtained at the time of the ICE encounter, 11 September 1985. The slit was oriented along the tail axis. The spectrum covers the column containing the ICE spacecraft *exactly* at the time of encounter, 7,800 km tailward of the nucleus. The extraction is from 7,000 km to 9,000 km in the tail.

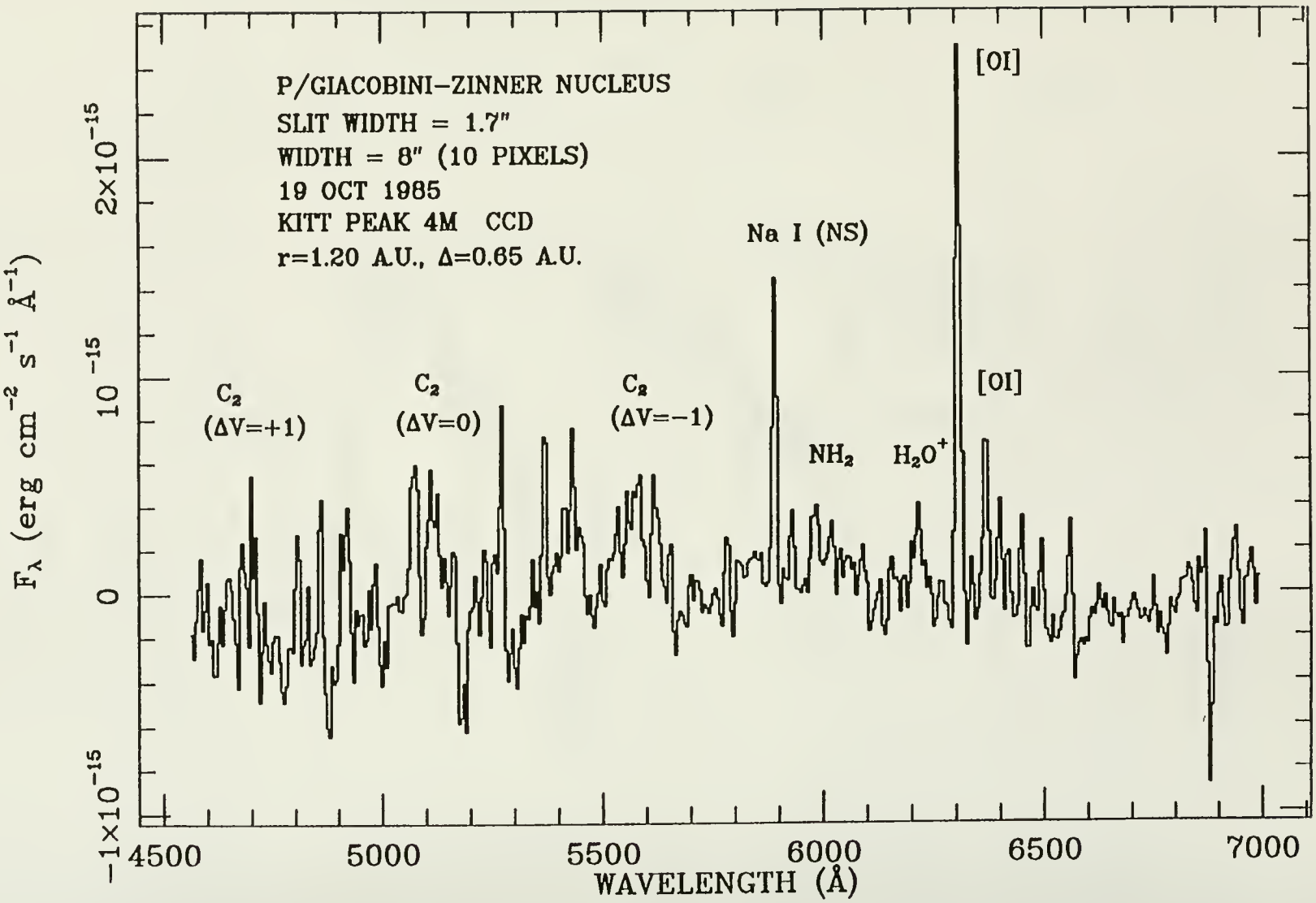


Figure 4. – Spectral extraction from a long-slit CCD spectrum of comet P/Giacobini-Zinner on 19 October 1985. The slit was oriented along the tail axis. The spectrum covers 8 arcsec (5,000 km) centered on the nucleus.

BRIGHTNESS PROFILES

The observed brightness profiles for NH_2(9-0) and $C_2(\Delta v = 0)$ extracted from the CCD spectrum on 11 September are shown in Figures 5 and 6 with profiles calculated using a Monte Carlo method. The parameters for the fits are shown in Table 9. The production rate for NH_2 was found to be $(5.1 \pm 2.5) \times 10^{24}$ molecules s^{-1} and for C_2 $(5.3 \pm 1.0) \times 10^{24}$ molecules s^{-1}.

TABLE 9. – PARAMETERS FOR THE NH_2 AND C_2 BRIGHTNESS PROFILES

	velocity (km s^{-1})	lifetime at 1.03 AU (s)	lifetime at 1.00 AU (s)	scale length at 1.00 AU (km)
NH_2 parent	1.0	2.5×4	$(2.4 \pm 0.7) \times 10^4$	$(2.4 \pm 0.7) \times 10^4$
NH_2	1.1	2.5×4	$(2.4 \pm 0.8) \times 10^4$	$(3.6 \pm 1.2) \times 10^4$
C_2 parent	1.0	8.0×4	$(7.5 \pm 1.5) \times 10^4$	$(7.5 \pm 1.5) \times 10^4$
C_2	0.5	1.0×5	$(9.4 \pm 1.9) \times 10^4$	$(1.1 \pm 0.2) \times 10^5$

The lifetime of the NH_2 parent was found to be $(2.4 \pm 0.7) \times 10^4$ s. The calculated photodissociation lifetime of NH_3 is 5.9×10^3 s at 1 AU from the sun (Huebner and Carpenter, 1979). Thus the calculated NH_3 lifetime is a factor of 4 smaller than the observed lifetime of the NH_2 parent. This difference may indicate that NH_3 can be excluded from the candidates for the parent of NH_2. Delsemme and Combi (1983) have obtained the lower limit for the lifetime of the NH_2 parent to be 2.7×10^4 s from observations of comet Kohoutek by reinterpreting the Haser scalelengths using the average random walk model (Combi and Delsemme 1980a) assuming the parent speed $v = 0.58\ r^{-1/2}$ km s^{-1}. If, instead, $v = 1.0\ r^{-1/2}$ is used, their lower limit reduces to 1.6×10^4 s, which is still a factor of about 3 larger than the NH_3 photodissociation lifetime. It has been suggested by Huebner *et al.* (1989) that NH_2 may come from polymers embedded in grains.

We obtained a lifetime for the C_2 parent at 1 AU of $(7.5 \pm 1.5) \times 10^4$ s. Huebner and Carpenter (1979) have calculated the photochemical lifetimes of C_2H_4 and C_2H_2. Possible reactions which may ultimately produce C_2 are:

(1) $C_2H_4 + h\nu \rightarrow C_2H_2 + H_2(or H + H); \tau = 2.1 \times 10^4$ s (98%)

(2) $C_2H_2 + h\nu \rightarrow C_2H + H; \tau = 1.0 \times 10^5$ s (74%)

(3) $C_2H_2 + h\nu \rightarrow C_2 + H_2; \tau = 3.7 \times 10^5$ s (20%)

(4) $C_2H + h\nu \rightarrow C_2 + H; \tau = 3.3 \times 10^4$ s (estimate, Schmidt et al., 1987)

Here the values in the parentheses are the branching ratios. If C_2 is produced by the reactions that take the path (1) followed by (3), the process takes at least 3.9×10^5 s. This time scale is 5 times larger than the lifetime observed for the C_2 parent(s). Therefore, we can probably exclude this process as a dominant production mechanism for C_2. In the case that C_2 is produced by the reactions (1), then (2), then (4), 1.5×10^5 s is required, which is two times longer than the lifetime we observed for the parent of C_2. The shortest process to make C_2 is process (4), but C_2H is very unlikely to be present in the comet nucleus, therefore, the most likely path is the process (2) followed by (4), which takes 1.3×10^5 s. We see then that both C_2H_4 and C_2H_2 take times about twice as long as the observed C_2 parent lifetime. We must remember, however, that the model fit to the observation is not very good near the nucleus which suggests that either C_2 may be the third generation or it has multiple parents, or both. Yamamoto (1981) and O'Dell *et al.* (1988) have shown that a Haser model for C_2 as the third generation fits very well with observations and therefore C_2 is likely the third generation of the original comet nucleus composition. C_2 may also come from dust grains. It is very likely that C_2 comes from several parent or grandparent molecules mostly from the nucleus and partly from dust.

DISCUSSION

C_2 and C_3 emissions have been shown to be weak with respect to CN in Giacobini-Zinner by Herbig (1976), and these results have been confirmed during the recent apparition by Schleicher (1985), Cochran and Barker (1987), and

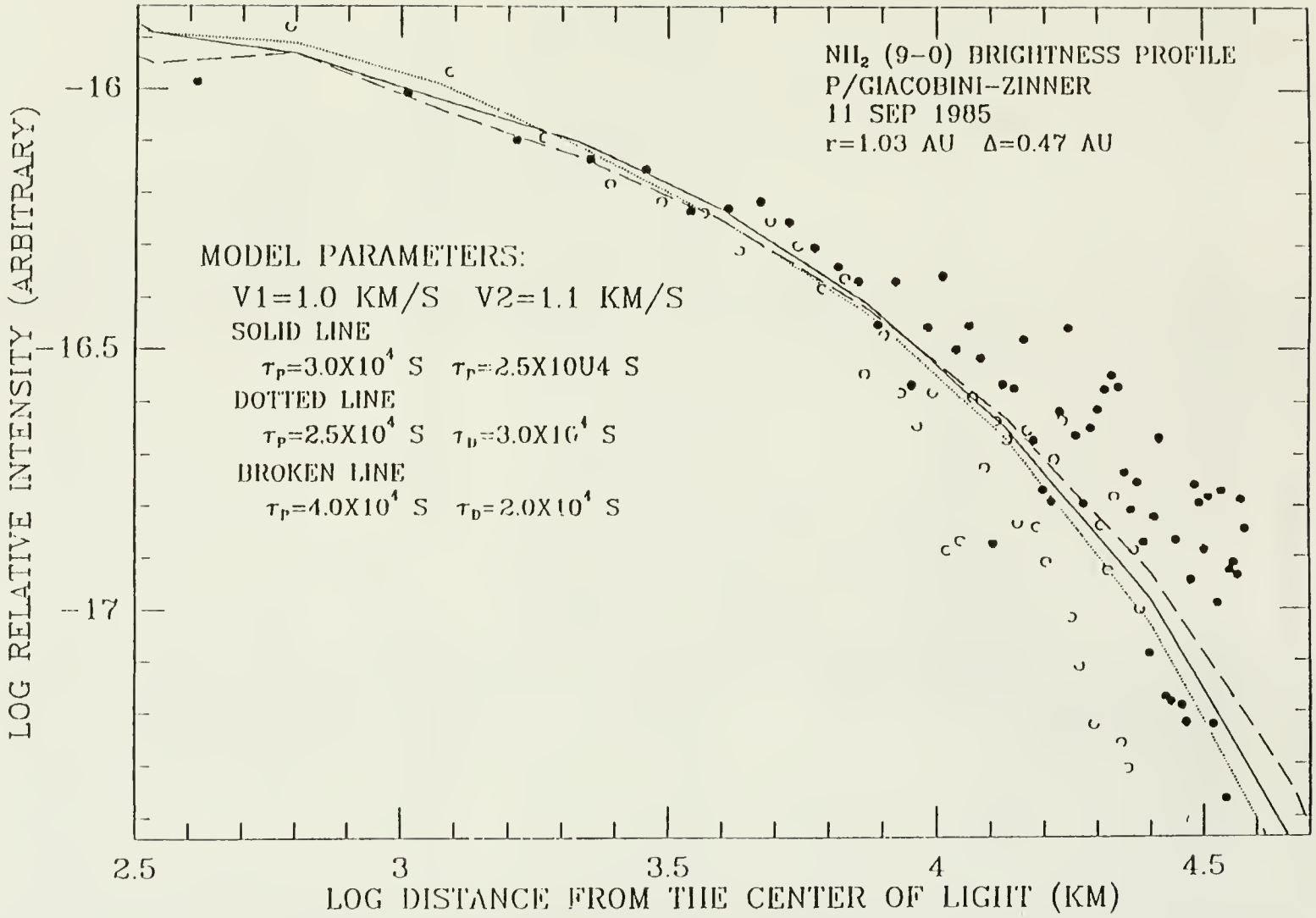


Figure 5. – Observed and calculated brightness profiles for NH_2. *open circles*: sunward profile; *filled circles*: tailward profile. *solid line*: best fit. Intensity is in orbitrary units.

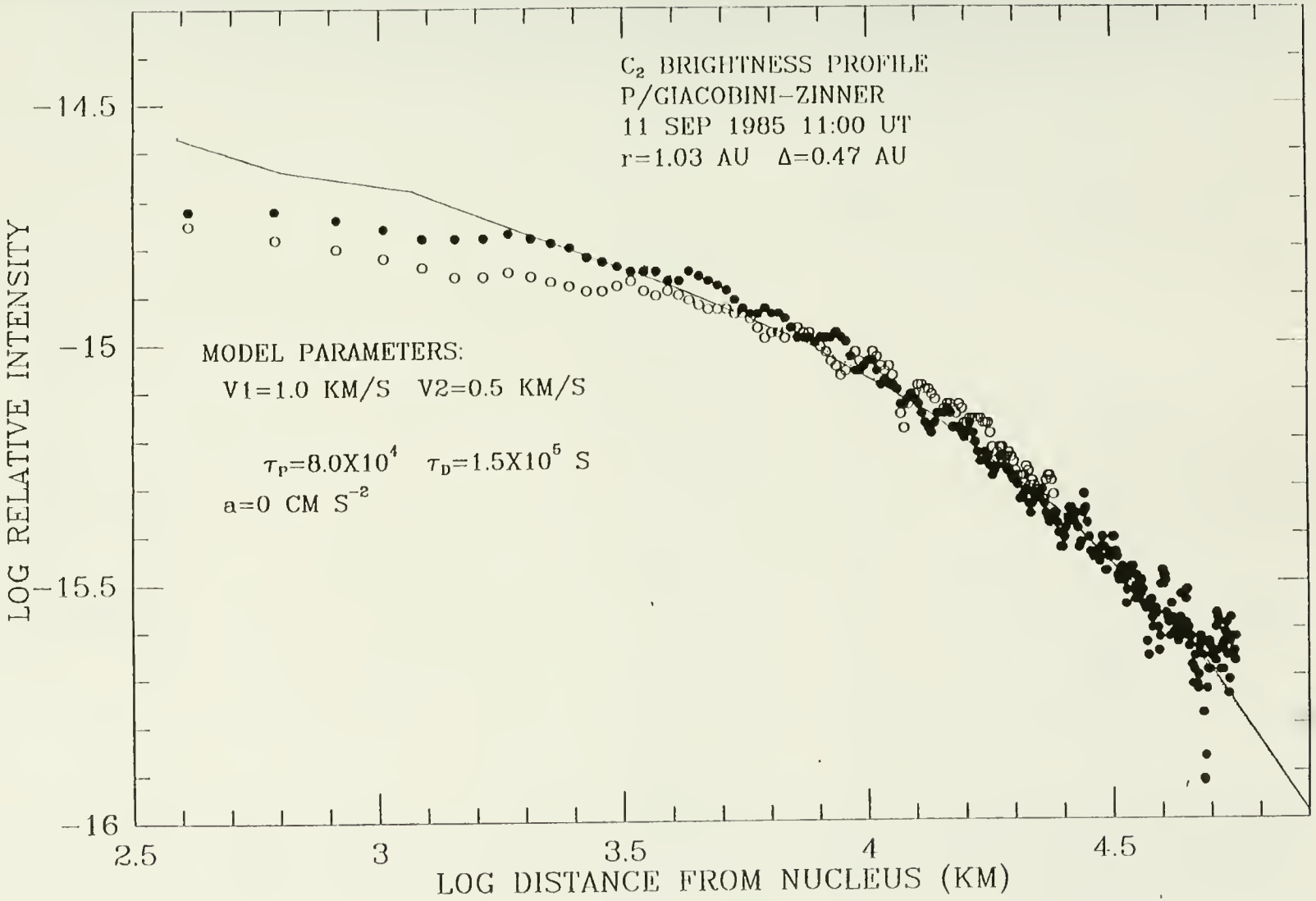


Figure 6. – Observed and calculated profiles for C_2. The circles and the line have the same meanings as in Figure 5. Intensity is in arbitrary units.

Schleicher *et al.* (1987). The production rates obtained in this work show that in Giacobini-Zinner, C_2 and NH_2 are depleted by a factor of 10 and 5, respectively, relative to H_2O compared with the values for an average comet obtained by Schleicher *et al.* (1987). Water production rates were obtained (see Figure 7) from the measurements of the [O I] 6300 Å line using the method developed by Spinrad (1985,1987). The water production rate for 11 September 1985 was found to be $(2.4 \pm 0.2) \times 10^{28}$ molecules s^{-1}, in agreement with the spacecraft results of $2\text{-}5 \times 10^{28}$ molecules s^{-1} by IUE and Pioneer Venus Orbiter (Stewart *et al.* 1985). The depletion of C_2 and C_3 in Giacobini-Zinner may be related to the low dust production rate. Wagner *et al.* (1987) have estimated the dust-to-gas mass ratio to be ~ 0.07, which is a factor of 3 lower than the average of the 17 comets observed by Newburn and Spinrad (1985). If dust grains are the source of observed C_2 and C_3 molecules, there may be a correlation between the dust-to-gas mass ratio and the relative abundances of carbon species. The data obtained by Newburn and Spinrad (1985) do not show an obvious correlation between the dust-to-gas mass ratio and the C_2/OH abundance ratio among the observed comets. In several comets, however, the abundance of C_2 does vary with the dust-to-gas mass ratio. Therefore dust may be responsible for at least part of the C_2 and C_3 production in some comets. But, since the method used to determine the dust-to-gas mass ratio in comets introduces an error of about a factor of three, it is difficult to derive the correlation between the dust-to-gas mass ratio and the production rates of any species. Comet Halley, however, has much higher C_2 abundance and its dust-to-gas mass ratio is in the range of 0.1 to 0.25 (Sagdeev *et al.* (1986), which is 3 to 8 times higher than Giacobini-Zinner. If dust grains are responsible for most of the production of C_2 and C_3 molecules, then the low production rates of these molecules in Giacobini-Zinner may be explained by the low dust production rate in this comet.

It was found that NH_2 is also depleted in Giacobini-Zinner. Wyckoff *et al.* (1988) have shown that NH_2 abundance is very low in comets they observed, suggesting the low NH_3 abundance in comets in general. As it was shown in the previous section, however, the lifetime for the NH_2 parent was found to be too long for NH_3 to be the parent. Therefore NH_2 seen in spectra of comets probably does not come from NH_3, which may be more abundant than found from the NH_2 abundance, but polymers embedded in dust grains, may be responsible for NH_2 in comet spectra. The low abundance of NH_2 in Giacobini-Zinner might also be related to the low dust-to-gas ratio in this comet.

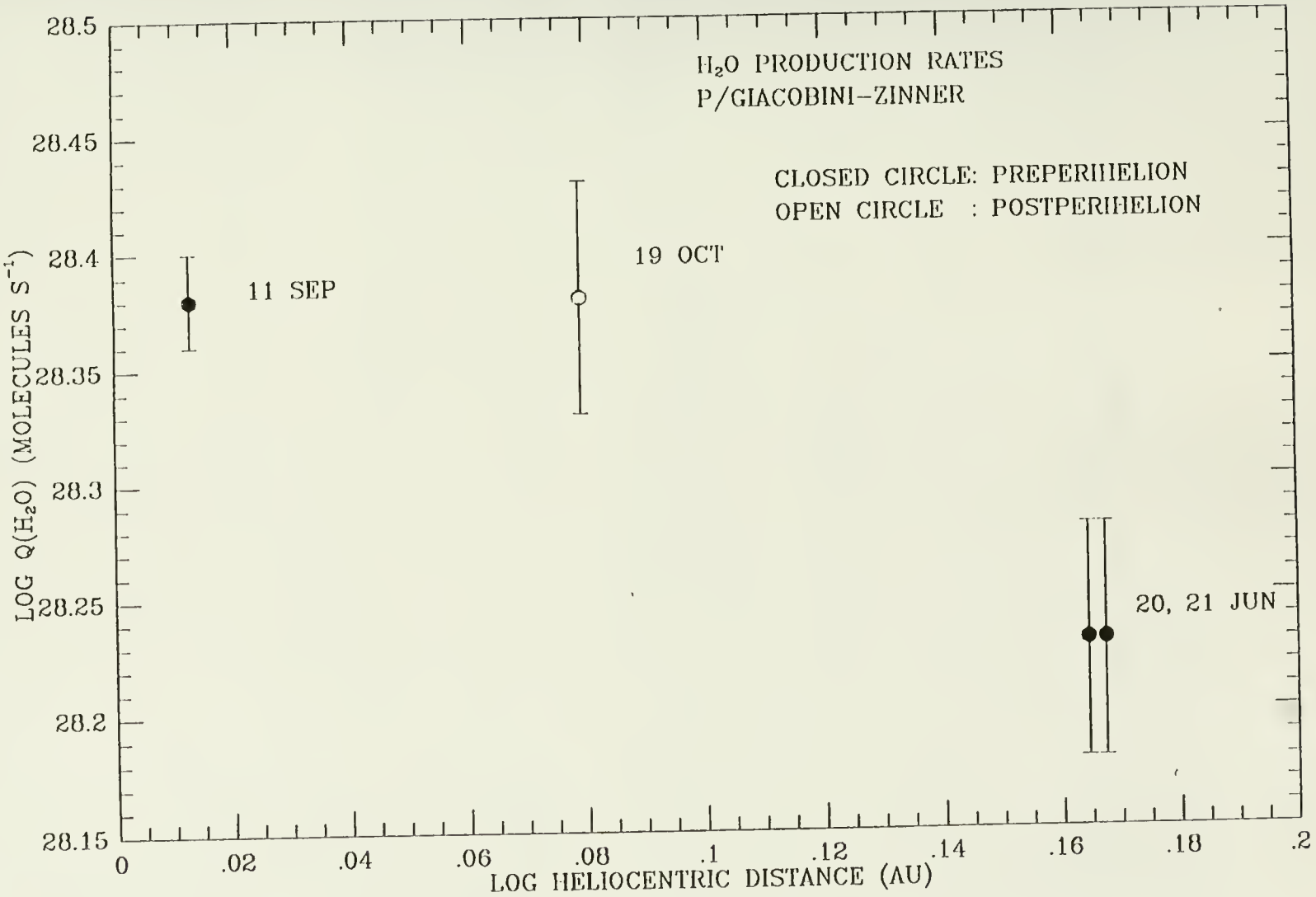


Figure 7. – Variation of water production rates for comet P/Giacobini-Zinner.

REFERENCES

A'Hearn, M.F.: Spectrophotometry of Comets at Optical Wavelengths. in *Comets*, ed. Laurel L. Wilkening, The University of Arizona Press, 1982, pp. 433-460.

A'Hearn, M.F.; and Millis, R.L.: Abundance Correlations among Comets. *A. J.*, vol. 85, 1980, pp. 1528-1537.

Cochran, A.L.; and Barker E.: Comet Giacobini-Zinner: A Normal Comet? *A. J.*, vol 92, 1987, pp. 239-243.

Combi, M.R.; and Delsemme, A.H.: Neutral Cometary Atmospheres I. An average Random Walk Model for Photodissociation in Comets. *Ap. J.*, vol. 237, 1980, pp. 633-640.

Cooper, D.M.; and Jones, J.J.: An Experimental Detection of the Cross Section the Swings Band System of C_3. *J. Quant. Spect. Rad. Trans.*, vol. 22, 1979, pp. 201-208.

Delsemme, A.H.; and Combi, M.R.: Neutral Cometary Atmospheres IV. Brightness Profiles in the Inner Coma of Comet Kohoutek 1973 XIII. *Ap. J.*, vol. 271, Aug. 1, 1983, pp. 388-397.

Feldman, P.D.; and Brune, W.H.: Carbon Production in Comet West (1975n). *Ap. J.*, vol. 209, 1976, pp. L45-L48.

Festou, M.C.; and Feldman, P.D.: The Forbidden Oxygen Lines in Comets. *Astron. Astrophys*, vol. 103, 1981, pp. 154-159.

Herbig, G.: Review of Cometary Spectra. In *The Study of Comets*. eds. B. Donn, M. Mumma, W. Jackson, M. A'Hearn, and R. Harrington (Washington: NASA SP-393), 1976, pp. 136-158.

Huebner, W.F.; and Carpenter, C.W.: Solar Photo Rate Coefficients. *Los Alamos Scientific Lab Report*, LA-8085-MS, 1979

Huebner, W.F.; Boice, D.C; and Korth, A: Halley's Polymeric Organic Molecules. *Advances in Space Research*, in print.

Luts, Barry L.: Fluorescence Efficiency Factors for Ionized Water Vapor. *Ap. J.*, vol. 315, no.2, April 15, 1987, pp. L147-L150.

Magnani, L.; and A'Hearn, M.F.: CO^+ Fluorescence in Comets. *Ap. J.*, vol. 302, 1986, pp. 477-487,

Newburn, R.L.Jr.; and Spinrad, H.: Spectrophotometry of Seventeen Comets. II. The Continuum. *A. J.*, vol. 90, no. 12, Dec. 1985, pp. 2591-2608.

O'Dell, C.R.; Robinson, Ronald R.; Swamy, K.S. Krishna; McCarthy, Patrick J.; Spinrad, H.: C_2 in Comet Halley: Evidence for Its Being Third Generation and Resolution of the Variational Population Discrepancy. *Ap. J.*, vol. 334, Nov. 1, 1988, pp. 476-488.

Sagdeev, R.Z.; Blamont, J.; Galeev, A.A.; Moroz, V.I.; Shapiro, V.D.; Shevchenko, V.I.; and Szegö, K.: Vega Spacecraft Encounters with Comet Halley. *Nature*, vol. 321, no. 6067, 15-21 May, 1986a, pp. 259-262.

Schleicher, D.G.: Ph.D. Dissertation, University of Maryland, 1983.

Schleicher, D.G.: *Bull. Am. Astron. Soc.*, vol. 17, 1985, p. 686.

Schleicher, D.G.; and A'Hearn, M.F.: Fluorescence of OH in Comets. *Ap. J.*, vol. 258, 1981, p. 864.

Schleicher, D.G.; Millis, R.L.; Birch, P.V.: Photometric Observations of Comet P/Giacobini-Zinner. *Astron. Astrophys.*, vol. 187, 1987. pp. 531-536.

Schmidt, H.U.; Wegmann, R.; Huebner, W.F.; and Boice, D.: Cometary Gas and Plasma Flow with Detailed Chemistry. *Computer Physics Communications*, vol. 49, 1988, pp. 17-59.

Spinrad, H.: Observations of the Red Auroral Oxygen Lines in Nine Comets. *Publ. Astron. Soc. Pacific*, vol. 94, Dec. 1982, pp. 1008-1016.

Spinrad, H.: Comets and Their Composition. *Ann. Rev. Astr. Ap.*, vol. 24, 1987.

Stewart, A.I.F.; Combi, M.R.; and Smyth, W.H.: *Bull. Am. Astron. Soc.*, vol. 17, 1985, p. 686.

Wagner, R.M.; Lutz, Barry L.; Wyckoff, S.: Groundbased Constraints on the H_2O^+/CO^+ Abundance Ratio and Dust Impact Rate in Comet P/Giacobini-Zinner: Comparison with the Spacecraft Results. *Ap. J.*, vol. 322, Mac. 1, 1987, pp. 544-548.

Wyckoff, S.; Tegler, S.; and Engel, L.: Ammonia Abundances in Comets. *Proceedings of 29th COSPAR*, 1989. in print.

Yamamoto, Tetsuo: On the Photochemical Formation of CN, C_2, and C_3 Radicals in Cometary Comae. *The Moon and the Planets*, vol. 24, 1981, pp. 453-463.

PHYSICAL PROCESSING OF COMETARY NUCLEI

Paul R. Weissman
Earth and Space Sciences Division
Jet Propulsion Laboratory

S. Alan Stern
Laboratory for Atmospheric and Space Physics, and
Department of Astrophysical, Planetary, and Atmospheric Sciences
University of Colorado

Abstract

Cometary nuclei preserve a cosmo-chemical record of conditions and processes in the primordial solar nebula, and possibly even the interstellar medium. However, that record is not perfectly preserved over the age of the solar system due to a variety of physical processes which act to modify cometary surfaces and interiors. Possible structural and/or internal processes include: collisional accretion, disruption, and reassembly during formation; internal heating by long and short-lived radionuclides; amorphous to crystalline phase transitions, and thermal stresses. Identified surface modification processes include: irradiation by galactic cosmic rays, solar protons, UV photons, and the Sun's T Tauri stage mass outflow; heating by passing stars and nearby supernovae; gardening by debris impacts; the accretion of interstellar dust and gas and accompanying erosion by hypervelocity dust impacts and sputtering; and solar heating with accompanying crust formation. These modification processes must be taken into account in both the planning and the interpretation of the results of a Comet Nucleus Sample Return Mission. Sampling of nuclei should be done at as great a depth below the surface crust as technically feasible, and at vents or fissures leading to exposed volatiles at depth. Samples of the expected cometary crust and near-surface layers also need to be returned for analysis to achieve a better understanding of the effects of these physical processes. We stress that comets are still likely less modified than any other solar system bodies, but the degree of modification can vary greatly from one comet to the next.

1. INTRODUCTION

It has become almost a matter of faith among solar system astronomers that "comets are the best obtainable source of original solar nebula material." There will be a temptation to quickly apply many of the new findings from a comet sample return mission to a description of the primordial solar nebula at the time the comets were forming. But, the comets, like every other solar system body we have studied with flyby and orbiter spacecraft, are evolved bodies. Over the history of the solar system comets have been subjected to a variety of physical processes which have modified them, admittedly much less than the larger planets and satellites, but still in very significant ways.

To fully understand and interpret the results of a comet sample return mission it is necessary to consider the target comet's complete physical and dynamical history, and the processes which have likely acted to modify it from its original "pristine" state. This is necessarily a statistical exercise, considering those "likely" processes which we can conjecture from our current understanding of the solar system, the Oort cloud, and the galaxy. One cannot foresee unique, low probability events in the history of any individual comet that might have modified it in some significant fashion, different from that generally experienced by the majority of other comets. Nor can we rule out that the comet itself is a unique body, formed (or captured) in some unique way that again does not represent the majority of the cometary population.

The situation has been additionally complicated recently by the suggestion that the source of the short-period (SP) comets is dynamically distinct from that of the long-period (LP) comets. Duncan et al. (1988) showed that SP comets dynamically evolved from the randomly oriented orbits of LP comets would preserve their random inclination distribution, contrary to the

relatively modest inclination, direct orbits which are observed. They have also shown that a more likely source for the SP comets is a flattened ring of $\sim 10^8$ to 10^9 comets beyond the orbit of Neptune, a remnant of the solar system's nebula accretion disc. They have named this the Kuiper belt, for Kuiper's (1951) suggestion that such an extended accretion disk might exist. Because the Kuiper belt is much closer to the Sun, the processing history of comets in the belt, which is partially if not totally within the Sun's heliosphere may be somewhat different than comets in the more distant Oort cloud.

A comet's evolutionary history can be broken into four distinct periods: 1) formation, presumably coincident with the formation of the Sun and planetary system; 2) initial processing, prior to ejection to the Oort cloud; 3) dynamical storage in the Kuiper belt or the Oort cloud at moderate to large solar distances for most of the history of the solar system; and 4) processing upon re-entry into the planetary system and the observable region, $r < 5$ AU. Each of these periods will be discussed below. In addition, the uncertainty associated with the various dynamical paths by which comets may evolve from the Kuiper belt or the Oort cloud to SP orbits, and the possible dynamical history of SP comets will be briefly examined.

Exactly what constitutes a "pristine" cometary nucleus has different meanings to different investigators. Even the interstellar medium prior to the comet's formation might not be considered truly "pristine" because of the complex chemistry that occurs when volatile ices condense on interstellar grains and are irradiated by UV photons and galactic cosmic rays (Greenberg and D'Hendecourt, 1985). Material in interstellar clouds has been processed in and by stars, shocked in supernova explosions, irradiated, etc., so it is meaningless to speak of truly pristine material. Given that the interstellar medium we observe today has already undergone similar processing, we will assume that condition as our starting point. It will be seen that the degree of modification as the comet forms and evolves can usually only be defined in a relative

sense. The object of this paper is to survey the possible physical processes, to rank them in relative importance, and to make recommendations regarding sampling strategies, leaving the detailed quantitative evaluation to future work.

2. COMETARY FORMATION

Hypotheses of cometary origin fall into two major categories (Weissman, 1985a): primordial hypotheses in which comets formed at the same time, and as part of the formation of the Sun and planets, and hypotheses in which comets are formed or captured episodically at essentially random times, often as a result of catastrophic processes, and possibly repeatedly over the history of the solar system. In general, the episodic hypotheses have not gained very wide acceptance, and will not be discussed further here (c.f. Bailey et al., 1986).

All primordial hypotheses agree on one basic fact: comets formed far from the Sun in the cooler regions of the solar nebula. The high volatile content of comets, largely in the form of ices, and the relatively small sizes of cometary nuclei, provide proof of that fact. Disagreement exists in just how far away the formation zone actually was. The suggestions range from the Uranus-Neptune zone at 20 to 30 AU from the Sun, to neighboring fragments of the proto-solar nebula, at distances of 10^4 AU or more.

Formation of comets among the outer planets was first suggested by Kuiper (1951) who noted that water ice would not condense any closer to the Sun than about Jupiter's orbit. But dynamical studies (Safronov, 1969; Fernandez and Ip, 1981) have shown that Jupiter and Saturn tend to eject the majority of the icy planetesimals in their zones to interstellar space, whereas Uranus and Neptune with their smaller masses and larger semimajor axes are more likely to place a sizeable fraction of planetesimals into distant bound orbits with dimensions $\sim 10^3$ to

10^5 AU or more, the region of the Oort cloud. Temperatures in the Uranus-Neptune zone are expected to have been $\leq$ 100 K during cometary formation, allowing volatile ices such as H_2O, CO, CO_2, NH_3, and CH_4 to condense and/or to be trapped as clathrate hydrates in the icy matrix (Delsemme, 1982).

According to the standard planetary formation scenario (Greenberg et al., 1984) ice and silicate grains in the infalling solar nebula descend to the equatorial plane of the nebula due to gas drag, forming an accretion disc. Agglomeration of grains leads to the growth of larger particles, both during the fall towards the nebula plane, and while circulating in the accretion disc (Weidenschilling, 1980), leading to growth of initial icy-conglomerate objects as large as 10 meters. When the density of material in the plane reaches a sufficient value, gravitational instabilities (Goldreich and Ward, 1973) lead to fragmentation of the disc and collapse into planetesimals several kilometers in dimension, within about 10^4 to 10^5 years after the start of nebula collapse. These objects were presumably the proto-comets. The total initial mass of planetesimals in the Uranus-Neptune zone is estimated to be on the order of 10 times the combined present masses of those two planets (Safronov, 1969; Lissauer, 1987). The proto-comets were ejected to the Oort cloud or to interstellar space by the growing proto-planetary cores.

The degree to which interstellar material is modified as it is brought together by the processes described above is highly uncertain. Infalling nebula material in the Uranus-Neptune zone may be moving inward with a velocity of a few km s^{-1}, and is likely slowed and shocked as it reaches the denser parts of the nebula around the accretion disc. This could raise the temperature of the material significantly, vaporizing icy particles and driving volatiles off of refractory grains. The degree of heating is also affected by the opacity of the accretion disc: how well it traps the heat generated at the shock boundary.

The grains cool rapidly as they begin to agglomerate and settle towards the nebula plane. The interparticle velocities at this point are very low, and material is brought together with relatively little compaction (Goldreich and Ward, 1973). This is expected to lead to a highly porous, low density, loosely bound structure composed of a heterogeneous mixture of ice and dust grains covering a wide range of particle sizes (Donn and Rahe, 1982; Greenberg, 1986).

The breakup of the accretion disc and collapse into planetesimals due to gravitational instabilities is also expected to be a relatively gentle process, with interparticle velocities on the order of only a few m s^{-1} at most. The total gravitational potential energy of a 10 km diameter icy conglomerate planetesimal is not enough to raise the average temperature of the material by even one Kelvin, when it is brought together with a mean density of 1.0 g cm^{-3}. Some local compaction and heating might be expected at interfaces where larger particles come together, probably resulting in a "welding" of the particles into a loosely bound agglomerate of icy chunks covering a fairly wide size range.

The precise structure of the cometary nucleus created in this fashion is still a matter of considerable debate. Figure 1 shows four suggested models for cometary nuclei (Whipple, 1950; Donn et al., 1985; Weissman, 1986; Gombosi and Houpis, 1986). Common features of all the models are the irregular shape of the nucleus, the heterogeneous mixture of icy and nonvolatile materials, and the existence of substantial voids within the nucleus. Differences exist over the exact degree and scale of the heterogeneity, and the degree to which the initial agglomeration of particles has been modified into a single, well compacted body. The initial nucleus structure will be important to its subsequent evolution, in particular to the way energy is deposited in, or liberated from the nucleus interior, and to its survivability against collisional destruction. Mixed in with the icy conglomerate material of the Uranus-Neptune zone will be some material formed closer to the Sun and then dynamically ejected by the growing proto-Jupiter and proto-Saturn.

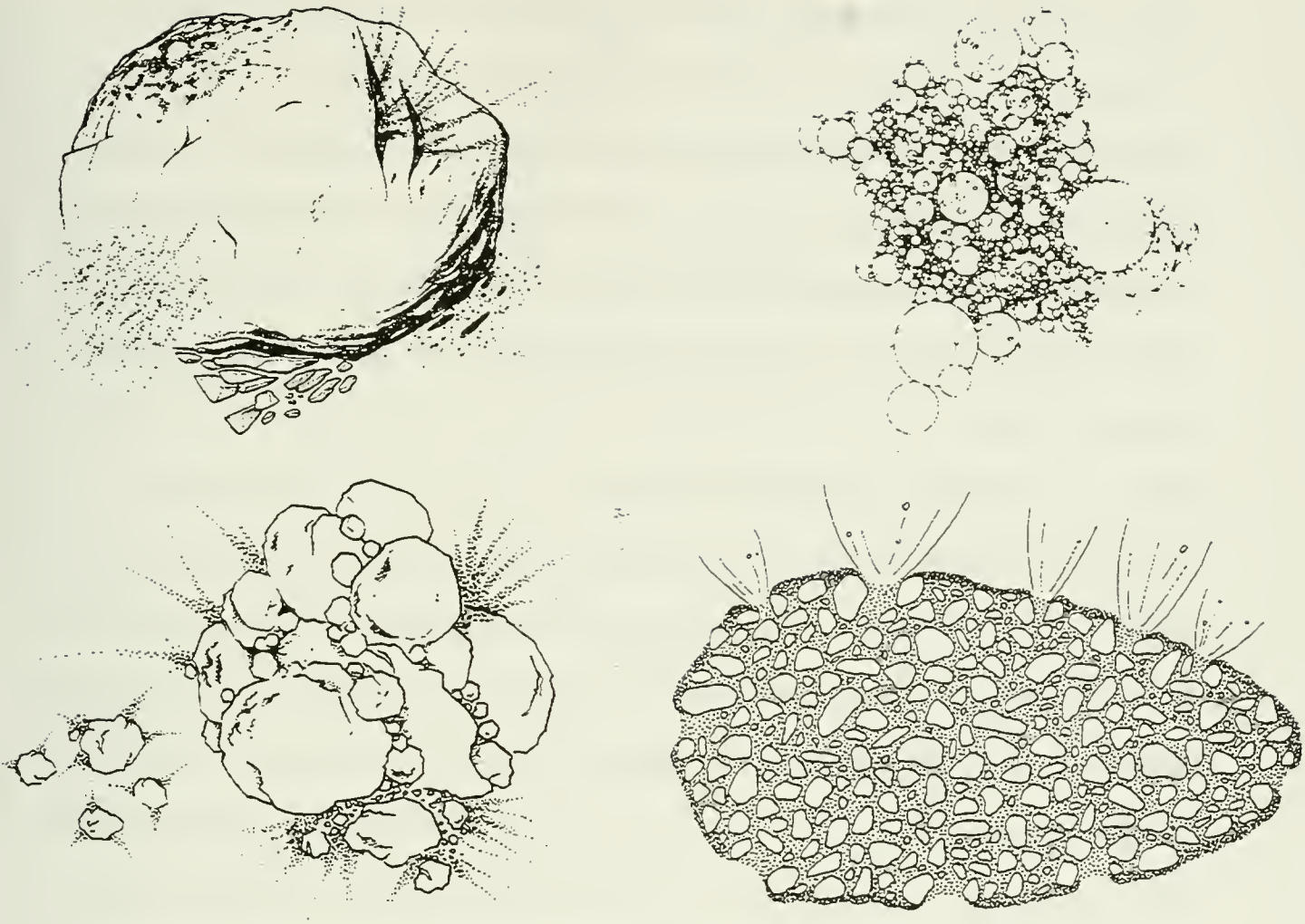


Figure 1. Four suggested models for the structure of cometary nuclei: a) the icy conglomerate model (Whipple, 1950); b) the fractal model (Donn et al., 1985); c) the primordial rubble pile (Weissman, 1986); and d) the icy-glue model (Gombosi and Houpis, 1986). All but d) were suggested prior to the Halley spacecraft encounters in 1986.

Some contamination might even be possible with material from the terrestrial planets zone, but it is likely that Jupiter will be a strong dynamic filter that ejects most of that material hyperbolically, rather than placing it in the Uranus-Neptune zone (material from the terrestrial planets zone approaches Jupiter with a high relative velocity as compared with the low velocity of material already in the Jupiter-Saturn zone, and thus has an even higher probability of dynamic ejection). Thus, any initial chemical differentiation in the solar nebula due to the radial temperature gradient will be blurred somewhat but will not be erased by dynamic exchange between different proto-planetary accretion zones.

Once the nuclei form they will continue to circulate in their orbits with low relative velocities. Collisions should initially be highly efficient in growing larger bodies. But as the larger accretion cores grow they will also serve to perturb the orbits of the remaining small icy planetesimals, increasing their relative velocities and decreasing the accretion efficiency. Higher velocity collisions will result in more destructive collisions, creating large amounts of debris which will quickly be swept up again by the planetesimals. Collisions which are not totally disruptive will result in crushing and compaction of the initial nucleus structure. The nuclei will thus likely go through a period of competing accretionary and destructive forces.

This process will slow when the runaway growth of one of the planetary embryos becomes sufficient to start ejecting comets to inner Oort cloud distances, on the order of 5×10^3 AU. At those distances galactic and stellar perturbations will be able to detach the proto-comets' perihelia from the Uranus-Neptune zone and make them semi-permanent residents of the inner Oort cloud. As material was either ejected or incorporated into the proto-planetary cores, the density of planetesimals remaining in the planetary zone would drop dramatically and collisional evolution would decrease accordingly.

Alternative hypotheses place the formation zone for the cometary nuclei farther from the

Sun. Among the attractive features of such hypotheses are the facts that the nebula material will undergo less heating prior to being incorporated into the icy planetesimals, and that subsequent evolution will also likely be milder with lower collision rates and collision velocities between planetesimals, and less acceleration of velocities since no large proto-planets grew (as far as we know) beyond the Uranus-Neptune zone. The principal drawback of these hypotheses involves the difficulty of bringing 10 km sized icy planetesimals together at large solar distances in a reasonable period of time.

One suggestion (Cameron, 1962, 1978) is that the nebula accretion disc did not stop at the orbit of Neptune, but rather extended out several hundred AU or more. The lack of giant planets beyond Neptune (Pluto is presumed to be an example of the largest icy conglomerate body to grow in its zone) was not a result of the nebula disc running out of material, but rather of it running out of sufficient time to build a giant planet. Accretionary times are dependent on the orbital period as well as the density of material, both of which act against planet building processes in the outer solar system.

Observational support for this concept has come from the IRAS discovery of dust shells around some young main sequence stars in the solar neighborhood (Aumann et al., 1984). An optical photograph of the β Pictoris disc edge-on (Smith et al., 1988) shows a flat disc extending up to 10^3 AU from the star, with a maximum thickness of about 50 AU. Estimates of the mass of these discs range from a minimum of $\sim$ 15 Earth masses ($M_\oplus$), to possibly 200 to 300 $M_\oplus$ if an asteroidal size distribution can be assumed.

This extended accretion disc is expected to become the Kuiper belt of comets beyond Neptune, as proposed by Duncan et al. (1988). However, some comets in the belt will be perturbed to Neptune and Uranus crossing orbits, and along with the comets formed in that zone will be ejected on long-period orbits. Duncan et al. (1987) showed that once the semimajor axes

of orbits reached about 5 x 10^3 AU, galactic and stellar perturbations would raise the perihelia of the orbits and gravitationally detach them from the major planets. Comets initially ejected to distances greater than 2 x 10^4 AU would form the primordial Oort cloud. However, most of those comets will be lost over the history of the solar system due to major perturbations from stars and giant molecular clouds in the galaxy (Hut and Tremaine, 1985). The outer Oort cloud will be replenished by comets from the inner Oort cloud reservoir, those comets initially ejected to orbits between 5 x 10^3 and 2 x 10^4 AU. They will be pumped up to the outer cloud by the same major perturbations that strip comets from the outer Oort cloud (Fernandez, 1985; Weissman, 1985b; Shoemaker and Wolfe, 1986).

An entirely different formation process involves differential radiation pressure on distant nebula fragments, perhaps 5 x 10^3 AU from the forming proto-Sun (Whipple and Lecar, 1976; Hills, 1982; Cameron, 1985). Because of the opacity of the nebula fragments, they will feel a net radiation pressure from the proto-Sun, forcing material together. At some point the density of the fragment will rise sufficiently for self-gravity to take over and for the fragment to collapse to form the proto-comet. In this manner comets could be formed in isolation and very cold, with virtually no processing of material from its primitive interstellar state.

The suggestion has also been made that distant nebula fragments may form their own, less massive accretion discs, in which comets would form within a relatively benign environment (Cameron, 1973). Or perhaps the comets formed in neighboring nebula fragments around other stars in the same open cluster in which the Sun formed. Initial relative velocities between the stars might be $\leq$ 1 km s^{-1}, low enough to allow capture of comets from the other stars (Donn, 1976).

There is no good way at present to discriminate between these various hypotheses. Each has its particular strong points and advocates, and each its weak areas and detractors. Comets

may be a direct consequence of planetary formation in the outer solar system, or they may be a largely unrelated by-product of far more distant nebula processes. Most likely, a fraction of the present day comets may have formed through each of the suggested processes, and what we observe is a truly heterogeneous mixture of material from different formation sites and with different degrees of physical processing.

Some attempts have been made to look for "cosmic thermometers" in comets that might indicate the heliocentric distance of their formation zones, or isotopic anomalies that could be interpreted as evidence for formation elsewhere in the galaxy. In the case of the former, observations of S_2 in comets have been put forward as evidence for a low temperature formation, $T < 25$ K (A'Hearn and Feldman, 1985). Also, measurement of the ortho-para ratio for water vapor in Comet Halley by Mumma et al. (1988) found values of 2.2 - 2.3, interpreted as implying a nuclear spin temperature of 25 K. This, in turn, was interpreted as implying the temperature in the Halley formation zone, placing it beyond the Uranus-Neptune zone, possibly in the Kuiper belt. Similar measurements for Comet Wilson, a dynamically new comet from the Oort cloud found a higher ortho-para ratio of 3.2, consistent with statistical equilibrium. Mumma et al. interpret this higher value as a resetting of the ortho-para ratio in the comet's outermost layers by cosmic ray bombardment while the object was resident in the Oort cloud. However, this is still a relatively new technique and both the Halley and Wilson interpretations need to be checked against the statistics of a larger number of objects.

As for isotopic ratios, Eberhardt et al. (1987) measured the deuterium-to-hydrogen ratio in Comet Halley from the Giotto spacecraft and found a value of $0.6 \times 10^{-4} \leq D/H \leq 4.8 \times 10^{-4}$. This range of values, shown in Figure 2 along with D/H measurements for other solar system and galactic reservoirs, is comparable to that for the Earth's oceans and for primitive meteorites, possibly indicating a related origin. Eberhardt et al. also measured the $^{18}O/^{16}O$ ratio in Halley

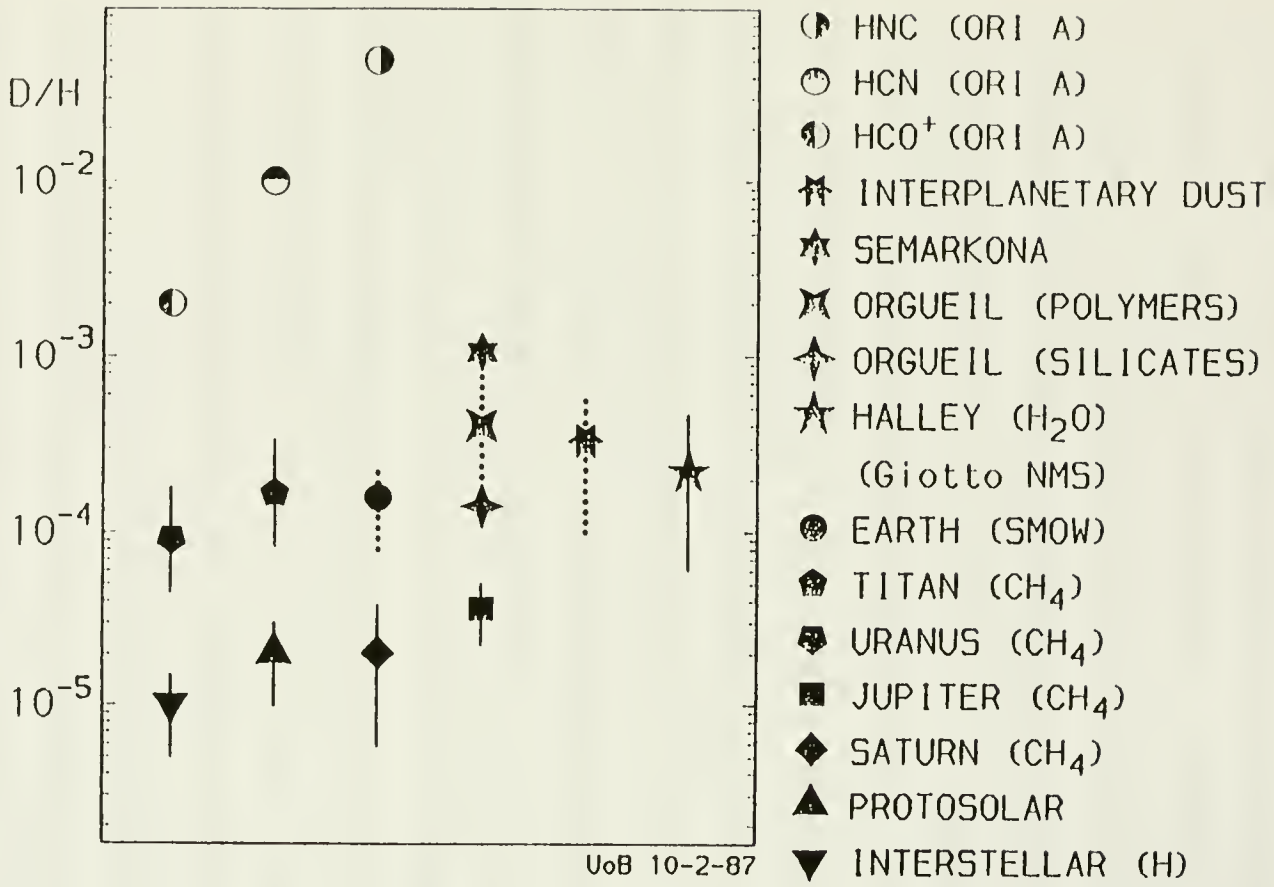


Figure 2. Deuterium/hydrogen ratios as measured for Comet Halley by the Giotto spacecraft, as compared with other solar system and galactic reservoirs (Eberhardt et al., 1987).

and found a value of 0.0023 ± 0.0006, in agreement with the terrestrial value of 0.00205. Both the D/H and $^{18}O/^{16}O$ ratios suggest that comets formed out of material that was isotopically similar (if not identical) to the solar system. Similarly, early measurements of the $^{12}C/^{13}C$ ratio in comets yielded values around 100, close to the terrestrial value of 89 (Vanysek and Rahe, 1978). However, spectral measurements of the $^{12}C/^{13}C$ ratio in Comet Halley (Wyckoff et al., 1989) found a somewhat lower value of 63 -65, less than the terrestrial value but comparable to that for interstellar clouds near the Sun. At the same time Wyckoff et al. found nitrogen isotope ratios > 200, consistent with the bulk solar system value of 250. Thus, most isotopic evidence gives a good match to terrestrial and/or solar system values, but there are still unexplained differences.

3. INITIAL PROCESSING OF COMETARY NUCLEI

Following their formation, however it might occur, the cometary nuclei will undergo warming due to long and short-lived radionuclides mixed in with the other nonvolatiles. A study of the internal temperatures of icy satellites and planetesimals in the outer solar system by Lewis (1971), assuming a chondritic composition diluted 3:1 by ices and with K, U, and Th as radioactive heat sources, and no solar heating, found that the internal temperatures of objects < 300 km in radius would be < 25 K. That study assumed a thermal conductivity typical of solid water ice, considerably higher than the conductivities suggested for cometary interiors. However, assuming more reasonable conductivities would still result in very little internal heating for bodies < 30 km in radius (about five times the mean radius of the nucleus of Comet Halley).

However, if short-lived radionuclides are present, then the results can be very different.

^{26}Al with a half-life of 7.4 x 10^5 yr has been suggested as an early solar system heat source, and evidence for it has been found in inclusions in carbonaceous chondrites. If similar concentrations were incorporated into the comets, then, assuming a low thermal conductivity, it would be possible to melt the interiors of nuclei greater than 3 to 6 km in radius (Wallis, 1980; Prialnik et al., 1987). This could lead to an interesting nucleus structure, melted and refrozen at the center, and least modified in the near surface layers. Such a comet may display interesting changes in behavior as it aged and the outer layers sublimed away.

Or, it may be that the cometary formation process took long enough that short-lived radionuclides were exhausted before they could be buried in large (kilometer sized) bodies. However, planetesimal formation times in the outer solar system are estimated to be $\sim 10^4$ to 10^5 years, and so ^{26}Al likely has played some role in the early internal heating of the cometary nuclei, at least those formed in or near the planetary region.

One stage in the cometary formation process that has received very little attention to date is the effect of the Sun's T Tauri phase on the comets. This period is characterized by the development of a very strong stellar wind and substantial mass outflow, presumably clearing away the remnants of the solar nebula. Already formed planetesimals and planetary embryos will likely survive this period, but all gas and fine dust will be swept away. The T Tauri stage is expected to begin within $\sim 10^6$ years of the initial nebula collapse, and thus favors hypotheses which lead to rapid giant planet formation. That time scale is much less than the very long dynamical clearing times for planetesimals in the Uranus-Neptune zone. Thus, most comets will likely still be relatively close to the Sun and will suffer considerable near-surface modification as a result of the intense solar wind. The modifying processes will be similar to the irradiation by galactic cosmic rays in the Oort cloud (see section 4 below) which causes sputtering of volatiles and polymerization of hydrocarbons in the upper several meters of the

nucleus surface. Even if comets formed farther from the sun, the T Tauri stage may still result in significant physical modification. As noted above, this is an area that deserves further study.

A second area that has received relatively little consideration is the collisional evolution of the cometary nuclei in the Uranus-Neptune zone prior to their ejection to the Oort cloud. As described above, the growth of planetary embryos in that zone will accelerate the remaining cometesimals, raising encounter velocities and causing a transition from accretionary to disruptive collisions. Low velocity collisions can be expected to cause compaction at contact interfaces and some local heating (Donn and Meakin, 1988), while high velocities will result in shock, intense heating, and fragmentation. By the time the nuclei are finally ejected to the Oort cloud they will likely have been disrupted and reassembled several times, resulting in a chaotic collection of collisionally processed and unprocessed materials. Clearly, this area merits further study as well.

4. DYNAMICAL STORAGE IN THE OORT CLOUD

At first glance, the Oort cloud would appear to present a relatively benign environment. The average spacing between comets is on the order of 15 AU or more in the outer, dynamically active cloud, and about 1 AU in the inner Oort cloud. The maximum surface temperature on cometary nuclei 10^3 AU from the Sun is only 13 K; comets at greater distances would be even colder.

However, four physical processes have been identified which modify the outer layers of cometary nuclei while they are in the Oort cloud. These are: irradiation by galactic cosmic rays and solar protons, heating by luminous passing stars and supernovae, gardening by debris impacts within the Oort cloud, and accretionary and erosive interactions with the interstellar

medium. As described below, each of these processes acts on the outermost 0.2 - 20 meters of all comets in the Oort cloud.

The study of radiation bombardment of icy surfaces has been undertaken in a number of laboratories (Shulman, 1972; Lanzerotti et al., 1978; Greenberg, 1982; Moore et al., 1983; Lanzerotti, 1983; Draganic and Draganic, 1984; Calcagno et al., 1985; Johnson et al. 1987; and Thompson et al., 1988). Energetic particles penetrate the nucleus surface to a depth which depends on both the energy of the particles and the density of the nucleus surface layers. Assuming a unit density material, low energy solar protons of a few, to a few hundred KeV penetrate only the first millimeter of surface or less; cosmic ray protons with typical energies $\sim$ 2 MeV penetrate about one meter. Since penetration depth goes inversely as density, lower density ices suffer damage to proportionately greater depth. The compositional and structural evolution occurs in the uppermost $\sim$ 100 g cm^{-2} of the cometary surface layers.

The effect of the irradiation is to break chemical bonds, producing volatile free radicals, some of which recombine to form a dense, dark polymer which is far less volatile than the original material, and some of which provide a latent energy source when the ices are warmed. Polymerization occurs particularly if hydrocarbons (e.g., CH_4, NH_3) are present. At the nucleus surface the energetic particle bombardment results in a net erosion by sputtering, and likely escape of the more volatile species, leaving behind a low volatility residue. At depth the volatiles are retained, but changed. One important result is the development of nonvolatile crusts (also sometimes referred to as mantles) on comets while they are still in the Oort cloud and before they ever enter the planetary region. This crust may begin the process of sealing off the nucleus surface against sublimation, well before the expected crustal development from solar heating during perihelion passage (see section 6, below).

Comets in the Kuiper belt likely experience a less intense cosmic ray processing history

than those in the inner and outer Oort cloud. Because the expected location of the Kuiper belt is partially, if not totally, within the Sun's heliosphere, the comets are likely shielded from the full effect of galactic cosmic rays. Thus, the degree of processing at depth will be somewhat less than that for the more distant Oort cloud comets.

The second process which acts to modify cometary surfaces in the Oort cloud is the passage of luminous stars through or near the cloud (Stern and Shull, 1988). It has long been recognized that random passing stars regularly penetrate the Oort cloud (Weissman, 1980). This process results in the ejection of comets close to the path of the passing star ($\sim$ 500 AU for one $M_\odot$ stars), diffusion of comets from the inner cloud to the outer cloud, and the randomization of orbits in the outer cloud. Stern and Shull (1988) calculated the importance of such encounters for the heating of comets in the cloud. They found that although the number of stellar encounters with the Oort cloud (several times 10^3) is dominated by solar type stars and white dwarfs, these stars are not sufficiently luminous to heat a significant fraction of the comets. Also, the effective ejection radius for solar mass stars exceeds the heating radius.

However, luminous O and supergiant stars were found to be capable of heating the entire Oort cloud to temperatures sufficient to induce selective mobilization of species such as CO, Ar, Ne, and CH_4 in the outermost layers of the nuclei. For example, a typical O star with luminosity 5 x 10^5 $L_\odot$ can heat all the comets in the Oort cloud to $\sim$ 20 K from about a parsec away. At such distances, its gravitational perturbations on the cloud are modest. Such encounters typically last a few times 10^3 years and can raise the temperature of cometary surfaces to between 16 and 24 K. Because vapor pressures are exponential in their temperature dependence, this temperature regime contrasts sharply with the ambient background temperature of 5 - 6 K in the Oort cloud between luminous star encounters. Stern and Shull estimated that there has been a 100% probability of an encounter with a luminous star which raised the Oort

cloud to 19 K, and a 10% chance of an encounter which heated the cloud to 34 K.

Stern and Shull also estimated the effects of nearby supernovae on Oort cloud heating. They found that a Type I supernova exploding at 19 parsecs can raise comet surface temperatures to 30 K. Using supernovae luminosity and formation rate statistics (Tammann, 1982; Narayan, 1987), it was found that all comets in the Oort cloud have been heated by supernovae to 50 K, and that there is a 50% probability that they have been heated to 60 K. Stern and Shull's results are summarized in Figure 3. Although supernovae can heat comets to higher temperatures than O stars, supernova events last only a few weeks. The thermal skin depth during a typical 3×10^3 year stellar encounter with a luminous O star is 20 to 140 meters, depending on the porosity and the amorphous/crystalline nature of the surface ices. Supernova encounters, while hotter, are briefer (about 10^7 sec); therefore, their heating pulse is estimated to propagate only 0.1 to 1 meter into the comets. Heating of Kuiper belt comets by passing stars and supernovae will likely not be significant since their closer distance to the Sun already warms them to comparable temperatures.

Collisions between comets, and between comets and small debris in the Oort cloud, is the third process affecting their evolution (Stern, 1988). A characteristic collision velocity in the inner Oort cloud is $\sim$ 1 km s^{-1}. Although individual comet-comet collisions were found to occur every few months in the inner Oort cloud and every few centuries in the outer cloud, less than one comet in 10^4 suffers such a collision over the age of the solar system. However, using constant area and constant mass per bin power-law size distributions, bracketing the size distribution for main belt asteroids, Stern showed that collisions between comets and small debris in the Oort cloud occur quite frequently. Such collisions provide a strong feedback mechanism for the production of additional small debris in the Oort cloud. For comets in the inner Oort cloud the frequency of collisions is sufficient to have overturned the entire surface several times

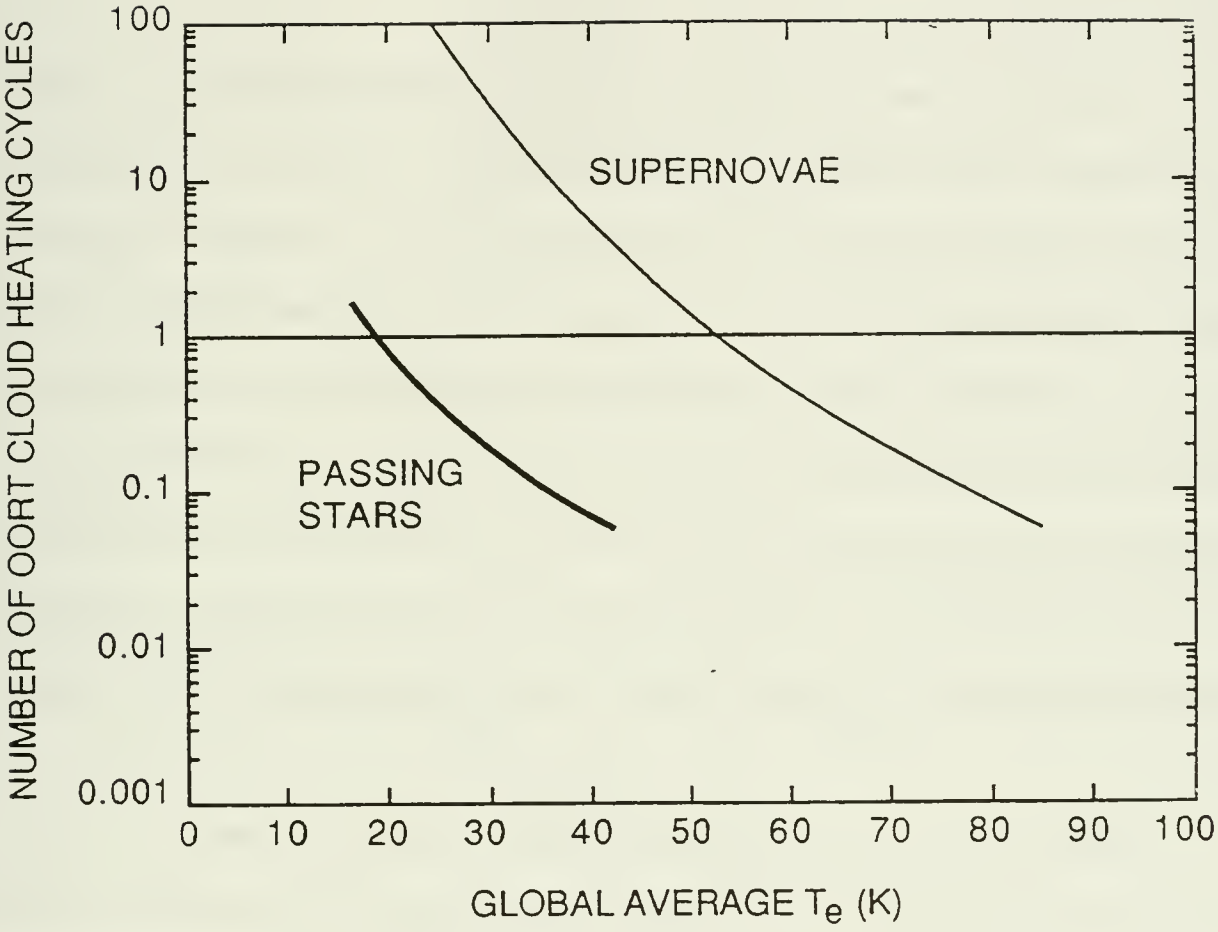


Figure 3. Fraction of comets heated by all types of passing stars as a function of processing temperature (heavy curve); all comets have been heated to ~ 16 K, and there is a 10% chance that the cloud may have been heated to ≥ 34 K. Fraction of comets heated by supernovae as a function of T during encounters (light curve); all comets have been heated to ≥ 45 K, and there is a 10% chance that a supernova has occurred close enough, < 8 parsecs, to heat the Oort cloud to ~ 60 K. A surface emissivity of 0.8 and an albedo of 0.05 were assumed. Adapted from Stern and Shull (1988).

to a depth of 0.5 to 5 meters (assuming a surface density of 1 g cm^{-3}), thereby promoting regolith development during residence in the Oort cloud. Collision rates in the Kuiper belt may even be higher.

The fourth and final processes known to cause cometary evolution in the Oort cloud is the interaction of comets with the interstellar medium (ISM). O'Dell (1971) investigated the accretion of interstellar dust and gas and found that a layer of 10 - 100 micrometers thickness would be built up over a period of 4.5×10^9 years. It had been speculated (Whipple, 1978) that this layer of interstellar volatiles accounted for the anomalous brightness of dynamically new LP comets on their first pass through the planetary region. However, Stern (1986) showed that erosion due to hypervelocity dust impacts is some 700 to 1000 times more efficient than gas accretion, causing comets to actually loose material due to the ISM interaction. The rate and energy of the impacts is controlled by the Sun's peculiar velocity through the ISM, $\sim$ 20 km s^{-1}.

A more recent and comprehensive study which includes grain erosion, accretion due to molecular sticking, gas sputtering, and thermal evaporation due to grain impacts, and which employs a realistic model of the various gas and cloud phases of the ISM, including giant molecular clouds, has been completed (Stern 1989). Taking into account the results of laboratory studies of micro-cratering in ices (Cintala, 1981; Croft, 1982; Lange and Ahrens, 1987), Stern found that erosion causes comets in the Oort cloud to lose 1.0 to 5.0 meters of surface material (for a density of 1.0 g cm^{-3}) over 4.5×10^9 years (Figure 4). Thus, erosion may remove some or all of the radiation and heat processed crust on the cometary surfaces.

On the other hand, recent laboratory experiments simulating capture of cometary dust grains during high speed spacecraft flybys have suggested that impacts into a very low density, "fairy castle" surface structure may lead to intact capture of the particles, with little net mass

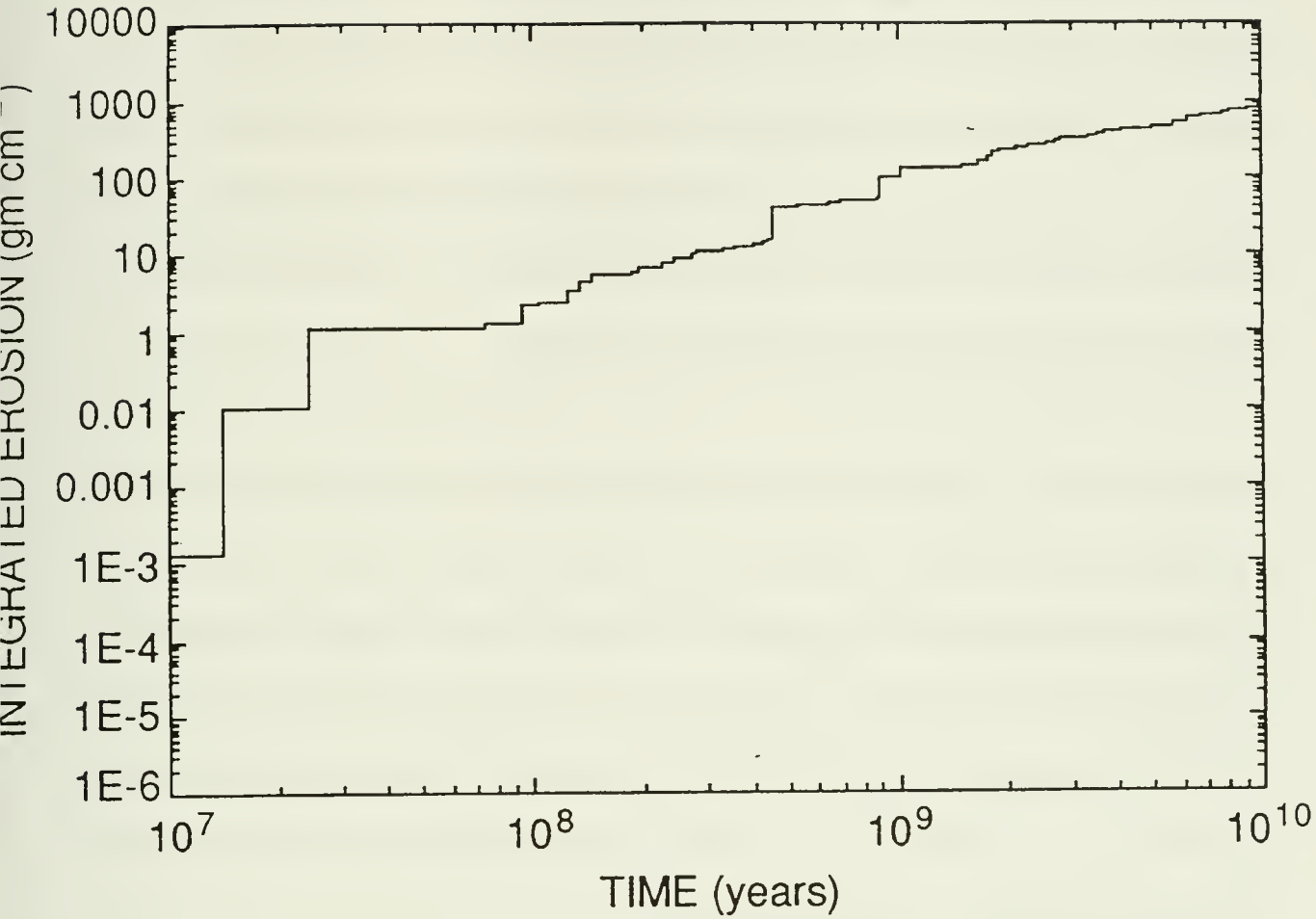


Figure 4. Integrated surface mass loss due to hypervelocity dust impacts experienced by comets and other debris in the Oort cloud, as described by Stern (1989). This model assumes an icy cometary surface and a four-phase ISM consisting of coronal gas, warm H I gas, and atomic and molecular clouds distributed in proportion to their galactic volume filling factors is assumed. The greatest erosion results from passages through giant molecular clouds.

loss (Tsou et al., 1984). The experiments have generally been done for relatively modest velocities, on the order of a few km s^{-1}. Whether or not the same effect would be true for the 20 km s^{-1} or more velocity expected for interstellar grains is open to some doubt. But it is possible that continued experiments might show that the erosion is not as significant as described above, and that there is, in fact, a net mass gain, as well as a slow compacting of materials, in the surface layers of cometary nuclei (Ostro et al., 1986).

It is clear that the Oort cloud is not just a storage bin in which comets reside in suspended animation. Instead, a number of important effects operate in an interrelated manner to evolve cometary surfaces. In addition to the four modifying processes discussed here, there may be other as yet undiscovered processes which affect the comets during their long residence in the Oort cloud. For example, creep of icy materials in the weak cometary gravitational field may lead to a compacting and densification of the nucleus. Thus, although comets may be ejected to the Oort cloud as low density, fractal-structured objects, they may return after 4.5 Gyr as single, well compacted nuclei with a density more typical of ordinary water ice, or at least a compacted snow bank.

5. THE SOURCE OF THE SHORT-PERIOD COMETS

There are a variety of dynamical paths that a LP comet might take from the Kuiper belt, or the inner or outer Oort clouds, to become a visible SP comet. The relative efficiencies of the different paths vary by orders of magnitude, but because of the very large number of comets in the Oort cloud reservoir, any of the major paths discussed below have a finite probability of producing a particular SP comet.

Put another way, it is not possible to integrate the orbit of a known SP comet backwards

in time to learn how it evolved into the planetary system. Small errors in the initial orbit determination or in the masses of the perturbing planets, unpredictable nongravitational forces from jetting of volatiles on the nucleus surface, and other unmodeled forces lead to a monotonic growth of uncertainty as the orbit is integrated backward.

Thus, the problem is limited to probabilistic arguments based on the relative efficiency of the various dynamical paths. In addition to evolution inward from the Kuiper belt, two other dynamical routes have been identified for the origin of the SP comets: 1) repeated perturbation of dynamically new LP comets from the Oort cloud passing through the observable region (Everhart, 1969); or, 2) repeated perturbation of dynamically new LP comets with perihelia in the Jupiter-Saturn zone, with a final dumping of cometary perihelia into the terrestrial planets zone (Everhart, 1972). The advantage of the second path over the first is that it allows comets to spend most of their dynamical evolution at solar distances where water ice sublimation is negligible, preserving the comets physically so that they are still active when they become SP comets. However, both paths are estimated to be a factor of 10^2 to 10^3 less efficient than the Kuiper belt for producing SP comets (Fernandez, 1980; Bailey, 1983).

Once deposited in a SP orbit, through whatever dynamical path, a comet will continue to random walk in both perihelion distance and semimajor axis as a result of planetary perturbations. For example, Monte Carlo studies of the evolution of meteoroids in the planetary region (Arnold, 1965) showed that 82% of all meteors which struck the Earth had at one time or another been within Mercury's orbit. To first order, those studies are equally applicable to the random walk of SP comet orbits. Similar evidence can be found among the observed SP comets. Since its discovery in 1902, periodic comet Grigg-Skjellerup has evolved from an initial perihelion distance of 0.753 AU, to 1.003 AU in 1967, and 0.989 AU currently (Marsden, 1986). Even more dramatic is the case of comet P/Lexell. It was discovered in 1770 when it

approached to within 0.015 AU of the Earth, with an orbit perihelion of 0.67 AU. Integration of the orbit backwards in time (Kazimirchak-Polonskaya, 1972) showed that Lexell had passed within 0.02 AU of Jupiter in 1767, and had previously had a perihelion of about 3 AU. After two passages around the Sun in its new orbit, the comet re-encountered Jupiter in 1779 at a distance of 0.0015 AU (half the radius of Io's orbit) and was perturbed to a new orbit with a perihelion beyond Jupiter's orbit.

Thus, for any observed SP comet, it is impossible to say where in the solar nebula it formed, and where it has been since the time of formation. A comet could have spent a part of its past in the inner solar system, then have been returned to the Oort cloud, and subsequently evolved back into the planetary region a second time. The fact that a comet's current perihelion is relatively large is no proof that the comet has not been much closer to the Sun in the not too distant past. Similarly, comets which presently have small perihelia may be recently arrived at those close solar distances, and may not yet have been heated very deep within the nucleus.

A possible example of the latter is P/Wild 2. The comet was deposited in its present orbit with a perihelion of 1.49 AU by a 0.0061 AU encounter with Jupiter in 1974 (Carusi et al., 1985). Prior to that time the comet had a perihelion near Jupiter's orbit. Integration of the orbit further backwards shows it being captured from a near-parabolic orbit about 400 years ago. However, as described above, such integrations are not reliable. They provide a representative example of possible cometary motion, rather than a detailed reconstruction of it.

6. RETURN OF COMETS TO THE PLANETARY REGION

When cometary nuclei return to the planetary region as LP and SP comets, their physical

evolution is dominated by the heating they receive from direct solar radiation. Other processes such as irradiation by solar wind protons and impacts by interplanetary dust particles will also intensify with decreasing heliocentric distance, but they do not compare in either mass removal rate or depth of penetration with the changes brought about by solar heating. The effect of the heating will manifest itself in a number of ways.

First will be conversion of amorphous water ice to the crystalline form. Prialnik and Bar-Nun (1987) showed that the slow heating of the surface of an amorphous ice nucleus, presumably formed at low temperature, < 100 K, would cause a transition to crystalline ice at about 5 AU inbound on its first perihelion passage. The amorphous to crystalline phase transition occurs at $\sim$ 140 K. Since this is an exothermic reaction, an additional heat pulse would push inward converting a layer 10 to 15 meters thick to crystalline ice. Prialnik and Bar-Nun showed that a chain reaction converting the entire nucleus to crystalline ice does not occur: the pulse is eventually dissipated as it reaches colder ice layers at greater depths, and by warming of nonvolatile dust mixed with the ice. The amorphous to crystalline ice transition may supply sufficient energy to blow off pieces of the primitive irradiated crust, resulting in the anomalously bright behavior at large solar distance often displayed by dynamically "new" LP comets. Subsequently, the amorphous-crystalline transition does not repeat for several orbits, until a sufficiently thick layer of the overlying crystalline ice is sublimated away, and the orbital heat pulse can penetrate to the buried amorphous core. A more detailed model by Prialnik and Bar-Nun (1988) which includes the effect of a nonvolatile dust crust on the nucleus surface (see below) found that the minimum thickness of the crystalline ice layer overlying the amorphous ice was $\sim$ 15 meters, and was often much thicker, $\sim$ 25 to 40 meters.

The second process is the sublimation of volatile ices at the nucleus surface, which results in the development of the extended cometary atmosphere, the coma. The evolving gases will

carry with them solid grains of dust and ice, creating the dust coma and (perhaps) an icy-hydrocarbon halo around the nucleus, respectively. Larger grains of nonvolatiles that are not carried off will begin to form a lag deposit on the nucleus surface, accumulating to form a crust that will begin to seal the nucleus off against further mass loss, and thermally insulate the nucleus ices interior to it (Brin and Mendis, 1979; Prialnik and Bar-Nun, 1988).

There are thus, two possible scenarios for crust formation. The comet may retain some or all of its original cosmic ray irradiated crust, and this serves as the foundation for additional crust growth. Or, debris gardening and the energy release from the amorphous-crystalline ice phase transition may blow away all of the primitive crust, and the comet then grows a new lag deposit of heavy nonvolatile grains, possibly glued together by complex organics.

Violent rupture of the crust due to the pressure of evolving gases below it may result in visible outbursts or even disruption of the nucleus. Further heating of amorphous ice within the nucleus will result in sporadic transitions to crystalline ice, also possibly resulting in visible outbursts. Thermal stresses on the nucleus caused by substantial temperature gradients within the ice may also result in cracking and exposure of "fresh" ices, and possibly outburst or disruption phenomena.

More subtle effects will include the migration of highly volatile molecules, both outward through the still frozen water ice matrix, and inward towards cooler regions of the nucleus where they will recondense. Also, as mass is lost from the rotating nucleus, its moments of inertia will change and the nucleus will precess, changing the orientation of the rotation pole and the balance of solar insolation across the nucleus surface, with perhaps additional interesting implications. For example, the changing axis orientation will change the centrifugal stresses on weakly bonded nucleus fragments, perhaps resulting in their breaking off and appearing as secondary nuclei.

For the purpose of analyzing the relative pristinity of cometary nuclei for a sample return

mission, the important factor will be the heating of the cometary nucleus at depth. The "thermal skin depth," δ, is defined as

$$\delta = (KP/\pi\rho C)^{1/2} \qquad (1)$$

where K is the conductivity, P is the period (length of day for diurnal skin depth, orbital period for orbital skin depth), ρ is the density, and C is the specific heat. The thermal skin depth is the distance over which a temperature perturbation at the surface will decrease by a factor of 1/e. For conductivities typical of solid, crystalline water ice, δ = 20 cm for a rotation period of 24 hours, or 9.2 meters for an orbital period of 6 years. However, conductivity decreases sharply for porous, low density structures as are suspected for cometary nuclei, and actual values of δ may be considerably smaller. Most measured values of surface conductivity in the solar system, including the icy Galilean satellites, are extremely low. If comets are similar, then a more realistic estimate of the orbital thermal skin depth may be $\sim$ 1 meter. This is a key measurement that can be made by the CRAF Penetrator experiment.

Internal temperature profiles for cometary nuclei are a complex function of the comets' orbital parameters, rotation pole obliquity, and the thermal properties of the comet surface materials. For example, the variation of temperature with depth for a typical 1 km radius SP comet nucleus, ignoring the diurnal temperature cycle and sublimation, and assuming solid crystalline ice, is shown in Figure 5 for four points around the comet's orbit (Herman and Weissman, 1987). Although the surface layer undergoes extreme temperature variations, the temperature several orbital thermal skin depths below the surface is virtually constant. Below this depth the nucleus has been heated to its average orbital temperature, but not appreciably higher.

Temperature profiles in a real case will not be as smooth as shown in Figure 5. Because of the typically low values of conductivity, many returns will be required for a comet to be

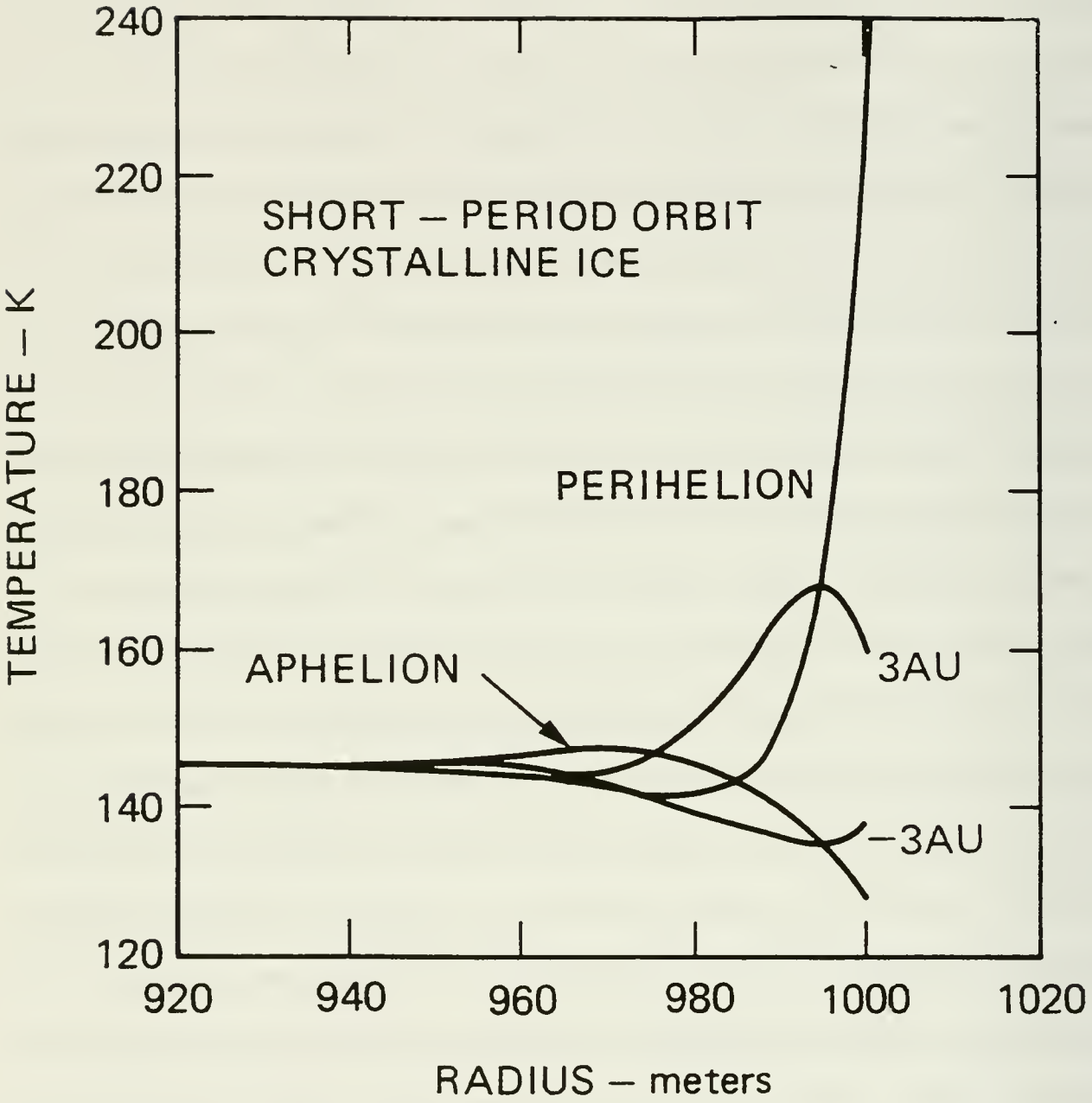


Figure 5. Equilibrium temperature profiles in the near surface layers of a hypothetical 1 km radius crystalline ice comet in a short-period orbit, for four points around the orbit. From Herman and Weissman (1987).

heated to its equilibrium internal temperature. But the comet's orbit is likely to change significantly over that same period of time. Since the changes are essentially random, some will result in additional internal heating, while others will result in a net cooling of the cometary nucleus. The final result might be a fairly complex interweaving of warm and cooler layers. Nevertheless, the equilibrium internal temperature of cometary nuclei can be approximated to within $\pm 10\%$ by the mean temperature for a nucleus in a circular orbit with the same semimajor axis

$$T_m = 280\ (1 - A)^{1/4}\ a^{-1/2}\ \epsilon^{-1/4} \quad K \qquad (2)$$

where A is the bond albedo of the nucleus surface, a is the semimajor axis in AU, and ϵ is the surface emissivity. For comets in non-circular orbits the problem cannot be solved analytically, so numerical techniques must be employed.

The intense solar heating near perihelion and increased time for cooling near aphelion, as well as the temperature dependence of the thermal conductivity, lead to a complex behavior of the central temperature as a function of semimajor axis and eccentricity. That behavior is illustrated in Figure 6 for the case of a 1 km radius crystalline ice nucleus (Herman and Weissman, 1987) where the "normalized temperature" is the calculated central temperature divided by the mean temperature from Equation 2.

The final central temperature which the nucleus reaches is also a function of the magnitude of the thermal conductivity, but is not a function of the nucleus radius (Herman and Weissman, 1987). However, larger nuclei could take hundreds or even thousands of orbits to reach equilibrium, longer than the time constant for appreciable changes in the comet's orbit due to Jupiter perturbations.

As a result of this internal warming, volatile ices with sublimation points below the central temperature will diffuse through the icy matrix and possibly escape the nucleus, unless

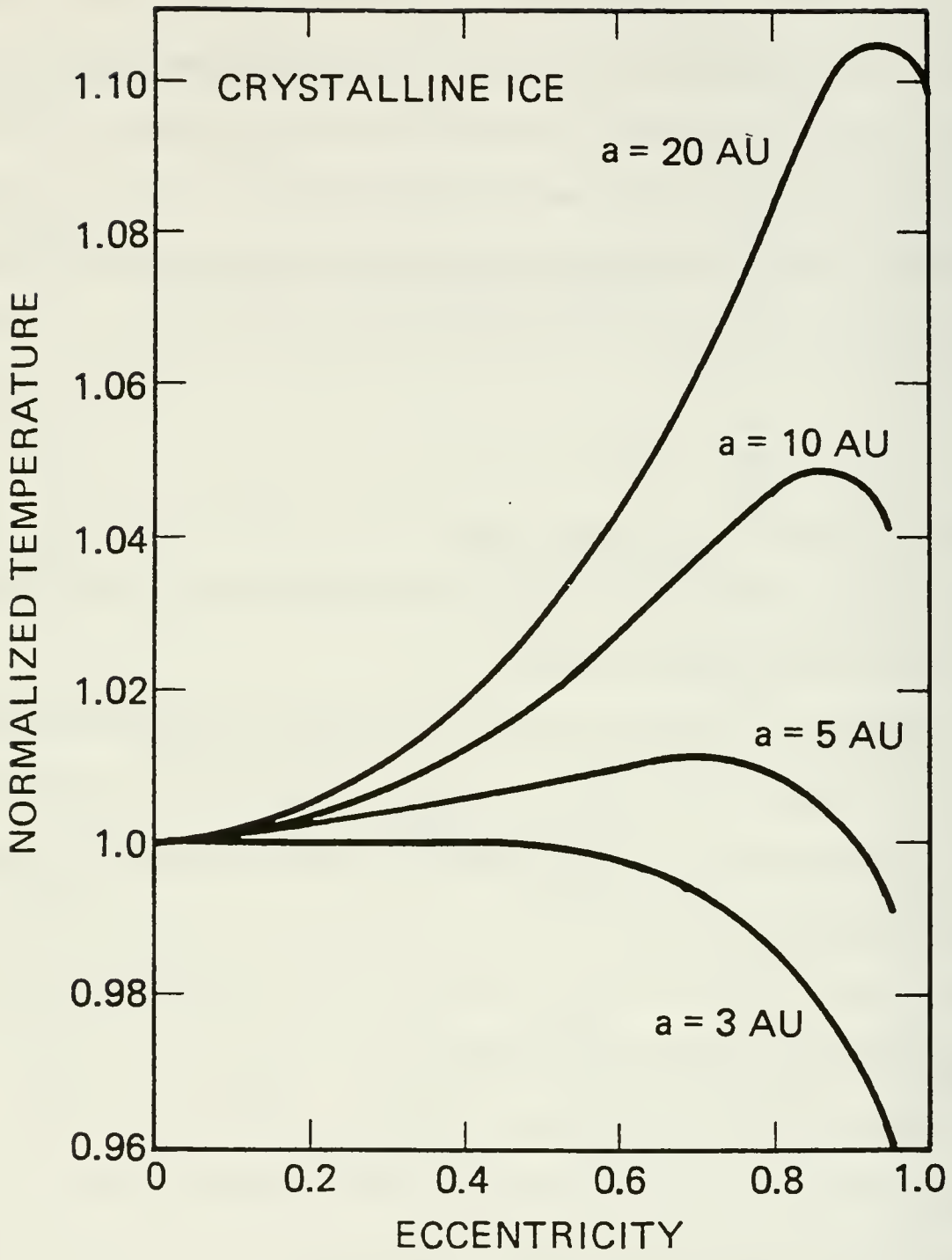


Figure 6. Variation of central temperature for short-period comets as a function of orbital semimajor axis and eccentricity. The normalized temperature is that for a comet in a circular orbit: see text. From Herman and Weissman (1987).

they are trapped as clathrate hydrates. The near surface layers will certainly be depleted in many of the more volatile ices. As a result, gas production rates for some volatile species may show a temporal dependence: as the comet approaches perihelion, the more volatile ices may not appear until the thermal wave has penetrated deep enough into the nucleus to reach undepleted layers. In addition, some deeper layers in the nucleus may be enriched in certain volatiles which were sublimated from the warm near-surface layers, and were able to diffuse to, and recondense in the cooler interior.

Calculated central temperatures for eight well known SP comets, most of which are under consideration as targets for comet rendezvous and/or sample return missions, are given in Table 1. The quantity T_c is the equilibrium central temperature for the comet's present orbit, assuming normal water ice sublimation over the entire nucleus surface. T_c' is the same but assuming no sublimation, a condition the comet would evolve to as it built up a nonvolatile crust covering most of the nucleus surface.

Note that with the exception of P/Halley, all the SP comets in Table 1 have a central temperature above 140 K, the transition temperature for amorphous to crystalline water ice. Thus, it is highly unlikely that any comet sample return mission will bring back a sample of amorphous ice; this certainly represents a major departure from the state in which the comet formed. For a low albedo nucleus, Equation 2 gives a central temperature of 140 K at a semimajor axis of 4.0 AU, or an orbital period of 8.0 years. Of 135 known periodic comets in the most recent catalog (Marsden, 1986), 82 have periods less than that value. Thus, those comets can be expected to have completely converted to crystalline ice in their interiors.

For those comets with longer orbital periods, or those comets recently arrived in the inner planets region, a sizeable fraction of the nucleus interior can still be expected to be amorphous ice (provided that the comet has not been significantly closer to the Sun in the past).

Table 1. Estimated central temperatures for several short-period comets.*

Comet	q - AU	P - yrs	T_c - K	T_c' - K
Encke	0.341	3.30	171.0	183.4
Honda-Mrkos-Pajdusakova	0.581	5.28	149.8	154.9
Tempel 2	1.381	5.29	150.8	156.9
Wild 2	1.491	6.17	144.7	148.9
D'Arrest	1.291	6.38	141.9	146.1
Kopff	1.572	6.43	143.4	147.0
Churyumov-Gerasimenko	1.298	6.59	140.8	145.2
Halley	0.587	76.10	67.8	68.7

*From Herman and Weissman (1987).

However, according to Prialnik and Barn-Nun (1988), the amorphous ice is located at least 15 meters, and possibly 40 meters, beneath the surface.

A variety of models have been developed to study crust growth on cometary nuclei. Calculations have shown that a layer only one or two centimeters thick would probably be sufficient to insulate the ices below and to greatly reduce the sublimation rate (Brin and Mendis, 1979; Fanale and Salvail, 1984; Horanyi et al., 1984). Estimates of the number of returns required to form the crust range from $\sim$ 1 to 20. Various theories have proposed that the crust is either porous, allowing continued gas diffusion through it to the surface, or sealed, resulting in a buildup of pressure beneath it that might cause violent rupture events. The results of the spacecraft flybys of Comet Halley have produced strong evidence for the existence of an insulating crust on the nucleus surface (Sagdeev et al., 1986, Keller et al., 1986), but at the same time have presented us with several apparent paradoxes. The fraction of active area on the nucleus of the comet has been estimated at 20 - 30% of the sunlit surface, based on spacecraft imaging and predictions of the gas production rate (Weissman, 1987). However, it is not clear why such a small fraction of the Halley nucleus is active. Virtually all predictions for Halley were that the nucleus surface would be crust free, the crust having been blown away by the high gas production.

Given that 70 - 80% of the nucleus surface was crusted over, why was it not 100%? Did the few active areas serve as pressure release points for the entire nucleus, implying a highly porous nucleus structure? Did the active areas change as the comet moved along its orbit, or from one perihelion passage to another? Earth-based observations of the comet suggested that the active areas did turn on and off irregularly, and Giotto imaging suggested at least one surface structure that may be a crusted over, former active area. On the other hand, some observers alleged a link between active areas observed in 1985-86, and locations of active areas derived

from 1910 observations (Sekanina and Larson, 1986), a very tenuous possibility which is exceedingly difficult to prove.

A further question is whether or not the allegedly inactive areas on the Halley nucleus were really inactive? Clearly, the sources of the dust jets appear to be confined to relatively small areas. But is it possible that gas from sublimating ices is still diffusing through the dark porous crust in other areas, while being unable to carry entrained dust with it? The relatively poor resolution of the Halley images does not permit an answer to this question.

Another piece of this complex puzzle comes from estimates of nongravitational forces on the motion of Comet Halley. The highly elongated nucleus seen in the spacecraft imaging, with its irregular and asymmetrically distributed active areas, would be expected to precess rapidly. But the fitted nongravitational forces on the comet have been virtually constant over the past 2,200 years (Yeomans and Kiang, 1981). How then can the nongravitational forces be so constant when the nucleus appears to be so dynamic and ever-changing?

Perhaps the best illustration of the complexity of this problem is to cite a real example. In Alaska, a volcanic deposition of ash over a snowbank at the base of a glacier resulted in the unusual cone shaped sublimation features shown in Figure 7 (photograph courtesy of M. Malin). Note that this strange topography is local to one area on the glacier, suggesting a unique combination of both location and lighting that led to it. It is highly unlikely that any scientist would have predicted such a topography from first principles, even knowing far more about the detailed conditions in Alaska versus our current, relatively poor knowledge of cometary nuclei.

What this all must lead to is a major rethinking of the physics and chemistry of the crust formation and removal process. Present models simply cannot explain the observations of the Halley nucleus. Further analyses of the Halley spacecraft data will yield a refined definition of the problem. But extensive laboratory work and theoretical modeling, as well as *in situ*



Figure 7. Sublimation induced features due to deposition of volcanic ash over a snowbank at the snout of one of the Knife Creek Glaciers in the Valley of Ten Thousand Smokes, Katmai, Alaska. Local melting may also have played a role in formation of these unusual cones. It is highly unlikely that such features could be predicted from an examination of the theory of ice sublimation. What then will sublimation features on cometary nuclei look like? This illustrates the complexity of the processes and interactions that may occur, and the reason why *in situ* measurements are imperative. Photograph courtesy of M. Malin (VTTS83-7-18).

observations of an evolving cometary nucleus over a sizeable fraction of its orbit, as will be provided by the Comet Rendezvous Asteroid Flyby (CRAF) mission, are needed to completely understand crust formation.

Another area of considerable interest is that of thermo-mechanical stresses on cometary nuclei (Kuhrt, 1984; Green, 1986; Tauber and Kuhrt, 1987). The dust jets in the Halley spacecraft images appear to be highly collimated, and appear to occur along linear features (Sagdeev et al., 1987). This suggests deep crevices opened up by stresses on the nuclei, or perhaps freshly exposed voids in a fractal structure. These crevices may penetrate sufficiently deep in the nucleus to reach relatively unmodified volatile rich layers, several thermal skin depths below the crusted surface. They also may be the best sites for obtaining samples of the cometary nucleus. But little is known yet about thermal stresses and the two groups working on the problem can not even agree on whether the stresses are tensional or compressional. More work in this area is clearly needed.

7. DISCUSSION

The sections above have described a number of physical processes, summarized in Figure 8, which have modified cometary nuclei since their formation in the primordial solar nebula, 4.5 Gyr ago. Many of these processes are restricted to the nucleus surface or to near-surface layers. But others affect the entire nucleus, and in at least one case, short-lived radionuclides, affect the center of the nucleus the most. The evidence appears to be that comets have only received modest heating over their histories, so as to drive off and/or mobilize a fraction of the more volatile ices, but leaving the nonvolatile constituents, in particular those at depth, relatively unmodified. The two qualifications on that statement are the possible early melting of cometary

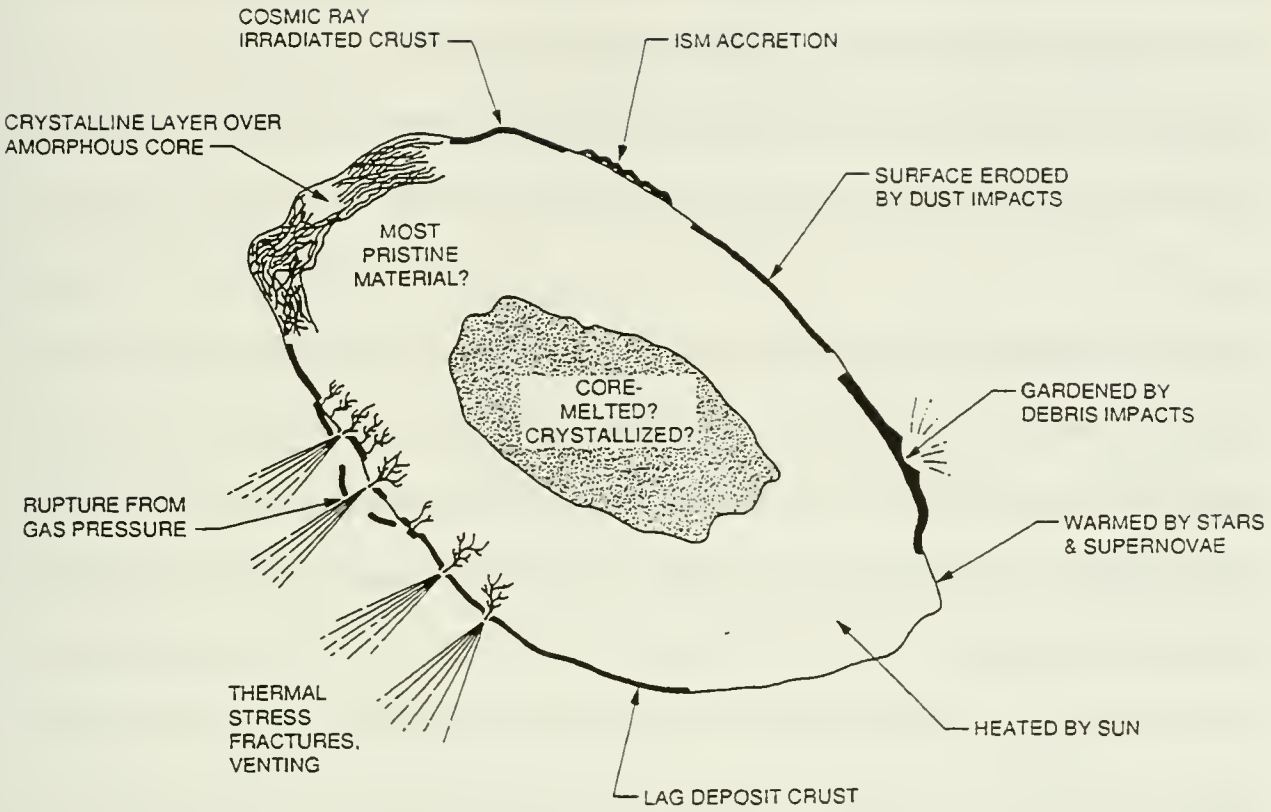


Figure 8. Conceptual diagram of the many different processes which act to modify cometary nuclei over their history. The important question is to understand how these various individual processes interact. For a nucleus sample return mission, the most primitive samples are likely to be found at least 5 to 10 meters beneath the surface, or even deeper, but well away from the core.

interiors by short-lived radionuclides, though the effects of this are hidden deep below the nucleus surface, and the polymerization of hydrocarbons and other materials in the upper 1 to 10 meters of the nucleus surface, though the polymerized layer may have since been lost.

The greatest degree of processing has almost certainly occurred at and near the nucleus surface, as a result primarily of solar heating, gardening from small debris impacts, and cosmic ray bombardment. To find relatively unprocessed materials requires penetrating beneath those processed layers. In the case of solar heating that would likely require a depth of several to tens of meters. For gardening the expected depth is 5 - 10 meters, but that layer may have already sublimated away. For cosmic ray bombardment the required depth would again be several meters, but it is again likely that the modified layer may have already been completely lost due to sublimation and crust blow-off. Or, it may have provided the basis for later crust growth and thus, could still be there.

The important question is how do all these various processes interact? For example, debris impacts in the Oort cloud would repeatedly break up the cosmic ray irradiated crust, with most of the ejecta escaping in the weak cometary gravity field. Hypervelocity dust impacts into an underdense regolith may lead to dust capture, crust compaction, and densification, which in turn may then lead to erosion by subsequent dust impacts, and so on. More complex models of these processes seem necessary, but our current knowledge of cometary materials is likely too poor to create adequately constrained models.

Observational evidence provides considerable support for the belief that comets still retain a very large fraction of their original volatile and nonvolatile constituents. The most abundant molecules detected in interstellar clouds have also been detected in cometary spectra (Irvine et al., 1985). Compositional measurements of solid grains during the Halley flybys show a mix of high temperature refractory grains and pure hydrocarbon grains, as well as more complex

grains with a heterogeneous composition (Kissel and Krueger, 1987; Jessberger and Kissel, 1987). Recovered interplanetary dust particles, which are believed to come from comets, have a botryoidal or fractal structure of sub-micron grains, much like Figure 1b, with a composition similar to the most primitive, undifferentiated meteorites (Fraundorf et al., 1982). In some cases the observations cited here are for "fresh" LP comets from the Oort cloud, but in other cases the evidence has also been found in SP comets, particularly when observers have looked hard enough.

An understanding of the modification processes discussed above is important to the planning of targeting and sampling strategies for a comet nucleus sample return mission. Although the ultimate choice of target comet will be made with numerous operational considerations in mind, processing considerations should also be factored into the selection. The optimum choice is a comet new to the inner planetary region, though there is still the problem of drilling through the meters-thick cosmic ray, thermal, and collisionally modified surface layers. If the target comet has been resident in a SP orbit for hundreds or even thousands of returns, it will have built up a substantial lag deposit crust and solar heated near-surface layers that may be several to tens of meters thick (Fanale and Salvail, 1984; Herman and Weissman, 1987). Unfortunately, most SP comets reachable by planetary exploration spacecraft fall into this latter category. P/Wild 2 may be a notable exception, because of its recent perturbation into a small perihelion orbit.

Concerning sampling strategy itself, any sample returned from the uppermost few meters of a short-period comet will reflect the damage of a variety of modifying processes; it will likely be quite far from pristine. To obtain the most primitive sample possible, two strategies are suggested. First, the maximum technically feasible drilling depth should be obtained. Because most processing scale lengths are on the order of a few meters and because damage should

generally decrease exponentially with depth, one needs to sample many meters below the surface to have a reasonable chance of obtaining primitive materials. Indeed, without a deep drill sample return, one cannot even know how damaged the surface samples are. A particular advantage of deep drilling is that the bore hole can be fitted with instrumentation to measure heat transport and radiation penetration at depth as the comet orbits the Sun, continuing to monitor the nucleus after the sample return vehicle has left.

Second, it is recommended to sample material excavated naturally at cometary vents or fissures. Vents may reach material at depths greater than can be reached by feasible spacecraft drilling techniques. Vent-excavated material might be acquired by sampling the outflow gas and dust before it contacts sunlight, i.e., from within the vent or during outflow after sunset. Although both deep drilling and vent sampling are technologically challenging, they represent the best chance for obtaining primitive material with a comet nucleus sample return mission.

Finally, it is clear that collected samples should be preserved at temperatures at or below the temperatures at which they are collected, to minimize any further processing during the return voyage to Earth.

Acknowledgments: We thank M. Malin for the use of his photograph of unusual ice sublimation features in Alaska. S. A. Stern acknowledges support under NGT-50236 and wishes to thank Sherwood Chang for supporting his travel to this Workshop. This work was supported, in part, by the NASA Planetary Geology and Geophysics Program, and was performed, in part, at the Jet Propulsion Laboratory under contract with the National Aeronautics and Space Administration.

REFERENCES

A'Hearn, M. F., and Feldman, P. D. 1985. S_2: a clue to the origin of cometary ice. In Ices in the Solar System, eds. J. Klinger, D. Benest, A. Dollfus, and R. Smoluchowski, D. Reidel, Dordrecht, pp. 463-472.

Arnold, J. R. 1965. The origin of meteorites as small bodies. Astrophys. J. 141, 1536-1556.

Aumann, H. H., Gillett, F. C., Beichman, C. A., de Jong, T., Houck, J. R., Low, F., Neugebauer, G., Walker, R. G., and Wesselius, P. 1984. Discovery of a shell around alpha Lyrae. Astrophys. J. 278, L23-L27.

Bailey, M. E. 1983. Comets, planet X and the orbit of Neptune. Nature 302, 399-400.

Bailey, M. E., Clube, S. V. M., and Napier, W. M. 1986. The origin of comets. Vistas in Astronomy 29, 53-112.

Brin, G. D., and Mendis, D. A. 1979. Dust release and mantle development in comets. Astrophys. J. 229, 402-408.

Calcagno, L., Foti, G., Torrisi, L., and Strazzulla, G. 1985. Fluffy layers obtained by ion bombardment of frozen methane: Experiments and applications to Saturnian and Uranian satellites. Icarus 63, 31-38.

Cameron, A. G. W. 1962. The formation of the sun and planets. Icarus 1, 13-69.

Cameron, A. G. W. 1973. Accumulation processes in the primitive solar nebula. Icarus 18, 407-450.

Cameron, A. G. W. 1978. The primitive solar accretion disc and the formation of the planets. In The Origin of the Solar System, ed. S. F. Dermott, John Wiley & Sons, New York, pp. 49-75.

Cameron, A. G. W. 1985. Formation and evolution of the primitive solar nebula. In Protostars and Planets II, eds. D. C. Black and M. S. Matthews, Univ. Arizona Press, Tucson, pp. 1073-1099.

Carusi, A., Kresak, L., Perozzi, E., and Valsecchi, G. B. 1985. Long-Term Evolution of Short-Period Comets. Adam Hilger, Bristol, 350 pp.

Cintala, M. J. 1981. Meteoroid impact into short-period comet nuclei. Nature 291, 134-136.

Croft, S. W. 1981. Hypervelocity impact cratering in icy media. Lunar and Planet. Sci. Conf. 12, 190-192 (abstract).

Delsemme, A. H. 1982. Chemical composition of cometary nuclei. In Comets, ed. L. L. Wilkening, Univ. Arizona Press, Tucson, pp. 85-130.

Donn, B. 1976. Comets, interstellar clouds, and star clusters. In The Study of Comets, NASA SP-393, pp. 663-672.

Donn, B., and Rahe, J. 1982. Structure and origin of cometary nuclei. In Comets, ed. L. L. Wilkening, Univ. Arizona Press, Tucson, pp. 203-226.

Donn, B., Daniels, P. A., and Hughes, D. W. 1985. On the structure of the cometary nucleus. Bull. Amer. Astron. Soc. 17, 520 (abstract).

Donn, B., and Meakin, P. 1988. The accumulation and structure of the cometary nucleus: the fluffy aggregate model. Bull. Amer. Astron. Soc. 20, 840 (abstract).

Draganic, I. G., and Draganic, E. D. 1984. Some radiation-chemical aspects of chemistry in cometary nuclei. Icarus 60, 464-475.

Duncan, M., Quinn, T., and Tremaine, S. 1987. The formation and extent of the solar system comet cloud. Astron. J. 94, 1330-1338.

Duncan, M., Quinn, T., and Tremaine, S. 1988. The origin of short-period comets. Astrophys. J. 328, L69-L73.

Eberhardt, P., Dolder, U., Schulte, W., Krankowsky, D., Lammerzahl, P., Hoffman, J. H., Hodges, R. R., Berthelier, J. J., and Illiano, J. M. 1987. The D/H ratio in water from comet Halley. Astron. Astrophys. 187, 435-437.

Everhart, E. 1969. Close encounters of comets and planets. Astron. J. 74, 735-750.

Everhart, E. 1972. The origin of short-period comets. Astrophys. Let. 10, 131-135.

Fanale, F. P., and Salvail, J. R. 1984. An idealized short-period comet model: surface insolation, H_2O flux, dust flux, and mantle evolution. Icarus 60, 76-511.

Fernandez, J. A. 1980. On the existence of a comet belt beyond Neptune. Mon. Not. Roy. Astron. Soc. 192, 481-491.

Fernandez, J. A., 1985. The formation and dynamical survival of the comet cloud. In Dynamics of Comets: Their Origin and Evolution, eds. A. Carusi and G. B. Valsecchi, D. Reidel, Dordrecht, pp. 45-70.

Fernandez, J. A., and Ip, W.-H. 1981. Dynamical evolution of a cometary swarm in the outer planetary region. Icarus 47, 470-479.

Fraundorf, P., Brownlee, D. E., and Walker, R. M. 1982. Laboratory studies of interplanetary dust. In Comets, ed. L. L. Wilkening, Univ. Arizona Press, Tucson, pp. 383-409.

Goldreich, P., and Ward, W. R. 1973. The formation of planetesimals. Astrophys. J. 183, 1051-1061.

Gombosi, T. I., and Houpis, H. L. 1986. The icy-glue model of the cometary nucleus. Nature 324, 43-44.

Green, J. R. 1986. Stress, fracture, and outburst in cometary nuclei. Bull. Amer. Astron. Soc. 18, 800 (abstract).

Greenberg, J. M. 1982. What are comets made of? A model based on interstellar grains. In Comets, ed. L. L. Wilkening, Univ. Arizona Press, Tucson, pp. 131-164.

Greenberg, J. M. 1986. Fluffy comets. In Asteroids, Comets, Meteors II, eds. C.-I. Lagerkvist, B. A. Lindblad, H. Lundstedt, and H. Rickman, Uppsala Univ. pp. 221-223.

Greenberg, J. M. and D'Hendecourt, L. B. 1985. Evolution of ices from interstellar space to the solar system. In Ices in the Solar System, eds. J. Klinger, D. Benest, A. Dollfus, and R. Smoluchowski, D. Reidel, Dordrecht, pp. 185-204.

Greenberg, R., Weidenschilling, S. J., Chapman, C. R., and Davis, D. R. 1984. From icy planetesimals to outer planets and comets. Icarus 59, 87-113.

Herman, G., and Weissman, P. R. 1987. Internal temperatures of cometary nuclei. Icarus 69, 314-328

Hills, J. G. 1982. The formation of comets by radiation pressure in the outer protosun. Astron. J. 87, 906-910.

Horanyi, M., Gombosi, T. I., Cravens, T. E., Korosmezey, A., Kecskemety, K., Nagy, A., and Szego, K. 1984. The friable sponge model of a cometary nucleus. Astrophys. J. 278:449-455.

Hut, P., and Tremaine, S. 1985. Have interstellar clouds disrupted the Oort comet cloud? Astron. J. 90, 1548-1557.

Irvine, W. M., Schloerb, F. P., Hjalmarson, A., and Herbst, E. 1985. The chemical state of dense interstellar clouds: an overview. In Protostars and Planets II, eds. D. C. Black and M. S. Matthews, Univ. Arizona Press, Tucson, pp. 579-620.

Jessberger, E. K., and Kissel, J. 1987. Bits and pieces from Halley's comet. In Lunar and Planet. Sci. Conf. 18, 466-467 (abstract).

Johnson, R. E., Cooper, J. F., Lanzerotti, L. J., and Strazzula, G. 1987. Radiation formation of a non-volatile comet crust. Astron. Astrophys. 187, 889-892.

Kazimirchak-Polonskaya, E. I. 1972. The major planets as powerful transformers of cometary orbits. In The Motion, Evolution of Orbits, and Origin of Comets, eds. G. A. Chebotarev, E. I. Kazimirchak-Polonskaya, and B. G. Marsden, D. Reidel, Dordrecht, pp. 373-397.

Keller, H. U., Arpigny, C., Barbieri, C., Bonnet, R. M., Cazes, S., Coradini, M., Csomovici, C. B., Delamere, W. A., Huebner, W. F., Hughes, D. W., Jamar, C., Malaise, D., Reitsema, H. J., Schmidt, H. U., Schmidt, W. K. H., Seige, P., Whipple, F. L., and Wilhelm, K. 1986. First Halley multicolour camera imaging results from Giotto. Nature 321, 320-326.

Kissel, J., and Krueger, F. R. 1987. The organic component in dust from comet Halley as measured by the PUMA mass spectrometer on board Vega 1. Nature 326, 755-760.

Kuhrt, E. 1984. Temperatures profiles and thermal stress on cometary nuclei. Icarus 60, 512-521.

Kuiper, G. P. 1951. On the origin of the solar system. In Astrophysics, ed. J. A. Hynek, McGraw Hill, New York, pp. 357-424.

Lange, M. A., and Ahrens, T. J. 1987. Impact experiments in low-temperature ice. Icarus 69, 506-521.

Lanzerotti, L. J., Brown, W. L., Poate, J. M., and Augustyniak, W. M. 1978. Low energy cosmic ray erosion of ice grains in interplanetary and interstellar media. Nature 272, 431-433.

Lanzerotti, L. J., Brown, W. L., and Johnson, R. E. 1983. Implications of Voyager data for energetic ion erosion of the icy satellites of Saturn. J. Geophys. Res. 68, 8765-8770.

Lewis, J. S. 1971. Satellites of the outer planets: their physical and chemical nature. Icarus 15, 174-185.

Lissauer, J. J. 1987. Timescales for planetary accretion and the structure of the proto-planetary disk. Icarus 69, 249-265.

Marsden, B. G. 1986. Catalogue of Cometary Orbits, 5th Edition, Smithsonian Astrophys. Observatory, Cambridge, 102 pp.

Moore, M. H., Donn, B., Khanna, R., and A'Hearn, M. F. 1983. Studies of proton irradiated cometary type ice mixtures. Icarus 54, 388-405.

Mumma, M. J., Blass, W. E., Weaver, H. A., and Larson, H. P. 1988. Measurements of the ortho-para ratio and nuclear spin temperature of water vapor in comets Halley and Wilson (1986l) and implications for their origin and evolution. Bull. Amer. Astron. Soc. 20, 826 (abstract).

Narayan, R. 1987. Supernovae rates in external galaxies. Astrophys. J. 319, 162-179.

O'Dell, C. R. 1971. A new model for cometary nuclei. Icarus 19, 137-146.

Ostro, S. J., Tsou, P., and Stephens, J. B. 1986. Impact cavities in underdense regoliths? Meteoritics 21, 476 (abstract).

Prialnik, D., and Bar-Nun, A. 1987. On the evolution and activity of cometary nuclei. Astrophys. J. 313, 893-905.

Prialnik, D., Bar-Nun, A., and Podolak, M. 1987. Radiogenic heating of comets by ^{26}Al and implications for their time of formation. Astrophys. J. 319, 993-1002.

Prialnik, D., and Bar-Nun, A. 1988. The formation of a permanent dust mantle and its effect on cometary activity. Icarus 74, 272-283.

Safronov, V. S. 1969. Evolution of the Protoplanetary Cloud and Formation of the Earth and

Planets, Moscow, Nauka Press, (NASA TT-F-667, 1972).

Sagdeev, R. Z., Szabo, F., Avanesov, G. A., Cruvellier, P., Szabo, L., Szego, K., Abergel, A., Balazs, A., Barinov, I. V., Bertaux, J.-L., Blamont, J., Detaille, M., Demarelis, E., Dul'nev, G. N., Endroczy, G., Gardos, M., Kanyo, M., Kostenko, V. I., Krasikov, V. A., Nguyen-Trong, T., Nyitrai, Z., Reny, I., Rusznyak, P., Shamis, V. A., Smith, B., Sukhanov, K. G., Szabo, F., Szalai, S., Tarnopolsky, V. I., Toth, I., Tsukanova, G., Valnicek, B. I., Varhalmi, L., Zaiko, Yu. K., Zatsepin, S. I., Ziman, Ya. L., Zsenei, M., Zhukov, B. S. 1986. Television observations of comet Halley from Vega spacecraft. Nature 321, 262-266.

Sagdeev, R. Z., Smith, B., Szego, K., Larson, S., Toth, I., Merenyi, E., Avanesov, G. A., Krasikov, V. A., Shamis, V. A., Tarnapolski, V. I. 1987. The spatial distribution of dust jets seen during the Vega 2 flyby. Astron. Astrophys. 187, 835-838.

Sekanina, Z., and Larson, S. M. 1986. Dust jets in comet Halley observed by Giotto and from the ground. Nature 321, 357-361.

Shoemaker, E. M., and Wolfe, R. F. 1986. Mass extinctions, crater ages, and comet showers. In The Galaxy and the Solar System, eds. R. Smoluchowski, J. N. Bahcall, and M. S. Matthews, Univ. Arizona Press, Tucson, pp. 338-386.

Shulman, L. M. 1972. The chemical composition of cometary nuclei. In The Motion, Evolution of Orbits, and Origin of Comets, eds. G. A. Chebotarev, E. I. Kazimirchak-Polonskaya, and B. G. Marsden, D. Reidel, Dordrecht, pp. 263-270.

Smith, B. A., Fountain, J. W., and Terrile, R. J. 1988. The beta Pictoris disk. Bull. Amer. Astron. Soc. 20, 875 (abstract).

Stern, S. A. 1986. The effects of mechanical interaction between the interstellar medium and comets. Icarus 68, 276-283.

Stern, S. A. 1988. Collisions in the Oort cloud. Icarus 73, 499-507.

Stern, S. A. 1989. ISM induced erosion and gas dynamical drag in the Oort cloud. Icarus, submitted.

Stern, S. A., and Shull, J. M. 1988. The thermal evolution of comets in the Oort cloud by passing stars and stochastic supernovae. Nature 332, 407-411.

Tammann, G. A. 1982. Supernova statistics and related problems. In Supernovae: A Survey of Current Research, eds. M. J. Rees and R. J. Stoneham, D. Reidel, Dordrecht, pp. 371-403.

Tauber, F., and Kuhrt, E. 1987. Thermal stresses in cometary nuclei. Icarus 69, 83-??.

Thompson, W. R., Sagan, C., and Khare, B. N. 1987. Coloration and darkening of methane clathrate and other ices by charged particle radiation: Applications to the outer solar system. J. Geophys. Res. 92, 14933-14947.

Tsou, P. D., Brownlee, D., and Albee A. 1984. Experiments on intact capture of hypervelocity particles. Lunar & Planet. Sci. Conf. 15, 866-867 (abstract).

Vanysek, V., and Rahe, J. 1978. The $^{12}C/^{13}C$ isotope ratio in comets, stars, and interstellar matter. Moon & Planets 18, 441-446.

Wallis, M. K. 1980. Radiogenic melting of primordial comet interiors. Nature 284, 431-433.

Weidenschilling, S. J. 1980. Dust to planetesimals: settling and coagulation in the solar nebula. Icarus 44, 172-189.

Weissman, P. R. 1980. Stellar perturbations of the cometary cloud. Nature 288, 242-243.

Weissman, P. R. 1985a. The origin of comets: implications for planetary formation. In Protostars and Planets II, eds. D. C. Black and M. S. Matthews, Univ. Arizona Press, Tucson, pp. 895-919.

Weissman, P. R. 1985b. Cometary dynamics. Space Sci. Revw. 41, 299-349.

Weissman, P. R. 1986. Are cometary nuclei primordial rubble piles? Nature 320, 242-244.

Weissman, P. R. 1987. Post-perihelion brightening of Halley's comet: Springtime for Halley. Astron. Astrophys. 187, 873-878.

Whipple, F. L. 1950. A comet model I: The acceleration of comet Encke. Astrophys. J. 111, 375-394.

Whipple, F. L. 1978. Cometary brightness variation and nucleus structure. Moon & Planets 18, 343-359.

Whipple, F. L., and Lecar, M. 1976. Comet formation induced by the solar wind. In The Study of Comets, NASA SP-393, pp. 660-662.

Wyckoff, S., Lindholm, E., Wehinger, P. A., Peterson, B. A., Zucconi, J.-M., and Festou, M. C. 1989. The $^{12}C/^{13}C$ abundance ratio in comet Halley. Astrophys. J. 339, 488-500.

Yeomans, D. K., and Kiang, T. 1981. The long term motion of comet Halley. Mon. Not. Roy. Astron. Soc. 197, 633-643.

THE ORGANIC MATTER OF COMET P/HALLEY AS INFERRED BY JOINT GAS AND SOLID PHASE ANALYSIS

F. R. Krueger
Ing. -Buero Dr. Krueger, Messelerstr. 24, D-6100 Darmstadt 12
Frankfurt, Germany

A. Korth
Max–Planck–Institut fuer Aeronomie, D-3411 Katlenburg–Lindau 3
Frankfurt, Germany

J. Kissel
Max–Planck–Institut fuer Kernphysik, D-6900 Heidelberg 1
Frankfurt, Germany

THE ORGANIC MATTER OF COMET p/HALLEY AS INFERRED BY JOINT GAS AND SOLID PHASE ANALYSIS

F. R. Krueger", A. Korth*, and J. Kissel+

" Ing.-Buero Dr. Krueger, Messelerstr. 24, D-6100 Darmstadt 12 / FRG
* Max-Planck-Institut fuer Aeronomie, D-3411 Katlenburg-Lindau 3/ FRG
+ Max-Planck-Institut fuer Kernphysik, D-6900 Heidelberg 1/ FRG

ABSTRACT:
During the encounters with comet Halley, PICCA on GIOTTO measured the gas phase organic ion composition of the coma, and PUMA on VEGA1 measured the dust composition. Joining those results a consistent picture of the parent organic matter from which dust and gas is produced can be obtained. One recognizes a complex unsaturated polycondensate, which splits during coma-formation into the more refractory C=C, C-N-containing dust part, and the more volatile C=C, C-O-containing gas part. The responsible exothermal chemical reactions, triggered by the sun light may play a major role in the dynamics of coma formation. The latent heat and reactivity may cause problems regarding a sample return mission.

1. Introduction

A wealth of organic molecular information has been obtained during the encounters of the GIOTTO and VEGA spacecrafts with comet p/Halley by means of mass spectrometry. Analyzing the refractory organic dust composition PUMA on board VEGA1 was the most successful one of the three impact mass spectrometers flown (1), so that a gross characterization of the organic residue was possible (2). Due to the breakdown of an amplifier PIA onboard GIOTTO was not sensitive enough to measure molecular ions. However, when now comparing the VEGA solid phase fwith the GIOTTO gas phase measurements, in both cases data were used refering to distances of several 10,000 km from the nucleus as well.

The organic gas composition was measured, i.a., by the PICCA ion mass spectrometer on board GIOTTO (3). The latter one succeeded especially well in analyzing higher mass gas phase ions up to m/z=100 (4), which ion data are now interpreted in detail with respect to the possible and compatible parent neutrals in this paper. It is obvious that both instruments not only analyze different phases (condensed and gas, respectively) but thus also, at least in part, different components of the parent cometary organic matter, separated due to different regimes of vapor pressure. However, we are able to show that under this respect both mass spectrometric results are well compatible with each other inferring a common parent matter. As an additional result we will show that a major part of the organic matter may have been produced in an exothermic polycondensation reaction under the elimination of water, thus forming the coma during the passage of the inner solar system.

2. The PICCA coma ion analysis

2.1 Instrumentation

The Positive Ion Cluster Composition Analyzer (PICCA) on board the spacecraft GIOTTO, which is part of the RPA-Copernic plasma instrument, was designed to determine the composition and the energy distribution of positively charged ions in the direction of the spacecraft motion (ram direction) in the coma of comet Halley. PICCA measures E/z (energy/charge) instead of the mass (8); however, ions in the inner coma are cold, so their motion with respect to the spacecraft is highly collimated along the ram direction at the relative flyby velocity of 68.4 km/s.

Most of these ions are apparently singly charged, as there are no traces of half-integer lines found in the high-resolution mass regime (see below). So the measurements of E/z are, to a very good approximation, proportional to the ion mass.

The mass resolution of the instrument is Δm = 0.4 amu (atomic mass units) in the mass range 10 - 50 amu, and Δm = 1 amu in the mass range 51 - 210 amu. Outside the ionopause, which is the outer boundary of the magnetic cavity region detected at a cometocentric distance of about 4600 km, the thermal energy spread of the incoming ions is larger than the instrumental energy resolution. The effective mass resolution amounts there to about 3 amu.

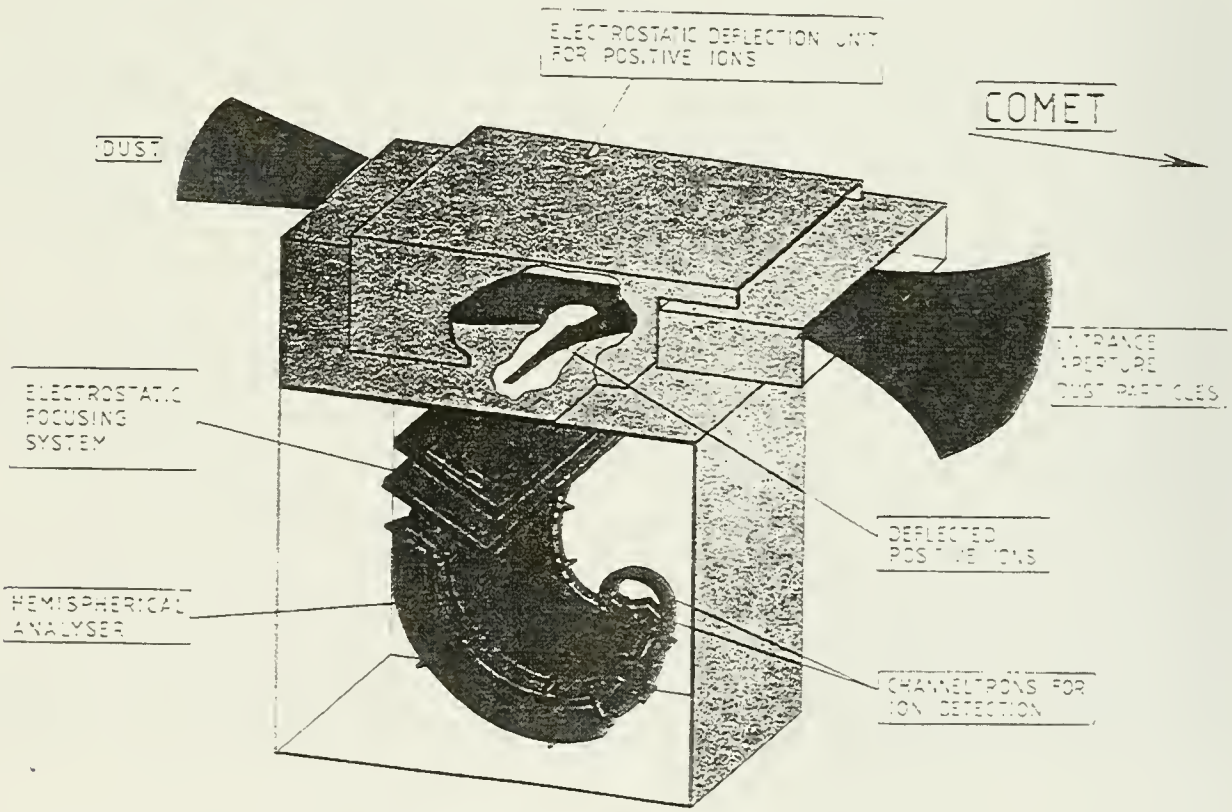


Fig. 1: The PICCA coma ion mass analyzer

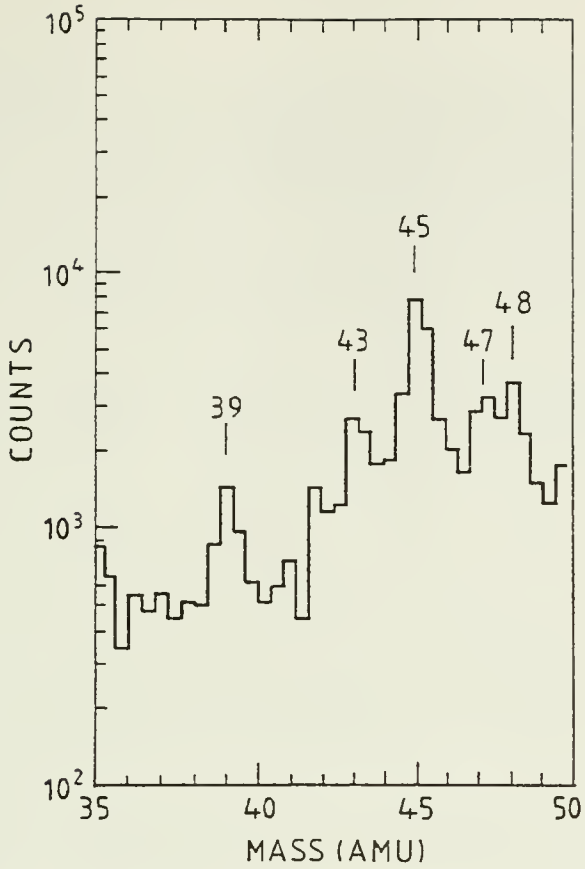


Fig. 2:
PICCA ion mass spectrum in the well resolved mass regime.

2.2 Ion observations in the gas phase

As mentioned above the ion resolution outside the ionopause (>4600 km) is poor due to the thermal spread of the measured ions. Between 25,000 km cometocentric distance and the ionopause the spectrum shows indeed broad mass groups but with clear peaks at 31, 45, 61, 75, 90 and 105 amu (4). Between 20,000 km and the closest approach of the spacecraft (605 km) the mass peaks from 30 - 33 amu are saturated whereas the mass peak at 45 amu is only saturated at about 11,000 km close to the intensity maximum of all ion species (9).

Inside the ionopause where the thermal spread of the incoming ions is comparible to the instrumental energy resolution we observe in the mass range between 23 amu and 50 amu the following mass peaks (10): 26, 28, 30-33 (saturated), 35, 37, 39, 42, 43, 45, 47, 48. Above 50 amu the instrumental mass resolution decreases and the dominent masses between 50 and 70 amu were determined by a least-square fitting procedure (4). The fits show peaks at 57, 61, and 63 amu. Above 70 amu the broad mass peaks could not be resolved due to the presence of a hot ion background which increased rapidly near the ionopause.

The unambiguous identification of the given peaks in the spectra with a particular ion is not possible, however we will list the dominant ion species that are expected from a C-H-O-N dominated medium. The measured peaks show a strong preference for odd mass numbers over even mass numbers. The ratio is difficult to derive because of the limited mass resolution. However, an estimation in the mass range from 36 - 49 amu

is possible and amounts to about 0.3 or less. The odd mass peaks give an indication for a nitrogen-poor and non-radical ion mixture: Namely, if radical and non-radical species would both contribute significantly, no such an overrepresentation of one even-odd character would occur. As it is consistent with gas phase measurements of other authors, nitrogen is depleted in the gas phase. If it were not, then again a clear preference in even-odd character could not be expected, due to the odd number of valences of an odd number of N atoms, and an even numer of valences of an even number of N atoms in the molecule. As a consequence also the PICCA-ions apparently contain little N. However, as they are preferably odd mass numbers, they are non-radical species when containing no other elements than H, C, O, and S.

In the following we will try to identify the different m/z peaks and will take, as pointed out earlier, only singly charged ions (z=1). We start with the less abundant even mass numbers, which may of course contain nitrogen, if not being accounted for a minor radical contribution which, however, is ruled out, as major radical species frequently seen in any electron impact spectrum are missing here. As therefore only non-radical ions are taken into account for analysis, most of them can at least formally described as protonation products of stable neutral molecules. This does in turn not necessarily mean, that protonation in the gas phase is the dominant mechanism of ion production. Another mechanism is proton exchange in the solid state and further disintegration of that solid state, which is known (9) to always produce such species. As we will see, this mechanism is also accounted for in Halley's coma formation, because further chemical ionization in the gas phase is by far not possible due to kinetic reasons.

m/z	
26, 28	non-radical ions which belong to the hydrocyanic acid such as CN+ and H2CN+
42	acetonitrile ion CH3CNH+
48	unsure, possibly non-radical aminomethanol, HOCH2NH3+
30, 32	reduction products of hydrocyanic acid like methylimine CH3NH+, and methylamine CH3NH3+ ; (also sulphur, S, may contribute) Mass peaks are included in the broad mass peak 30-33 amu where the instrument shows saturation. The maximum is at 31 amu.

The following odd mass numbers will not contain any nitrogen

31, 45	These are the highest maxima in the surroundings. Formaldehyde, H2COH+, and acetaldehyde, H3CHCOH+ or in principle it could also be protonated alkanes like ethane, C2H7+ and propane, C3H9+. However, due to its non coordinative binding state these ions are very labile and will never show up as the largest peak.
35, 37	water compounds like H2O.OH+ and H2O.H3O+
39	aromatic cyclopropenyl C3H3+ (10)

43, 45, 47, 57, 61,
63, 75, (89, 91) the abundance of these ions indicate that the parents are unsaturated hydrocarbons with none or one oxygen-heteroatom. If the parents were carbon-homo-atomic hydrocarbons than we will not find the peaks at m/z 45 and 47 amu. The pattern m/z 61 and 63 missing 59 amu and 75, 89 and 91 point to hydrocarbons CnHm+ with a comparible low m like C5H+, C5H3+, C6H3+, C7H5+, and C7H7+ .

The measured peaks in the mass spectra indicate that the ions were not generated by photoionization from neutral molecules in the gas phase. Collisions, however, in the gas phase could produce the observed ions, but the probability from gas kinetic reasons are low. Therefore we conclude that the formation of these ions could only be from decomposition of the dust.

It should be pointed out already here that the above ions certainly are fragment ions produced from larger molecules in the solid state of the comet. Namely, speaking about a "molecular ion" in that space analysis only means distinguishing against "atomic ions". Moreover, in terms of a mass spectrometrist we would even not expect molecular ions, as those are generally radical. Protonation would only produce quasi-molecular ions (M+H)+. These we can only assign for species from which we know by other analyses that they really exist as neutral molecules, too, namely water (H3O+), Ammonia (NH4+), Hydrocyanic acid (H2CN+) and so on.

3. The PUMA dust particle analysis

3.1 Measurement - method and objectives

The dust impact mass analyzer PUMA was flown i.a. on the Soviet spacecraft VEGA1 and obtained a wealth of data, especially also molecular ones. The detailed description of the instrument and the analysis strategy has been already published (2). Consequently a short overview may be sufficient here.

With the PUMA instrument ions are generated by the impacting dust particle on a silver target. Due to the high relative velocity between the dusty coma and the spacecraft of v = 78 km/s, any impacting dust particle is nearly completely vaporized and ionized, and so is some target material, too. From the number of atomic projectile ions (due to each element) one can infer (5) the elemental composition of that very particle - together with the number of atomic target (Ag) ions one can also determine mass and density of that particle.

However, there is a slight probability in the very first moment when the impact shock wave reaches the outermost layers that from those molecules and molecular ions are ejected with only minor decomposition. It is known that all the ionization mechanisms from solid surfaces in such rapid dissipation processes are very much comparable with each

other (9), i.e. yield similar results. Namely, one generally obtains preferably non- radical stable ion-species, under which those carrying local charges (due to N-sites, or to a lesser extent, O-sites) are very much overrepresented. Molecular lines evidently showed up in the PUMA mass spectra, and consequently an analysis was performed, using these ion formation rules as a basis.

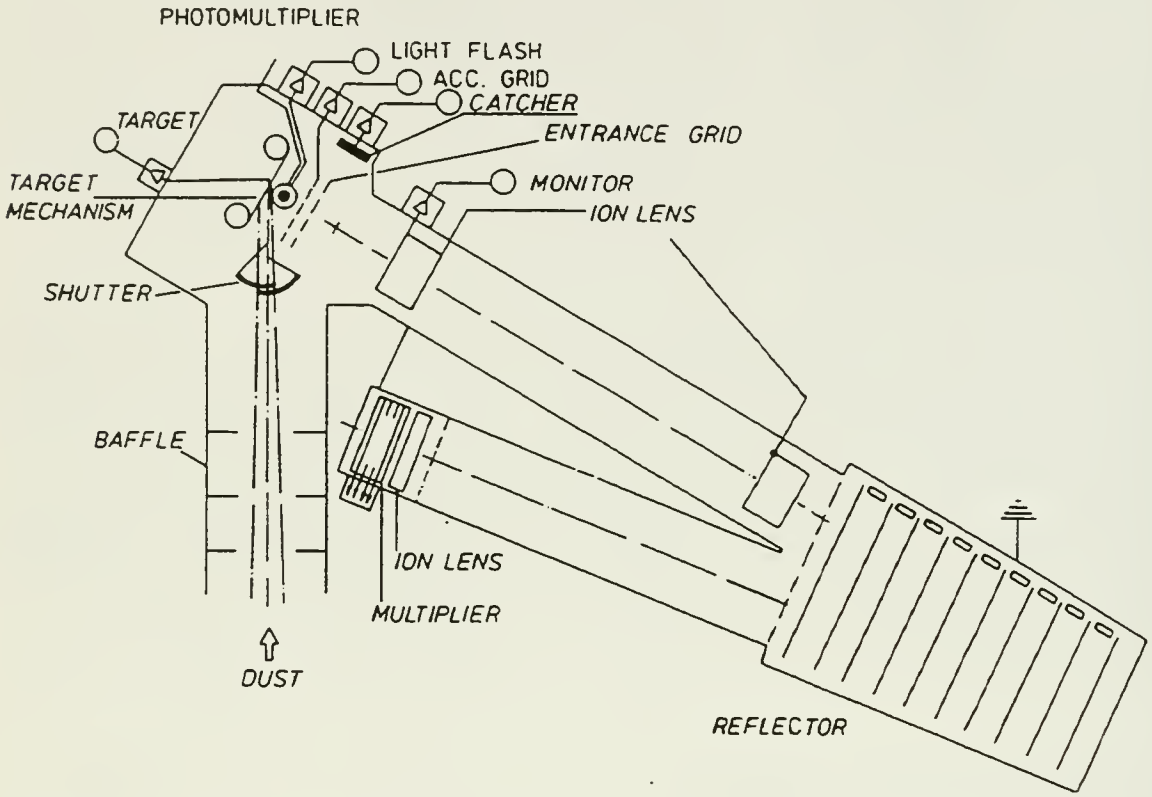


Fig. 3: The PUMA dust particle impact time-of-flight mass spectrometer

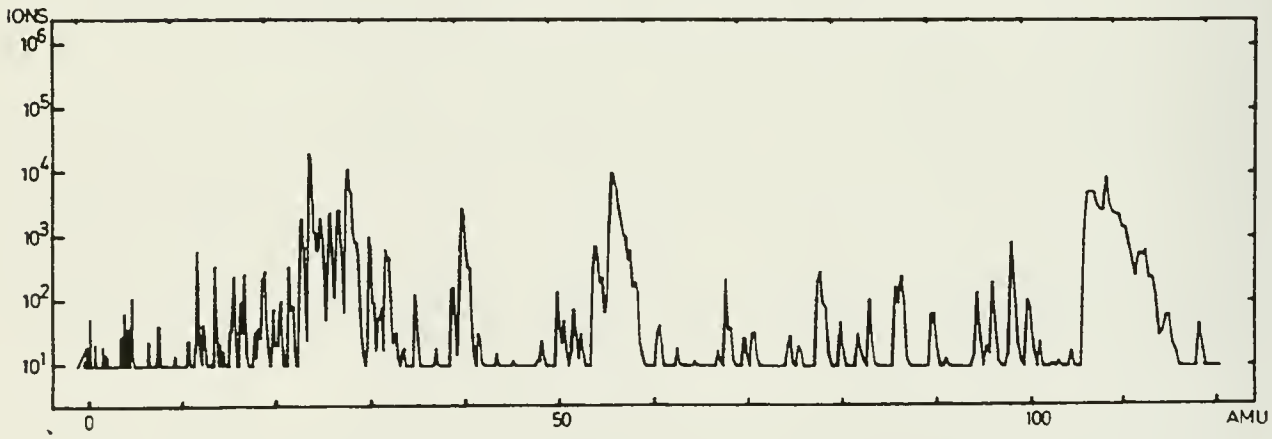


Fig. 4: A typical converted PUMA mass spectrum showing atomic and molecular ions

Element	Moles total	Moles thereof in sub-fractions [val]					
Organic fraction		Water	Unsaturated hydrocarbons without heteroatoms	Unsaturated nitrogen-containing species	Oxygen-containing species	Sulfur-cont. species (unsure)	
H	600	180	250	70	80	20	
C	500		375	80	40	15	
N	20			20			
O	150	90			60		
S	10					10	

Anorganic fraction		Water	Carbon	Anions					Kations	(val)
H	180	160					20			
C	100		80		20					
O	500	80		300	60	40	20	2		
Na	2								2 Na^+	(2)
Mg	70								70 Mg^{2+}	(140)
Al	5		Sulfur						5 Al^{3+}	(15)
Si	100	Troilit		100						
P	0.5							0.5		
S	40	20	10			10				
Cl	1							1		
K	0.1							Cl^-	0.1 K^+	(0.1)
Ca	4								4 Ca^{2+}	(8)
Ti	0.5		Iron	SiO_3^{2-}	CO_3^{2-}	SO_4^{2-}	OH^-	PO_4^{3-}	0.5 Ti^{2+}	(1)
Cr	1								1 Cr^{3+}	(3)
Mn	1								1 Mn^{2+}	(2)
Fe	70	20	5						45 $Fe^{2+/3+}$	(104)
Co	0.5								0.5 Co^{2+}	(1)
Ni	3								3 Ni^{2+}	(6)
Zn	0.1								0.1 Zn^{2+}	(0.2)
val:				200	40	20	20	2.5		(282.3)

Fig. 5 : The most probable mean composition of the dust particles as measured by PUMA.

3.2 Results - Ion correlations

When all the apparent atomic ion signals had been subtracted, those residual signals were assigned to mass lines, which time-of-flight were consistant with integer mass and which amplitude was above noise level. These resultant mass spectra have been compared with a random mass distribution.

Several m/z numbers apparently showed up to be overrepresented in the PUMA mass spectra (after subtraction of the atomic ions) when compared with random, namely

m/z = 18, 25, 26, 28, 29, 42, 43, 44, 46, 60, 63, 65, 67, 68, 71, 78, 79, 81, 87, 89, 118, 122,

other underrepresented, namely

m/z 45, 47, 49, 51, 52, 59, 61, 76, 80, 82, 83, 90, 94, 100, 101

- both significant when comparing with Poisson statistics.

However, this is not sufficient to determine the class of substances, although it gives at least some hints. A much more powerful technique is looking for ion-ion-correlations in the mass spectra, i.e., how often appears a certain mass line in one mass spectrum together with another certain mass line - and this far more frequently than independent chance would suggest.

The following m/z ion-ion-correlations have been found to be statistically strongly overrepresented:

m/z(1)-m/z(2) = 26-28, 26-70, 28-62, 28-64, 28-78, 28-89, 42-66, 42-67, 42-71, 42-77, 42-78, 48-68, 48-89, 64-81, 66-81, 68-71, 68-97, 71-77, 71-78, 78-88, 78-97, 78-98, 85-91, 89-91, 89-98, 91-93, 95-97.

From this list some key mass numbers are recognized to be very often members of such correlations, and thus are to be considered as key decomposition (fragment) ions of the impacting (certainly larger) molecules, namely:

m/z 28, 42, 71, 78, 91, and, to a minor extent, m/z 48, 77, 89.

It was the task to reveal the information, certainly accumulated in those mass numbers, about the parent molecule class yielding these ionic decomposition products.

3.3 Refractory organic molecule species

Yielding the ion formation processes valid as known from other rapid dissipation processes near solid surfaces, a first glance especially to the above key ions show that saturated hydrocarbons without heteroatoms cannot be responsible for this ion decomposition pattern. Namely, such ions would prefer odd mass numbers, which is not seen. Also unsaturated hydrocarbons without heteroatoms cannot account for, because they also strongly prefer odd mass numbers; but they could be distinguished from saturated ones by the exact m/z values: saturated prefer CnH2n+m ions with m=+3, +1, -1, whereas unsaturated prefer those with m=-1, -3, -5,..

The importance of m/z 28 and 42 in any reaction chains is always recognized if nitrogen plays an important role in the parent molecules being decomposed down to the nitrile ions (m/z 30, 44, and 58, less important with the PUMA spectra, would show a decomposition only down to the imine ions). Whereas amines would yield the latter ones, iminies, enamines or nitriles would yield the, observed, former ones. Consequently, many of the molecular ions seen can be accounted to unsaturated N-containing hydrocarbons.

O-containing hydrocarbons generally yield key ions with m/z 31, 45, 59, which were not found; moreover, they occured even statistically underrepresented (31 is however totally accounted as P atomic ion within the cosmic abundance).

If one thus assumes the correlational ions mostly as unsaturated ions containing one or (with larger m/z) sometimes two N heteroatoms, nearly all correlations are easily explained as members of reaction chains with, at least formally, hydro-dehydro and HCN or C2H2 addition-elimination exchange reactions. This formal result is at least consistent with a general chemical matter being built up from acetylene and hydrocyanic monomers ionized during impact by proton transfer reactions.

However, we must strongly point out here again, that N-containing ion species are much more probable to be seen in such mass spectra than ions from hydrocarbons without heteroatoms. According to the low N/C atomic ratio we found in the dust (4%), we conclude that there must have been a lot of precursor fragments not containing N and thus not showing up as ions.

So, we cannot recognize the refractory organic as a hydrocyanic (HCN) polymer or a acetonitrile (CH3CN) polymer, though both being unsaturated. The low N/C ratio forbids this. However, it is completely within the results of the above analysis to say, that the refractory organic consists of an unsaturated hydrocarbon polymer with (not too much) nitrogen heteroatoms. In contrary it cannot consist of an aldehyde or keto-polymer, whether saturated or not, as O seems not be a major part of the molecular ions, and other analysis shows (2), that the oxygen in the organic part may mainly be due to water ice or some acids, at least in the large distances of VEGA1 from the nucleus in the outer coma (GIOTTO measurements give hints of an elimination of CO and other O-containing species in the inner coma nearer than 10,000 km from the nucleus).

Before we combine the results of gas phase and solid phase measurements, respectively, let us first make some remarks about polymer vapor pressures.

4. Polymers and their vapor pressures

It takes some hours time for the dust and gas after ejection to reach a several thousand km distance from the nucleus. It is obvious that the vapor pressure of the organic material determines whether it will find itself in the coma gas phase or in the dust particles. Materials of medium vapor pressure will give rise to an extended source of gas, because its vapor pressure may be too low to be ejected directly into the gas phase, and too high to survive in the condensed phase of the dust.

Let us now discuss more quantitatively the kinetics of vaporization of polymers as found with PICCA and PUMA. For simplicity we can regard the isothermal (T) behaviour of the vapor pressure as follows: The probability P per unit time that a molecule leaves the surface, where it is bound to, is proportional to the product of the conditional probabilities w_i that any structural element of the polymer possess in that very time interval a vibrational energy higher than a certain limit value dependent on the nature of that element. (i: structural element number). For large molecules the w are independent from each other and Boltzmann's theory yields

$$w_i = c_i \exp(-E_i/kT)$$

with E_i the limit vibrational energy. The total probability P is then given as

$$P = C \prod_i \exp(-E_i/kT) \quad \text{or} \quad \log P = \log C + \sum_i (-E_i/kT)$$

Due to kinetic gas theory that probability P is directly proportional to the vapor pressure p via the Hertz-Knudsen-equation we will need in a moment, so that with constant temperature T we can simply rewrite as follows:

$$- \log p = C' + \sum_i a_i$$

with $a_i = E_i/kT$ and $C' = -4$ if p is measured in atm (log is natural logarithm). It is now the task to determine at least roughly the mean contributions a of any structural element. This is done by comparing the vapor pressures at T=300 K (which is a reasonable dust temperature) of two molecules differing in that one structural element (7). (With other temperatures slight changes are due to a recalculation using Clausius-Clapeyron's equation for dp/dT.)

For each additional CH2-group in an alkane chain it is approximately a=1; an exchange of an -ane into an -ene or an -yne group (introduction of a double or triple bond into the chain) an additional a=0.5 has to be applied.
Nitrogen bearing species are very potent in reducing the vapor pressure. An additional N-atom bound as nitrile yields approximately a=5, as amine or imine a=4.
Oxygen bearing species are less potent in reducing the vapor pressure; only O bound as an -ole (alcohol) or -ale (aldehyde) group yields approximately a=4, as keto-groups a=3, and as ethers only a=1.5

Introducing now explicitly the Hertz-Knudsen-equation we have a relation between the number of desorbing molecules per unit time and unit surface d Z/(dt dO), the vapor pressure at temperature T expressed in numbers n of molecules per unit volume, and the mass m of the molecules:

$$r = d^2Z/(dt\ dO) = n\sqrt{kT/(2\pi m)}$$

If that rate density r is about 10^{14} /cm^2/s, a lot of the material of a 1 µm diameter dust particle is evaporated in the above discussed coma development times. This corresponds to vapor pressures of several 10^{-10} atm. This means that materials with vapor pressures lower than 10^{-10} atm ($\sum a > 27$) will preferably be found in the condensed (dust) phase, whereas those higher than 10^{-9} atm ($\sum a < 25$) will preferably be found in the gas phase.

For instance, a pure CH2O-polymer (polyoxymethylene) must possess at least 11 chain elements (molecular mass M=330 amu) to survive in the dust particles. Such large pure C/O molecules are, however, very unlikely due to elemental abundances. Smaller ones are possible in the gas phase, and are found, although only to a minor extent when comparing with pure CH-polymers, in the PICCA mass spectra (in contrary to an earlier finding of other authors, 13)

In contrary, a pure HCN-polymer (polymethylenimine) must possess at least only 5 chain elements to survive in the dust, and there are a lot of indications for decomposition products of such species in the PUMA ion-correlation mass spectra found. Within the gas phase species containing N-atoms cannot be very large if abundant. Consequently besides the abundant HCN (hydrocyanic acid) and aceto- nitrile not very many N-bearing species are found.

5. The organic parent substance of gas and dust

5.1 Inferred polymeric parent species

The above results together with the measured element ratios in the comet (which are actually solar, 5) now allow a better characterization of the cometary matter before (!) coma formation. A remarkable point is the low O/C-ratio in the molecular ions found (about 0.6 in the gas, probably below 0.3 in the dust), although the total O/C-ratio is above 1., also in the organic component alone. Apparently most of the oxygen is bound in water molecules and not in polymeric molecules. From the above measurements, however, one can not deduce, whether the huge amount of water seen in the coma is already chemically present as water in the comet nucleus, or whether it has been produced by any reaction out of the pristine matter.

Nevertheless, at least shortly after evaporation of the comet's nucleus we observe a fairly unsaturated polymeric organic matter with about 35% C-atoms, 18% O-atoms, 2% N-atoms, and 45% H-atoms (the latter deduced from the mean degree of saturation). The mean chain length (or ring magnitude) may be about 10 nuclear (CNO) atoms, so that molecular weights of 100 - 200 amu may be typical. This can be concluded from the organic matter dust to gas ratio, together with the vapor pressures, and the mean travel time from the nucleus to the loci of detection.

Together with this polymeric material there is a lot of small molecular matter containing much oxygen, especially water, HOH, but possibly also formic acid, HCOOH and/or other oxidized species forming CO under decomposition processes.

5.2 Possible polycondensate formation mechanism

If one looks to a fairly unsaturated polymer accompanied by water, one may think that it was polycondensation rather than polymerization how such a species may have been formed. It is an open question up to now (11), whether these organics have been produced by irradiation processes of frozen gases in the inner solar system, or whether the comet consists of organics already in the Oort's cloud. If the latter is the case, water (and to a lesser extent CO) may be driven out at higher temperatures by polycondensation mechanisms, especially if latent heat is present in the organic matter (e.g. due to free radicals). Anyway, the ultimate result of such reactions in laboratory simulation are apparently unsaturated products, and water is driven out.

6. Consequences and recommendations for ROSETTA or any CNSR

There are a lot of precautions to be taken with any comet nucleus sample return (CNSR) mission, e.g. ROSETTA, which results from the chemical properties of that matter.
First of all, at least the organic fraction (if not both) are not yet in an equilibrated state, so that temperature and pressure rise is expected to trigger chemical reactions. By no means a liquid state should be achieved neither during transport nor during subsequent analysis, because thence a series of chemical reactions would take place completely altering the primordial matter.
Another problem may cause the material of the containers, as catalytic action with the cometary matter has to be strictly avoided.
Sealing and flanging may not be trivial as well, because there is a wide range of size distributions of the matter.

It seems that there may be a rather hard crust like a compact polymeric plastics with minerals embedded, covering the comet's surface, which thus may be hard to overcome. In contrast to it, the primordial matter below will be very soft and fluffy. As neither the thickness nor the elastic and inelastic modules of that crust is known, such a layered structure may cause severe problems when penetrating it: Namely, if the force acting is too small the penetrator may not penetrate at all, if it is too large the penetrator may vanish in the comet's interior.

7. Conclusion

It has been clearly shown that the molecular gas phase ions are not arising from small parent molecules, but from larger polymers in the cometary matter the more volatile of which forming the gas phase, the less volatile the dust.

The volatile component contains an appreciable amount of oxygen. If nitrogen is present only small molecular ions are formed in the gas phase. The volatile matter is apparently not totally saturated, but bears generally some double or triple bonds.

The involatile component apparently contains less oxygen in the polymer species rather than in smaller molecules. It consists mainly of unsaturated hydrocarbons with some nitrogen present.

Both components may be highly reactive under normal conditions, i.e., in a liquid water environment, under which it can form a lot of prebiotic chemical species (2,11) with large free energy, especially with the help of the catalytic action of the large specific area doped silicatic backbone of the dust grains. Consequently, a series of special precautions have to be taken with a comet nucleus sample return.

REFERENCES:

(1) Kissel, J., Sagdeev, R. Z. & al., Nature 321, 280 (1986)
(2) Kissel, J. & Krueger, F. R., Nature 326, 755 (1987)
(3) Korth, A., Richter, A. K., & al., Nature 321, 335 (1986)
(4) Mitchell, D. L. et al., to appear in Adv. Space Res., 1988
(5) Jessberger, E. K., Kissel, J., Fechtig, H. & Krueger, F. R., In: Comet Nucleus Sample Return Workshop Proc. ESA SP-249, 27 (1986)
(6) Krueger, F. R., Z. f. Naturforschung 38a, 385 (1983)
(7) CRC-Handbook of Chemistry and Physics, 56th Ed. (1976)
(8) Korth, A. et al., J. Phys. E. Sci. Instr., 20, 787, 1987
(9) Korth, A. et al., Eur. Space Ag., SP-250, 199, 1986
(10) Korth, A. et al., to appear in Nature, 1989
(11) Ferris, J. P., Origins of Life and Evolution of the Biosphere 18, 161 (1988)
(12) Strazzulla, G., In: Laboratory Simulation of Organic Cometary Material, Catania (1987)
(13) Huebner, W. F., Boice, D. C. & Sharp, C. M., The Astrophysical J. 320 (1987), L149; Huebner, W. F., Science 237 (1987), 628

ON THE MEASUREMENT OF COSMOGENIC RADIONUCLIDES IN COMETARY MATERIALS

G. F. Herzog
Rutgers University

P. A. J. Englert
San Jose State University

R. C. Reedy
Los Alamos National Laboratory

K. Nishiizumi, C. P. Kohl, and J. R. Arnold
University of California, San Diego

ON THE MEASUREMENT OF COSMOGENIC RADIONUCLIDES IN COMETARY MATERIALS

G. F. Herzog
Rutgers University

P. A. J. Englert
San Jose State University

R. C. Reedy
Los Alamos National Laboratory

K. Nishiizumi, C. P. Kohl, and J. R. Arnold
University of California, San Diego

ABSTRACT

Determinations of the cosmogenic nuclide concentrations in cometary material will help to define the recent surface history of the comet and its exposure to cosmic rays. In particular, the rates for the removal or mixing of surface material could be studied, and any variations in cosmic-ray intensity implied by the data could be used to infer orbital changes during the last few million years. The measurement of the shorter-lived isotopes poses technical challenges that should be addressed now. The measurement of longer-lived isotopes will be straightforward provided that rates of mass loss are not too high.

INTRODUCTION

An important goal of solar system exploration is to obtain for laboratory study cometary material that has been subjected to a minimum of post-accretional processing. The proposed Rosetta mission (Ahrens et al., 1987), for example, would achieve this goal by recovering core, volatile, and non-volatile surface samples. Close to the comet's surface, solar and cosmic-ray irradiation will have induced nuclear reactions that produce a wide variety of cosmogenic nuclides, both radioactive and stable. We consider here some strategies for the measurement and interpretation of the cosmogenic nuclide record in returned cometary material. Our main purpose is to point out how cosmogenic radionuclide data may help in reconstructing the recent history of the cometary surface. Few other approaches would provide comparable information.

In the sections to follow we 1) list some isotopes of interest and the ways in which they are produced; 2) review current analytical capabilities for these isotopes; 3) describe some semi-empirical calculations of production rates in a quiet comet, calculations that may serve as a convenient framework for discussion; 4) consider some processes that would perturb the comet's surface and how they would affect the cosmogenic nuclide record; 5) point out the kinds of samples and measurements we think best suited for the reconstruction of the irradiation history and 6) identify those gaps in present, relevant knowledge that pre-launch research should fill.

1. ISOTOPES OF INTEREST AND THEIR MANNER OF PRODUCTION

The cosmogenic radionuclides of particular interest for unravelling the histories of cometary surfaces are listed in Table 1 along with half-lives, major target elements, current detection limits and methods of measurement. As shown in Table 1, these nuclides may be produced by nuclear interactions with galactic cosmic rays (GCR) or solar cosmic rays (SCR) or by the capture of thermal neutrons (Reedy and Arnold, 1972; Reedy et al., 1983). Because of the variety of the cosmic-ray particles and of their modes of interactions, the effective depths of the interactions and their products vary considerably. This diversity in the types of products and their depths will be very useful in studying the cosmic-ray record of the comet (cf., Reedy et al., 1983). In particular the concentrations of SCR products furnish a most sensitive measure of surface disturbance (see below). An examination of the target elements listed in Table 1 shows further that most of the nuclides are produced primarily in dust particles: i.e., silicate or possibly metal grains. Production of ^{14}C and ^{10}Be may also occur in icy and/or organic material.

TABLE 1. PROPOSED MEASUREMENTS

	Half-life	Target Elements	Detection Limit (10^6 atom)	Detection Method	Principle Means of Production#
^{7}Be	53.3 d	C, O, Mg, Si	0.05*	Counting	GCR
^{56}Co	77.7 d	Fe	0.01*	Counting	SCR
^{54}Mn	312 d	Fe	0.05*	Counting	GCR+SCR
^{22}Na	2.61 y	Mg, Si	1.*	Counting	SCR+GCR
^{60}Co	5.27 y	Co	2.*	Counting	N_{th}
^{3}H	12.3 y	O, Mg, Si, Fe	0.1	Mass spec.	GCR
^{14}C	5730 y	O, N	0.2	AMS	GCR
^{41}Ca	0.10 My	Ca, Fe	1.?	AMS	GCR+N_{th}
^{36}Cl	0.30 My	Cl, K, Ca, Fe	0.4	AMS	GCR
^{26}Al	0.71 My	Al, Si	0.4	AMS	SCR+GCR
^{10}Be	1.5 My	C, O, Mg, Si	0.2	AMS	GCR
^{53}Mn	3.7 My	Fe, Ni	100	NAA	SCR+GCR

* These numbers are based on laboratory measurements; in situ detection limits may be an order of magnitude higher. # GCR=Galactic cosmic rays, SCR=Solar cosmic rays, N_{th}=thermal neutron capture.

2. CURRENT ANALYTICAL CAPABILITIES

The isotopes listed in Table 1 have a wide range of half-lives. This range is advantageous because it opens observational windows on a correspondingly broad range of rates for cometary processes. From a technical standpoint, it implies a need to employ a number of different experimental methods. In the text below, we will take 5 y as the half-life that operationally separates long-lived species which, as we will see, are readily amenable to terrestrial measurement, from short-lived species.

Short-lived isotopes - In practice it will be difficult to measure the nuclides with shorter half-lives for several reasons. A major difficulty is the long transportation time (~3 years) of the sample return. The original radioactivity produced in the comet will decay appreciably during transit from comet to laboratory, while at the same time measurable amounts of the nuclides will be produced by cosmic ray bombardment of the sample in the space probe. Two possible alternatives to laboratory measurement are discussed in section 5.

The precision attainable for the short-lived nuclides would not match that for the longer-lived species. The detection limits for the short-lived nuclides listed in Table 1 are based on laboratory measurements after chemical separation. The detection limits for in-situ measurements or nondestructive counting in the space probe may be more than an order of magnitude higher. Nonetheless, the importance of obtaining the activities of these short-lived nuclides warrants further investigation of the feasibility of the two approaches described in section 5.

Long-lived isotopes - Determinations of longer lived radionuclides should present few technological challenges either in sample preparation or measurement. The detection limits for nuclides measured by accelerator mass spectrometry (AMS; see Table 1) are typically 10^6 atoms, 2-4 orders of magnitude lower than achievable by decay counting (Elmore and Phillips, 1987). The detection limit of ^{53}Mn by neutron activation is about 10^8 atoms (Nishiizumi, 1983) but AMS may lower this value to 10^6 atoms within a few years. The nuclides ^{10}Be, ^{26}Al, and ^{53}Mn have been measured in 100 μg size samples of deep sea spherules and in mg size samples of lunar rocklets by AMS and by neutron activation (Raisbeck et al., 1985; Nishiizumi, 1983). The size of the cometary sample required for our study will depend on the rate of surface mass loss and on the depth of the material below the cometary surface. If the rate of mass loss is less than 10^{-3} g/cm^2-y, all of the long-lived nuclides proposed could be measured with an error of less than 10% in a sample of 10-50 mg. The chemical procedures needed to separate these nuclides from silicate and ice are well established and have been widely applied. Means for the separation of ^{10}Be from CO_2 and organic material will have to be tested before actual sample preparation. A second developmental question concerns ^{41}Ca. Fink et al. (1988) have reported a minimum detectable ^{41}Ca/^{40}Ca ratio of 5×10^{-16} (see also Kubik et al., 1986). This nuclide is expected to be measurable at the level given in Table 1 within a year. Small amounts of ^{3}H can be detected by mass spectrometric measurements but only if ^{3}He is allowed to accumulate for suitable times in the sample and if most of the ^{3}He initially present can be removed (Clarke et al., 1976).

3. PRODUCTION RATES IN A QUIET CORE

Nature of the interaction - Cosmogenic nuclides are normally not present in appreciable quantities in material buried beneath many meters of overburden. When a piece of comet is exposed to cosmic-ray particles, concentrations of cosmogenic nuclides steadily increase until, after several half-lives, radionuclide activities approach an equilibrium value where the rate of decay equals the production rate. In contrast, stable isotopes such as ^{3}He and ^{21}Ne and tracks made by heavy ($Z > 20$) cosmic-ray nuclei may continue to accumulate indefinitely and can be used to determine the total length of time that a sample was exposed to cosmic rays.

Two types of energetic particles can induce nuclear reactions in matter, the galactic cosmic rays (GCR), which have low fluxes but high ($E \sim$ GeV) energies, and the solar cosmic rays (SCR) (often called solar energetic particles), which are emitted irregularly from the Sun with low ($E \sim$ 10-100 MeV) energies but high fluxes (cf., Reedy and Arnold, 1972; Reedy et al., 1983). The nuclei in both types of cosmic rays are mainly protons and α particles (with a proton/α-particle ratio of about 10-20), with about 1% heavier nuclei.

The energy, charge, and mass of a cosmic-ray particle and the composition of the target material determine which interaction processes are important and which cosmogenic products are formed. Energetic nuclear particles interact with matter mainly in two ways: ionization energy losses and reactions with nuclei. All charged particles continuously lose energy by ionizing the matter through which they pass. A nuclear reaction between an incident particle and a target nucleus generally involves the formation of new, secondary particles (such as neutrons, protons, pions, and photons) and of a residual nucleus that is usually different from the initial one. One-GeV protons have a range of about 400 g/cm^2 and a nuclear-reaction mean free path of ~100 g/cm^2, so only a few percent go their entire range without inducing a nuclear reaction.

SCR Products - The depth profiles of cosmogenic nuclides made by SCR particles are very different from those made by the galactic cosmic rays. The relatively low-energy solar protons and α particles are usually stopped by ionization energy losses near (top few millimeters) the surface. The SCR particles that induce nuclear reactions as a rule produce few secondary particles and the masses of the reaction

products are close to those of the target nuclei: e.g., ^{56}Co from iron (Reedy and Arnold, 1972). The fluxes of SCR particles as a function of depth can be calculated accurately from ionization-energy-loss relations, so a nuclide's production rates can be predicted well if the cross sections for its formation are known. Like the densities of heavy-nuclei tracks, the activities of SCR-produced nuclides decrease rapidly with depth, most being made within a centimeter of the surface (Reedy and Arnold, 1972; Reedy et al., 1983).

GCR Products - The GCR particles that produce nuclear reactions can roughly be divided into four components: high-energy (E > 1 GeV) primary particles, medium-energy (about 0.1 to 1 GeV) particles produced partially from the first component, a low-energy group (E < 100 MeV) consisting mainly of energetic secondary neutrons, and slow neutrons with energies below about a keV. The fluxes of the high-energy primary GCR particles decrease exponentially with depth as they are removed by nuclear reactions. The numbers of secondary particles as a function of depth build up near the surface, where most of them are made, but eventually decrease roughly exponentially. In the moon, the rate of neutron production is about 13/s-cm^2 (Lingenfelter et al., 1972). This neutron production rate may be compared to an average omnidirectional flux of about 3/s-cm^2 for the GCR primaries in space (Reedy et al., 1983). The difference between the two fluxes shows the importance of the large cascade of nuclear reactions that produces numerous secondary particles.

Neutron products - Neutrons slowed to energies of keV or eV can produce nuclides by neutron-capture reactions. Some reactions of interest are $^{59}Co(n,\gamma)^{60}Co$, $^{14}N(n,p)^{14}C$, and $^{58}Ni(n,\gamma)^{59}Ni$ and others leading to stable isotopes such as ^{150}Sm and ^{158}Gd (Lingenfelter et al., 1972). Most GCR-induced reactions involve incident particles with energies of 1 MeV or more, emit one or more nucleons either individually or in clusters like α particles, and are called spallation reactions. Such products are referred to as "spallogenic" nuclides. Sometimes the spallation reactions are divided into low-energy and high-energy groups. High-energy spallation reactions involve particles with energies above about 100 MeV, produce numerous secondaries, and can make, in relatively low yields, many different product nuclides. Examples of high-energy spallation reactions are $^{16}O(p,X)^{3}He$ or $^{24}Mg(p,X)^{10}Be$, where X can be any one of a large number of possible outgoing particle combinations. Low-energy spallation reactions usually involve particles with energies below 100 MeV and can produce certain nuclides in high yields because both the fluxes of particles and the cross sections are relatively large. The reaction $^{24}Mg(n,\alpha)^{21}Ne$ is such a low-energy reaction and is the major source of ^{21}Ne in most stony objects. Because the distributions of low-energy and high-energy GCR particles are not the same for all locations, the production rate-versus-depth profiles for different cosmogenic nuclides can vary. A high-energy product like ^{3}He has a depth-versus-concentration profile that is fairly flat near the surface, whereas a low-energy product, like ^{21}Ne, builds up in concentration considerably with increasing depth near the surface (Reedy and Arnold, 1972; Reedy et al., 1983).

Model calculations - Reedy (1987a) reviews several approaches that have been used to predict the rates, ratios, or profiles for the production of cosmogenic nuclides. Simulations using thick targets bombarded by a beam of high-energy protons have been used to model the production rates and profiles of several cosmogenic nuclides (Englert et al., 1987). Several research groups have developed semi-empirical models from measured concentrations of cosmogenic nuclides. Several models for the production rates of cosmogenic nuclides are based on particle fluxes estimated inside the object and cross sections for the nuclear reactions of interest. The most important parts of these models are the expressions adopted for the fluxes of cosmic-ray particles as a function of particle energy and sample depth. For SCR particles, ionization-energy-loss relations can be used to calculate the particle fluxes (Reedy and Arnold, 1972). For GCR particles in the moon, Reedy and Arnold (1972) derived particle spectra that varied with depth. Cross sections used for the production of a nuclide are measured ones, if available; if not they can be estimated from nuclear models or other systematics, such as spallation formulae (Reedy, 1987a).

In a few cases, production rates and profiles have been calculated from theoretical expressions for nuclear interactions. Armstrong and Alsmiller (1971) used a Monte Carlo code for intranuclear cascades to calculate the distribution of cosmic-ray particles and product nuclides in the moon. Drake et al. (1988) have used a similar code to calculate particle fluxes in Mars. Rates for neutron-capture reactions

have been calculated for the moon, meteorites, and Mars using several neutron-transport codes. Given an initial distribution of secondary neutrons, which are made with energies of the order of 1 MeV, these calculations transport the neutrons through the object and follow the scattering reactions that slow the neutrons to thermal energies (E < 1 eV) (Lingenfelter et al., 1972; Drake et al., 1988). The production rates for neutron-capture reactions vary much more with sample depth and peak more deeply than do those for spallation reactions (Reedy et al., 1983). This large variability with radius and depth makes neutron-capture products, like SCR products, useful in determining sample histories. However, the composition of the medium, especially its hydrogen and carbon content, can strongly affect neutron transport (Drake et al., 1988).

Comparison of models with experiments - The absolute rates calculated with the models are sometimes not very reliable and are generally normalized to measured ones. When, as is often the case, the activity of a radionuclide in an extraterrestrial sample is in equilibrium with its production rate, measured activities can directly be used as production rates, assuming no complications in the sample's history. A measured activity of a cosmogenic radionuclide and a production ratio can also be used to infer the production rate for a stable nuclide, especially if the pair of nuclides are made by similar reactions or if the stable nuclide is the decay product of the radionuclide. Radioactive/stable pairs used in this way include $^{3}H/^{3}He$, $^{22}Na/^{22}Ne$ (with care to correct for variations in ^{22}Na activity over an 11-year solar cycle), $^{36}Cl/^{36}Ar$, $^{39}Ar/^{38}Ar$, and $^{81}Kr/^{83}Kr$.

To a good first approximation, the cosmogenic nuclide depth profiles in the cometary surface should be analogous to those observed in the lunar surface because the irradiation geometry is 2π in both cases. Fig 1 shows ^{10}Be, ^{26}Al, ^{36}Cl, and ^{53}Mn depth profiles measured for the Apollo 15 drill core (Nishiizumi et al., 1984a,b) along with model calculations (Reedy and Arnold, 1972) for both SCR and GCR production of these nuclides.

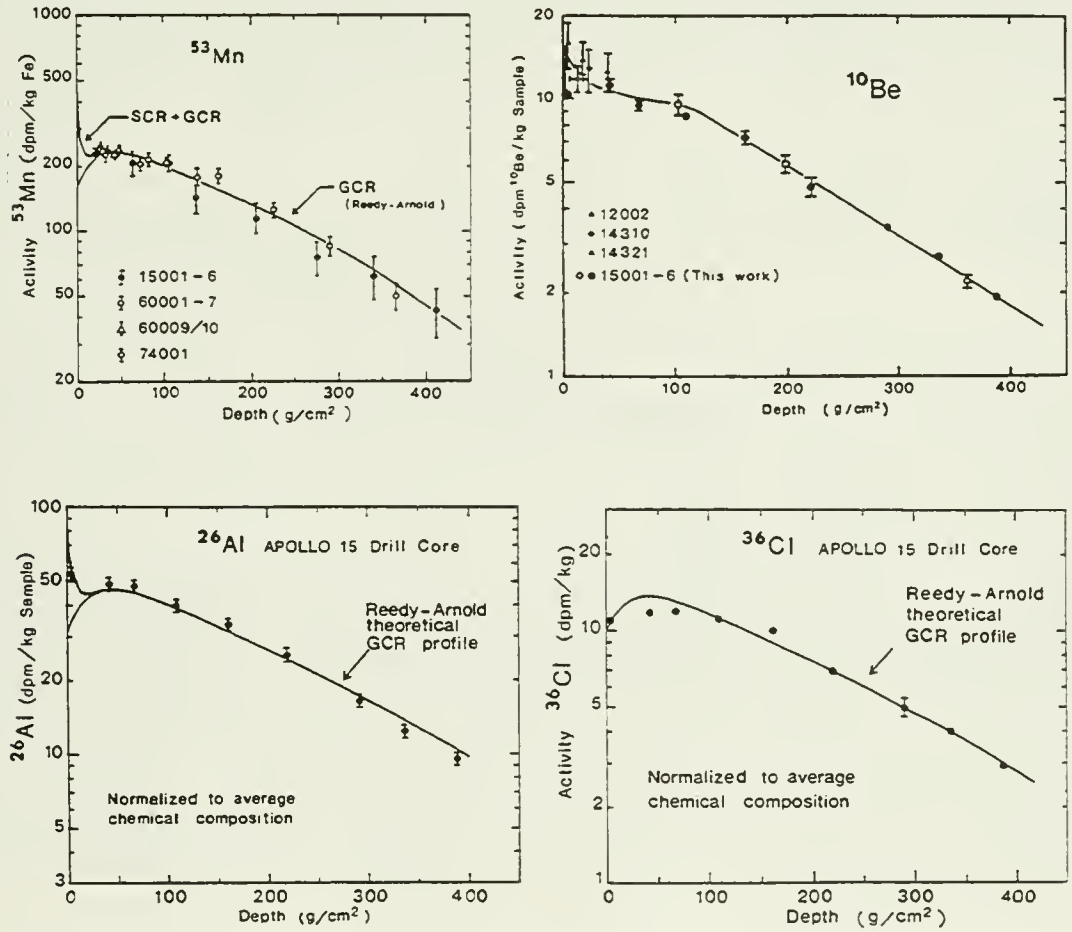


Figure 1. Measured and calculated cosmogenic nuclide profiles in the lunar surface. For references, see text.

4. PERTURBATIONS OF THE CORE

We can expect three sources of perturbations to the baseline production rates for cosmogenic radionuclides: 1) mass loss, which may vary from phase to phase; 2) mixing as a result of cratering, gas release, or other processes; 3) variation in the cosmic ray flux that follows either orbital evolution or compositional change. Adjustments to model calculations can be made to allow for these effects. Such adjustments have worked well in the lunar case.

Mass Loss - The loss of matter from the surface of the comet will reduce the radionuclide inventory from its baseline value. The key parameter governing the size of the reduction is the ratio $\varepsilon\tau/\rho$ where ε is a nominal erosion rate, τ the half-life of an isotope and ρ the thickness of matter that will reduce the relevant production rate by a factor of two. Put another way, significant radioisotope losses will occur whenever the thickness of matter eroded during one half-life is comparable to the half-thickness. With the aid of the cosmogenic nuclide measurements one can in principle determine the sizes of the reductions and from them estimate the rates of mass loss. Is this goal achievable in practice?

The answer to this question will depend on the sampling strategy adopted. Weissman (1989) has proposed blasting surface material away prior to coring. Such an approach would almost surely obliterate the cosmic-ray record. A second strategy for retrieving deeper-lying material is to select as active a region as possible (Y. Langevin, pvt. comm.) on the theory that the least altered and most volatile-rich areas will have the greatest activity. While it is difficult to predict what the rate of mass loss will be, we do have some limiting cases to consider.

In meteorites, micrometeorite milling proceeds at rates corresponding to average values of ε of about 1 mm/My (Schaeffer et al., 1981). Lunar rates may be somewhat higher but in either case only isotopes with the longest half-lives and/or smallest half-thicknesses (e.g., SCR-produced ^{59}Ni, ^{26}Al, or ^{53}Mn in lunar surface rocks) show signs of much loss (Lanzerotti et al., 1973; Fruchter et al., 1981; Kohl et al., 1978). For a comet with a radius of 10 km, the global rates of mass loss given by, e.g., Glass (1982) and Ahrens et al. (1987), translate into average erosion rates between 0.001 and 2 g/cm^2-y.

TABLE 2. ESTIMATED GCR PRODUCED ACTIVITY

ISOTOPE	HALF-LIFE	EROSION RATE (g/cm^2-y)				
		0			0.001	
		Depth (g/cm^2)				
		0	0	200	0	200
		Activity *(atom/g)* or (dpm/kg)				
^{22}Na	2.61 y	*4.8x10^4*	24	15	24	15
^{14}C	5730 y	*6.1x10^7*	14	11	13	10
^{36}Cl	0.30 My	*3.4x10^8*	1.5	0.8	0.4	0.2
^{26}Al	0.71 My	*8.6x10^9*	16	12	2.4	1.7
^{10}Be	1.5 My	*1.9x10^{10}*	17	13	1.3	1.0
^{53}Mn	3.7 My	*3.4x10^{10}*	12	10	0.4	0.3
^{53}Mn (dpm/kg Fe)		*4.5x10^{11}*	161	136	5.1	4.4

To assess the impact of erosion in a comet nucleus, we have calculated cosmogenic nuclide concentrations at the surface and at a depth of 200 g/cm^2 (Table 2). The calculations are based on the computational model of Reedy and Arnold (1972) and the chemical composition reported for comet P/Halley by Jessberger et al. (1988). Two cases are presented here, the first with no mass loss and the second with a mass loss of 10^{-3} g/cm^2 year. The results show that the short-lived species are relatively insensitive to erosion, while long-lived species produced by cosmic rays are almost completely removed.

Even though the effects of solar cosmic rays may not be detected in the long-lived nuclides, it is of critical importance that the depths below cometary surface be known as exactly as possible for all samples.

Unfortunately from our point of view, imaging of comet P/Halley and other evidence indicate that only a small fraction - perhaps 10% - of the comet's surface is active at any time. This observation implies local erosion rates much higher (~20 g/cm^2-y) than the average considered above. With erosion rates so rapid, only the shortest-lived isotopes hold any promise of providing useful information. All SCR products, for which production is confined to the uppermost centimeter or so, and the bulk of the longer-lived isotopes will have vanished within a few apparitions.

There may be some mitigating factors. On the centimeter scale relevant to the behavior of a sampling site we do not know, for example, whether a specific location becomes active and remains so; or whether - as seems unlikely - activity occurs uniformly throughout. Moreover, depending on the comet selected, we may know little *a priori* about the total duration of the activity. Finally, and perhaps most important, the nature and durability of the crust widely believed to cover the comet's surface is uncertain. The crust may retain for long periods constituents tough enough to resist volatilization but porous enough to permit the escape of gases (Brin and Mendis, 1979; Horanyi et al., 1984). Simulation experiments and direct observation suggest that the crust includes silicates, polymeric organic material, and water ice (Sagdeev et al., 1986; Klinger et al., 1988; Wdowiak et al., 1989). Among these phases, the silicates certainly and the others possibly would retain cosmogenic nuclides.

Mixing Processes - Stern (1988) argues that comets undergo regolith formation, albeit at slow rates; Keller et al. (1986) present possible evidence for cratering on comet P/Halley. Cratering may lead to both vertical and horizontal mixing of material and thereby scramble the record of cosmogenic nuclides. Studies of the lunar regolith demonstrate that cosmogenic nuclide data can unscramble the record. Nishiizumi et al. (1983), for example, have shown that certain depth profiles on the lunar surface differ from profiles calculated for undisturbed material (e.g., Nishiizumi et al., 1983) but can be reconciled with them by allowing for the effect of meteoritic mixing with the model of Langevin at al., (1982). The effects extend to about 50 g/cm^2 over a 1-10 My time scale.

The devolatilization of comets may also lead to mixing of surface material. Dust lifted from one portion of the surface - perhaps by electrostatic processes (Flammer et al., 1986) - could return to another. Material may slide into depressions created by evaporation. Gas may recondense as the comet moves away from perihelion (Whipple, 1987). The explosive release of gas pockets in the interior (Bar-Nun, 1989) could lead to the extensive relocation of material.

Variations of the cosmic-ray flux - The galactic cosmic-ray flux has a positive radial gradient of about 2%/AU with little dependence on latitude (Venkatesan et al., 1984; Van Allen and Randall, 1985; Webber and Lockwood, 1986). The flux of solar cosmic rays decreases as $1/R^2$. For isotopes with half-lives longer than a few periods (15-20 y), the variation in production rates due to changing heliocentric distance will be minimal for the range of orbital parameters considered. On the other hand, longer-term orbit variations may be significant.

Mission planning assumes that as the comet orbit evolved over the last few million years its average heliocentric distance decreased in a stochastic but more or less monotonic way (Ahrens et al., 1987). At distances beyond the heliopause (> 50 AU), cosmic-ray fluxes may increase to ~4 times the values typical of the inner solar system (Reedy, 1987b). Such fluxes could raise production rates high enough to create observable effects in the longest-lived and stable isotopes provided that the comet achieved its rendezvous orbit or one much like it within a few half-lives of capture from the Oort cloud. Figure 2 illustrates the effect schematically for a case in which the comet went from an orbit with high fluxes to one with lower, local fluxes about 1,000 years ago. Figure 2 suggests that high concentrations of longer-lived isotopes alongside of normal inventories of shorter-lived isotopes in the same sample would constitute a signal for high fluxes beyond the heliopause. With careful analysis of radioisotope inventories as a function of half-life, we may be able to separate the effects of mass loss from those due to changes in the cosmic-ray flux.

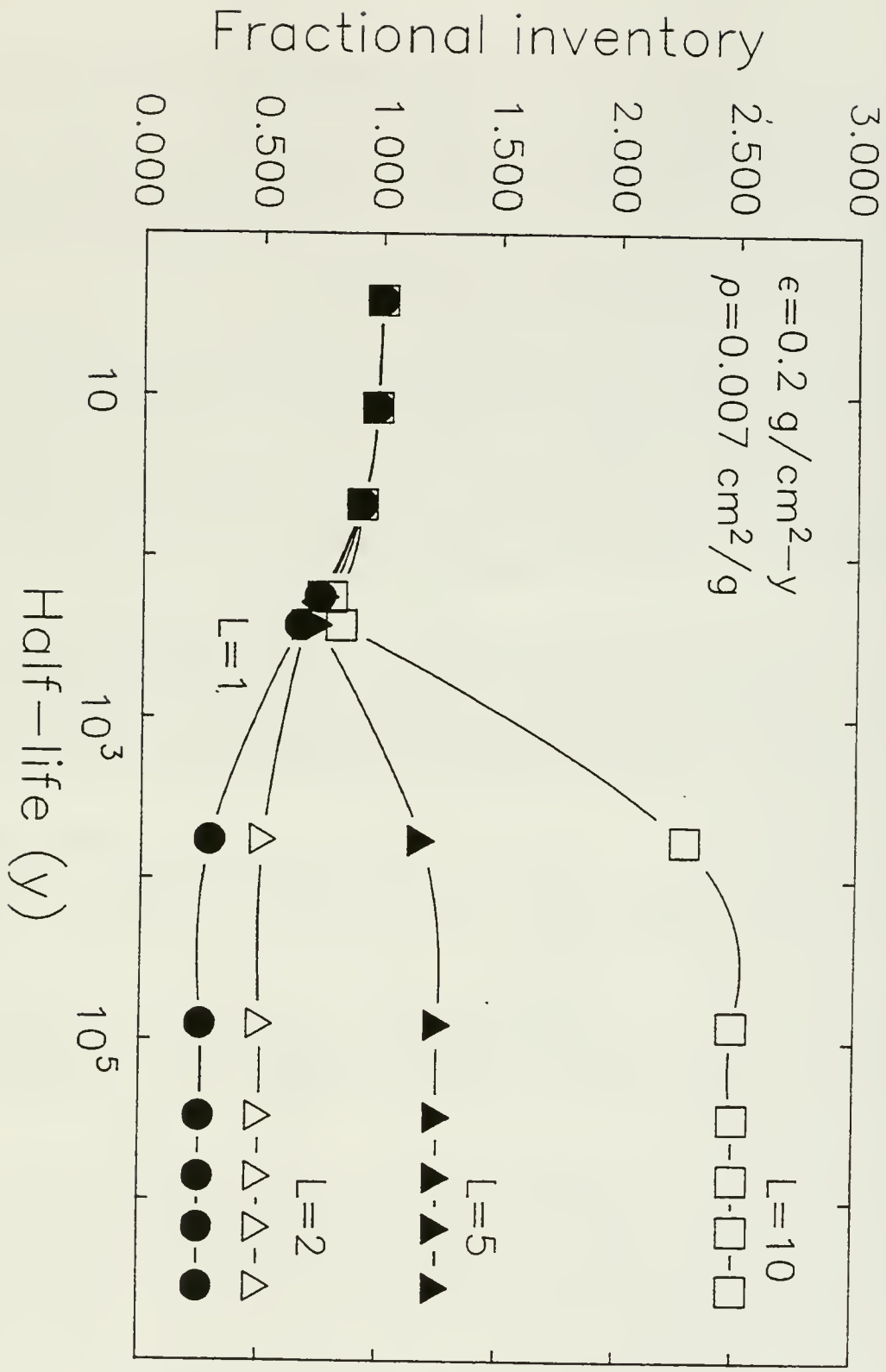


Figure 2. A schematic illustration of the expected inventories of cosmogenic radionuclides vs. their respective half-lives. The calculation assumes that the comet arrived in the inner solar system 1000 y ago from a region where the cosmic ray flux had a value L times its present one. ε is the erosion rate; ρ is the thickness of matter that reduces the nuclide production rate by a factor of two.

Another time-dependent effect of comparable magnitude but subtler origin may affect cosmogenic nuclide contents. Begemann and Schultz (1988) have argued that the development of the flux of secondary cosmic ray particles, which produce more than half the inventories of most isotopes, depends strongly on the composition of the matrix. Accordingly, if the composition of the matrix changes as ices vaporize or with regolith development (Cintala and Horz, 1987), so will the cosmogenic nuclide production rates. Fortunately the production rates are amenable to laboratory and computational study and it should be possible to infer initial and final compositions of the core from direct observation.

5. SAMPLES AND MEASUREMENTS

To decipher the cosmogenic record we will need to know the cosmogenic nuclide profiles for each of the separate phases and the petrography and stratigraphy of the core as a whole. We next consider sampling and measurement protocols that will allow us to obtain this information.

The total amount of cometary material returned to terrestrial laboratories may be very small. Magnani et al. (1989) list as the samples likely to be recovered: one deep segmented drill core; a 'pristine' sample from the bottom of the drill hole; and possibly a surface sample from a different location obtained with a "harpoon." B. Clark (pvt. comm.) believes that we may be able to recover a larger and more diverse set of samples. To be conservative, our suggestions for sampling sites, sampling procedures, and sample transportation and handling requirements are based on the sampling scenario of Magnani et al. (1989).

Sampling locations - If the core is to come from a location of high activity, then only the shorter-lived isotopes will cast light on the history of the material. The measurements are possible but challenging (see below). Accordingly, unless a reliable, alternative approach becomes available, we would urge that an effort be made to recover additional material from a less active and presumably older site. With such material we could more effectively address questions related to surface loss mechanisms, to orbital evolution, and to the variability of the cosmic ray flux.

For our purposes a narrower but longer core would be preferable to a shorter, thicker one. The reason is that if coring penetrates deeply enough to reach the regime where production rates decrease monotonically with depth then estimates of total inventories and hence of mass loss (vaporization) or gain (lateral transport) will be possible.

Documentation - The production rates of cosmogenic nuclides reflect the geometric conditions under which irradiation took place. In a column cored from a semi-infinite slab, production rates depend only on depth and chemical composition. In more complex topographic settings - valleys or mounds - production rates will also reflect the sample's "view" of the sky (Russ and Emerson, 1980). Therefore, in order to interpret the cosmogenic nuclide contents we will have to know the locations of all samples with respect to each other and to the surface. Toward this end, the neighborhood of each sampling site should be documented and the sampling sequence recorded by stereometric photography or other means (see also: Ahrens et al., 1987; Englert, 1988). In order to insure the fidelity of the stratigraphic record, coring procedures should be designed so as to minimize the physical disturbance. Maintenance of the core's integrity during transport and subsequent handling procedures is also important. If sample deterioration and the consequent loss of geometrical information seem likely due to acceleration, vibration, or heating, then it would be desirable to store separately subsamples for cosmogenic nuclide studies.

Extraterrestrial measurement of short-lived isotopes - The 2-3 year return to earth will occur with the samples exposed to altered irradiation conditions. As a result, cosmogenic nuclide contents will change as will other radiation-related properties of the material such as thermoluminescence and free radical concentrations. The effects will be largest for the cosmogenic nuclides with half-lives of a few years or less and in samples from greater depth where cometary production rates were low. Two kinds of measures could help to conserve the information potential of the isotopes with half-lives between 2 and 5 years, namely, optimization of shielding and monitoring of the nuclear-active flux *en route*. We consider each of these measures in turn.

Weight constraints eliminate the possibility of screening out cosmic rays entirely by the use of massive shielding. The obvious fallback, a moderately shielded location in, say, a heavy cargo compartment, would unfortunately also promote the development of a substantial flux of secondaries. As it turns out, the best practical way to limit cosmogenic nuclide production in transit is to place the samples in the least shielded location (Englert, 1988) consistent with temperature control requirements. At least part of the residual secondary radiation from the spacecraft - the thermal neutrons - could be eliminated by the judicious use of Cd, B, or Li shielding.

To monitor the remaining flux, the spacecraft should be equipped with active detectors for charged particles and neutrons. When the return trip begins the spacecraft should also have the capability to deploy passive detectors, i.e., foils with various activation thresholds that will accumulate short-lived ($t_{1/2}$ < 3 y) nuclear-reaction products that can be conveniently determined in the terrestrial laboratory. Track detectors that could be positioned over fissionable or alpha-emitting material at the time when samples are transferred to the spacecraft would also be useful (Woolum et al., 1975).

Even these measures will probably not suffice for the shortest-lived isotopes (Table 1) for their concentrations will have been too greatly altered by the time the mission returns with samples. Each isotope has some characteristic utility - ^{60}Co as a thermal neutron monitor and ^{7}Be and ^{22}Na as possible indicators of exposure age. In the case of ^{7}Be and, with some restrictions, ^{22}Na, extraterrestrial measurements, either on the comet or in the spacecraft, offer the only way to determine activities. The radiation environment in the spacecraft will be inhospitable to the measurement of short-lived radioactivity; large guard counters would be needed to reduce background rates. Nonetheless the technical feasibility of such measurements deserves further study. An alternative may be the measurement of cosmic-ray particle fluxes on the comet, at the sample site itself, by means of neutron-, gamma-, and/or charged particle spectrometry. Such an approach has proved useful on the moon (15) but will require further study for application to a comet.

Material requirements for non-destructive measurements - Upon return, the entire sample should be analyzed by non-destructive, low-level counting of γ radiation. As a bonus, the spectra could provide information about the naturally occurring radioactive species ^{40}K, Th, and U (provided they are abundant enough). The construction of low-level, low-temperature equipment suitable for this application should be carried out in advance of the mission.

Material requirements for destructive measurements - Most long-lived cosmogenic nuclides can be determined in small samples - less than 1 mg in favorable cases. For the analysis of a large suite of nuclides, samples of 20-40 mg would seem appropriate. The siliceous phases are the most likely to retain a coherent record of cosmic-ray effects and deserve the most intense study. Significant production of ^{3}H, ^{14}C and ^{10}Be will also occur in the icy and organic components of a comet. Therefore 40-mg samples of these phases, too, should be reserved for cosmogenic nuclide analysis.

We would request perhaps 20 samples from the core. The mass required would be a very small percentage of the total planned recovery. As the primary aim of the measurements is to understand surface processes, the sampling density close to the surface should be greater than in the presumably undisturbed depths of the comet. The distances between these samples should probably increase exponentially as depth along the core increases. Should older material be available, from the harpoon perhaps, then especially dense sampling of the topmost few centimeters would be useful for tracking the products of solar cosmic rays.

Information from related measurements - As noted in Table 1, many cosmogenic nuclides can be made from more than one of the elements that are present, so the chemical composition of a sample is needed to interpret a cosmogenic-nuclide measurement. Other related information of interest would include nuclear track densities, thermoluminescence results, free radical concentrations, and the concentrations of stable cosmogenic nuclides.

6. PRE-LAUNCH RESEARCH

We know little about the production and retention of cosmogenic nuclides in volatile materials like those observed in comets. To lay the groundwork for the interpretation of sample data, cosmogenic nuclide production in material rich in hydrogen and carbon should be studied by using both theoretical and experimental techniques. Accelerator bombardments (e.g., Englert et al., 1987) of volatile-rich material can simulate the cosmic-ray irradiation of comets. The computer codes developed to model high energy interactions and neutron transport should be tested against the results. The information now lacking includes the *numbers of secondary particles*, especially neutrons, made in cometary-like material and the *energy spectra* of these particles from the eV to the GeV range. Also missing are cross sections for many nuclear reactions, such as that for the production of ^{10}Be from carbon.

Related work is already under way. There are gamma-ray and neutron spectrometers scheduled to go to Mars in 1992 on the Mars Observer. Measurements by these instruments over the Martian poles and perhaps elsewhere on the planet will broaden our experience with planetary surfaces that are rich in hydrogen and carbon (Drake et al., 1988).

The behavior of the cosmogenic nuclides in material subject to volatilization deserves study. Refractory isotopes (such as ^{10}Be) may be left behind if the surrounding material is slowly lost by volatilization. By using material with the composition of a comet, we may be able to carry out the appropriate simulation experiments.

Finally, we should assess carefully the kinds of spacecraft instrumentation that might allow the determination of the shorter-lived nuclides. Even if direct counting proves impractical for them, appropriate monitoring of the cosmic ray flux would enhance the information conveyed by isotopes with somewhat longer half-lives.

CONCLUSION

The utility of cosmogenic nuclide measurements in returned cometary material will depend, finally, on the rate of mass loss in the area selected for sampling. If that rate turns out to have been low to moderate, then the return of information available from the analyses will amply justify the necessary investment of material and time. In anticipation of a favorable outcome, we would urge that the definition of curatorial responsibilities and the equipping of the curatorial facility allow specifically for the needs associated with the measurement of the cosmogenic radionuclides. A modest program of terrestrial research in preparation for the mission would yield results applicable in a variety of planetary contexts.

REFERENCES

Ahrens, T. J.; Atzei, A.; Begemann, F.; Brownlee, D. E.; Campins, H.; Chang, S.; Coradini, A.; Eberhardt, P.; Festou, M. C.; Grun, E.; Harris, A. W.; Hechler, M.; Kerridge, S. J.; Langevin, Y.; McDonnell, J. A. M.; Pillinger, C. T., Schwehm, G.; Stoffler, D.; Wanke, H.; Wasserburg, G. J.; West, R. M.; and Wood, J. A.: Rosetta - The comet nucleus sample return mission. SCI(87)3, Plan. European Space Agency, 1987.

Armstrong, T. W.; and Alsmiller, Jr., R. G.: Calculation of cosmogenic radionuclides in the Moon and comparison with Apollo measurements. Proc. Lunar Sci. Conf. 2nd, 1971, pp. 1729-1745.

Bar-Nun, A.: Experimental studies of gas trapping in amorphous ice and thermal modelling of comets - implications for Rosetta. Abstract in Workshop on analysis of returned comet nucleus samples. Lunar Planet. Inst. Contrib. 691, 1989, pp. 5-7.

Begemann, F.; and Schultz L.: The influence of bulk chemical composition on the production rate of cosmogenic nuclides in meteorites. Lunar Planet. Sci., vol. 19, 1988, 51-2.

Brin, G. D.; and Mendis, B. O.: Dust release and mantle development in comets. Astrophys. J., vol. 229, 1979, 402-408.

Cintala, M. J.; and Horz. F.: The effects of impact velocity on the evolution of experimental regoliths. Proc. 18th Lunar Planet. Sci. Conf., Cambridge Univ. Press, 1987, pp. 409-422.

Clarke, W. B.; Jenkins, W. J.; and Top, Z.: Spectrometric measurement of ^{3}He. Int. J. Appl. Rad. Iso., vol. 27, 1976, 515- 522.

Drake, D. M.; Feldman, W. C.; and Jakosky, B. M.: Martian neutron leakage spectra. J. Geophys. Res., vol. 93, 1988, 6353-6358.

Elmore, D.; and Phillips, F. M.: Accelerator mass spectrometry for measurement of long-lived radioisotopes. Science, vol. 236, 1987, 543-550.

Englert, P. A. J.: Cosmogenic nuclides in the Martian surface: constraints for sample recovery and transport. Lunar Planet. Inst. Tech. Rep. 88-07, 1988, 75-76.

Englert, P.; Reedy, R. C.; and Arnold, J. R.: Thick-target bombardments with high- energy charged particles: Experimental improvements and spatial distribution of low-energy secondary neutrons. Nucl. Instrum. & Methods, vol A262, 1987, 496-502.

Fink, D.; Middleton, R.; Sharma, P.; and Klein, J.: AMS measurements of ^{41}Ca in terrestrial samples without pre-enrichment. Abstract presented at V.M. Goldschmidt Conf., Baltimore, MD, May 11-13, 1988 (Geochem. Soc.).

Flammer, K. R.; Jackson, B.; and Mendis, D. A.: On the brightness variation of comet Halley at large heliocentric distance. Earth Moon Planet., vol. 35, 1986, 203-212.

Fruchter, J. S.; Reeves, J. H.; Evans, J. C.; and Perkins, R. W.: Studies of lunar regolith dynamics using measurements of cosmogenic radionuclides in lunar rocks, soils and cores. Proc. Lunar Planet. Sci Conf., 12th, 1981, 567-575.

Glass, B. P.: Introduction to Planetary Geology, Cambridge Univ. Press, 1982, p. 346.

Horanyi, M.; Gombosi, T. I.; Cravens, T. E.; Korosmezey, A.; Nagy, A. F.; and Szego, K.: (1984) The friable sponge model of a cometary nucleus. Astrophys. J., vol. 278, 1984, 449-455.

Jessberger, E. K.; Christoforidis, A.; and Kissel, J.: Aspects of the major element composition of Halley's dust. Nature, vol. 332, 1988, 691-695.

Keller, H. U.; Arpigny, C.; Barbieri, C.; Bonnet, R. M.; Cazes, S.; Coradini, M.; Cosmwici, C. B.; Delamere, D. A.; Heubner, W. F.; Hughes, D. W.; Jamar, C.; Malaise, D.; Reitsema, H. J.; Schmidt, H. U.; Schmidt, W. K. H.; Seige, P.; Whipple, F. L.; and Wilhelm K.: First Halley multicolour imaging from Giotto. Nature, vol. 321, 1986, 320-326.

Klinger, J.; Benkhoff, J.; Espinasse, S.; Grun, E.; Ip, W.; Joo, F.; Keller, H. v.; Kochan, H.; Kohl, H.; Roessler, K.; Sebold, W.; Spohn, T.; and Thiel, K.: (1988) How far do results of recent simulation experiments fit with current models of cometary nuclei? Lunar Planet. Sci., vol. 19, 1988, 611-612.

Kohl, C. P.; Murrell, M. T.; Russ, G. P. III; and Arnold, J. R.: Evidence for the constancy of the solar cosmic ray flux over the past ten million years: ^{53}Mn and ^{26}Al measurements. Proc. Lunar Sci. Conf. 9th, 1978, 2299-2310.

Kubik, P. W.; Elmore, D.; Conard, N.; Nishiizumi, K.; and Arnold, J. R.: Determination of cosmogenic ^{41}Ca in a meteorite with tandem accelerator mass spectrometry. Nature, vol. 319, 1986, 568-570.

Langevin, Y.; Arnold, J. R.; and Nishiizumi, K.: Transport processes on the lunar surface: comparison of model calculations with radionuclides data. J. Geophys. Res., vol. 87, 1982, 6681-6691.

Lanzerotti, L. J.; Reedy, R. C.; and Arnold, J. R.: Alpha particles in solar cosmic rays over the last 80,000 years. Science, vol. 179, 1973, 1232-1234.

Lingenfelter, R. E.; Canfield, E. H.; and Hampel V. E.: The lunar neutron flux revisited. Earth Planet. Sci. Lett., vol. 16, 1972, 355-369.

Magnani, P. G.; Gerli C.; and Colombina, G.: Candidate sample acquisition systems for the Rosetta mission. Abstract in: Workshop on analysis of returned comet nucleus samples. Lunar Planet. Inst. Contrib. 691, p. 47.

Nishiizumi, K.: Measurement of ^{53}Mn in deep-sea iron and stony spherules. Earth Planet. Sci. Lett., vol. 63, 1983, 223-228.

Nishiizumi, K.; Murrell, M. T.; and Arnold, J. R.: ^{53}Mn profiles in four Apollo surface cores. Proc. Lunar Planet Sci. Conf., 14th, J. Geophys. Res., Suppl., vol. 88, 1983, B211-B219.

Nishiizumi, K.; Elmore, D.; Ma, X. Z.; and Arnold, J. R.: ^{10}Be and ^{36}Cl depth profiles in an Apollo 15 drill core. Earth Planet. Sci. Lett., vol. 70, 1984a, 157-163.

Nishiizumi, K.; Klein, J.; Middleton, R.; and Arnold, J. R.: ^{26}Al depth profile in Apollo 15 drill core. Earth Planet. Sci. Lett., 70, 1984b, 164-168.

Raisbeck, G. M.; Yiou, F.; Klein, J; Middleton, R; and Brownlee, D.: ^{26}Al/^{10}Be in deep sea spherules as evidence of cometary origin. In "Properties and Interactions of Interplanetary Dust" R. H. Giese and P. Lamy, eds., D. Reidel, 1985, 169-174.

Reedy R. C.: Predicting the production rates of cosmogenic nuclides in extraterrestrial matter. Nucl. Instrum. & Methods, vol. B29, 1987a, 251-261.

Reedy, R.C.: Nuclide production by primary cosmic-ray protons. Proc. 17th Lunar Planet. Sci. Conf, Part 2, J. Geophys. Res., vol. 92, 1987b, E697-E702.

Reedy, R. C.; and Arnold J. R.: Interaction of solar and galactic cosmic-ray particles with the moon. J. Geophys. Res., vol. 77, 1972, 537-555.

Reedy, R. C.; Arnold J. R.; and Lal, D.: Cosmic-ray record in solar system matter. Annu. Rev. Nucl. Part. Sci., vol. 33, 1983, 505-537: and Science, 219,127-135.

Russ, G. P.; and Emerson, M. T.: ^{53}Mn and ^{26}Al evidence for solar cosmic ray constancy - an improved model for interpretation. Proc. Conf. Ancient Sun, Pergamon, 1980, pp. 387-399.

Sagdeev, R. Z.; Blamont, J.; Galeev, A. A.; Moroz, V. I.; Shapiro, V. D.; Shevchenko, V. I.; and Szego, K.: Vega spacecraft encounters with comet Halley. Nature, vol. 321, 1986, 259-273.

Schaeffer, O. A.; Nagel, K.; Fechtig, H.; and Neukum, G.: Space erosion of meteorites and secular variation of cosmic rays (over 10^9 y). Planet. Space Sci., vol 29, 1981, 1109-1118.

Stern, S. A.: (1988) Collisions in the Oort cloud. Icarus, vol. 73, 499-507.

Van Allen, J. A.; and Randall B. A.: Interplanetary cosmic ray intensity: 1972-1984 and out to 32 AU. J. Geophys. Res., vol. 90, 1985, 1399-1412.

Venkatesan, D.; Decker R. B.; and Krimigis S. M.: Radial gradient of cosmic ray intensity from a comparative study of data from Voyager 1 and 2 and IMP 8. J. Geophys. Res., vol. 89, 1984, 3735-3746.

Wdowiak, T. J.; Robinson, E. L.; Flickinger, G. C.; and Boyd, D. A.:(1989) Ion bombardment experiments suggesting an origin for organic particles in pre-cometary and cometary ices. Abstract in: Workshop on analysis of returned comet nucleus samples. Lunar Planet. Inst. Contrib. 691, pp. 79-80.

Webber, W. R.; and Lockwood J. A.: Interplanetary cosmic-ray radial and latitudinal gradients derived in 1984 using IMP 8, Voyager, and Pioneer data. Astrophys. J., vol. 302, 1986, 511-516.

Weissman, P. R.: Physical processing of cometary nuclei. Abstract in: Workshop on analysis of returned comet nucleus samples. Lunar Planet. Inst. Contrib. 691, pp. 81-82.

Whipple, F. L.: The cometary nucleus: current concepts. Astron. Astrophys., vol. 187, 1987, 852-858.

Woolum D. S.; Burnett, D. S.; Furst, M.; and Weiss, J. R.: Measurement of the lunar neutron density profile. The Moon, vol. 12, 1975, 231-250.

MORPHOLOGY AND COMPOSITIONAL DIFFERENTIATION OF THE SURFACE OF COMETS

W. F. Huebner
D. C. Boice
Southwest Research Institute
San Antonio, Texas

Morphology and Compositional Differentiation of the Surface of Comets

W. F. Huebner and D. C. Boice, Southwest Research Institute, San Antonio, TX 78284

Giotto images reveal many features on the nucleus of Comet Halley, including gas- and dust-producing sources surrounded by an inactive region. In the inactive region, crater-like structures can be seen that may be extinct sources. These structures may develop by surface erosion of an active area and deposition of some excavated material on the periphery, creating crater-like rims. These rims are formed from "clumps" of comet regolith that can be lifted by the escaping gas. The lack of lift caused by the divergence of the gas flow near the boundary of an active region lets them fall back on the nucleus and create a rim. This may be a continuous process during perihelion passage.

Supplementing the original concept of investigating the active and inactive regions, we conclude that three compositionally distinct areas should be sampled during the Rosetta mission: (1) The active regions rich in frozen gases and unprocessed dust. (2) The inactive region covered by a thin layer of fine dust enriched in organics that may be sintered. (3) The crater-like rims containing "clumps" of processed organics, silicates, and trapped frozen gases.

To assess the concepts of gas production we consider Comet Halley for comparison. The measured rate of gas production was $Q \simeq 7\ 10^{29}$ molecules s^{-1} during the Giotto encounter at a heliocentric distance of $r = 0.9$ AU. About 80 to 85% of the gas was water. For an albedo of 0.03 and a 30° average angle of sunlight incidence, the specific gas production rate is $Z_a \simeq 1.4\ 10^{22}$ molecules $m^{-2}\ s^{-1}$. The active area is therefore about 45 km^2. Since the total surface area of P/Halley is approximately 400 km^2, the active area is about 20% of the illuminated surface. On the Halley Multicolour Camera (HMC) images, no dust production is evident from the inactive area (see Fig. 1). Nevertheless, if we assume that as much as 10% of the gas is produced on the inactive area, then the specific gas production on the inactive area, which covers about 80% of the illuminated surface, is only 3% of that of the active area. A reasonable result is $Z_i = (0.03 \pm 0.03)$ Z_a. Such a low gas production rate cannot entrain large dust particles. It is therefore reasonable to assume that all the dust comes from the active area. Figure 1 is consistent with this interpretation.

For other short-period comets the total gas production rate is smaller than that of P/Halley. If comet compositions are similar, this suggests that the total active area is smaller than that on P/Halley. Nothing definitive can be said about the specific gas production rates, but it appears reasonable that both Z_a and Z_i are similar to the values of P/Halley.

Since the gas production rate is higher for the active areas than for the inactive areas, an overpressure tends to develop over the active regions. Pressure equilibration then causes a surface wind to develop. This wind carries fine dust rich on CHON with it. The smallest dust particles can be moved laterally out of the dust "jet" by a few collisions with the gas, while the large dust particles require many collisions and therefore remain in the dust "jet". In support of this argument, the HMC images show an intensity gradient across the nucleus. As can be seen in Fig. 1, the intensity decreases from the active regions in the antisolar direction. Some of the fine dust may settle on the surface, particularly on the night side. When this side faces the Sun again during the comet's rotation, the organic dust may get sintered.

The gas over the active areas entrains the dust. The entrainment can be approximated in two limiting cases (Huebner, 1970): If the mean free path, Λ, of the gas is large with respect to



Fig. 1. A composite of six images of Comet Halley obtained with the Halley Multicolour Camera on the Giotto spacecraft (Keller et al., 1988). The resolution increases toward the brightest part. Illumination by the Sun is from the left at about 28° above the horizontal and 12° behind the image plane. Most of the visible surface is not illuminated. The light intensity gradient from the top left on the nucleus to the bottom right is apparent. The dust emission is concentrated in jet-like features emanating from the subsolar hemisphere. Structural details of the surface are visible down to the resolution limit of about 100 m. A crater-like structure is visible on the nucleus between the two brightest dust emissions.

the dust particle size of effective radius a, i.e., $\Lambda = v/(Z\sigma) > a$, free molecular flow is a good approximation. In the other limit, when $\Lambda < a$, fluid dynamics is a good approximation.

The equation of motion for a dust particle in the **free molecular flow** approximation is

$$\frac{4\pi}{3}a^3\rho_{\rm d}\frac{d^2R}{dt^2} = m_{\rm u}M(v - \frac{dR}{dt})^2\pi a^2\frac{Z_{\rm a}}{v}\left(\frac{R_{\rm N}}{R}\right)^2 - \frac{(4\pi/3)^2a^3\rho_{\rm d}R_{\rm N}^3\rho_{\rm N}G}{R^2}, \qquad (1)$$

where R is the radial position of the particle in the coma, $R_{\rm N}$ is the effective radius of the nucleus, a the radius of the particle, v the gas velocity, M the molecular weight of the gas, $m_{\rm u}$ the unit atomic mass, $\rho_{\rm d}$ the density of the dust particle, $\rho_{\rm N}$ the density of the nucleus, $Z_{\rm a}$ the specific gas production rate of an active area, and G the universal gravitational constant. The term on the left side of Eq. (1) is mass times acceleration of the dust particle. The first term on the right represents the time rate of change of momentum of the dust particle caused by collisions with gas molecules and the second term on the right represents the weak gravitational pull of the nucleus. The centripetal acceleration can be neglected since it contributes only a few percent at

the equator. To solve for the maximum particle size, a_m, that can be entrained by the gas at the surface, $R = R_N$, we set $d^2R/dt^2 = dR/dt = 0$ and obtain

$$a_m = \frac{9Mm_u Z_a v}{16\pi R_N \rho_d \rho_N G}. \quad (2)$$

For $R_N \simeq 5$ km, $v \simeq 100$ m s^{-1}, $M \simeq 18$, $\rho_d \simeq \rho_N \simeq 500$ kg m^{-3}, $Z \simeq 10^{22}$ m^{-2} s^{-1} at 1 AU, we find $a_m \simeq 0.1$ m.

A similar equation can be solved in the **fluid dynamic limit**. In that case

$$a_m = (\frac{27\eta v}{8\pi G \rho_d \rho_N R_N})^{1/2}, \quad (3)$$

where

$$\eta = \frac{1.8510^{-6}T^{1/2}}{1 + 680/T}, \quad (4)$$

is the viscosity. For the same parameters as above and with $T \simeq 200$ K, $A \simeq 0.1$ m and $a_m \simeq 0.1$ m, i. e., free molecular flow does not apply, but the fluid dynamic limit has not yet been reached.

It is interesting to note that the fluid dynamic limit also gives an upper limit to the dust size distribution. Even for large gas production rates at smaller heliocentric distances, the maximum size of particles that can be lifted from the surface by gas entrainment remains nearly constant since the temperature of the gas and dust does not significantly change.

Centimeter- and decimeter-sized "clumps" of dust are easily entrained by the gas in the center of an active region. Gas production will fluctuate. During a small decrease in the gas production the lift by the gas will be reduced and a "clump", under the action of the weak gravity, falls back to the nucleus. Similarly, the divergent flow of the gas over an active region results in a reduction of lift and the "clumps" fall back. This process has also been suggested by Sekanina (1983). The tendency will be to fall outside of the active area, where they will accumulate into a rim structure. Even though centimeter-sized particles are less sensitive to these two actions then decimeter-sized particles, they move only slowly to some height above the nucleus. As the nucleus rotates under them the lift from the gas "jet" is removed and they will fall back to the nucleus on the evening side of the active area. Thus any rim that may form will be imperfect. Figure 1 shows several crater-like structures. One structure is clearly visible on the nucleus between the two brightest jet-like features. It may be an extinct active area or one that has not yet turned on in the early morning on the nucleus. It is very shallow and about 2 km in diameter. The rim is not perfectly circular and may be open on two sides. Figure 2 presents an intensity trace perpendicular through the northern jet-like feature about 50 to 100 m above the nucleus. The feature is optically thin, so that the intensity is directly proportional to the column density of the dust through the "jet". A Gaussian curve has been drawn through the intensity profile. The deviations to this Gaussian are filaments that persist to large distances from the nucleus. The details in the intensity profile are not sensitive to the height of the intensity trace above the surface.

The "clumps" in the rim will be rich on unprocessed dust, i.e., dust that contains silicates as well as CHON. The "clumps" may still contain some trapped frozen gases, while their surface may be depleted of the ices.

We conclude that large particles are lifted from the surface near the center of an active region. A small reduction in the gas production causes the largest particles to fall back on the nucleus, while the smallest particles are carried by the surface wind and may fall back to the surface over

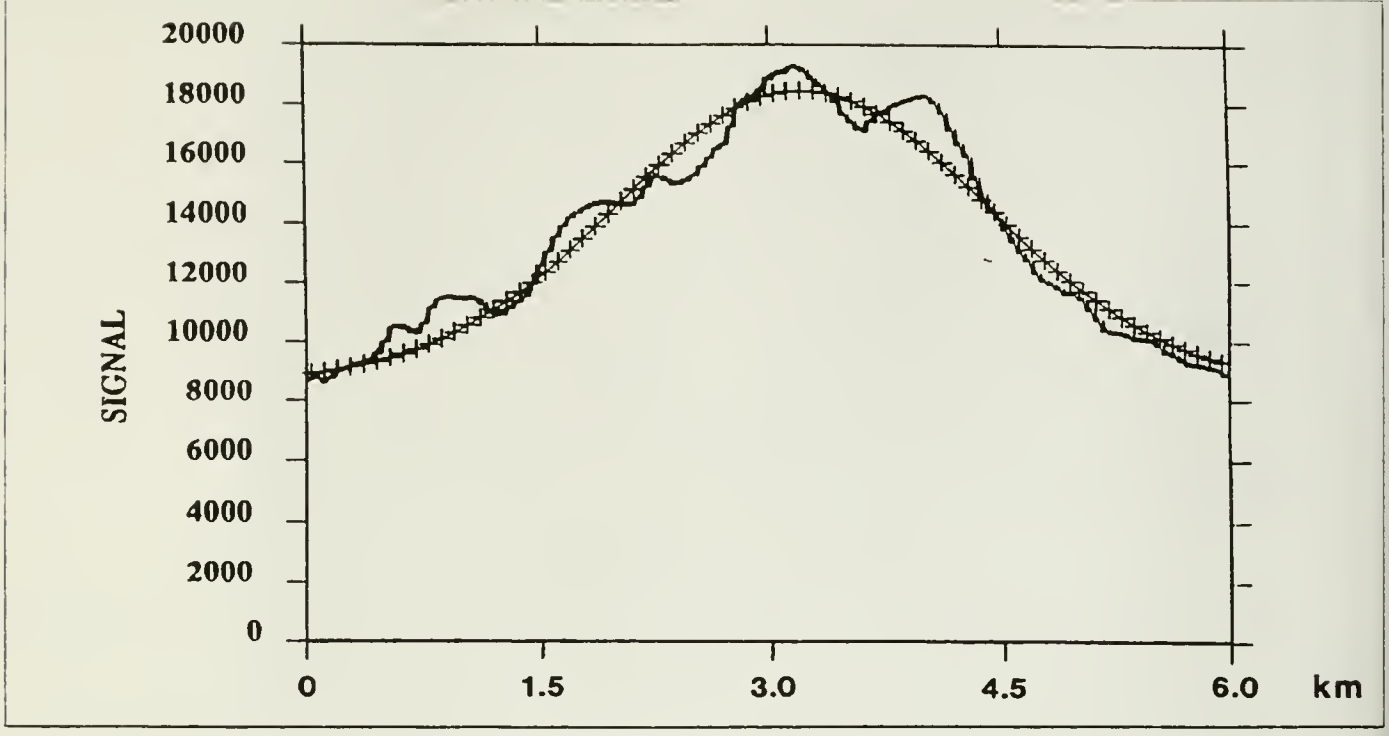


Fig. 2. An intensity trace about 50 to 100 m above the nucleus perpendicular through the top jet-like feature seen in Fig. 1 (Reitsema, 1989). A Gaussian curve has been fitted to the intensity data. The structural deviation from the Gaussians are filaments of dust in the jet-like feature; they are reproducable at different heights above the surface.

the inactive region. The intermediate dust with particle size of the order of 1 μm stays in the dust-like features and is carried into the coma and eventually into the dust tail. Centimeter-sized particles can be lifted to some height above the nucleus. However, since the nucleus rotates under the particles, they lose their lift from the entraining gas and fall back on the nucleus toward the evening side.

Erosion of an active region is of the order of tens of meters per apparition. On the same time scale the rim formation may be of the order of a few meters. At least three different regions on a nucleus should be sampled. The original plan for the Rosetta mission was to sample two different regions on the nucleus: One area was an active region which is expected to be rich on frozen gases and unprocessed dust. A core sample from such a region is most desirable. The second sample is from an inactive region which is rich on inert material that possibly is covered by a thin layer of fine, organic dust. This dust may be sintered on the surface. A thin surface sample would be most desirable. A third region that should be sampled is the rim around an active area. It may contain coarse material with some trapped ices. It will give information about the formation of "clumps" in or on a comet nucleus.

This work was supported by funds from the NASA Planetary Atmospheres Program.

Huebner, W. F., Astron. Astophys. 5, 286 (1970).
Keller, H. U., Kramm, R., and Thomas, N., Nature 331, 227 (1988).
Reitsema, H. J., private communication (1989).
Sekanina, Z., Adv. Space Res. 2, 121 (1983).

THE IN-SITU PARTICULATE SIZE DISTRIBUTION MEASURED FOR ONE COMET: P/HALLEY

J. A. M. McDonnell
G.S. Pankiewicz
P. N. W. Birchley
S. F. Green
C. H. Perry
Unit for Space Sciences
University of Kent
Cantebury, Kent, U. K.

THE IN-SITU PARTICULATE SIZE DISTRIBUTION MEASURED FOR ONE COMET: P/HALLEY.

J.A.M. McDonnell, G.S. Pankiewicz, P.N.W. Birchley, S.F. Green, C.H. Perry.
Unit for Space Sciences, University of Kent, Canterbury, Kent CT2 7NR, U.K.

ABSTRACT

The comet Halley dust mass distribution measured by the Giotto DIDSY and PIA experiments is used to derive the dust to gas mass ratio μ for the nucleus material. The excess of grains observed for masses > 10^{-9} kg places μ in the range 1-200 if the observed size distribution is representative of the average properties of the coma. The lower bound corresponds to integration up to the largest particle (~1g) impacting Giotto. The mass and area distributions at the nuclear surface for distributions with and without this large particle excess are compared.

INTRODUCTION

The close approach of Giotto to comet P/Halley during its 1986 apparition offered a unique opportunity to study the distribution of particulates of masses up to one gram. Data acquired by the dust shield detector system, DIDSY [1] and the front end channels of the highly sensitive mass spectrometer PIA [2], provide definition of the detected distribution as close as 1000km to the nucleus. Measured particles extend from 10^{-19}kg (~ 0.02μm) to some 30mg (~ 2mm) and can also be inferred for masses up to the region of 1g (~ 5mm) by virtue of the spacecraft deceleration of 23.05 cm s^{-1} [3].

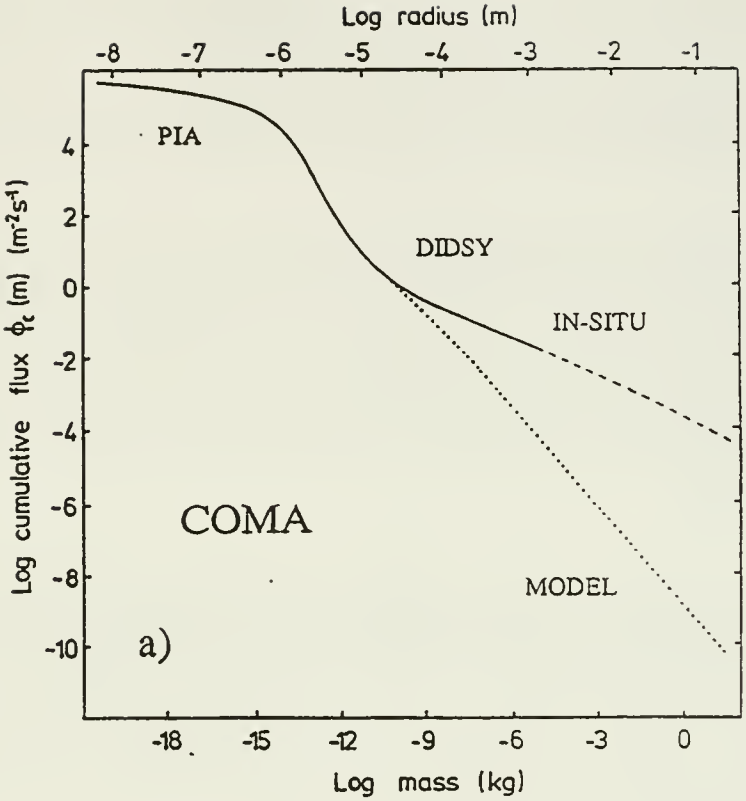
This work examines implications of the measured data with respect to:

1. The flux and size distribution of particles leaving the nucleus surface.
2. The dust to gas mass ratio in the nucleus matrix as a function of mass, $\mu(m)$.
3. The mass and area distributions of grains in the nucleus matrix.

The results may be applied to the task of remote sensing of a cometary nucleus to locate active areas. In a **Comet Nucleus Sample Return Mission** such as CNSR - ROSETTA, the identification of a fresh production surface by reflectance or emission properties at wavelengths from optical to radar depends upon the scale depth of absorbing material and the detectability of ice in the matrix.

DUST MASS DISTRIBUTIONS IN THE COMA AND NUCLEUS

Calculation of dust fluxes from Giotto DIDSY and PIA impact data is described by McDonnell et al [4]. Figure 1a shows the measured cumulative flux $\Phi_c(m)$ (number of particles of mass > m impacting the spacecraft per m^2 per second) of particles observed by DIDSY and PIA in the coma at a mean distance from the nucleus of 5240km determined from post encounter measurements in the period +60 to +120s. The solid line (IN-SITU) represents the distribution as measured, with the same slope assumed for m>10^{-5}kg (~ largest measured particle derived from DIDSY data, [4]). The dotted line (MODEL) indicates the distribution assuming that the observed excess of large masses is not representative of the average properties of the coma. Distributions of this form have



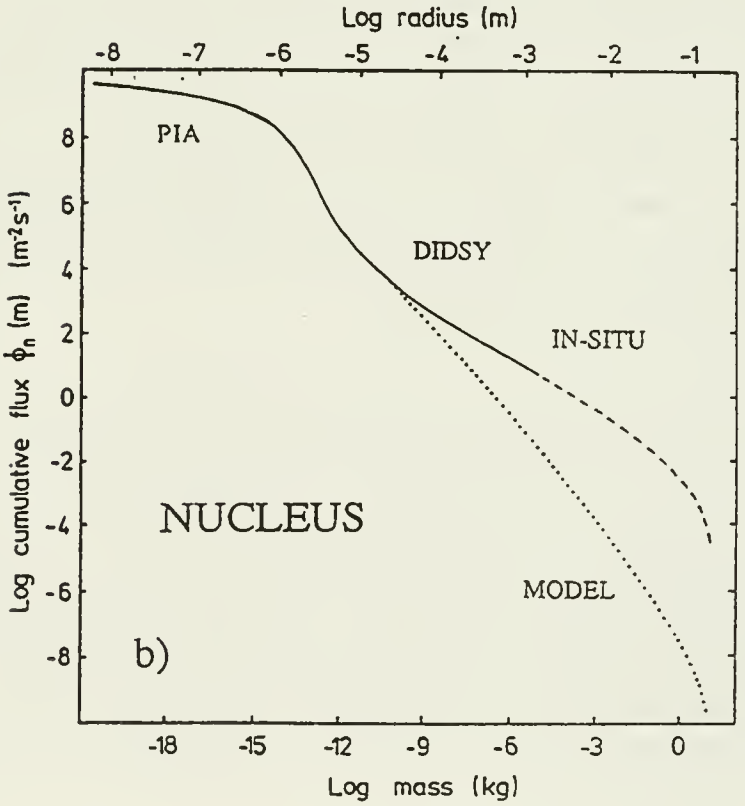


Figure 1
Cumulative mass distibutions
a) in the coma,
b) at the nucleus.
The solid curve is for Giotto data (nuclear distance of 5240km post-encounter) and the dotted line for a model with uniform mass index at large masses.

generally been assumed from interpretation of remote sensing data and were used for pre-encounter modelling [5] with a constant size index at large masses of u = 3.7 (α = 0.9)

The dust cumulative flux $\Phi_n(m)$ at the nucleus surface is given by

$$\Phi_n(m) = \int_0^m n_n(m)\,dlogm = \int_0^m n_c(m)\,\frac{v(a)}{v_s}\,\left(\frac{R}{R_n}\right)^2\,dlogm$$

where the grain velocity v(a) is taken from figure 2, R_n=5.2km is the effective nucleus radius (derived from model of Sagdeev et al, [6]) and v_s is the spacecraft velocity = 68.4 km s^{-1}, $n_n(m)$ and $n_c(m)$ are the differential fluxes in the nucleus and coma respectively. We derive the cumulative flux distribution at the nucleus (figure 1b) assuming radial trajectories and a velocity distribution of the form shown in figure 2. Dust velocities are calculated using the approximation of Divine [7] with a maximum liftable mass of radius 15cm (assuming a nucleus density = 800 kg m^{-3} and an active fraction of the nucleus of 10% of the total surface area, [8]). The grain density is assumed to take the form

$$\rho(a) = 3000 - 2200\,\left(\frac{a}{a+a_o}\right) \quad kg\ m^{-3}$$

[5] where a_o=2x10^{-6}m.

DUST TO GAS MASS RATIO

The resultant fluxes are then integrated over all relevant masses and used to obtain a dust production rate that may be directly compared to the measured gas production rate of 2.55 x 10^4 kg s^{-1} [9] to yield a dust to gas mass ratio as a function of mass (figure 3). The dust to gas mass ratios $\mu(m)$ are shown here as a function of the mass of the largest grains included. The shaded region indicates the limits of the likely value of $\mu(m)$ where

$$\mu(m) = \frac{4\pi R^2}{Q_g \mathcal{M}} \int_o^m n_n(m')\ m'\ dlogm'$$

whereas the dotted line (MODEL distribution) may be compared with previously derived results from remote sensing. Q_g is the gas production rate = 6.9x10^{29} mol s^{-1} [9] and $\mathcal{M}$ is the mean molecular mass = 3.7x10^{-26}kg [5]. Although the nucleus is known to comprise localised active areas on a predominantly inactive surface the gas production rate is an average value for the data measured during the whole encounter. Likewise, since DIDSY and PIA data show relatively small flux variations they can be treated as an average value for the period +60 to +120 seconds. During this period the sub-satellite track was over the sunlit hemisphere.

The MODEL distribution produces a bulk dust to gas ratio of ~ 0.2 but figure 3 clearly shows how the measured large mass distribution enhances the total mass of dust to produce a bulk ratio in the range 1-200. The lower limit to the shaded region is based on the IN-SITU distribution but with no grains more massive than the largest inferred from the total spacecraft deceleration (~1g). The largest particles measured by DIDSY indicate

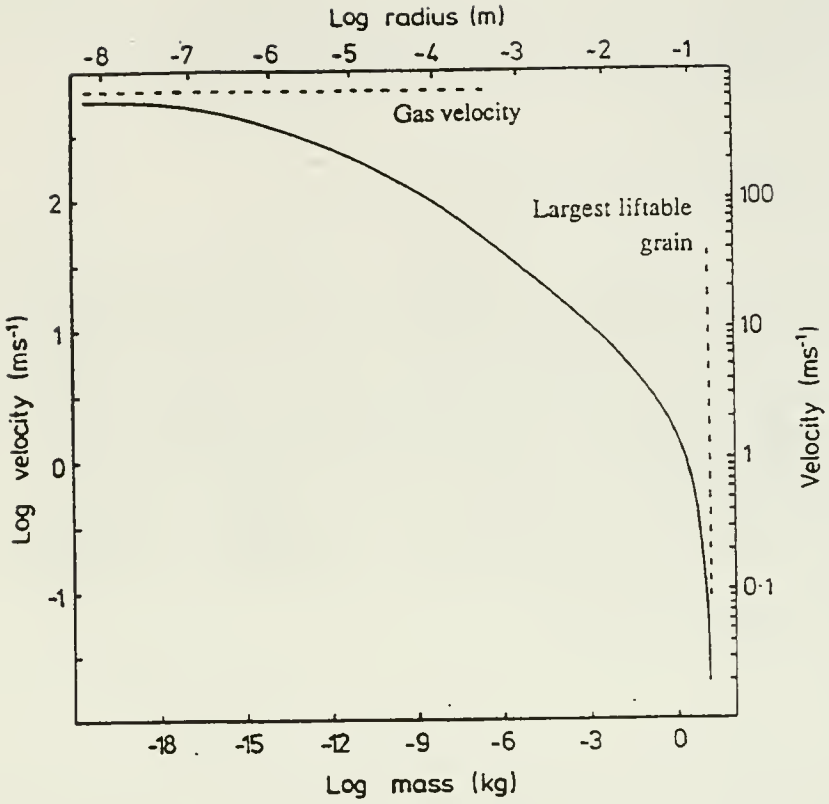


Figure 2
Grain velocity distribution from [7].

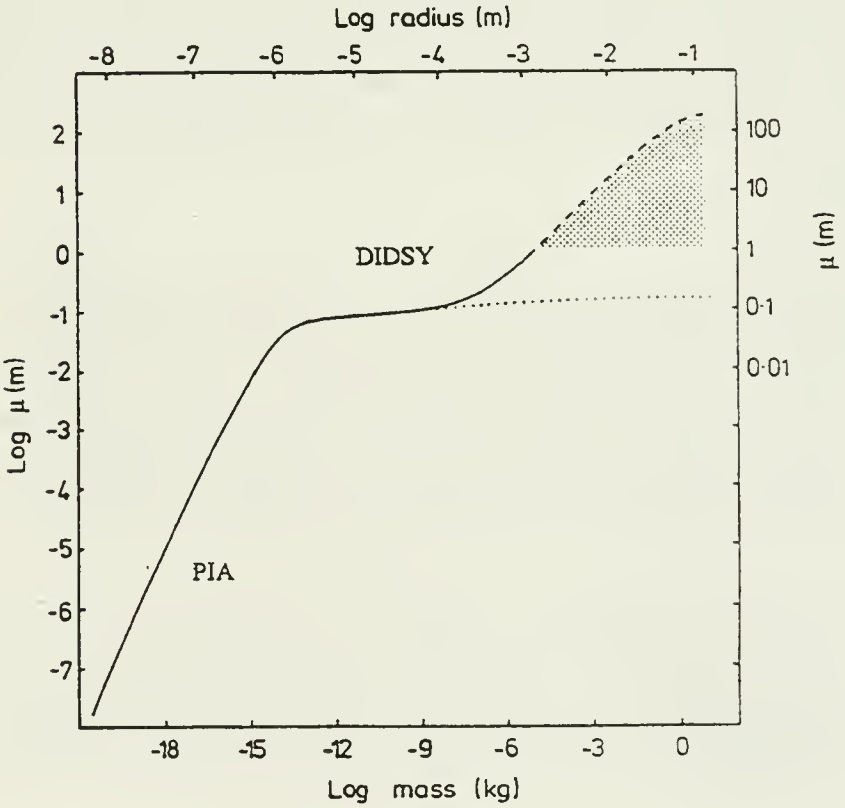


Figure 3.
Dust to gas mass ratios μ as a function of the largest grains included.

a lower limit of 1.0 to the bulk ratio, with expected values in the shaded region, but only if the observed large mass excess is representative of the coma as a whole. There is considerable evidence for an abundance of mm - cm sized grains in cometary comae [10,11], but ground-based infrared observations of silicate emission (e.g. [12]) indicate that for much of the time grains <20μm in size dominate the coma.

AREA AND MASS DISTRIBUTIONS

Using the above distributions the numbers of dust particles embedded in any volume of interest may be calculated. Figures 4 and 5 display the number, area and mass distributions in $1m^3$ in the coma (5240km from the nucleus) and in the nucleus matrix itself. The differential distributions $n_c(m)$, $\mathcal{A}_c(m)$ and $m_c(m)$ are shown for the IN-SITU distribution (solid line), and the MODEL distribution (dotted line) in figure 4. The number of particles per m^3 per log mass interval

$$n_c(m)\ \mathrm{dlogm} = (n_c(m)/v_s)\ \mathrm{dlogm},$$

the area of particles per m^3 per log mass interval

$$\mathcal{A}_c(m)\ \mathrm{dlogm} = (n_c(m)\pi a^2/v_s)\ \mathrm{dlogm}$$

and the mass of particles per m^3 per log mass interval

$$m_c(m)\ \mathrm{dlogm} = (n_c(m)m/v_s)\ \mathrm{dlogm}.$$

Although the majority of grains are of mass $< 10^{-9}$ kg, the total grain mass is dominated by the largest grains. Remote sensing observations, which are dependent on the cross-sectional area, indicate dominant grain masses $\sim 10^{-14}$kg. The DIDSY data indicate that a significant contribution to the cross-sectional area could come from large grains. Figure 5 shows similar differential distributions for the nucleus material where the number of particles per m^3 per log mass interval

$$n_n(m)\ \mathrm{dlogm} = (n_n(m)/V)\ \mathrm{dlogm},$$

the area of particles per m^3 per log mass interval

$$\mathcal{A}_n(m)\ \mathrm{dlogm} = (n_n(m)\pi a^2/V)\ \mathrm{dlogm}$$

and the mass of particles per m^3 per log mass interval

$$m_n(m)\ \mathrm{dlogm} = (n_n(m)m/V)\ \mathrm{dlogm},$$

where V is the total volume of material ejected per m^2 per second from the nucleus (see fig 6). The nucleus mass distribution is dominated by the largest grains. The maximum mass plotted is the calculated largest liftable mass ~10kg. In reality, the true dust to gas mass ratio will depend on the largest grains present in the nucleus which may be larger *or smaller* than this value of maximum liftable mass. The total cross-sectional area of grains at the nucleus for the MODEL distribution is dominated by grains $\sim 10^{-14}$kg.

APPEARANCE OF THE NUCLEUS SURFACE

The large masses measured by DIDSY significantly enhance the nucleus area and mass distributions above $\sim 10^{-9}$kg and reduce the effective areas and masses from smaller particles because of the lower volume available for such particles. This results in an optically thinner nucleus matrix on the scale of several microns, as is evident from the boxes of nucleus material represented schematically in figure 6. Each window depicts the

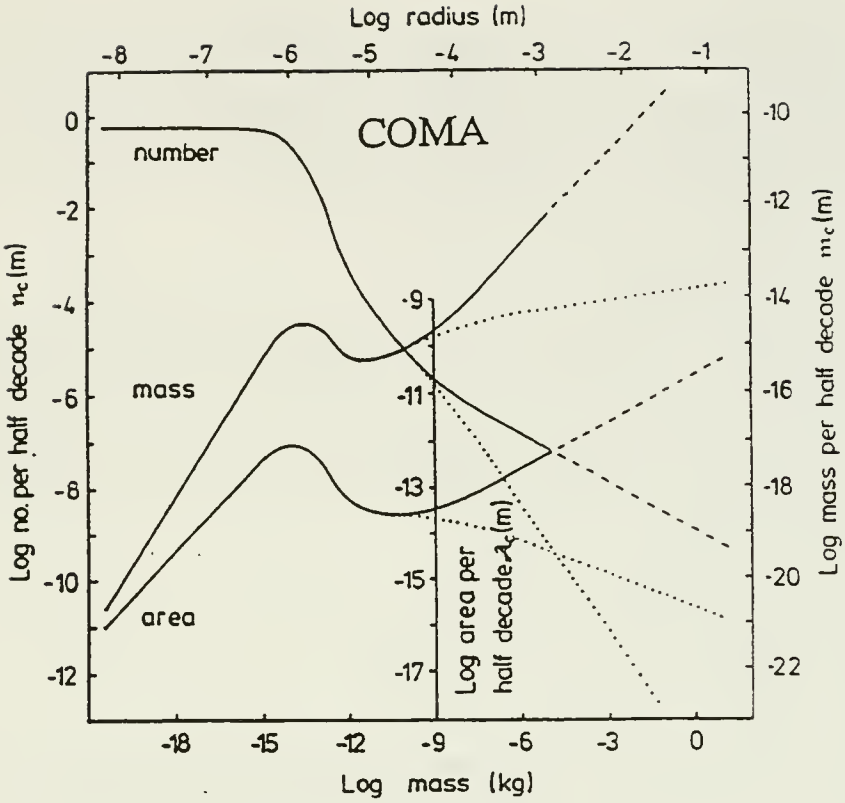


Figure 4.
Differential number, cross-sectional area and mass distributions of dust grains in the coma. Solid line - IN-SITU distribution; dotted line - MODEL distribution.

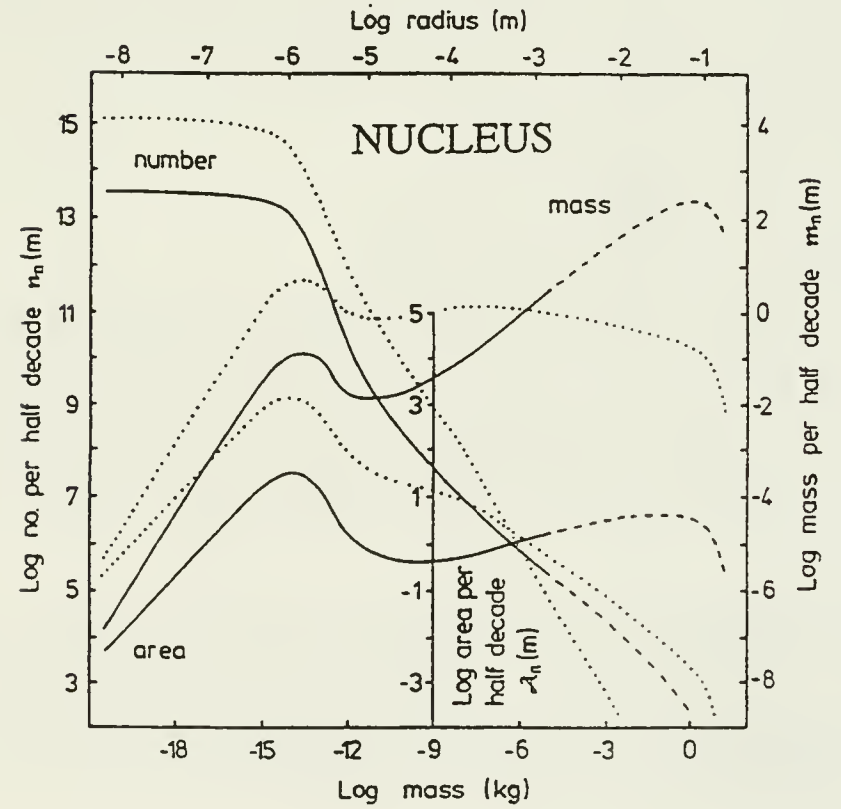


Figure 5.
Differential number, cross-sectional area and mass distributions of dust grains on the nucleus. Solid line - IN-SITU distribution; dotted line - MODEL distribution.

number of grains in a 1mm slice of the surface at scales of 1m, 1cm, 100μm and 1μm. The number of grains of mass m per m^3 of the surface material

$$n_n(m) = \frac{\Phi_n(m)}{\int \Phi_n(m) \frac{m}{\rho} \left(\frac{1+\rho}{\mu \rho_{gas}}\right)}$$

where the denominator is the volume occupied by gas and dust. The dust to gas mass ratio μ is taken from figure 3 at m=10kg and ρ_{gas} assumed to be 200 kg m^{-3}. The grains represented in each case have a range of radii from 0.5 to 10^{-3} of the respective scale sizes. The model distribution is optically thick (optical depth τ=1 implying 63% attenuation) at a depth of 0.1mm with grains of size <50μm dominating. The presence of large mass grains in the IN-SITU distribution (figure 5) reduces the optical depth (τ=1 at a depth of 4mm), allowing incoming radiation to penetrate further into the nucleus. The MODEL distribution gives a very dark sooty appearance for a box 100μm on each side and 1mm deep as it is dominated by micron sized particles (the scale depth at which the optical depth τ = 1.0 in this case is 98μm). The measured DIDSY number distribution however produces a **clearer** matrix (the scale depth calculated is 3.3mm), even though the distribution is dominated by larger grains.

CONCLUSIONS

The appearance of the nuclear surface depends critically on the true distribution of large mass grains at the nucleus. Giotto data indicate an excess up to m~1g along its trajectory but give no information for larger grains or for the coma as a whole.

REFERENCES

[1] McDonnell, J.A.M., 1987. *J. Phys. E.: Sci. Instrum.*, **20**, 741-758.

[2] Kissel, J., 1986. *ESA SP-1077,* 67-83.

[3] Edenhofer, P., Bird, M.K., Brenkle, J.P., Buschert, H., Kursinsiki, E.R., Mottinger, N.A., Porsche, H. & Stelzried, C.T., 1987. *Astron. Astrophys.*, **187**, 712-718.

[4] McDonnell, J.A.M., Alexander, W.M., Burton, W.M., Bussoletti, E., Evans, G.C., Evans, S.T., Firth, J.G., Grard, R.J.L., Green, S.F., Grün, E., Hanner, M.S., Hughes, D.W., Igenburgs, E., Kissel, J., Kuczera, H., Lindblad, B.A., Langevin, Y., Mandeville, J.C., Nappo, S., Pankiewicz, G.S.A, Perry, C.H., Schwehm, G.H., Sekanina, Z., Stevenson, T.J., Turner, R.F., Weishaupt, U., Wallis, M.K. & Zarnecki, J.C., 1987. *Astrophys. J.*, **187,** 719-741.

[5] Divine, N., Fechtig, H., Gombosi, T.I., Hanner, M.S., Keller, H.U., Larson, S.M., Mendis, D.A., Newburn, R.L., Rheinhard, R., Sekanina, Z. & Yeomans, D.A., 1986. *Space Sci. Rev.*, **43**, 1-104

[6] Sagdeev, R.Z., Krasikov, V.A., Shamis, V.A., Tarnopolski, V.I., Szego. K., Toth, I., Smith, B., Larson, S. & Merenyi, E., 1986. *ESA SP-250, Vol II*, 335-338.

[7] Divine, N., 1981. *ESA SP-174,* 25-30.

Figure 6. Schematic of the appearance of dust grains on the nucleus surface on different size scales. See text for details.

[8] Keller, H.U., Delamere, W.A., Huebner, W.F., Reitsema, H.J., Kramm, R., Thomas, N., Arpigny, C., Barbieri, C., Bonnet, R.M., Cazes, S., Coradini, M., Cosmovici, C.B., Hughes, D.W., Jamar, C., Malaise, D., Schmidt, K., Schmidt, W.K.H. & Siege, P., 1987. *Astron. Astrophys.* **187**, 807-823.

[9] Krankowsky, D. Lammerzahl, P., Herrwerth, I., Woweries, J., Eberhardt, P., Dolder, U., Herrmann, U., Schulte, W., Berthellier, J.J., Iliano, J.M., Hodges, R.R. & Hoffman, J.H., 1986. *Nature,* **321**, 326-330.

[10] Eaton, N., Davies, J.K. & Green, S.F., 1984. *Mon. Not. R. astr. Soc.* **211** 15p-19p.

[11] Harmon, J.K., Campbell, D.B., Hine, A.A., Shapiro, I.I. & Marsden, B.G., 1989. *Astrophys. J.,* in press.

[12] Hanner, M.S., Tokunaga, A.T., Golisch, W.F., Griep, D.M. & Kaminski, C.D., 1987. *Astron. Astrophys.,* **187**, 653-660.

ORGANIC CHEMISTRY IN INTERSTELLAR ICES: CONNECTION TO THE COMET HALLY RESULTS

W. A. Schutte
Laboratory Astrophysics, Leiden, the Netherlands
NASA Ames Research Center, Moffet Field, California

V. K. Agarwal
Rensselaer Polytechnic Institute
Troy, New York

M. S. de Groot
J. M. Greenberg
Laboratory Astrophysics
Leiden, the Netherlands

P. McCain
J. P. Ferris
Rensselaer Polytechnic Institute
Troy, New York

R. Briggs
Center for Laboratories and Research
New State Department of Health, Albany, New York

Organic Chemistry in Interstellar Ices; Connection to the Comet Halley Results.

W.A. Schutte*#, V.K. Agarwal@, M.S. de Groot*,
J.M. Greenberg*, P. McCain@, J.P. Ferris@ and R. Briggs~

* Laboratory Astrophysics, Leiden, the Netherlands.
\# NASA Ames Research Center, Moffett Field, Ca..
@ Rensselaer Polytechnic Institute, Troy, N.Y..
~ Center for Laboratories and Research, N.Y. State Department of Health, Albany, N.Y.

Abstract

Experiments simulating the photolysis of ice mantles on grains in dense clouds produce organic molecules similar to the ones observed by Giotto's Picca heavy ion analyzer near Comet Halley.

1. Introduction.

Mass spectroscopic measurements on the gas and dust in the coma of Comet Halley revealed the presence of considerable amounts of organic species (Mitchell et al. 1987, 1988, Kissel et al. 1987). Greenberg (1973) proposed that prior to the formation of the comet UV processing of the ice mantles on grains in dense clouds could lead to the formation of complex organic molecules. Theoretical predictions of the internal UV field in dense clouds (Prasad et al. 1983) as well as the discovery in interstellar ices of species like OCS and OCN- which have been formed in simulation experiments by photoprocessing of interstellar ice analogues (Geballe et al. 1985, Grim and Greenberg 1987, see also fig. 1) point to the importance of such processing. We undertook a laboratory simulation study of the formation of organic molecules in interstellar ices and their possible relevance to the Comet Halley results. A detailed review is given in Schutte (1988).

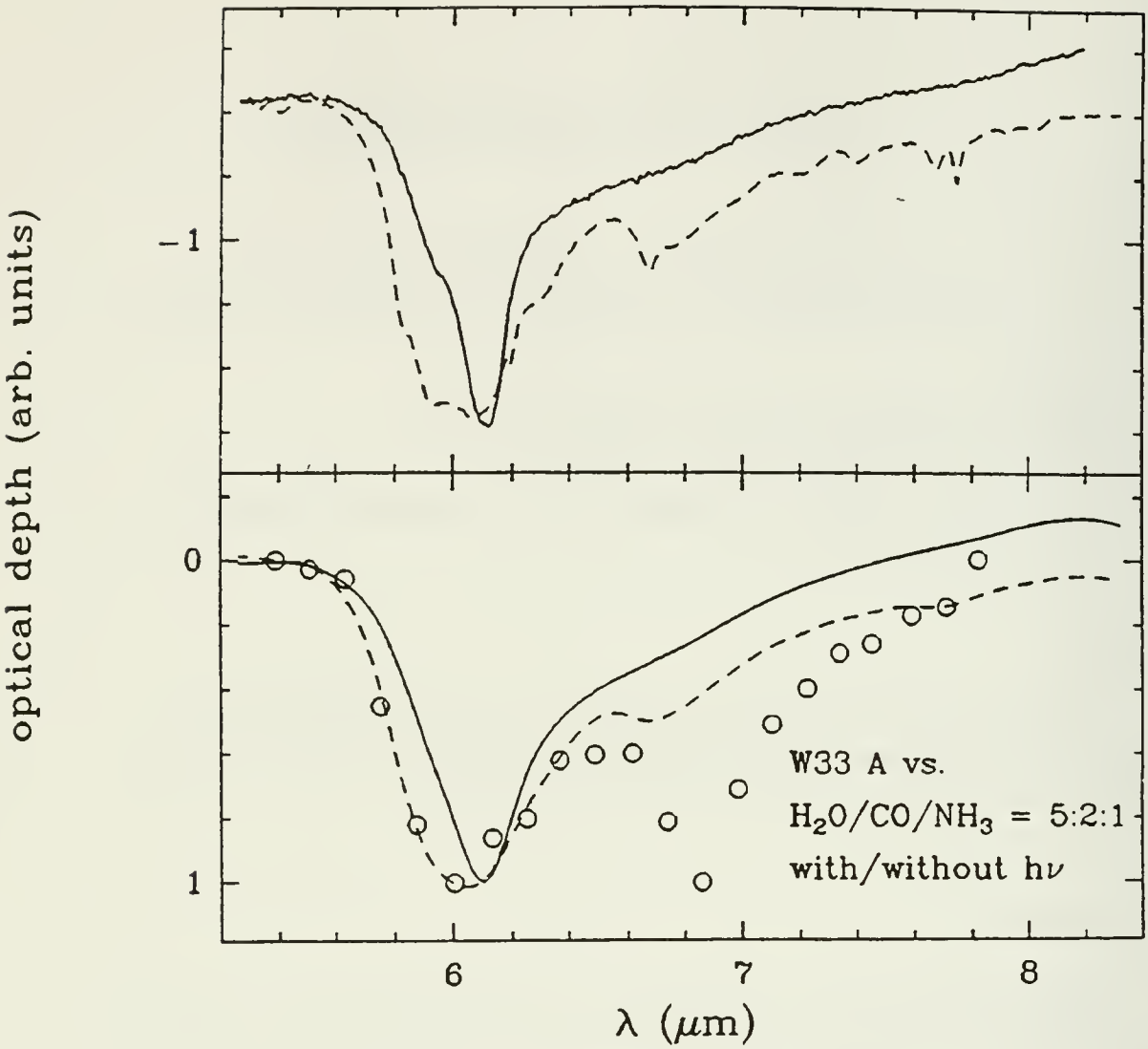


Figure 1. *Lower part*: A comparison of the 6 μm interstellar ice feature observed towards the embedded source W33 A (circles; Tielens et al. 1988) with the ice mixture H20/CO/NH3 = 5:2:1, before and after UV irradiation (solid and dashed line respectively). The growth of features from photoproducts substantially increases the match with the interstellar band. The laboratory spectra were smoothed to the resolution of the observations. *Upper part*: The laboratory spectra at their original resolution.

2. Experimental

Mixtures of astrophysically relevant molecules (H20/CO/NH3 ≈ 5:2:1) were deposited on a cold finger (12 K) with simultaneous UV irradiation. About 0.2 UV photons were absorbed in the ice per molecule in this experiment. In the interior of molecular clouds this corresponds to about 106 years of irradiation (Prasad et al. 1983). Subsequently, the sample was slowly warmed up (0.5 K min-1), the changes being monitored in situ with an I.R. spectrometer. The refractory yellow residue remaining on the substrate at room temperature was investigated with Gas Chromatography / Mass Spectrometry.

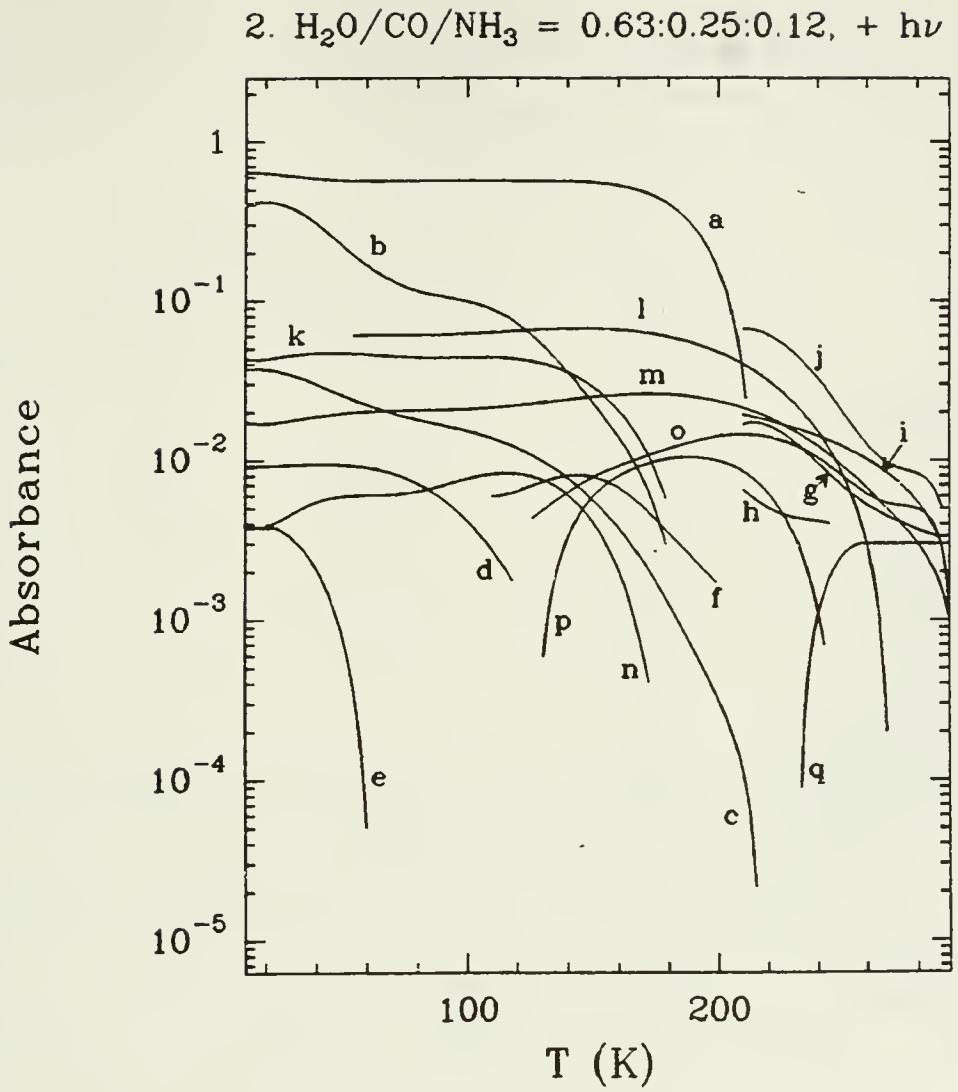


Figure 2. The appearance and disappearance of species during warm-up of the photolysed sample H20/C0/NH3 = 5:2:1, monitored by following the depth of a characteristic I.R. feature (assignments from Hagen 1982, Schutte 1988 and Grim et al. 1989; R denotes carbon chain or H atom). a. H20 (3300 cm-1); b. CO (2138 cm-1); c. 13CO2 (2278 cm-1); d. H2CO (1499 cm-1); e. HCO (1848 cm-1); f. CH3OH (1020 cm-1); g. HCOOH/HCONH2 (1686 cm-1); h. HOCH2CH2OH (1030 cm-1); i. unidentified (1580 cm-1); j. unidentified (2400 - 3350 cm-1); k. NH3 (1060 - 1200 cm-1); l. OCN- (2167 cm-1); m. NH4+ (1410 - 1520 cm-1); n. NO3- (1388 cm-1); o. NH4NO3 (1330 cm-1); p. R-NO2 (1540 cm-1); q. R3-C-H (2900 cm-1).

3. Results.

A large number of molecules are formed in the laboratory sample during the photolysis and from reactive photoproducts during warm-up. The appearance and sublimation during the warm-up of the species detected by I.R. was monitored by following the intensity of a characteristic feature (fig. 2). Table 1 lists the organic species that were observed in the ice and in the non-volatile residue. The are composed of 1 - 3 C atoms with -NH2, -OH and -(C=O)- functional groups. A large number of volatile organic species can however have escaped detection due to the confusion of the numerous features in the I.R. spectrum. About 3% of the available carbon was converted to organic species that are volatile at room temperature and about 2.5% to residue material.

Table 1. Photochemically produced organic species from deposited H2O, CO and NH3 (from Agarwal et al. 1985, Schutte 1988).

Molecule	Mass (amu)	volatile (at 293 K)
CH3OH	32	+
HCONH2	45	+
HCOOH	46	+
NH2CONH2	60	-
NH2CH2CH2OH	61	-
R-NO2	>61	+
HOCH2CH2OH	62	+
HOCH2CONH2	75	-
HOCH2COOH	76	-
NH2COCONH2	88	-
NH2COCOOH	89	-
HOCH2CHOHCH2OH	92	-
HOCH2CHOHCONH2	105	-
HOCH2CHOHCOOH	106	-

4. Comparison of the Experimental Results with Comet Halley Data.

Giotto's PICCA heavy-ion analyzer detected molecules rich in C, H, O and N in the gas near comet Halley (Mitchell et al. 1987, 1988). The spectra showed masses in the range 30 - 120 amu with a total abundance of the order of a few percent of that of the water ions. Furthermore, Vega's PUMA dust impact mass spectrometer tentatively identified species like formic acid (HCOOH) and oxalic acid (HOCOCOOH) in the cometary grain mantles (Kissel et al. 1987).

There is a good correspondence between the elemental composition of the laboratory residue material and the elemental composition inferred from the PICCA mass spectra (table 2). Although the residue species are not expected to sublimate at the dust temperatures during the Giotto and Vega encounters (≈ 300 K; e.g., Tokunaga et al. 1989), the more volatile organic component produced in the experiment should have similar elemental composition since it is formed by similar chemical processes (Schutte 1988). The detected abundances are in good agreement with the amount of organic material that could form in interstellar ice mantles over astrophysical time scales.

Table 2. Comparison between the elemental composition of the laboratory organic residue and the organic species detected by PICCA near Comet Halley.

	rel. abundance	
Element	residue	Halley
C	1.0	1.0
H	2.2	
O	1.3	1.2 - 1.4
N	0.24	≤0.27

Conclusions.

We simulated the photoprocessing of interstellar ices in dense clouds in connection with the detection of organic species by PICCA in the coma of Comet Halley. The following conclusions can be drawn:

- The simulation experiments produce organic molecules of mass between 30 and 110 amu rich in -(C=O), -OH, and -NH2 molecular groups.
- The elemental composition of the organic species detected by PICCA is similar to that of the experimentally produced molecules.
- The production efficiency of organics in molecular clouds could be sufficient to explain the observed abundance of organic species in the coma of Comet Halley.

References.

Agarwal, V. K., Schutte, W., Greenberg, J. M., Ferris, J. P., Briggs, R., Connor, S., van de Bult, C. P. E. M., and Baas, F. 1985, *Origins of Life*, **16**, 21.

Butchart, I., McFadzean, A. D., Whittet, D. C. B., Geballe, T. R., and Geballe, T. R., Baas, F., Greenberg, J. M., and Schutte, W. 1985, *Astr. Ap. (Letters)*,**146**, L6.

Greenberg, J. M. 1986, *Astr. Ap. (letters)*, **154**, L5.

Greenberg, J. M. 1973, in *Molecules in the Galactic Environment*, ed. Gordon and Snyder (Wiley Interscience), p. 94.

Grim, R. J. A., and Greenberg, J. M. 1987, *Ap. J.*, **321**, L91.

Grim, R. J. A., Schutte, W. A., Greenberg, J. M., Baas, F., and Schmitt, B. 1989, *Astr. Ap.*, in press.
Hagen 1982, Ph.D. thesis, University of Leiden, the Netherlands.
Kissel, J., and Krueger, F. R. 1987, *Nature*, **326**, 755.
Lacy, J. H., Baas, F., Allamandola, L. J., Persson, S. E., McGregor, P. J., Lonsdale, C. J., Geballe, T. R., and van de Bult, C. E. P. 1984, *Ap. J.*, **276**, 533.
Mitchell, D. L., Lin, R. P., Anderson, K. A., Carlson, C. W., Curtis, D. W., Korth, A., Reme, H., Sauvaud, J. A., d'Uston, C., and Mendis, D. A. 1987, *Science*, **237**, 626.
Mitchell et al. 1988, preprint.
Prasad, S. S., and Tarafdar, S. P. 1983, *Ap. J.*, **267**, 603.
Schutte 1988, Ph.D. thesis, University of Leiden, the Netherlands.
Tielens et al., 1989, *Ap. J.*, in preperation.
Tokunaga, A. T., Golisch, W. F., Griep, D. M., Kaminski, C. D., and Hanner, M. S. 1988, *Astron. J.*, **96**, 1971.

EVOLUTION OF CARBONACEOUS CHONDRITE PARENT BODIES: INSIGHTS INTO COMETARY NUCLEI?

Harry Y. McSween, Jr.
University of Tennessee, Knoxville
Knoxville, Tennessee

EVOLUTION OF CARBONACEOUS CHONDRITE PARENT BODIES: INSIGHTS INTO COMETARY NUCLEI?

Harry Y. McSween, Jr.

University of Tennessee, Knoxville

INTRODUCTION

"More than ever, comets appear to be made of a pristine material older than the planets, preserved in its primitive state by the very deep cold of interstellar space and able to give us information about the chemistry of the early solar nebula." (Delsemme, 1988)

Much of the excitement about obtaining cometary samples accrues from the conventional view, expressed eloquently in the statement above, that they comprise the most primitive materials that we are likely to get our hands on. But is this true? Although "parent body" alteration of such samples would not necessarily detract from this interest, we should keep in mind the possibility that certain kinds of secondary processes may have affected cometary nuclei. Weissman (1986) has proposed some mechanisms by which comet nuclei might be altered, but observational evidence supporting the physical processing of comets is not yet generally available. This paper will take another approach: inferences about the kinds of modifications that might be encountered can be drawn from data on the evolution of carbonaceous chondrite parent bodies. The following observations suggest that, of all the classes of chondrites, these meteorites are most applicable to the study of comets:

(1) Carbonaceous chondrites are chemically the most primitive meteorites. The elemental abundances of CI chondrites, normalized to silicon, provide the closest match with the composition of the solar photosphere (Holweger, 1977; Anders and Grevesse, 1989).

(2) Spectral reflectivity surveys of asteroids suggest that carbonaceous chondrite-like bodies reside primarily in the more distal portions of the asteroid belt (Gradie and Tadesco, 1982). Their formation locations thus lie at greater solar distances than those of other meteorite types, closer to inferred sites for comet accretion (Weissman, 1985; Hartmann et al., 1987).

(3) Petrographic studies of carbonaceous chondrites indicate that they formed in volatile-rich environments (McSween, 1979; Kerridge and Bunch, 1979), and H_2O and other volatile components may have been incorporated

initially as ices (Bunch and Chang, 1980; Prinn and Fegley, 1988).

(4) Some types of chondritic porous interplanetary dust particles (IDPs), which may be solid debris from short period comets, are mineralogically similar to carbonaceous chondrites (Bradley and Brownlee, 1986; Tomeoka and Buseck, 1988), although some compositional distinctions occur (Schramm et al., 1987). Moreover, both of these materials appear to be broadly similar in composition to Comet Halley dust (Rietmeijer, 1987; Blanford et al., 1988).

It seems increasingly unlikely that carbonaceous chondrites are comet nucleus samples. However, these meteorites were probably derived from planetesimals that originally contained ices, though possibly in lesser proportions than comets, so the compositional distinction between carbonaceous chondrite parent bodies and comets may be one of degree. The possibility of an orbital evolution of cometary bodies into asteroidal orbits has also been suggested (Wetherill, 1979). For these reasons, it seems prudent to examine the processes which have affected carbonaceous chondrite parent bodies as possible analogs for the evolutionary history of comets.

THERMAL PROCESSES

Most carbonaceous chondrites show evidence of parent body heating, either in the form of thermal metamorphism or, more commonly, aqueous alteration (Zolensky and McSween, 1988). Although aqueous alteration clearly took place at low temperatures near the freezing point of water (Clayton and Mayeda, 1984), heat was necessary to produce water from ice. Aqueous alteration at low temperatures may also have affected some IDPs (Reitmeijer and Mackinnon, 1985a).

The source of heat for chondrite parent bodies is still controversial. Decay of short-lived radionuclides like ^{26}Al is one plausible mechanism (Lee et al, 1977; Hutcheon et al., 1987) that could presumably affect asteroids and comets. External heat sources such as electromagnetic induction by a massive solar wind (Herbert and Sonett, 1979) have also been suggested, but the decrease in effectiveness of this mechanism with solar distance renders this heat source unlikely for cometary bodies. The time scale for aqueous alteration in carbonaceous chondrites (Macdougall et al., 1984) was fairly short and commenced soon after accretion, as would be appropriate for either heating mechanism.

Melting of ice in carbonaceous chondrite parent bodies has resulted in profound mineralogical changes. The original (presumed anyhydrous) chondrite assemblage has been altered to nonequilibrium mixtures of fine-grained phyllosilicate minerals like serpentine, smectite, and chlorite, as well as poorly crystallized oxides, hydroxides, sulfides, carbonates, and carbonaceous phases (e.g. Barber, 1981; Mackinnon, 1982;

Tomeoka and Buseck, 1985, 1988). High-resolution transmission electron microscopy has revealed intimate intergrowths of complex phases (Fig. 1) that are extremely difficult to characterize. CI chondrites are cut by veins containing sulfate and carbonates (Richardson, 1978) precipitated from fluids of differing compositions (Fig. 2).

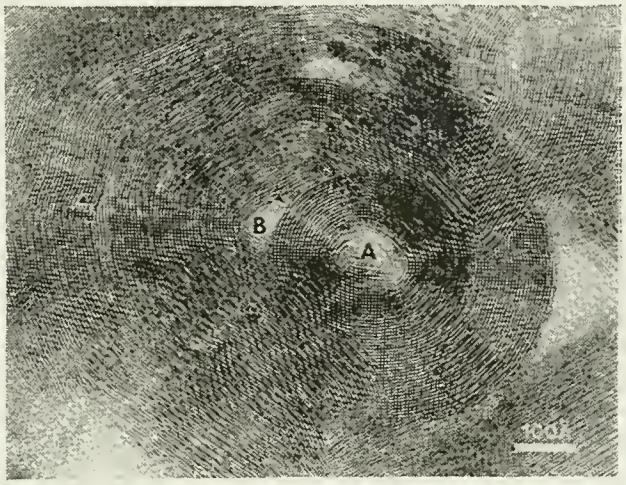


Figure 1. HRTEM photomicrograph of tubular phyllosilicate phase with 5 A lattice spacing in the Mighei CM carbonaceous chondrite. Two distinct core regions are indicated by A and B. This phase formed by aqueous alteration. From Tomeoka and Buseck (1983).

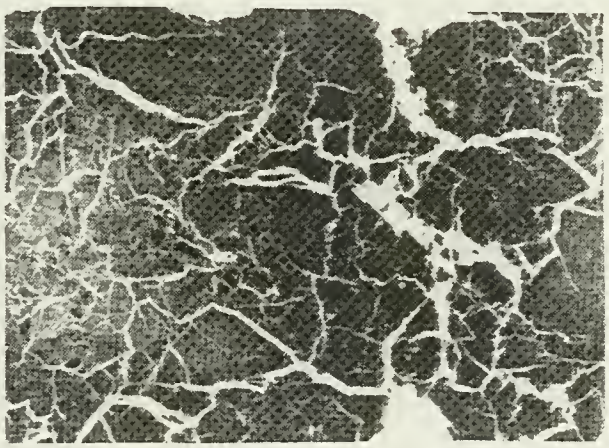


Figure 2. Sulfate and carbonate veins crosscutting a thin section of the Orgueil CI carbonaceous chondrite. The section is approximately 10 mm wide. From McSween (1979).

It is generally believed that chemical changes accompanying aqueous alteration were minor (McSween and Richardson, 1977), although this conclusion is based primarily on similarities to solar elemental abundances which are not precisely measured. However, observed modifications of the isotopic composition of oxygen (Clayton and Mayeda,

1984), which constitutes nearly half of mass of these meteorites, suggests the likelihood of other chemical changes. Bunch and Chang (1980) noted that the strongest reported enrichments of the heavy isotopes of O, N, and C occur in chondrites which have been exposed to aqueous alteration.

Grimm and McSween (1987) constructed thermal models for ice-bearing planetesimals. Not surprisingly, the presence of ice was found to act as a thermal buffer for such bodies, possibly accounting for the difference in metamorphic history between parent bodies for ordinary and carbonaceous chondrites. More recent work suggests that exothermic hydration reactions may have significant thermal effects which should be included in thermal modeling. Grimm and McSween (1989) have developed an interior-alteration model driven by ^{26}Al decay and a regolith-alteration model powered by either ^{26}Al or impacts. Both models are capable of producing homogeneously altered materials in relatively short time spans.

SYNTHESIS OF CARBONACEOUS MATERIALS

Because carbonaceous chondrites contain carbon in carbonates and organic compounds extractable by water and solvents, Bunch and Chang (1980) raised the possibility of organic synthesis during aqueous alteration. Fischer-Tropsch type reactions in the nebula or in interstellar clouds have been suggested to have produced many hydrocarbons in carbonaceous chondrites (Hayatsu and Anders, 1981), but other, secondary mechanisms are worthy of consideration.

Organic compounds are much more abundant in altered carbonaceous chondrites than in unaltered ones (Cronin et al., 1988). Pelzer et al. (1984) noted that the presence of both amino acids and hydroxy acids in these meteorites suggests formation by a Strecker-cyanohydrin synthesis in an aqueous, ammonia-containing medium, which might be reasonably expected to accompany aqueous alteration. Thermodynamic calculations by Shock (1988) indicate that carboxylic and amino acids should be produced by reactions with water and ammonia at 25°C. The Miller-Urey synthesis, which is capable of producing many other organic compounds, is postulated to have taken place on parent body surfaces, although its link with aqueous altertion is tenuous.

Poorly graphitized carbon is also present in carbonaceous chondrites and IDPs (Mackinnon and Rietmeijer, 1987). This material may either have been derived from, or alternatively, be the remnants of interstellar organic phases. The carbonization reaction involves removal of O and N and the subsequent graphitization of hydrocarbons. Rietmeijer and Mackinnon (1985b) showed that this process could occur at temperatures of several hundred degrees or less.

IMPACT PROCESSES

Virtually all classes of meteorites show the effects of impact processes, so it seems possible that cometary materials may also show shock effects. The results of impact phenomena in carbonaceous chondrites take many forms.

Shock metamorphic effects include partial destruction of the crystal structures of many minerals, easily recognizable from their optical and X-ray diffraction properties. The breakup of chondrules to produce isolated mineral grains (Richardson and McSween, 1978) may have been facilitated by both shock and aqueous alteration. Uniaxial compaction and deformation of chondrules in a few carbonaceous chondrites have also been recognized (Cain et al., 1986). Although this has been attributed to overburden on the parent asteroid, similar strain effects in ordinary chondrites are clearly related to shock (Sneyd et al., 1988).

Most, if not all, carbonaceous chondrites are breccias, containing clasts with variable alteration histories (Nagy, 1975; McSween and Richardson, 1977; Olsen et al., 1988). Many of these formed in regoliths although some, such as that shown in Figure 3, may be accretional breccias (Kracher et al., 1985). Mixing of different kinds of materials within the outer parts of comets might also have occurred, even if impacts were infrequent.

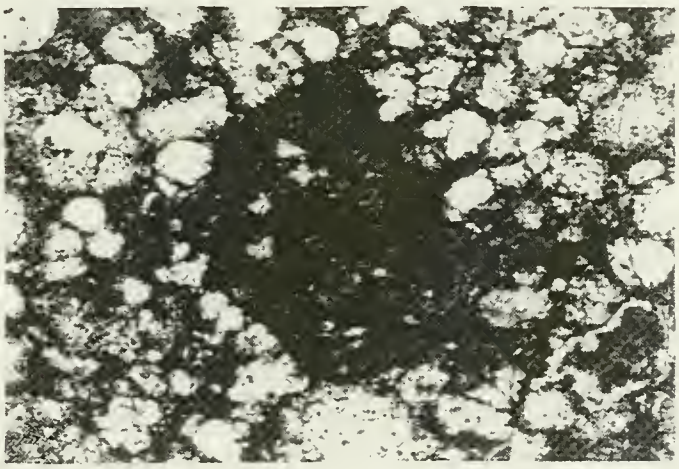


Figure 3. Photomicrograph of the Leoville CV carbonaceous chondrite, illustrating dark carbonaceous clast in lighter colored host. This meteorite is thought to be an accretionary breccia. The clast is approximately 2 mm across. From McSween (1977).

Lange and Ahrens (1982) showed experimentally that shock can cause dehydration of serpentine and suggested that impacts into carbonaceous chondrite bodies may result in devolatilization. Loss of structural water from minerals in carbonaceous chondrites has been documented in at least one meteorite (Akai, 1988), although this was attributed to heating.

IRRADIATION PROCESSES

Many chondrites have been irradiated by solar-wind, solar-flare, and cosmic-ray particles. The penetration depths for these particles vary with their energies (galactic cosmic rays 1 m, solar cosmic rays 1 mm, solar wind <1 um), but none can penetrate to appreciable depths. For this reason, most chondrite irradiation occurred in regoliths on parent body surfaces or during exposure as small meteoroids in space.

A high proportion of carbonaceous chondrites contain solar-wind implanted noble gases, as well as significant amounts of cosmogenic nuclides and solar flare tracks in mineral grains (Fig. 4). All of these features are indicative of irradiation. More information on the multi-stage exposure histories of these meteorites can be obtained if compaction ages are available. For the few carbonaceous chondrites for which exposure histories have been measured, the solar-wind and solar-flare irradiations occurred before 4.2-4.4 b.y. ago (Macdougall and Kothari, 1976). Exposure may have occurred in small bodies that were precursors to the carbonaceous chondrite parent asteroids, in small fragments of disrupted parent bodies that subsequently reaccreted, or in asteroid megaregoliths (Goswami et al., 1984).

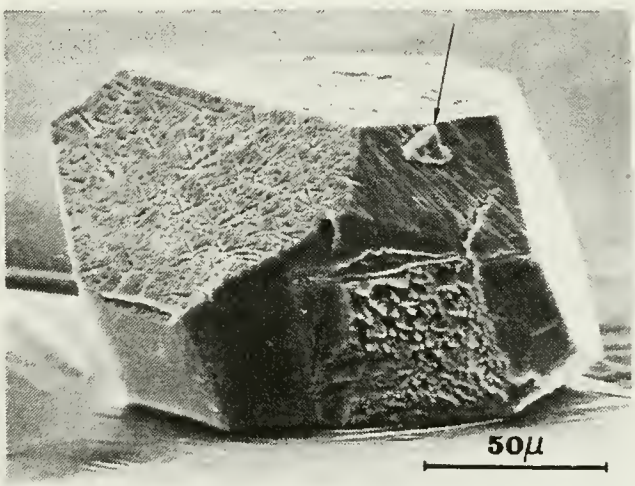


Figure 4. Olivine crystal with tracks (enlarged by etching) on some faces, caused by irradiation. Arrow points to an included chromite grain. From Macdougall and Kothari (1976).

IMPLICATIONS FOR COMET EVOLUTION

How applicable, if at all, are these processes to comets? Based on

our present lack of data on and detailed understanding of cometary nuclei, we probably cannot afford to rule any of them out.

Calculations of the thermal effect of decay of long-lived radionuclides in comets suggest that interior temperatures could reach above 50 K for 10-km-diameter objects (Yabushita and Wada, 1988). If the proportion of possible short-lived radionuclides such as ^{26}Al in cometary materials were similar to those in chondrites, and if the time scale of comet accretion was fast enough to permit incorporation of "live" radionuclides, comets might have reached significantly higher temperatures. Rietmeijer (1985) has considered the possibility of cryogenic ($<0^{o}C$) alteration in comet nuclei, owing to the presence of thin interfacial water layers. Even modest temperature excursions in cometary nuclei might result in thermal histories somewhat like those of carbonaceous chondrite parent bodies. We might then predict that cometary dust should contain some phyllosilicate minerals and other phases formed by aqueous alteration at low temperatures. At least some chondritic IDPs contain phyllosilicates and carbonates (Rietmeijer and Mackinnon, 1987), and aggregate IDPs may closely approach CI chondrites in bulk composition (Blanford et al., 1988). The occurrence of graphitized carbon in some IDPs suggests that these particles may have experienced temperatures of up to several hundred degrees (Rietmeijer and Mackinnon, 1985b). Based on a chemical comparison between Comet Halley dust and cosmic abundances, Anders and Grevesse (1989) suggested that non-solar Fe/Si and Mg/Si ratios indicate that the Halley dust component cannot be pristine interstellar matter. On the other hand, similarities between the chemical compositions of anhydrous IDPs and Comet Halley dust (Rietmeijer, 1987) may suggest that aqueous alteration processes have not appreciably affected this cometary nucleus. Detailed mineralogical characterization of returned comet samples may be required to resolve this question.

Thermal effects in comet nuclei may also result from repeated close passage to the sun (Weissman, 1986), or near passing stars in the Oort cloud (Stern, 1986). Spectral observations from the Giotto mission indicate dust temperatures at the surface of comet Halley may have reached $80^{o}C$ at 1 A.U. (Gombosi and Houpis, 1986). These temperatures are certainly sufficient for aqueous alteration processes, provided that the kinetics of such reactions are reasonably rapid. The chemical and mineralogical diversity of chondritic IDPs suggests that their sources are heterogeneous or differ in degree of thermal processing (Mackinnon and Rietmeijer, 1987). If all IDPs are derived from comets, they may have different thermal histories because of their orbits or other factors.

It is difficult to say anything about the origin of carbonaceous compounds in comets. Comet Halley shows the C-H stretch band at 3.4 microns in emission, indicating the presence of organic matter on its nucleus (Combes et al., 1986), but specific compounds have not been identified. IDPs also show this C-H stretching feature (Sandford and Walker, 1985). Organic constituents in IDPs are still poorly characterized, though evidence of some thermal processing in the form of graphitized carbon is present (Rietmeijer and Mackinnon, 19885b). Understanding of carbon compounds in comets has been greatly improved by

the recognition that much of this material resides in the dust fraction (Delsemme, 1988), and return of a condensed sample may allow chemical and isotopic studies which address this problem.

Impact processes probably affected cometary materials during their initial accretion. Low number densities of comets in the Oort cloud may have minimized subsequent collisions, but their ejection from the outer solar system into the Oort cloud may have been catastrophic. We should be prepared to find that comets are heterogeneous, consisting of rock fractions with different thermal and shock histories. In fact, the comet nucleus itself may ultimately be viewed as a megabreccia, comprised of rock and ice blocks and clasts.

Suggestions that dusty regoliths may persist on cometary surfaces suggest that irradiation of cometary materials is likely. Conceptions of comet surfaces that envision refractory lag deposits or icy pedestals capped by dust also offer opportunities for sample irradiation, and the shielding characteristics of ice are less than that of rock. Beyond the heliopause, comets may be exposed to increased amounts of galactic cosmic rays. Moreover, progressive devolatilization of comets during passages close to the sun should expose increasing amounts of rocky material to solar radiation, and "extinct" comets might have irradiation histories similar to asteroids. It is noteworthy that cosmic-ray tracks have been observed recently in chondritic IDPs (Bradley and Brownlee, 1986), although these tracks were probably implanted during exposure to solar flares while the particles were in interplanetary orbits rather than on the parent objects.

Comets may indeed turn out to be pristine materials, as stated in the quotation that opened this paper, but we are not yet positive of that. Their formation and storage at great solar distances does not automatically guarantee them immunity from the kinds of processes that have affected other solar system bodies, and repeated approaches to the inner solar system may offer other opportunities for alteration processes to affect those comets that we will be able to sample.

REFERENCES

Akai J. (1988) Incompletely transformed serpentine-type phyllosilicates in the matrix of Antarctic CM chondrites. Geochim. Cosmochim. Acta 52, 1593-1599.

Anders E. and Grevesse N. (1989) Abundances of the elements: Meteoritic and solar. Geochim. Cosmochim. Acta, in press.

Barber D. (1981) Matrix phyllosilicates and associated minerals in C2M carbonaceous chondrites. Geochim. Cosmochim. Acta 45, 945-970.

Blanford G.E., Thomas K.L, and McKay D.S. (1988) Microbeam analysis of four chondritic interplanetary dust particles for major elements, carbon and oxygen. Meteoritics 23, 113-121.

Bradley J.P. and Brownlee D.E. (1986) Cometary particles: Thin sectioning and electron beam analysis. Science 231, 1542-1544.

Bunch T.E. and Chang S. (1980) Carbonaceous chondrites-II. Carbonaceous chondrite phyllosilicates and light element geochemistry and indicators of parent body processes and surface conditions. Geochim. Cosmochim. Acta 44, 1543-1577.

Cain P.M., McSween H.Y., and Woodward N.B. (1986) Structural deformation of the Leoville chondrite. Earth Planet. Sci. Lett. 77, 165-177.

Clayton R.N. and Mayeda T.K. (1984) The oxygen isotope record in Murchison and other carbonaceous chondrites. Earth Planet. Sci. Lett. 67, 151-161.

Combes M. and 15 coauthors (1986) Detection of parent molecules in comet Halley from the VEGA experiment. In Proc. 20th ESLAB Symp. on the Exploration of Halley's Comet, vol. 1, ESA SP-250, pp. 353-358.

Cronin J.R., Pizzarello S., and Cruikshank D.P. (1988) Organic matter in carbonaceous chondrites, planetary satellites, asteroids and comets. In Meteorites and the Early Solar System, ed. J.F. Kerridge and M.S. Matthews, Univ. of Arizona Press, Tucson, pp. 819-857.

Delsemme A.H. (1988) The chemistry of comets. Phil. Trans. R. Soc. Lond. A 325, 509-523.

Gombosi T.I. and Houpis H.L.F. (1986) An icy-glue model of cometary nuclei. Nature 324, 43-44.

Goswami J.N., Lal D., and Wilkening L.L. (1984) Gas-rich meteorites: Probes for particle environment and dynamical processes in the inner solar system. Space Sci. Rev. 37, 111-159.

Gradie J.C. and Tedesco E.F. (1982) The compositional structure of the asteroid belt. Science 216, 1405-1407.

Grimm R.E. and McSween H.Y. (1987) Water and the thermal history of the CM carbonaceous chondrite parent body. Lunar Planet. Sci. XIX, 427-428.

Grimm R.E. and McSween H.Y. (1989) Water and the thermal evolution of carbonaceous chondrite parent bodies. Icarus, submitted.

Hartmann W.K., Tholen D.J., and Cruikshank D.P. (1987) The relationship between active comets, "extinct" comets, and dark asteroids. Icarus 69, 33-50.

Hayatsu R. and Anders E. (1981) Organic compounds in meteorites and their

origins. In Topics in Current Chemistry Vol. 99, ed. F.L. Boschke, Springer, 1-37.

Herbert F. and Sonett C.P. (1979) Electromagnetic heating of minor planets in the early solar system. Icarus 40, 484-496.

Holweger H. (1977) The solar Na/Ca and S/Ca ratios: A close comparison with carbonaceous chondrites. Earth Planet. Sci. Lett. 34, 152-154.

Hutcheon I.D., Hutchison R., and G.J. Wasserburg (1987) Evidence of the in-situ decay of ^{26}Al in a Semarkona chondrule. Lunar Planet. Sci. XIX, 523-524.

Kerridge J.F. and Bunch T.E. (1979) Aqueous activity on asteroids: Evidence from carbonaceous meteorites. In Asteroids, ed. T. Gehrels, Univ. of Arizona Press, Tucson, pp. 745-764.

Kracher A., Keil K., Kallemeyn G.W., Wasson J.T., Clayton R.N., and Huss G.I. (1985) The Leoville (CV3) accretionary breccia. J. Geophys. Res. 90 Suppl., D123-126.

Lange M.A. and Ahrens T.J. (1982) Shock release adiabat measurements on volatile bearing minerals and implications for an impact generated atmosphere. Lunar Planet. Sci. XIII, 421-422.

Lee T., Papanastasiou D.A., and Wasserburg G.J. (1977) Aluminum-26 in the early solar system: Fossil or fuel? Astrophys. J. 211, L107-110.

Macdougall J.D. and Kothari B.K. (1976) Formation chronology for C2 meteorites. Earth Planet. Sci. Lett. 33, 36-44.

Macdougall J.D., Lugmair G.W., and Kerridge J.F. (1984) Early solar system aqueous activity: Sr isotope evidence from the Orgueil CI meteorite. Nature 307, 249-251.

Mackinnon I.D.R. (1982) Ordered mixed-layer structures in the Mighei carbonaceous chondrite matrix. Geochim. Cosmochim. Acta 46, 479-489.

Mackinnon I.D.R. and Rietmeijer F.J.M. (1987) Mineralogy of chondritic interplanetary dust particles. Rev. Geophys. 25, 1527-1553.

McSween H.Y. (1977) Petrographic variations among carbonaceous chondrites of the Vigarano type. Geochim. Cosmochim. Acta 41, 1777-1790.

McSween H.Y. (1979) Are carbonaceous chondrites primitive or processed? A review. Rev. Geophys. Space Phys. 17, 1059-1078.

McSween H.Y. and Richardson S.M. (1977) The composition of carbonaceous chondrite matrix. Geochim. Cosmochim. Acta 41, 1145-1161.

Nagy B. (1975) Carbonaceous Meteorites. Elsevier Pub. Co., Amsterdam.

Olsen E.J., Davis A.M., Hutcheon I.D., Clayton R.N., Mayeda T.K., and Grossman L. (1988) Murchison xenoliths. Geochim. Cosmochim. Acta 52, 1615-1626.

Pelzer E.T., Bada J.L., Schlesinger G., and Miller S.L. (1984) The chemical conditions on the parent body of the Murchison meteorite: Some conclusions based on amino, hydroxy and dicaroxylic acids. Adv. Space Res. 4, 69-74.

Prinn R.G. and Fegley B. (1988) Solar nebula chemistry: Origin of planetary, satellite, and cometary volatiles. In Origin and Evolution of Planetary and Satellite Atmospheres, ed. S. Atreya, J. Pollack, and M. Matthews, Univ. of Arizona Press, Tucson, in press.

Richardson S.M. (1978) Vein formation in the C1 carbonaceous chondrites. Meteoritics 13, 141-159.

Richardson S.M. and McSween H.Y. (1978) Textural evidence bearing on the origin of isolated olivine crystals in C2 carbonaceous chondrites. Earth Planet. Sci. Lett. 37, 485-491.

Rietmeijer F.J.M. (1985) A model for diagenesis in proto-planetary bodies. Nature 313, 293-294.

Rietmeijer F.J.M. (1987) A quantitative comparison of fine-grained chondritic interplanetary dust and Comet Halley dust. Lunar Planet. Sci. XIX, 980-981.

Rietmeijer F.J.M. and Mackinnon I.D.R. (1985a) Layer silicates in a chondritic porous interplanetary dust particle. J. Geophys. Res. 90 Suppl., D149-155.

Rietmeijer F.J.M. and Mackinnon I.D.R. (1985b) Poorly graphitized carbon as a new cosmothermometer for primitive extraterrestrial materials. Nature 315, 733-736.

Sandford S.A. and Walker R.M. (1985) Laboratory infrared transmission spectra of individual interplanetary dust particles from 2.5 to 25 microns. Astrophys. J. 291, 838-851.

Schramm L.S., Brownlee D.E., and Wheelock M.M. (1987) The elemental composition of interplanetary dust. Lunar Planet. Sci. XIX, 1033-1034.

Shock E.L. (1988) Relative abundances of amino acids in the Murchison meteorite: Clues to synthesis pathways or sampling bias? EOS 69, No. 44, 1287.

Sneyd D.S., McSween H.Y., Sugiura N., Strangway D.W., and Nord G.L. (1988) Origin of petrofabrics and magnetic anisotropy in ordinary chondrites. Meteoritics 23, 139-149.

Stern S.A. (1986) Cometary capture rates and extra-solar Oort cloud

encounters. Lunar Planet. Sci. XVIII, 950.

Tomeoka K. and Buseck P.R. (1983) A new layered mineral from the Mighei carbonaceous chondrite. Nature 306, 354-356.

Tomeoka K. and Buseck P.R. (1985) Indicators of aqueous alteration in CM carbonaceous chondrites: Microtextures of a layered mineral containing Fe, S, O and Ni. Geochim. Cosmochim. Acta 49, 2149-2163.

Tomeoka K. and Buseck P.R. (1988) Matrix mineralogy of the Orgueil CI carbonaceous chondrite. Geochim. Cosmochim. Acta 52, 1627-1640.

Weissman, P.R. (1985) The origin of comets: Implications for planetary formation. In Protostars and Planets II, ed. D.C. Black and M.S. Matthews, Univ. of Arizona Press, Tucson, 895-919.

Weissman, P.R. (1986) How pristine are cometary nuclei? Proc. Comet Nucleus Sample Return Mission Workshop, ESA SP-249, pp. 15-25.

Wetherill, G.W. (1979) Steady-state populations of Apollo-Amor objects. Icarus 37, 96-112.

Yabushita S. and Wada K. (1988) Radioactive heating and layered structure of cometary nuclei. Earth Moon Planet. 40, 303-313.

Zolensky M. and McSween H.Y. (1988) Aqueous alteration. In Meteorites and the Early Solar System, ed. J.F. Kerridge and M.S. Matthews, Univ. of Arizona Press, Tucson, pp. 114-143.

INTERPLANETARY DUST PARTICLES OPTICAL PROPERTIES: A CLUE TO COMETARY DUST STRUCTURE?

A. C. Levasseur–Regourd
Service d'Aéronomie
Varriéres, France

R. Dumont
Observatoire de Bordeaux
Floirac, France

J. B. Renard
Service d'Aéronomie
Varriéres, France

INTERPLANETARY DUST PARTICLES OPTICAL PROPERTIES : A CLUE TO COMETARY DUST STRUCTURE ?

A.C. LEVASSEUR-REGOURD[1], R. DUMONT[2], J.B. RENARD[1]

1. Service d'Aéronomie, Verrières, France 2. Observatoire de Bordeaux, Floirac, France

Both the solar light scattered by interplanetary dust particles and the thermal emission from these particles have been extensively observed. Techniques of inversion of the line-of-sight brightness allow to derive local optical properties of the interplanetary dust.

In the ecliptic plane near 1 au, the heliocentric gradients of local polarization, temperature and albedo are found to be of the order, respectively, of 0.8, - 0.3, and - 0.7. Towards the ecliptic pole, the local polarization is found to be much smaller than in the ecliptic at the same solar distance. Also the temperature decreases faster with increasing distance than it does in the ecliptic, whence an increase in bulk albedo.

Some optical properties of the dust particles may be inferred from these results. They are consistent with a scenario of evolution of dark fluffy cometary grains evaporating as they spiral towards the Sun.

INTRODUCTION

Zodiacal light

Our present knowledge of the distribution of brightness and polarization of light scattered by interplanetary dust particles (= zodiacal light), as seen from the Earth's orbit, comes from extended ground based programmes, together with space observations. Zodiacal light is a faint extended source, which is collected along the line of sight together with atmospheric airglow (negligible for space observations), starlight, galactic light and diffuse galactic light (negligeable at high galactic latitudes). The results are usually given as a function of ecliptic latitude β and helioecliptic longitude $\lambda - \lambda_\odot$ of the line of sight (fig. 1). There is a fairly good agreement between the observations published since the mid seventies (see for instance compilations by Levasseur and Dumont, 1980 or Fechtig et al., 1981).

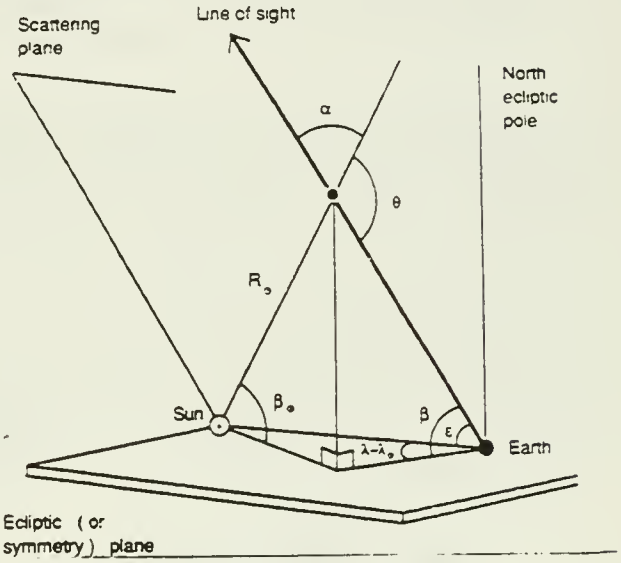


Fig. 1. Geometry of IDP observations

The main feature for the zodiacal light brightness in an increase towards the Sun, together with a secondary increase due to some backscattering in the antisolar region (gegenschein). The zodiacal light is found to be rather stable with time, but for some annual temporal variations at high and medium ecliptic latitudes ; these oscillations originate in the slight inclination (about 1.5°) of the symmetry surface of the zodiacal cloud upon the ecliptic plane.

The polarization distribution is characterized by a region of strong linear polarization near 60° elongation. The Fresnel vector is in the scattering plane (observer-Sun, observer-line of sight), but for the antisolar region which exhibits a negative polarization.

Thermal emission

With a spectrum that is almost solar like, zodiacal light prevails below 5 μm. In the 5 to 50 μm range, the thermal emission of the interplanetary dust cloud turns out to be the most prominent component of the sky, at least for high and medium galactic latitudes.

Thermal emission has been observed at various wavelengths since the beginning of the eighties from balloons or rockets and from IRAS satellite (Hauser et al., 1984 ; Murdock and Price, 1985 ; Salama et al., 1987).

Due possibly to calibration problems, there is a discrepancy by a factor of about 2 between the satellite and rocket emissivities, while the thermal emission is most likely to be stable with time. The survey performed by IRAS, even though limited to elongation angles ε in a 60° to 120° range, clearly confirms that the zodiacal cloud symmetry surface is slightly inclined upon the ecliptic (Dumont and Levasseur-Regourd, 1978 ; Hauser et al., 1985) and that it is not entirely smooth, due to narrow dust trails ahead or behind cometary nuclei and to dust bands of asteroidal origin (Levasseur and Blamont, 1976 ; Sykes et al., 1986 ; Dermott et al., 1986).

Need for an inversion

The measurements of both zodiacal light and thermal emission provide integrals along a line of sight of local brightnesses. To interpret these measurements in terms of local properties, it is necessary to develop model fitting or, even better, inversion methods.

We present here new results for the "nodes of lesser uncertainty" inversion method, which may be of interest to derive some physical properties of the interplanetary dust and of its cometary or asteroidal sources.

HELIOCENTRIC DEPENDENCE OF PHYSICAL PROPERTIES IN THE ECLIPTIC PLANE

Nodes of lesser uncertainty on a secant to the Earth's orbit

Once surveys of zodiacal light or of thermal emission are available in the ecliptic plane,

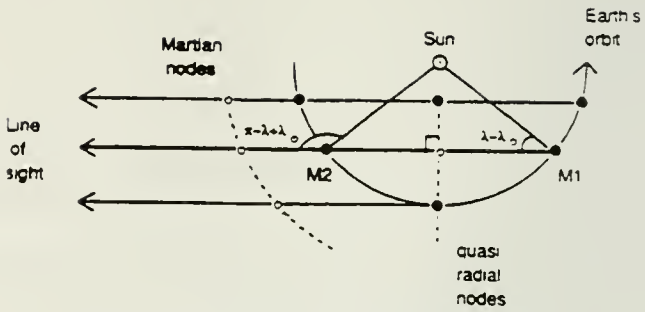


Fig. 2. Nodes in the ecliptic plane

integrated brightnesses can be obtained along the same line of sight (that intersects the Earth's orbit in M_1 and M_2) for a given helioecliptic longitude and for the supplementary angle (fig. 2). The knowledge of integrated brightnesses along $M_1 \infty$ and $M_2 \infty$ offers some possibility of partly inverting the brightness integral under limited assumptions.

The inversion is indeed feasible without any assumption only for the first section (from where the observation is performed) of a line of sight tangent to the orbit of the Earth (or of a moving spacecraft). For any other location and direction, various assumptions are required.

We assume here a steady state and a rotational symmetry of the interplanetary dust cloud, as strongly suggested by the absence of seasonal dependence of optical and infrared brightnesses after correction for the oscillations of the Earth on either side of the symmetry plane. The local optical brightness can therefore be written as $F \times C_{vis}(R_\odot, \theta)/ R_\odot^2$, where F is the solar intensity and where C_{vis} (directional scattering cross-section of the unit volume) is only a function of the heliocentric distance $R_\odot$ and the scattering angle θ. Also the local infrared brightness can be written as $F \times C_{IR}(R_\odot,\lambda)/R_\odot^2$ where C_{IR} (monochromatic thermal cross-section of the unit volume) is only a function of the distance $R_\odot$ and the wavelength λ.

We also assume the functions that characterize the scattering or thermal cross-sections to be positive (optically thin medium) and rather monotonous (relative smoothness of the cloud, at least to the first order), and to decrease asymptotically to zero with increasing $R_\odot$ (absence of interplanetary dust far away from the Sun). From the whole of set of constraints (integrals along $M_1 \infty$ and $M_2 \infty$ lines of sight, plus values and derivatives at infinity), it can be demonstrated that the curves which represent all the possible C_{vis} or C_{IR} functions for a given line

of sight have to constrict in two foci or nodes, where the local scattering or thermal cross-section of the unit volume can be determined with less uncertainty than elsewhere. Details on the method can be found in Dumont and Levasseur-Regourd (1985a) for the optical case or in Dumont and Levasseur-Regourd (1988) for the infrared case.

One of the nodes, always located at an heliocentric distance of the order 1.5 au, is called the martian node. In the visual case, the determination of C_{vis} ($R_\odot \approx 1.5$ ua, θ) at the martian node allows to disregard the heliocentric dependence and therefore to retrieve the scattering phase function near 1.5 ua.

The other node, which remains located near the middle of M_1M_2 chord, is called the quasi radial node. In the visual case, the determination of $C_{vis}(R_\odot, \theta \approx 90°)$ at this node allows to disregard the scattering angle dependence and to retrieve the scattering cross-section at ≈ 90°, at least in the 1 to 0.5 au range.

In the infrared case, the simultaneous determinations of $C_{IR}(R_\odot, \lambda_1)$ and $C_{IR}(R_\odot, \lambda_2)$ at the quasi radial node, together with the values of the thermal cross-section for the same two wavelengths at the martian node, provide (with a grey-body assumption) the radial dependence of the local colour temperature.

Decrease of polarization degree with decreasing heliocentric distance

The nodes of lesser uncertainty method allows to derive local parallel and perpendicular scattering cross-sections from the measured zodiacal light polarized components (parallel and perpendicular to the scattering plane, i.e. to the ecliptic plane). The local polarization degree is then computed from the two local scattering cross-sections.

The inversion at the martian node provides the evolution of the local polarization degree at 1.5 au from the Sun as a function of the scattering (or phase) angle (Dumont and Levasseur-Regourd, 1985b). It may be of interest to mention that the smallest values on the negative branch and the slope at inversion compare quite well with the cometary data, as presented in Dollfus et al. (1988).

The inversion at the quasi-radial node provides the evolution of the local polarization

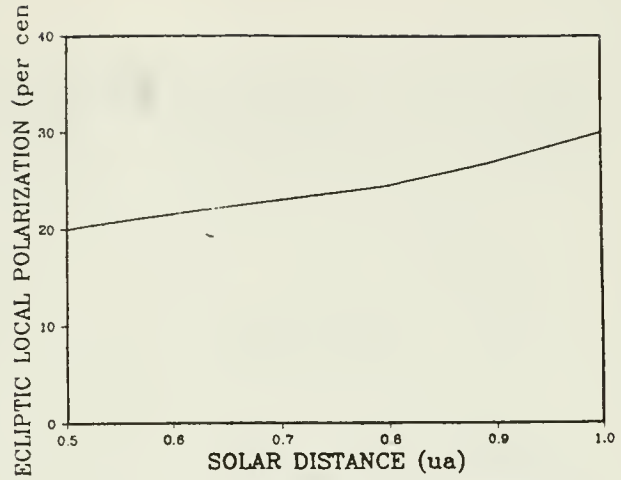


Fig. 3. Solar dependence of local polarization

degree at 90° scattering angle as a function of the heliocentric distance. As can be seen on fig. 3, it drops from ≈ 30% at the Earth's level to ≈ 20% at 0.5 au. Such a decrease is in excellent agreement with Helios 1 and 2 measurements (Leinert, 1975).

This result clearly demonstrates that the interplanetary dust particles properties depend upon their heliocentric distance. It is most likely that their surfaces are quite rough (negative branch in polarization) and that their porosity decreases with decreasing heliocentric distance.

Increase of albedo with decreasing heliocentric distance

As previously mentionned, the inversion method also allows to derive local temperatures from the thermal emissions measured at two wavelengths. There is indeed a discrepancy (even after correction for the effective bandpasses) in local temperatures as deduced from IRAS or rocket observations, which reflects the discrepancy in the raw data. However, the agreement on the gradient of temperature with heliocentric distance (-0.35±0.05) is excellent. It should be noted that the deviation of the gradient from the value that could be expected in a grey-body case (-0.5) is likely to originate in the distinct heliocentric changes of C_{IR} and C_{vis}.

Once both the thermal energy reemitted by unit volume in the infrared and the energy scattered by unit volume in the optical domain are known, the local albedo can be computed. The former is deduced from the local temperature and from a monochromatic thermal cross-section C_{IR}. The latter is precisely the directional scattering cross-section C_{vis} which, from zodiacal light observations, is mostly derived at

90° scattering angle. The albedo at 90°, as defined by Hanner et al. (1981) by analogy with the geometric albedo, is therefore accessible for various heliocentric distances.

The gradient of albedo is negative from all observational data, in agreement with our preliminary analyses (Levasseur-Regourd and Dumont, 1985) and with similar suggestions made, from very different approaches, by Fechtig (1984) or Lumme and Bowell (1985). Fom IRAS survey, the local albedo at 90° scattering angle is found to be of the order of 0.7 $R_\odot^{-0.7}$. This result is in good agreement with the evolution of local polarization previously mentioned, since increases in albedo are usually correlated with decreases in polarization on various planetary surfaces (Dollfus, 1985).

Once both the local temperature and albedo are obtained as a power law function of heliocentric distance, an empirical law of evolution of the bulk albedo A versus the local colour temperature T is derived in the ecliptic plane. IRAS leads to $A \approx 10^{-6} \times T^2$.

These previous results demonstrate that the in-ecliptic dust is most likely to originate in rough, porous and dark grains. When the particles spiral towards the Sun under Poynting-Robertson effect, their roughness, porosity, darkness and size may decrease, possibly because of some breaking off and evaporation due to sublimation and sputtering.

DIFFERENCE IN LOCAL POLARIZATION OR ALBEDO OUT OF THE ECLIPTIC PLANE

Nodes of lesser uncertainty towards the ecliptic poles

As well as the ecliptic case, various constraints are imposed to the polarized components of the local optical brightness and to the monochromatic thermal brightnesses. The integrals towards the ecliptic pole are known, together with the local values at the Earth (found by differenciation of the measurements performed in the ecliptic plane) and the derivatives at the Earth (assumed to be equal to zero for symmetry reasons). Also, the local values and their derivatives at infinity are equal to zero (absence of dust and flattened dust cloud).

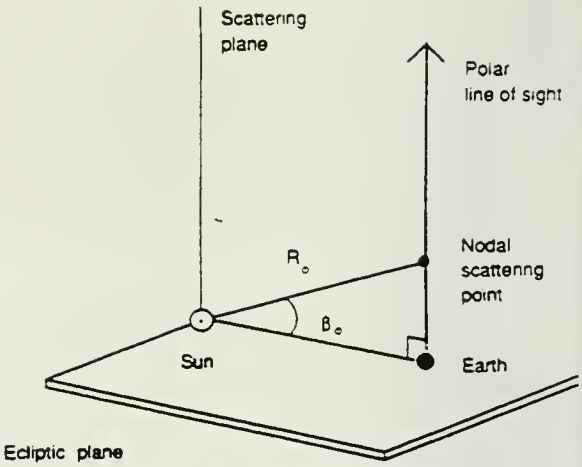


Fig. 4. Observations towards the ecliptic pole

It has been already noticed (Levasseur-Regourd and Dumont, 1988) that all the curves which represent the local functions have to be constricted at a node of lesser uncertainly, the ecliptic latitude of which is of the order of 20° (fig. 4). A partial inversion can therefore be performed at this node for the visual local brigthnesses and polarization, for the thermal local brightnesses and temperature, and ultimately for the local albedo.

Smaller polarization out of the ecliptic plane

From Dumont and Sanchez (1975) optical observations, the smallest uncertainty is obtained for the ecliptic latitude 21°, i.e. for a nodal scattering point at 1.07 au from the Sun and at 0.36 au above the Earth and the ecliptic plane. The corresponding local polarization at 111° scattering angle is found to be of the order of 9%. Comparable results are obtained from Fechtig et al.(1981) compilations, with a local polarization at 110° scattering angle of the order of 11%.

Since the polarization curves (as measured on different interplanetary samples, or deduced from various modellings) are usually flat in the 80° to 110° scattering angles range, these results can be compared to the values obtained in the ecliptic plane at 90° scattering angle. At the same heliocentric distance, the local polarization is equal to 30.5%, much greater than at the nodal point towards the ecliptic pole.

This result demonstrates that the interplanetary dust particles found at 0.35 au towards the pole are different from the grains observed at 1 au in the ecliptic plane. It is likely that their porosity is significantly smaller.

Larger albedo out of the ecliptic

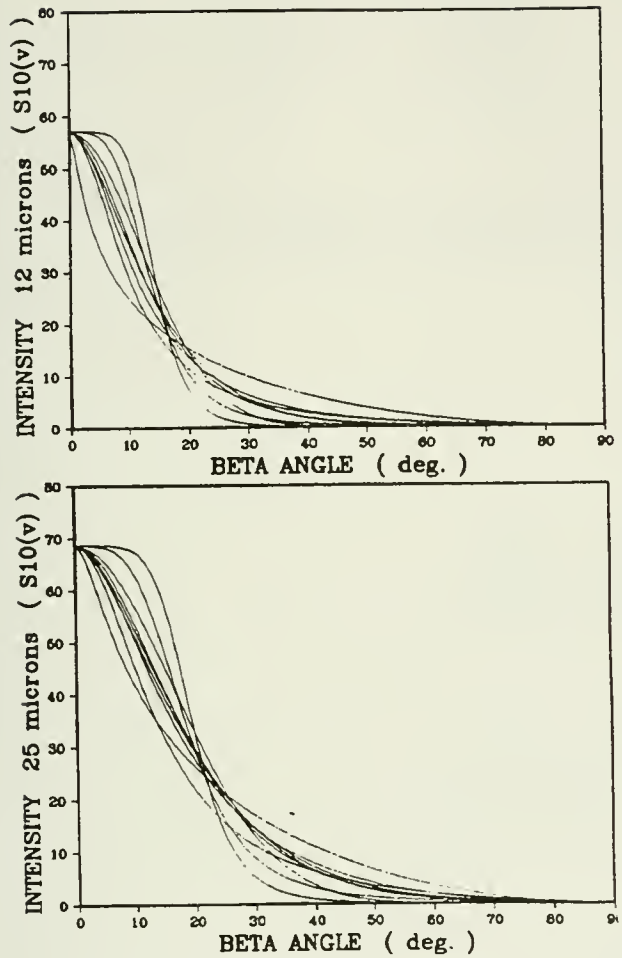


Fig. 5. Nodes for thermal emission towards the pole

As can be seen on fig. 5, the same inversion method is used to derive local thermal brightnesses at various wavelengths, whence a local colour temperature. From IRAS data, the lesser uncertainty on the temperature is obtained for the ecliptic latitude $\beta_\odot$ = 18°, i.e. for a nodal point at 1.05 au from the Sun and at 0.32 au above the Earth's orbit. The temperature has to be in a 195-240 K range, much smaller than it would be in the ecliptic plane at the same heliocentric distance.

From both the visual and thermal brightnesses, a local albedo near $\beta_\odot$ = 20° is derived for 110° scattering angle. As could be suspected from the steep decrease of temperature, this albedo, with a value of the order of 11%, is greater than in the ecliptic plane at the same solar distance.

As noticed previously, the decrease in the local polarization goes together with an increase in bulk albedo. The dust particles found at 0.35 au above the Earth's orbit are less porous or dark and, maybe, smoother and smaller than in the ecliptic at the same heliocentric distance.

CONCLUSION

The optical properties of the interplanetary dust grains are found to strongly depend upon their location in the zodiacal cloud. They are consistent with a scenario of evolution of dark porous cometary grains evaporating as they spiral towards the Sun and, later, being isotropically pushed away as small light β meteoroids under the solar radiation pressure. However, our purpose here is not to propose speculative interpretations of observational results, but rather to present some constraints on polarization and albedo of cometary dust, and to emphasize the evolution of porosity and fluffyness of cometary grains as their age and surface temperature increases.

REFERENCES

DERMOTT, S.F, NICHOLSON, P.D, WOLVEN, B. in : Asteroids, comets, meteors II, ed. C.I. Lagerkvist et al., HSC, Uppsala, 583-594,1986

DOLLFUS, A., Photopolarimetric sensing of planetary surfaces, Adv. Space Res., 5, 8, 47-58 1985

DOLLFUS, A., BASTIEN, P., LE BORGNE, J.F. , LEVASSEUR-REGOURD, A.C., MUKAI, T., Optical polarimetry of P/Halley : synthesis of the measurements in the continuum, Astron. Astrophys., 206, 348-356,1988

DUMONT, R. and LEVASSEUR-REGOURD, A.C., Zodiacal light gathered along the line of sight ; retrieval of the local scattering coefficient from photometric survey of the ecliptic plane, Planet. Space Sci., 33, 1-9, 1985 a

DUMONT, R. and LEVASSEUR-REGOURD, A.C., Remote sensing of the zodiacal cloud along secants to Earth's orbit, in : Properties and interactions of interplanetary dust, ed. R.H. Giese and P. Lamy, D. Reidel, Dordrecht, 207-213 ,1985 b

DUMONT, R. and LEVASSEUR-REGOURD, A.C., Properties of interplanetary dust from infrared and optical observations I, Astron. Astrophys., 191, 154-160, 1988
DUMONT, R. and SANCHEZ-MARTINEZ, F., Zodiacal light photopolarimetry II, Astron. Astrophys., 38,405-412,1975
FECHTIG, H.,The interplanetary dust environment beyond 1 au, and in the vicinity of the ringed planets, Adv. Space Res. 4, 9, 5-11, 1984
FECHTIG, H.,LEINERT, C., GRÜN, E., Interplanetary dust and zodiacal light, in Landolt-Bornstein, Springer, VI, 2a, 228-243, 1981
HANNER, M.S., GIESE, R.H, WEISS,K., ZERULL, R., On the definition of albedo and application to irregular particles, Astron. Astrophys., 104, 42-46,1981
HAUSER, M.G., GILLET,F.C., LOW, F.J., GAUTIER,T.N., BEICHMAN, C.A., NEUGEBAUER, G., AUMANN, H.H., BAUD, B., BOGGESS, N., EMERSON, J.P., HOUCK,J.R., SOIFER, B.T., WALKER, R.G., IRAS observations of the diffuse infrared background, Astrophys. J., 278, L15-L18,1984
HAUSER, M.G., Models for infrared emission from zodiacal dust, in : Comets to cosmology, ed. A. Lawrence, Springer-Verlag, Berlin, 27-39,1988
LEINERT, C., Zodiacal light - a measure of the interplanetary environment, Space Sci. Rev., 18, 281-339,1975
LEVASSEUR-REGOURD, A.C. and BLAMONT, J.E., Evidence for scattering particles in meteor streams, in : Interplanetary, dust and zodiacal light, ed. H. Elsässer and H. Fechtig, Springer-Verlag, Berlin, 58-62,1976
LEVASSEUR-REGOURD, A.C. and DUMONT, R., Absolute photometry of zodiacal light, Astron. Astrophys. 84, 277-279,1980
LEVASSEUR-REGOURD, A.C. and DUMONT,R., Détermination des températures locales et de gradient d'albédo dans le nuage zodiacal à partir des données radiométriques d'IRAS, Compt. Rend. Acad. Sci. Paris, 300, II, 109-112,1985
LEVASSEUR-REGOURD, A.C. and DUMONT, R., IRAS observations and local observations of interplanetary dust, Adv. Space Research, to be published,1988
LUMME K and BOWELL, E., Photometric properties of zodiacal light particles, Icarus, 62, 54-71,1985
MURDOCK, T.L. and PRICE, S.D., Infrared measurements of zodiacal light, Astron. J. 90, 375-386,1985
SALAMA, A., ANDREANI, P., DALL'OGLIO, G., DEBERNARDIS, P., MASI, S., MELCHIORRI, B., MELCHIORRI,F., MORENO, G., NISINI, B., SHIVANANDAN, K., Measurements of near and far infrared zodiacal dust emission, Astron. J. 92, 467-473,1987
SYKES, M.V., LEBOFSKY, L.A., HUNTEN, D.M., LOW, F.J., The discovery of dust trails in comets, Science, 232, 1115-1117,1986

COMETARY EVOLUTION: CLUES ON PHYSICAL PROPERTIES FROM CHONDRITIC INTERPLANETARY DUST PARTICLES

Frans J. M. Rietmeijer
Department of Geology
University of New Mexico
Albuquerque, New Mexico

Ian D. R. Mackinnon
Electron Microscope Centre
University of Queénsland
St. Lucia, QLD 4067, Australia

COMETARY EVOLUTION: CLUES ON PHYSICAL PROPERTIES FROM CHONDRITIC INTERPLANETARY DUST PARTICLES. (*)

Frans J. M. Rietmeijer,

Department of Geology, University of New Mexico, Albuquerque, NM 87131, USA

and

Ian D. R. Mackinnon,

Electron Microscope Centre, University of Queensland, St. Lucia, QLD 4067, Australia.

INTRODUCTION.

The degree of diversity or similarity detected in comets depends primarily on the lifetimes of the individual cometary nuclei at the time of analysis. It is inherent in our understanding of cometary orbital dynamics [Weissman, 1985] and the seminal model of comet origins by Oort [Oort, 1950] that *cometary evolution* is the natural order of events in our Solar System. Thus, predictions of cometary behaviour in terms of bulk physical, mineralogical or chemical parameters should contain an appreciation of temporal variation(s). Previously, Rietmeijer and Mackinnon [1987] developed mineralogical bases for the chemical evolution of cometary nuclei primarily with regard to the predominantly silicate fraction of comet nuclei. We suggested that alteration of solids in cometary nuclei should be expected and that indications of likely reactants and products can be derived from judicious comparison with terrestrial diagenetic environments which include hydrocryogenic and low-temperature aqueous alterations. In a further development of this concept, Rietmeijer [1988] provides indirect evidence for the formation of sulfides and oxides in comet nuclei. Furthermore, Rietmeijer [1988] noted that timescales for hydrocryogenic and low-temperature reactions involving liquid water are probably adequate for relatively mature comets, e.g. P/comet Halley.

In this paper, we will address the evolution of comet nuclei physical parameters such as solid particle grain size, porosity and density. In natural environments, chemical evolution (e.g. mineral reactions) is often accompanied by changes in physical properties. These concurrent changes are well-documented in the terrestrial geological literature, especially in studies of sediment diagenesis [Berner, 1980] and we suggest that similar basic principles apply within the upper few meters of active comet nuclei.

The database for prediction of comet nuclei physical parameters is, in principle, the same as used for the proposition of chemical evolution [Rietmeijer and Mackinnon, 1987]. We use detailed mineralogical studies of chondritic interplanetary dust particles (IDPs) as a guide to the likely constitution of mature comets traversing the inner Solar System. While there is, as yet, no direct proof that a specific sub-group or type of chondritic IDP is derived from a specific comet [Mackinnon and Rietmeijer, 1987], it is clear that these particles are extraterrestrial in origin [Bradley *et al.*, 1988] and that a certain portion of the interplanetary flux received by the Earth is cometary in origin [Brownlee, 1985]. Two chondritic porous (CP) IDPs, sample numbers W7010A2 and W7029C1, from the Johnson Space Center Cosmic Dust Collection have been selected for this study of putative cometary physical parameters. This particular type of particle is considered a likely candidate for a cometary origin [Bradley *et al.*, 1988] on the basis of mineralogy, bulk composition and morphology. While many IDPs have been subjected to intensive study over the past decade, we can develop a physical parameter model on only these two CP IDPs because few others have been studied in sufficient detail [Mackinnon and Rietmeijer, 1987].

OBSERVATIONS.

The data used in this analysis have been obtained solely from Analytical Electron Microscope studies of individual CP IDPs W7010A2 and W7029C1. The latter IDP was provided in two separate allocations W7029A23 and W7029A24 by the JSC Curatorial Facility. In each case the majority of grains within each allocation has been examined for mineral identity (i.e. structure and composition determinations) and grain size and shape. The dimensions of typically platey grains in both IDPs have been measured from transmission electron micrographs (with a precision of ~1%) and calculated as the root-mean-square (rms) grain size. This size is calculated by the relation $(a^2+b^2)^{1/2}$ where a and b are two orthogonal dimensions across a grain.

Further details on individual mineral analyses and abundances, as well as their interpretations, are given in Mackinnon and Rietmeijer [1984, 1987], Rietmeijer and Mackinnon [1985a] and Rietmeijer [1989]. For simplicity, not all grains within each IDP are utilised in this study. Only non-carbonaceous grains and grains which are part of the IDP matrix are included in the grain size histograms shown in Figures 1 and 2. Thus, the data for IDP W7010A2 excludes measurements of large (> 1.0 μm) euhedral and rod-shaped silicate crystals [Rietmeijer, 1989] while the data for IDP W7029C1 exclude poorly graphitised carbon [PGC] grains which constitute ~45% of all grains in this IDP [Rietmeijer and Mackinnon, 1985a].

The ultrafine platey grains in IDP W7010A2 are embedded in amorphous carbon and, as yet, unidentified hydrocarbons [Bradley, 1988; Rietmeijer, 1989]. The presence of these carbonaceous species suggests a low thermal regime (< ~250°C) in the anhydrous IDP parent body(ies) [Rietmeijer, 1986; Rietmeijer and Mackinnon, 1985b]. In the case of IDP W7029C1, the degree of ordering inferred from the PGC basal spacing is consistent with a thermal regime of ~300°C in this IDP [Rietmeijer and Mackinnon, 1985b]. While this IDP is nominally an anhydrous variety, ~11% of all grains are layer silicates and qualitatively, the mineralogy of IDP W7029C1 is similar to that interpreted from the chemical signature of ultrafine-size silicate dust in P/comet Halley [Rietmeijer *et al.*, 1989].

The omission of grain size data for carbonaceous phases, as well as data related to the presence of Ti-rich minerals which have pseudomorphic textures due to a temperature dependant transformation, limits a thorough interpretation of grain size distributions for these two CP IDPs. Nevertheless, the choice of grains for this size distribution comparison implies an analysis of processes which have affected the bulk of the IDP (and, by implication, the IDP parent body(ies)). The size distribution for 254 grains in IDP W7010A2 and for 157 grains in IDP W7029C1 are shown in Figures 1 and 2, respectively.

DISCUSSION.

Interpretations of grain size distributions are, to a first approximation, model dependant and for the sake of discussion, we list below important assumptions for these interpretations:
(1) chondritic porous IDPs are samples of cometary dust,
(2) hydrocryogenic and low-temperature aqueous alterations of anhydrous IDPs occurs on comet nuclei,
(3) the chemical and mineralogical diversity of chondritic IDPs is a good argument for similar diversity in comet nuclei.

While we have argued for mineralogical diversity, and thus evolution, in cometary nuclei [Rietmeijer and Mackinnon, 1987], there is as yet little understanding of the spatial variations of comet mineralogy with time. Nevertheless, if we compare the behaviour of terrestrial sediments during diagenesis, it is apparent that grain size distributions follow well-defined and predictable trends [Berner, 1980]. For example, grain sizes during terrestrial diagenesis generally show initially a strongly peaked size

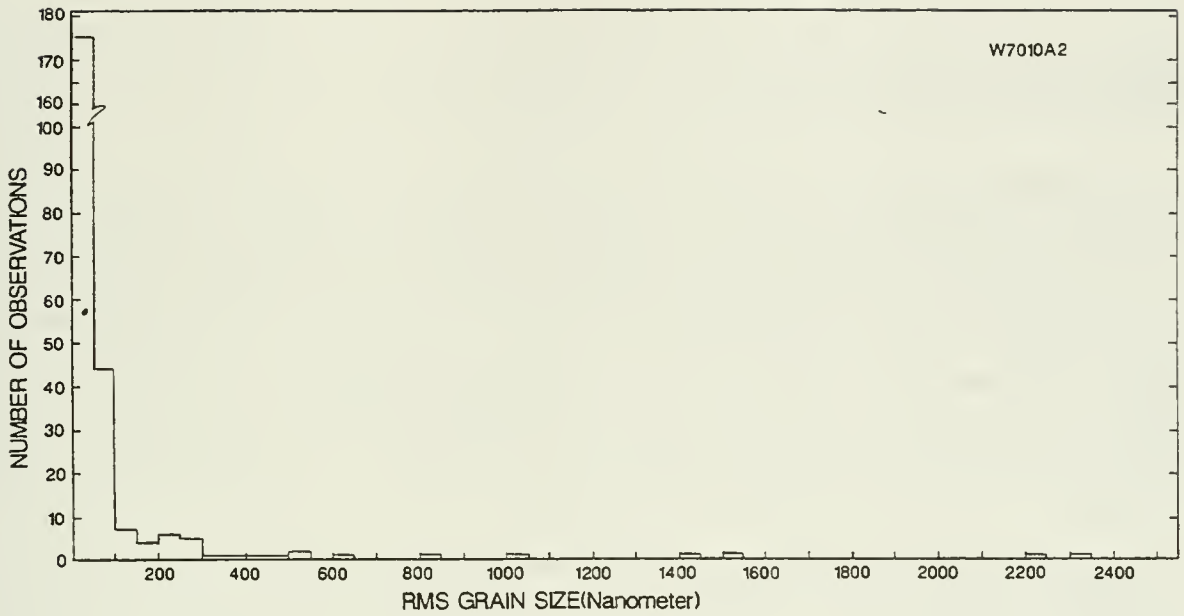


FIGURE 1: Root-mean-square grain size distribution for 254 mineral grains in chondritic porous interplanetary dust particle W7010A2.

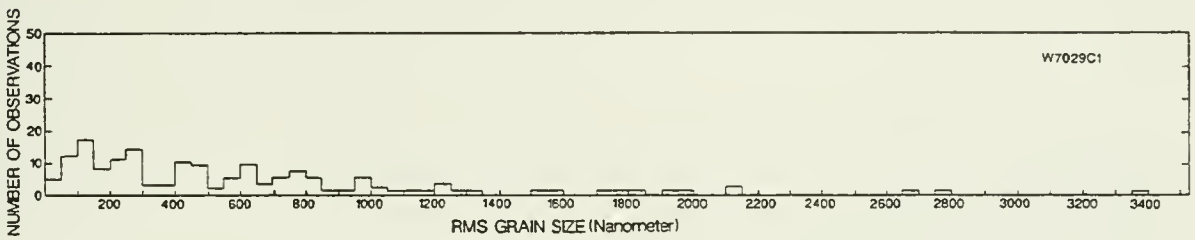


FIGURE 2: Root-mean-square grain size distribution for 157 mineral grains in chondritic porous interplanetary dust particle W7029C1.

distribution in the original sediment which flattens and shifts to a higher mean grain size with further diagenesis. Also a concomittant decrease in porosity accompanies an increase in the median grain size in terrestrial sediments [Berner, 1980].

The rms grain size distribution for IDP W7010A2 [Figure 1] shows a distinct positive skewness which is markedly different from the much flatter distribution for IDP W7029C1 [Figure 2]. Also, the mean rms grain size for each distribution differs, viz. 96.85 nm (W7010A2) and 562.1 nm (W7029C1). These data suggest comparatively advanced diagenesis for IDP W7029C1 relative to IDP W7010A2 and is consistent with the higher thermal regime indicated for the former. Both IDPs are of the chondritic porous subtype. Yet, the moderately higher median grain size for IDP W7029C1 (1325 nm) compared to 1125 nm for IDP W7010A2 indicates a slightly lower porosity for the former and suggests that mineralogical evolution of cometary nuclei will be accompanied by subtle changes in grain size, and consequently also in nucleus porosity and density. Measured densities for chondritic IDPs are between 0.7 and 2.2 $g.cm^{-3}$ [Flynn and Sutton, 1988; van der Stap, 1986]. Unfortunately, the porosity of chondritic IDPs is poorly known but it may be as high as 90% for anhydrous chondritic IDPs and ~70% for a layer silicate-rich IDP [Mackinnon *et al.*, 1987].

Assuming that (1) terrestrial diagenesis can be used to model the chemical, mineralogical and physical evolution of chondritic IDPs and (2) chondritic IDPs are samples of cometary dust, it will be a prerequisite to assess grain size distributions of chondritic IDPs. Comet nucleus models should consider differences in physical properties (grain size, porosity and density) on length-scales of at least ~60 μm which is the size of the largest chondritic IDP presently collected from the Earth's stratosphere. The extent and spatial variations with time of these differences within cometary nuclei will be different for individual comets and will depend on inherent comet nucleus properties such as ice-dust ratios, the structural state of dust, the evolution of comet orbits and comet lifetime.

CONCLUSIONS.

Petrological analyses of chondritic porous IDPs suggest that grain size, density and porosity of comet nuclei may evolve during their lifetime in the Solar System. Effects of physical evolution, as well as chemical and mineralogical evolutions, in cometary nuclei may be subtle. The extent and spatial variations with time are presently unknown but it seems imperative for models of active short-period comets to consider the possibility of dust evolution.

We believe that Analytical Electron Microscope analyses of chondritic IDPs, in conjunction with astronomical observations and theoretical modelling, will yield the data to model comet nucleus evolution. It seems obvious that putative evolutions of comet nucleus physical properties can place engineering constraints on a Comet Nucleus Sample Return Mission. For example, the mode of penetration (rotation or percussion) selected for a "smart nucleus penetrator" as a function of resistance encountered during descent into the nucleus may critically depend on pre-programmed density differences. Modelling the physical, chemical and mineralogical evolution of cometary dust properties will have a qualitative character until a successful Comet Nucleus Sample Return Mission. However, the possibility of comet nucleus evolution may have important implications for mission planning and the type of sample that will be returned.

REFERENCES.

Berner, R. A.: Early Diagenesis. A theoretical Approach. Princeton University Press, 1980.
Bradley, J. P.: Analysis of chondritic interplanetary dust thin-sections. Geochim. Cosmochim. Acta, vol.

52, 1988, pp. 889-900.
Bradley, J. P.; Sandford, S. A.; and Walker, R. M.: Interplanetary Dust Particles. In: Meteorites and the Early Solar System (Kerridge, J. F. and Matthews, M. S., Eds.), University Arizona Press, 1988, pp. 861-898.
Brownlee, D. E.: Collection of cosmic dust: Past and future. In: Properties and Interactions of Interplanetary Dust (Giese, R. H. and Lamy, P., Eds), D. Reidel Publ. Co, Dordrecht, Holland, 1985, pp. 143-147.
Flynn, G. J.; and Sutton, S. R.: Cosmic dust particle densities inferred from SXRF elemental measurements. Meteoritics, vol. 23, 1987, pp. 268-269.
Mackinnon. I. D. R.; and Rietmeijer, F. J. M.: Bismuth in interplanetary dust. Nature, vol. 311, 1984, pp. 135-138.
Mackinnon. I. D. R.; and Rietmeijer, F. J. M.: Mineralogy of chondritic interplanetary dust particles. Reviews Geophys., vol. 25, 1987, pp. 1527-1553.
Mackinnon. I. D. R.; Lindsay, C.; Bradley, J. P.; and Yatchmenoff, B.: Porosity of serially sectioned interplanetary dust particles. Meteoritics, vol. 22, 1987, pp.450-451.
Oort, J. H.: The structure of the cometery cloud surrounding the solar system and a hypothesis concerning its origin. Bull. Astron. Inst. Netherlands, vol. 11, 1950, pp. 91-110.
Rietmeijer, F. J. M.: Olivines and iron-sulfides in chondritic porous aggregate U2015*B formed at low-temperature during annealing of amorphous precursor materials. Meteoritics, vol. 21, 1986, pp. 492-493.
Rietmeijer, F. J. M.: Sulfides and oxides in comets. Astrophys. J., vol. 331, 1988, pp. L137-L138.
Rietmeijer, F. J. M.: Ultrafine-grained mineralogy and matrix chemistry of olivine-rich chondritic interplanetary dust particles. Proc. 19th Lunar Planet. Sci. Conf., 1989, pp. 513-521.
Rietmeijer, F. J. M.; and Mackinnon. I. D. R.: Layer silicates in a chondritic porous interplanetary dust particle. Proc. 16th Lunar Planet. Sci. Conf., part 1, J. Geophys. Res., vol. 90, Suppl., 1985a, pp. D149-D155.
Rietmeijer, F. J. M.; and Mackinnon. I. D. R.: Poorly graphitized carbon as a new cosmothermometer for primitive extraterrestrial materials. Nature, vol. 316, 1985b, pp. 733-736.
Rietmeijer, F. J. M.; and Mackinnon. I. D. R.: Cometary evolution: Clues from chondritic interplanetary dust particles. European Space Agency, SP-278 (September 1987), 1987, pp. 363-367.
Rietmeijer, F. J. M.; Mukhin, L. M.; Fomenkova, M. N.; and Evlanov, E. N.: Layer silicate chemistry in P/Comet Halley from PUMA-2 data. Lunar Planet. Sci., vol. 20, 1989, pp. 904-905.
van der Stap, C. C. A. H.: Experimental studies of meteorites and cosmic dust, Ph.D. thesis Free University, Amsterdam, the Netherlands, 1986.
Weissman, P. R.: The origin of comets: Implications for planetary formation. Protostars & Planets II (Black, D. C. and Matthews, M. S., Eds.) University of Arizona Press, Tucson, 1985, pp. 895-919.

(*) This work was supported by NASA Grant NAG 9-160.

LABORATORY SIMULATIONS: THE PRIMORDIAL COMET MANTLE

R. E. Johnson
Department of Nuclear Engineering and Engineering Physics
University of Virginia
Charlottesville, Virginia

Laboratory Simulations: The Primordial Comet Mantle

R.E. Johnson
Dept. of Nuclear Engineering and
Engineering Physics
University of Virginia
Charlottesville, VA 22901

Abstract

Laboratory data are needed to understand the formation of organics in cometary and precometary materials and for deciding on the fate of the volatiles. Appropriate experiments were described in the talk at Milipitas. Because of its importance for the comet sample return mission, I discuss here the relevance of this data for predicting the thickness, nature, and ability to survive of the cosmic-ray produced primordial comet mantle ('crust') . That part of the mantle which becomes predominantly refractory is ~ 30 gm/cm^2 thick. The tensil strength of this outer mantle is such that it might survive the comet's entrance into the inner solar system. In addition, important modifications to the ices occur to depths ~ 300 gm/cm^2. Based on this it is expected that a deep probe is needed to obtain minimally altered material.

Introduction

The outer layers of a comet, the comet's mantle, will be sampled during the proposed Rossetta comet-sample-return mission. It has been pointed out by a number of authors that this region of the comet is significantly altered by cosmic-ray particle processing of the ices and organics during the comet's 4.5×10^9 years residence time in the Oort cloud[1-4]. That such an alteration occurs would appear to be reenforced by the recent measurements of the ortho-para ratio of water molecules effusing from a new comet[5]. Since a prime goal of the proposed mission is, as indicated by its name, to establish the connections between the comet constituent materials and the precursor materials, any post-formation alterations to the region from which the sample is taken is of great importance. There are, of course, other processes, some of which were recently described by Stern[6,7], that can also affect the structure and state of the comet mantle before the comet is ejected from the Oort cloud into the inner solar system. These will not be dealt with here: see paper by Weissman in this volume. Whereas estimates of the effect of the Stern processes are based on statistical considerations involving a number of likely interactions but involving uncertain physical quantities (e.g. Oort cloud comet densities, supernova events near our solar system, etc.), determination of the cosmic-ray particle processing of the mantle is based on spacecraft measurements of cosmic-ray particle fluxes and on laboratory measurements of energetic particle alterations of materials. Therefore, the effect of cosmic-ray particles on the comet mantle can, in principle, be described with some certainty, especially if this mantle is static during the comet's life in the Oort. If other mantle altering processes are also important then the effects described here are superimposed on them.

In my talk in Milipitas I described the general nature of the laboratory simulations of interest to comet science, I attempted to outline the various stages in the 'history' of comet materials during which charged-particle alterations occurred, and I discussed the differences between UV and charged-particle irradiations. In this paper I will not discuss those topics in any depth as that material has been recently incorporated into a chapter on particle irradiation effects for the volume to be published following the Bamberg meeting this year[8] and some of that material also occurs in a recently completed text on charged particle irradiation effects to appear shortly[9]. One of the most important topics from my talk for the proposed Rossetta sample-return mission is the nature of the primordial comet mantle, and the survivability and evolution of this mantle when the comet is ejected into the inner solar system. Therefore, this paper will be devoted primarily to this topic. In the next section I will review the laboratory data relevant to mantle formation and mantle stability. I will then combine this with the cosmic-ray particle energy deposition profile in order to expand on the picture of the mantle described in an earlier paper[1]. Finally I will consider the fate of this mantle and its relevance for the Rossetta mission.

Laboratory Results

There has been a considerable body of literature devoted to the study of energetic particle alterations of materials. Whereas the GeV energies of interest for the primordial mantle formation are not easily obtainable in the laboratory it has been shown that the effects of interest generally scale with the electronic energy deposition per unit path length in the material, $(dE/dx)_e$[10]. This energy produces, primarily, ionizations and excitations of the electrons on the molecules in the sample. The decay of these excitations

leads, with high frequency, to bond breaking and atomic displacements. In ices or organics this can initiate chemical activity, whereas in more refractory materials structural alterations and defects may occur. Because the nature of the primary excitation processes produced in the laboratory by keV electrons and MeV ions are the same as the dominant processes for GeV particles, laboratory data can be applied to describe the comet mantle formation knowing only the total dose of electronic energy deposited. The GeV cosmic-ray particles produce nuclear reactions more efficiently than the MeV ions, but much of the energy lost in such processes is eventually also transferred to the electrons by the stopping of the energetic products and it has been shown the net effect of the nuclear alteration is small[11].

Alterations produced in molecular ices, organic solids and liquids, and molecular gases are often characterized by G values[10]. G is the average number of a particular type of alteration (e.g., 2 $CH_4 \rightarrow C_2H_6 + H_2$) per 100eV of electronic energy deposited in the material. Such results have been published for those gas and liquids relevant to biological processes[12]. Typical G-values are in the range 0.1 - 2 depending on the process. However, in most cases studied diffusion of some species (i.e. temperature) plays a role. The low temperatures in the Oort cloud inhibit such effects, therefore, only studies on ices and organics at low temperature (<30K) are relevant. In this region thermal diffusion of any species except H_2 and He is highly inhibited. Irradiation induced 'diffusion', due to jostling of the atoms following displacement events, does occur, however. Further, only experiments involving low fluxes in which events happen on a particle-by-particle basis are relevant. In such an environment unrecombined radicals can be relatively stable in the solid matrix, as has been shown experimentally[13]. Of course, even though the mobilities are small, extrapolating them to 4.5×10^9 years is

risky. In this regards, one of the major effects of the Stern-processes mentioned earlier is a temporary elevation of temperatures in the mantle region which may allow radical recombination. Such chemical activity also adds heat and, therefore, a super nova shock or a comet-comet collision might enhance the alteration of the comet mantle.

In a closed system long-term irradiation will lead to a material which is a stable mixture of species, as bonds are broken and reform. However, the presence of a vacuum interface allows the continuous ejection of volatile species from the surface. Therefore, the material is driven to an end point, a highly refractory material resistant to alteration by subsequent irradiation. The most volatile species formed, H_2, is lost 'immediately' by diffusion through the damaged solid to the vacuum. Other volatile species formed in an ice mixture or from organics (e.g. CO, O_2, N_2, etc.) are 'lost' more slowly at these low temperatures by incident particle assisted diffusion and ejection from the surface[9]. However, the loss of H is the controlling effect. In a mixture with atomic composition of C, H,O,N,S, the removal of H permits the enhanced formation of for example C-C, C-N, C-O, C-S and S-S bonds. This converts ice mixtures (e.g. H_2O, NH_3, CO, CH_4, H_2S, etc.) to 'organics' with residual volatiles (e.g. O_2, CO) and some unrecombined radicals.

In this irradiation process the solid also becomes inhomogeneous so that the material partially segregates due to preferential bonding. Therefore, local carbonized regions form and, possibly, regions with enhanced S content. As the material becomes altered the efficiency of the radiation eventually decreases[14], and in almost all mixtures studied, containing either C or S atoms, refractory solids, referred to as residues, result after long-term irradiation[15,16]. Further, the refractory materials themselves experience enhanced adhesion due to the irradiation[17]. In an organic solid such

processes happen more efficiently (i.e. at lower doses). This residue material, superimposed on damaged refractory grains (e.g. silicates), is the material that forms the outer part of the mantle.

In order to quantify the above it is sufficient to note that in gases of small molecules an ionization event is produced, on the average, for every 30 eV of energy deposited ($G \tilde{} 3$). One such event generally leads to breaking of a typical covalent bond and the formation of a radical. In solids and liquids ionizations (electron-hole pairs) are produced more efficiently. In charged particle irradiation the average primary excitation energies are of the order of 60 eV/molecule resulting in pairs of ionization events occurring in close proximity due to the secondary electrons produced. Therefore, in addition to radical formation and hot-atom chemistry, prompt reactions can occur between the affected neighbors. Based on the results of Foti et al.[16] the polymerized fraction of an organic component at low doses varies, roughly, as

$$f \approx (1 - \exp(-\sigma\phi)) \qquad (1)$$

where ϕ is the fluence of MeV ions (ions/cm^2; a dose). They find $\sigma \propto (dE/dx)_e$. Writing $\sigma \approx (dE/dx)_e/n_M W_c$, where n_M is the molecular number density and W_c is the energy deposited per molecule for loss of H, formation of new C-C bonds, or cross-linking[18]. In this form

$$\sigma\phi \approx D_M/W_c \qquad (2)$$

where D_M is the dose in eV/molecule and $W_c \approx 140$ eV based on their data for MeV ions, or $G \approx 0.7$. This energy is about twice the average energy deposited per

methane molecule found by Lanzerotti et al.[19] for initiating the loss by diffusion of newly formed H_2 from the complete depth of penetration of the ion in solid methane. The G-value above energy corresponds to about two primary ionization events per initial small molecule. In an ice mixture, the average energy deposition for forming C-C bonds will increase somewhat due to reduced concentration.

Water is lost from a low temperature solid both by sputtering and conversion, $H_2O \rightarrow H_2 + (1/2)\ O_2$. The G for the latter process is ~ 0.7 for α-particles and 0.3 for β-particles. These are comparable to the values for organic alteration above. As GeV ions have very low $(dE/dx)_e$, more comparable to the β's, the smaller values may be more relevant at large depths into the mantle. The H_2 is lost by diffusion through the lattice 'immediately' after a dose ~ 60 eV/molecule is received (G ~ 1.5) and then the accumulated O_2 is driven off.

Cosmic-Ray Doses

The energy deposited by cosmic rays in the comet mantle has been estimated by a number of authors[2,11,20]. As cosmic ray fluxes have been measured in the earth's atmosphere for years the measured energy deposition vs thickness, given in grams/cm^2, can be used as a lower limit and applied to the comet, as was done initially by Whipple[2].

Since the primary energy loss mode for fast ions is to the electrons, the standard Bethe-Born expression for energy deposition, with relativistic corrections at high speeds,can be used to calculate the energy loss. A recommended expression for protons for energies of the order of or greater than 1 MeV[21] is

$$\left(\frac{dE}{dx}\right)_e = (5.1\times10^{-19})\ (\text{eV cm}^2)\ (Z_B n_B) \times \left[\ln\left(\frac{7.52\times10^4\beta^2}{I'(1-\beta^2)}\right)-\beta^2\right]/\beta^2 \qquad (3)$$

which is shown for water in Fig (1). Here $\beta=(v/c)$, c is the speed of light, $Z_B n_B$ is the number of electrons on the typical target atom or molecule having number density n_B, and I′ is called the mean ionization energy, here given relative to the hydrogen atom. Since $(dE/dx)_e$ is only weakly dependent on I′, approximate expressions are useful ($I'\approx 5.5$ for water, $I' \approx 1.2\ Z_B^{0.9}$ for refractory components). In addition there is a small component of stopping due to nuclear elastic collisions and a large component due to <u>inelastic</u> nuclear interactions, since the inelastic nuclear interaction length is ~ 100 g/cm^2 for 1 GeV protons in most materials[22]. For an average energy loss in such processes of ~ 100 MeV the mass stopping would be ~ 1 MeV cm^2/gm in water or about half the minimum in the ionization effect in Fig(1).

The dose of electronic energy deposited vs. depth is calculated from the particle flux spectrum, $\phi(E)$, and the total stopping power, $(dE/dx)_T$, and the energy loss by the primary and all subsequent particles. If the $(dE/dx)_T$ mostly relaxes to electronic loss then it can be used alone. Giving the dose in energy deposited per initial molecule, D_M, for a depth z into the comet

$$D_M(z) \approx \frac{1}{n_M}\int_{E_m(z)}^{\infty} \phi(E')\left[\left(\frac{dE}{dx}\right)_T\right]_z dE' \qquad (4a)$$

Ignoring deflections, the energy of a ion of initial energy E at depth z is E(z), so that

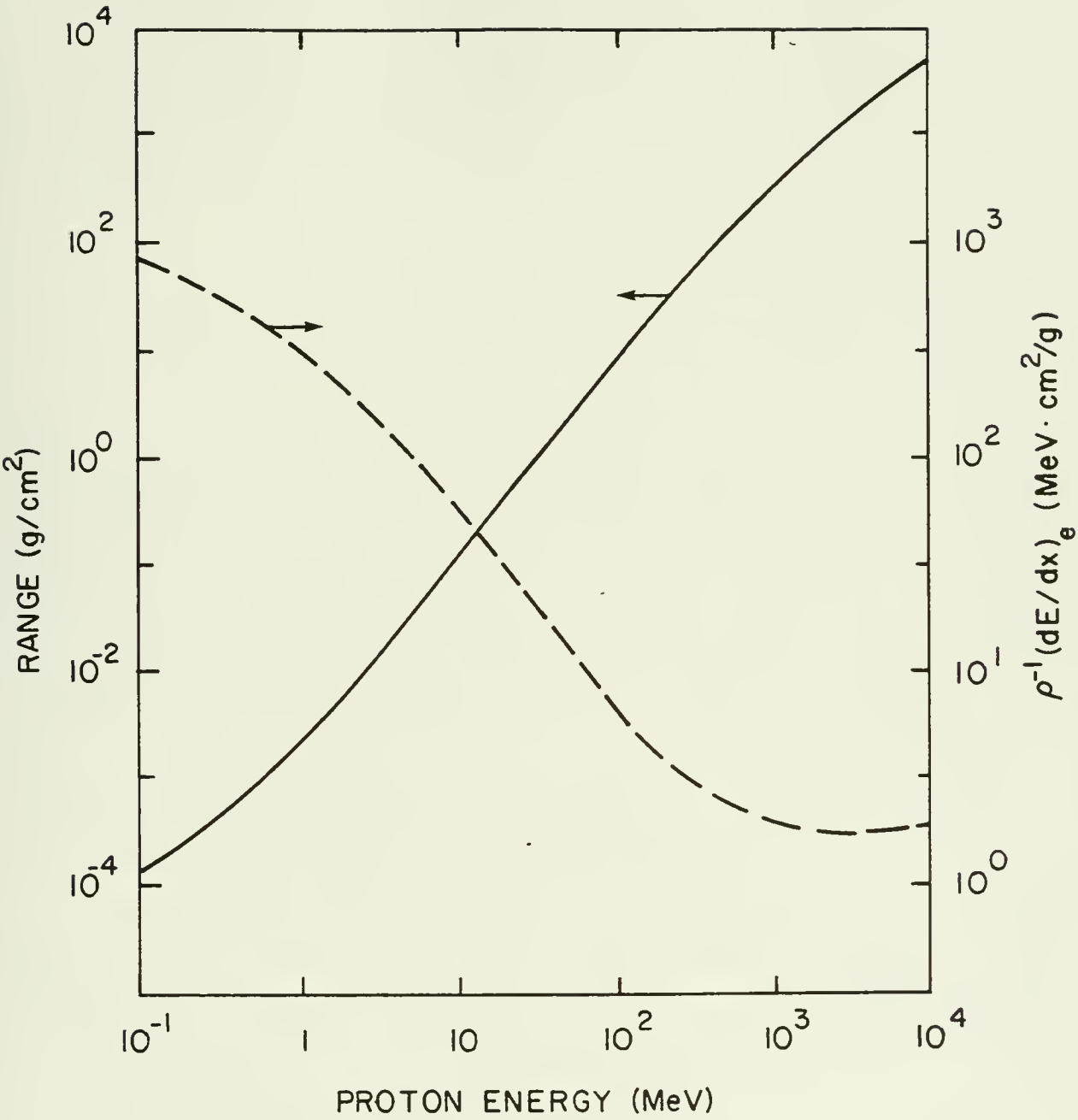


Fig.1 The electronic stopping power from Eq.(3) and the penetration depth using this. Axes as indicated.

$$z \approx \int_{E(z)}^{E} dE'/(dE/dx)_T \qquad (4b)$$

In Eq (4a) E_m is the minimum ion energy, an ion which reaches depth z with E(z)=o. Using Eq (4a) and (4b) with $(dE/dx)_T$ equal to $(dE/dx)_e$ an approximate D_M at large penetration depths was obtained by Moore[23] for an incident flux

$$\phi(E)=k\ e^{-a}\ (\text{ions}/(m_2\ \text{sec ster MeV/nucleon})) \qquad (5)$$

where a=2.5, k=2.5x10^8, and e=E+m_0c^2. At z ≈ 10 cm , D_M ≈ 100 eV/mol, for E < 1GeV. Ryan and Draganic[11] approximated the nuclear aspect of the stopping for E > 1GeV. The results given in ref (1) based on ref (11) were too large as the data in ref (11) were plotted incorrectly. Strazzulla[4] obtained alteration depths which were too large due to neglect of the high velocity energy loss effects.

The actual atmospheric measurements can be used as lower bounds to D_M in Eq (4a) at large z. Since ionization, due to the incident particles or the secondaries, is the dominate energy loss mode and is directly connected to material alteration, the measurements of ion pairs (ion plus electron) produced per cm^3 per sec in air[2] can be used. Assuming the atmospheric molecules (O_2, N_2, CO_2, H_2O, etc.) exhibit energy loss curves similar to that of an average comet material (H_2O, CO, C_2O, SiO_2, etc.), the number of times an 'original' molecule would be ionized in 1.4 x 10^{17} sec (4.5 x 10^9 years) can be calculated. Accounting for the differences in stopping between water and air and for the differences in W values results about (1.5) times Whipple's estimates are obtained and are given in Fig (2) for energy deposition in water. Assuming ~ 30 eV deposited per ionization, the right hand axis gives the number

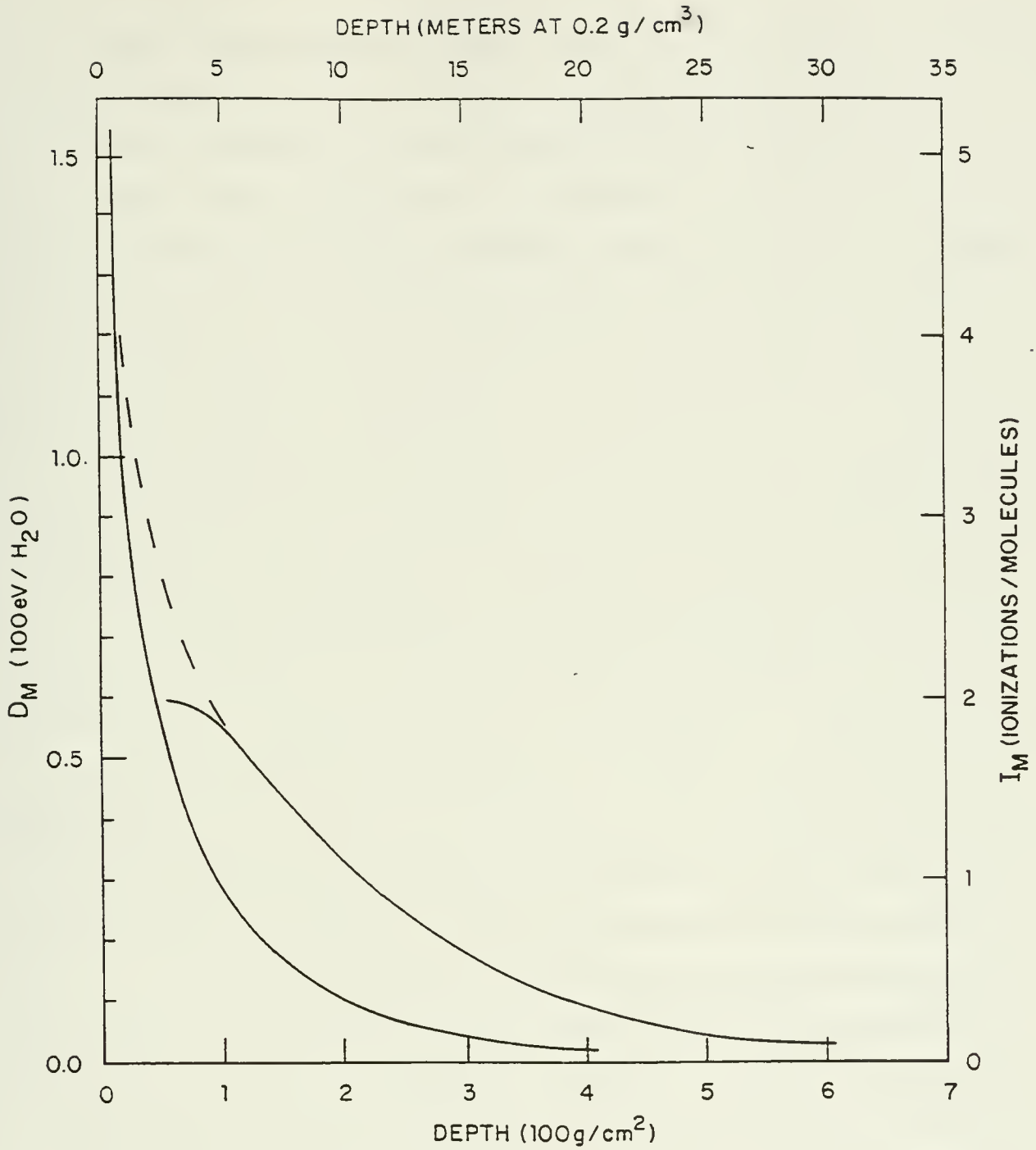


Fig.2 Cosmic-ray dose. Solid curves:W Whipple's estimate from the atmospheric measurements multiplied by 1.5 due to accounting for differences of ionization and stopping in air and water. MDRD sum of the Moore and Donn results and the Ryan and Draganic' results as discussed. Dashed curve an interpolation.

of times, on the average, an original water molecule has been ionized. (In the solid electron/hole pair formation requires, on the average, less energy.)

The Ryan and Draganic[11] results for E > 1GeV are combined with the Moore[23] results, E < 1 GeV, in Fig (2). The depth is given in g/cm^2 since stopping is roughly proportional to the mass density in any solid (i.e. the number of electrons is roughly proportional to the mass). Therefore, for water ice $100g/m^2$ implies 1m depth; for a comet mantle or 'dust' density ($\tilde{}0.2g/cm^3$), $100g/cm^2$ is $\tilde{}$5m. The choice of this density accounts for some of the confusion in stating mantle 'thickness'. The latter results provide lower limits to the dose at small depths and the results obtained from air provide lower limits at large depths. The dashed line interpolates between these (note that these doses are lower than those in ref.(1) for the reasons discussed).

The Comet Mantle

It is seen that at a depth of 100 g/cm^2 into the comet any original water, methane, ammonia, etc. molecule will have been 'ionized' at least once in its life in the Oort cloud. Using Eqs. (1) and (2) with the net dose in Fig (2), the fraction of the initial organic material in the mantle which is polymerized is shown vs. depth into the mantle in Fig (3) based on G $\tilde{}$ 0.7.

Water molecules are depleted from the mantle due to ion bombardment. This depletion is due to sputtering and chemical conversion $H_2O \rightarrow H_2 + (1/2)\ O_2$ with the latter process dominating. The loss of H_2O is likely to be given by something in between the solid ($G\tilde{}0.7$) and dashed curves ($G\tilde{}0.3$). As the damage to water occurs in a mileau containing other species the back reactions are less likely so that the larger G value may be more relevant. Conversion of CO_2 to $CO + (1/2)O_2$ is even more efficient[9,10], affecting greater depths.

Regions containing sulfur molecules such as CS_2, H_2S and SO_2 in a water or

carbon mix will be converted to sulfur suboxide, S_2, or chain-sulfur with G-values comparable to those used for obtaining Fig (3). Therefore, the observation of S_2 near the nucleus of a new comet may be understandable.

The recent observations of the altered ortho-para ratio[5] can be understood by noting that at low temperatures H transfer occurs efficiently on ionization ($\tilde{}$ 30 eV/mol., G $\tilde{}$ 3). If this is the case then the alteration depth ($f \tilde{} e^{-1}$) is $\tilde{}$ 200-300 gm/cm^2. This is a region of little water loss. Writing the fraction of the original water which remains and has its ortho-para ratio changed ($\exp(-D_M/W_c) - \exp(-D_M/W)$) with $W_c \approx 140$eV and $W \approx 30$eV, that fraction of the initial water which has an altered ortho-para ratio is given in Fig (4). At small depths the water is lost, at large depths the ortho-para ratio is altered. Therefore, it is seen that a considerable volume of ice is so altered. This region is also a region in which stored radicals are produced which may result in additional activity on first pass[2,3].

Conclusions

Because the proposed comet-sample return penetration does not go very deep into the mantle, it is not clear from the above results that the Rossetta mission can obtain a record of early solar system or pre-solar system (ISM) material with a shallow probe. A number of observations on new comets are indicative of outer mantle alterations. However, a key issue is the tensil strength of the refractory material in the altered layers which would indicate whether the primordial mantle would survive. The region of depth < 30 gm/cm^2 has received a total dose of radiation comparable to that experienced by an IPDP (interplanetary dust particle) prior to collection at earth[25]. These particles are structurally sound, due in part to the irradiation produced adhesion[17]. Therefore, a tensil strength in the outer layer equivalent to

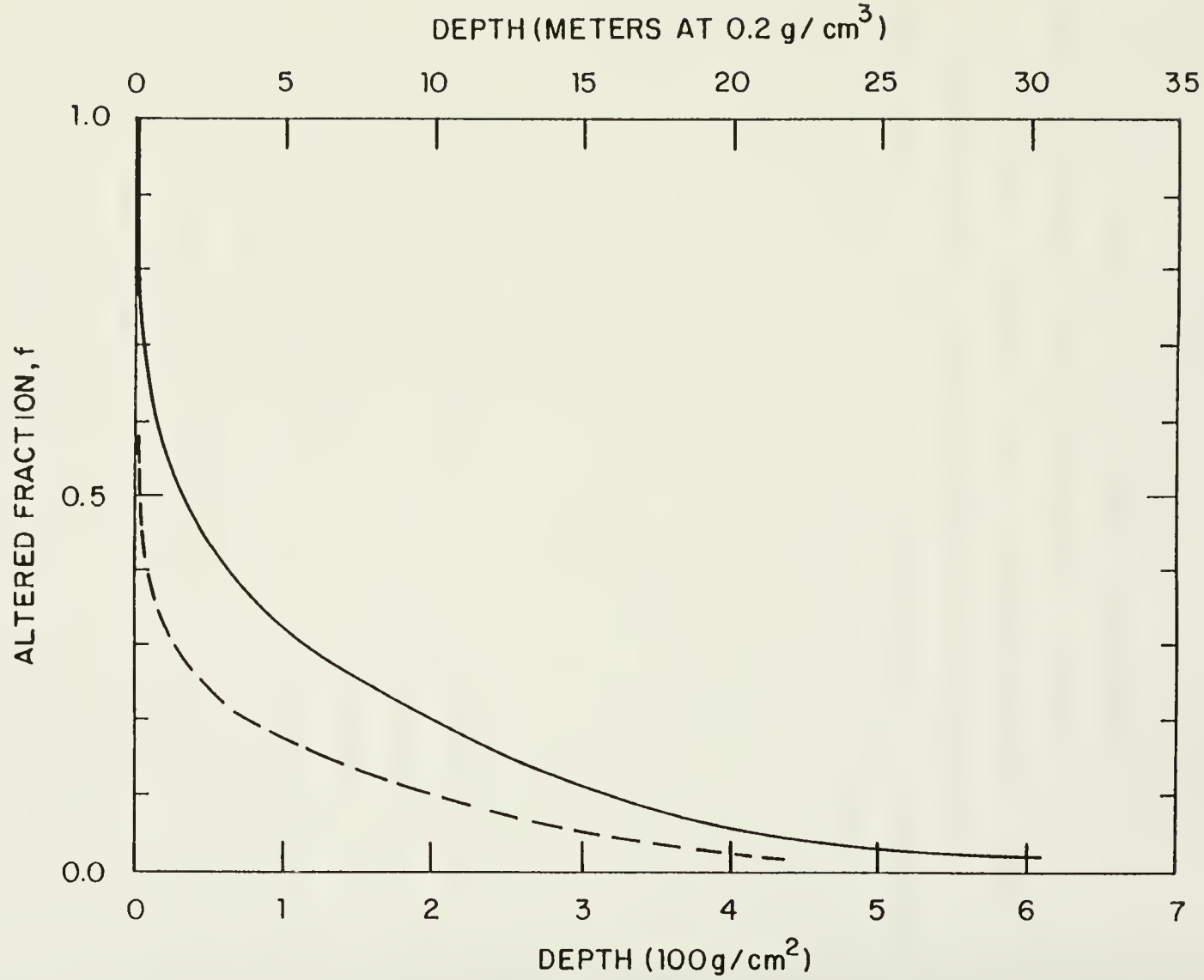


Fig.3 Altered fraction: solid curve G~0.7 ; dashed curve G~0.3.

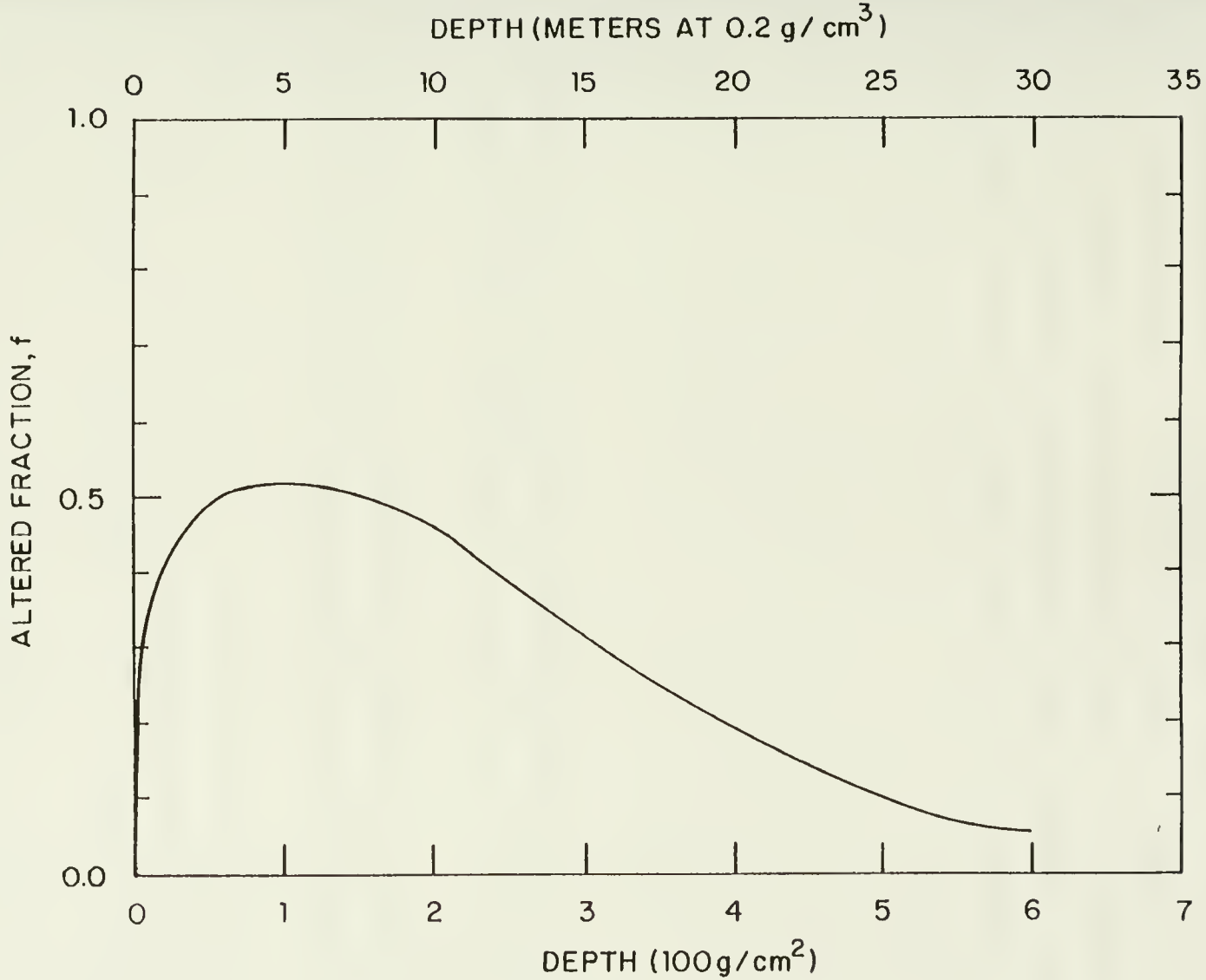


Fig.4 Altered fraction for estimating the change in the ortho-para ratio for the water ice.

such particles would be expected. As pointed out earlier[1], the outer mantle ('crust') will not be uniform, due to the initial irregularity of the surface which allows shadowing. Therefore, there will be unstable regions of the mantle which will be lost quickly and crevices may exist allowing volatiles to have access to the vacuum. These form the active regions which will be controlled by inner solar system mantle forming processes[25]. Such processes will also increase the thickness of the mantle in the regions from which the primordial mantle it is not lost. The comet then acts like a large reservoir for volatiles and loose dust with a few active spots, as was observed to be the case for Halley. The warming of the comet fills the reservoirs below the active region and increasing temperature near perihelion makes these regions active.

Acknowledgement: The author acknowledges the support of NASA grant NAGW 186 and discussions with M. Moore and R. Streitmatter about cosmic-ray doses.

References

(1) Johnson, R.E., J.F. Cooper, L.J. Lanzerotti and G. Strazzulla (1987) Radiation formation of a non-volatile comet crust Astron. Astro. 187 889-892.

(2) Whipple, F.L. (1977) The constitution of cometary nuclei in Comets, Asteroids, Meteorites: ed. A.H. Delsemmone, (Univ. of Taledo Press) pp. 25-32.

(3) Donn, B. (1976) The nucleus: panel discussion in The Study of Comets (B. Donn et al., eds.) (NASA SP-393) pp 611-621.

(4) Strazzulla, G. (1986) "Primitive" galactic dust in the early solar system? Icarus 67 63-70.

(5) Mumma, M.J., W.E. Blass, H.A. Weaver, and H.P. Laron (1989) Measurements of the ortho-para ratio and the nucleus spin temperature of water vapor in comets Halley and Wilson and the implication for their origin and evolution. (submitted).

(6) Stern, S.A. and M.J. Shull (1988) The reflectance of supernovae and passing stars on comets in the Oort cloud Nature 332 407-411.

(7) Stern, S.A. (1988) Collisions in the Oort cloud. Icarus 73 499-507.

(8) Strazzulla, G. and R.E. Johnson (1989) Irradiation effects on comets and cometary debris (submitted).

(9) Johnson, R.E. (1989) Energetic Charged-Particle Interactions with Atmospheres and Surfaces (Springer-Verlag, Berlin) in press.

(10) Magee, J.L. and A. Chatterjee, (1987) Track reacting of radiation chemistry in Kinetics of non homogeneous processes (ed. G.R Freeman) (J. Wiley and Sons, N.Y.) pp. 171-214.

(11) Ryan, H.P. and I.G. Draganic (1986) Radiation dosimetry of a cometary nucleus Astron. Space Sci. 125 49-69.

(12) Cooper, D.C. and R.W. Wood (1974) Physical Mechanisms in Radiation Biology

(CONF-721001, U.S. Dept. of Commerce, Wash.)

(13) Hart, E.J. and R.L. Platzman (1961) Radiation Chemistry, in Physical Mechanisms in Radiation Biology 1 (Academic Press, N.Y.) pp. 93-120.

(14) Lanzerotti, L.J., W.L. Brown and K.J. Marcantonio (1987). Experimental study of erosion of methane ice by energetic ions and some consideration for astrophysics. Astrophys. J., 313 910-919.

(15) Moore, M.H. and B. Donn (1982). The infrared spectrum of a laboratory-synthesized residue: implications for the 3.4 micron interstellar absorption feature. Astrophys. J. 257 L47-L50.

(16) Foti, G., L. Calcagno, K.L. Sheng and G. Strazzulla (1984) Micrometer-sized polymer layers synthesized by MeV ions impinging on frozen methane. Nature 310 5973-5974.

(17) Johnson, R.E. (1985) Comment on the evolution of interplanetary grains in Ices in the Solar System (eds. J. Klinger) (D. Reidel, Amsterdam) pp. 337-339.

(18) Foti, G., L. Calcagno, F.Z. Zhu, and G. Strazzulla (1987). Chemical evolution of solid methane by keV ion bombardment. Nucl. Inst. and Meth. B 24/25, 522-525.

(19) Lanzerotti, L.J., W.L. Brown and R.E. Johnson (1989) Threshold for H_2 release from methane Astrophys. J. (submitted)

(20) Moore, M.H. and B. Donn (1983). Studies of proton-irradiated ice mixtures Icarus 54 388-392.

(21) Inokuti, M. J.L. Dehmer, T. Baer, and J.D. Hauson (1981) Oscillator-strength moments, stopping powers, and total inelastic-scattering cross sections of all atoms through strontium. Phys. Rev. A 23 95-109.

(22) Particle data Group (1984) Review of particle properties. Rev. Mod. Phys. 56 supplement.

(23) Moore, M.H. (1982) Ph.D. Thesis. University of Maryland:

(24) A'Hearn, M.F. P.D. Feldman, and D.G. Scheicher (1983) The discovery of S_2 in comet IRAS-ARAKI-ALCOCK 1983d.

(25) Johnson, R.E. and L.J.Lanzerotti (1986) Ion bombardment of interplanetary dust. Icarus 66 619-624.

(26) Prialnik, D. and A. Bar-nun (1988) The formation of a permanent dust mantle and its effects on cometary activity Icarus 74 272-283.

METAMORPHISM OF COSMIC DUST: PROCESSING FROM CIRCUMSTELLAR OUTFLOWS TO THE COMETARY REGOLITH

Joseph A. Nuth III.
Astrochemistry Branch
Laboratory for Extraterrestrial Physics
NASA Goddard Space Flight Center
Greenbelt, Maryland

Abstract

Nucleation is a non-equilibrium process: the products of this process are seldom the most thermodynamically stable condensates but are instead those which form fastest. It should therefore not be surprising that grains formed in a circumstellar outflow will undergo some degree of metamorphism if they are annealed or are exposed to a chemically active reagent. Metamorphism of refractory particles continues in the interstellar medium (ISM) where the driving forces are sputtering by cosmic ray particles, annealing by high energy photons and grain destruction in supernova generated shocks. Studies of the depletion of the elements from the gas phase of the interstellar medium tell us that if grain destruction occurs with high efficiency in the ISM, then there must be some mechanism by which grains can be formed in the ISM. Various workers have shown that refractory mantles could form on refractory cores by radiation processing of organic ices. A similar process may operate to produce refractory inorganic mantles on grain cores which survived the supernova shocks. Most grains in a cloud which collapses to form a star will be destroyed; many of the surviving grains will be severely processed. Grains in the outermost regions of the nebula may survive relatively unchanged by thermal processing or hydration. It is these grains which we hope to find in comets. However, only those grains encased in ice at low temperature can be considered pristine since a considerable degree of hydrous alteration might occur in a cometary regolith if the comet enters the inner solar system. Some discussion of the physical, chemical and isotopic properties of a refractory grain at each stage of its life cycle will be attempted based on the limited laboratory data available to date. Suggestions will be made concerning the types of experimental data which are needed in order to better understand the processing history of cosmic dust.

Introduction

Silicate dust is observed in a wide variety of astrophysical environments: in dense, circumstellar shells and the diffuse interstellar medium, in the cold, dark interiors of molecular clouds and in the energetic plasma of planetary nebulae. It would seem only logical that each of these environments could "leave its mark" on grains which once resided within. If a large enough sample of interstellar grains were collected it might be possible to distinguish features which could reveal something of the history of an individual grain based on that grain's deviation from characteristics common to an "average" grain. Such general techniques are already used to distinguish pre-solar components of meteorites (Anders, 1988) and interplanetary dust particles (Zinner, 1988) from more common matrix material. In these studies specific isotopic anomalies are thought to be correlated with grain formation in particular astrophysical environments.

There is no doubt that individual components of any class of meteorite have undergone a significant degree of processing during the formation and evolution of the meteorite parent body. In addition the processes used to concentrate "pre-solar" meteoritic material in the laboratory completely destroy the petrographic context of the individual grains. Similarly, the IDP's have undergone a number of processing steps which make it difficult to distinguish primitive features from more recent processes including the possibility for metamorphism on the comet, in the cometary coma and the interplanetary medium or upon entry into the earth's atmosphere. The return of samples from a cometary nucleus promises to eliminate many of these impediments to interpretation of the astrophysical context of such grains provided

that the samples are carefully chosen. In this paper I will discuss the characteristics which might be observable in grains from a sample of the cometary nucleus based on both theoretical considerations of the life cycle of refractory grains and laboratory experiments using simple analogs to the more complex natural system.

In section II the lifecycle of a typical silicate grain is briefly discussed, from condensation in a circumstellar outflow to incorporation into a cometary parent body. In Section III I discuss the possibility for grain metamorphism within the cometary environment together with the results of relevant laboratory experiments which have been performed to date. In Section IV, the results of experiments which may have implications for the properties of interstellar grains are presented together with some speculative comments concerning the likelihood that evidence for any of these characteristics might be observable in cometary grains. Section V is a summary of what might be learned about pre-solar refractory grains by studying samples returned from a cometary nucleus.

II. Lifecycle of Refractory Silicates

a. The Circumstellar Environment

At equilibrium in the photosphere of a cool star of normal (oxygen-rich) composition, most of the grain forming elements exist as atoms or diatomic molecules (Tsuji, 1973). SiO, atomic Fe and atomic Mg are present in approximately equal amounts and together account for more than about 75% of the material which will nucleate to form circumstellar grains. Other materials, e.g., Al, Ca or Na, together account for less than 5% of the grain mass and are therefore unimportant as a first approximation (Duley, Millar and Williams, 1979). Most of the remaining mass of the initially nucleated grains will be derived from reaction of the grain cores with OH. The initially nucleated grains will be oxygen poor since nucleation is an inherently non-equilibrium process, and much of the mass of the grain forming material exists in the gas phase as metal atoms.

Once the grain nuclei begin to form in the supersaturated stellar outflow (due to the nucleation of SiO), a sufficient surface area becomes available for many of the remaining metal atoms to condense rapidly: this is especially true of metals such as Fe and Al which have low vapor pressures. More volatile metals such as Mg, Ca or Na may not condense until later depending upon the exact temperature and pressure at which the nucleation of the initial grains occurs. Both SiO and Al are efficient reducing agents and will tend to become more oxidized at the expense of other metals (such as Fe or Mg). Both of these species will tend to react rapidly with OH or H_2O molecules which impinge on the growing surface. If grain formation occurs rapidly, then it is unlikely that either the SiO or Al will have sufficient time to become fully oxidized before they are shielded from directly impinging OH by the growing grain surface. Rapid grain formation will also result in a large number of grain defects and unsaturated chemical valences.

The grain temperature in typical outflows appears to be on the order of 500-1000K (Rowan-Robinson and Harris, 1982) and it would therefore seem unlikely that the grains would be thermally annealed to a more stable "glassy" structure (Nuth and Donn, 1984). However, because the grains are already at a relatively high

temperature they should be quite readily heated by the absorption of UV-visible photons. Depending upon the oxidation and structural state of the grain at the moment of heating it is possible that a significant amount of chemical energy could be released as the grain anneals, (e.g., Clayton, 1980) leading to large degree of internal mobility of the grain constituents. This would result in the formation of tetrahedrally coordinated silicon and aluminum oxides, the reduction of some of the iron and magnesium oxides to metal, some degree of segregation between metallic and oxide phases and the formation of a glassy silicate.

In the outermost regions of circumstellar winds, thermally driven annealing reactions have been completely quenched for a considerable time and the glassy silicate grains may undergo some degree of low temperature surface reaction with volatile species such as OH, HS, H_2O or H_2S. If the (C + Si)/O ratio is approximately equal to one, sulfides will be more prevalent than oxides as carriers of the other metals and the silicate grains will develop sulfide crusts as metallic magnesium and iron react with SH or H_2S (Nuth et al., 1985). These effects have been observed in a number of stars (Goebel and Moseley, 1985). However, as the sulfide coated grains mix into the general interstellar medium, one would expect such coatings to be destroyed via reaction with the large abundance of water and OH in the ISM. Such reactions would produce MgO or FeO from any unoxidized metal atoms near the grain surface. Only metal nuggets which are well shielded from possible gas-grain surface reactions would be expected to survive as metals. Of course, in stars with (C + Si)/O considerably less than one, most of the exposed metal atoms will have been oxidized before the grains enter the ISM.

Despite the wide variation in the structures of the silicate grains added to the interstellar medium by each class of oxygen-rich star, one might expect that conditions in the interstellar medium would tend to drive all silicate grains toward some steady-state average. The primary forces responsible for grain metamorphism are cosmic-ray induced radiation damage, annealing by the absorption of UV photons and the reaction of grain surfaces with oxidizing vapor-phase species. The later would tend to fully oxidize SiO and any metals such as iron or magnesium which remain exposed at grain surfaces. Constituents buried within grains are not likely to be effected by such processes since rapid diffusion below the grain surface would be inhibited due to the low grain temperatures and low pressures in the interstellar medium. Cosmic ray bombardment would tend to destroy any crystalline structure in silicates which formed by annealing in very hot stellar environments. Conversely, chaotic amorphous silicates could become more ordered after cosmic ray bombardment or the absorption of a UV photon if the absorbed energy is greater than the activation energy for the formation of glassy silicates. Experimental observations have been reported which support both effects: Kratschmer and Huffman (1979) used high energy ions to convert crystalline olivine to glassy olivine while DeNatale and Howitt (1983) have shown that a degree of crystallinity may be introduced in some glasses due to bombardment by 100 keV electrons in an electron microscope.

The net observational effect of these processes would be to homogenize the properties of interstellar grains condensed in different circumstellar outflows. Effects of peculiar stellar chemistry, such as the formation of a MgS crust on otherwise normal silicate grains, would be quickly eliminated in the ISM. Similarly,

the preservation of highly crystalline or extremely chaotic silicates would be equally unlikely. Interstellar silicates would tend to be glassy and have a higher overall oxidation state than that of an average of silicates in circumstellar outflows. Iron metal inclusions might be preserved if they become buried within the glassy silicate grain. Magnesium and iron on grain surfaces would tend to oxidize.

b. Destruction and Reformation of Silicates in the ISM

Until recently, it was assumed that grains which formed in circumstellar outflows comprised the bulk of the interstellar grain population: the masses of these grains might be increased by the accretion of both volatile and refractory organic mantles, but the silicate cores were expected to survive most interstellar processes intact. Several years ago, Seab and coworkers presented a series of calculations which indicate that the lifetime of a typical silicate grain might be much shorter than had previously been expected (Seab and Shull, 1985). In fact, some of these calculations indicate that as many as 10 times the number of grains are destroyed in the ISM as are replaced by circumstellar condensates. Unless these calculations are grossly in error, a significant fraction of the interstellar grain population may have formed in the ISM rather than in circumstellar outflows. What properties might be used to distinguish grains formed in the interstellar medium from those formed in a circumstellar environment?

If a large fraction of interstellar grains were atomized in a shock wave, recondensation would occur slowly on the surfaces of the surviving grain cores. As the metals (e.g., Si, Fe and Mg) are accreted onto such surfaces, reaction with the more abundant molecules (e.g., H_2O, CO or NH_3) or with adsorbed hydrogen atoms could be more probable than reactions which yield silicates (A.G.G.M. Tielens, personal communication, 1984). Such reactions would undoubtedly produce a variety of metal radicals (e.g., SiOH, FeCO, or MgH) as well as silanes (Si_nH_{2n+2}), metal hydrides or metal carbonyls. These species would coexist in the grain mantle with ices of water, ammonia and various organic compounds. Exposure of these mantles to cosmic rays and ultraviolet radiation would increase the concentration of metallic radicals in the matrix and create a variety of new organic radicals as well. As this ice/radical mixture warms, reaction of the radicals will produce a refractory residue. Experiments by Greenberg and coworkers (See Greenberg, this volume) and by Moore and Donn (1983) on organic/ice mixtures have demonstrated the formation of refractory organic residues, while experiments by Nuth and Moore (1988a,b) on metallic/ice mixtures have shown that silicate residues can be formed by such processes. Experimental studies of organic/metallic/ice mixtures are needed before a realistic assessment can be made of the importance of this process compared to a scenario in which silicates are made by epitaxial growth of individual atomic species onto surviving grain cores. The properties of these inorganic residues will be discussed in Section IV.

c. Processing in the Solar Nebula

Undoubtedly the bulk of the grains present in the portion of the giant molecular cloud which formed the sun were destroyed as they became incorporated into the solar interior. Grains which passed close to the sun before being carried into the outer nebular regions could have been annealed to crystallinity, partially melted or even distilled to a more refractory composition. Implantation of ions from the

intense solar wind into these crystalline grains is likely to have occurred at many different times as the sun underwent outbursts during the accretion process and during its T-Tauri phase. Gas-solid reactions must have occurred between grains and active molecular species such as O, OH, H_2O, S, HS or H_2S. These reactions could have been mediated by nebular lightning, intense UV radiation from the sun or the nebular corona as well as by the elevated temperatures in the disk. All of these processes will be represented in the grains returned from a cometary nucleus provided that turbulent mixing in the disk was sufficiently vigorous.

For comets, the accretion process itself is unlikely to have been energetic enough to have effected the grains: the process was sufficiently gentle that a significant quantity of volatile material remained within the comet. It is also unlikely that the comet underwent a period of intense radioactive heating: again because comets today retain a large volatile inventory which would have been lost during any period of even moderately high temperature (e.g., $T \gtrsim 250K$). Cometary grains sampled by CNSR will therefore be representative of the population of grains present in the outer solar nebula at the time the comet accreted provided that no grain metamorphism occurs on the comet over its lifetime. The probability of metamorphism in such an environment will be assessed below.

III. Grain Metamorphism in the Cometary Environment

a. Cosmic-ray bombardment

Comets have spent roughly 4.5 billion years in the unshielded environment of the Oort Cloud without benefit of the protection from cosmic rays provided by the Sun's magnetic field. Over this time period it is probable that at least the topmost 10 meters of cometary ice and dust have received a significant dose of radiation (Moore and Donn, 1982). The above estimate assumed a cometary density of ~ 1 g/cm^3 and so might underestimate the depth to which such radiation penetrates if the density of the nucleus is significantly lower. It is usually assumed that this topmost layer is lost within the first one or two orbits through the inner solar system and so might not be of interest in a mission to an older (periodic) comet. Unfortunately, this may not be completely correct: the extent to which radiation processed dust is a component of the cometary regolith will depend a great deal on the mechanism by which volatiles escape from the cometary interior. It may even be possible that a significant fraction of this processed refractory material remains in the regolith if most outgassing comes from vents to the comet's interior rather than from a more or less continuous mass flux through the regolith (and random opening of vents which are nearly at the comet's surface). These possibilities will be discussed further in Section V.

The effects of cosmic-ray interactions on the structure of refractory grains is relatively straight forward. Energetic particles may destroy the crystallinity of refractory minerals by creating defects in the previously ordered structure: this could be a simple matter of a few cosmic ray tracks in an olivine grain or could result in the complete loss of all order in a less stable phyllosilicate. On the other hand, the energy deposited within an amorphous silicate grain by the passage of a cosmic ray particle may sufficiently exceed the activation energy required to initiate oxidation/reduction reactions in a chemically inhomogeneous particle that

these reactions could become self-sustaining. The resultant energy release might be sufficient to partially anneal the previously amorphous grain.

b. Thermal Annealing

Except in the case of sun grazing comets, it is fairly safe to assume that thermal annealing of even nanometer sized amorphous silicates will play little or no role in the metamorphism of cometary grains. Prior to the time when such materials were incorporated into the comet however it is probable that at least some thermal metamorphism will have occurred either in the circumstellar environment, the interstellar medium or the solar nebula. The rate and the effects of such processing depend upon both the chemical composition and initial structure of the grains.

The technological importance of fiber optics has led to numerous studies of the kinetics of devitrification of various glass compositions. It has been shown by several authors that the rate at which polymorphs of SiO_2 crystallize is dependent upon the initial structure (Wagstaff, 1968; 1969), the presence of trace impurities (Zaplatynsky, 1974, 1988; Bihuniak, 1983; Boden et al., 1984), the bulk composition of the glass (Brown and Kistler, 1959) and the ambient atmosphere in which it is annealed (Wagstaff and Richards, 1966). All of these factors are important in considering the effect of thermal annealing on an initially amorphous grain of "cosmic" composition which passes through several very different astrophysical environments between the time it nucleates in a circumstellar outflow and the time at which it finally becomes incorporated into a comet. A more detailed understanding of the initial composition and structure of refractory condensates is needed before accurate predictions of the rate at which such grains crystalline can be attempted. Very preliminary x-ray diffraction studies of the rate at which amorphous Mg-SiO smokes become crystalline (Nuth and Donn, 1983) show an extreme temperature dependence. Because we have few constraints on the temperature history of an individual grain in the solar nebula before it was incorporated into the comet it will be difficult to directly unravel the temperature-time dependence of such material if it is well crystallized. More amorphous samples however, may provide upper limits to the time-temperature history of associated materials.

Nuth and Donn (1984) have carried out a series of experiments designed to place limits on the stability of initially amorphous Si_2O_3 and Mg-SiO condensates as a function of temperature and time. In these experiments changes in the infrared spectra of the samples were monitored as a function of processing history. Figure 1 (taken from Nuth and Donn, 1982) shows the changes in the infrared spectrum of amorphous Mg-SiO smoke annealed in vacuo at 1000K for 0, 1, 2, 4, 8, 16.5 and 30 hours (top to bottom). Three aspects of these spectra should be noted. First, no sharp features (indicative of crystalline material) appear in the spectra for at least 16.5 hours. Second, one of the earliest changes to occur in this series is the loss of a minor absorption feature near 11.5 microns. Third, a series of very large shifts in both the positions and relative intensities of the major silicate features at 10 and 20 microns occur as the sample anneals: these latter changes indicate an increased level of polymerization and chemical equilibration within the sample.

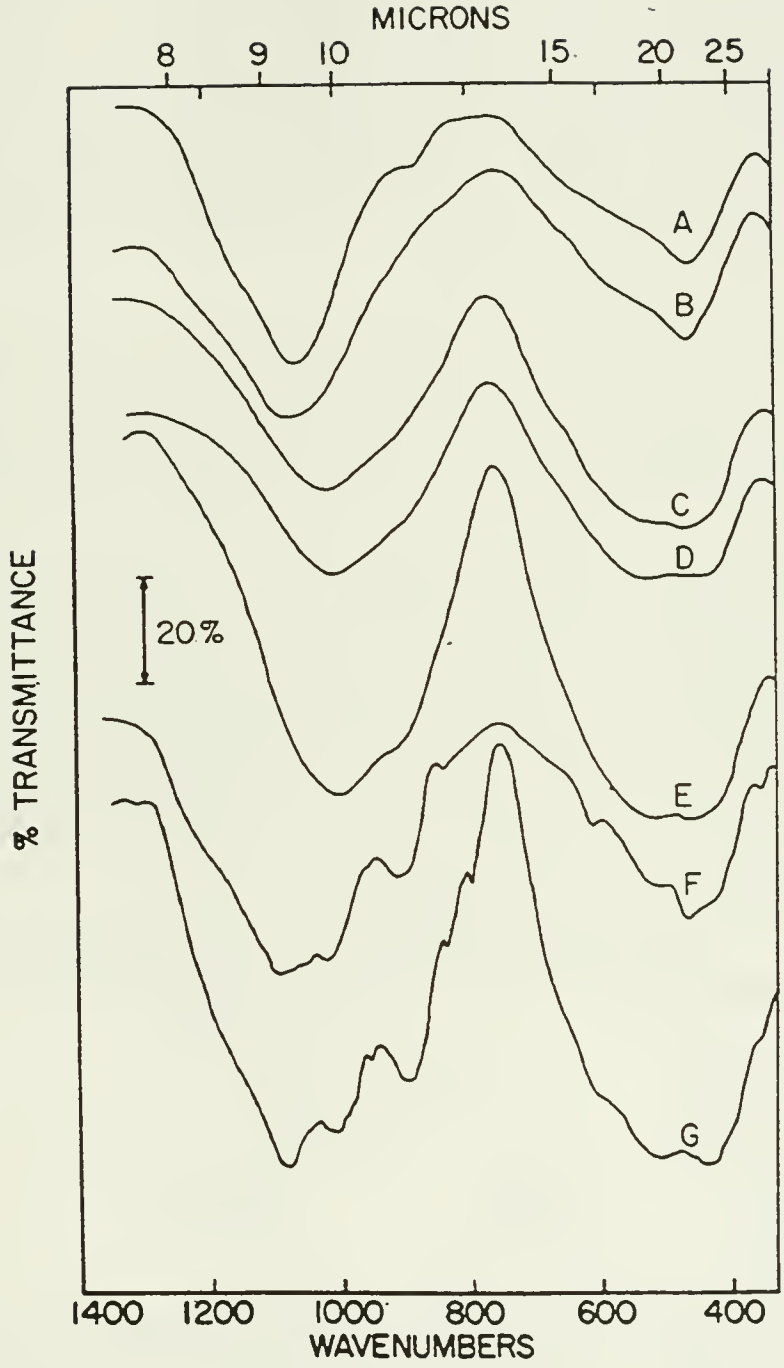


Figure 1. Infrared spectrum of an unannealed Mg-SiO smoke (A) and of smoke samples annealed in vacuo at 1000K for 1 hr. (B), 2 hrs. (C), 4 hrs. (D), 8 hrs. (E), 16.5 hrs. (F), and 30 hrs. (G) (Nuth and Donn, 1982).

Nuth and Donn (1984) have measured the rate at which the 11.5 micron feature (due to Si_2O_3) disappears as a function of temperature. The rate of this reaction is given by $k(hr^{-1}) = 10^9 \exp(-40 \text{ kcal/mole/RT})$ and represents a lower limit on the stability of an amorphous condensate. As the example in Figure 1 shows, if the 11.5 micron feature is still present in the amorphous Mg-SiO condensate then one can infer that little metamorphism had occurred since the material nucleated. The half-life for survival of the 11.5 micron feature calculated using the above rate equation is given in Table 1 as a function of temperature. It is obvious from this table that if nucleation occurs at temperatures less than 1000K and transport to cooler environments occurs relatively rapidly then the grains will remain amorphous and may preserve internal chemical heterogeneities which could lower the activation energy for other processes such as hydration.

Infrared spectroscopy is sensitive to small changes in the average chemical bonding in the solid and is therefore very sensitive to the earliest stages of metamorphism (e.g., transitions from a chaotic state to a more ordered glassy structure). Unfortunately, because infrared spectroscopy averages over a sample containing millions of small grains, conclusions derived from such studies apply only to "average" grains and cannot easily constrain the range of the deviations which might occur in an individual grain during processing.

Rietmeijer et al. (1986) have shown using analytical election microscopy that although the bulk Mg-SiO sample is indeed amorphous as shown by its infrared spectra, some degree of microcrystallinity exists in even the unannealed smokes. The crystalline fraction increases as a function of annealing time. It should be noted however that the initial crystalline components (Olivine and tridymite) are not predicted to be the most thermodynamically stable mineral assemblage. As annealing continues, olivine and tridymite gradually convert to the more stable clinopyoxene. Several alternative explanations for these observations are discussed in the paper by Rietmeijer et al. (1986) and will not be further discussed here.

Table 1

Half-life of Si_2O_3 Disproportionation vs. Temperature

Temperature (K)	Si_2O_3 half-life
1200	43 seconds
1000	20 minutes
800	50 hours
600	24 years
400	0.4 billion years

c. Hydration

The first general misconception which must be dealt with in any discussion of the hydration of cometary grains is that macroscopic quantities of liquid water are necessary for hydration to occur. Rietmeijer (1985) has argued, based on analogy with weathering studies of antarctic soils, that a significant degree of alteration can be expected in the presence of ice at temperatures below the freezing point of water. In addition Clayton and Mayeda (1984) have shown that hydration in at least one meteorite parent body occurred at temperatures which may have been below 273K. Such conditions may occur at the base of the cometary regolith in contact with the

"icy snowball" surface in older models of a cometary nucleus. Hydration may also occur within the regolith as water vapor percolates outward through ever hotter grains to the cometary surface. It is well known to anyone who has ever worked with a high vacuum system that water bonds quite strongly to both silica and metal surfaces; transport of water vapor from the interior of a comet to its surface through a silicate regolith will therefore result in some degree of H_2O absorption on grain surfaces. Studies of antarctic weathering have shown that significant hydration can occur from the presence of a single monolayer of water (see Rietmeijer, 1985). If the regolith pores are not "well connected" then water vapor percolation will be slow, the surface coverage will be higher, and the probability of hydration will be increased.

Studies of the rate at which amorphous Mg-SiO smokes hydrate in the presence of liquid water have been performed in order to set limits on the rate at which hydration may occur in a cometary regolith (Nelson, Nuth and Donn, 1987) or a meteorite parent body (Nuth et al., 1986). These studies used amorphous smokes as a starting material since these smokes are likely to be more reactive than cometary grains due both to their large surface to volume ratio and to the metastability of amorphous materials. In addition, liquid water was used rather than water vapor to ensure complete surface coverage of each grain by water. Reaction was followed by monitoring changes in the infrared spectra of the exposed samples as a function of both temperature and time. Results of these experiments are presented in Table 2 using several different infrared bands as indicators of the hydration process.

As can be seen from Table 2, little hydration occurs below about 200K and therefore grains which are encased in ice at the temperatures postulated for the nucleus ($T \leq 170K$) will probably not be affected by hydration unless they are much more reactive than our amorphous Mg-SiO analogs. From these results it would appear that more crystalline materials which may have been produced in the solar nebula via several processes will be preserved quite well if encased in ice. Grains in the regolith however may be severely altered if the temperatures reported for Comet Halley ($T \geq 400K$) are typical of most comets (Combs et al., 1986). Our amorphous materials are altered on timescales of hours at such high temperatures so that it would seem likely that more crystalline material would be altered to some extent over the longer periods available to grains in such a regolith. Alteration would of course proceed faster at higher temperatures or with shocked grains.

Table 2

Half-life of Mg-SiO Infrared Features in Liquid Water

Temperature (K)	11.5 micron decay	16 micron growth	20 micron growth
1250	4.1 seconds	0.03 seconds	41.4 seconds
1000	12.2 seconds	0.16 seconds	1.6 minutes
750	1.3 minutes	2.2 seconds	6.6 minutes
500	51.2 minutes	7.6 minutes	1.8 hours
400	13.5 hours	6.8 hours	15.2 hours
300	56.3 days	220 days	21.5 days
200	1541 years	360,000 years	67.8 years

IV. Grains Produced in the Interstellar Medium

As mentioned in Section II.b, Greenberg has long discussed the possibility that refractory organic mantles or "yellow stuff" will be formed on the surfaces of silicate grains in the interstellar medium. The properties of such material is

discussed in the review by Johnson (this volume) and will therefore not be treated further here. However, a similar process may act to produce refractory inorganic grains in the interstellar medium (Nuth and Moore, 1988) or in the solar nebula as previously irradiated grains are gradually warmed during the collapse phase. The measured and expected properties of these grains are discussed briefly below.

Infrared spectra of the amorphous iron silicate residues have been reported (Nuth and Moore, 1988a,b) and show strong and very broad absorption features near 10 and 20 microns due to the silicate stretching and bending fundamentals, respectively. Also evident in the laboratory spectra are features at 4.6 and 4.9 microns due to the SiH stretch and the CO stretch. Both of these features are quite stable and are easily observed in the residues even after vacuum annealing to 400K for 30 hours. Features at these wavelengths are also observed in the spectrum of W33A, a strong infrared emission source thought to be a young protostar. The persistence of reactive entities such as SiH or volatile species such as CO after vacuum annealing and exposure to air at room temperature implies that silicates produced by slow reaction of icy radicals may serve as very efficient traps for more volatile materials.

Experiments to measure the efficiency with which noble gases are trapped in these grains are currently in progress. Preliminary measurements show that both Kr and Xe are very efficiently trapped in the growing silicate matrix while Ne and Ar are trapped much less efficiently (Hohenberg, private comm.). It may be possible that the "planetary" component of the noble gases trapped in meteorites formed via these processes in the interstellar medium. Trapping would therefore have occurred both in carbonaceous and in inorganic grains. If noble gases are trapped then it might easily be possible to trap more reactive species such as CO or H_2O. Interstellar materials may have been a major source of volatile materials for planetesimals in the early solar nebula.

The morphology of the grains produced in our experiments is also quite interesting. Some grains produced from irradiated mixtures of SiH_4-H_2O show quite distinct rhomboidal structure indicative of crystallinity even though these grains were never heated above 300K (Mackinnon, personal comm.). This blocky texture is also evident in grains produced from $Fe(CO)_5$-SiH_4-H_2O mixtures. In addition we have observed a number of iron poor fibrous grains comprising approximately 10-15% of our sample. These grains probably also contain additional light elements such as carbon, oxygen, and hydrogen. More detailed analysis of the composition, crystal structure and morphology of these materials is in progress (Mackinnon, personal comm.). In comets these materials would be identified as an inorganic coating over a refractory core much in the same way that "yellow stuff" would be expected to occur on silicate cores in the interstellar medium.

V. Sample Collection Strategy

The major uncertainty in developing a strategy for the collection of samples of refractory cometary particles is the thickness and history of the regolith. Of course this consideration is also of major importance in collecting samples of cometary ices since, if the regolith is too thick, then a core sample may not extend down to the ice layer. In the old "dirty snowball" model of the cometary nucleus it was assumed that any dust which came to the surface was quickly lost. Despite evidence for a very high surface temperature ($T > 400K$ at 1 AU) many models for the

cometary surface still assume a very thin regolith which has a very low thermal conductivity. These models also assume that the active jets are "bare spots" in the regolith where the ice resides at the surface. If these models are correct then the Comet Nucleus Sample Return mission described at this workshop will be successful. Unfortunately the current mission does not have a viable backup sample collection strategy if the current model of the cometary nucleus is incorrect.

The very low apparent density of Halley's Comet (< 0.5 g/cc) supports the fractal model of a cometary nucleus proposed by Donn (1981, 1987). Such a comet would have numerous internal voids which could interconnect to allow the escape of volatiles from the nucleus and the transport of energy into the interior via gas transport. Laboratory experiments in which comet-like mixtures of ice and dust have been allowed to sublime into a vacuum (Saunders et al., 1986; Storrs et al., 1988; reports of the KOSI team in this volume) have shown that the resulting residue may occupy nearly the same volume after loss of its volatile component as it did initially and that this residue can be surprisingly strong. If we combine Donn's model with the laboratory experiments one possible result is that the active jets are vents to the interior of the comet through which volatiles escape. It is quite conceivable that the outside of the comet could be almost all regolith - a large number of completely degassed - but still largely intact - dust balls which adhere to one another because the dust filaments of adjacent "units" are interconnected.

In the above scenario the "jets" which are observed could still become active or dormant due to the opening or closing of interior connections via the condensation or evaporation of volatiles or the shearing caused by shrinkage of individual ice-dust balls during loss of the unit's volatiles. Stephens (this volume) has noted that if individual ice-mineral mixtures contain organics then the resulting residue is even sturdier than a typical ice-dust residue. Given the large number of CHON particles detected during the Halley encounter (Kissel and Kruger, this volume) one might suppose that the dust regolith could be quite strong and that once the regolith formed it would be quite difficult to erode. If a layer of cosmic-ray produced organic residue were produced in the Oort cloud (e.g., Johnson, this volume) then this organic glue might serve to hold a large number of near surface grains together as the comet first approached the sun by increasing the relative proportion of the stickier organics in the near surface region relative to the more volatile organics. Once this regolith forms it can only grow.

If the model just described is more realistic than the thin regolith models, then several predictions can be made about the nature of the refractory particles returned from the nucleus and about the likelihood of recovering any ice using a 3m coring device. To take this latter point first, it would be very unlikely that such a short core would succeed in recovering an ice sample since it would seem more likely that in an older comet the top 10 to 100 meters of the comet would be completely degassed. Grains near the surface (e.g., the top 10 meters or so) may contain cosmic ray tracks from the time the comet spent in the Oort cloud. Grains in the regolith should also be completely hydrated. Cometary grains ejected in jets may be pristine materials newly released from the interior ice core or may be hydrated grains swept out of the interior from the walls of the regolith: both populations of grains are likely to be represented in such material. Cryogenic collection and preservation of grains ejected in jets may be one of the only ways to return "pristine" unaltered refractory grains to earth for analysis since grains collected near the surface may have undergone some degree of metamorphism within the cometary environment.

References

Anders, E., 1988 in Meteorites and the Early Solar System, eds. J. Kerridge and M. Matthews (Univ. Ariz. Press, Tucson) Chap. 13.1.

Bihuniak, P. P., 1983, J. Am. Cer. Soc. 66, C-188.

Boden, G., Richter, E. and Wollschlager, K., 1984, Silikattechnik 35, 149.

Brown, S. D. and Kistler, S. S., 1959, J. Am. Cer. Soc. 42, 263.

Clayton, D. D., 1980, Ap. J. 239, L37.

Clayton, R. N. and Mayeda, T. K., 1984, EPSL 67, 151.

Combs, M. and 19 co-authors, 1986, Nature 321, 266.

DeNatale, J. F. and Howitt, D. G., 1983, Proc. 41st Annual Meeting of the Microscopy Society of America (San Francisco Press, San Francisco) p. 354.

Donn, B. D., 1981 in Comets and the Origin of Life, ed. C. Ponnemperuma (D. Reidel, Dortrecht) p. 21.

Donn, B. D., 1987 in Exploration of Halley's Comet, eds. B. Battrick, E. J. Rolfe and R. Reinhard (ESA SP-250, Vol. III) p. 523.

Duley, W. W., Millar, T. J. and Williams, D. A., 1979, Astrophys. Space Sci. 65, 69.

Goebel, J. H. and Moseley, S. H., 1985, Ap. J. (Lett.) 290, L35.

Kratschmer, W. and Huffman, D. R., 1979, Astrophys. Space Sci. 61, 195.

Moore, M. H. and Donn, B. D., 1983, Icarus 54, 388.

Nelson, R. N., Nuth, J. A. and Donn, B. D., 1987, Proc. 17th Lun. Plan. Sci. Conf., in J. Geophys. Res., 92, E657.

Nuth, J. A. and Donn, B. D., 1982, Ap. J. (Lett.) 257, L103.

Nuth, J. A. and Donn, B. D., 1983, Proc. 13th Lun. Plan. Sci. Conf., in J. Geophys. Res. 88, A847.

Nuth, J. A. and Donn, B. D., 1984, Proc. 14th Lun. Plan. Sci. Conf., in J. Geophys. Res. 89, B657.

Nuth, J. A., Moseley, S. H., Silverberg, R. F., Goebel, J. H. and Moore, W. J., 1985, Ap. J. (Lett.) 290, L41.

Nuth, J. A., Donn, B. D., DeSeife, R., Donn, A. and Nelson, R. N., 1986, Proc. 16th Lun. Plan. Sci. Conf., in J. Geophys. Res. 91, D533.

Nuth, J. A. and Moore, M. H., 1988a, Ap. J. (Lett.) 329, L113.

Nuth, J. A. and Moore, M. H., 1988b, Proc. 19th Lun. Plan. Sci. Conf., (LPI, Houston) in press.

Rietmeijer, F. J. M., 1985, Nature 313, 293.

Rietmeijer, F. J. M., Nuth, J. A. and Mackinnon, I. D. R., 1986, Icarus 66, 211.

Rowan-Robinson, M. and Harris, S., 1982, Mon. Not. Roy. Astr. Soc. 200, 197.

Saunders, R. S., Fanale, F. P., Parker, T. J., Stephens, J. B. and Sutton, S., 1986, Icarus 66, 94.

Seab, C. G. and Shull, J. M., 1985 in Interrelationships Among Circumstellar, Interstellar and Interplanetary Dust, eds. J. Nuth and R. Stencel (NASA CP 2403, GPO, Wash. DC) p. 37.

Storrs, A. D., Fanale, F. P., Saunders, R. S. and Stephens, J. B., 1988, Icarus 76, 493.

Tsuji, T., 1973, Astr. Astrophys. 23, 411.

Wagstaff, F. E., 1968, J. Am. Cer. Soc. 51, 449.

Wagstaff, F. E., 1969, J. Am. Cer. Soc. 52, 650.

Wagstaff, F. E. and Richards, K. J., 1966, J. Am. Cer. Soc. 49, 118.

Zaplatynsky, I., 1974, NASA TM X-2969.

Zaplatynsky, I., 1988, NASA TM-101335.

Zinner, E., 1988 in Meteorites and the Early Solar System, eds. J. Kerridge and M. Matthews (Univ. Ariz. Press, Tucson) Chap. 13.2.

EXPERIMENTAL STUDIES OF GAS TRAPPING IN AMORPHOUS ICE AND THERMAL MODELING OF COMETS—IMPLICATIONS FOR ROSETTA

A. Bar–Nun
D. Prialnik
I. Kleinfeld
D. Laufer
Department of Geophysics and Planetary Sciences
Tel Aviv University
Tel Aviv, Israel

EXPERIMENTAL STUDIES OF GAS TRAPPING IN AMORPHOUS ICE AND THERMAL MODELLING OF COMETS - IMPLICATIONS FOR ROSETTA

A. Bar-Nun, D. Prialnik, I. Kleinfeld and D. Laufer

Dept. of Geophysics and Planetary Sciences
Tel Aviv University, Tel Aviv, Israel

I. INTRODUCTION

The realization that water ice at low temperatures is the major constituent of comets, the satellites of the outer planets and their rings particles, and of icy grain mantles in dense interstellar clouds, prompted in recent years a number of groups to study experimentally the properties and behavior of ice at very low temperatures and apply their findings to icy bodies. Among them are the groups of Delsemme, Donn and Moor, Fanale, Greenberg, Ibadinov, Kajmakov, Klinger, Mayer, Miller, Rossler, Sanford and Allamdola, Schmitt and Wallis. Because of the limitation on the space of this article, the over 100 works of these groups will not be included in the list of references.

In most of these experiments, several microns to several cm thick ice samples were studied under, presumably, isothermal conditions. Thus, almost no experimental data exists on the processes by which a heat wave penetrates into the ice, the formation of a dust crust by partial water sublimation and other large scale phenomena. The works of Kajmakov, Ibadinov and their groups were aimed mainly at the formation of a filamentry residue when the ice sublimated completely, as were the works of Storrs, Fanale and Stephans. A major step in the direction of measuring bulk behavior of large (~15 cm thick, ~30 cm diameter) ice-gas-dust samples was made in recent COSI (Comet Simulation) experiments. These results will be described by Grun in this volume.

All this experimental and theoretical effort would not have led anywhere without some knowledge of the structure, composition and behavior of icy bodies. In this field, major advances were made by the two Voyagers' flybys among the icy satellites of Jupiter, Saturn and Uranus, with Neptune yet to come. A tremendous advance in our knowledge of comets was obtained by the six spacecrafts which studied comet Halley, with Giotto and Vega contributing most of the new and surprising data. Only the combined efforts of the spacecrafts experimenters, modellists and laboratory experimenters could lead to the far better understanding of comets which we now have. The next major advances will certainly occur during the coming CRAF and ROSETTA missions.

In what follows, because of space limitations, we will describe only the experimental results obtained at the Comet Simulation Laboratory of Tel Aviv University (1-5), as well as our thermal models (6-10), which incorporate the experimental results. These will be applied to the temperature and composition of the nebula in the region of comet formation; the timescale of comet formations; the small explosions observed on Comet Halley and the formation of its large active craters, as well as to Miranda's chaotic terrain; the possible contribution of comets to the noble gas inventory on the terrestrial planets and finally, to a detailed model of the thermal evolution of comet P/Temple-1.

II. EXPERIMENTAL PROCEDURE

The experimental setup and procedures were described in detail in our papers (1-6) and will therefore be described here only very briefly. A premixed gas-water vapor mixture was flowed onto a cold plate at 20- 100K and was co-deposited on it, at a pressure of ~10^{-6} Torr, for ~45 min., through a capillary tubing with a diffuser on its tip. When an ice layer containing 10^{17} -10^{20} water molecules was formed, the chamber was pumped for ~10 min, until a constant pressure of ~10^{-8} Torr was reached. The plate was then uniformly warmed, at a constant rate of 0.1-1K min^{-1}.

The evolution of gas and water vapor from the ice was monitored by a precalibrated quadrupole mass-filter and the amounts of gas and water vapor emerging at each temperature range were obtained by integrating their fluxes over the time of their evolution from the ice. The sensitivity of the mass-filter spanned 8-9 orders of magnitude of gas flux. Thus, very subtle changes in the ice, which were manifested by gas evolution, could be detected. During the evolution of gas at the various temperature ranges, spikes of water and gas were monitored by the quadrupole mass-filter. Each spike corresponds to a gas jet or to an ice grain, which enter the mass filter's probe.

III. RESULTS AND DISCUSSION

A. Structure of the amorphous ice (3-4)

When a layer of amorphous ice is viewed from the edge or at an oblique angle, a hairlike structure is revealed (Fig. 1). The ice looks like a shaggy woolen carpet, which explains its very large surface area - 86 m^2 g^{-1}. The amorphous ice needles, which grow by ballistic deposition of water vapor, are smooth, with no side branches, unlike the dendritic structure of hexagonal ice, which grows on a cold surface by diffusion of water vapor in air. The same structure is formed with water vapor deposition rates between 10^{16} and 10^{19} water molecules cm^{-2} min^{-1}, at temperatures between 20 and 100K. Below this deposition rate, the ice layer is too thin for anything to be seen. It is estimated that about 80% of the ice is in the form of needles. The ice needles are not altered during the evaporation of the ice, between ~140 and ~180K and retain their shape until their complete evaporation.

B. Gas trapping in the ice and its release upon warming (3-4)

The trapping of various gases in amorphous ice and their stepwise release when the ice is warmed up, was used to probe the ice's structure and dynamics. A typical plot of gas release from ice which was co-deposited with argon (H_2O water vapor Ar=1:1) is shown in Figure 2. *Eight* regions of gas release, labelled a-g can be seen. The first one (a) is due to the evaporation of gas which was not trapped internally, and froze on the surface. Range (c) which starts at 44K is due to the desorption of the last monolayer of adsorbed gas from the surface. From the amount of gas released in range (c), a surface area of 86 m^2 g^{-1} is found for ice at 44K, diminishing to 78, 55 and 38 m^2 g^{-1}, for ice which was deposited at 75, 100 and 120K, respectively. Ranges (b), (d) and (d') which start at 35K ~85K and ~120K, respectively, are attributed to three distinct annealing processes in the amorphous ice. Each one proceeds in a stepwise, temperature dependent, manner. Thus, if the temperature is kept constant for tens of hours in the middle of these three ranges, gas emission declines slowly, until it reaches the limit of detections - 10^9 molecules cm^{-2} sec^{-1}. A temperature increase by a mere 2-3 degrees results in the



Fig. 1 - A view of an amorphous ice layer, seen at an oblique angle. Needles about 0.1 mm long are seen, with an ice layer containing ~10^{20} water molecules/cm^2.

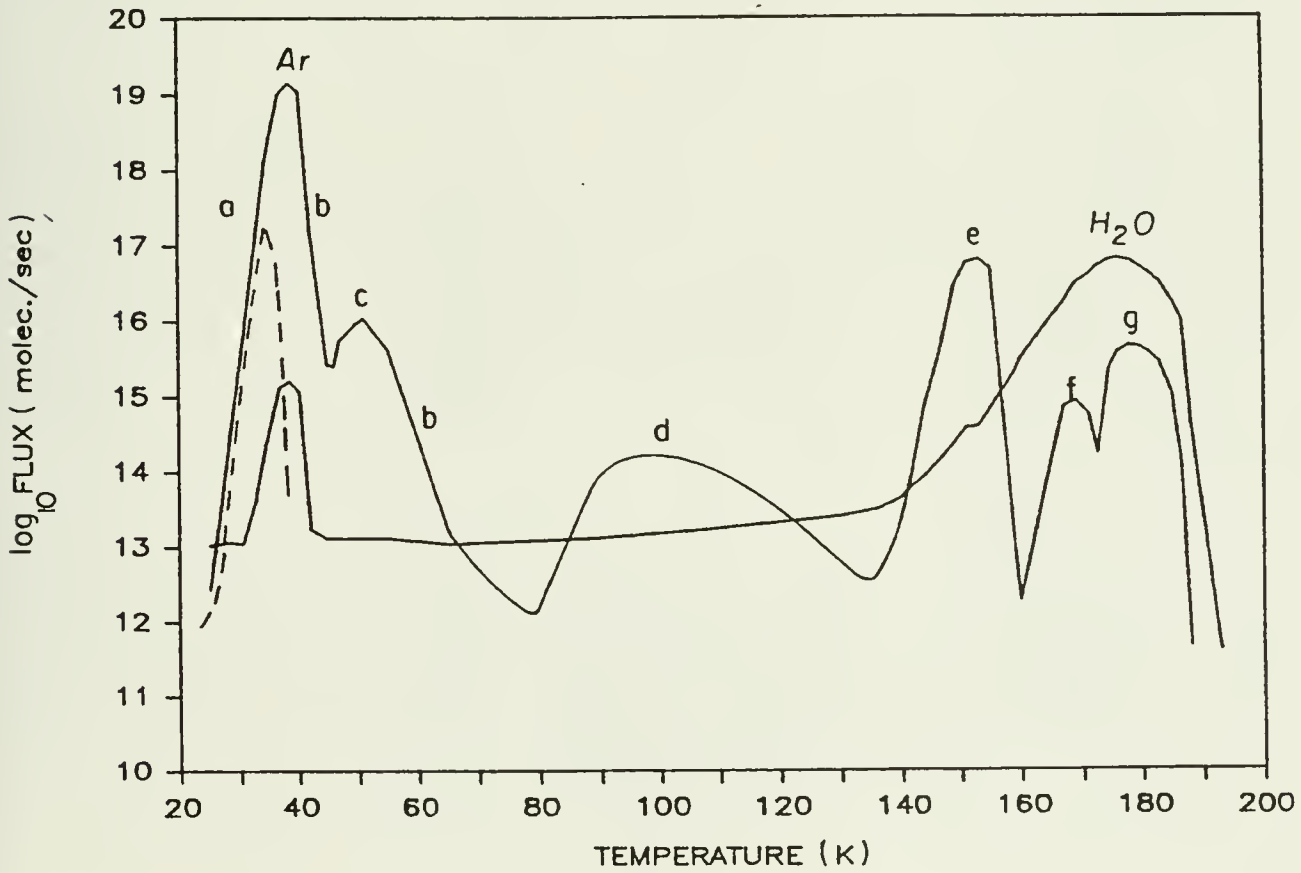


Fig. 2 - A plot of the fluxes of evolved argon and water vs temperature, representing the eight ranges of gas evolution. The fluxes vary by up to 8 orders of magnitude as the ice temperature varies. The rise in the water flux at 30K is due to ice-grain ejection. An evaporation curve of frozen argon from an ice-free plate (----) is added for comparison.

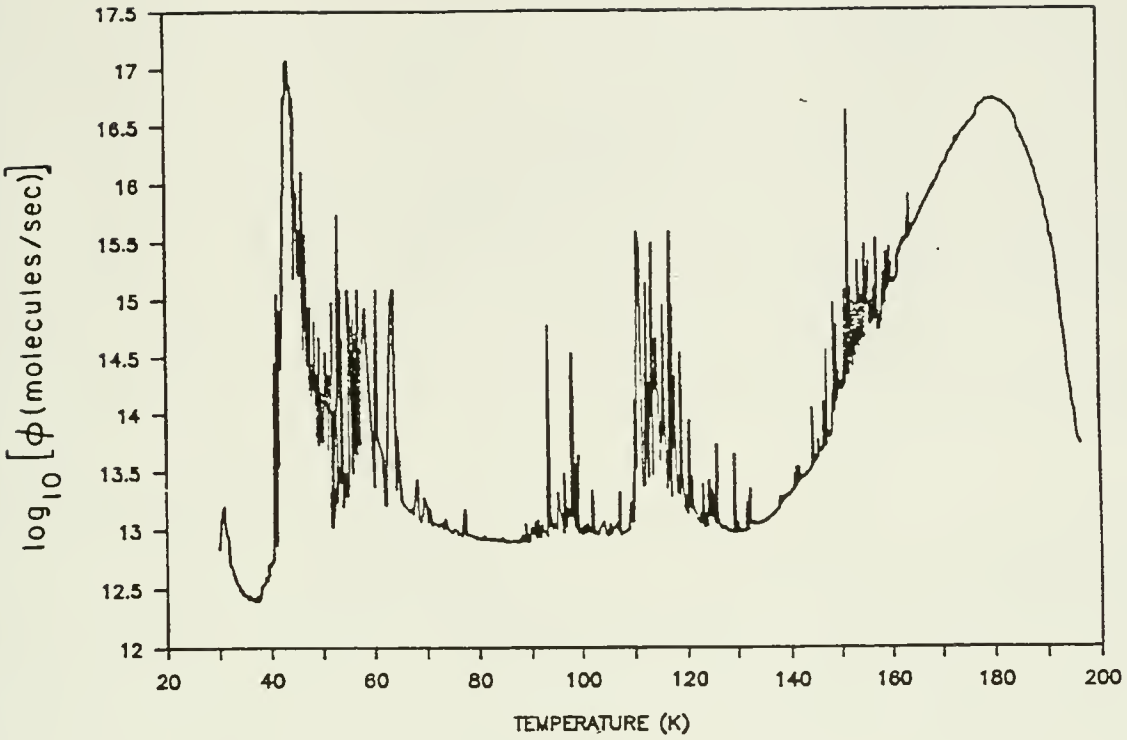
resumption of gas emission at the level reached before the temperature was kept constant. Range (e) is due to the release of gas during the exothermic transformation of the amorphous ice into cubic ice. The onset of the transformation occurs at 137K. If the ice is kept at a constant temperature anywhere in range (e), all the gas which was supposed to come out in this range leaks out and, unlike in ranges (b), (d) and (d'), a slight increase in temperature does not cause another surge of gas. At 160K, the cubic ice transforms into hexagonal ice, in an almost thermoneutral process. During this transformation, an additional portion of the trapped gas comes out in range (f). Gas release in range (g), which follows, is symmetrical with the evaporation of the ice (Fig. 1). It is attributed to the evaporation of the clathrate hydrate, where the water cages evaporate, releasing the gas molecules which were trapped in each cage.

Very large fluxes of gas jets, each containing about 5×10^{10} gas molecules, and ice grains, each containing about 10^{10} water molecules, are emitted from the ice under a variety of conditions (Fig. 3): whenever Ar, CO, CH_4, N_2 and Ne, but not H_2 or D_2, are emitted from gas- rich ice; during the deposition of a 1:1 gas- water-vapor mixture below 29K; and during gas flow into pure amorphous ice, below 29K at a pressure exceeding 2.6 dyn cm^{-2}. With an ice layer containing $\sim 10^{19}$ water molecules cm^{-2}, the ice needles are ~1 μm long and ~0.2 μm wide, and their speed is at least 1.67 m sec^{-1}. In addition to the large gas jets, all gas emission in the various ranges is not quiescent, but consists of numerous minijets, ~100 times smaller than the large ones, which result in a "noisy" gas signal at a frequency of $\sim 10^{3}$ sec^{-1}. Whenever a large flux of ice grains is emitted, the ice remaining on the plate is not hairlike, but has a very rough texture. Therefore, it seems that the ice grains are indeed the ice needles, which are broken from their base and are propelled by the large gas jets. The frequency of ejection of the needles is correlated with the amount of gas trapped in the ice.

Up to 63% (by number) of H_2, D_2 and Ne are trapped in the ice at 16-25K (Figure 4). Three ranges of gas release are observed for these three gases: 16-35K, 35-85K and 85-120K. The second and third ranges of gas release correspond to ranges (b) and (d), whereas the first range corresponds to the penetration of the narrow H_2 and D_2 molecules or the somewhat bigger Ne atom into the hexagonal channels of the ice. According to Hobbs (12), in cubic ice, the hexagons which are formed by the oxygen atoms have the configuration shown in Figure 5. With a radius of 1.4 Å between adjacent oxygen atoms, the free channel through each hexagon has a diameter of 2.5 Å. The diameters of Ar, Ne, H and D atoms are 4.7, 3.8 and 2.2 Å respectively. Therefore, hydrogen and deuterium molecules, but not neon or argon, can penetrate freely the lattice of cubic ice. Only the ***amorphous*** ice lattice, in which the distances between adjacent oxygen atoms are larger, is permeable to neon, and some channels are even large enough to allow argon atoms to penetrate the ice lattice.

This is clearly demonstrated by the reversible trapping in the first range, of H_2 and D_2 in cubic ice, which was cooled to 19K, and the failure of Ne and Ar to be trapped under these conditions. Yet, considerable amounts of H_2 and D_2 are held in the ice until ranges (b) and (d) are reached, even though the ice matrix is open to them. Apparently, some of the open channels are blocked by domains in the ice which are perpendicular to each other. Hence the amounts of H_2 and D_2 which are emitted in (b) and (d) versus the amount in the first range, provide a measure of the fraction of blocked domains in the ice. Of the 0.63 H_2 molecules per water molecule in the ice, 0.42 reside in open channels and 0.21 reside in blocked regions, which open when the ice anneals in ranges (b) and (d).

As for the larger argon atoms, when gas is flowed into preexisting amorphous



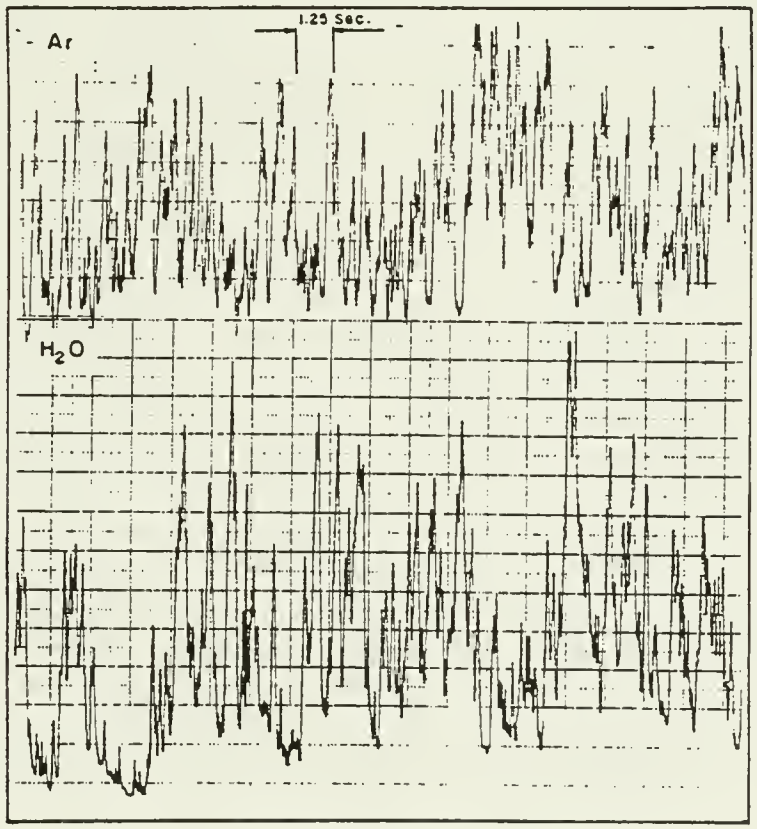


Fig. 3 - (top) A plot of the fluxes of water vs temperature, from a co-deposition of a 1:1 Ar-H_2O mixture at 25K, showing the ranges of ice-grain ejection. The timescale in this measurement did not allow the separation of single grains, which is shown at the bottom.

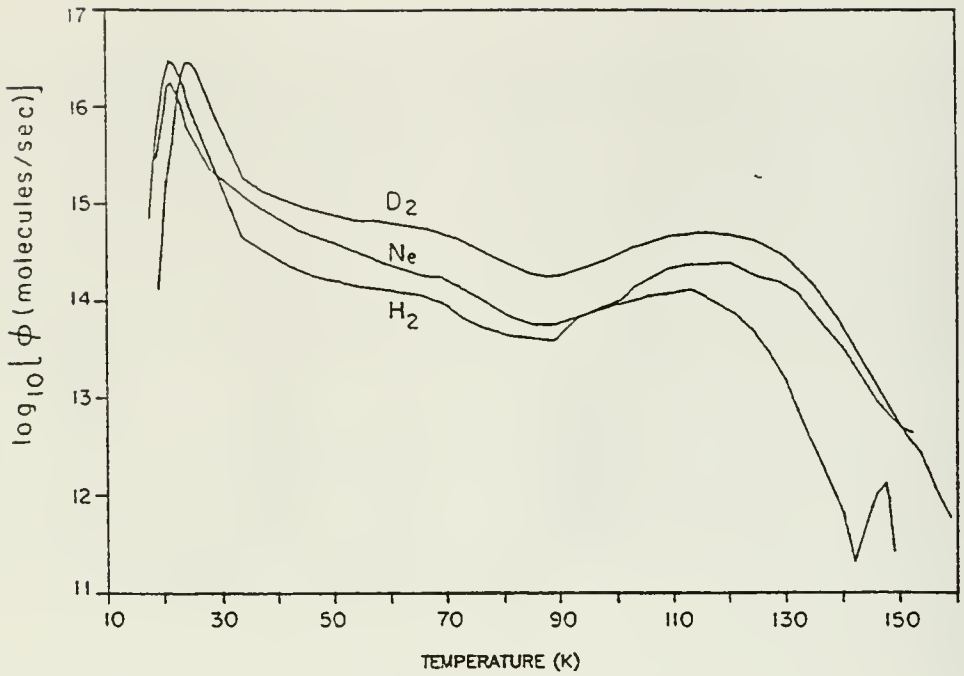
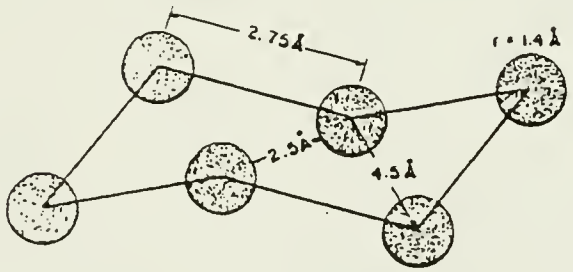


Fig. 4 - A plot of the fluxes of evolved H_2, D_2 and Ne vs temperature, from co-deposition, at 16-18K, of 1:1 gas-H_2O mixtures.



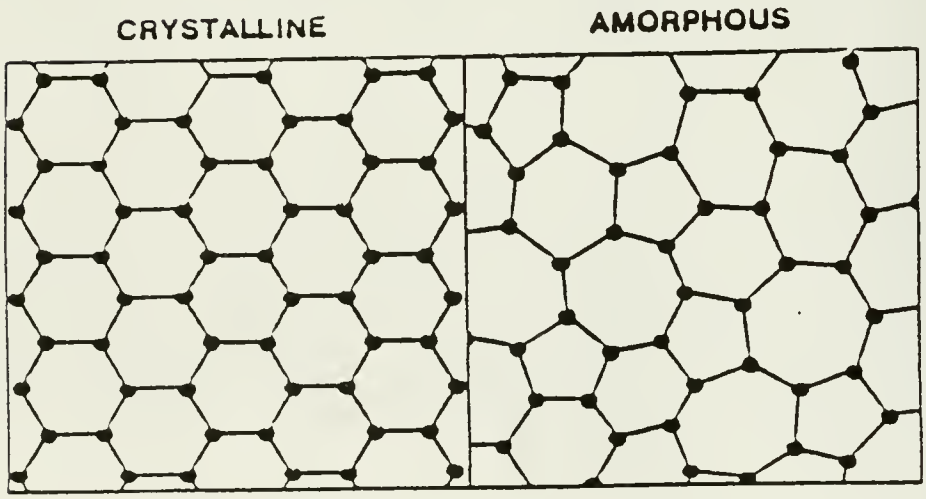


Fig. 5 - (top) The configuration of a hexagon of oxygen atoms in a cubic ice lattice (after Ref. 12). Two hydrogen atoms (not shown) are adjacent to each oxygen atom. The diameter of the free channel through the hexagon is 2.5 Å. (bottom) a schematic drawing of the hexagonal channel in crystalline and amorphous ice.

ice, the channels are blocked by the constant annealing of the ice, whereas in co-deposition of gas-water-vapor mixtures, the underlying gas-filled channels are blocked by the added layers of ice as well as by the annealing of the ice. Thus, the argon atoms are locked inside the wide channels in the amorphous ice matrix, either completely isolated from each other or in small clusters. Upon warming, when the ice anneals, the rearrangement of the water molecules opens some of the blocked channels. However, only when a channel opens all the way to the ice surface can the gas in it escape out. Thus, a dynamic percolation behavior results, where only a connection of many gas- filled domains in the ice, up to the surface, forms a minijet. While the larger gases (Ar, CO, CH_4, N_2 and Ne) emerge in minijets, the smaller H_2 and D_2 molecules emerge continuously and reversibly, since the channels in both amorphous and cubic ice are wide enough for them to get through without obstruction. The large jets are formed when many small channels open simultaneously, not to the surface, but to a weak region in the ice, where the gases build-up a pressure large enough to rupture the overlying ice. This rupture breaks the ice needles from their base and the outflowing gas propels them.

C. Competition among CO, CH_4, N_2 and Ar (5)

Up till now we discussed the trapping of ***single*** gases in the ice, where the gas could occupy all the available sites in the ice. With ***gas mixture***, however, the gases have to compete on these sites. With co-deposition of a mixture of H_2O: CH_4: Ar: CO (or N_2) = 1: 0.33: 0.33: 0.33, the results shown in Figure 6 were obtained. It can be seen that all three gases come out at exactly the same temperature ranges, but differ in their quantities. The quantities of trapped gases from this mixture as a function of ***deposition temperature*** between 28 and 100K are shown in Figure 7. It can be clearly seen that, while at 28K all four gases are trapped in the ice indiscriminantly, at 50-100K there are strong enhancements among the gases. These enhancements are observed with a 1:1 gas-water vapor mixture, where there is a competition among the various gases on the available trapping sites in the ice. With a gas-poor mixture (water vapor: gas = 100), the gases are trapped in the ice exactly in their proportion in the gas mixture, because there are sufficient trapping sites in the ice. The reasons for these enhancements include factors such as gas- water molecules interaction energy, size of the trapped gas atom or molecule and type of clathrate-hydrate formed (I for CH_4 and CO and II for N_2 and Ar). Note that between 28 and 100K, the total amount of trapped gas in the ice drops exponentially by many orders of magnitude. This sharp temperature dependance, together with the gas content found for comet Halley, might serve as an indicator to the temperature in the region of comet Halley's formation: several percent of trapped gas may suggest a formation temperature of about 50K (Figure 7).

This formation temperature is only for condensation of water vapor in the presence of various gases and their subsequent trapping in the amorphous ice, which is very temperature sensitive. The question then arises whether ice which was formed at higher temperatures and, consequently, trapped very little gas, was cooled in the solar nebula to 50K or even lower and then trapped some additional gases, bringing the gas content to the observed value. This situation was studied by us as well. In these experiments, pure water ice was condensed from the gas phase at various temperatures, was cooled down to 25K and gas was then flowed into it. These experiments show very clearly that the amount of gas which is trapped in the ice depends only on the highest temperature which the ice reached at some time and not on the temperature at which the gas was flowed into it. This is because the amorphous ice anneals in a stepwise, temperature dependant process, which closes a fixed fraction of the available trapping sites at each temperature. The conclusion from these experiments, regarding the formation of comets, is straightforward and

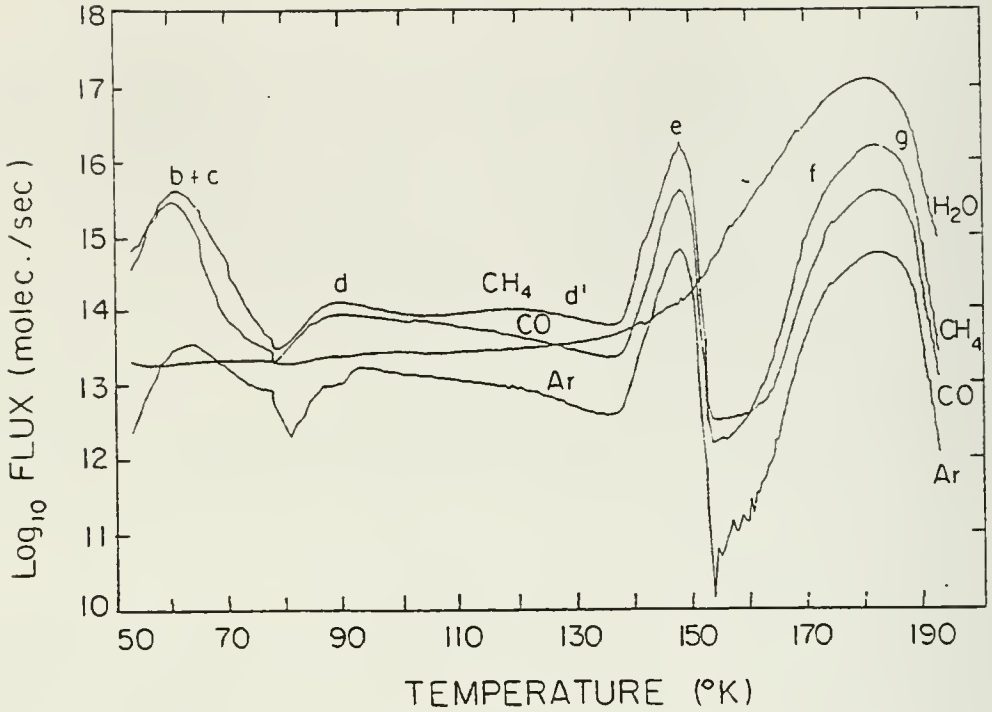


Fig. 6 - A plot of the fluxes of gas and water vapor vs temperature. The gas-rich amorphous ice was condensed at 50K. from a $H_2O:CH_4:CO:Ar$ = 1:0.33:0.33:0.33 mixture. The various ranges of gas evolution (b)-(g) are laoeled. Note the changes in gas evolution over 6 orders of magnitude.

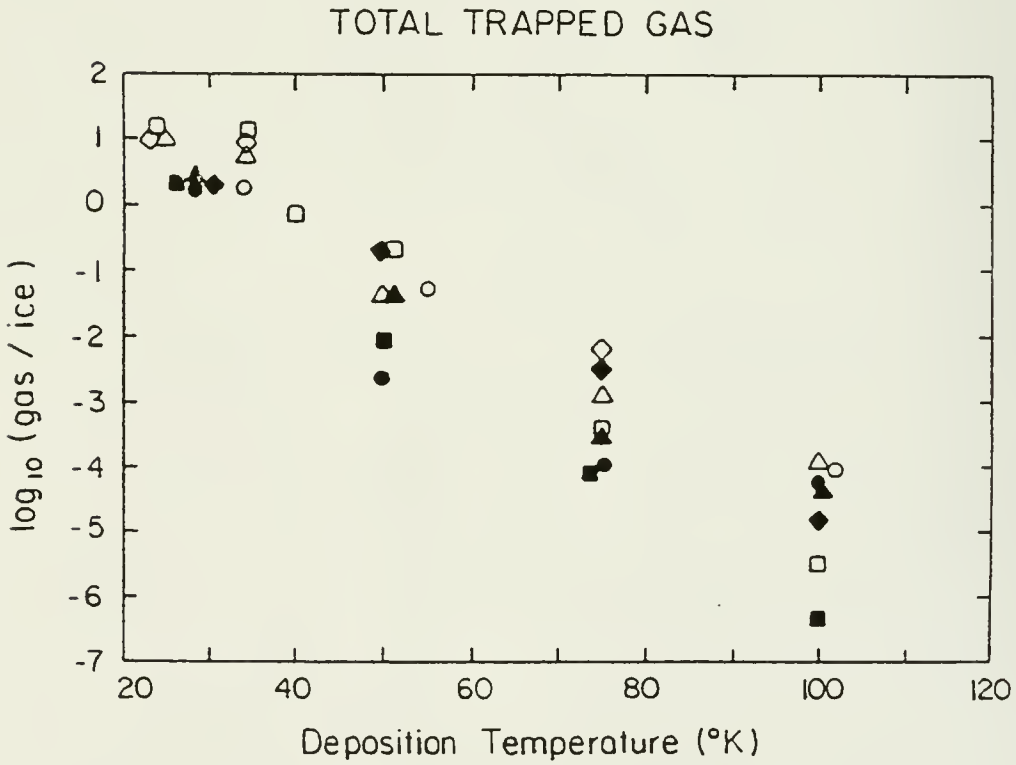


Fig. 7 - The total amounts of trapped gases vs deposition temperature of the water vapor-gas mixtures. - CH_4, Δ - CO, - N_2 and - Ar. Open symbols represent the results of the deposition of 1:1 single gas-water vapor. Solid symbols represent the results of the deposition of gas mixtures $H_2O:CH_4:Ar:CO$ (or N_2) = 1:0.33:0.33:0.33. Each point is an average of at least two experiments. (Some points were moved slightly on the temperature scale, to prevent overlapping).

will be discussed below.

Since the Giotto, Vega, IUE and sounding rockets observations all showed that CO is the major gas component of comet Halley, and it is more abundant than CH_4 by a factor ~3.5, (13) we focused our attention on the CO/CH_4 ratio in the gas which was trapped in the ice, at 50K, as a function of this ratio in the gas mixture. The amount of CH_4 which is trapped in the ice at 50K drops below that of CO only when the CO/CH_4 ratio in the gas mixture is increased to 100. The implication to the composition of the solar nebula is obvious, and will be discussed below. Hydrogen, diluting 35 times a 1:1 gas: water vapor mixture, had no effect on any of the gases. Hydrogen itself is trapped in the ice only below 20K.

D. Competition among the noble gases Ar, Kr and Xe

The competition among the noble gases was studied, with a mixture containing Ar:Kr:Xe = 10,000: 8:1, similar to the solar ratio of 20,000:8:1 (Table 2). This mixture was co-deposited with water vapor (1:1) between 30 and 75K. The enhancement factors for Kr/Ar and Xe/Ar (the ratio of the amounts of trapped gases divided by their ratio in the gas mixture), as a function of deposition temperature, are shown in Table 1. A hundredfold dilution with CO did not affect these enhancement factors.

Table 1
Trapping of an Ar:Kr:Xe = 10,000:8:1 mixture at 50-75K
resulted in the following enrichment factors

$T_{DEPOSITION}$	Kr/Ar	Xe/Ar
30K	1.0	1.0
50K	57.5	19.0
53K	92.5	25.0
60K	362.5	83.0
70K	812.5	780.0
75K	987.5	3600.0

The possible implications of these, temperature dependent, enrichment factors to the noble gas distributions on the terrestrial planets will be discussed later.

IV. THERMAL MODELLING OF COMETS AND ICY SATELLITES

Our experimental work was complemented by models, which describe the heating of comets and icy satellites by solar radiation or by the radionuclides in their dust. The experimental results on gas release were, of course, incorporated into these models.

A. Thermal models of pure ice (6)

Assume that at a given time t a cometary nucleus is a fast rotating perfect sphere of mass M(t) and radius R(t), consisting of water ice, either amorphous (at low temperatures), or crystalline.

If the mass m is chosen as the independent space variable ($0 \leq m \leq M$), the structure of the nucleus will be given by the following time dependent functions: the temperature T(m,t), the density $\rho(m,t)$, and the mass fractions of amorphous (A) and crystalline (C) ice $X_A(m,t)$ and $X_C(m,t)$ respectively. In a pure ice nucleus, $X_A + X_C = 1$, but, in principle, other constituents of the nucleus may be included, such

as gases, radioactive isotopes or dust.

The rate of change of the internal energy at each point of the nucleus is determined by the heat flux F(m,t) and the local energy sources (or sinks) q(m,t):

$$\partial u(m,t)/\partial t = \partial F(m,t)/\partial m + q(m,t), \quad (1)$$

where

$$F(m,t) = \kappa(T)\partial T(m,t)/\partial m \text{ ergs } s^{-1} \quad (2)$$

with $$F(0,t) = 0 \quad (3)$$

at the center, and at the surface:

$$F(M,t)=4\pi R(t)^2[(1 - A)S\langle\cos\phi\rangle/d_H(t)^2 - \varepsilon\sigma T(M,t)^4], \quad (4)$$

where A is the albedo, S is the solar constant, $\langle\cos\phi\rangle$ is the average value of the local solar zenith angle, which will be taken as 0.25 (the value corresponding to a uniformly illuminated sphere), d_H is the heliocentric distance (in AU), ε is the emissivity, and σ the Stefan- Boltzmann constant.

The crystallization reaction, which sets in when amorphous ice is heated to 136.8K, is practically instantaneous and may be described by

$$\partial X_A(m,t)/\partial t = -\lambda X_A(m,t), \quad (5)$$

where the time constant λ^{-1} should be short (on the order of seconds to minutes) for $T > 136.8K$ and infinite for $T < 136.8K$. The definition adopted for λ was

$$\lambda = \begin{cases} 1/10\ s^{-1}, & T \geq 136.8K, \\ 0, & T < 136.8K \end{cases} \quad (6)$$

Equations (1) - (5), constitute the evolution equations for the cometary nucleus, to be solved numerically for an assumed orbit, i.e. a given function $d_H(t)$.

The orbit of comet P/Halley was chosen. Other relevant parameters were: R = 2500 m, $\rho = 0.7$ g cm^{-3}, porosity p = 0.3, A = 0.1, $\varepsilon = 0.5$ and the latent heat of sublimation H = 2490 J·g^{-1}. The density and porosity were assumed constant and uniform throughout the calculations. The gas content of comet Halley (gas/water $\geq$ 0.2), together with our experimental results, suggest that Halley-type comets were formed in a region of the solar nebula where the temperature was ~50K. This is well below the transition point from amorphous to cubic ice (136.8K ± 1.6K). Hence, it seems quite certain that the water ice of cometary nuclei was formed in the amorphous state. In the region where the comets spent ~4.5 x 10^9 yr, they had ample time to cool down to the ambient temperature of ~10K. Therefore, the initial model for the evolutionary calculations was an amorphous ice sphere at a uniform temperature of 10K.

B. Thermal model with dust (7)

In numerical simulations of dust-covered cometary nuclei, it is generally assumed that the water vapor may escape freely through the dust mantle. Indeed, in the experiments of Storrs et al. the entire dusty ice ball evaporated, although more slowly than from a ball made of pure ice, leaving behind the fluffy network of dust. Thus, even if the entire comet is enveloped in a dust mantle, the cometary activity is not completely quenched. The dust layer, if sufficiently thin to permit easy diffusion of water vapor and gases, provides mainly thermal insulation. The main question addressed is, then, to what extent would the secular cometary activity be impaired by a growing, permanent dust mantle, permeable to water vapor? The initial stages of mantle formation would proceed as follows: Consider an outer layer of mass Δm of a spherical cometary nucleus. Assume that a fraction X_d of the mass is dust and the rest $X_i = 1 - X_d$ is water ice and other volatiles. The ratio X_d/X_i in comets is of the order of 1. When the ice sublimates and the gases escape, the

small dust particles are carried away with the gas flux. Only a fraction η of the dust mass $\Delta m_d = X_d \Delta m$ will be stored on the surface, forming a permanent dust mantle. It can be envisioned that η will increase with time, as more dust particles will stick to the thickening dust mantle. This process might be augmented if the dust particles are covered by a layer of organic material which, when initially cold, behaves like the minerals but, when warmed up near the surface, becomes sticky. The variation of the dust mantle's thickness and the rate of erosion of the nucleus with repeated revolutions may be obtained by numerical simulations of the evolution of a cometary nucleus in a given orbit for given η. The initial model for the one-dimensional ("fast rotator") numerical simulations is a homogeneous sphere of ice and dust, with an initial radius of 2500 m (the assumed radius is of no significant consequence). The crucial parameters of the model are the density of the nucleus ρ_n, the mass fractions of ice and dust X_i and X_d, respectively, and η - the fraction of dust mass which is assumed not to be blown away. Evolutionary sequences were calculated for different combinations of these parameters, to be compared with the pure ice model. The method of computation was described above, with some changes, (e.g. heat capacity, thermal conductivity) which take account of the dust.

C. Solar heating and crystallization (6,7)

A major feature of the comet model is the penetration of a crystallization front inward. When, due to solar heating, the outer layer of amorphous ice reaches 136.8K, it crystallizes into cubic ice. The energy released by this transformation, 90 J gr^{-1}, further heats the ice to 160K, where it transforms into hexagonal ice and, also, drives the transformation wave inward, until a layer is reached, where the temperature is lower than 136.8K. The next transformation event occurs when the surface has sublimated far enough so that solar heating will raise the temperature of an underlying amorphous ice layer to 136.8K, thus triggering another wave of transformation. A typical distance between the surface and the underlying amorphous ice boundary at which transformation can be triggered is 15 m.

Due to the insulating effect of the dust mantle, the rate of erosion of the surface is much slower than in the case of a bare nucleus and is constantly, although slowly, decreasing. The inward propagating heat wave, generated by the onset of crystallization, is weaker than in the case of pure ice. An appreciable fraction of the absorbed solar energy is absorbed by the dust, and only part of the energy induces further crystallization. Consequently, the thickness of the crystalline ice layer varies between ~15 and ~40 m. These findings are summarized in Figure 8, where the variation with time, over many orbits, of the outer radius R, due to sublimation and of r_c, the boundary between the outer-crystalline ice layer and the inner-amorphous ice core, are shown for a comet in Halley's orbit. Note the effects of ice density (ρ), dust to ice ratio (X_d/X_i) and the fraction of dust which remains permanently on the surface (η). The variation of temperature with heliocentric distance in comet Halley's orbit at the dust surface (T_d) and the ice surface (T_s) just below the dust mantle are shown in Figure 9. T_{max} = 400K, is the temperature reached by the dust surface at perihelion.

D. Radiogenic heating (8)

Both comets and icy satellites have considerable amounts of dust mixed with their ice. In the dust are incorporated radionuclides such as ^{40}K, ^{232}Th, ^{235}U and ^{238}U, all with decay constants of the order 10^{-10} - 10^{-11} yr^{-1}. In addition, the dust is very likely to contain ^{26}Al, (whose decay constant is 9.37 10^{-7} yr^{-1}) as suggested by the Mg excesses in the Allende meteorite and, independently, by the γ-ray detectors on the HEAO3 and SMM satellites. The radioactive heat output per gram

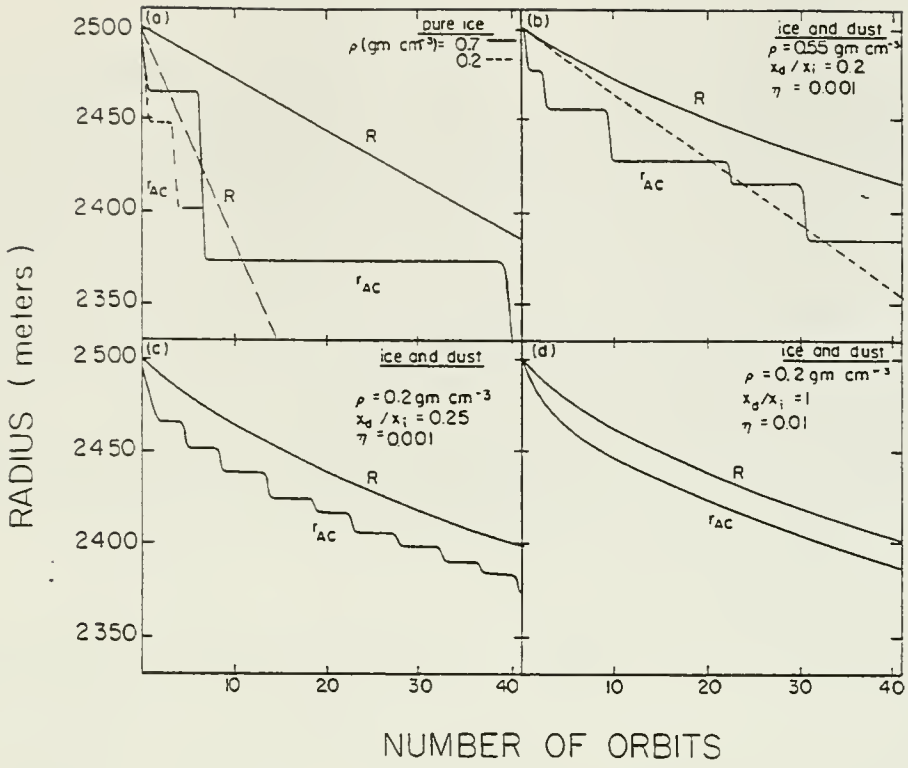


Fig. 8 - Variation with time of the outer radius R (initially 2.5 km) and the boundary r_{AC} between amorphous and crystalline ice within a comet nucleus model. The orbit assumed is comet Halley's and the time is measured in units of orbital periods. (a) corresponds to pure ice models of different densities: 0.7 g cm^{-3} (solid lines) and 0.2 g cm^{-3} (dashed lines). (b), (c) and (d) correspond to models of mixed composition; the density, dust to ice mass ratio and value of η are indicated. The dashed line in (b) represents the outer radius of a pure ice model of similar properties.

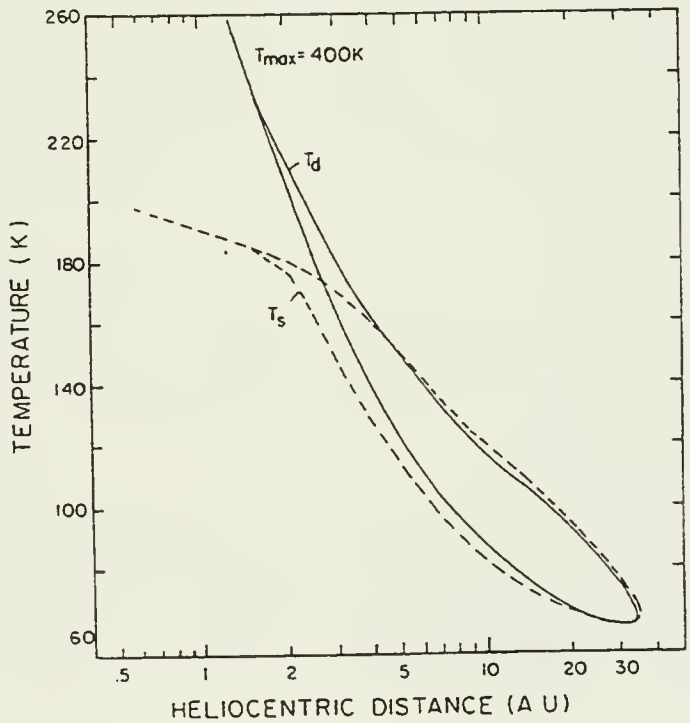


Fig. 9 - Variation of temperatures with heliocentric distance in comet Halley's orbit for the dust surface T_d (solid line) and the ice surface T_s below the dust mantle (dashed line). T_{max} is the maximum temperature reached by the dust surface at perihelion.

of comet nucleus material as a function of time is shown in Figure 10. The dust to ice ratio is 1 and the mass fractions of the radionuclides: $X(^{26}Al) = 5.6 \times 10^{-8}$, $X(^{40}K) = 5.65\ 10^{-7}$, $X(^{232}Th) = 2.76 \times 10^{-8}$, $X(^{235}U) = 3.13 \times 10^{-9}$ and $X(^{238}U) = 1.09 \times 10^{-8}$. Contrary to solar heating, which propagates from the surface inward, the heating of comets or icy satellites by the decay of radionuclides is most effective at the center, because the outer layers get rid of the heat more easily through the surface. Therefore, in an icy body made of amorphous ice, once a temperature of 137K is reached at the center, a wave of transformation from amorphous into crystalline ice will propagate outward. Similarly, melting will also begin at the center, if enough heat is generated.

V. IMPLICATIONS TO COMETS AND ICY SATELLITES

A. The temperature in the region of comet Halley's formation (11)

The results of the measurements of the Giotto and Vega spacecrafts, together with our experimental findings on the amount of gas trapped in ice at various temperatures, can set a rather strict limit on the temperature of the solar nebula in the region of comet Halley's formation: From the latest results on gas emission from comet Halley, as summarized by Lammerzahl (13), CO is the major gas released directly from the nucleus . Its amount, relative to water, is 5-7%. In order to trap in comet Halley's ice this much CO, its formation by condensation of water vapor in the presence of CO, had to take place in a region of the solar nebula where the temperature was 48±2K, as seen from Figure 7. The very steep slope of the curve of the amount of trapped gas vs deposition temperature sets a strict limit on this temperature. As shown in section IIIC, the condensation of water vapor into amorphous ice could not have taken place at a higher temperature, with subsequent cooling and flow of gas into the ice, since in this case, as shown experimentally, the amount of trapped gas depends only on the highest temperature at which the ice was formed or resided.

The experimental results on the amount of gas trapped in amorphous ice which was deposited at various temperatures from a 1:1 gas:water vapor mixture, are directly applicable to the gas content of comet Halley, since in the solar nebula the ratio of CO or CH_4 to water vapor was near unity, as shown in Table 2.

Table 2
Abundances of gases in the solar nebula, relative to H_2, calculated from the atomic abundances of Anders, F. and Ebihara, M. (Geochim. Cosmochim. Acta. 46, 2363-2380, (1982)) assuming that the molecules listed are the major ones in the nebula

All C as CH_4			All C as CO
H_2O*	1.48×10^{-3}		5.9×10^{-4}
CH_4	8.9×10^{-4}		0
CO	0		8.9×10^{-4}
N_2		9.1×10^{-5}	
Ne		$2.83\ 10^{-4}$	
Ar		$7.65\ 10^{-6}$	
Kr		$3.33\ 10^{-9}$	
Xe		$3.2\ 10^{-10}$	

*If other oxygen bearing molecules, such as MgO, are taken into account, the H_2O abundance should be lower by about 20%.

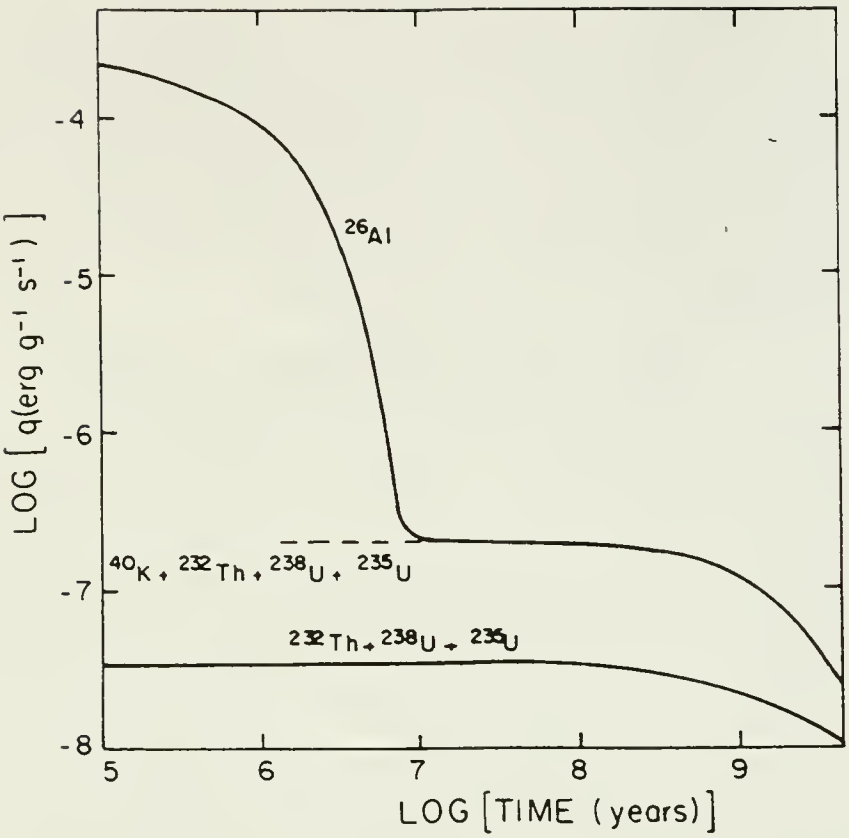


Fig. 10. - Radioactive heat output per gram of comet nucleus material as a function of time. The mass fraction of ^{26}Al is 5.6×10^{-5}; those of ^{40}K, ^{232}Th, ^{235}U and ^{238}U are given in the text. Before $t = 10^7$ yr, when the decay of ^{26}Al is the main energy source, the contribution of the other radioisotopes is shown by the dashed line. Lower curve shows the heat ourput due to the heavy elements alone.

A formation temperature for comet Halley of 48K is surprisingly close to the temperatures observed by IRAS for the circumstellar dust shells around α PsA (55K) and ε Eri (45K). The temperatures of the dust shells around α Lyr (Vega - 85K) and β Pic (100K) are considerably higher, and comets formed there would have gas/ice ratios of 10^{-3} - 10^{-4}. The agreement between the comet formation temperature which was deduced from the present experimental study, and those observed for two out of four circumstellar dust shells, lends credence to the suggestion that Halley type comets were formed outside the region of planet formation. Moreover, Duncan et al. (14), Weismann (16) and Delsemme (15) propose that the orbits of short and long period comets can be explained by two different regions of formation: the short period comets were formed in the extended dust shell (the "Kuiper belt") at ~40K and remained there unpreturbed, whereas the long period comets were formed in the Uranus-Neptune region, at ~80K and were ejected from there into the Oort cloud and, simultaneously, into the inner region of the solar system. Consequently, a much larger flux of high temperature comets, as compared with the flux of low temperature comets, can be expected on the Terrestrial Planets. A formation temperature of 80K for the long period comets should mean that their gas content is in the ~10^{-4} range, as compared with 10^{-1}-10^{-2} for the short period comets.

B. The gas composition in the region of comet Halley's formation (11)

With a ratio of CO or CH_4 to H_2O in the nebula being close to 1 (Table 2), the regime of competition among the various gases on the available trapping sites in the amorphous ice should be applied. As discussed in section III C, at 50K, the trapping of CO overcomes the trapping of CH_4 only in a mixture with CO: CH_4 = 100. Thus, in order for CO to be the dominant gas in the icy nucleus of comet Halley, the CO/CH_4 ratio in the region of comet formation had to be $\geq$ 100. Simonelli et al. (17) also reach the conclusion that CO comprised 75- 90% of the carbon in the outer solar nebula, if Pluto and Charon were formed directly from the solar nebula. Lunine (18) also reaches the conclusion that the CO/CH_4 in the solar nebula was 100. Knacke et al. (19) set a limit of CO/CH_4 > 100 in several molecular clouds.

C. On the timescale of comet formation and thermal evolution of icy satellites (8)

A study of the radiogenic heating of icy bodies by ^{26}Al, ^{40}K, ^{232}Th, ^{235}U and ^{238}U (section IV D), showed that in order to maintain the cometary ice in the amorphous and, hence, gas-rich form, the main heat generating radioisotope - ^{26}Al - had to be in an initial abundance of $<4\times10^{-9}$. This initial abundance is a 100 times lower than that in the Allende meteorite. Hence, a lower limit of ~5×10^{6} years for the formation time is implied, in order for the ^{26}Al to decay from its initial abundance. In addition, the coexistance of molten cometary cores and extended amorphous, gas- rich, ice mantles is ruled out.

Larger icy spheres (r > 100 km) reach the transformation temperature even in the absence of ^{26}Al, due to the decay of the other radionuclides. As a result, the outermost icy satellites in the solar system, which might have been formed from ice in the amorphous state, have probably undergone crystallization. Since this process proceeds from the center outward, huge amounts of trapped gases are pushed in front of the outward propagating transformation wave. This could give rise to eruptive activity when the gas is released near the surface, and to chaotic terrain such as observed on Miranda.

D. Could have comets provided the terrestrial planets with their noble gases?

The experimental results on the trapping of Ar, Kr and Xe in amorphous ice are discussed in section III D. The enrichment factors Kr/Ar and Xe/Ar, as a function of deposition temperatures are shown in Table 1. On Earth, these enrichment factors are: $Kr/^{36}Ar = 74$ and $Xe/^{36}Ar = 48$. From Table 1, they can be obtained (from an Ar:Kr:Xe = 10,000:8:1 mixture) by co-deposition this noble gas mixture with water vapor at 52-55K, quite close to the 48±2K, which was deduced to be the formation temperature of comet Halley, from its CO content. Thus, the Earth could have obtained its entire budget of Ar, Kr and Xe from a single hit by a R = 42 km, ρ = 0.5 g cm^{-3} comet, which was formed around 50K. Mars, which has a similar $Kr/^{36}Ar$ ratio, could have been supplied with its noble gases by a smaller comet which, still, had to be formed at about 50K. On Venus, the $Kr/^{36}Ar$ and $Xe/^{36}Ar$ ratios are solar and the abundance of ^{36}Ar is 2-3 orders of magnitude larger than on Earth. The solar ratio could have resulted from a hit by a comet which was formed at 30K, since at this temperature the noble gases are trapped in the ice in their proportion in the gas mixture. (Table 1). Moreover at 30K, Ar, Kr and Xe are trapped 2 to 3 orders of magnitude more efficiently than at 50K (Figure 6). Hence, the larger amounts of these gases on Venus.

In conclusion, the Ar, Kr, Xe patterns on the Terrestrial Planets could have been obtained by a single hit of each planet by a comet which was formed at either ~30K (Venus) or ~50K (Earth and Mars). A single hit is required since, if many hits are required, mixing between 30K and 50K comets could not be avoided. These low temperature comets came from the stable Kuiper Belt, from which a large flux of comets should not be expected. The large flux of comets which hit the Terrestrial Planets and the icy satellites originated in the Uranus- Neptune region, from which they were scattered both inward and outward, into the Oort cloud. These, however, were formed at 80- 90K and their noble gas content was 3-4 orders of magnitude smaller (Figure 6).

E. The activity of cometary nuclei (6,7)

The experimental results on gas release from the ice upon its warming, were combined with the modelling results on the penetration of a heat wave into the nucleus, to produce a reasonable picture of the activities observed on comet Halley:

In our dusty comet models (section IV C) an outer layer of crystalline ice, about 15-40 m thick, was found to overlay the inner amorphous ice bulk of the nucleus. With comets formed at 48K, most of the trapped gas (except the clathrate-hydrate) is released from the ice in ranges (e) and (f) - during the transformations of the amorphous ice into cubic and then hexagonal ice (Figure 2). As shown experimentally, with only a ~100 μm thick ice layers (section III B), gas emission from the ice cannot proceed freely and is accompanied by the ejection of ice grains, which are propelled by gas jets. A 15-40 m thick crystalline ice layer would certainly block gas escape more efficiently than a 100 μm thick ice layer. Hence, it can be easily envisioned that gas filled pockets will be formed in the ice, when the gases will be released from the amorphous ice upon its transformation into cubic and hexagonal ice. These pockets could be permanent or form temporarily by dynamic percolation processes. When the pressure in such a pocket exceeds the tensile strength of the overlying crystalline ice layer, an explosion will occur. Numerous such explosions were indeed observed on comet Halley both from the ground and by IUE. In one (20) an amount of gas equivalent to a frozen 30x30x10 m^3 chunk was observed. These dimensions are in good agreement with our calculation of a 15-40 m

thick crystalline ice layer.

Such an explosion will remove the overlying, choking, dust layer. Moreover, its vibrations might trigger the explosion of adjacent gas- filled pockets. Thus, by enhanced evaporation of a single small crater or by combination of several adjacent small craters, a large crate such as observed on comet Halley can be produced.

F. The possible formation of a hydrogen coma around comets at large heliocentric distances (9)

An experimental test - the detection of a hydrogen coma around comets at large heliocentric distances - can be proposed for determining whether comets were formed by the agglomeration of unaltered, ice-coated, interstellar dust grains. The laboratory experiments (section III B) showed that amorphous water ice traps H_2, D_2 and Ne below 20K and does not release them completely until the ice is heated to 150K (Figure 4). Gas/ice ratios as high as 0.63 are obtainable. Thus, if the ice-coated interstellar grains were not heated above ~110K prior to their agglomeration into cometary nuclei, the inward propagating heat wave, when the comets approach the sun, should release from the comets a continuous flux of molecular hydrogen. This flux would exceed that of water molecules (and, hence, H_2 production by photolysis) at ~3 AU preperihelion and ~4 AU post-perihelion.

G. Thermal evolution of comet P/Temple 1 (10)

Comet P/Temple 1 was chosen for detailed thermal modelling, as a representative of the group of targets for the CRAF and ROSETTA missions. It has a period of 5.5 years, an eccentricity of 0.52 and a perihelion distance of 1.5 AU. The model was constructed in the same manner as the ones described in sections IV B and C. Several evolutionary tracks were computed, spanning more than 100 revolutions, for various combinations of the following parameters: ρ = 0.2 or 0.55 g cm^{-3}; dust/ice ratio Xd/Xi = 1 or 0.2; the fraction of dust mass which accumulates permanently on the surface η = 0.001, 0.01 or 1. Six parameters were calculated for each combination: T_s - the temperature of the dust layer on the surface; T_i - the ice temperature of the ice just underneath the dust layer; T_{-10} - the ice temperature 10 m below the surface; $R_o - R_s$, in m - the difference between initial radius (5 km) and surface radius at a given orbit, or the thickness of the ice which has been lost by sublimation; $R_s - r_{ac}$, in m - the difference between the surface radius and the radius of the interface between crystalline and amorphous ice or, the thickness of the crystalline ice layer overlying the inner core of amorphous ice, Δr, in cm - the thickness of the dust mantle.

The following conclusions may be drawn from these results:

1. The temperature at the surface of the dust layer is weakly dependant on the assumed parameters, for given albedo (0.04) and emissivity (0.5). Thus, at perihelion, T_s varies between 235 and 268K, with an average value of 252±17K.

2. The temperature of the ice surface just beneath the dust mantle is very nearly constant. T_i at perihelion is between 176 and 187K, except for the extreme case of η = 1.

3. For all models T_s increases, T_i decreases and $\dot{R}$ decreases slowly with repeated revolutions, because of the growth of the dust mantle, which is of the order of cm-m, depending on η.

4. The temperature at a depth of 10 m is practically constant with time and varies very little from one set of parameters to another. Thus, we may expect a temperature of 163K with an uncertainty of 3%. Moreover, because this temperature is above the transition point from amorphous into crystalline ice, the ice down to 10 m below the surface is crystalline.

5. The crystalline ice shell overlying the inner core of gas- laden amorphous ice is at least 40 m thick and may be as thick as 240 m. The crucial parameter in this respect is the dust to ice ratio. The higher this ratio, the thinner the crystalline ice layer becomes. The layer thickens with number of revolutions.

In conclusion, since even the lower limit of 40 m for the thickness of the crystalline ice layer is significantly larger than the depth of penetration currently planned for the CRAF and ROSETTA probes, we may conclude that they will, most probably, sample crystalline ice. They may tap a gas-filled pocket, with unpredictable results - explosions etc. If the target comet resembles comet Halley, where several active craters were found, it might be worthwhile to dig into such a crater, at the bottom of which the more active gas-laden amorphous ice should be exposed.

VI. REFERENCES

1. A. Bar-Nun, G. Herman, M.L. Rappaport and Yu. Mekler. Ejection of H_2O, O_2, H_2 and H from water ice by 0.5-6 KeV H^+ and N_e^+ ion bombardment. Surface Sci., 150, 143-156 (1985).

2. A. Bar-Nun, G. Herman, D. Laufer and M.L. Rappaport. Trapping and release of gases by water ice and implications for icy bodies. Icarus, 63, 317-332 (1985).

3. A. Bar-Nun, J. Dror, E. Kochavi and D. Laufer. Amorphous water ice and its ability to trap gases. Phys. Rev. B. 35, 2427-2435 (1987).

4. D. Laufer, E. Kochavi and A. Bar-Nun. Structure and dynamics of amorphous water ice. Phys. Rev. B. 36, 9219-9227 (1987).

5. A. Bar-Nun, I. Kleinfeld and E. Kochavi. Trapping of gas mixtures in amorphous water ice. Phys. Rev. B. 38, 7749-7754 (1988).

6. D. Prialnik, and A. Bar-Nun. On the evolution and activity of cometary nuclei. Astrophys. J. 313 893-905 (1987).

7. D. Prialnik and A. Bar-Nun. The formation of a permanent dust mantle and its effect on cometary activity. Icarus, 74, 272-283 (1988).

8. D. Prialnik, A. Bar-Nun and M. Podolak. Radiogenic heating of comets by ^{26}Al and implications for their time of formation. Astrophys. J. 319, 993-1002 (1987).

9. A. Bar-Nun and D. Prialnik. The possible formation of a hydrogencoma around comets at large heliocentric distances. Astrophys. J. Lett. 32, L31-L34 (1988).

10. A. Bar-Nun, E. Heifetz and D. Prialnik. Thermal evolution of comet P/Temple-1, representing the group of targets for the CRAF and ROSETTA missions. Icarus, in press (1989).

11. A. Bar-Nun and I. Kleinfeld. On the temperature and gas composition in the region of comet formation. Icarus, in press (1989).

12. P.V. Hobbs. Ice Physics, Clarendon Press, Oxford (1974).

13. P. Lammerzahl. Gas emission from Comet Halley. in E. Grun. 3 Kometenwerstatt. 14-15 Nov. 1988.

14. M.T. Duncan, T. Quinn and S. Tremain. The origin of short period comets. Astrophys. J. 328, L69-L73 (1988).

15. A.H. Delsemme. Have comets played a role in the primary organic synthesis. Preprint F.7.1.2 COSPAR, Helsinki (1988).

16. P.R. Weissman. The Oort cloud and the galaxy: dynamical interactions. in The Galaxy and the Solar System, eds. R. Smoluchowski, J.N. Bachall and M.S. Matthews. University of Arizona Press, pp.204-237 (1986).

17. D.P. Simonelli, J.B. Pollack, C.P. McKay, R.T. Reynolds and A.L. Summers. The carbon budget in the outer solar nebula. Submitted to Icarus (1988).

18. J.I. Lunine. Primitive bodies: molecular abundances in comet Halley as probes of cometary formation environments. Preprint (1989).

19. R.F. Knacke, Y.H. Kim, K.S. Noll and T.R. Geballe. Search for interstellar methane. Astrophys. J. 298, L67-L69 (1985).

20. P.D. Feldman, H.A. Weaver, T.N. Woods, M.F. A'Hearn, L.A. McFadden and M.C. Festou. The 18-19 March 1986 outburst of Comet Halley as observed by the IUE. Abstract No. 20.10, DPS Meeting, Paris. Bull. Amer. Astron. Soc. 18, 795 (1986).

MODIFICATIONS OF COMET MATERIALS BY THE SUBLIMATION PROCESS: RESULTS FROM SIMULATION EXPERIMENTS

E. Grün, et al.
Max-Planck-Institut für Kernphysik
Heidelberg, FRG

MODIFICATIONS OF COMET MATERIALS BY THE SUBLIMATION PROCESS: RESULTS FROM SIMULATION EXPERIMENTS

E. Grün[1], J. Benkhoff[2], A. Bischoff[2], H. Düren[2], H. Hellmann[3], P. Hesselbarth[1], P. Hsiung[4], H.U. Keller[5], J. Klinger[6], J. Knölker[2], H. Kochan[3], G. Neukum[7], A. Oehler[7], K. Roessler[4], T. Spohn[2], D. Stöffler[2] and K. Thiel[8]

[1]Max-Planck-Institut für Kernphysik, Heidelberg, FRG; [2]Institut für Planetologie, WWU, Münster, FRG; [3]Institut für Raumsimulation, DLR, Köln-Porz, FRG; [4]Institut für Chemie I, KFA, Jülich, FRG; [5]Max-Planck-Institut für Aeronomie, Katlenburg-Lindau, FRG; [6]Laboratoire de Glaciologie et Geophysique de l'Environment, Saint-Martin-d'Heres, France; [7]Institut für Optoelektronik, DLR, Oberpfaffenhofen, FRG; [8]Abteilung Nukelarchemie, Universität Köln, Köln, FRG.

Abstract

Sublimation experiments with ice–mineral mixtures were carried out at the DLR Space Simulator in order to study cometary processes. First experiments were done with cylindrical samples of 30 cm diamter and 15 cm thickness which consisted of water-ice or water- and CO_2-ice mineral mixtures. These experiments have already yielded important and new insights into the modifications of the sample which are caused by the sublimation of the ices due to insolation: (1) Spectral reflectance measurements show the reduction of volatile materials in the surface layers of the sample and the formation of a permeable refractory dust mantle, (2) the dust mantle as well as the residuals of emitted dust particles have a low density (~ 0.1 g/cm^3) aggregate structure, (3) metamorphosis of the original non-coherent ice into hard but still porous water ice has been observed under the dust mantle and (4) fractionation of ices of different volatility occurs during their sublimation. A qualitative model is described which can explain the observed modifications of the sample material.

Key words: Comet simulation, sublimation fractionation, ice-mineral mixtures

Introduction

Halley measurements. An active comet like comet Halley loses by sublimation a surface layer of the order of 1 m thickness per perihelion passage. In situ measurements (Krankowsky and Eberhardt, 1989) showed that water ice is the main constituent which contributes to the gas emission although even more volatile species have been identified (Table 1).

Dust particles which were embedded in the ices are carried by the sublimating gases. Measurements of the chemical composition of cometary grains indicate that they are composed of silicates of approximate chondritic composition (Jessberger et al., 1988) and of refractory carbonaceous material (Kissel and Krüger, 1987) at a mass ratio of about 2:1.

Table 1: Gas composition of Comet Halley (Krankowsky and Eberhardt, 1989) and typical sublimation temperatures (i.e. temperature at a vapor pressure of 0.1 Pa).

Species	Abundances (Vol%)	Temperature (K)
H_2O	80	196
CO	10-12	37
CH_4	~2	48
NH_3	1-2	124
CO_2	1.5	105
N_2	<2	33
H_2CO	~1	99
HCN	~0.1	152

Previous comet simulations. In the past there have been several attempts to experimentally study the sublimation process of mixtures of ices, minerals and carbonaceous compounds. Extensive work was carried out by Soviet groups in Dushanbe and Leningrad, who heated up ice samples electrically or irradiated them with light sources inside a cold chamber (Kajmakov and Sharkov, 1972; Ibadinov, 1989). Among the interesting findings was the formation and ablation of dust mantles during the sublimation process. In another approach (Saunders et al., 1986; Storrs et al., 1988), silicate minerals and organic compounds covered with water ice were exposed in a vacuum chamber. After sublimation of the water ice highly porous filamentary sublimate residues were found for some classes of phyllosilicate minerals or in cases when organic compounds (tar) were present.

KOSI experiments. The approach by the KOSI-team (Kometensimulation) (Grün et al., 1987; Kochan et al., 1989a; Klinger et al., 1989a) focuses on the investigation of cometary processes at relevant scales. The scale of the simulation experiments is determined by the scale for the heat transport into the interior (diurnal thermal skin depth) and the scale of the gas interaction (mean free path length) above the surface which both have been estimated to be of the order of 10 cm. Comet simulation experiments are performed in the big Space Simulator of DLR, Cologne, which allows the study of model comets of up to one meter dimensions.

Experimental Set-Up

Space Simulator. The Space Simulator is a large vacuum chamber with an inner liquid nitrogen cooled shroud and a separate light source (Xenon lamps) which insolates a <1 m sized target with up to 1.3 kW light power (Kochan et al., 1989b). The spectrum of the lamps matches roughly the solar spectrum in the visible wavelength regime. The background pressure in the chamber is $\leq 10^{-4}$ Pa. The shroud keeps the background temperature at ~77 K and thereby acts as an effective pump for less volatile gases like water and CO_2.

Sample container. The cylindrical sample container for the first 3 KOSI experiments has a diamter of 30 cm and a hight of 15 cm (Fig. 1). For easy charging the container with the ice-dust mixture is mounted horizontally, while during the experiment it is tilted by 45° in

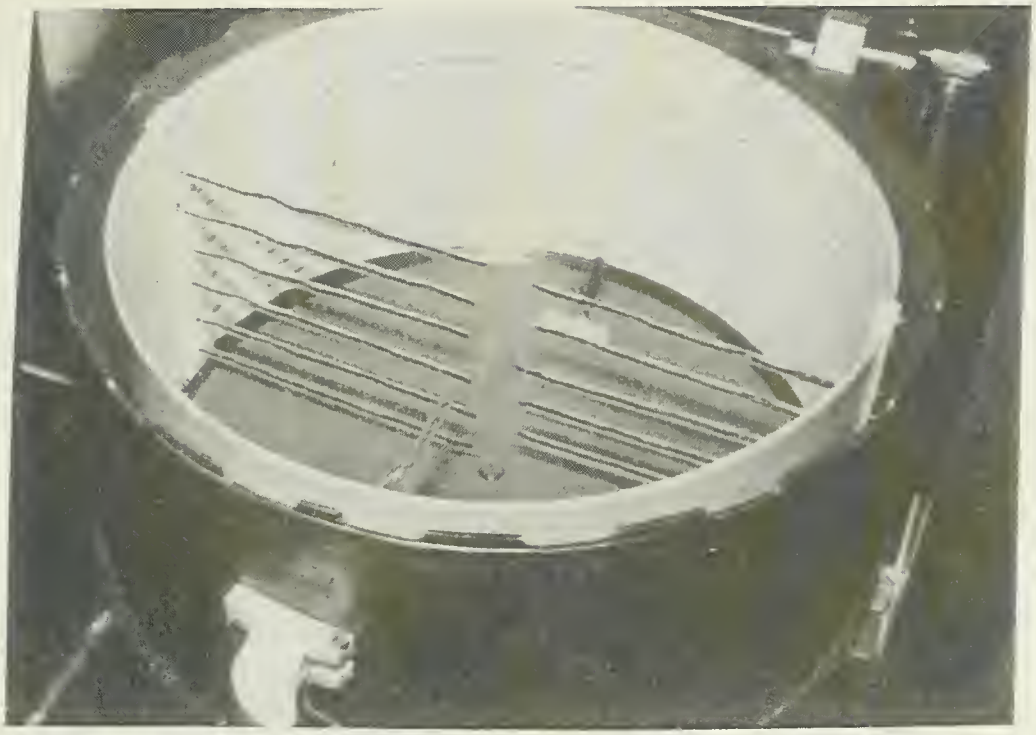


Fig. 1 Sample container used for the comet simulation experiments. Its dimensions are 30 cm diameter and 15 cm depth. Thermocouples sticking from both sides into the interior. A teflon cylinder insulates the sample from the liquid nitrogen cooled outer copper shell.

order to be effectively insolated. The bottom of the sample container is a liquid nitrogen cooled copper plate. The inner wall of the container is made out of teflon in order to shield the sample material from the outer copper wall. A motor driven cover protects the sample during preparation from ambient temperature and contaminants. Several temperature sensors are installed in order to measure the sample temperatures at various depths.

Diagnostics. At some distance from the sample container a range of instruments are mounted to a rectangular support structure in order to analyse the emitted gas and dust as well as to observe in situ the modifications of the sample during insolation (Fig. 2). Dust collectors, piezo-electric impact detectors as well as television cameras determine the rate, the size and the speed of the emitted dust particles. Ionization gauges and mass spectrometers measure the flux, the composition and the speed of the released gases. The sample itself is monitored by TV cameras.

Sample materials. The sample material consists of ices (H_2O, CO_2) and minerals simulating cometary dust. The dust analogue materials were selected on the basis of (1) the observed mineralogical composition of solar system materials and (2) the availability of the analogue materials in large quantities. The mineralogy of carbonaceous chondrites (Kerridge and Matthews, 1988), of interplanetary dust particles (Mackinnon and Rietmeijer, 1985; Sandford and Walker, 1985), and the data of the comet Halley obtained by the GIOTTO mission (Jessberger et al., 1988) justify the selection of Mg-rich silicates of olivine and pyroxene composition, of sheet silicates and of carbonaceous material. Carbon (soot) has been chosen as a simple substitute for carbonaceous matter, and montmorillonite and kaolinite as representatives of the sheet silicates. Olivine and pyroxene are the main constituents of powdered dunite. The dust components, compositions and grain size characteristics are listed in Table 2. All components are in fact mineral mixtures as they contain accessory minerals in the order of 5 to 10%. Carbon which has a grain size of only 23 nm is suspended in water activated by a sodium salt of a naphtaline sulfoacid condensation product. The grain size of the other mineral powders is predominantly below ~ 4 μm.

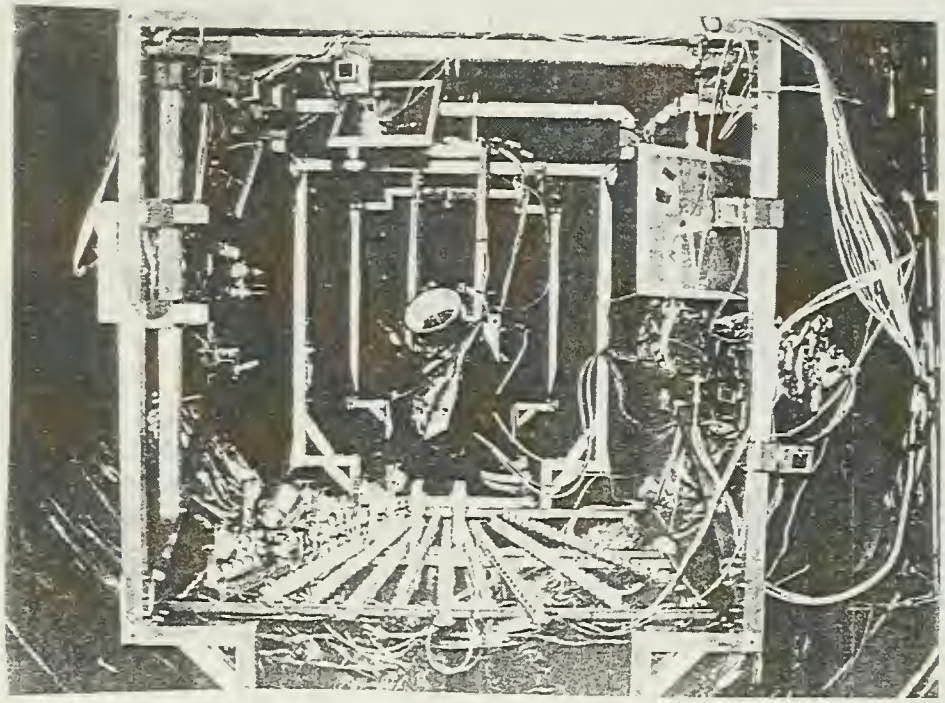


Fig. 2 View into the opened Space Simulator. In the center the sample container is visible. The rectangular structure supports mirrors (top and right), gas diagnostics (upper left) and dust detectors and collectors (bottom). Outside the cylindrical cold shroud can be seen.

Sample preparation technique. So far, all samples were prepared from dust mixtures suspended in water. Non-coherent, fluffy ice-dust mixtures were prepared by spraying these suspensions into liquid nitrogen (cf. Saunders et al., 1986). This method was chosen for simplicity and efficiency (abuot 10 kg of sample material are needed for a simulation). Because of the high content of minerals in the water (ca. 10% by weight) the individual grains were not completely separated from each other in the suspension. Therefore dust aggregates found after sublimation of the ice were preformed during the freezing of the suspension. Sample preparation techniques which avoid the mutual contact of dust particles in the presence of liquid water are under development (e.g. condensation from the gas phase).

The propellant gas used for the spraying was nitrogen in the first two experiments (KOSI-1 and 2). For the KOSI-3 experiment we used CO_2 as propellant gas. Thereby another volatile ice component was produced. The content of CO_2-ice in the mixture was measured by gas chromatography of released CO_2-gas upon heating of witness samples (Roessler et al., 1989). The composition of the samples of the first 3 KOSI experiments is given in Table 3.

The technique of sample preparation has been standardized. The water-mineral suspensions were treated for 8 - 12 hours by shaking and were kept for 15 minutes in an ultrasonic bath at a frequency of 20 kHz (Bischoff and Stöffler, 1988). The grain size distribution of the mineral dust was controlled by a laser granulometer. In mixtures of all components including carbon the median grain size was ~4 µm. The control of the grain sizes in the suspension together with the variation of the dust composition was intended to get an idea of the effects caused by the contact of liquid water with the different mineral grains which could not be avoided in these initial experiments.

For spraying the suspension we used a special device which is shown in Fig. 3. The suspension was constantly stirred before it flowed through an ultrasonic bath and

Table 2: Properties of mineral components for synthetic cometary samples (weight %)

Material name	Mineralogical composition	Nominal grain size parameters	Density of the individual minerals (g/cm^3)
HD-Ton	90-92% kaolinite 5% illite 93% montmorillonite	min. 90% < 2 µm	2.58-2.68
Bentonite ASB 350	93% montmorillonite 3% feldspar 2% mica 2% quartz and cristobalite	median diameter: 4 µm 99% < 35 µm	1.95-2.06 2.53-2.62 2.77-2.94 2.65 2.30-2.35
Dunite	84-91% olivine 5-11% orthopyroxene 1.7-2.2% chlorite 1.0-2.2% serpentinite 0.1-0.4% talc 0.5% spinel	median diameter: 4 µm 95% < 30 µm	3.3 3.2 2.64-2.74 2.51-2.56 2.73-2.82 3.60-3.95
Derussol VU 25/L	25% soot in H_2O with ion activated wetting agent	ca. 23 nm	max. 2.23

Table 3: KOSI samples; initial composition (main constituents) and properties

	KOSI-1 May 87	KOSI-2 April 88	KOSI-3 Nov. 88
Composition (weight %)			
H_2O ice	90%	90%	78%
CO_2 ice	-	-	14%
total dust content	10%	10%	8%
Relative mineral composition			
olivine	-	70	90
montmorillonite	-	30	10
kaolinite	100	-	-
carbon	1*	1	1
albedo	~ 0.2	0.06	0.18
density (g/cm^3)	0.4	0.6	0.5
porosity	n.d.	0.4	0.5
penetration strength (MPa)	n.d.	0.2	0.2

* formed large aggregates; n.d.: not determined

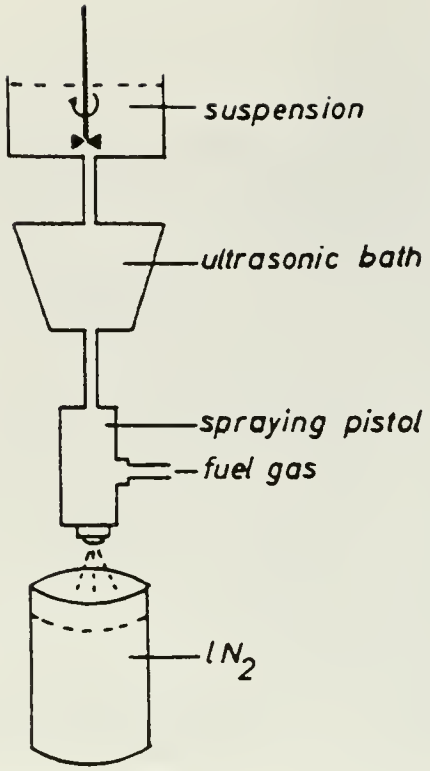


Fig. 3 Method for the production of synthetic cometary samples (schematic).

entered a spraying pistol (nozzle diameter: 1.5 mm) which was directed into a sieve catcher positioned at some depth within the liquid nitrogen. The produced "snow" was taken directly into the sample container of the space simulator. At the same time a second sample container was filled in the same way and analysed in a glove box (Roessler et al., 1989). There it was cooled by liquid nitrogen and finally kept in a low temperature room at about 250 K for physical characterization of the sample.

Considering the relatively short times the minerals were exposed to liquid water and ice before the sublimation experiment is performed we can exclude chemical reactions between H_2O and olivine, pyroxene and montmorillonite, respectively. Such reactions may take place in permafrost over geological time periods (Rietmeijer, 1985).

Sample characterization. Analyses performed with the samples before and after the sublimation experiment include the measurement of reflectance spectra (albedo) both at visual and near-infrared wavelengths, determination of the penetration strength (Thiel et al. 1989) and of the density and porosity (cf. Table 3). Attempts to produce polished sections of aliquots of KOSI-2 samples were made (Stöffler et al., 1989) based on techniques used in snow research (e.g. Good, 1982, 1987). In this method the porous samples are impregnated with liquid diethylphtalate at ~268 K and then frozen at ~255 K. Polished sections are prepared by a sledge microtome. Preliminary studies of these sections with a polarized microscope indicate that the dust grains are contained either in spherical aggregates of dust and ice or in irregular polycristalline sections of ice where they occupy the grain boundaries of the ice crystals preferably (Fig. 4). The spherical aggregates ranging from some 100 μm to more than 2 mm (Bischoff and Stöffler, 1988) are obviously formed when the dust-water suspensions are sprayed into liquid nitrogen.

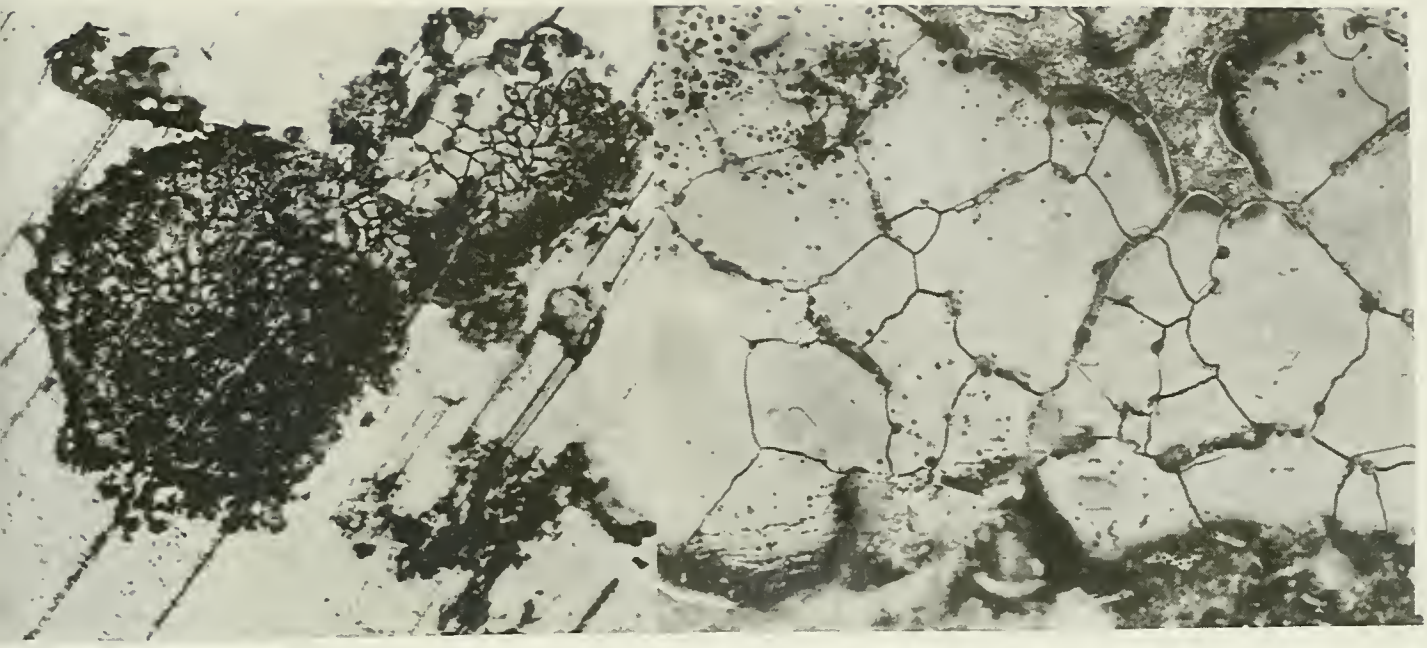


Fig. 4 Micrographs of a polished section of a KOSI-2 sample obtained by the polarizing microscope in reflected light, horizontal width of microphotograps: 1.4 mm. (a) In the center: spherical dust-ice aggregate; upper right corner: polycristalline ice with interstitial dust; white matrix with diagonal lines: pore space filled with crystallized diethylphtalate. (b) Polycristalline ice; dark lines: grain boundaries between ice crystals where some dust aggregates are located (worm-like features).

Initial Results

Experimental sequence. Besides with different sample materials the KOSI experiments were conducted with different insolation profiles. During the KOSI-1 experiment, the main purpose of which was technology verification, the sample was insolated with 1.1 SC (Solar Constant, light power onto surface) for 13 hours. The insolation profile during KOSI-2 was more complex: 1 SC for 16.5 h, off 4 h, 1 SC 4 h, off 4 h, 1 SC 4 h, off 4 h, ~2 SC 2 h and during KOSI-3: 1.3 SC 10.3 h, off 6 h, 1.3 SC 30.8 h. As an example for the in-situ measurements we want to discuss in some detail the temperature and the released gas data.

Temperature measurements. Figure 5 shows the time-history of the temperatures within the sample during the KOSI-3 experiment. The temperatures are taken at 1 cm distance intervals from the backplate of the sample container (no measurements at 0 and 3 cm have been taken). The higher the temperatures the closer they are measured to the sample surface. The thermoelement at 13 cm from the backplate penetrates the surface of the sample after about 3 h and becomes exposed to direct irradiation, at which time the trace is discontinued. The measurement at 12 cm never became exposed to direct light but reached temperatures as high as 300 K in the upper layers of the sample. The sensitivity of the temperatures to the incident light in the lower part of the sample is an experimental artefact. Two distinct levels of temperatures are recognized within the sample: at the beginning of the experiment at about 120 K and in the later stages just below 210 K. They are attributed to the discrete levels of sublimation of CO_2 and H_2O, respectively (cf. Spohn and Benkhoff, 1989).

Emitted gas. The gas release during the KOSI-3 experiment is shown in Fig. 6. Immediately after the initial switch-on of the irradiation both CO_2 and H_2O emission rates jumped to

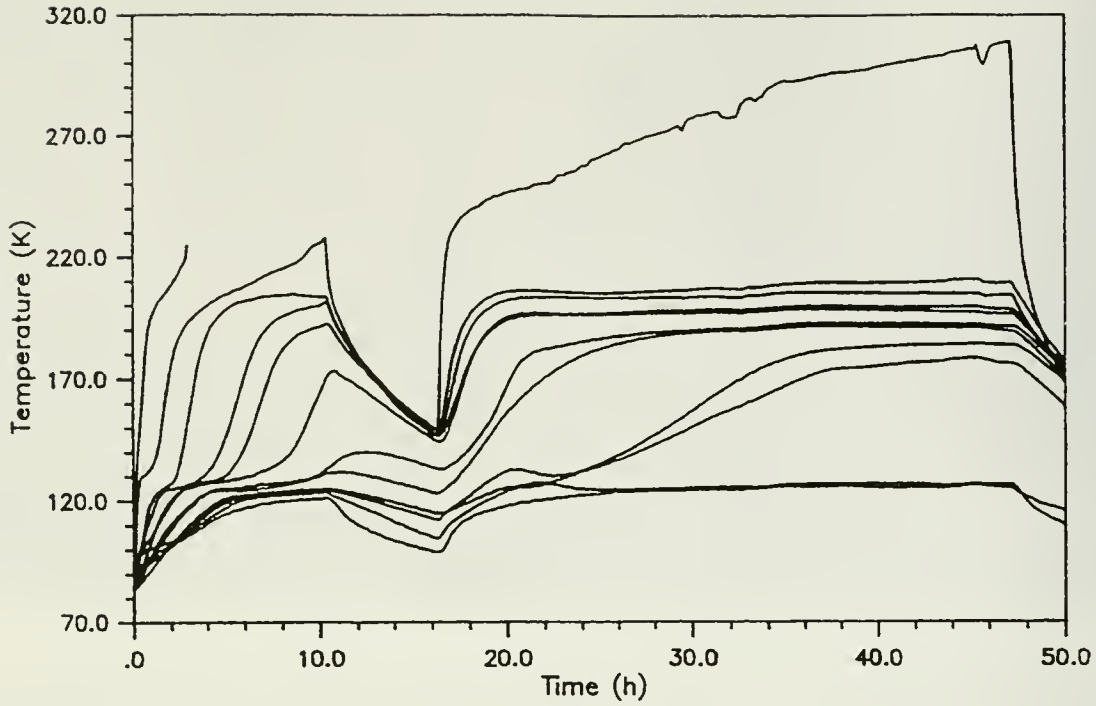


Fig. 5 Evolution of temperatures in the KOSI-3 sample. The sample had been insolated with 1.3 SC 0 h to 10.3 h and from 16.3 h to 47.1 h. Temperature measurements are shown at distances 1, 2, 4, 5, 6, 7, 8, 9, 10, 11, 12 and 13 cm from the back plate. The trace of the measurement at 13 cm is discontinued at ~3 h when it became exposed to direct irradiation.

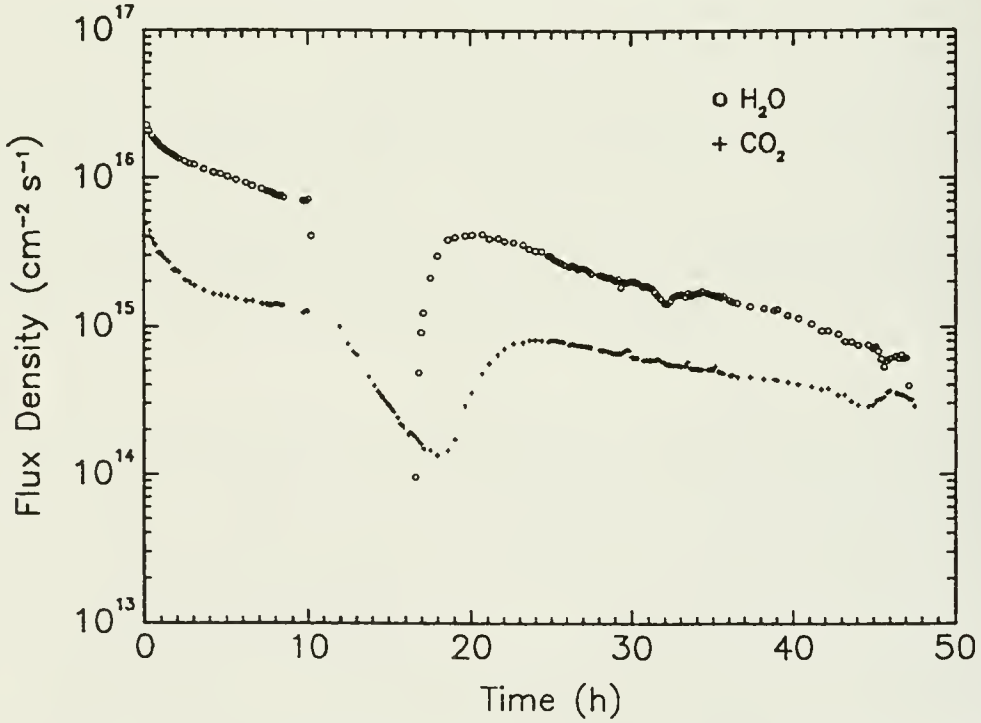


Fig. 6 Measurement of the H_2O and CO_2 gas flux density at 90 cm distance from the sample and at an angle of 38 from the surface normal (KOSI-3). For the insolation periods cf. Fig. 5.

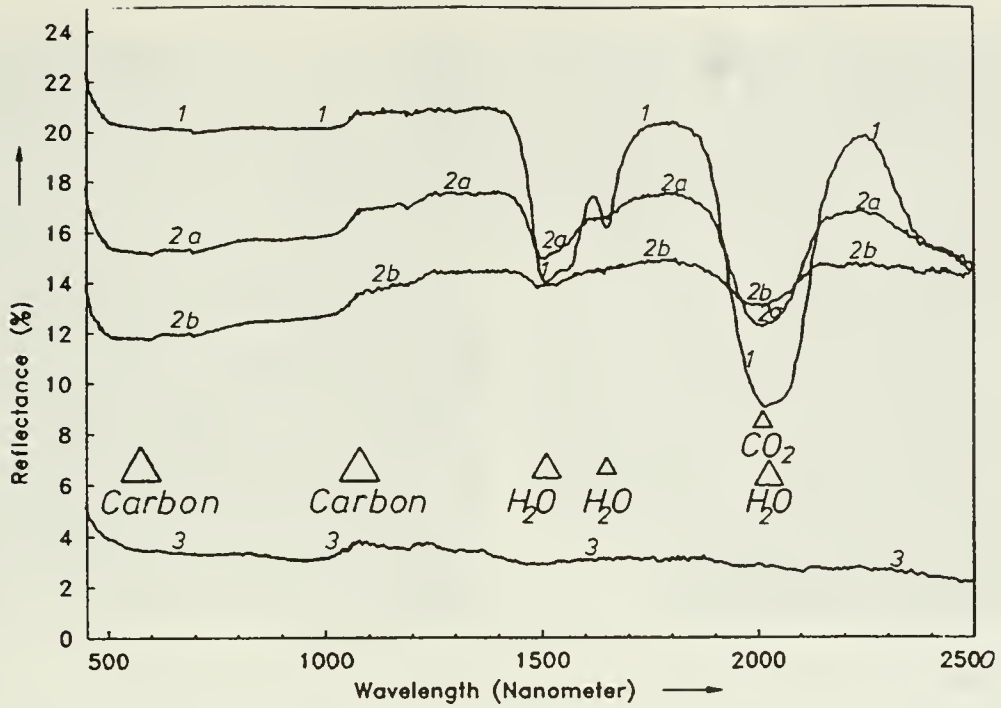


Fig. 7 Reflectance spectra of the KOSI-3 sample. Trace 1: original sample; traces 2: irradiation processed sample (2a upper and 2b lower part of the inclined sample surface); trace 3: pure carbon. Sample temperature ≈ 130 K, measurement in sample normal, illumination at 32° phase angle.

maximum values. Thereafter both emission rates decreased with time. The ratio of H_2O/CO_2 emission decreased with time from about 6 to 3 at the end of the experiment, although the mole fraction of both constituents was ~14 in the original sample material. During the off-period of irradiation and shortly thereafter this ratio varied over a large range. When the lamps were switched off the water emission ceased rapidly, while the CO_2 emission followed much more slowly. During the sun-off period only CO_2 emission was observed. After switch-on of the lamps water emission started immediately, reaching its maximum value about three hours later. CO_2-emission continued to decrease for two more hours after switch-on before it started to increase again. This is an indication that CO_2 sublimates in deeper layers of the sample. After it had reached its maximum value about 5 hours after switch-on the CO_2-emission declined roughly in proportion with the water emission. From the evaluation of the gas flux data we estimate that about 60% of the total CO_2 content left the sample during the experiment.

Optical properties. The samples are characterized by optical reflectance spectroscopy. The radiance coefficient (Hapke, 1981) is measured in the wavelengths range from 0.45 μm to 2.5 μm. The spot size on the sample is about 4 cm diameter. The sample is contained in a glove box and is liquid nitrogen cooled. The sample is illuminated and viewed through four quartz windows which allows the measurement of reflectance spectra at phase angles of 32°, 50° and 70°. Fig. 7 shows reflectance spectra of the sample before and after insolation at 32° phase angle. The reflectance (albedo) averaged over the wavelength range is 18.3% for the original KOSI-3 sample, 16.0% in the upper part and 13.7% in the lower part of the irradiation processed sample. For comparison pure carbon powder has an average reflectance of 3.1%. The albedo of the KOSI-3 sample was much higher than that of the KOSI-2 sample (6%) because of the admixture of bright CO_2-ice. In the KOSI-1 experiment a different type of carbon was used which formed large agglomerates and therefore was not as effective.

The reflectance spectra show characteristic absorption bands for carbon as well as for CO_2 and H_2O ice. The abundances of the minerals olivine and montmorillonite are too low in

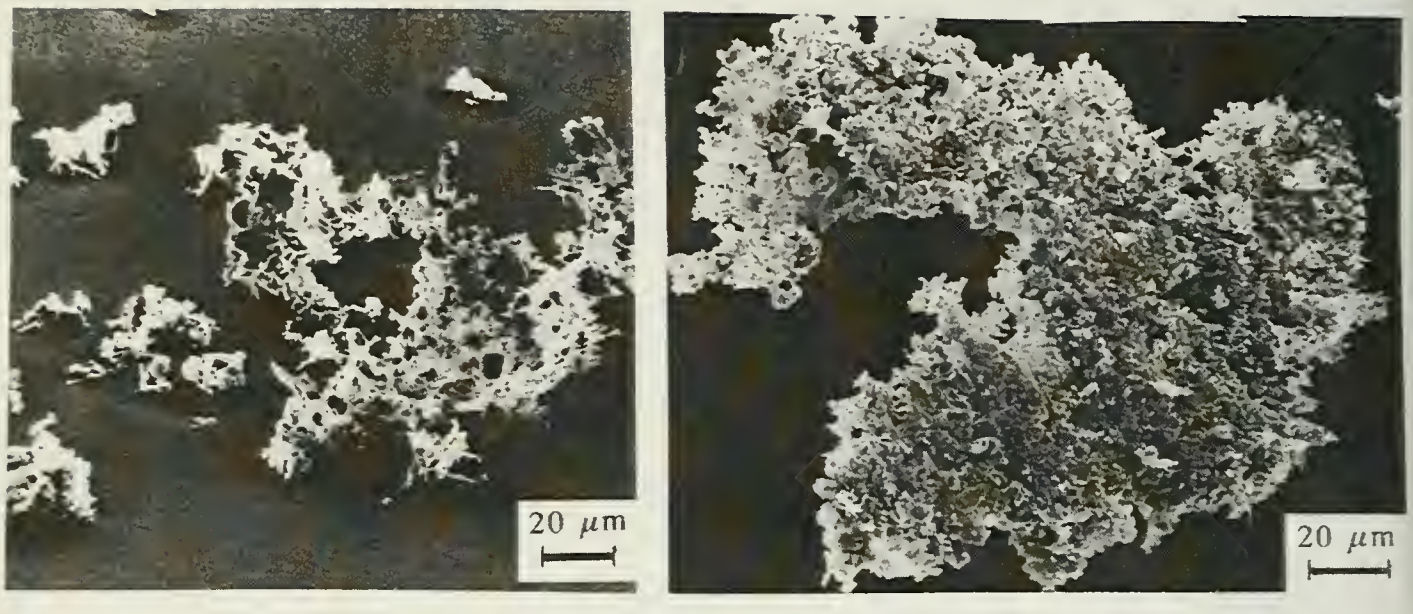


Fig. 8 SEM micrographs of dust grains emitted during the KOSI-3 experiment. The dust composition is 90 % (by weight) olivine and 10 % montmorillonite. (a) Fluffy grain. (b) Compact grain.

order for their absorption bands to be noticeable in the presence of the dark carbon. Narrow absorption bands of CO_2-ice at 2020 nm can barely be seen in the original sample on top of the heavy absorption band of water ice at 2000 nm. Because of the high transmission of both ice components between 450 nm and 1000 nm wavelength and because of the low concentration of the silicates the spectrum in this range is dominated by carbon. Below 500 nm the carbon shows a strong increase of its reflectance. This increase is caused by Rayleigh scattering of the very small carbon grains. This increase at short wavelength is also visible for the KOSI sample material but the effect of carbon is somewhat reduced because of an opposite effect of the silicates. The balance between the reddening by the minerals and the increase towards shorter wavelengths by the carbon depends on the distribution of both minerals in the mixture and is therefore dependent on details of the sample preparation technique.

A comparison of the spectra of the original sample and the processed sample shows a decrease of the total reflectance as well as a reduction of the water absorption bands. The CO_2-signature vanishes already after little processing by insolation. The difference in the spectra from the upper and lower parts of the surface of the processed sample are explained by the formation of a dust mantle of variable thickness on top of the ices.

Dust mantle. Inspection of all samples after insolation shows that a layer of dry dust of a few mm to ~1 cm thickness had formed overlaying the ice mixtures. This layer was generally thicker on the lower parts of the sample surface than on the upper parts. Observations of the sample during insolation showed that some of the bigger particles which were not completely dragged away by the gas stream just rolled down the inclined surface of the sample and accumulated on the lower portions of the sample surface.

SEM analysis of the mantle material (Thiel et al., 1989) and the residues of emitted dust particles (Fig. 8) which were collected during the experiment showed that both were of very similar structure. The density of the mantle material is of the order of 0.1 g/cm^3. The fluffy texture of the mantle indicates an almost complete lack of volatiles in it. This structure is mainly controlled by (1) the mineralogical composition of the dust component in the ice-mineral mixture, (2) by the consistency of the original material and (3) by the preparation method.

As mentioned above phyllosilicates (montmorillonite, kaolinite) and nesosilicates (olivine) are mainly used to simulate the comet nucleus analogue. SEM-investigations reveal that the fraction of phyllosilicates relative to olivine is the main parameter that determines the final structure of the residuals (cf. Storrs et al., 1988). Higher fractions of phyllosilicates yield spongy particles of regular pore shape, the pores being separated by straight partition walls made of silicate platelets. A high olivine fraction on the other hand leads to irregular fluffy material made up of roundish constituents glued delicately together, forming completely irregular pore spaces.

The structure of the dust mantle as a whole is influenced by the consistency of the original ice (snow) dust mixture. Starting with a massive block of dirty ice yields a fine-grained coherent dust mantle occasionlly separated in series of fine layers. Compact snow with small pores (mud-like appearence) produces a loose dust layer of small grain sizes (~1 μm to ~100 μm), spongy snow with large pores (snow-like appearance) leads to a highly fluffy dust mantle of medium to large grain sizes (100 μm to >1000 μm).

Hardness test. Both before and after a KOSI experiment the hardness of the sample is measured. The measuring device is a motor driven force-meter which pushes a cylindrical piston of 5 mm diameter into the sample (Thiel et al., 1989). The penetration force is recorded as function of depth. After the KOSI-3 experiment it was found that right beneath the dust mantle a hard crust had formed. The hardness had risen from originally ~0.2 Mpa to 1.3-5.1 Mpa over a thickness of 28 to 70 mm. The actual values varied over a large range with the location on the sample, however, the general trend that the hardness of a sub surface layer increased considerably during insolation has been confirmed by a number of experiments. In addition, the thickness of this layer increased with time. Below this hard layer the hardness showed the original value. This observation indicates that a major metamorphosis of the near surface layer of the sample material occured during the sublimation experiment.

Sample structure and composition. After transfer of the irradiated KOSI sample to the glove box (Roessler et al., 1989) the sample was inspected and a number of small specimen including drill cores were taken from different positions within the sample. These specimen were used for chemical, isotopic and petrographic characterization of the different phases of the sample.

Visual inspection of the KOSI-3 sample showed beneath the dust mantle the several cm thick, hard and coherent but porous ice crust. This material was somewhat brighter than the non-coherent material underneath the crust which resembled most the original sample material. The bottom layer (of several mm to cm thickness) was very bright and contained some larger ice platelets.

The CO_2-content at various depths was determined by gas chromatography (Roessler et al., 1989). Except for the bottom ~2 cm no significant CO_2 abundance was measured within the KOSI-3 sample. Even there it was mostly reduced from its original value of ~14% to about 2% except for the lowest few mm where it had even increased to 20%.

The isotopic ratios $^{18}O/^{16}O$ and D/H have been measured at various depths of the KOSI-2 sample (Klinger et al., 1989b). It turned out that in the near surface layers ($\leq$ 4 cm) a strong enrichment of heavy isotopes occured, whereas in the deeper layers the depletion was smaller or even negligible. But these results need further confirmation.

The mass densities were determined on volumetrically defined aliquots. For the KOSI-3 samples the density before the sublimation experiment was 0.5 g/cm^3 and afterwards it differed distinctly between the ice crust (0.5 g/cm^3) and the non-coherent lower layer (0.3 g/cm^3). The results from the first attempts of a petrographic characterization of the

ice-mineral mixtures have been discussed above (cf. Fig. 4). Several specimen were molten for grain size measurements of the dust component by laser granulometry. The dust in the suspensions from which the KOSI-3 sample was prepared had a median grain diameter of 4.9 μm, a rather large standard deviation and a slight excess of coarse grains. The suspensions produced by melting the ice-dust samples after the sublimation experiments had a median grain diameter of ~6.4 μm and a slight excess of fine grains. Comparison with measurements made with KOSI-2 samples showed that the CO_2 admixture had a major effect on the mean grain size measured after the sublimation experiment.

Discussion

The results from the sublimation experiments are discussed in terms of a proposed qualitative model which accounts for the observed temperature profile, the gas release characteristics and the metamorphosis of the sample material (i.e. the formation of a dust mantle and an ice crust)

Sublimation fractionation model. The KOSI sample material had a density of about 0.5 g/cm^3. Such a low density material necessarily contains a great number of pores that communicate with each other. As long as such a system is confined in a closed volume and kept at a constant temperature, the pressure in the pores is equal to the vapor pressure of the ice at the given temperature. When a thermal gradient is maintained within the sample material, a pressure gradient builds up as a result of the variation of the vapor pressure of the ice as a function of temperature. This pressure gradient acts as a driving force for the diffusion of the vapor phase through the pore system. In this way a supersaturation occurs locally and leads to a recondensation of the vapor phase. This phenomenon can persist in deeper layers of the sample material even when the vapor phase can leave the sample through a semi-permeable top surface. In this case a net sublimation occurs in the near-surface ice layers. The vapor phase that circulates through the pore system contributes to the heat exchange between the surface and the deeper layers of the sample (Smoluchowski, 1982, Klinger et al., 1989a, Spohn and Benkhoff, 1989). This heat transfer to colder ice layers has three components, heat conduction by solids (1) and by gas (2) and (3) deposition of latent heat due to the net mass transport by recondensation. A consequence of the redeposition of water vapor is the hardening of the initially non-coherent material. This mass and heat transport occurs both for water and CO_2, for the latter only at greater depth within the sample and at a lower temperature level.

Figure 9 demonstrates the result of sublimation fractionation of the KOSI sample after some period of insolation and the corresponding temperature and pressure profiles. The two top panels show the stucture and the composition of the sample. At the bottom of the sample (depth 4) it is still in its original state. At depth 3 effective sublimation of CO_2 occurs, inwards of which its concentration is slightly increased due to inward migration, outward this level no CO_2-ice is found. Water sublimation occurs at depth 2, outward of which a dust mantle has formed.

The temperature profile reflects the energy input at the top surface of the dust mantle. Its surface temperature is determined by the balance between absorbed light energy, emitted thermal radiation and heat conducted into the interior by solid state and gas heat conduction. The temperature of the sublimation surface of water ice is elevated above the temperature of an ice surface which sublimates freely into vacuum, although the energy flux into that surface is already reduced from the energy absorbed by the dust mantle. A flat temperature profile characterizes the heat transport by the water vapor down to some distance from the water sublimation surface (Spohn et al., 1989). A similar behaviour of the temperature profile is seen inward the CO_2 sublimation surface. Only at great depth the temperature profile has the steep gradient expected for solely solid state heat conduction.

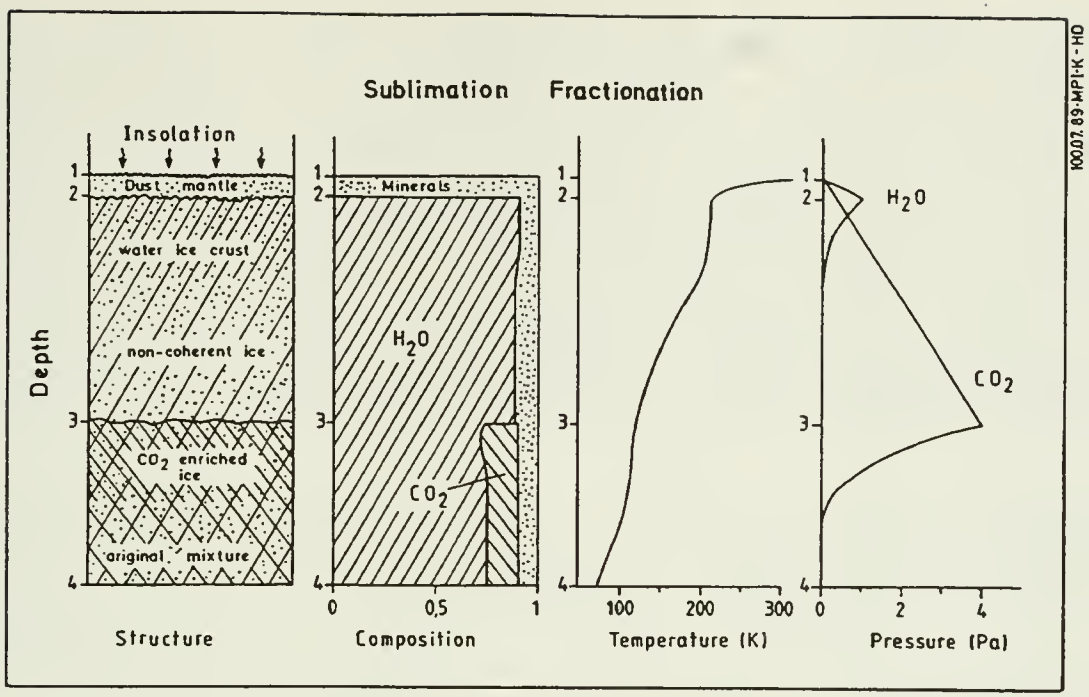


Fig. 9 Model of sublimation fractionation: sample structure, composition and internal temperature and pressure profiles. The conditions of the KOSI-3 experiment are shown after some time of insolation.

The pressure profile follows the temperature profile insofar as inside sublimation surfaces the partial pressure corresponds to the vapor pressure at this temperature. Outside sublimation surfaces the pressure is controlled by the flow through the partially permeable overlaying material.

Future developments. Because of the close coupling of the energy and mass transport within the sample a quantitative model has to describe both effects together. Since the system is evolving, ultimately, non-stationary solutions have to be investigated. Also the experiments have to be improved in order to determine quantitatively the energy and mass balance of the KOSI experiments. Methods have to be developed to measure the thermal emission from the surface and the heat flux into the back plate of the sample container as well as to determine the mass loss from the sample container. In addition the sample materials and their phases have to be better characterized: both thermal conductivity, heat capacity, porosity and permeability for gases have to be determined. It is estimated that for the present sample dimensions the temperatures at the sublimation level of CO_2 are affected by the back plate temperature already after a few hours of experiment time. Therefore, an increase of the dimensions of the sample by at least a factor of two would allow us to follow the development of the temperature wave for longer times and at lower temperature levels.

Relevance to comets. There are two lines of evidence that cometary nuclei in general and their near-surface layers in particular are of high porosity (≥ 0.5). Firstly, estimates of the mean density of Halley's and other comets' nuclei indicate that their densities are low (< 1 g/cm^3), lower than any reasonable solid non-porous ice-dust mixture would have. Secondly, the detection of gases more volatile than water suggests that these gases are released from greater depths than water and that these gases have to percolate through the overlaying material. Therefore, the fractionation effects which we have found to take place during the sublimation of porous ice-dust mixtures in the laboratory should occur also under cometary conditions.

However, there is a major difference between the simulation experiments and the cometary situation which has to be taken into account. That is the about 10^4 times higher gravity in the simulation experiments. The effect of which is, that only grains smaller than 10 µm to a few 100 µm (depending on their densities, cf. Grün et al., 1989) will be draged away by the gas flow. Under cometary conditions the limit will be 10cm to 100 cm sized particles. In addition, the thickness of a layer which is able to sustain by its weight alone the pressure of the evaporating gases has to be much thicker in the cometary case. Therefore, the maximum pressure gradient will be only $\sim 10^{-4}$ of that in the simulation experiments and the scale lengths will be accordingly larger. Because of these larger scale lengths the time period to reach quasi stationary equilibrium will be much longer than in the simulation experiments and it will only be reached if the insolation period (~ nuclear spin period) is long enough. However, this time scale applies only to the upper layers of a few diurnal skin depths deep. For the more volatile ices which sublime even further down the relevant time scale is the time period of perihelion passage (~ orbital period).

The thickness which is required for a layer to sustain a given pressure gradient will be reduced if the cometary surface material has some coherence. Since we have found in our simulation experiments that at least icy materials develop coherence during the sublimation process some effects of the low cometary gravity will be reduced. Another conclusion from our sublimation experiments is, that clathrates or other trapped mixtures of volatile gases in water (cf. Bar-Nun, 1989) will probably be separated during the sublimation fractionation process and therefore will not be found in the surface layers of cometary nuclei. These inferences have to be confirmed by future comet simulation experiments.

Acknowledgement

This research has been supported by DFG within the SPP 'Kleine Körper im Sonnensystem'.

References

Bar-Nun A., 1989: Experimental studies of gas trapping in amorphous ice and thermal modelling of comets- Implications for Rosetta; Workshop on Analysis of Returned Comet Nucleus Samples, Milpitas, USA

Bischoff A. and Stöffler D., 1988: Comet nucleus simulation experiments: Mineralogical aspects of sample preparation and analysis; Lunar and Planet. Sci. XIX, Lunar and Planetary Insitute, Houston, 90-91

Good W., 1982: Structural investigations of snow and ice on core III from the drilling on Vernagtferner, Austria; Z.f. Gletscherkunde u. Glazialgeologie *18*, 53-64

Good W., 1987: Thin sections, serial cuts and 3-D analysis of snow; Avalanche Formation, Movement and Effects, IAHS Publ. *182*, 35-48

Grün E., Kochan H., Roessler K. and Stöffler D., 1987: Simulation of cometary nuclei; Proc. Symposium on Diversity and Similarity of Comets, eds. E.J. Rolfe and B. Battrick, ESA-SP 278, 501-508

Grün E., Benkhoff J., Fechtig H., Hesselbarth P., Klinger J., Kochan H., Kohl H., Krankowsky D., Lämmerzahl P., Seboldt W., Spohn T. and Thiel K., 1989: Mechanisms of dust emission from the surface of a cometary nucleus, Proc. COSPAR workshop on Comet Nucleus Modeling and Cometary Materials, Adv. Space Res., *Vol. 9. No. 3*, 133-137

Hapke B., 1981: Bidirectional reflectance spectroscopy, 1. Theory, J. Geophys. Res., *86*, 3039-3054

Ibadinov K.I., 1989: Laboratory investigation of the sublimation of comet nucleus models, Adv. Space Res., *Vol. 9, No. 3*. 97-112

Jessberger E.K., Christoforidis A. and Kissel J., 1988: Aspects of the major element composition of Halley's dust; Nature, *332*. 691-695

Kajmakov E.A. and Sharkov V.I., 1972: Laboratory simulation of icy cometary nuclei; in The Motion, Evolution of Orbits, and Origin of Comets, eds. Chebotarev et al., Reidel Publ. Comp., Dordrecht, 308-314

Kerridge J.F. and Matthews M.S., (editors), 1988: Meteorites and the Early Solar System, Univ. of Arizona Press, Tuscon

Kissel J., Krueger F.R., 1987: The organic component in dust from comet Halley as measured by the PUMA mass spectrometer on board Vega 1, Nature, *326*, 755-760

Klinger J., Benkhoff J., Espinasse S., Grün E., Ip W., Joo F., Keller H.U., Kochan H., Kohl H., Roessler K., Seboldt W., Spohn T. and Thiel K., 1989a: How far do results of recent simulation experiments fit current models of cometary nuclei?, Proc 19th Lunar Planet. Sci. Conf., Lunar and Planetary Institute, Houston, 493-497

Klinger J., Eich G., Bischoff A., Joo F., Kochan H., Roessler K., Stichler and Stöffler D., 1989b: "KOSI" comet simulation experiment at DFVLR: Sample preparation and the evolution of the $^{18}O/^{16}O$ and the D/H ratio in the icy component, Proc. COSPAR workshop on Comet Nucleus Modeling and Cometary Materials, Adv. Space Res., *Vol. 9. No. 3.* 123-125

Kochan H., Benkhoff J., Bischoff A., Fechtig H., Feuerbacher B., Grün E., Joo F., Klinger J., Kohl H., Krankowsky D., Roessler K., Seboldt W., Thiel K., Schwehm G. and Weishaupt U, 1989a: Laboratory simulation of a cometary nucleus: Experimental setup and first results, Proc. 19th Lunar Planet. Sci. Conf., Lunar and Planetary Institute, Houston, 487-492

Kochan H., Feuerbacher B., Joo F., Klinger J., Seboldt W., Bischoff A., Düren H., Stöffler D., Spohn T., Fechtig H., Grün E., Kohl H., Krankowsky D., Roessler K., Thiel K., Schwehm G. and Weishaupt U., 1989b: Comet simulation experiments in the DFVLR Space Simulators, Proc. COSPAR workshop on Comet Nucleus Modeling and Cometary Materials, Adv. Space Res., *Vol. 9, No. 3*, 113-122

Krankowsky D. and Eberhardt P., 1989: Evidence for the composition of ices in the nucleus of comet Halley; Comet Halley 1986, World-Wide Ivestigations, Results and Interpretations, Ellis-Horwood Limited, Chichester, in press

Mackinnon I.D.R. and Rietmeijer F.J.M., 1987: Mineralogy of chondritic interplanetary dust particles; Review of Geophysics, *25*, 1527-1553

Rietmeijer F.J.M., 1985: A model for diagenesis in proto-planetary bodies; Nature, *313*, 293-294

Roessler K., Hsiung P., Heyl M., Neukum G., Oehler A., Kochan H., 1989: Handling and analysis of ices in cryostats and glove boxes in view of cometary samples; Workshop on Analysis of Returned Comet Nucleus Samples, Milpitas, USA

Sandford S.A. and Walker R.M., 1985: Laboratory infrared transmission spectra of individual interplanetary dust particles from 2.5 to 25 microns; Astrophys. J., *291*, 838-851

Saunders R.S., Fanale F.P., Parker T.J., Stephens J.B. and Sutton S., 1986: Properties of filamentary sublimation residues from dispersions of clay in ice; Icarus, *66*, 94-104

Smoluchowski R., 1982: Heat transport in porous cometary nuclei; J. Geophys. Res., *87*, Supp. A., 422-424

Spohn T., Benkhoff J., Klinger J., Grün E. and Kochan H., 1989: Thermal modeling of two KOSI comet nucleus simulation experiments; Proc. COSPAR workshop on Comet Nucleus Modeling and Cometary Materials, Adv. Space Res., *Vol. 9, No. 3*, 127-131

Spohn T. and Benkhoff J., 1989: Thermal history of models for KOSI sublimation experiments, submitted to Icarus

Stöffler D., Düren H. and Knölker J., 1989: Concepts for the curation primary examination, and petrographic analysis of comet nucleus samples returned to Earth; Workshop on Analysis of Returned Comet Nucleus Samples, Milpitas, USA

Storrs A.D., Fanale F.P., Saunders R.S. and Stephens J.B., 1988: The formation of filamentary sublimate residues (FSR) from mineral grains, Icarus, *76*, 493-512

Thiel K., Kochan H., Roessler K., Grün E., Schwehm G., Hellmann H., Hsiung P. and Kolzer G., 1989: Mechanical and SEM analysis of artificial comet nucleus samples; Workshop on Analysis of Returned Comet Nucleus Samples, Milpitas, USA

THE NATURE OF COMET MATERIALS AND ATTACHMENT TO THEM

James Stephens
Planetology and Oceanography Section
Jet Propulsion Laboratory
Pasadena, California

The Nature of Comet Materials and Attachment to Them

James Stephens
Planetology and Oceanography Section
Jet Propulsion Laboratory
Pasadena, California 91109-8099

Because cometary surfaces are likely to be far colder and of a different composition and surface topography than other planetary surfaces with which we have experience, there are some new considerations that must be examined in regards to placing and attaching instrumented packages or sample return devices in or on their surfaces. The qualitative analysis of the problem of embedding hardware in a comet icy core is limited to only one of several means for the purposes of this discussion. This means can be characterized as a kinetic impact piercing device. Such kinetic impact piercing device may be used to attach the feet of an instrumented package on the surface or it may be the means for implanting the package in the icy core below the mantle.

The functional requirement is to implant a device in the icy core and by mechanical means, prevent the device from being ejected back into space. The requirement can be divided into two parts.

The first requirement is to pierce the mantle and obtain access to the icy core because the mantle may not be attached to the core and instrument sensors must have access to the icy core. The impact piercing device may ricochet off of the mantle if it cannot be directed approximately perpendicular to the impact surface (Fig. 1). The surface geometry may be closer to the local vertical than to the horizontal because solar heat focusing, fluid dynamic channeling and electrostatic filament forming forces will likely prevail over the low comet gravity to form very grotesque surface topography. Furthermore, if the mantle that covers the icy core has mineral particles that are bonded together by a tar-like substance and if the surface tension forces of this "tar" prevail over other bonding forces; then the mantle may shrivel under solar heating to form an "asphalt" like brittle, high density, high strength material. In addition, old cometary mantles may be formed

Piercing device impacts comet surface at steep angle and ricochets off of the surface

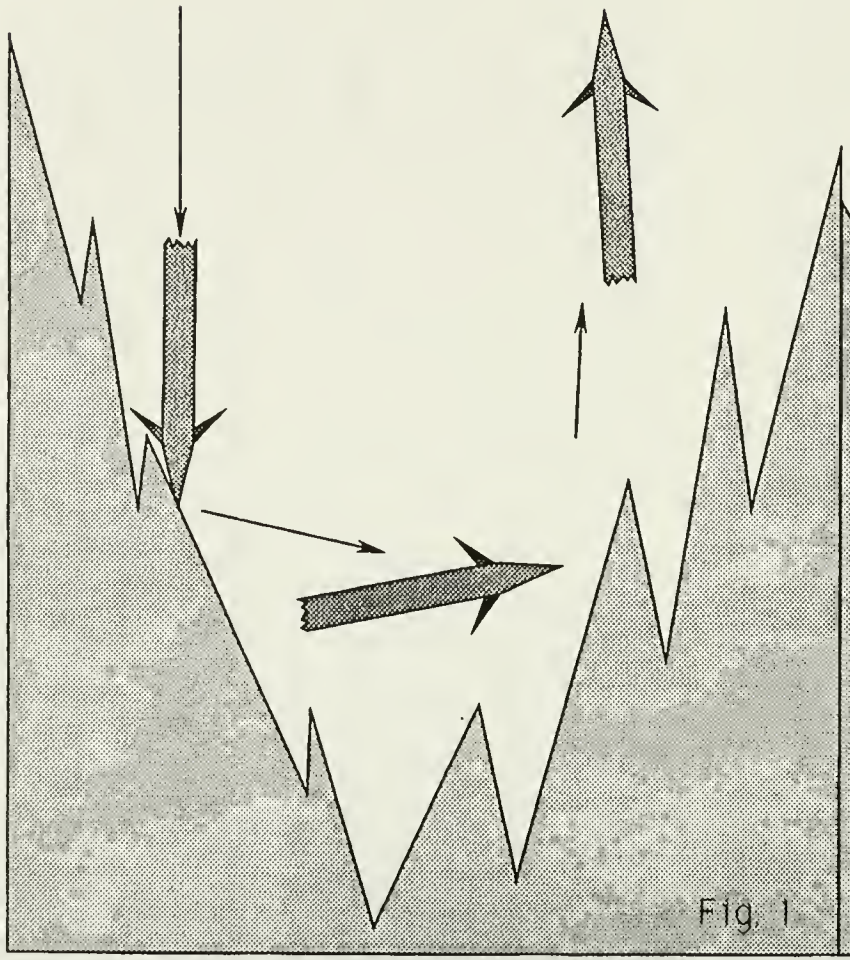


Fig. 1

Piercing device impacts comet surface and shatters adjacent mantle and icy core material

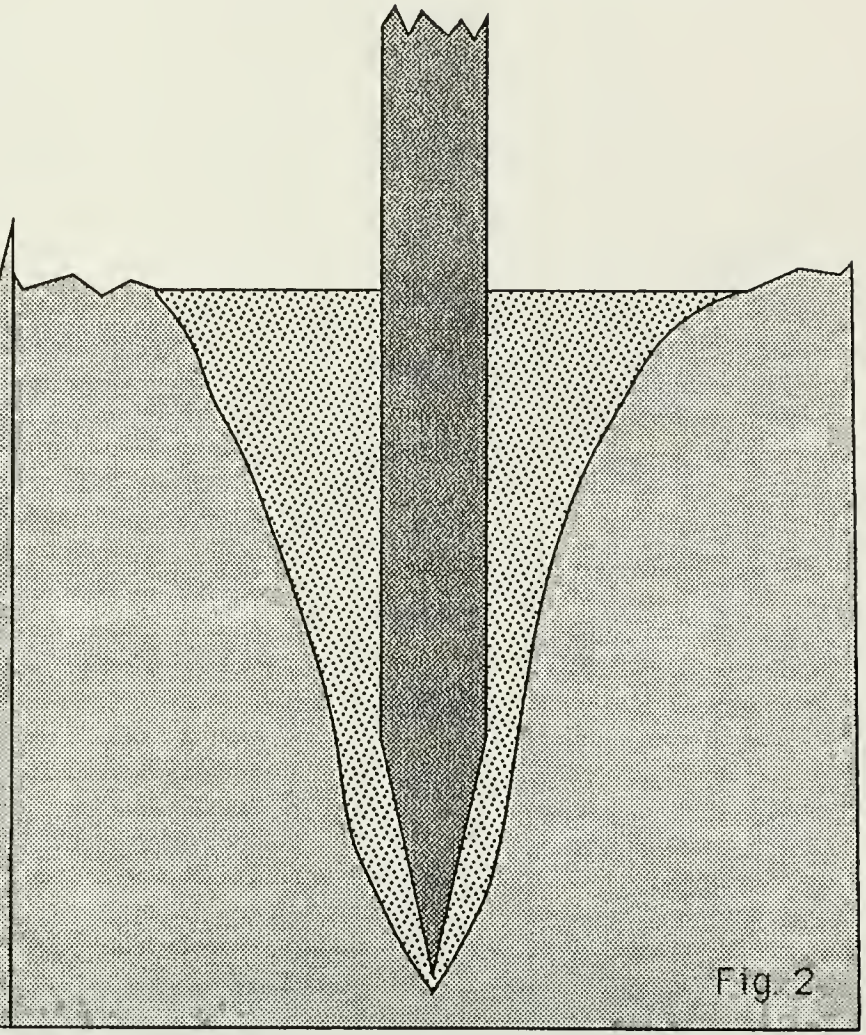


Fig. 2

from the thermally stress-fractured remnants of earlier mantles. Radar observations of comet mantles and laboratory experimental investigations into the formation of comet mantles suggests that such non horizontal surface structures are likely to exist.

The second requirement is to overcome the forces produced by the transformation of the impact kinetic energy into forces that try to eject the piercing device back into space. The mantle and icy core can absorb some of the impact kinetic energy in the form of fracture formation and friction energy (Fig. 2). What energy that is not absorbed in these two ways is for the most part stored by the icy core as elastic deformation of the icy core. This elastic deformation energy is returned to the piercing device and the fragmented mantle and fragmented core material that surrounds it after the piercing device comes to zero velocity. The elastic deformation rebounding force is assisted by the pressure force of the gas that is formed by the previously mentioned fracture formation and friction energy. Much of the fracture formation and friction energy is converted into heat that is ultimately converted into gas because the icy core is more than likely to be in thermodynamic equilibrium with its under-mantle environment. An additional source of gas pressure is supplied by the new equilibrium that the core must achieve when the conductance through the mantle is increased by the additional venting of the mantle by the piercing device. Only if the icy core is subcooled to below the new equilibrium temperature will the production of additional gas not occur. Clathrate, free radical, and/or phase change produced gas may also be triggered by the impact.

The impact piercing device must develop hold-down forces that can overcome the elastic deformation rebounding force and the pressure force of the evolved gas.

Hold-down forces that depend upon friction between the piercing device and the icy core may be insignificant because a gas bearing may form at the contact

between the piercing device and the icy core. Experiments in drilling simulated comet icy core materials in vacuum suggest that gas bearing lubrication is to be expected between highly loaded metal objects and ice containing materials.

Hold-down forces that depend upon cohesion between the piercing device and the icy core are likely to be insignificant because there are no liquids that are likely to form at the interface and upon refreezing bond the piercing device to the core. Even if the icy core can rebound in the horizontal direction and clamp the piercing device in the crater, the friction forces and the cohesive forces remain small.

Hold-down forces that depend upon fixed or deployed barbs may be insignificant because they are likely to shatter the core material (Fig. 3) during entry as does the piercing device and it is unlikely that the material that they engage will still be attached to the core. It is unlikely that the shattered material will rebond because no liquid can form at the expected comet pressure and temperature.

Even if anchoring devices could be deployed horizontally below the surface of the unfractured icy core, the hold-down force might be as little as the gravity force of the pieces of the core that may be fractured by the deployment forces of the barbs (Fig. 3). Such fracturing is possible because subsurface wedging forces are likely to be very large in a low porosity icy core and the resulting cracks are likely to extend to the surface. Observations of comet fracturing and laboratory experimental investigations into the fracturing of simulated comet cores suggest that brittle fracture behavior of comet icy core material is to be expected.

It is concluded that:

1) because the comet mantle topography is likely to be non horizontal and thus may deflect the kinetic impact piercing device; some means must be devised to assure perpendicular entry into the local mantle,

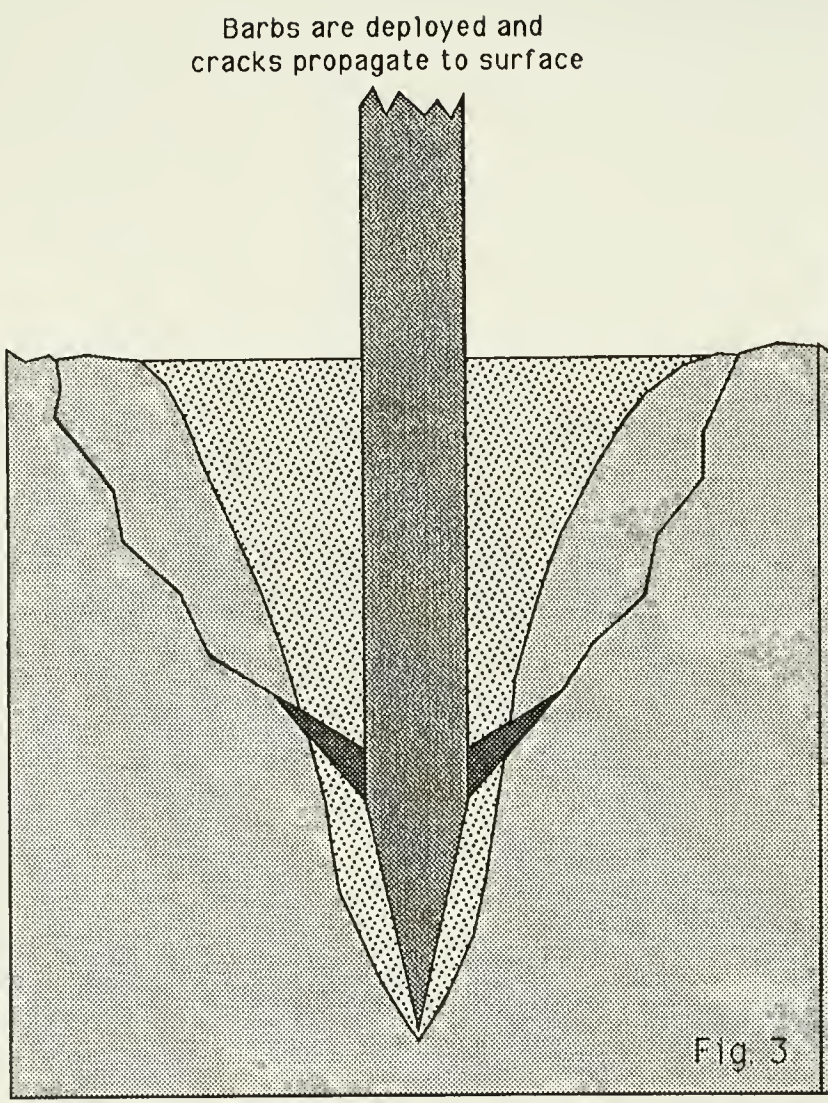

Barbs are deployed and
cracks propagate to surface

Fig. 3

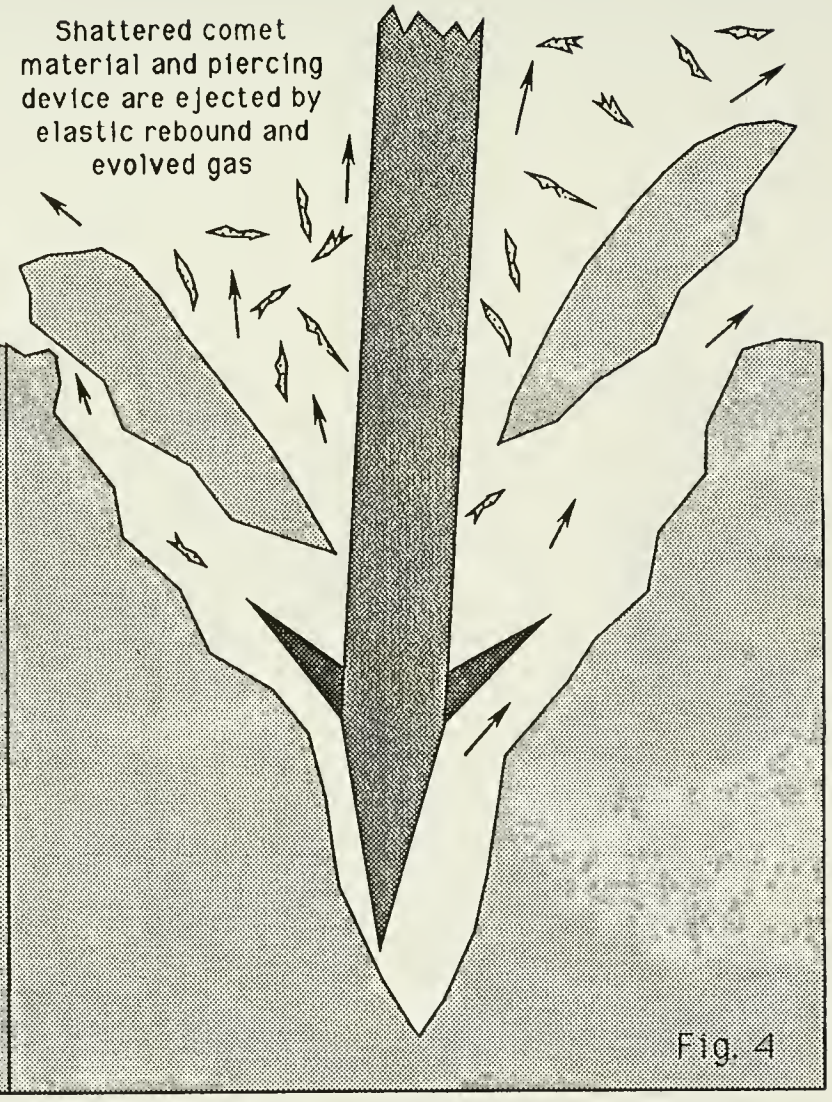

Shattered comet
material and piercing
device are ejected by
elastic rebound and
evolved gas

Fig. 4

2) because the comet mantle and icy core are almost certainly brittle, the icy core is likely to be self lubricating and nonbonding; the elastic rebound and gas pressure expulsion forces produced by an impact piercing device must be counteracted by forces greater than those that may be provided by a piercing device with fixed or deployable barbs (Fig. 4).

MECHANICAL AND SEM ANALYSIS OF ARTIFICIAL COMET NUCLEUS SAMPLES

K. Thiel
Abt. Nuklearchemie
Universität Köln
Köln, FRG

H. Kochan
Institut für Raumsimulation
Köln, FRG

K. Roessler
Institut für Chemie, Nuklearchemie
Jülich, FRG

E. Grün
Max-Planck-Institut für Kernphysik
Heidelberg, FRG

G. Schwehm
European Space Agency
Noordwijk, The Netherlands

H. Hellmann
Institut für Raumsimulation
Köln, FRG

P. Hsiung
Institut für Chemie, Nuklearchemie
Jülich, FRG

G. Kölzer
Abt. Nuklearchemie
Universität Köln
Köln, FRG

MECHANICAL AND SEM ANALYSIS OF ARTIFICIAL COMET NUCLEUS SAMPLES*

K. Thiel[1], H. Kochan[2], K. Roessler[3], E. Grün[4], G. Schwehm[5], H. Hellmann[2], P. Hsiung[3], and G. Kölzer[1].

[1]Abt. Nuklearchemie, Universität Köln, D-5000 Köln 1, FRG
[2]Institut für Raumsimulation, DLR WB-RS, D-5000 Köln 91, FRG
[3]Institut für Chemie, Nuklearchemie, KFA, D-5170 Jülich, FRG
[4]Max-Planck-Institut für Kernphysik, D-6900 Heidelberg, FRG
[5]European Space Agency, NL-2200 Noordwijk, The Netherlands

THE KOSI PROJECT

In 1987 approx. 20 scientists from different disciplines started a 6 year program (KOSI) to simulate physically and chemically relevant processes of cometary nuclei (E. Grün et al., 1989, H. Kochan et al., 1988;). The experiments are mainly carried out in two simulation chambers of the German Aerospace Research Establishment, DLR at Cologne, FRG. Experiments in the Big Space Simulator are dedicated to effects and processes induced by artificial solar irradiation (~ 1 solar constant) on a 30 cm diameter model comet of well-defined properties. Supporting investigations are performed in a smaller space simulation chamber with ice-dust targets of typically 10 cm diameter. A detailed description of the chambers is given by Kochan et al. (1988). Several groups of theorists who are part of the KOSI-team process the experimental results and provide relevant boundary conditions for the design of new experiments.

The main objective of these studies is a better understanding of

- the temperature behaviour of ice-dust mixtures under given irradiation conditions
- the total mass and energy budget of the target
- the mobilization of material (dust and gas) within the target body
- physical and chemical alterations of the sample as a function of the experimental parameters, especially:
- crust formation
- gas emission
- dust emission and dust properties
- gas-dust interaction

The KOSI-project is intended to allow a better interpretation of ground based and space mission gained cometary data and to support the planning of future sample return missions.

*) This work is financially supported by Deutsche Forschungsgemeinschaft Bonn, under 9 different contracts.

On-line Monitoring of Crustal Strength

During experiments in the small simulation chamber the development of a near surface ice crust is monitored by hardness measurements using a remote-controlled hardness tester. The force meter can be equipped with cylindrical boring tools of various dimensions, depending on the penetration forces to be measured (typical diameter of the boring head: 5 mm). The observation of an *in-situ* crust development during artificial sunlight exposure was a first step to confirm diffusion and re-freezing of water vapor in the porous sample as expected from theoretical considerations (Klinger et al., 1988; Grün et al., 1988a). The crustal strength as a function of irradiation time (using 1 solar constant intensity) was found to gradually increase during the first 50 minutes. After 1 hr of light exposure strength values rapidly raised by a factor of ~6 relative to the initial value and again showed a slower increase for longer irradiation times (see also figure 1).

Off-line Measurement of Crustal Strength

Before and after experiments in both simulation chambers the hardness of the different sample materials was measured by means of a motor driven boring device supplied by ESA (fig. 2a). A boring tool similar to that used in the on-line investigation in the small chamber is propelled vertically into the sample with a penetration velocity of 0.2 mm/s. The penetration force is measured and recorded on an x-y-plotter as a function of penetration depth. The resulting depth profiles of mechanical stress provide a feasible diagnostic means to check the reproducibility of the sample preparation procedure in the case of not irradiated samples. In the case of irradiated

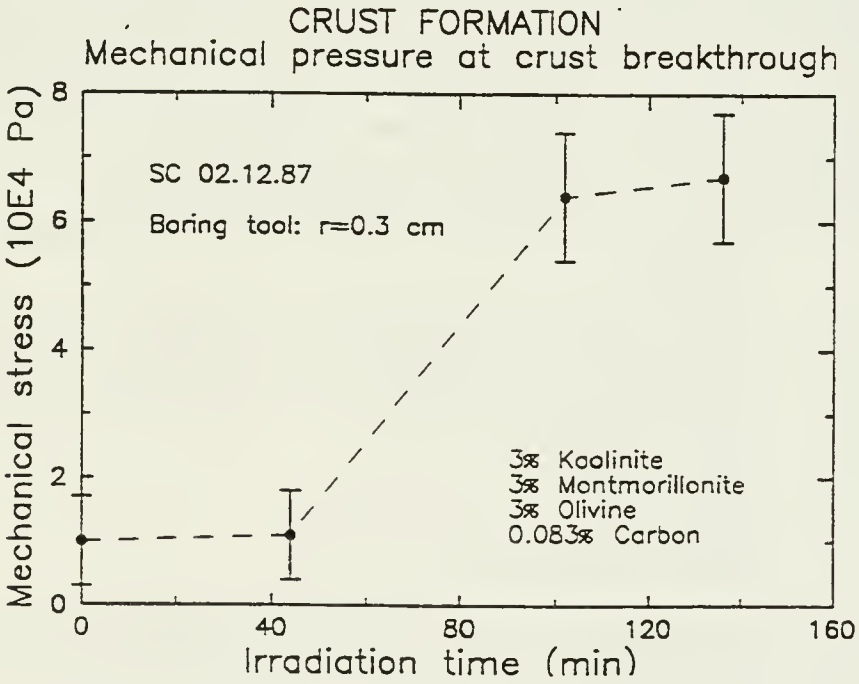


Figure 1: In-situ crust formation as a function of irradiation time

samples stress depth profiles are the most direct way of measuring crustal evolution of the comet nucleus analogues induced by radiation.

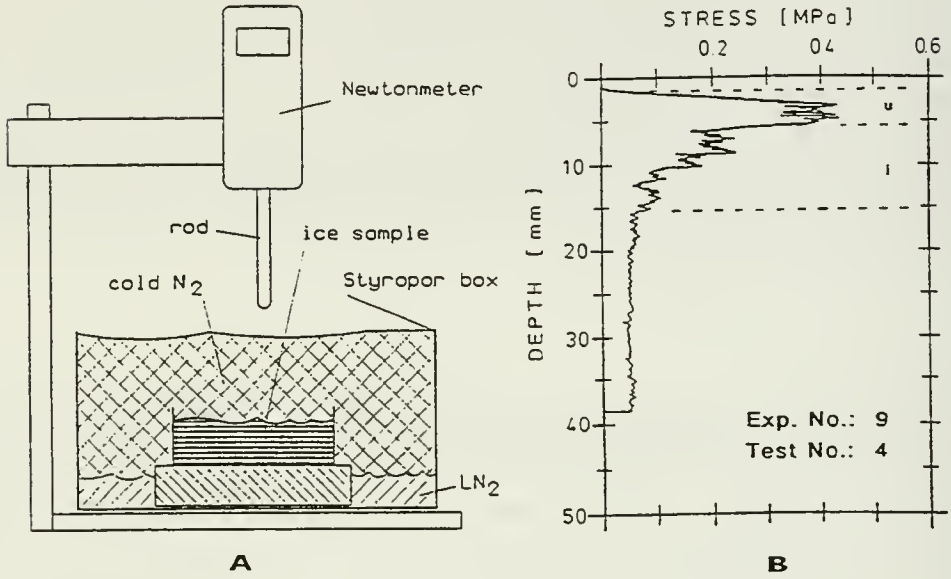
It was found that soil mechanical data of a given sample are closely related to the method of sample preparation. The present procedure of sample production is based on a simple spraying technique using aqueous suspensions of mineral powder. For a more detailed discussion of the technique cf. Roessler et al. (1989). The following parameters affect the structure and texture of the sample: (1) ultrasonic treatment of the aqueous suspension, (2) type of the propellant spray gas [N_2 or CO_2], (3) pressure of the propellant gas [variations of a few hundred Pa are essential], (4) flow rate of the suspension in the spray gun at zero propellant gas pressure (5) distance between spray gun nozzle and surface of the liquid nitrogen the suspension is sprayed into, (6) content of CO_2-ice in case of two-component ice samples [H_2O and CO_2-ice].

Table 1: Typical parameters of small chamber experiments 8-12 (18.10., 19.10., 20.10., 25.10., 28.10.1988) and the big chamber experiment KOSI 3 (29.11.-02.12.1988)

EXPERIMENT	8	9	10	11	12	KOSI 3
Mineral composition, (olivine:montmorillonite)	7 : 3	9 : 1	7 : 3	7 : 3	9 : 1	9 : 1
Content of CO_2-ice [wt%]	6.5	4.0	5.0	14.0	13.0	13.8
Density [g/cm^3]	0.41	0.43	0.38	0.36	0.41	0.48
Porosity [%]	-	-	59	63	60	57
Texture	mud	snow	snow	mud	snow	mud
Intensity of irradiation [SC]	2.0 - 2.4	2.0	2.0 - 2.4	2.0 - 2.4	2.0 - 2.4	1.3 - 1.6
Period of irradiation [h:min]	3:38	2:12	2:15	2:45	3:38	41:10
T_i, T_f [K] 2 cm below surface *)	149 - 196	143 - 209	151 - 218	163 - 211	164 - 222	~100-~150
Max. dust activity [μg/cm^2/min]	-	132	19	607	173	-
Thickness of crust [mm]	20 - 25	16 - 18	20 - 24	10 - 26	20 - 42	28 - 70
Strength of crust [MPa]	0.30 - 1.3	0.43 - 0.55	0.15 - 0.19	0.75 - 1.10	0.35 - 0.88	1.3 - 5.1
Strength below crust [MPa]	0.1 - 0.3	0.04 - 0.06	0.03 - 0.05	0.08 - 0.24	0.03 - 0.08	0.2 - 0.5
No. of strength measurements	4	7	9	5	6	7

*) T_i, T_f initial and final temperature of the sample during the experiment

Figure 2: a: Sketch of the ESA/ESTEC boring device. During measurements the sample is shielded against room temperature and air humidity by flooding with 77-100 K nitrogen gas.
b: Stress depth profile of a sample which was irradiated for 2.2 hrs with an intensity of 2 solar constants (olivine : montmorillonite ratio 9:1).



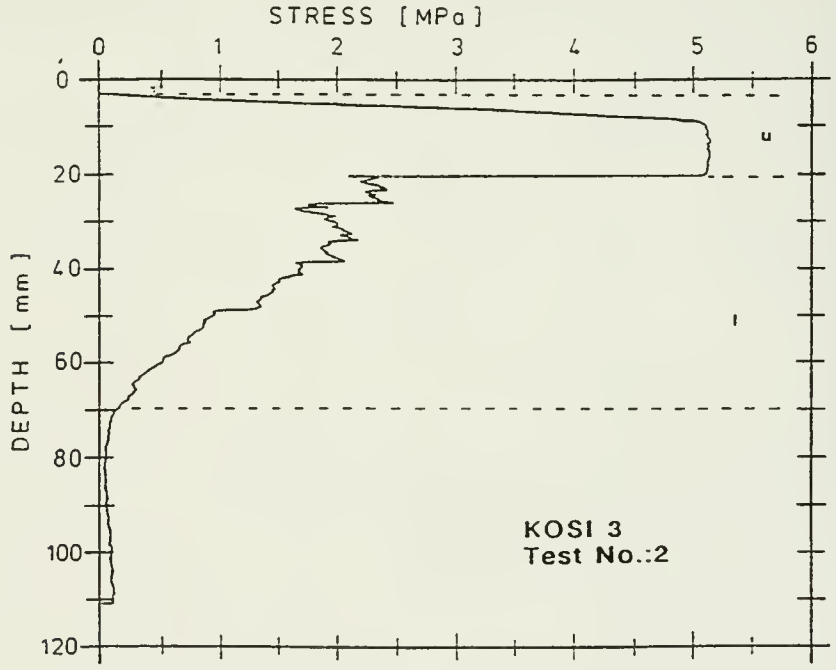


Figure 3: Stress depth profile of a sample which was irradiated for 41.2 hrs with an intensity of 1.3-1.6 solar constants (olivine : montmorillonite ratio 9:1).

In some cases a complex interrelation between these parameters make it difficult to produce ice-dust mixtures that meet the essential requirements of a comet nucleus analogue at the same time (low mass density, high porosity, desired mineral dust admixture, content of CO_2-ice etc.). The present technique does not allow to produce e.g. "fluffy" material of a snow-like consistency with a nesosilicate to phyllosilicate ratio of the dust admixture of 7 : 3 and an overall CO_2-content of ~ 15 wt%.

In table 1 a summary is given of experiment parameters and some soil mechanical data obtained during a series of test runs in the small simulation chamber and during the KOSI 3 experiment in the Big Simulator at DLR. One of the main factors controlling the gas and dust emission of a sample when irradiated with light is the composition of the dust admixture. Most of the samples investigated so far contained nesosilicates (olivine) and phyllosilicates (montmorillonite) in ratios (by weight) of 7:3 and 9:1. The samples listed in table 1 all contained CO_2-ice in the range of 4 to 14 wt%. Experiment no. 11 gives an example of a high CO_2-content in a fine grained sample of "mud"-like appearance when stored in liquid nitrogen. With the spray technique used for the sample preparation it is difficult to produce "snow"-like samples with CO_2-contents > 10 wt% and phyllosilicate contents > 3 wt%.

The strength data cover a relative wide range between 150 kPa and 5.1 MPa due to lateral and vertical inhomogeneities with respect to the sample hardness. Especially the depth variation of stress shows some general features which become obvious in typical depth profiles of the different target materials investigated after the experiment (cf. figures 2 and 3). The presence of a loose ice-free dust mantle is indicated by low compressive forces during the first few mm of penetration depth. When the solidified ice-dust layer ("crust") is reached 3-5 cm below the surface a steep increase of the stress values is observed in the depth profile. A common feature of most of the samples is the occurrence of a stronger upper crust and a weaker lower crust where the stress values drop by a factor of ~2. A more thorough study of material transport within the sample is devoted to the question of a possible alteration of the target structure due to moving depth layers of vapor re-freezing.

SEM INVESTIGATION OF DUST MANTLE AND EMITTED DUST RESIDUALS

Dust Mantle

All samples investigated so far showed the formation of a surface dust layer (dust "mantle") when irradiated with light. There are however differences in the appearance of the mantle depending on the original structure of the sample:

(i) Compact, pore free ice-dust mixtures suffer ice sublimation only at the outermost surface. Samples containing initial dust fractions of ≥ 10 wt% form a thin ice-free dust "skin" of low porosity made up of tightly cohering mineral grains. This "skin", due to the lack of ice, can now be heated to higher surface temperatures. Eventually the gas pressure of the sublimating ice underneath

exceeds the cohering forces of the mineral grains of the "skin" and an extended dust "sheet" of ~50-200 μm thickness is slowly peeled off, releasing the gas pressure.

This process may recur several times leading to a periodic separation of up to ~10 "skin" generations. The dust "mantle" of such samples is a sequence of loosely bound thin dust layers showing a typical substructure. In several cases single layers were regularly covered with "bubbles" of some 10 μm in diameter, similar to "blister" phenomena induced by energetic gas implantation in solids. Most of the "bubbles" were burst open, indicating the effect of gas pressure. A cracked dust "bubble" as seen from the bottom is shown in the SEM-micrograph figure 4.

(ii) Compact but porous ice-dust samples, which have a "mud"-like appearance when stored in liquid nitrogen (cf. table 1) produce quite different dust mantles. A sample made of "mud"-like material, due to its fine porosity, undergoes ice sublimation in a surface layer of several 100 μm thickness when irradiated with light. This leads to the formation of a porous but coherent crust of mineral residuals covering the ice-containing material underneath (fig. 5). Due to its greater thickness (mechanical rigidity) and higher porosity (gas permeability) compared to massive ice-dust samples this mineral "mantle" can not easily be lifted by the gas stream originating from deeper ice layers.

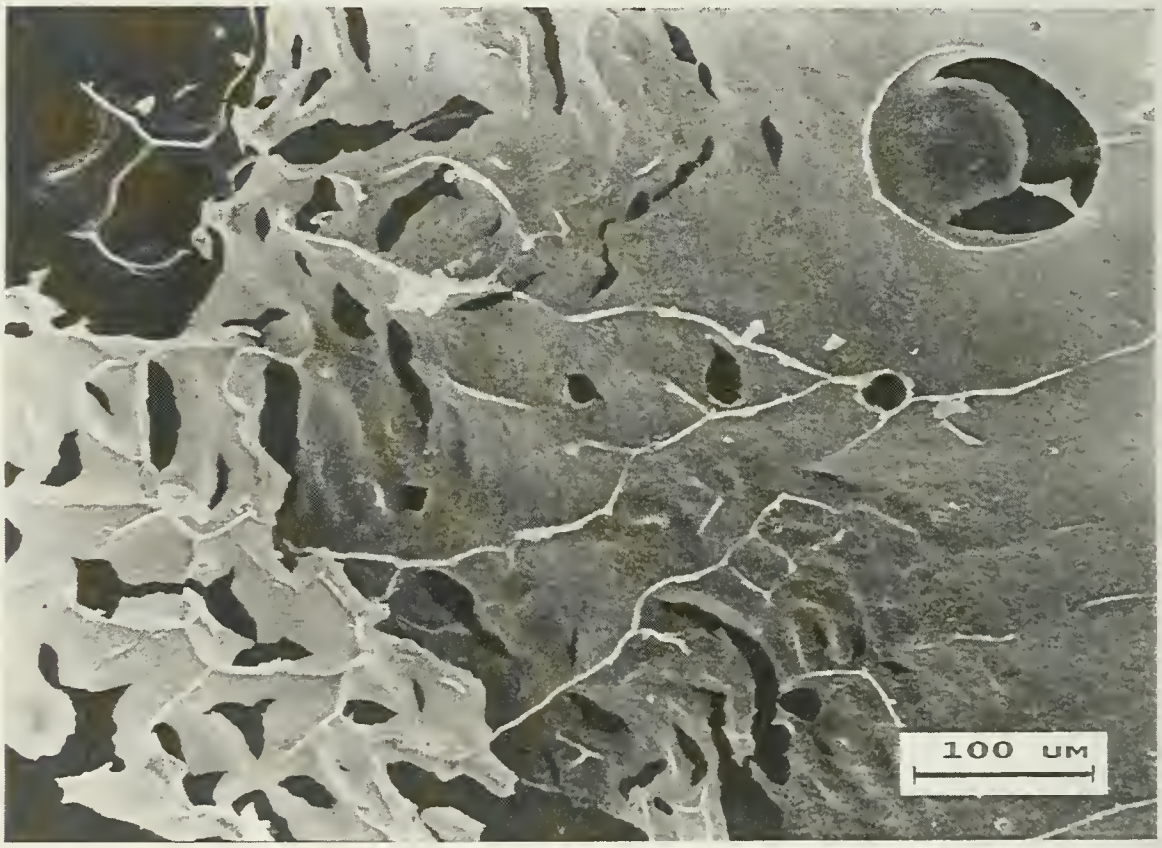


Figure 4: Coherent dust layer showing features of deformation caused by gas pressure. The SEM-micrograph shows the high pressure side of the layer, which is part of a multi-layer dust mantle formed on a compact dust-ice block under light exposure (~2 solar constants). Upper right: broken "pressure bubble".

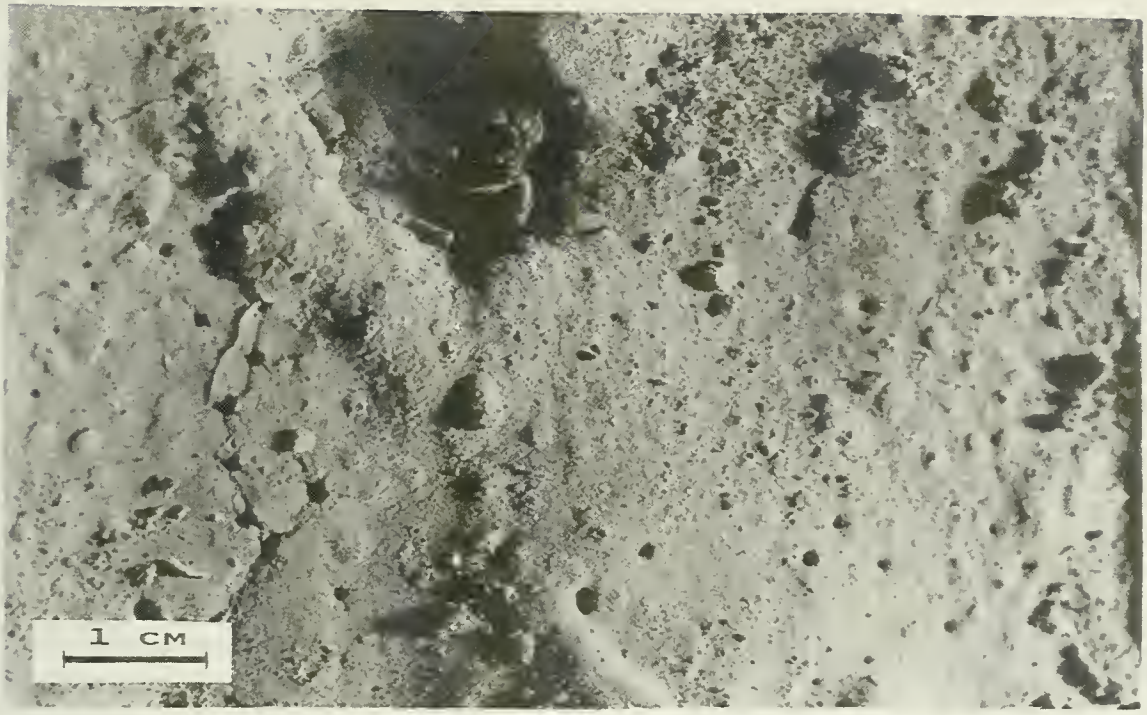


Figure 5: Dust mantle of a sample with "mud"-like texture.

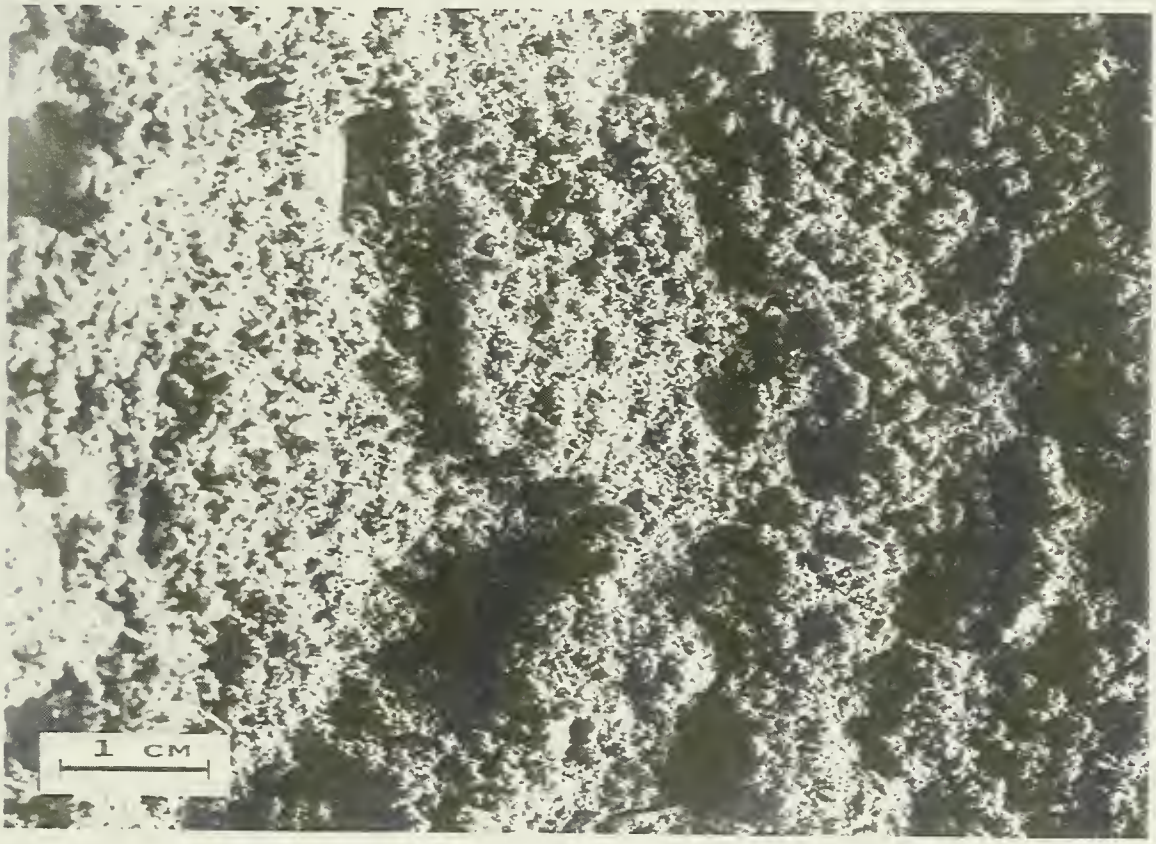


Figure 6: Dust mantle of a sample with "snow"-like texture.

The dust mantle quenches the sublimation of ice, the gas emission of the sample is reduced, and dust emission completely stops. By increasing the irradiation intensity, the surface temperature and consequently the vapor pressure of the deeper ice layers can be raised to high values. When the pressure forces due to enhanced ice sublimation exceed the mechanical strength of the mantle, big flakes of the dust mantle (diameters > 1 cm) are blown off, and dust emission abruptly starts again ("dust activity threshold").

(iii) Highly porous ice-dust mixtures of a "snow"-like texture (cf. table 1) suffer ice sublimation in a much thicker surface layer than compact samples, when exposed to light. The emanating gas stream is sufficiently strong to carry away particles which are only weakly attached to the surface or which become loose due to the steady ice corrosion by sublimation. Dust emission activity is maintained for much longer time periods (days) and the quenching of ice sublimation by a dust cover is effectively delayed by heat transport into greater depths via the vapor phase. Structural and compositional changes of "fluffy" snow samples are mainly controlled by their porosity and heat permeability. The typical surface texture of a "snow"-like sample is demonstrated in figure 6.

Residuals of Emitted Dust Particles

Ice-free dust particles deposited on the dust collectors during the experiments look very similar to the grains found in the dust mantle of the target. The emission process obviously causes no structural alteration of the residuals. Their structure and texture is mainly controlled (1) by the mineral composition of the dust in the original ice-dust mixture and (2) by the sample preparation technique which may lead to very specific target materials (cf. "Dust Mantle").

(1) The amount of clay minerals (e.g. montmorillonite and kaolinite) contained in the dust component strongly influences the appearance of the residuals. Especially phyllosilicates of the montmorillonite mineral group carrying a small negative charge on their cleavage planes may strongly adsorb traces of cations present in the water of the sample suspension. It is assumed that montmorillonite platelets are "glued" together by electrostatically effective water layers in a parallel orientation and on a scale of many grain diameters. The formation of parallel oriented grain agglomerates is obviously favored by shock freezing during the sample preparation process (cf. (2)). The resulting texture of the dust in the ice matrix (which is essentially preserved in the texture of the ice-free residuals) is characterized by highly regular pores and a delicate network of straight or bent walls made up of phyllosilicate platelets.

Reducing the phyllosilicate fraction and increasing the amount of nesosilicates, which are represented by olivine in the samples investigated so far, yields residuals of less regular texture and commonly smaller pores. This can be achieved e.g. by changing the ratio olivine : montmorillonite from 7:3 to 9:1.

(2) In the KOSI simulation experiments a comet nucleus analogue material is used, which is produced by spraying aqueous suspensions of mineral dust into liquid nitrogen (cf. also Roessler et al., 1989). The parameters of the spraying process (cf. "Off-line Measurements of Crustal Strength"), especially the pressure of the propellant gas, and the flow rate of the sample suspension control the droplet size of the spray and thus the grain size of the ice-dust mixture. A

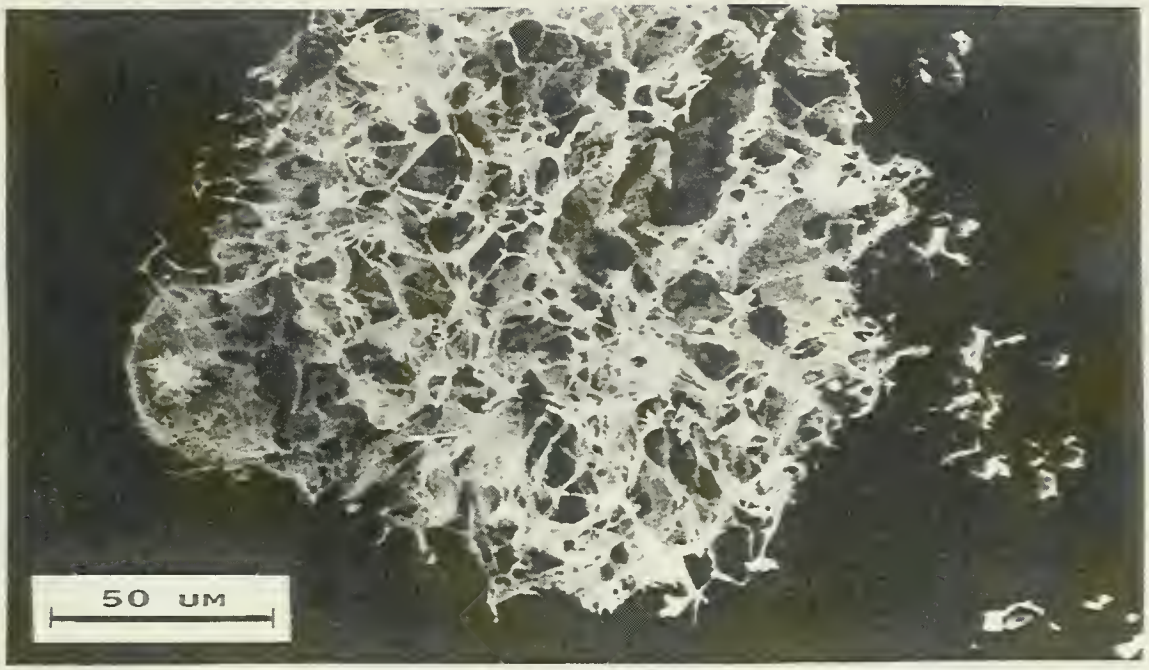


Figure 7: SEM-micrograph of a coarse porous dust residual containing 30 wt% phyllosilicates



Figure 8: SEM-micrograph of a fine porous dust residual containing 10 wt% phyllosilicates

higher gas pressure generally yields smaller grain sizes and *vice versa*. In the case of a two-component ice mixture of H_2O and CO_2 the carbon dioxide is used as a propellant gas and the fraction of both ices can be controlled by the gas pressure.

The droplets which are injected into the liquid nitrogen suffer shock freezing. The freezing starts at the surface of the droplets and rapidly proceeds into the interior. Suspended mineral grains may be predominantly oriented along proceeding ice fronts yielding the textures described above. Typical dust residuals with different amounts of phyllosilicates are shown in figures 7 and 8. One of the objectives of the sample preparation is, to produce material that yields dust residuals which resemble stratospheric Brownlee particles of the "fluffy" type. With the spraying technique used in the KOSI experiments this is achieved only for a phyllosilicate fraction in the dust component of < 10-30%. To overcome the disadvantages due to the presence of liquid water during sample preparation, a method to produce material from the vapour phase is presently being developed.

REFERENCES

Grün, E. and KOSI team: Modifications of comet materials by the sublimation process: Results from simulation experiments, Workshop on Analysis of Returned Comet Nucleus Samples, Jan. 16-18, 1989, Milpitas, Cal.

Grün, E., J. Benkhoff, H. Fechtig, P. Hesselbarth, J. Klinger, H. Kochan, H. Kohl, D. Krankowsky, P. Lämmerzahl, W. Seboldt, T. Spohn, and K. Thiel: Mechanisms of dust emission from the surface of a cometary nucleus, Proc. of the twenty-seventh plenary meeting of the Committee on Space Research (COSPAR), 18-29 July 1988, Espoo, Finland, Advances in Space Research, (1988a), Pergamon Press, Oxford (in press)

Klinger, J., J. Benkhoff, S. Espinasse, E. Grün, W. Ip, F. Joo, H. U. Keller, H. Kochan, H. Kohl, K. Roessler, W. Seboldt, T. Spohn, and K. Thiel: How far do results of recent simulation experiments fit current models of cometary nuclei ?, Proc. of the Nineteenth Lunar and Planetary Science Conf. (1988) (in press)

Kochan, H., J. Benkhoff, A. Bischoff, H. Fechtig, B. Feuerbacher, E. Grün, F. Joo, J. Klinger, H. Kohl, D. Krankowsky, K. Roessler, W. Seboldt, K. Thiel, G. Schwehm, and U. Weishaupt: Laboratory simulation of a cometary nucleus: Experimental setup and first results, Proc. of the Nineteenth Lunar and Planetary Science Conf. (1988) (in press)

Roessler, K., G. Eich, M. Heyl, H. Kochan, A. Oehler, A. Patnaik, W. Schlosser, R. Schulz: Handling and analysis of ices in cryostats and glove boxes in view of cometary samples, Workshop on Analysis of Returned Comet Nucleus Samples, Jan. 16-18, 1989, Milpitas, Cal.

ION BOMBARDMENT EXPERIMENTS SUGGESTING AN ORIGIN FOR ORGANIC PARTICLES IN PRE-COMETARY AND COMETARY ICES

Thomas J. Wdowiak
Edward L. Robinson
Gregory C. Flickinger
David A. Boyd
Physics Department
University of Alabama at Birmingham
Birmingham, Alabama

ION BOMBARDMENT EXPERIMENTS SUGGESTING AN ORIGIN FOR ORGANIC PARTICLES IN PRE–COMETARY AND COMETARY ICES

Thomas J. Wdowiak, Edward L. Robinson,
Gregory C. Flickinger, and David A. Boyd

Physics Department, University of Alabama at Birmingham
Birmingham, Alabama 35294

ABSTRACT

Simple molecules frozen as mantles of interstellar and circumstellar grains and incorporated into comets are subjected to ion bombardment in the form of cosmic rays, stellar flares, stellar winds, and ions accelerated in stellar wind shocks. The total expected dosage for the variety of situations range from 10 eV/molecule for interplanetary dust subjected to solar flares to 10^6 eV/molecule for material in the T Tauri environment. Utilizing a Van de Graaff accelerator and a target chamber having cryogenic and mass spectrometer capabilities, we have bombarded frozen gases in the temperature range of 10 K to 30 K with 175 keV protons. After irradiation, removal of the ice by sublimation at an elevated temperature in vacuum reveals a fluffy residue. These experiments suggest that processes resulting in the formation of organic particles found in the coma of Comet Halley ,"CHON", may have included ion bombardment. Also, the moderate energy (100 keV to 500 keV) shock accelerated ion environment of bipolar outflow of stars in the planetary nebula stage such as the Red Rectangle, could produce complex molecular species which emit the observed unidentified infrared bands at 3.3 μm, 6.2μm, 7.7μm, 8.6μm, and 11.3μm.

INTRODUCTION

During the Giotto and Vega encounters with Comet Halley, mass spectrometers were used to determine the elemental compostion of impacting dust particles (Kissel et al. 1986a; 1986b). A significant component of the dust population was found to be free of mineral constituents and was composed of carbon, hydrogen, oxygen, and nitrogen. The name "CHON" has been coined to identify this apparent organic material. The formation of these organic solids and their incorporation into a comet nucleus are among the more interesting questions of cometary science. Greenberg, in many discussions, (see Greenberg 1989) argues for the mechanism of photoprocessing of precursor interstellar grain mantles. However, other processing mechanisms such as charged particle irradiation warrant consideration. Inventories of possible charged particles fluxes in various environments (Strazzula, 1988; Johnson, 1989) indicate particle fluxes from 10 cm^{-2} s^{-1} for low energy galactic cosmic rays to 10^{10} cm^{-2} s^{-1} for solar flares at 1 AU. The estimated ion irradiation dosage for interstellar, circumstellar, and interplanetary situations are listed in Table 1.

TABLE 1. DOSE ESTIMATES[a]

	Ion Energy	Penetration Depth	Dose (eV/molecule)
Interplanetary Dust	100 keV	0.1 μm	10^1–10^2
Comet in Oort Cloud	> 1 MeV	$\leq$ 0.5 m	10^2
Interstellar Dust	> 1 MeV	total	10^3 (10^9yr)
Interplanetary Dust	1 keV	100 Å	10^5
T Tauri Flare Environment	$\leq$ 1 MeV	1 μm	10^6

[a]Johnson 1989

Still to be explored are the ion environments associated with shock activity in the bipolar outflow and rotating molecular disk during the T Tauri stage of the sun. In addition, it is important to remember the sun was most likely formed as a member of a galactic cluster, and hence, the solar nebula could have been subjected to bipolar outflows of other members of cluster. Perhaps at some point the sun may have been in the Herbig–Haro object of a nearby massive protostar. This scenario seems to have neglected in discussions regarding the formation of the solar system, and one only has to consider the current situation in Orion to recognize its possible impact on models.

The acceleration of 1 keV ions in the solar wind to $\geq$ 100 keV energies in shocks is well established from spacecraft measurements of solar system phenomena (see papers in volume edited by Arons, McKee, and Max, 1979). The diversity of situations involving shocks as particle accelerators in the solar system has been catalogued by Verkatesan (1985) and includes: coronal shocks, bow shocks, interplanetary propagating shocks, corotating interaction forward and reverse interplanetary shocks, and the solar wind termination shock. Voyager 2 measurements in a propagating interplanetary shock have demonstrated that shock energy is translated into accelerated ion energy at an efficiency of approximately 40 percent (Sarris and Krimigis, 1985). During the T Tauri stage of the sun the solar wind mass flow could have been 7 to 8 orders of magnitude greater than its present value. This suggests an intense moderate energy ($\geq$ 100 keV) ion environment as probable.

Attempts have been made to characterize the ion environment in the early solar system through examination of meteorites (Heyman and Dziczkaniec, 1976; Audouze et al., 1976) and observation of T Tauri stars (Worden et al., 1981). Using a scaling argument, Strazzulla (1985) has argued that ion–induced solid–state effects are important for the chemical evolution of planetary systems in their early stages. The difficulty in specific analysis of the ion environment and its impact on chemical processes is that its complexity of multiple sources requires more extensive analysis than that which estimates the outcome of photoprocessing. In the latter case an estimate of the available ultraviolet radiation is accessable from the parameters of photospheric temperature, luminosity, distance, and extinction. An attractive aspect of ion irradiation is that it is free of extinction by dust in the environment and hence should be an important process in dark clouds.

EXPERIMENTS

If ion–irradiation has been an important process in the chemical evolution of the early solar system, then comets are expected to be repositories of the products. Therefore, we have undertaken the task of determing the characteristics of materials processed by ion bombardment for eventual comparison with cometary samples and contemporary and future telescopic observations. Also, experience with laboratory analogs is necessary for planning with integrity the sampling techniques and examination procedures to be utilized in spacecraft missions to comets. Emphasis to date has been on obtaining infrared spectra of non–volatile residues produced by irradiation of ice mixtures with H_2^+ ions (175 keV/proton).

Gas mixtures composed of Ar, CO, H_2O, D_2O, N_2, CH_4, C_2H_2, and C_2D_2 are mixed in a one liter bulb to desired specifications. Typically, a total pressure of 400 torr is used. The gas mixture is bled through a glass capillary into the bombardment chamber where it is frozen onto a sapphire disk maintained in the temperature range of 10 K to 15 K. A one hour deposition results in approximately 200 torr liters being deposited on the 2.5 cm diameter sapphire disk that is cooled by an Air Products Incorporated model 202 closed cycle refrigerator. After deposition, the refrigerator and sapphire are rotated 90^0 bringing the sample into view through two quartz windows. As shown in Figure 1 an ion beam from the Van de Graaff accelerator can bombard the frozen matrix at an incident angle of 45^0. Material eroded from the matrix during ion bombardment can enter the ionizer of the quadrupole mass spectrometer. Prior to cooling the sapphire to cryogenic temperatures, the chamber is evacuated to a pressure of $\leq 1 \times 10^{-7}$ torr using a Varian Star Cell triode ion pump. Also prior to gas deposition, the sapphire is raised briefly to a temperature of 60 K to remove any residual gases other than H_2O and CO_2 that may have condensed during the cooling phase of the experiment.

Concern about contamination in the form of hydrocarbons from the accelerator beam line led to control experiments where Ar and Ar/H_2O mixtures were irradiated with H_2^+ ions accelerated by a potential of 350 KV (175 keV/proton). Negligible amounts or an abscence of residue on the sapphire after sublimation of the Ar or Ar/H_2O mixture leads to the conclusion that the level of contamination is < 1% of residues formed from reactive gases.

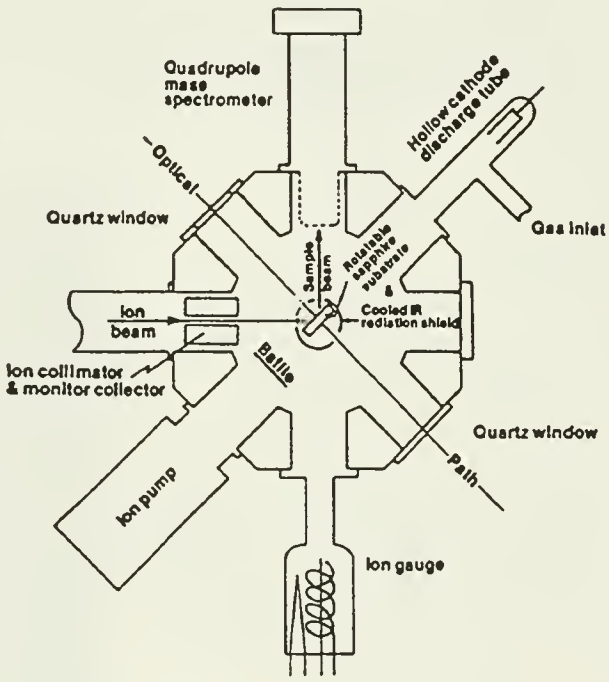


Figure 1. Astrophysics bombardment chamber for the preparation of species by the bombardment of cryogenic ice mixtures with 175 keV protons. The beam collimator on the left serves to reduce contamination from the beam line by a reduction in conductance. Gas mixtures may be ionized by electrical discharge prior to deposition and may be exposed to UV radiation after deposition.

Quadrupole mass spectroscopy of ejected species (Figure 2.) during 175 keV proton bombardment (as H_2^+ ions accelerated by a potential of 350 KV) of an ice mixture of in parts: 170 CO, 170 Ar, and 25 H_2O indicates the formation of species at m/q peaks 29, 30, 32, and 44 suggestive of the CHO radical, CH_2O, CH_3OH, and CO_2.

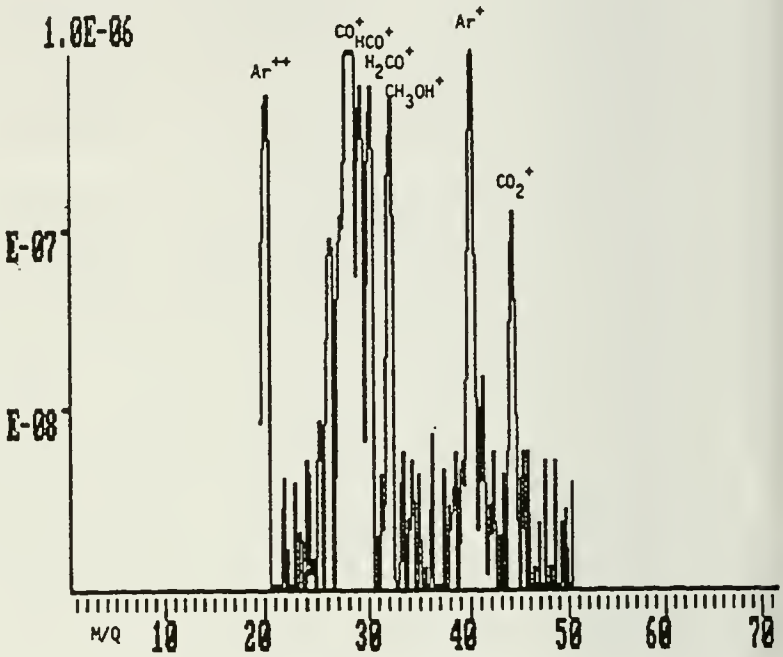


Figure 2. Mass spectrum of species ejected from a CO, Ar, and H_2O ice at 20 K during ion bombardment. The CO^+ and Ar^+ peaks are in excess of the partial pressure scale.

Figure 3 is an SEM image of the residue remaining after sublimation of bombarded ice composed in parts of: 170 CO, 25 H_2O, 20 N_2, and 15 CH_4. This mixture was chosen to reflect cosmic molecular abundances (Wdowiak et al. 1989). The SEM image was made with 1.1 keV electrons and the sample was not coated with a conductive film. This indicates it may not be necessary to coat samples while using a spacecraft SEM avoiding an obvious complication. Strazzula (1988) warns that conclusions regarding morphology of samples prepared at high dose rates may not be valid for astrophysical situations.



Figure 3. SEM image.

INFRARED SPECTRA OF RESIDUES

H_2^+ ion beam currents of less than 1 μamp to as great as 10 μm are used to irradiate a target area of approximately 0.25 cm^2. This translates into a proton flux between ~ 1 x 10^{13} cm^{-2} s^{-1} and ~ 5 x 10^{14} cm^{-2} s^{-1} or an integrated flux between ~ 2 x 10^{16} cm^{-2} and ~ 4 x 10^{18} cm^{-2}. Assuming a maximum penetration of 10 μm, dose estimates range from ~ 700 eV/molecule to ~ 1.4 x 10^5 eV/molecule for 175 keV protons incident on a CO ice. The experiments cover the higher part (~ 10^3 – ~ 10^5 eV/molecule) of the dose range listed in Table 1. The integrated flux of 4 x 10^{18} cm^{-2} compares well with the estimate of Andouze et al. (1976) of ~ 3 x 10^{18} cm^{-2} for the irradiation of the amorphous grains of carbonaceous chondrites with protons having energies $\geq$ 100 keV.

The color of the residues depends upon dosage and range from brownish yellow to black with a brown tinge on the periphery. Samples are prepared for FTIR absorption spectroscopy by dispersing the residue into 100 mg spectroscopic grade KBr in a two ball agate vibrating mill. The mixture is pressed into a 0.25 cm^2 pellet at a pressure of 20,000 PSI. Spectra are obtained with a Mattson Polaris FTIR spectrometer operating in the 4000 cm^{-1} to 400 cm^{-1} (2.5μm to 25μm) range.

The spectrum of the bombarded ice brown residue (displayed in Figure 3) is shown in Figure 4 along with material vaporized from the acid insoluble residue of the Orgueil C1 carbonaceous chondrite onto a KBr crystal (Wdowiak et al., 1988). The ice residue exhibits aliphatic C–H stretch at 2940 cm^{-1} (3.4 μm), C=O stretch at 1710 cm^{-1} (5.85 μm), C=C stretch at 1620 cm^{-1} (6.2 μm), and features at 1380 cm^{-1} (7.24 μm) and 1100 cm^{-1} (9.1 μm). These features are in common with some of those of the volatile fraction of the acid insoluble residue of the Orgueil C1 carbonaceous chondrite. This particular residue was prepared at an estimated dose of ~ 1 x 10^4 eV/molecule composed of parts: 170 CO, 25 H_2O, 20 N_2, and 15 CH_4.

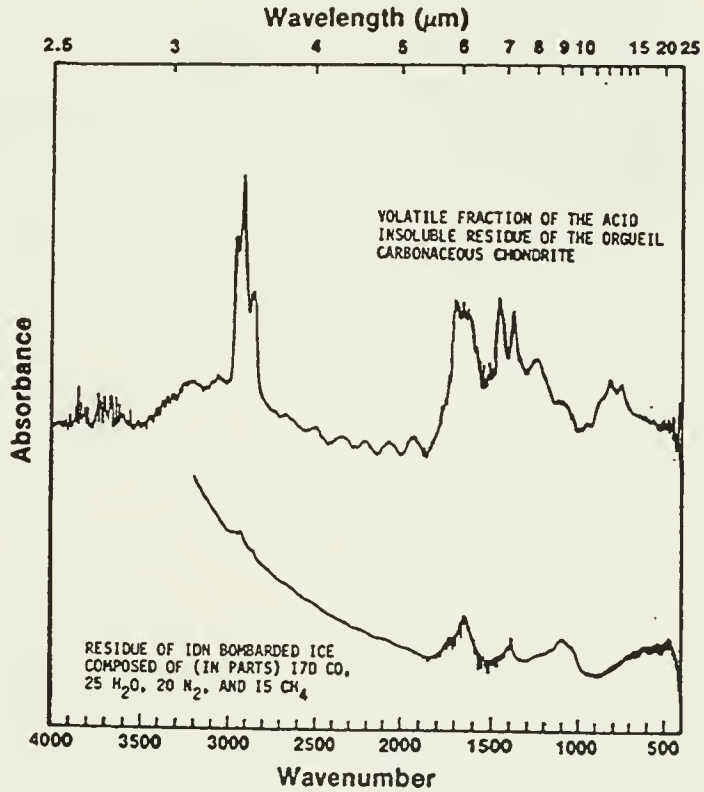


Figure 4. FTIR spectrum of bombarded ice residues prepared at a dose of ~ 1 x 10^4 eV/molecule using 175 keV protons, and that of the acid insoluble residue of the Orgueil C1 meteorite.

Irradiation at a current and duration leading to an estimated dose of ~ 5 x 10^4 eV/molecule results in black with brown tinged periphery residue prepared from an ice in parts of: 170 CO, 170 Ar, 25 H_2O, 20 N_2, and 15 CH_4. The FTIR spectrum (Figure 5) besides exhibiting aliphatic C–H stretch at 2940 cm^{-1} (3.4μm) and the feature at 1400 cm^{-1} (7.1μm), is significant in that it has strong features that correlate with the observed celestial unidentified infrared bands (UIRs) emitted by numerous cosmic sources ranging from bipolar nebulae to galaxies. First discovered by Gillett, Forrest, and Merrill (1973) the UIRs are found in emission at 3.3 μm (3030 cm^{-1}), 6.2 μm (1620 cm^{-1}), 7.7 μm (1300 cm^{-1}), 8.6 μm (1163 cm^{-1}), and 11.3 μm (885 cm^{-1}). Because the laboratory material has a brown component, the two aliphatic (and non–UIR) features may be due to that component and not the material responsible for the features at UIR wavelengths. That possibility is currently under investigation. Figure 6 shows the high degree of correlation of the features of the laboratory material with the four of the five predominant UIRs. Especially significant is the exact coincidence with the 7.7 μm and 8.6 μm UIRs. The principle deviation is with the 11.3 μm UIR thought to be due to the out–of–plane aromatic hydrogen wag (Cohen et al., 1985). However, the 11.6 μm feature of the laboratory material is a better match than that of the 11.9 μm feature of coronene as proposed by Leger and Puget (1984), although not as good as the 11.3 μm match achieved by thermal treatment of the Orgueil C1 acid insoluble residue (Wdowiak et al., 1988).

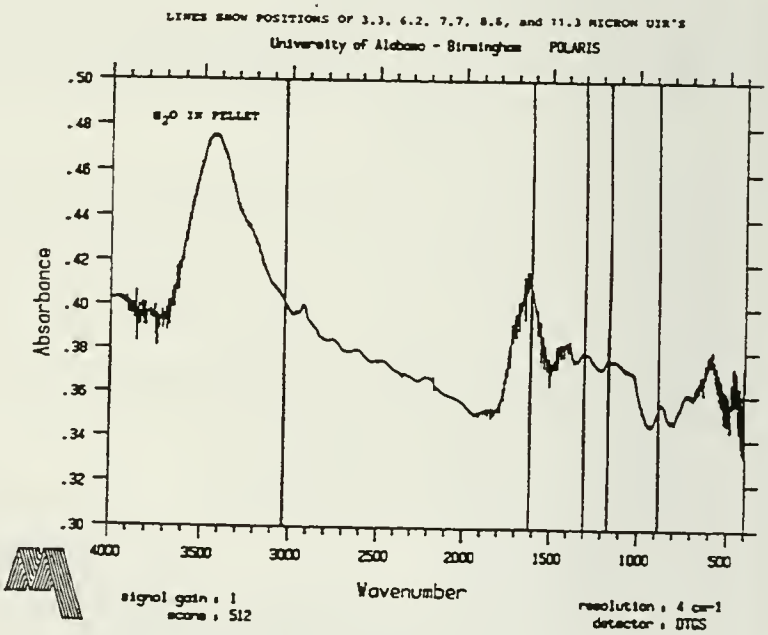


Figure 5. FTIR spectrum of bombarded ice residue prepared at a dose of ~ 5 x 10^4 eV/molecule showing coincidence with four of the five UIR bands at frequencies marked by vertical lines.

CONCLUSIONS

The formation of solid material from the ion bombardment of reactive cryogenic ices is of interest as a laboratory analog for the CHON particles detected during the Giotto and Vega encounters with Comet Halley (Kissel et al., 1986a; 1986b). During the T Tauri stage of the sun, extensive flare activity and a solar wind mass flow of 7 to 8 orders of magnitude of its present value would have produced an intense moderate energy ion

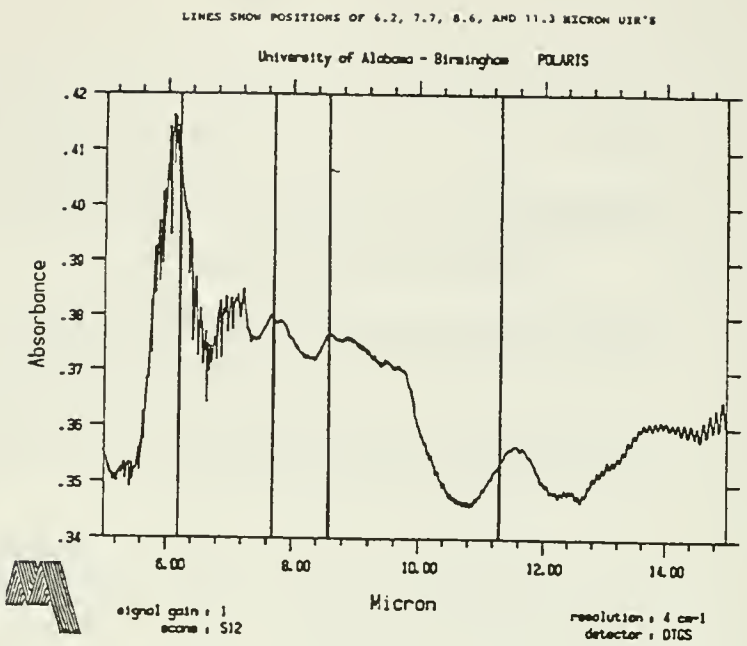


Figure 6. FTIR spectrum shown in Fig. 5 plotted against a micron scale showing the high degree of coincidence with four of the five UIR bands.

environment. Considerable shock activity would have been present resulting in 1 keV T Tauri wind ions accelerated by shock processes to $\geq$ 100 keV. These ions impacting on cryogenic reactive ice mantles of dust grains and centimeter size ice "chunks" would produce organic solids. Aggregation of the bombarded ice mantled grains and "chunks" into a cometary nucleus would result in particulates being distributed throughout. The chemical nature of the organic solids would depend upon the dosage with aliphatics dominant at low dosage and aromatics at higher dosage. Aromatic material has been detected by nuclear magnetic resonance in the acid insoluble residue of the Orgueil C1 carbonaceous chondrite (Cronin et al., 1986), and by Raman spectroscopy in the interplanetary dust particle (IDP) Essex (Allamandola et al., 1987). Bipolar outflow appears to be ubiquitous occurring in planetary nebulae such as the Red Rectangle (Schmidt et al., 1980; Warren–Smith et al., 1981) and would be expected to be accompanied by shock activity. Ion acceleration in shocks and the irradiation by these ions of cryogenic reactive ice mantles may be a mechanism through which the species responsible for the UIR bands are formed. Ion irradiation may also be an important mechanism in active galaxies such as M 82 and in dusty regions in general.

Continuing experiments are focusing on the relationship between dosage and the development of infrared spectral features as suggested by comparison of the ice residue spectra in Figures 4 and 5.

TJW and GCF wish to acknowledge the support of NASA Grant NAGW–749.

REFERENCES

Allamandola, L. J., Sanford, S. A., and Wopenka, B. (1987) Interstellar Polycyclic Aromatic Hydrocarbons and Carbon in Interplanetary Dust Particles and Meteorites. Science, 237, 56–59.

Arons, J., McKee, C., Max, C., eds (1979); Particle Acceleration Mechanisms in Astrophysics, American Institue of Physics.

Audouze, J., Bibring, J. P., Dran, J. C., Maurette, M., and Walker, R. M. (1976) Heavily Irradiated Grains and Neon Isotope Anomalies In Carbonaceous Chondrites. Ap. J. (Letters) 206, L185–L189.

Cohen, M., Tielens, A. G. G. M., and Allamandola, L. J., (1985) A New Emission Feature in IRAS Spectra and the Polycyclic Aromatic Hydrocarbon Spectrum. Ap. J. (Letters) 299, L93.

Cronin, J. R., Pizzarello, S., and Frye, J. S. (1987) ^{13}C NMR Spectroscopy of the Insoluble Carbon of Carbonaceous Chondrites. Geochim. Cosmochim. Acta 51, 299–303.

Gillett, F. C., Forrest, W. J., and Merrill, K. M. (1973) Ap. J. 183, 87.

Greenburg, J. M. (1989) From Interstellar Dust To Comets. LPI Contribution No.691. Analysis of Returned Comet Nucleus Samples, 22–23.

Heymann, D., and Dziczkaniec, M. (1976) Early Irradiation of Matter in the Solar System: Magnesium (Proton, Neutron) Scheme. Science 191, 79–81.

Johnson, R. E. (1989) Radiation Modification of Cometary Materials: Laboratory Simulations. LPI Contibution No. 691, Analysis of Returned Comet Nucleus Samples, 32.

Kissel, J., Sagdeev, R., Bertaux, J., Angarov, V., Audouze, J., Blamont, J., Buchler, K., Evlanov, E., Fechtig, H., Fomenkova, M., von Hoerner, H., Inogamov, N., Khromov, V., Knabe, W., Krueger, F., Langevin, Y., Leonas, V., Levasseur–Regourd, A., Managadze, G., Podkolzin, S., Shapiro, V., Tabaldyev, S., Zubkov, B. (1986a) Composition of Comet Halley Dust Particles from Vega Observations. Nature 321, 280–282.

Kissel, J., Brownlee, D., Buchler, K., Clark, B., Fechtig, H., Grun, E., Hornung, K., Igenbergs, E., Jessberger, E., Krueger, F., Kuczera, H., McDonnell, J., Morfill, G., Rahe, J., Schwehm, G., Sekanina, Z., Utterback, N., Volk, H., Zook, H. (1986b) Nature 321, 336–337.

Leger, A., and Puget, J. L. (1984) Identification of the Unidentified IR emission features of Interstellar Dust? Astr. Ap. 137, L5–L8.

Sarris, E. T., and Krimigis, S. M. (1985) Quasi–Perpendicular Shock Acceleration of ions to ~ 200 MeV and Electrons to ~ 2 MeV Observed by Voager 2. Ap. J. 298, 676–683.

Schmidt, G. D., Cohen, M., and Margon, B. (1980) Discovery of Optical Molecular Emission From the Bipolar Nebula Surrounding HD 44179. Ap. J. (Letters) 239, L133–L138.

Strazzulla, G. (1984) Modifications of Grains by Particle Bombardment in the Early Solar System. Icarus 61, 48–56.

Strazzulla, G. (1988) Ion Bombardment: Techniques, Materials and Applications. In Experiments on Cosmic Dust Analogues (eds. E. Bussoletti, C. Fusco, and G. Longo). Klower Academic Publishers, Dordrecht, 103–113.

Venkatesan, D. (1985) Cosmic Ray Picture of the Heliosphere. Johns Hopkins APL Technical Digest 6 No. 1, 4–19.

Warren–Smith, R. F., Scarrott, S. M., and Murdin (1981) Peculiar Optical Spectrum of the Red Rectangle. Nature 292, 317–319.

Wdowiak, T. J., Flickinger, G. C., and Cronin, J. R. (1988) Insoluble Organic Material of the Orgueil Carbonaceous Chondrite and the Unidentified Infrared Bands. Ap. J. (Letters) 328, L75–L79.

Wdowiak, T. J., Donn, B., Nuth, J. A., Chappelle, E., and Moore, M. (1989) Laboratory Experiments On Carbonaceous Material As a Source For the Red Rectangle Visual Emissions. Ap. J. 336, 838–842.

Worden, S. P., Schneeberger, T. J., Kuhn, J. R., and Africano, J. L. (1981) Flare Activity On T Tauri Stars. Ap. J. 244, 520–527.

ON THE ISOTOPE ANALYSIS OF COMETARY DUST

Friedrich Begemann
Max-Planck-Institut für Chemie
Mainz, FRG

ON THE ISOTOPE ANALYSIS OF COMETARY DUST

Friedrich Begemann

Max-Planck-Institut für Chemie, Mainz, FRG

The understanding was that this presentation should consist of two parts, one about what one may hope to learn from the isotopic analysis in the laboratory of cometary matter, and a second part on whether present-day analytical methods are adequate to reach these goals, where improvements are required and what needs to be developed in order to optimize the scientific return. The understanding was, furthermore, that I should report on isotopics and the analysis of heavy elements and noble gases by conventional mass spectrometry, but that I should neither concern myself with light elements like H, C, O and N, nor should I deal with the potential of ion probes.

I. Problems of interest

Comets are still believed to be a conglomerate of ices and meteoritic dust in a ratio of about 5:1 (if we take the ratio ices/dust to be equal to the ratio gas/dust). When Whipple proposed his "dirty snowball" model in 1950 he envisaged a single, well consolidated body; recent refinements are the icy-glue model for the cometary nucleus of Houpis and Gombosi (1986) or the "primordial rubble pile" of Weissman (1986). These refinements appear to pertain essentially to the macroscopic structure of the nucleus on the scale of tens of centimeters to hundreds of meters, however, so they need not concern us in the present context, since we are interested in the structure on a much smaller scale. What we should like to know is the size distribution of non-gaseous matter ("gaseous" at elevated temperatures like room temperature) which we may expect in a kg-sized sample. The most recent and most comprehensive data available on this topic are those obtained for comet Halley which may or may not be typical of comets - but then we do not know, of course, how "typical" the first returned cometary sample will be either.

According to McDonnell et al. (1987) the grain size distribution, at the cometary surface, is such that the number of grains decreases steeply with increasing grain size, but the exponent in the power law distribution appears to be ≤ 3 over the whole size range analysed which is from about 1 μm to 1 cm, corresponding to a range in mass from ca. 10^{-15}g to 1 g. The fact that the exponent in the power-law is < 3 means, of course, that most of the mass occurs in large grains. Still, if one kg of cometary matter were to be returned, it should contain a hundred gram or so of silicates, and a few milligram of these would be grains with masses of 10 μg or less.

The question what one can do with these grains, and what one may hope to learn from their analysis, is related to the nature of the grains. We anticipate to find brittle, friable, loosely connected aggregates of primordial grains, a collection of "stardust" and of pristine grains from the proto-solar cloud. And we hope that the "yellow stuff" of Greenberg [cf. e.g. Greenberg and Grim, 1986] plays a minor role, at least in the sense that individual fragments of the fragile grains may be covered by it, but the grains as a whole are not. Presumably, this would make the disintegration of the grains into their original constituents much easier as if everything were embedded in "yellow stuff".

The reason why one would wish to do this and why one wants to have a look at the grains in their original state is, of course, the experience we have with carbonaceous chondrites. From several of them, in particular the CM 2's Murray and Murchison, it has been possible to isolate rare constituents which are more or less anomalous in the isotopic composition of all their elements (H, C, N, Ne, Si, Kr, Xe; (Swart et al., 1983; Lewis et al., 1983; Yang and Epstein, 1984; Zinner et al., 1987; Ott et al., 1988; Tang Ming and Anders, 1988). Since the anomalies are as they are predicted for different processes of nucleosynthesis, the explanation is that these grains are "stardust", i.e., that they are unadulterated primary condensates from the stars in which the elements were produced. Such "stardust" as it is known from astronomical observations and from meteorites is in the sub-micrometer size range, and it is therefore grains of this size which should be analysed, one by one, or which should be pooled. The only reason why this has been possible in meteorites is that nature has been kind to us by providing the isotopically anomalous elements in phases with an extreme chemical resistivity - carbonaceous matter, diamonds, SiC (Zinner et al., 1987, and references therein) - which makes them the insoluble residue when one subjects the carbonaceous chondrites to an extended and harsh chemical treatment. But there is no a priori-reason why all "stardust" should be chemically refractory; perhaps the inertness of a few such components is just meant as a hint for us to look for others which might be as interesting and as rewarding as the ones which have been found so far.

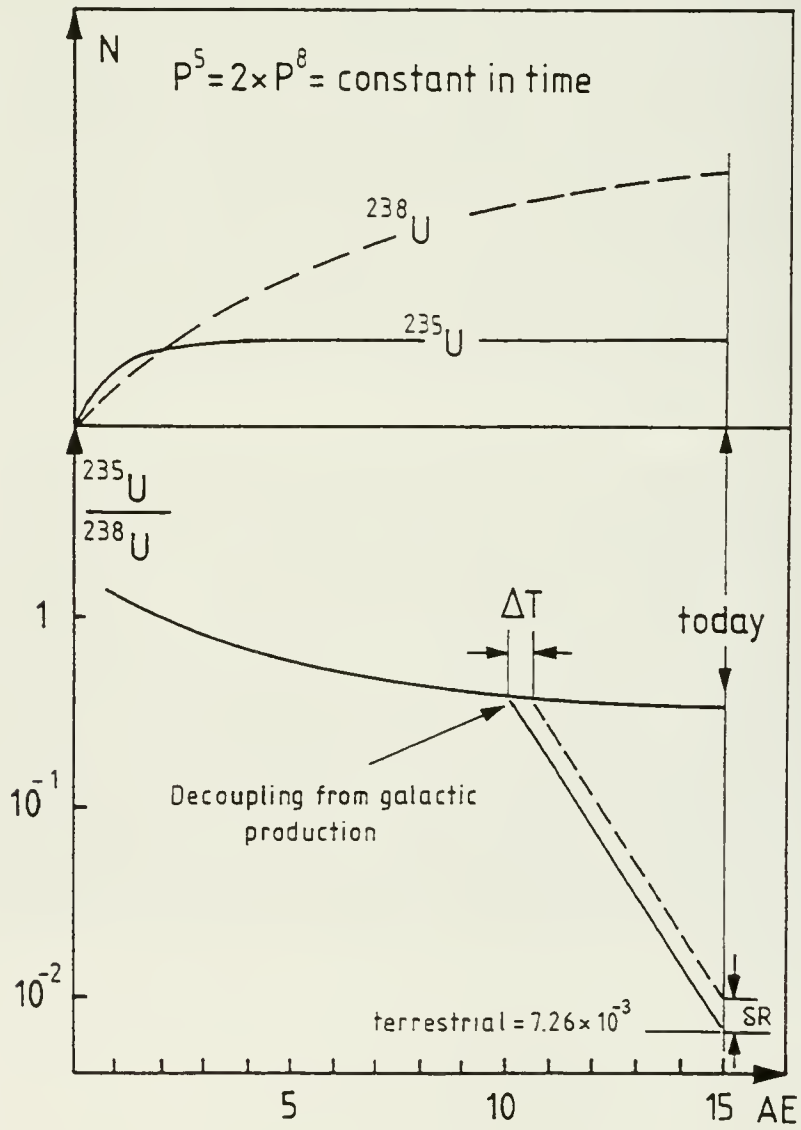
Aside from attempts to identify and isotopically analyse individual grains in order to better characterize the different nucleosynthetic contributions to the proto-solar nebula there are other questions which can perhaps be answered by looking at larger ensembles of grains. One is the age of the solid matter. There may be two problems, however. The first is related to the small grain size of the "stardust". Since all radiometric clocks depend on one kind or other of radioactive decay, there is always a certain fraction of the total decay energy imparted to the daughter product and this may make it recoil out of where it belongs. How serious this problem is depends on which decay one wants to utilize - fission transfers a much larger kinetic energy to its fragments than does α-decay which, in turn, is orders of magnitude more effective than β-decay. Typical ranges of the recoil particles are 15 μm for fission fragments, 15 nm ($\hat{=}$ 150 Å) for α-decay and distances of a few atomic diameters for β-decay. The severity of the problem of losses by recoil

depends then on the commensurability of these recoil ranges with the grain size of the host material, on the average distance between grains, and on what the interstitial space is filled with. What should be done in order to avoid these problems is a "whole rock" analysis on chunks of cometary matter which include all the original constituents - solid, liquid and gaseous (under normal lab conditions). And one might look at the ices separately and see whether they are enriched in radiogenic nuclides which would give an indication whether the effect is something to worry about.

The second problem is one of interpreting the data. If the meteoritic part of cometary matter was never isotopically and elementally equilibrated it will not be possible to determine an internal isochron, which would date the time since equilibration, and the meaning of an age will not be immediately obvious. After all, if cometary matter were a representative sample of pre-solar system matter, it would make no difference whether the radiometric clocks were running in the dilute pre-solar cloud or in the condensed cometary matter, except that condensed matter would be cut off from galactic nucleosynthesis. As to this latter point it would be interesting to know the time since cometary matter was decoupled from galactic nucleosynthesis. One way to measure this is to look at the relative abundance of radionuclides like ^{40}K and ^{87}Rb, or to measure the $^{235}U/^{238}U$ abundance ratio. Both U-isotopes are produced in the r-process of nucleosynthesis which is, of course, spotty in time and space, but on time scales of the half life of ^{235}U and ^{238}U it is fairly regular. In the simplest case of a production rate constant in time the situation is as depicted in Fig. 1. The concentration of both isotopes increases with time until an equilibrium is reached where the production rate equals the decay rate. ^{235}U, because of its shorter half life, will reach this equilibrium faster than ^{238}U and consequently the abundance ratio $^{235}U/^{238}U$ changes with time, it slowly decreases. Once uranium is cut off from its source so that nothing is being produced any more the ratio decreases much faster, almost with the half life of ^{235}U. Actually, the ratio changes so fast that its exact value is rather sensitive to the time of decoupling: a difference of 100 Ma ensues in a change of the ratio of ca. 8%.

The results presently available for solar system matter are notoriously messy. For terrestrial and lunar samples the ratio has invariably been found to be constant, but for meteorites different laboratories have measured quite contradictory results (cf. Shimamura and Lugmair, 1981 and references therein). Still, for bulk samples the total range reported so far is less than 2% which would indicate that meteoritic, terrestrial and lunar matter all were decoupled from r-process nucleosynthesis within 20 Ma or so. (It should be mentioned, though, that most of the production of the U isotopes occurs via their radioactive precursors and that there are other explanations possible for variations in the $^{235}U/^{238}U$ ratio (cf. e.g. Tatsumoto and Shimamura, 1980)). For cometary matter one might expect a less strict contemporaneity, be it because the outer reaches of the proto-solar cloud were still in contact with interstellar matter at a time when the inner parts had been decoupled already, or because (some) comets are errant messengers from other worlds altogether.

Figure 1: Idealized sketch of the development of r-process ^{235}U and ^{238}U and of their abundance ratio. a) The absolute concentrations increase with time until an equilibrium is reached between production and decay. Note, that the assumption of a production rate constant in time is an oversimplification and that the exact value for the ratio of the production rates (which include production via radioactive precursors) as well as the duration of r-process nucleosynthesis are contentious [Thielemann et al., 1983,; Fowler, 1987; Clayton, 1988]. This, however, does not affect the essential point discussed here. b) The abundance ratio $^{235}U/^{238}U$ in interstellar matter decreases with time because ^{238}U ($T_{1/2}$ = 4.47 x 10^9a) approaches its equilibrium concentration slower than does ^{235}U ($T_{1/2}$ = 7.04 x 10^8a). At the time, matter is decoupled from galactic production the ratio starts to change very fast, due to the much faster decay of ^{235}U as compared to ^{238}U. If the decoupling of two parcels of matter is separated in time by ΔT, the present-day $^{235}U/^{238}U$ ratio in the two parcels will be different by δR.



II. Experimental requirements

A solution of the problems I have been sketching requires mass spectrometric isotope abundance analyses. Since we do not know what to expect, it is difficult to say which accuracy will be necessary in order to reach meaningful conclusions. What we should strive for, however, are uncertainties in isotope abundance ratios of less than 1 percent. If we take this number as a basis for our discussion what, then, is the minimum amount of material required to reach this goal?

A mass spectrometric analysis consists essentially of three steps

Ionisation
Transmission of ions
Detection of ions.

Independent of the exact mode of detection, whether it is measuring currents or ion counting, the entity which determines the ultimate precision that can be reached is the number of collected ions. Since the statistical error connected with registering n independent events is $\sqrt{n}$ the relative error is $\sigma = \sqrt{n}/n = 1/\sqrt{n}$ so that a statistical uncertainty of 1 percent requires that 10^4 ions be registered. Let us assume that the relative abundance of the particular isotope we want to measure is 10% and that the atomic weight of the element is 60. What is needed then is $10^4 \times 1/0.1 \times 60/6 \times 10^{23} = 10^{-17}$g of ions of the element in question. If we assume further that the abundance of our element in the grains is 1% by weight, then the grain must have a mass of 10^{-15}g which corresponds to a diameter of ca 0.1 μm.

This is the absolute minimum amount of material required since the estimate implies, first, that there are no errors other than the statistical ones connected with the number of counted ions and, second, that all atoms are ionized and registered. In reality the total efficiency for detection is

$$\eta_{total} = \eta_{ionisation} \times \eta_{transmission} \times \eta_{registration}$$

Table 1 shows a compilation of data from the literature for the product $\eta_{ionisation} \times \eta_{transmission}$. All measurements were performed with modern mass spectrometers for which the transmission is better than 50% so that, within a factor of two, the entries in column 3 are essentially the ionisation efficiencies. Note that in all cases except the noble gases, emitters have been used which for some not well-understood reason greatly enhance the ionisation efficiency. Actually, they do this in such an irregular way as to obliterate the dependance on ionisation energy of the ionisation probability as one finds it for thermal ionisation without emitter, and they do it in such an unpredictable way that so far trial and error is just about the only way to find efficient emitters.

From this compilation it is obvious that, using present technologies, the amount of matter required is typically at least hundred times the minimum amount calculated above. "At least", since the registration efficiency is not unity which would require, first, that all ions at the receiving end of the mass spectrometer are collected and, second, that the sample is run to exhaustion. Collecting all ions is not possible in the normal sequential

scanning mode where the magnetic field is changed in steps and one isotopic species is collected while all others go undetected. It rather necessitates using a multicollector which has the additional advantage that, at least in principle, irregularities in the ion beam intensity cancel out so that abundance ratios can be measured even if the signal is very noisy. Modern technology is sufficiently advanced that one need not worry any more about the vagaries of working with a number of independent amplifiers or counting systems, at least not at the level of precision we are talking about.

Table 1. IONISATION YIELD TIMES TRANSMISSION FOR SOME SELECTED ELEMENTS.

Element	E_J[eV]	$n_{ion} \times n_{trans.}$	Emitter	Reference
Mg	7.6	1×10^{-2}	Si-gel, H_3PO_4	-
Ca	6.1	1×10^{-3}	Ta_2O_5	(1)
Ti (as TiO+)	-	10^{-4}	Ta_2O_5	(2)
Cr	6.7	2×10^{-3}	Si-gel, H_3PO_4	(3)
Ni	7.6	2×10^{-3}	Si-gel, Ge-Oxide	(4)
Ru	7.7	2×10^{-3}	Si-gel, H_3PO_4	(5)
Sn	7.3	1×10^{-3}	Si-gel, H_3PO_4	-
Pb	7.4	1×10^{-2}	Si-gel, H_3PO_4	-
U	(6.1)	1×10^{-2}	Graphite	(6)
Ar	15.6	0.5	e^--bombardment	(7)
Xe	12.1	0.7	e^--bombardment	(7)

(1) Jungck, M.H.A. et al., 1984
(2) Niederer, F.R. et al., 1980
(3) Birck, J.L. and Allègre, C., 1984
(4) Birck, J.L. Lugmair, G.W., 1988
(5) Poths, H. et al., 1987
(6) Chen, J.H. and Wasserburg, G.J., 1980
(7) Hohenberg, C.M., 1980 Kirschbaum, C. 1988

Running a sample to exhaustion may not appear to be difficult. Presently, however, the emphasis is more on stable ion beams, and for many elements these have only been attained at rather low intensities. In this case running a sample to exhaustion means long times of measurements. This, by itself, is no problem, but any ion detection device has its background and it clearly would be advantageous to have a signal which normally lasts for 20 hours compressed into, say, 20 minutes if one had a corresponding increase in the signal/noise ratio. Again, use of a multicollector should alleviate much of the need for stable ion beams, but it remains to be shown how much compression in time of the signal can be done without deterioration of the ionisation yields.

Finally, in order to avoid contamination, handling of the cometary samples should be kept to an absolute minimum. Preferably, individual crystals should be loaded directly onto the filament of the ion source whithout any chemical treatment whatsoever. Lee et al. (1977) have shown that <0.4ng of Mg from an anorthite crystal with Al/Mg >280 can be isotopically analysed with a precision of better than 1 percent. But again, it remains to be shown that "direct loading" can be done without much reduction in ion yields and in particular that a combination of "direct loading" and signal compression still allows to distinguish between a genuine anomalous isotopic composition of an element and an apparent one caused by compromising interferences on one or more of the masses.

Problems with such compromising interferences must indeed be anticipated once the analyses are performed in such a way that control measurements are not possible. One way to regain specificity in the sense that only one element at a time is ionized and detected is to utilize laser resonance ionisation. This together with laser evaporation of the samples would certainly be a very clean method of analysis. Samples could be measured without doing chemistry, thus avoiding the inevitable problem of contamination, and the amount of hot structural material in the ion source would be kept to a bare minimum which again would help to reduce contamination. Of course, this would make it impossible to take advantage of the enhancement by orders of magnitude of the ion yield by using emitters so that it remains to be seen whether the advantages outweigh the drawbacks. And it must be realized that by this method it will be a non-trivial matter to analyse more than one element per grain which makes the search for correlated anomalies difficult, if not impossible.

For noble gases the situation is somewhat different and in a sense much more advanced already and closer to the theoretical limits. High-sensitivity ion sources require only ca. 15 000 atoms of Ar or Xe to yield a count rate of 1 count per second (cps) which should be compared with a background count rate of 0.1 cps or less (Kirschbaum, 1988). Transmission x ionisation yield are >0.5 (Baur, 1980; Hohenberg, 1980) so that more than 50% of all gas atoms are available for registration. So far this potential has not been fully utilized, however, because ion collection is still done sequentially with single collectors. In the case of Kr and Xe with their many stable isotopes this means that a factor of 10 or more is given away in the total number of ions. Use of a multicollector would again be the way out but in the case of gases it would not only be beneficial. It would result in a considerable increase in volume of the mass spectrometer and, since noble gases are always measured under static conditions, a corresponding decrease of gas pressure in the spectrometer. A reduced particle density in the ion source, in turn, results in a lower ion beam intensity so that the advantage of the multicollector that a larger fraction of the total number of ions is collected is offset in part by a lower signal/noise ratio.

III. Conclusion

It would appear that no major break-throughs or innovations are required

in order to exploit the isotopic information we expect to be contained in cometary "solid" matter. What is needed, however, is combining a number of technologies into a single instrument and a demonstration that the whole is not more than but equal to the sum of its parts. Preferably, such an instrument should also provide the possibility to characterize by appropriate non-destructive means single grains prior to their destructive isotope analysis.

References:

Baur, H.: Numerische Simulation und praktische Erprobung einer rotationssymmetrischen Ionenquelle für Gasmassenspektrometer. Ph.D dissertation, Swiss Fed. Inst. Technology, 1980.

Birck, J.L.; and Allègre, C.J.: Chromium Isotopic Anomalies in Allende Refractory Inclusions. Geophys. Res. Lett., vol. 11, 1984, pp. 943-946.

Birck, J.L.; and Lugmair, G.W.: Nickel and Chromium Isotopes in Allende Inclusions. EPSL, vol. 90, 1988, pp. 131-143.

Chen, J.H.; and Wasserburg, G.J.: A Search for Isotopic Anomalies in Uranium. Geophys. Res. Lett., vol. 7, 1980, pp. 275-278.

Clayton, D.D.: Nuclear Cosmochronology within Analytical Models of the Chemical Evolution of the Solar Neighbourhood. Mon. Nat. R. astr. Soc. vol. 234, 1988, pp 1-36.

Fowler, W.A.: The Age of the Observable Universe. Quarterl. J. R. astr. Soc. vol. 28, 1987, pp. 87-102.

Greenberg, M.J.; and Grim, R.: The Origin of Comet Nuclei and Comet Halley Results.20th ESLAB SYMPOSIUM on the Exploration of Halley's Comet. Proceedings of the International Symposium Heidelberg, Germany 27-31 October 1986, pp. 255-263.

Hohenberg, C.M.: High Sensitivity Pulse-Counting Mass Spectrometer System for Noble Gas Analysis. Rev. Sci. Instrum., vol. 51, 1980, pp. 1075-1082.

Houpis, H.L.F.; and Gombosi, T.I.: An Icy-Glue Nucleus Model of Comet Halley. 20th ESLAB SYMPOSIUM on the Exploration of Halley's Comet. Proceedings of the International Symposium Heidelberg, Germany 27-31 October 1986, pp. 397-401.

Jungck, M.H.A.; Shimamura, T.; and Lugmair, G.W.: Ca Isotope Variations in Allende. Geochim. Cosmochim. Acta, vol. 48, 1984, pp. 2651-2658.

Kirschbaum, C.: Carrier Phases for Iodine in the Allende Meteorite and their Associated $^{129}Xe_r/^{127}I$ ratios: A Laser Microprobe Study. Geochim. Cosmochim. Acta, vol. 52, 1988, pp. 679-699.

Lee, Typhoon; Papanastassiou, D.A.; and Wasserburg G.J.: Mg and Ca Isotopic Study of Individual Microscopic Crystals from the Allende Meteorite by the Direct Loading Technique. Geochim. Cosmochim. Acta, vol. 41, 1977, pp. 1473-1485.

Lewis, R.S.; Anders, E.; Wright, I.P. et al.: Isotopically Anomalous Nitrogen in Primitive Meteorites. Nature, vol. 305, 1983, pp. 767-771.

McDonnell, J.A.M.; Alexander, W.M.; Burton, W.M. et al.: The Dust Distribution within the Inner Coma of Comet P/Halley 1982i: Encounter by Giotto's Impact Detectors. Astron. Astrophys. vol. 187, 1987, pp. 719-741.

Niederer, F.R.; Papanastassiou, D.A.; and Wasserburg, G.J.: Endemic Isotopic Anomalies in Titanium. Astrophys. J., vol. 240. 1980, pp. L73-L77.

Ott, U.; Begemann, F.; Jongmann Yang; and Epstein, S.: S-Process Krypton of Variable Isotopic Composition in the Murchison Meteorite. Nature, vol. 332, 1988, pp. 700-702.

Poths, H.; Schmitt-Strecker, S.; and Begemann, F.: On the Isotopic Composition of Ruthenium in the Allende and Leoville Carbonaceous Chondrites. Geochim. Cosmochim. Acta, vol. 51, 1987, pp. 1143-1149.

Shimamura T.; and Lugmair G.W.: U-isotopic Abundances. Lunar Planet.Sci. XII, 1981, p. 976-978.

Swart, P.K.; Grady, M.M.; Pillinger, C.T. et al.: Interstellar Carbon in Meteorites. Science, vol. 220, 1983, pp.406-410.

Tang Ming; and Anders, E.: Isotopic Anomalies of Ne, Xe, and C in Meteorites. III. Local and Exotic Noble Gas Components and their Interrelations. Geochim. Cosmochim. Acta, vol. 52, 1988, pp. 1245-1254.

Tatsumoto, M.; and Shimamura, T.: Evidence for live ^{247}Cm in the Early Solar System. Nature, vol. 286, 1980, pp. 118-122.

Thielemann, F.-K.; Metzinger J.; and Klapdor H.V.: Beta-Delayed Fission and Neutron Emission: Consequences for the Astrophysical r-Process and the Age of the Galaxy. Z. Phys. A - Atoms and Nuclei, vol. 309, 1983, pp. 301-317.

Weissman, P.A.: Are Cometary Nuclei Primordial Rubble Piles? Nature, vol. 320, 1986, pp. 242-244.

Whipple, F.L.: A Comet Model. I. The Acceleration of Comet Encke. Astrophys. J., vol. 111, 1950, pp. 375-394.

Yang, Jongmann; and Epstein, S.: Relic Interstellar Grains in Murchison Meteorite. Nature, vol. 311, 1984, pp. 544-547.

Zinner, E.; Tang Ming; and Anders, E.: Large Isotopic Anomalies of Si, C, N and Noble Gases in Interstellar Silicon Carbide from the Murray Meteorite. Nature, vol. 330, 1987, pp. 730-732.

ANALYSIS OF ORGANIC COMPOUNDS IN RETURNED COMET NUCLEUS SAMPLES

John R. Cronin
Arizona State University
Tempe, Arizona

ANALYSIS OF ORGANIC COMPOUNDS IN RETURNED COMET NUCLEUS SAMPLES

John R. Cronin

Arizona State University
Tempe, Arizona

INTRODUCTION

Comets are generally believed to be primitive bodies that preserve solar system matter in, or nearly in, its primordial state. This expectation has been at least partially borne out by the 1986 flyby missions to Comet Halley which provided data indicating that, with the exception of hydrogen, the light elements (C, N, O, and S) occur in approximately their solar abundances (Delsemme, 1988). Although mass spectrometers carried aboard the spacecraft provided much additional data from which to speculate about the molecular forms of these elements (Kissel and Krueger, 1987), a detailed understanding of cometary organic chemistry will ultimately require the laboratory examination of returned samples. Some of the problems that will be encountered in such studies, for example, sensitivity to trace constituents, resolution of numerous isomeric forms, and avoidance of terrestrial contaminants, have already been faced in analyses of the organic compounds from carbonaceous chondrites. (See Cronin et al., (1988) for a recent review.) Furthermore, there is reason to believe that the progenitors of the carbonaceous chondrites were volatile-rich planetesimals (Bunch and Chang, 1980) similar to those which, at greater radial distances, formed comets. Thus, the organic chemistry of carbonaceous chondrites may represent the outcome of a process of chemical evolution that parallels, although is perhaps further advanced than, that which occurred in comets. These meteorites may then represent not only a useful model for the development and refinement of analytical methods, but also a guide to the types of organic compounds that may be encountered in analyses of cometary matter.

In what follows, I have (i) briefly reviewed the results of amino acid analyses of CM chondrites, (ii) discussed the origin of these compounds and the implications for comet organic chemistry, and (iii) described some recent developments in analytical instrumentation for amino acids and their implications for analyses of extraterrestrial materials. Although the emphasis is on amino acids, their general characteristics are common to the other classes of organic compounds in CM chondrites and inferences regarding their origins should be generally relevant (Cronin et al., 1988).

THE CHONDRITIC AMINO ACIDS

Amino acids can be extracted from crushed samples of CM chondrites with hot water and isolated, free of coextracted inorganics, by adsorption onto a cation exchange resin and elution with dilute NH_4OH (Kvenvolden et al., 1970). When analyzed by ion-exchange chromatography with o-phthalaldehyde detection, the Murchison extract gives a complex chromatogram (Cronin and Pizzarello, 1986). The majority of the amino acids, certainly all the more abundant ones, have now been positively identified by GC-MS using ion exchange and/or reverse phase chromatography

for preparative fractionation. All the amino acids identified to date fall into one of two general classes; they are either monoaminoalkanoic acids or monoaminoalkandioic acids. The monoaminoalkanoic acids also include cyclic forms and N-alkyl derivatives. Structures of these amino acids are illustrated in figure 1. It is interesting to note that, of the more than 80 amino acids now positively identified, only eight protein amino acids and 11 non-protein, but biologically occurring, amino acids have been found. Thus, the majority of the amino acids are uniquely extraterrestrial.

As might be expected, given the large number of amino acids and only two structural classes, they show little structural selectivity, that is, all the stable amino acid structures are apparently represented in the meteorite within the limits set by the two general classes. Analyses of the seven-carbon α-amino monocarboxylic acids have provided the most stringent test of this point (Cronin and Pizzarello, 1986). This group is comprised of 14 chain isomers, four of which have two chiral centers and thus have diastereomeric forms. As a result, there are 18 isomers separable by normal, i.e., achiral, chromatographic systems. All 18 isomers have been identified in extracts of the Murchison meteorite. It should also be noted that both amino acid enantiomers have been found to be present in many instances, and in nearly equal amounts (Kvenvolden et al., 1970).

Quantification of the Murchison amino acids is summarized in figure 2. Both the total amino alkanoic acids and the total α-amino alkanoic acids show declining amounts with increasing carbon number but with a pronounced maximum at C_4 (fig. 2A); the abundance of the amino position isomers is α>γ>β. When the α-amino acid abundances are presented as a function of carbon number within homologous series (fig. 2B), a smooth, exponential decline in content is observed within each homologous series. At each carbon number, the content of individual branched-chain isomers is greater than that of the straight-chain isomer. This fact seems to explain the maximum at C_4 in the plots of total amino alkanoic acids and total α-amino alkanoic acids, in that C_4 is the minimal chain length at which chain branching becomes possible. In summary, the Murchison amino acids have the general characteristics listed in figure 3. These characteristics are shared by many of the other classes of organic compounds found in carbonaceous chondrites, e.g., the mono- and dicarboxylic acids (Lawless and Yuen, 1979; Peltzer et al., 1984), thus we believe them to be products of a common synthetic process.

ORIGIN OF CHONDRITIC AMINO ACIDS

The origin of the organic compounds of carbonaceous chondrites has been a controversial question. Two hypotheses have dominated the discussion. The first involves reactions of CO and H_2 catalyzed by condensed particles in the solar nebula, the so-called Fischer-Tropsch type (FTT) process (Studier et al., 1968). The second is a planetary (parent body) process in which atmospheric reduced gases react under the influence of one or more possible energy sources, the so-called Miller-Urey (MU) synthesis (Wolman et al., 1972). A third possibility, that intact interstellar materials were incorporated into meteorites, was also suggested some time ago (Cameron, 1973), but has only recently received serious consideration with the discovery that some meteoritic carbonaceous materials are isotopically unusual. The latter possibility now appears to provide the key to understanding the origin of the chondritic amino acids, although parent body processes probably also played a role in their formation.

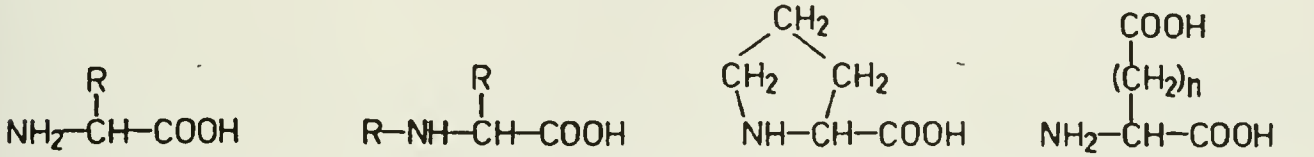


Figure 1. - General structures of amino acids of CM chondrites.

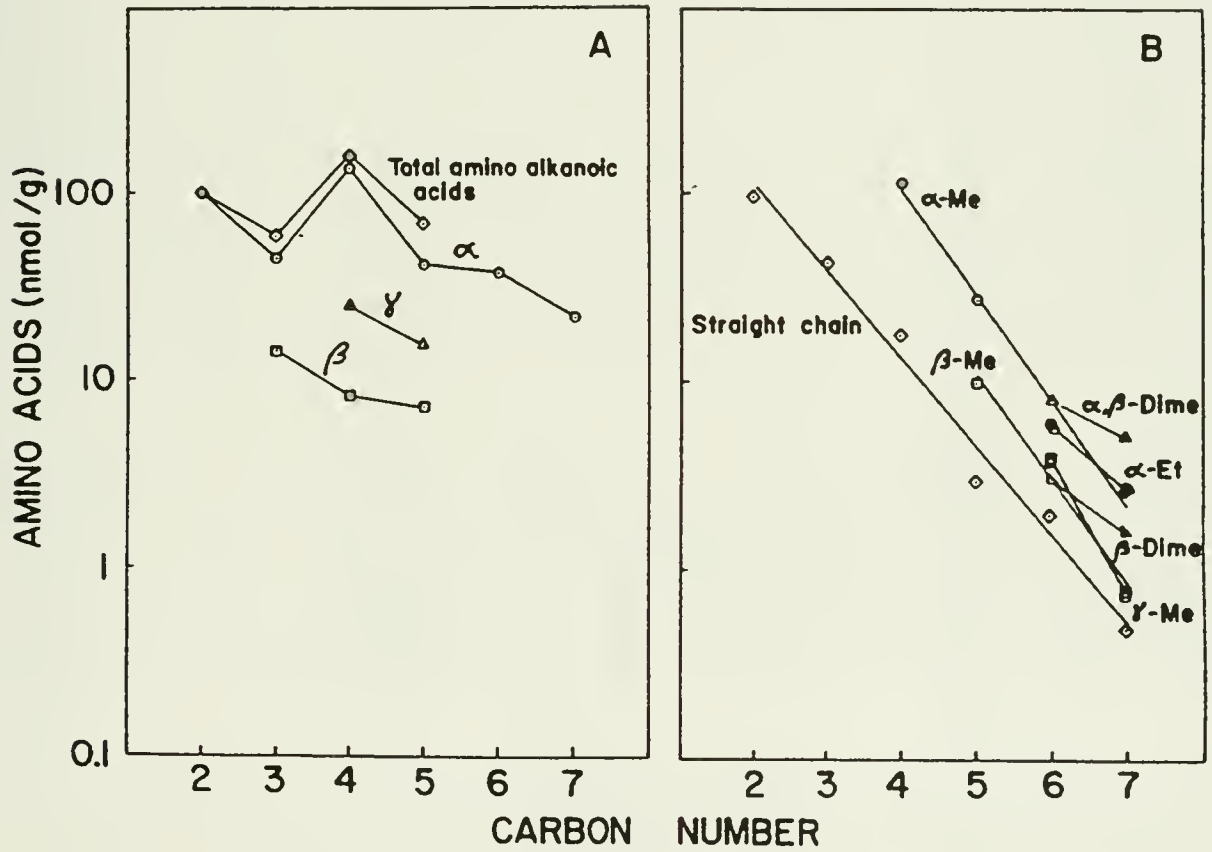


Figure 2. - Amino acid concentration in the Murchison meteorite related to carbon number.

Amino Acids of the Murchison Meteorite

Positively identified:	74	Protein: 8 Biological, non-protein: 11 Extraterrestrial: 55
Structural classes:		Monoamino alkanoic acids (includes cyclic & N-alkyl forms) Monoamino alkandioic acids
Content:		Total: 600 nmol gm^{-1} Individual: $\leq$ 100 nmol gm^{-1}
Characteristics:		Complete structural diversity Exponential decline in content within homologous series Branched chain predominance

Figure 3. – General characteristics of amino acids found in the Murchison meteorite.

Deuterium in Carbonaceous Chondrites

Inferences about meteorite synthetic processes based on molecular analyses are likely to be valid only insofar as the results accurately reflect the product yield of the synthetic process and are unaffected by secondary processing, decomposition, and contamination. In contrast, the stable isotopic signature of a particular synthetic process may survive substantial alteration of the original product mixture. (It can, of course, be seriously affected by contamination.) Consequently, increasing emphasis has been placed on determining stable isotope ratios of meteorite organics, i.e., ^{13}C, ^{15}N, and $^{2}H(D)$.

The results of selected deuterium analyses are given in Table 1. Deuterium content is expressed as δD.[1] The first analyses of deuterium in carbonaceous chondrites were carried out by Boato (1954). Hydrogen is found in meteorites in essentially three forms: hydrated salts, hydrous silicates, and organic compounds. The water associated with hydrated salts can undergo exchange with terrestrial water and is therefore of little interest, however, this water can be removed by heating the samples in a vacuum at 180°. As seen in table 1, the remaining hydrogen was found to be enriched in deuterium relative to terrestrial matter, although this is not always the case (Kerridge, 1985). Since two reservoirs of deuterium still remained after heating, the question became whether the deuterium enrichment was associated with the organic matter, the clay minerals, or both. Smith and Rigby (1981) attacked this question directly by carrying out isotopic analyses of the insoluble, kerogen-like matter obtained by demineralizing a carbonaceous chondrite sample with HF-HCl. They found this organic matter to be significantly enriched in deuterium in all five meteorites examined. Later, Robert and Epstein (1982) showed by stepwise pyrolysis/combustion that this material was not homogeneous, but contained a very D-rich component(s) diluted by less enriched material, and Becker and Epstein (1982) found the methanol-soluble compounds also to be quite D-rich.

Although several processes could have contributed, in principle, to deuterium enrichment in the early solar system, it is now generally believed that the deuterium enrichments observed in carbonaceous chondrites result from fractionation by ion-molecule reactions (Watson, 1976) in the gas phase of the precursive interstellar cloud, followed by condensation of D-rich compounds and their incorporation into the meteorite parent body(ies) (Geiss and Reeves, 1981), a possibility first suggested by Kolodny et al. (1980). Deuterium enrichment may be a hallmark of interstellar organosynthesis in low-temperature regimes as a consequence of the low zero-point energy of the D-C bond.

If meteorite amino acids were themselves interstellar molecules, or were derived from interstellar precursors, they might be expected to show a significant deuterium enrichment. Therefore, we extracted and isolated amino acids from the Murchison meteorite and, in collaboration with Epstein, obtained stable isotope ratios (Epstein et al., 1987). The results, given in table 1, showed the amino acids to be substantially enriched in deuterium.

1. $$\delta D\ (‰) = \left[\frac{(D/H)_{sample} - (D/H)_{stnd}}{(D/H)_{stnd}}\right] \times 10^3$$

Standard mean ocean water (SMOW) is taken as the standard for deuterium analyses; $(D/H)_{SMOW} = 0.0001557$. The terrestrial δD range is about -400 to +100 (Pillinger, 1984).

TABLE 1. - DEUTERIUM IN CARBONACEOUS CHONDRITES

Sample	Meteorite	δD	Reference
Whole rock, >180°	Ivuna	+297	b
HF-HCl residue	Murchison	+547	e
HF-HCl residue, 700°	Murchison	+2600	d
MeOH extract	Murchison	+486	a
Amino acids	Murchison	+1370	c

a) Becker & Epstein, 1982; b) Boato, 1954; c) Epstein et al., 1987;
d) Robert & Epstein, 1982; e) Smith & Rigby, 1981.

Formation Hypothesis

As before, this deuterium enrichment has been interpreted as indicating chemistry under interstellar cloud conditions. But how direct is the relationship to interstellar molecules? Are the meteorite amino acids themselves interstellar molecules, or are they derived from interstellar precursors? Thus far, amino acids have not been identified in interstellar clouds although glycine, the simplest amino acid, has been sought (Snyder et al., 1983).

It has been suggested that the meteorite amino acids are products of a Strecker-cyanohydrin synthesis (Peltzer and Bada, 1978), a reaction sequence shown in figure 4. These reactions generate both hydroxy acids and amino acids and both classes of compounds have been identified in the Murchison meteorite (Peltzer and Bada, 1978). Moreover, the ratios of four pairs of analogous hydroxy/amino acids are consistent with their equilibration at a common ammonia concentration as would be expected were the Strecker synthesis responsible for their formation (Peltzer et al., 1984). The facts that the reactants in this process, aldehydes or ketones, HCN, and ammonia, occur in interstellar clouds (Irvine and Hjalmarson, 1984) and have been shown to be D-rich (Penzias, 1980) can account, at least qualitatively, for the D-enrichment of the meteorite amino acids.

Where did the reactions occur? The coexistence of organic matter and clay minerals in carbonaceous chondrites was apparent to the chemists who first examined carbonaceous chondrites over 150 years ago and the analyses of numerous carbonaceous chondrites since then have shown this correlation to be without exception. Furthermore, there is substantial evidence that the clay mineralogy is secondary, that is, that clays were formed in a parent body by hydrothermal alteration of pre-existing anhydrous silicates (DuFresne and Anders, 1962; Bunch and Chang, 1980). These indications of liquid water in the meteorite parent body raise the question whether the synthesis of amino acids from interstellar precursors by the Strecker reaction, an aqueous phase process, occurred concomitantly. If so, might there not be a correlation between amino acid content and some petrologic indicator of hydrothermal activity? For example, it might be predicted that amino acid content would correlate with the meteorite matrix content since the matrix components, serpentine minerals plus complex Fe-Ni-S-O-bearing phases (so-called "poorly characterized phases" (PCP) now known to be composed of cronstedtite and tochilinite (MacKinnon and Zolensky, 1984; Tomeoka and Buseck, 1985)), are believed to have been produced by aqueous processes. Determination of the apparent matrix content (McSween, 1979) and amino acid content (Cronin and Pizzarello, 1983) for a set of CM chondrites have provided data with which this prediction can be tested. A correlation with matrix content was not found. However, more recently, McSween (1987) has determined the relative proportions of serpentine minerals and PCP in the matrices of several CM chondrites. Using these data along with the previously determined matrix contents it was possible to test for a correlation between amino acid content and PCP content. Interestingly, as shown in figure 5, there appears to be a positive correlation. Tomeoka and Buseck (1985) have proposed an alteration sequence in which PCP appears at an early stage and then is decomposed by further alteration. Thus, these results seem to suggest that amino acids were formed early in the aqueous alteration process and then were destroyed as alteration progressed further. (Their destruction may have involved a process akin to diagenesis of amino acids in terrestrial soils, shales, etc., i.e., incorporation into kerogen-like material.) In any case, both the evidence for a Strecker synthesis and the correlation of amino acid content with the aqueous alteration process are consistent with aqueous processing of interstellar precursors in the meteorite parent body.

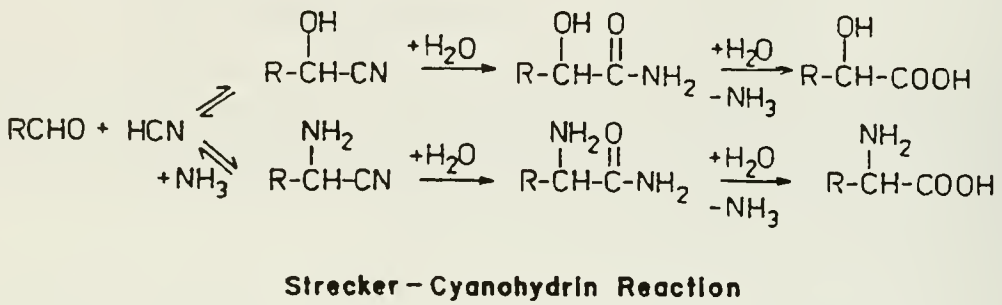


Figure 4. - Reactions of the Strecker-cyanohydrin synthesis of α-hydroxy acid and α-amino acids.

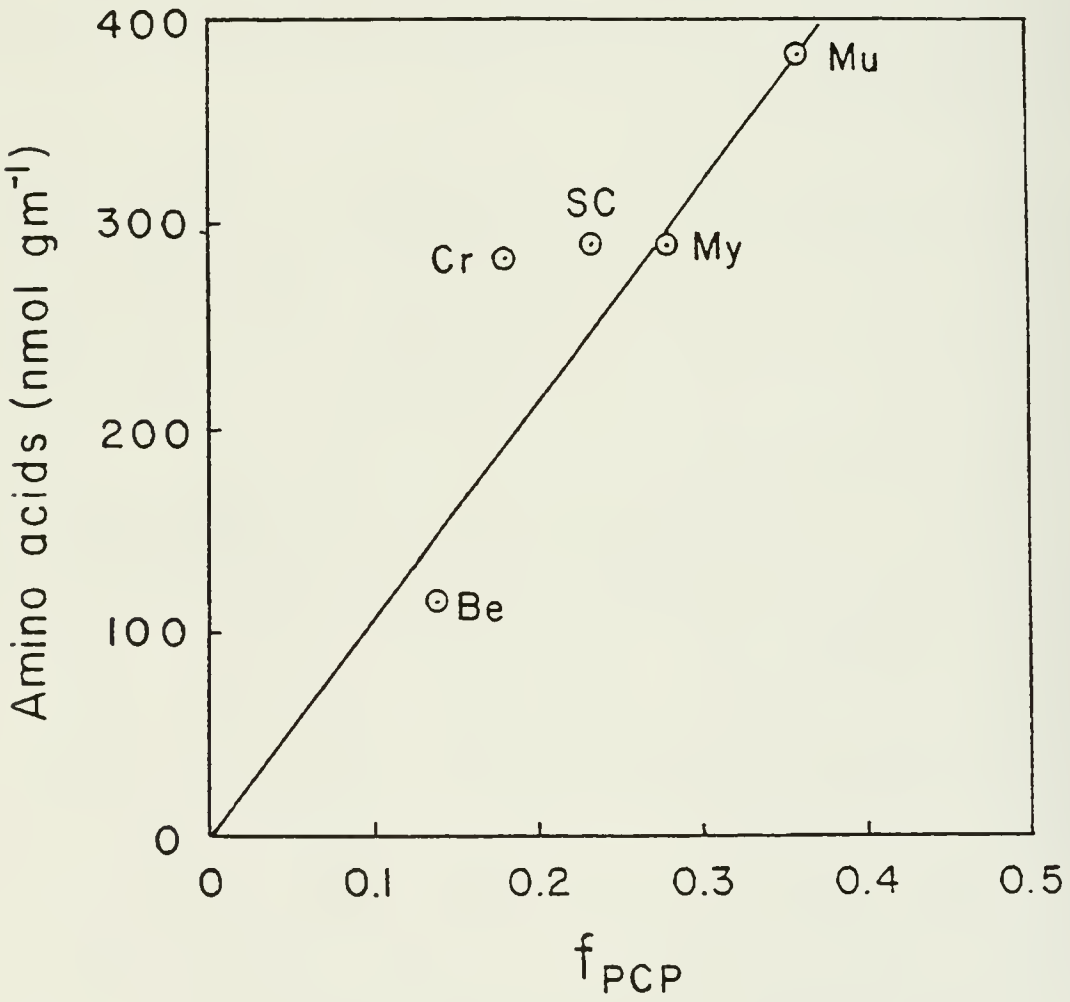


Figure 5. - Variation of amino acid content with PCP content of CM chondrites. The fractional volume of PCP (f_{PCP}) was obtained from McSween (1979, 1987).

The origin of the chondritic amino acids can be understood in the context of the general scenario outlined in figure 6. In this scheme, ion-molecule reactions in cold interstellar clouds generate simple precursors, aldehydes and ketones, ammonia, and HCN (IS Molecules) in the case of the amino acids. These precursors may or may not be processed to some degree in interstellar grain mantles, e.g., to form branched-chain aldehydes and ketones (IS Grain Molecules). Aggregation of grains and the condensation of gas-phase components give volatile-rich planetesimals which further agglomerate to form the meteorite parent body(ies) and comets. Warming of the parent body, perhaps by decay of short-lived radioisotopes, leads to the generation of an internal aqueous phase (DuFresne and Anders, 1963), the conversion of anhydrous silicates and metals to PCP, and the conversion of interstellar precursors to amino acids (Meteorite Organics). The final stage suggests the delivery of amino acids to the primitive earth by meteorite infall, a probable occurrence, but one of unknown significance for terrestrial chemical evolution.

IMPLICATIONS FOR COMETARY ORGANIC CHEMISTRY

The implications of this scheme for the organic chemistry of a pristine comet are straight-forward. Unless it has experienced sufficient heating to produce a liquid water phase, a comet nucleus would be expected to be rich in the small, volatile, highly reactive molecules, ions, and radicals that characterize the gas phase of interstellar clouds and to contain, in addition, a significant contribution from interstellar grain mantles where the gas-phase species may have been processed further (Greenberg, 1984). The irradiation of icy mantles by cosmic rays is expected to generate abundant hydroxyl radicals which would react in part with organic species to produce alcohols, polyols, hydroxy acids, etc. Indeed, a laboratory model of such a process has been found to produce a suite of oxygenated organics of this type (Agarwal et al., 1985).

If a comet were heated above the melting point of water, as may well be possible even in the Oort cloud (Weissman, 1989), numerous aqueous phase reactions would come into play. In addition to the rapid reaction of radicals and unstable ions, the formation of hydroxy nitriles by the Strecker reaction would be expected, and in the neutral pH range and above there would be a significant yield of amino nitriles. The hydrolysis of these compounds would produce hydroxy acid amides and amino acid amides, respectively, as intermediates in the formation of α-hydroxy acids and α-amino acids, the stable, hydrolytic end products found in carbonaceous chondrites. (See Fig. 4.)

It is interesting to inquire whether the conditions of a cometary melt would be suitable for amino acid formation. The necessary reactants, H_2O, HCN, NH_3 and at least one aldehyde (CH_2O) are well documented comet constituents. However, as mentioned above, amino acid formation by the Strecker reaction is pH dependent. Miller and Van Trump (1981) have calculated the hydroxy acid/amino acid ratio from a Strecker synthesis as a function of pH. They find that the ratio becomes favorable for amino acid formation only at pH values ≥ 5. Lunine (1988) has critically reviewed the Halley molecular abundance data from several types of observations. Based on these data, the pH of a melt of Halley composition would be set by the NH_3/CO_2 ratio. Based on the abundance ranges of these molecules given by Lunine, this buffer would have a pH in the range 5.3-6.4, sufficiently high to provide a significant yield of amino acids by a Strecker reaction. The conversion of anhydrous silicate grains in the melt to clay minerals, e.g., olivine to cronstedtite, is an acid-consuming process and would tend to drive the pH even higher if it were occurring concomitantly.

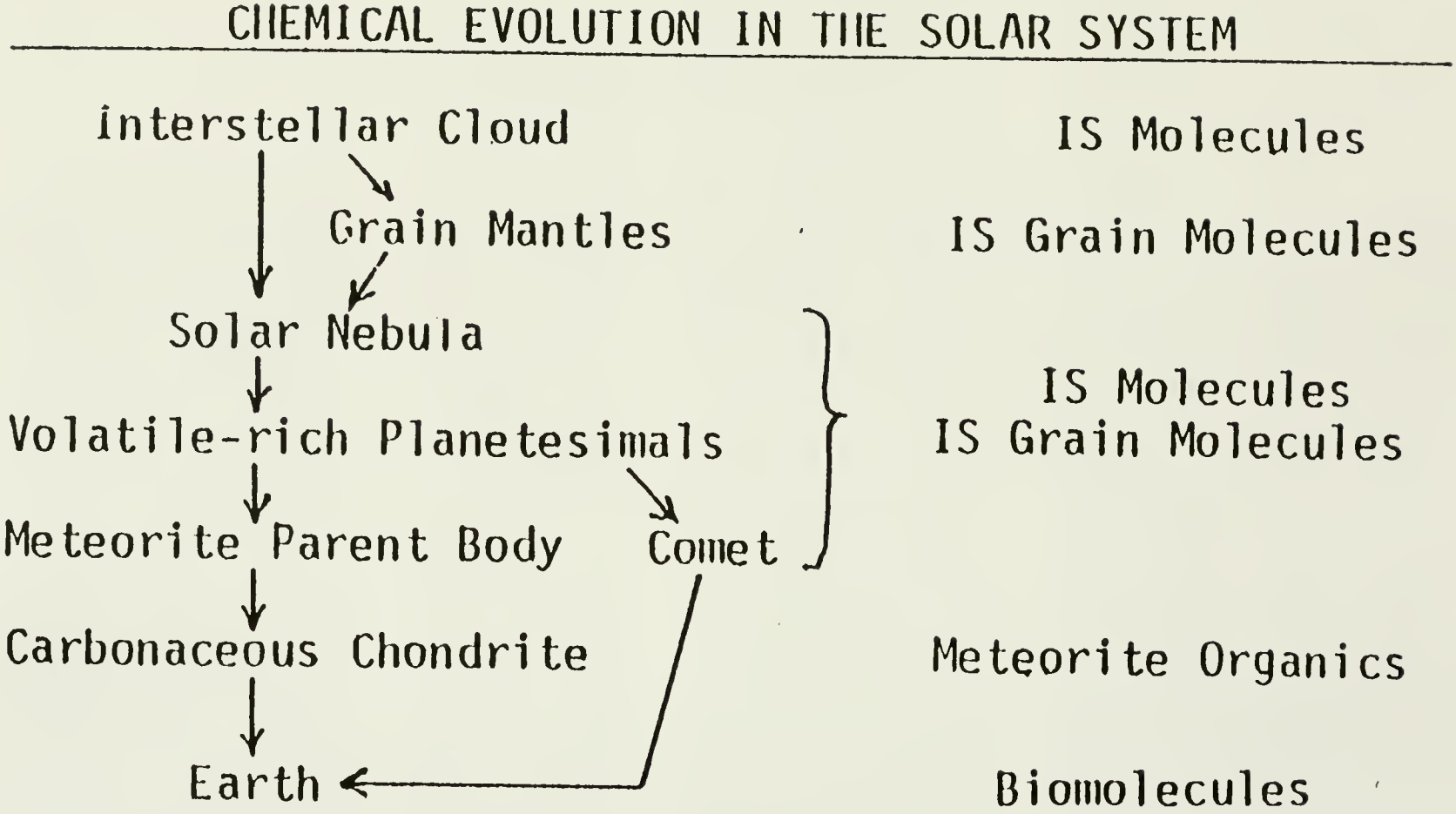


Figure 6. - A general scheme of organic chemical evolution in the early solar system as it affected carbonaceous chondrites, comets and possibly the early Earth.

In addition to the Strecker reaction, other hydrolytic and facile addition reactions among interstellar molecules can be envisioned, for example, the conversion of (i) alkyl nitriles to monocarboxylic acids, (ii) cyanate and ammonia or amines to various ureas and other amides, (iii) cyanoethylene and HCN to dinitriles and on to dicarboxylic acids, and (iv) cyanoacetylene to pyrimidines. The well-known HCN polymerization reactions that generate purines and amino acids, in addition to complex polymeric species (Sanchez et al., 1967), could also come into play. However, given a formaldehyde/HCN ratio of 10-100 (Lunine, 1988) these reactions would appear to be less favored than the Strecker reactions.

Thus, the nature of the organic analytical problem may depend on the extent to which an aqueous phase has conditioned the chemical evolution of comets. Assuming some parallel with the carbonaceous chondrites, the nature of silicate grains in comets can have important implications, since the secondary formation of hydrous silicates is indicative of the development of the typical chondritic organic chemistry. On the other hand, a comet in which an initial complement of interstellar molecules has remained locked in an icy matrix at Oort cloud temperatures may have had little opportunity for chemical evolution, and analyses must be primarily designed to detect volatile and reactive molecules, radicals, and ions. Intermediate possibilities can also be envisioned. A brief episode of melting would allow radical reactions and facile addition reactions to occur, generating what might be called transitional species such as hydroxy- and aminonitriles, imines (Schiff's bases), etc., without their extensive hydrolysis to stable end-products. The possibility of regimes within a comet that have differed significantly in their temperature history implies the presence of a range of organic compounds spanning the categories described above. The cometary surface, which is subject to the competing effects of cosmic radiation (accretion) and particle bombardment (erosion) even in the Oort cloud, provides unique conditions for organic reactions that have not been dealt with here.

AMINO ACID ANALYSIS OF EXTRATERRESTRIAL MATERIALS

Although developments in the technique and instrumentation of amino acid analysis have been driven mainly by the needs of biochemists and molecular biologists, the technology has been readily adapted for analyses of carbonaceous chondrites. Sensitivity is frequently a limiting parameter when considering the analysis of scarce and irreplaceable materials like meteorites, however, the development of instrumentation for amino acid analysis has been accompanied by such remarkable increases in sensitivity that sample size limitations have not generally been a hindrance. In figure 7, a time line is sketched illustrating the advances in sensitivity accompanying instrumental evolution in this area over the last 35 years. The progression begins with automation (Spackman et al., 1958) of the chromatographic amino acid analyzer invented by Moore and Stein (1951) and proceeds through the introduction of HPLC (high performance liquid chromatography) technology (Hare, 1977), the use of fluorescence rather than absorbance for detection (Benson and Hare, 1975), the formation of derivatives prior to chromatographic separation (Chang et al., 1977), the introduction of microcolumn technology (Einarsson et al., 1986), and finally, laser-induced fluorescence detection (Roach and Harmony, 1987). A parallel progression, beginning about 1980, has exploited capillary electrophoresis for the separation of fluorescent amino acid derivatives (Jorgensen and Lukacs, 1981). This technology has outstripped chromatographic techniques in sensitivity, at least temporarily, by the use of laser-induced fluorescence and a device "borrowed" from cell biology, the sheath-flow cell, as a detection system (Cheng and Dovichi, 1988). These developments have brought us to a point at which sensitivity can be as conveniently expressed in numbers of molecules as in fractional moles.

The earliest amino acid analyses of meteorite amino acids were made using commercial Moore-Stein analyzers. This early work was done without a full appreciation of the pitfalls of terrestrial contamination and was ultimately of little scientific value (Hayes, 1967), except as a lesson that must still be heeded, i.e., that each advance in detection sensitivity is accompanied by a correspondingly heightened risk that terrestrial contamination will confuse, distort, or obscure the analysis of indigenous amino acids.

The first valid analyses of chondritic amino acids were made by Kvenvolden et al. (1970) using a commercial Moore-Stein analyzer and GC/GC-MS instruments of comparable sensitivity. This level of sensitivity required meteorite samples of the order of grams for an analysis. For about the last ten years, we have been using an HPLC system with post-column fluorescent detection (Cronin and Hare, 1977) which has reduced the sample requirement for a single analysis to tens of milligrams. However, the recent advances in sensitivity now open the way, not only for further decreases in sample size requirements, which are always desirable, but also for new experiments that will be designed to answer questions at a petrologic level, i.e., the correlation of amino acid content with individual grains and particular mineral phases. In this regard, it will be very interesting to approach the question of correlation of amino acid content with PCP-phases by direct analysis. It will also be possible to analyze amino acids in materials that are available in only minute amounts, for example, IDP's, although such work will require the development of radically different techniques for sampling and contamination control. The fact that terrestrial sources of amino acids add almost exclusively the L-enantiomer has provided an effective way to assess contamination in extraterrestrial materials. It is important to note that enantiomeric separation has not been neglected in the development of ultra-sensitive methods (Gozel et al., 1987).

The implications of these analytical advances for chondrite and IDP sample size requirements are illustrated in Table 2. Here are listed the minimum number of molecules detected by Cheng and Dovichi (1988) using capillary electrophoresis with laser-induced fluorescence detection of fluorescein isothiocyanate derivatives. The weight of Murchison meteorite required to yield this number of molecules was calculated as well as the number of IDP particles. The latter calculation assumed an IDP of 20 μm diameter, density of 1.0 gm cm^{-3}, and amino acid content equivalent to the Murchison meteorite. It is clear that if detection at these levels can be achieved in practice, analyses of CM chondrites can be made on samples as small as a few picograms if the total sample can be transferred to the analytical system. In the case of an IDP, even if only a small fraction of the total extract were analyzed, e.g., 1/100, single particle analyses would be feasible.

Given the development of contamination-free techniques for sampling a comet nucleus specimen, transferring, and extracting the sample, it should be possible to analyze the amino acids in very small solid and liquid phase samples. As a result, the relationship between comet structure and organic composition could be ascertained with a high degree of spatial resolution.

Finally, for reasons discussed in preceding sections, it is by no means certain that amino acids will occur in a comet nucleus. Although these bodies are rich in the biogenic elements and appear to contain in abundance the reactants for amino acid and hydroxy acid synthesis via the Strecker pathways, whether the necessary aqueous phase has existed remains a crucial question. Even if this has not been the case, it will be important to attempt to verify the potential for such syntheses by carrying out experiments in which comet samples are melted, concentrated, and subjected to hydrolysis before amino acid analysis.

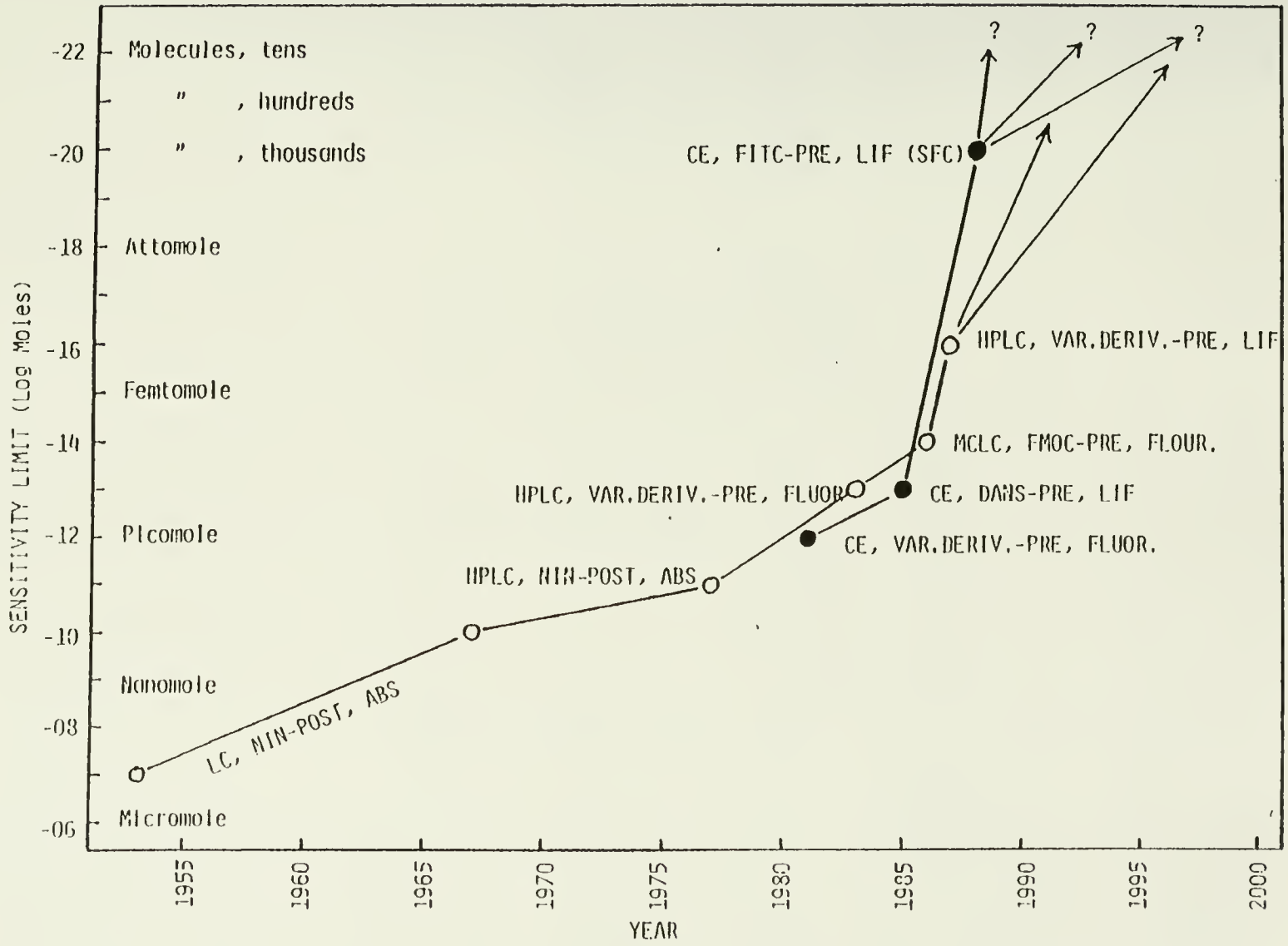


Figure 7. - Sensitivity increases accompanying the development of instrumentation for amino acid analysis.

TABLE 2. - AMINO ACID ANALYSIS (CE-LIF)

Amino Acid	Detection Limit		Murchison equivalent (picogram)	IDP equivalent (number)
	Moles ($x10^{20}$)	Molecules		
Alanine	4.6	27,000	1.0	.00024
Aspartic acid	6.8	41,000	13	.003
Glutamic acid	2.8	17,000	1.6	.00038
Glycine	3.7	22,000	0.4	.000095
Isoleucine	2.5	15,000	6.3	.0015
Leucine	10.0	61,000	25	.006

CONCLUSIONS

1. Analyses of amino acids in CM chondrites over the past 20 years have required the development of methods for quantification of these compounds in scarce and irreplaceable samples, at trace levels, as components of very complex mixtures, and in an environment where there is enormous potential for contamination. Analyses of returned comet nucleus samples pose similar problems and appropriate analytical methodology can build on, and be tested in, meteorite studies.

2. A current view of the origin of chondritic amino acids suggests their formation by aqueous processing of interstellar precursors, a scheme that may also be relevant to comets. Depending upon the prior existence of an aqueous phase, comets can be expected to contain organic molecules ranging from simple, volatile, reactive interstellar molecules, to the more complex and stable chondritic compounds. Organic analysts should be prepared to deal with this entire range of organic species, as well as grain mantle organics and possible intermediates formed in a transient aqueous phase. It may also be desirable to carry out analyses after laboratory simulation of aqueous processing.

3. Returned samples should represent the full range of comet structural and compositional diversity, i.e., samples taken at various depths and representing various material phases.

4. Maintaining sample integrity is essential, especially avoiding temperature increase and the introduction of contaminants.

5. Recent developments in analytical technology, e.g., for amino acid analysis, suggest that much information including spatial distribution will be obtainable from analyses of the small samples now made feasible by recent advances in analytical sensitivity.

REFERENCES

Agarwal, U. K.; Schutte, W.; Greenberg, J. M.; Ferris, J. P.; Briggs, R.; Connor, S.; Van de Bult, C. P. E. M.; and Baas, F.: Photochemical Reactions in Interstellar Grains - Photolysis of CO, NH_3, and H_2O. Origins of Life, vol. 16, 1985, pp. 21-40.

Becker, R. H.; and Epstein, S.: Carbon, Hydrogen and Nitrogen Isotopes in Solvent-Extractable Organic Matter from Carbonaceous Chondrites. Geochim. Cosmochim. Acta, vol. 46, 1982, pp. 97-103.

Benson, J. R.; and Hare, P. E.: o-Phthalaldehyde: Fluorogenic Detection of Primary Amines in the Picomole Range. Comparison with Fluorescamine and Ninhydrin. Proc. Nat. Acad. Sci. USA, vol. 72, 1975, pp. 619-622.

Boato, G.: The Isotopic Composition of Hydrogen and Carbon in the Carbonaceous Chondrites. Geochim. Cosmochim. Acta, vol. 6, 1954, pp. 209-220.

Bunch, T. E.; and Chang, S.: Carbonaceous Chondrites - II. Carbonaceous Chondrite Phyllosilicates and Light Element Geochemistry as Indicators of Parent Body Processes and Surface Conditions. Geochim. Cosmochim. Acta, vol. 44, 1980, pp. 1543-1577.

Cameron, A. G. W.: Interstellar Grains in Museums. In Interstellar Dust and Related Topics (J. M. Greenberg and H. C. Van de Hulst, eds.) IAU, 1973, pp. 545-547.

Chang, J.-Y.; Knecht, R.; and Braun, D. G.: Amino Acid Analysis in the Picomole Range by Precolumn Derivatization and High-Performance Liquid Chromatography. Meth. Enzymol., vol. XLVII, 1977, pp. 41-48.

Cheng, Y.-F.; and Dovichi, N. J.: Subattomole Amino Acid Analysis by Capillary Zone Electrophoresis and Laser-Induced Fluorescence, Science, vol. 242, 1988, pp. 562-564.

Cronin, J. R.; and Hare, P. E.: Chromatographic Analysis of Amino Acids and Primary Amines with o-Phthalaldehyde Detection. Anal. Biochem., vol. 81, 1977, pp. 151-156.

Cronin, J. R.; and Pizzarello, S.: Amino Acids in Meteorites. Adv. Space Res., vol. 3, 1983, pp. 5-18.

Cronin, J. R.; and Pizzarello, S.: Amino Acids of the Murchison Meteorite. III. Seven Carbon Acyclic Primary α-Amino Alkanoic Acids. Geochim. Cosmochim. Acta, vol. 50, 1986, pp. 2419-2427.

Cronin, John R.; Pizzarello, Sandra; and Cruikshank, Dale P.: Organic Matter in Carbonaceous Chondrites, Planetary Satellites, Asteroids and Comets. In Meteorites and the Early Solar System (J. F. Kerridge and M. S. Matthews, eds.), Univ. Arizona Press, 1988, pp. 819-857.

Delsemme, A. H.: The Chemistry of Comets. Phil. Trans. Roy. Soc. Lond. A, vol. 325, 1988, pp. 509-523.

DuFresne, E. R.; and Anders, E.: On the Chemical Evolution of the Carbonaceous Chondrites. Geochim. Cosmochim. Acta, vol. 26, 1962, pp. 1085-1114.

Einarsson, S.; Folestad, S.; Josefsson, B.; and Lagerkvist, S.: High-Resolution Reversed-Phase Liquid Chromatography System for the Analysis of Complex Solutions of Primary and Secondary Amino Acids. Anal. Chem., vol. 58, 1986, pp. 1638-1643.

Epstein, S.; Krishnamurthy, R. V.; Cronin, J. R.; Pizzarello, S.; and Yuen, G. U.: Unusual Stable Isotope Ratios in Amino Acid and Carboxylic Acid Extracts from the Murchison Meteorite. Nature, vol. 326, 1987, pp. 477-479.

Geiss, J.; and Reeves, H.: Deuterium in the Solar System. Astron. Astrophys., vol. 93, 1981, pp. 189-199.

Gozel, P.; Gassmann, E.; Michelsen, H.; and Zare, R. N.: Electrokinetic Resolution of Amino Acid Enantionmers with Copper (II)-Aspartame Support Electrolyte. Anal. Chem., vol. 59, 1987, pp. 44-49.

Greenberg, J. M.: Chemical Evolution in Space. Origins of Life, vol. 14, 1984, pp. 25-36.

Hare, P. E.: Subnanomole-Range Amino Acid Analysis. Meth. Enzymol., vol. XLVII, 1977, pp. 3-18.

Hayes, J. M.: Organic Constituents of Meteorites - A Review. Geochim. Cosmochim. Acta, vol. 31, 1967, pp. 1395-1440.

Irvine, W. M.; and Hjalmarson, A.: The Chemical Composition of Interstellar Molecular Clouds. Origins of Life, vol. 14, 1984, pp. 15-23.

Jorgenson, J. W.; and Lukacs, K. D.: Zone Electrophoresis in Open-Tubular Glass Capillaries. Anal. Chem., vol. 53, 1981, pp. 1298-1302.

Kerridge, J. F.: Carbon, Hydrogen and Nitrogen in Carbonaceous Chondrites: Abundances and Isotopic Compositions in Bulk Samples. Geochim. Cosmochim. Acta, vol. 49, 1985, pp. 1707-1714.

Kissel, J.; and Krueger, F. R.: The Organic Component in Dust from Comet Halley as Measured by the PUMA Mass Spectrometer on Board Vega 1. Nature, vol. 326, 1987, pp. 755-760.

Kolodny, Y.; Kerridge, J. F.; and Kaplan, I. R.: Deuterium in Carbonaceous Chondrites. Earth Planet. Sci. Lett., vol. 46, 1980, pp. 149-158.

Kvenvolden, K.; Lawless, J.; Pering, K.; Peterson, E.; Flores, J.; Ponnamperuma, C.; Kaplan, I. R.; and Moore, C.: Evidence for Extraterrestrial Amino Acids and Hydrocarbons in the Murchison Meteorite. Nature, vol. 288, 1970, pp. 923-926.

Lawless, J. G.; and Yuen, G. U.: Quantification of Monocarboxylic Acids in Murchison Carbonaceous Meteorite. Nature, vol. 282, 1979, pp. 396-398.

Lunine, J. I.: Abundances of Molecular Species in Halley's Comet--Their Role in Understanding the Chemistry of Cometary Formation Environments. In The Formation and Evolution of Planetary Systems (H. A. Weaver, F. Paresce, and L. Danly, eds.) Cambridge Univ. Press, 1988, pp. xxx.

MacKinnon, I. D. R.; and Zolensky, M. E.: Proposed Structures for Poorly Characterized Phases in C2M Carbonaceous Chondrite Meteorites. Nature, vol. 309, 1984, pp. 240-242.

McSween, H. Y.: Alteration in CM Carbonaceous Chondrites Inferred from Modal and Chemical Variations in Matrix. Geochim. Cosmochim. Acta, vol. 43, 1979, pp. 1761-1770.

McSween, H. Y.: Aqueous Alteration in Carbonaceous Chondrites: Mass Balance Constraints on Matrix Mineralogy. Geochim. Cosmochim. Acta, vol. 51, 1987, pp. 2469-2477.

Miller, S. L.; and Van Trump, J. E.: The Strecker Synthesis in the Primitive Ocean. In Origin of Life (Y. Wolman, ed.) D. Reidel Publ., 1981, pp. 135-141.

Moore, S.; and Stein, W. H.: Chromatography of Amino Acids on Sulfonated Polystyrene Resins. J. Biol. Chem., vol. 192, 1951, pp. 663-681.

Peltzer, E. T.; and Bada, J. L.: α-Hydroxycarboxylic Acids in the Murchison Meteorite. Nature, vol. 272, 1978, pp. 443-444.

Peltzer, E T.; Bada, J. L.; Schlesinger, G.; and Miller, S. L.: The Chemical Conditions on the Parent Body of the Murchison Meteorite: Some Conclusions Based on Amino, Hydroxy and Dicarboxylic Acids. Adv. Space Res., vol. 4, 1984, pp. 69-74.

Penzias, A. A.: Nuclear Processing and Isotopes in the Galaxy. Science, vol. 208, 1980, pp. 663-669.

Pillinger, C. T., Light Element Stable Isotopes in Meteorites--from Grams to Picograms. Geochim. Cosmochim. Acta, vol. 48, 1984, pp. 2739-2766.

Roach, M. C.; and Harmony, M. D.: Determination of Amino Acids at Subfemtomole Levels by High-Performance Liquid Chromatography with Laser-Induced Fluorescence Detection. Anal. Chem., vol. 59, 1987, pp. 411-415.

Robert, F.; and Epstein, S.: The Concentration and Isotopic Composition of Hydrogen, Carbon, and Nitrogen in Carbonaceous Meteorites. Geochim. Cosmochim. Acta, vol. 46, 1982, pp. 81-95.

Sanchez, R. A.; Ferris, J. P.; and Orgel, L. E.: Studies in Prebiotic Synthesis. II. Synthesis of Purine Precursors and Amino Acids from Aqueous Hydrogen Cyanide. J. Mol. Biol., vol. 30, 1967, pp. 223-253.

Smith, J. W.; and Rigby, D.: Comments on D/H Ratios in Chondritic Organic Matter. Earth Planet. Sci. Lett., vol. 54, 1981, pp. 64-66.

Snyder, L. E.; Hollis, J. M.; Suenram, R. D.; Lovas, F. J.; Brown, L. W.; and Buhl, D.: An Extensive Galactic Search for Conformer II Glycine. Astrophys. J., vol. 268, 1983, pp. 123-128.

Spackman, D. H.; Stein, W. H.; and Moore, S.: Automatic Recording Apparatus for Use in the Chromatography of Amino Acids. Anal. Chem., vol. 30, 1958, pp. 1190-1206.

Studier, M. H.; Hayatsu, R.; and Anders, E.: Origin of Organic Matter in Early Solar System - I. Hydrocarbons. Geochim. Cosmochim. Acta, vol. 32, 1968, pp. 151-173.

Tomeoka, K.; and Buseck, P. R.: Indicators of Aqueous Alteration in CM Carbonaceous Chondrites: Microtextures of a Layered Mineral Containing Fe, S, O, and Ni. Geochim. Cosmochim. Acta, vol. 49, 1985, pp. 2149-2163.

Watson, W. D.: Interstellar Molecule Reactions. Rev. Mod. Phys., vol. 48, 1976, pp. 513-552.

Weissman, P. R.; and Stern, S. A.: Physical Processing of Cometary Nuclei. This volume, LPI, 1989, pp. xxx-xxx.

Wolman, Y.; Haverland, W. J.; and Miller, S. L.: Nonprotein Amino Acids from Spark Discharges and Their Comparison with the Murchison Meteorite Amino Acids. Proc. Nat. Acad. Sci. U.S.A., vol. 69, 1972, pp. 809-811.

CONCEPTS FOR THE CURATION, PRIMARY EXAMINATION, AND PETROGRAPHIC ANALYSIS OF COMET NUCLEUS SAMPLES RETURNED TO EARTH

D. Stöffler
H. Düren
J. Knölker
Institut für Planetologie
Westfälische Wilhelms-Universität Münster
Münster, FRG

Concepts for the curation, primary examination, and petrographic analysis of comet nucleus samples returned to Earth*

D. Stöffler, H. Düren, and J. Knölker
Institut für Planetologie, Westfälische Wilhelms-Universität Münster, Münster, F.R. of Germany

INTRODUCTION

One of the fundamental requirements of the planned ESA/NASA Comet Nucleus Sample Return Mission (ROSETTA) is to develop concepts and instrumentations for the curation and analysis of the returned samples in an adequately equipped Receiving Laboratory. This laboratory must meet the condition that the handling, inspection, and analysis of the samples be performed at the temperature and pressure of the parental comet nucleus environment. This restriction must hold for the complete period of what may be called "Primary Sample Examination and Analysis" (PSEA). Only after this period subsamples may be released to less restrictive environments.

As foreseen in the "Sampling and sample storage requirements" of the ROSETTA mission definition report (ESA Publ. Div., 1987), different types of samples will be returned in sealed containers at a temperature of less than 160 K, preferably at 130 K. The total sample mass is expected to be near 15 kg. This sampling plan which includes a 1-3 m long core sample provides a first set of boundary conditions of a Receiving Laboratory. A second set of limiting conditions has to be derived from a "best estimate model" of the mineralogical composition and texture of the returned samples. It is the aim of this article to help defining (a) the objectives of a Primary Sample Examination and Analysis, (b) the properties of best estimate cometary model samples, and (c) the requirements and instrumentation for PSEA with special emphasis on microscopic bulk analysis of the samples.

CONCEPT AND OBJECTIVES OF THE PRIMARY SAMPLE EXAMINATION AND ANALYSIS

According to the ROSETTA mission goals (ESA Publ. Div., 1987) three types of cometary samples will be returned to Earth:

(1) A core sample of 1 to 3 m length and about 10 cm diameter; it will be stored most probably in segments of 0.5 m,

(2) a small sample of volatile material with a mass of up to 100 g, and

(3) a surface sample enriched in refactory materials with a mass of up to 5 kg.

Although the actual design of the sample containers is not yet known, it is clear that they will be under high vacuum and at temperatures as low as 130 K. In principle, the handling of the containers arriving at the Receiving Laboratory will require a facility which can transport and open the containers by remote operation without change of the P-T-conditions. Furthermore it must be capable of handling and subdividing samples and to transfer whole samples or aliquots to special inspection devices and analytical instruments by which all types of investigations considered to be necessary for the PSEA can be adequately performed with a minimum degradation of the samples.

The basic idea for the remotely operated primary examination and analysis of the samples (PSEA) is to proceed in two subsequent modes in a system of evacuated cryogenic cabinets and transfer locks:

(1) Non-destructive inspection and analysis by special tomographic methods (Albee, this volume) and non-destructive bulk chemical and physical analyses

* Contribution No. 12 of the Institut für Planetologie, Münster, work in part supported by the Deutsche Forschungsgemeinschaft (Sto 101/23-1)

by photometric and spectrocopic methods
(2) Inspection and analysis of the bulk samples by destructive methods such as cutting of samples and thin sectioning of specially prepared aliquots or mechanical separation of particular constituents

Basically PSEA should provide information on the bulk mineralogical and chemical composition, and on textural and fabric characteristics in the sense of an overall petrographic and chemical sample characterization. The aim of the PSEA is to provide a thorough assessment of the sample properties in as much detail as will be necessary for the definition of a post-PSEA sample analysis and allocation plan. In particular, PSEA should be capable of identifying heterogeneities of the bulk samples, textural subunits, and certain physical properties such as porosity and material strength in order to optimize the decision on type, mode, and sequence of further analyses.

This concept for PSEA undoubtedly requires the development of new laboratory techniques and robotic operations adapted to these techniques. Such instrumentation must be tested on artificially produced comet nucleus model samples which have to be defined on the basis of our present knowledge about comets, primitive solar system material, and interstellar matter.

MODEL COMPOSITION AND TEXTURE OF COMET NUCLEUS SAMPLES

Information which is relevant for a model of the composition and texture of comet nucleus material can be obtained from very different sources: (1) Direct observations of comets, meteors, and of interstellar and circumstellar dust (Wilkening, 1982; Grewing et al., 1988; ESA Public. Division, 1986; Jeßberger et al., 1988; Mathis, this volume), (2) laboratory analysis of primitive solar system material such as interplanetary dust particles (IDP's) and carbonaceous chondrites (Brownlee, 1985; Sandford and Walker, 1985; Mackinnon and Rietmeijer, 1987; Bradley, 1988; Kerridge and Matthews, 1988; Wasson, 1985; McSween, 1987), (3) theory and laboratory simulation of grain formation in solar and stellar nebulae and interstellar clouds (Black and Matthews, 1985; Nuth and Stencel, 1986; Morfill, 1985; Wood and Morfill, 1988; Cassen and Boss, 1988), and (4) accretion and evolution models of comets (Whipple, 1950; Wilkening, 1982; Fanale and Salvail, 1984; Klinger et al., 1985; Houpis et al., 1985; Weissmann, 1986, ESA Publ. Div., 1986; Stern, 1988).

How can we make use of this extreme diversity of information in defining model samples representative of the upper 3 to 5 m layer ("regolith") of a comet nucleus? Clearly, it is necessary to derive a "regolith model" which takes care of the sample properties on the macro- and microscale. The interpretation of the presently available data leads to the basic conclusion that the regolith is heterogeneous in vertical and horizontal sections on a macroscopic as well as microscopic scale. This model actually reflects the generally accepted idea of a stochastic nature of the processes that formed and reprocessed cometary nuclei. Consequently, the instrumentation for sample analysis has to be capable of dealing with the following potential macro- and microproperties of the regolith (Fig. 1):

(1) Fractal structure at all scale lengths
(2) Layered structure subparallel to the surface
(3) Existence of textural and compositional subunits at all scale lengths

This may be considered as a "worst case heterogeneity scenario" which we take as a basis for defining the range of variation of comet regolith model samples. If we consider such samples as petrographic objects it is obvious that we have to develop best estimates for three classes of bulk properties given the size and geometry of samples to be returned to Earth (see section above):

(1) The modal composition, i.e. the nature and volumetric abundance of the constituents
(2) The textural properties, i.e. the size, morphology, and intergrowth characteristics of the constituents and cavities (pore space)
(3) The fabric characteristics, i.e. the spatial distribution and orientation of

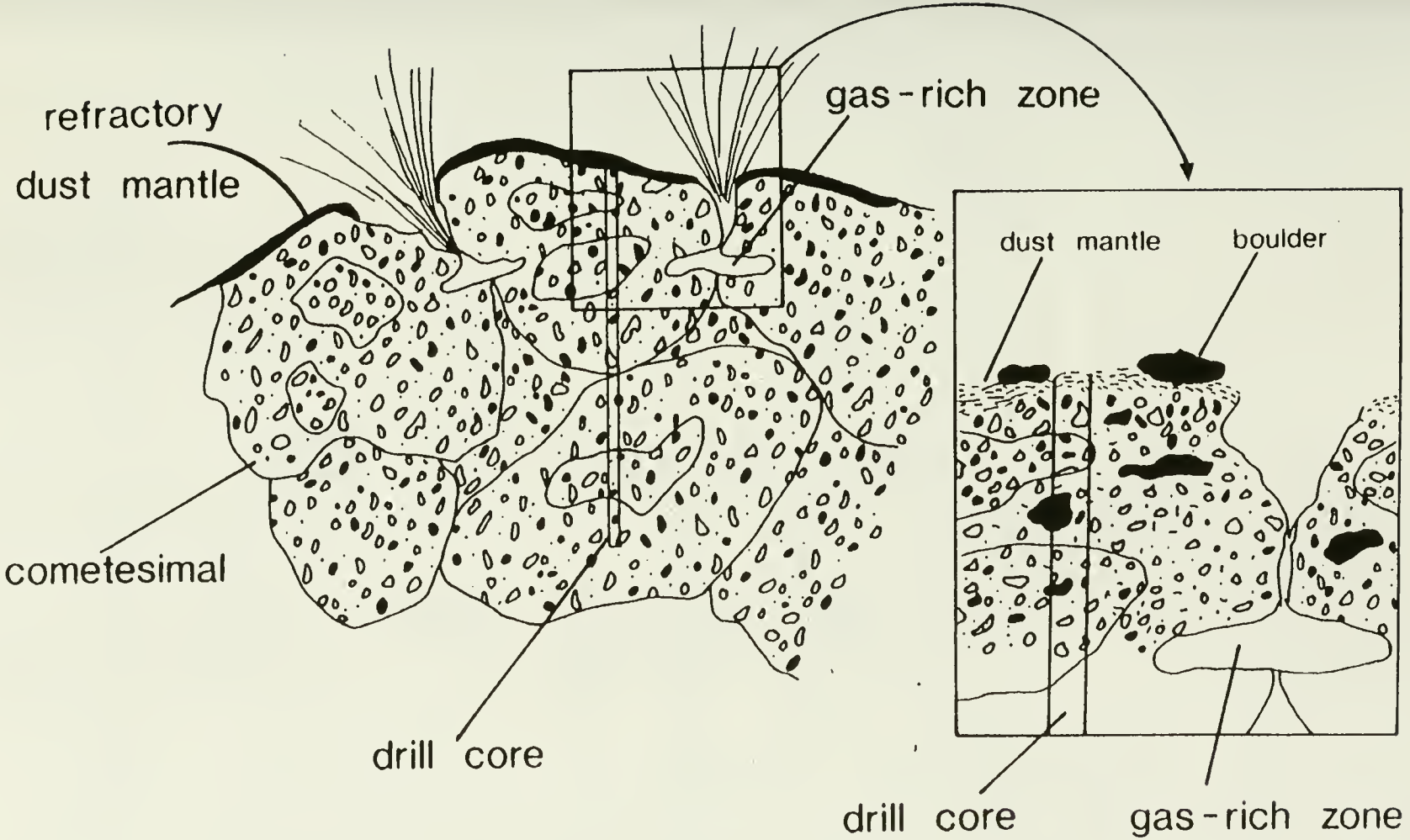


Figure 1.- Macroscopic model of the near surface zone of a comet nucleus at a potential landing site; solid vertical lines = drill core; see text for data sources

TABLE 1. - COMPOSITION AND TEXTURE OF COMETARY MODEL SAMPLES (SEE TEXT)

	End member constituents				
	Monophase grains	Coherent aggregates		Porous aggregates	
Phases (main elements)	(1) single crystals (2) disordered crystals (3) amorphous grains	(1) mantled monophase grains (2) polycrystalline grains (with crystals and amorphous grains)		(1) aggregates of monophase or multiphase grains (2) aggregates of composite mono- and multiphase grains	
Ices and clathrate hydrates (H, C, N, O, S)	H_2O, CO, CO_2, CH_4, NH_3 etc. and clathrates containing these and other molecules	polycrystalline ices and clathrates 		fluffy "snow" 	
Inorganic minerals (Si, Mg, Fe, Ca, Al, O, S, C)	Anhydrous silicates (olivine, pyroxene, feldspar and other Ca-Mg-Fe-silicates) Hydrated silicates (serpentine, smectite, kaolinite, talc, tremolite etc.) Oxides (Spinel, perovskite, magnetite etc.) Carbides (SiC, $(Fe,Ni)_xC$) Sulfides (FeS, pentlandite, etc.) Sulfates, carbonates, phosphates, and hydroxides of Mg, Ca, Fe Metals (Fe-Ni, noble metals, Ti etc.) Carbon (graphite, amorphous carbon	polycrystalline "rock-like" particles containing more than one type of inorganic minerals (or disordered or amorphous minerals) 	(a) grains containing ices and inorganic minerals (b) grains containing inorganic minerals and hydrocarbons (c) grains with all types of volatile and refractory phases 	fluffy dust aggregates 	porous aggregates of all types of mono- and multiphase grains
Hydrocarbon compounds (C, H, O, N)	simple hydrocarbons polycyclic hetero-aromatics etc.	coatings on other mono-phase grains matrix "cement" irregular bodies (?)		fluffy carbonaceous aggregates	

ices  inorganic minerals  hydrocarbons (+C) 

the constituents and the pore space.

These bulk porperties determine the chemical composition and the physical porperties which are therefore no variables to be defined independently. However, all properties depend now on the definition of the term "constituent". In a petrographic sense, constituents of a cometary sample can be homogeneous grains of variable composition, heterogeneous grains (e.g. mantled crystals or coherent multiphase particles), and aggregates of homogeneous and/or heterogeneous grains all of which can be considered as textural subunits formed as such by one particular process. At a smaller scale, we expect three kinds of solid phases as building blocks of the "constituents" : ices (including clathrates), inorganic minerals, and hydrocarbon compounds. Therefore, constituents of comet samples containing these phases are classified as follows (Table 1):

(1) Single monophase grains (crystalline to amorphous)
(2) Coherent aggregates of one type or different types of monophase grains
(3) Porous aggregates of either type (1) or type (2) particles or composites of both

The grain size of these constituents in the comet regolith may range from the nanometer to submillimeter level for type (1) constituents and from the submicron to the meter scale for type (2) and (3) constituents (compare Fig. 1). With these formalities in mind, a comet model samples can be seen as a comet nucleus subunit or regolith subunit with a particular volume proportion of "end member" constituents or components as they have been defined above and in Table 1. Therefore comet nucleus samples may differ in the following important parameters:

(1) The relative volume proportion of the end member constituents which includes the ratio of refactory to volatile material and of organic to inorganic material,
(2) the grain size distribution of the constituents, and
(3) the structure and porosity of the bulk sample.

TABLE II. - RANGES FOR COMPOSITION AND TEXTURAL PARAMETERS OF COMETARY MODEL SAMPLES

Parameter	Dimension	Range
Fraction of refractory dust	%	0 - 100
Mass ratio of refractory inorganic minerals to refractory carbonaceous compounds (includ. C)	-	1 - 4
Porosity of refractory surface material	%	0 - 95
Porosity below dust mantle	%	10 - 80
Density of dust mantle	g/cm^3	0.005 - 2.2
Density below dust mantle	g/cm^3	0.1 - 1.5
Grain size of monophase grains	µm	0.001 - 100
Grain size of multiphase grains and composite aggregates	µm - m	1 µm - 1 m
Compressive strength of bulk samples	MPa	10^{-4} - 10^{2}

Estimated ranges for these parameters of cometary model samples as established by the ROSETTA Science Definition Team are given in Table 2. The data and informations discussed so far (Fig. 1, Tables 1 and 2) translate into a comet regolith model which is visualized in Figs.1 and 2. The regolith can be seen petrographically as a polymict geological body defined as a mixture of 4 major textural components (Fig. 2). These components have a certain matrix-inclusion-relationship typical of polymict rocks with finer grained components forming the matrix and coarser grained components representing inclusions (Fig. 2). Any actual sample returned by the ROSETTA mission may represent only part of this multi-component system, e.g. a surface sample consisting only of refactory dust or a core sample segment composed solely of a rock-like aggregate of refactory material or alternatively of pure, non-porous polycrystalline ice. This must be kept in mind for the following discussion on required instrumentation of a comet sample receiving facility.

PROPOSED TECHNIQUES FOR THE PETROGRAPHIC CHARACTERIZATION OF COMET NUCLEUS SAMPLES

The basic technical requirements for an adequate handling and primary examination and analysis of returned comet nucleus samples (PSEA) depend on a variety of boundary conditions. They are dictated by the general scientific goals of the sample analysis (ESA Publ. Div., 1987) and by the mass, geometry, and nature of the samples themselves. Since most of these conditions cannot be exactly predicted, the instrumentation for an effective PSEA will be highly complex and demanding. The analytical capabilities of a Receiving Laboratory must meet any of the extreme conditions given by the wide range of possible sample properties discussed in the last section. Compared to the case of the preliminary examination of lunar samples (McKay, this volume) a much higher degree of quality and quantity of investigations must be achieved during the PSEA of cometary material because of the complexity and unusual P-T-state of the study objects.

A tentative and simplified concept of the mode and sequence of investigations during the PSEA of returned nucleus samples is sketched in the flow diagram of Fig. 3. It is based on a system of cryogenic cabinets and transfer locks providing the necessary environmental conditions with respect to temperature and pressure. Until the sample characterization has reached a stage where subsamples may be released into less restrictive environments, it is assumed that all studies are performed under cometary conditions, i.e. at 130-160 K and ultrahigh vacuum. The PSEA plan of Fig. 3 is subdivided into several steps or sections:

(1) Detailed assessment of all remote sensing data related to the sample acquisition on the comet nucleus; this includes the reduction and interpretation of data obtained from the photo documentation of the sampling site and of the sampling procedures, from the temperature monitoring during sampling, and from the borehole logging if available

(2) Inspection and analysis of the samples inside the closed containers by non-destructive methods, in particular by modern three-dimensional X-ray computer assisted tomography (CAT scans; Albee, this volume)

(3) Opening of the sample containers and further inspection of the samples by imaging and non-destructive microscopic, bulk chemical and physical analyses including reflection spectrophotometry and spectrometric analyses (e.g. X-ray fluorescence, gamma-ray and alpha-backscatter spectroscopy; e.g. Englert et al., 1987)

(4) Dissection of samples and recovery of suitable aliquots for further detailed petrographic and microchemical analysis based on destructive methods of sample preparation

(5) Preparation and investigation of sample aliquots in more specialized sections of the cryostat system; these comprise a preparation unit for polished section and thin section production with attached facilities for optical and electron microscopy and micro-chemical analysis; a mineral (or phase) separation unit; and a long-term storage unit

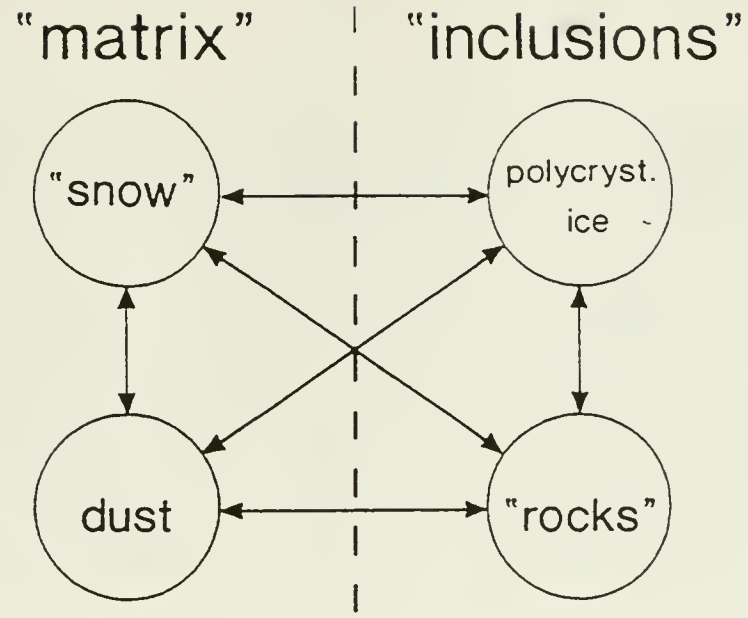


Figure 2.- Schematic representation of the mixing of "end member constituents" in a cometary model regolith

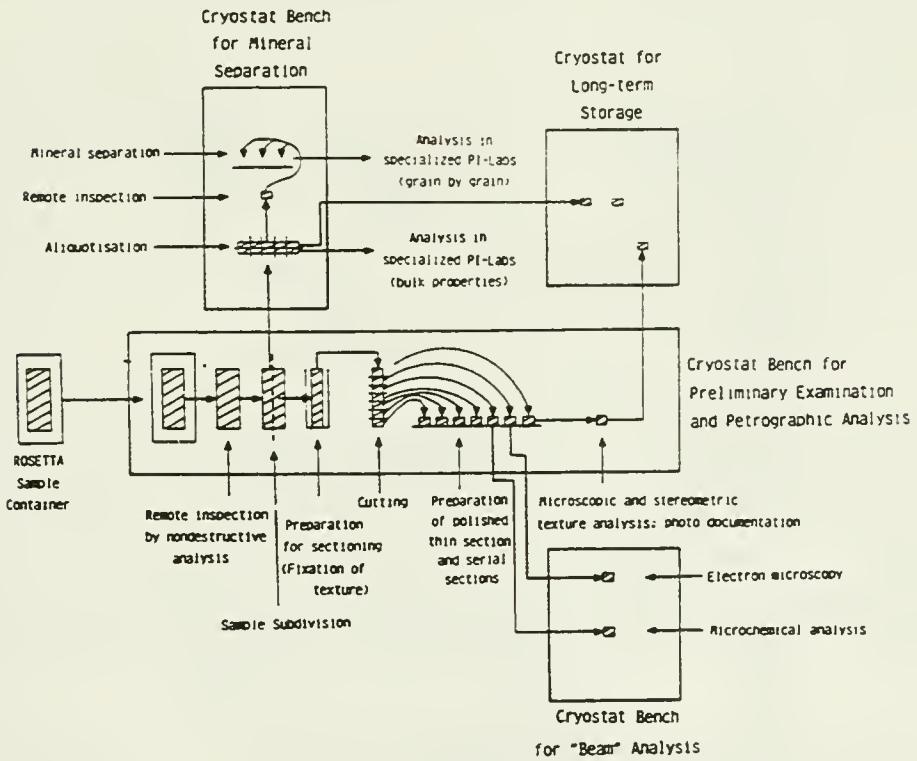


Figure 3.- Schematic plan for sample examination and analysis in a Comet Nucleus Sample Receiving Laboratory

(6) Transfer of samples to highly specialized instruments for further bulk or grain by grain analysis. Such instruments could be in part attached to the Receiving Laboratory or located in outside laboratories of principle investigators. Part of the sample suite will probably be released to non-cometary environmental conditions at this point.

It is obvious that most of the instrumentation needed for the PSEA is not yet available and must be developed in the next decade or existing analytical tools must be adapted to the extreme P-T-conditions of the cometary environment. For the petrographic (mineralogy, texture) and chemical bulk characterization of the samples the X-ray tomography and the non-destructive spectroscopy using sensor heads are the most important methods of non-destructive PSEA. They will not be discussed here in any detail and the reader is referred to other sections of this volume (Albee, this volume; Lindstrom and Lindstrom, this volume; Sutton, this volume) and to special literature (Englert et al., 1987). These non-destructive investigations however, are insufficient for a quantitative assessment of the texture and mineralogy of the bulk samples. A stereometric analysis in two-dimensional sections is required and will be discussed in the remaining part of this chapter.

Any combined stereometric and modal analysis of a sample must be performed on well-defined plane sections which are either polished sections of "thick samples" or polished thin sections. The analytical instruments will be either the polarizing microscope or any type of electron microscope with attached image analysis. Currently used techniques for snow and ice microscopy are the most appropriate starting point for further developments (Bader et al., 1939; De Quervain, 1954; Kinosita and Wakahama, 1960; Narita, 1969, 1971; Kry, 1975; Gubler, 1978; Good, 1980, 1982, 1987; Perla and Ommanney, 1985; Perla, 1985; Perla and Dozier, 1985; Dozier et al., 1987).

In snow and avalanche research the preparation of polished sections and thin sections is made in the following steps (Fig. 4; e.g. Good, 1987):

(1) Impregnation of the snow sample by an organic liquid (e.g. diethylphthalate, aniline) at moderately low termperature, e.g. at about -4°C in the case of diethylphthalate
(2) Freezing of the impregnated sample at -20 to -30 °C in order to crystallize the pore-filling liquid
(3) Cutting of the sample and preparation of polished sections by means of a sledge microtome at about -13 °C
(4) Staining of the impregnating medium for better discrimation of ice crystals and pore space in microphotographs
(5) Digital image analysis of microphotographs

The stereological analysis of the two-dimensional sections can be done by conventional methods of stereology and pattern recognition (Good, 1980, 1987; Dozier et al., 1987). It yields the volumetric fractions of the constituents (ice and pore space in the case of snow) as well as the textural parameters characterizing grain size and intergrowth properties. In recent years it was recognized that a more sophisticated three-dimensional analysis of the snow microstructure is required for a better understanding of the correlation of stereological parameters with the mechanical, thermal, and electromagnetic properties of snow. Therefore, the method of "serial cuts" was introduced (DeHoff, 1983; Perla et al., 1986; Good, 1987) which allowed the reconstruction of the three-dimensional snow microstructure (Fig. 5). The serial polished sections are typically taken with spacings of 50 to 100 μm (Fig. 4).

The application of the described techniques for the textural analysis of snow to the much more complex cometary samples requires several important changes of the method. The impregnation technique must be adapted to much lower temperatures that means liquids with freezing points near 160 K must be used or a completely different method has to be developed. A different sectioning techniques is necessary in order to cope with the expected wide range of hardness of the constituent phases in comet samples (Mohs hardness ranging probably from ~1.5 to ~7 or 8). Diamond tools will be needed for cutting and polishing. The whole preparation procedure must be performed at very low temperature and by remote robotic manipulation.

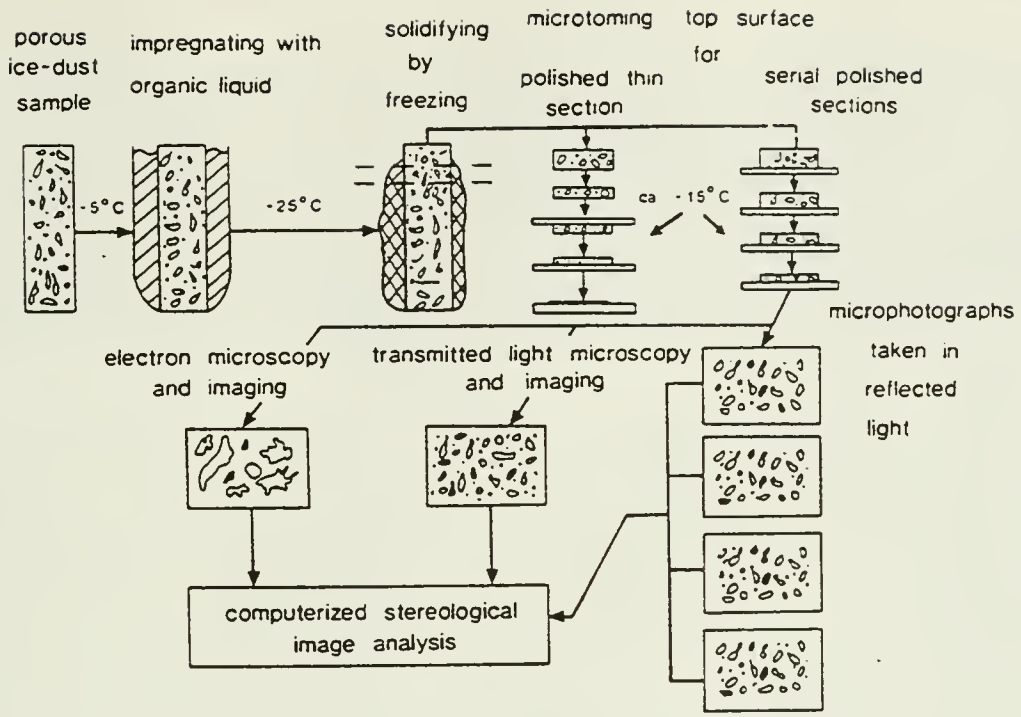


Figure 4.- Preparation of porous ice-dust samples for polished thin sectioning and polished serial sectioning, subsequent microscopy, and quantitative textural analysis; temperatures are those used for terrestrial snow (see text for references)



Figure 5.- Micrograph of snow taken in reflected light (ice crystals are black, pore space is white) and reconstruction of the three-dimensional shape of the center particle by stereological analysis of serial sections of the same area as shown in the top image; reproduced from Good (1987)

We have made first successful tests to prepare polished sections of synthetic cometary samples (Grün et al., this volume) which consisted of 90% H_2O-snow, 9% olivine, 1% montmorillonite, and 0.08% carbon and had a bulk density of about 0.5 g/cm^3. The sample was prepared according to steps (1) and (2) described above. For the polishing procedure a sledge microtome (Polycut E of Reichert and Jung, Cambridge Instruments Germany) equipped with a rotating double-diamond milling head was used while the sample temperature was varied between 100 K and 260 K. Additional samples which consisted of solid H_2O-ice and mineral powder (olivine, montmorillonite, carbon) were sectioned and polished by the same method. In some cases a sledge micotome with a tungsten carbide knife was used. The preparation work and the study of thin sections by a polarizing microscope was carried out in a low-temperature laboratory at about -15°C. Selected microphotographs of the samples are shown in Figs. 6 to 10.

Our preliminary findings can be summarized as follows. A method for producing polished thin sections of porous ice-silicate mixtures containing olivine can be developed by modifying commercially available microtomes which use rotating diamond tools (Grasenick and Warbichler, 1979). Sledge microtomes with metal knifes as used in snow research can only be used for samples with dust rich in sheet silicates (low Mohs hardness). Future developments must concentrate on new impregnation techniques for porous samples which can be applied at temperatures below 200 K, and on new techniques for better discrimination of ice, cemented pore space, and various types of mineral phases in optical microscopy. Also the problem of transferring polished thin sections at temperatures below 200 K from the preparation unit (e.g. microtome) to the optical or electron microscope needs attention. The microscopic investigations can be carried out with the aid of commercially available cryogenic tables where appropriate P-T-conditions can be achieved. Techniques applicable to optical microscopes have been reviewed by Roedder (1984).

CONCLUSIONS

Following the science goals and mission concepts for a Comet Nucleus Sample Return Mission as expressed by the joint ESA/NASA Mission Definition Team (ESA Publ.Div., 1987) we have reviewed the potential requirements for the curation and investigation of returned samples in a Receiving Laboratory. We arrive at the following main conclusions:

(1) The instrumentation of a Receiving Laboratory must be capable of handling, characterizing, subdividing, and transferring returned samples to special inspection devices and analytical instruments. All operations must be performed at cometary P-T-conditions by remotely operated robotic manipulators in a sustained system of cryogenic cabinets and transfer locks.

(2) A thorough and quantitative "Primary Sample Examination and Analysis" (PSEA) is required before any subsample will be released to non-cometary environments and subsequent specialized analyses. This PSEA will be more complex and demanding that the corresponding Preliminary Examination of lunar samples or of any other extraterrestrial samples.

(3) The PSEA must provide sufficient information on bulk sample properties (mineralogy, chemistry, texture) in a way that further destructive analyses of the samples can be carefully planned without loss of any global information.

(4) It is proposed to perform the PSEA in two subsequent modes with a first phase of non-destructive investigations by "tomographic" methods and remote bulk chemical and physical analyses and a second phase of optical and electron microscopy requiring destructive modes such as preparation polished sections and thin sections.

(5) The methodological and instrumental developments required for achieving the PSEA call for a test phase during which synthetic comet samples must be analyzed. Cometary model samples have to be defined on the basis of the current knowledge of comets and other relevant solar system, stellar, and interstellar matter.



Figure 6.- Polycrystalline ice produced from a water-carbon suspension (soot of ca. 25 nm grain size) with carbon aggregates occupying grain boundaries of ice crystals; polished section in reflected light; horizontal width of image: 0.7 mm

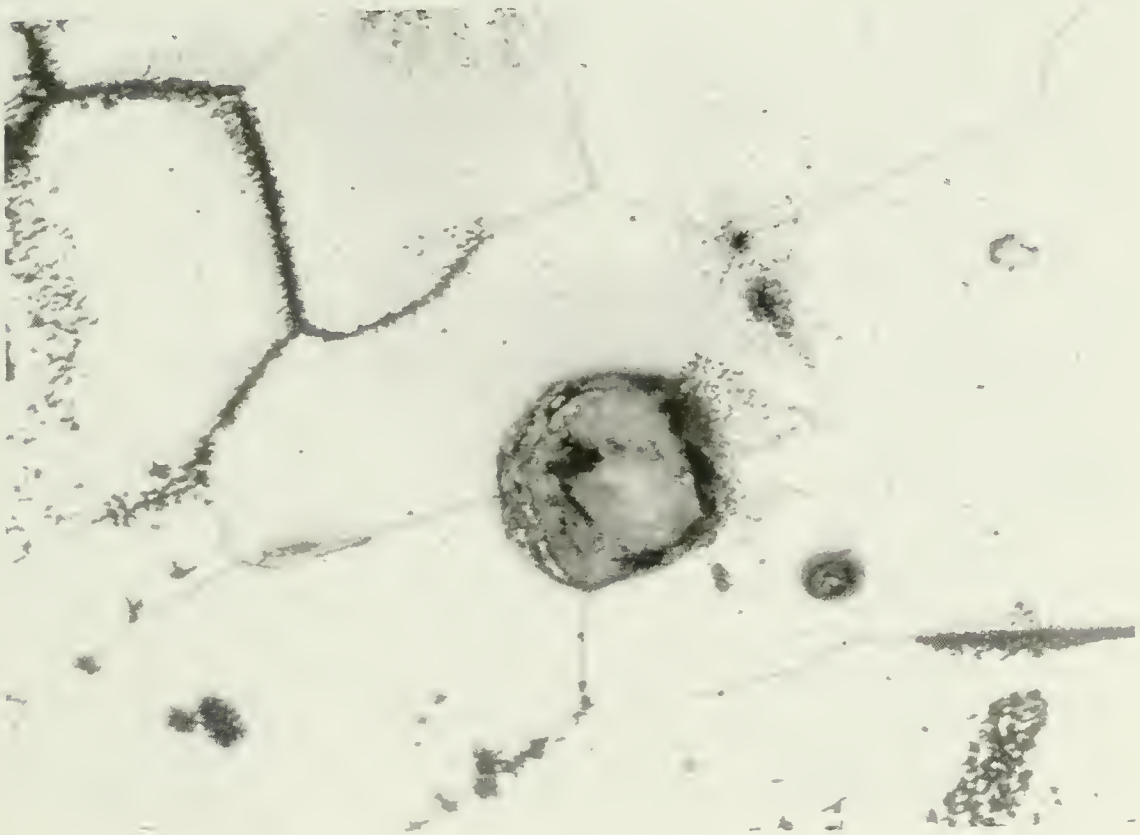


Figure 7.- Polycrystalline ice with interstitial olivine-powder (average grain-size: 4 µm); polished section in reflected light; horizontal width of image: 2.8 mm

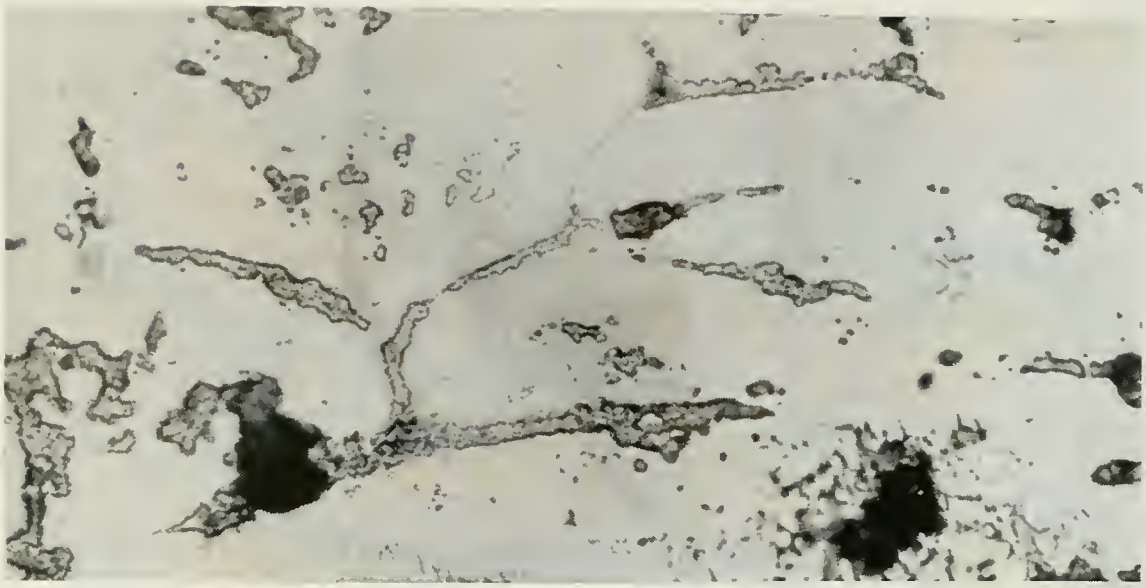


Figure 8.- Same as Figure 7 but with montmorillonite (average grain size: ~ 8 µm) instead of olivine; horizontal width of image: 0.7 mm

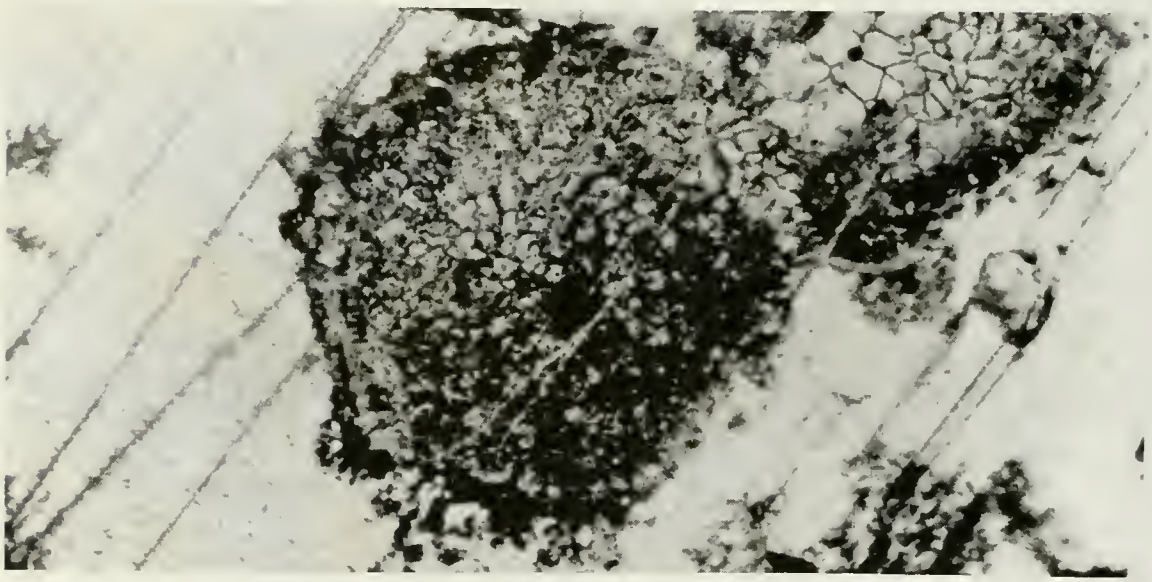


Figure 9.- Micrograph of a polished section of a synthetic cometary sample with 90 % H_2O-snow, 9% olivine (av. grain size: 4 µm), 1 % montmorillonite (av. grain size: 8 µm) and 0.08 % carbon (soot) by weight; reflected light; center: spherical dust-ice aggregate; upper right corner: polycrystalline ice with interstitial dust; white matrix with diagonal lines: pore space filled with crystallized diethylphthalate; horizontal width of image: 1.4 mm

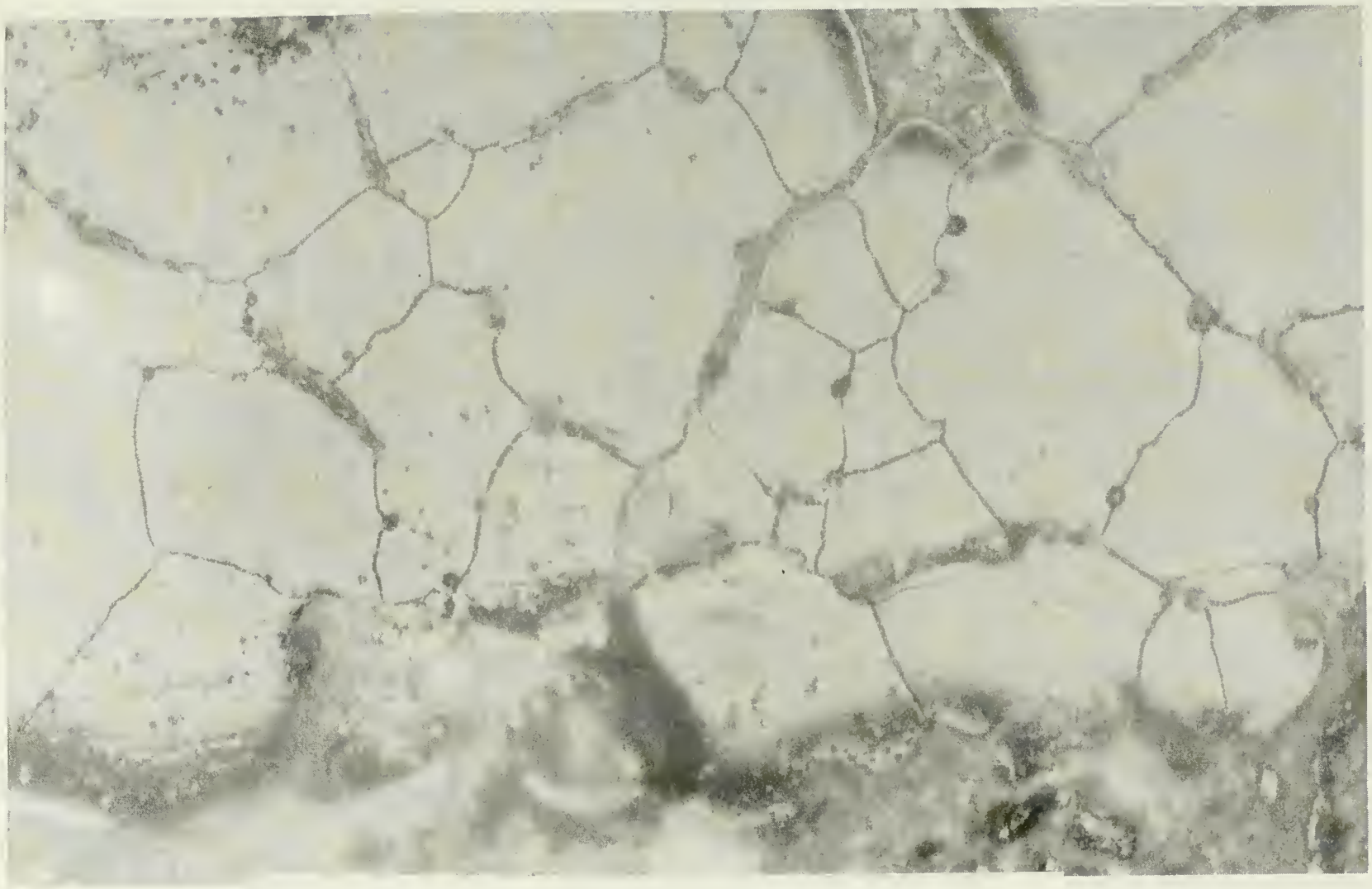


Figure 10.- Region of polycrystalline ice in the same eample as shown in Figure 9; micrograph taken in reflacted light; dark lines are grain boundaries between ice crystals where dust aggregates are concentrated (worm-like features); horizontal width of field: 1.4 mm

(6) Comet nucleus model samples have been defined on the basis of a four component cometary regolith model in which "snow", "polycrystalline ice", "dust grains" and "rock-like aggregates" are mixed in variable proportions. The constituent phases of these "end member" components are (1) ices and clathrates, (2) inorganic minerals, and (3) hydrocarbons. These phases may occur in 3 major textural subunits: single monophase grains, coherent aggregates of phases, and porous aggregates of mono- and multiphase grains.

(7) For the petrographic and microchemical characterization of cometary samples during the PSEA we propose to improve and modify techniques which are currently used in snow research for the fabrication of thin sections and serial sections and for the subsequent stereological analysis of microscopic images. Ongoing studies on olivine-smectite-carbon-snow mixtures in our laboratory show that such techniques can be developed.

REFERENCES

Albee, A.L.: Analytical study of comet nucleus samples. this volume, pp. 1-2, 1989

Bader, H.; Haefele, R.; Bucher, E.; Neher, J.; Eckel, O.; and Thams, C.: Der Schnee und seine Metamorphose. Beiträge zur Geologie der Schweiz, Geotechnische Serie, Hydrologie, 1939

Black, D.C.; and Matthews, M.S. (eds.): Protostars & Planets II. The University of Arizona Press, Tucson, 1985

Bradley, J.P.: Analysis of chondritic interplanetary dust thin-sections. Geochim. Cosmochim. Acta 52, pp. 889-900, 1988

Brownlee, D.E.: Cosmic dust: Collection and research. Ann. Rev. Earth Planet. Sci. 13, pp. 147-173, 1985

Cassen, P.; and Boss, A.P.: Protostellar collapse, dust grains and solar system formation. in J.F. Kerridge; and M.S. Mathews (eds.): Meteorites and the early solar system. The University of Arizona Press, Tucson, pp. 304-328, 1988

DeHoff, R.T.: Quantitative serial sectioning analysis: preview. J. Microsc. 131, pp. 259-563, 1983

De Quervain, M.R.: Snow as a crystalline aggregate. CRREL Trans. 21, pp. 1-7, 1954

Dozier, J.; Davis, R.E.; Perla, R.: On the objective analysis of snow microstructure. Avalanche Formation, Movement and Effects IAHS Publ. 162, pp. 49-59, 1987

Englert, P.; Brückner, J.; and Wänke, H.: Planetary gammaray spectroscopy, a special form of prompt charged particle and prompt neutron activation analysis. J. Radioanal. and Nucl. Chem. 112, pp. 11-22, 1987

ESA Publication Division: ROSETTA, The Comet Nucleus Sample Return Mission, Report of the Science Definition Team, Space Science Department of ESA, ESTEC, Noordwijk, The Netherland, 1987

ESA Publication Division: The Comet Nucleus Sample Return Mission Proc. Workshop, Canterbury, UK, 15-17 July 1986, ESA SP-249, 1986

ESA Publication Division: Symposium on the Diversity and Similarity of Comets, Brussels, Belgium, ESA SP-278, 1987

Fanale, F.P.; and Salvail, J.R.: An idealized short-period comet model: surface insolation, H2O flux, dust flux, and mantle evolution. Icarus 60, pp. 476-511, 1984

Good, W.: Structural investigation of snow, a comparison of different parameter sets. in E.S. Gelsema; L.N. Kanal: Pattern recognition in practice. North Holland Publ. Comp., 1980

Good, W.: Structural investigations of snow and ice on core III from the drilling on Vernagtferner, Austria, in 1979. Z. Gletscherk. und Glacialgeol. 18, pp. 53-64, 1982
Good, W.: Thin sections, serial cuts and 3-D analysis of snow. Avalanche Formation, Movement and Effects IAHS Publ. 162, pp. 35-48, 1987
Grasenick, F.; and Warbichler, P.: The effects of different methods of preparation on reproducing the surface of porous materials. Z. Prakt. Metallographie 16, pp.537-546, 1979
Grewing, M.; Praderie, F.; Reinhard, R. (eds.): Exploration of Halley's Comet. Springer-Verlag Berlin, 1988
Grün, E.; and KOSI-team: Modifications of comet materials by the sublimation process: results from simulation experiments. this volume, 1989
Gubler, H.: Determination of the mean number of bonds per snow grain and of the dependence of the tensile strength of snow on stereological parameters. J. Glaciol. 20, pp. 329-341, 1978
Houpis, H.F.L.; Ip, W.-H.; and Mendis, D.A.: The chemical differentiation of the cometary nucleus: the process and its consequence. Astrophy. J. 295, pp. 654-667, 1985
Jeßberger, E.K.; Christoforidis, A.; and Kissel, J.: Aspects of the major element composition of Halley's dust particles. Nature 332, pp. 691-695, 1988
Kerridge, J.F.; and Matthews, M.S. (eds.): Meteorites and the Early Solar System. The University of Arizona Press, Tucson, 1988
Kinosita, S.; and Wakahama, G.: Thin section of deposited snow made by the use of aniline. Contr. Inst. Low Temp. Sci. 15, pp. 35-45, 1960
Klinger, J.; Benest, D.; Dollfus, A.; and Smoluchowski, R.: Ices in the Solar System. D. Reidel Publ. Company, Dordrecht, 1985
Kry, P.R.: Quantitative stereological analysis of grain bonds in snow. J. Glaciol. 14, pp. 467-477, 1975
Lindstrom, D.J.; and Lindstrom, R.M.: Prompt gamma activation analysis (PGAA): Technique of choice for nondestructive bulk analysis of returned comet samples? this volume, 1989
Mathis, J.S.: Interstellar and cometary dust. this volume, 1989
McKay, D.S.: Description and analyses of core samples: the lunar experience. this volume, 1989
Mackinnon, I.D.R.; and Rietmeijer, F.J.M.: Mineralogy of chondritic interplanetary dust particles. Rev. Geophy. 25, pp. 1527-1553, 1987
McSween, H.Y., Jr.: Aqueous alteration in carbonaceous chondrites: Mass balance contraints on matrix mineralogy. Geochim. Cosmochim. Acta 51, pp. 2469-2477, 1985
Morfill, G.E.: Physics and chemistry in the primitive solar nebula. in R. Lucas; A. Omont; and L.R. Stora: The Birth and Infancy of Stars. North Holland Publ., Amsterdam, pp. 693-792, 1985
Narita, H.: Measurement of the specific surface of deposited snow I. Contr. Inst. Low Temp. Sci. A 27, pp. 77-86, 1969
Narita, H.: Measurement of the specific surface of deposited snow II. Contr. Inst. Low Temp. Sci. A 29, pp. 69-79, 1971
Nuth, J.A.; and Stencel, R.E. (eds.): Interrelationships among circumstellar, interstellar, and interplanetary dust. NASA Sci. Technol. Info. Branch, NASA Conf. Publ. 2403, 1986
Perla, R.: Snow in strong or weak temperature gradients, Part II: section-plane analysis. Cold Regions Sci. Technol. 11, pp. 181-186, 1985
Perla, R.; and Dozier, J.: Observations of snow structure. Proc. Int. Snow Sci. Workshop, pp. 182-187, 1985

Perla, R.; Dozier, J.; and Davis, R.E.: Preparation of serial sections in dry snow specimens. J. Microsc. 141, pp. 111-114, 1986
Perla, R.; and Ommanney, C.S.C.: Snow in strong and weak temperature gradients. Part I: experiments and qualitative observations. Cold Regions Sci. Technol. 11, pp. 23-35, 1985
Roedder, E.: Inclusion measurements - heating, cooling decrepitation and crushing. in Reviews in mineralogy 12, Fluid inclusions, pp. 182-219, 1984
Sandford, S.A.; and Walker, R.M.: Laboratory infrared transmission spectra of individual interplanetary dust particles from 2.5 to 25 microns. Astrophy. J. 291, pp. 838-851, 1985
Stern, S.A.: Collision in the Oort Cloud. Icarus 73, pp. 499-507, 1988
Sutton, S.R.: Non-destructive trace element microanalysis of as-received cometary nucleus samples using synchrotron x-ray fluorescence. this volume, 1989
Wasson, J.T.: Meteorites. W.H. Freemann and Company, New York, 1985
Weissman, P.R.: Are cometary nuclei primordial rubble piles? Nature 320, pp. 242-244, 1986
Whipple, F.L.: A comet model I: the acceleration of Comet Encke. Astsrophys. J. 111, pp. 375-394, 1950
Wilkening, L.L.: Comets. The University of Arizona Press, Tucson, 1982
Wood, J.A.; and Morfill, G.E.: A review of solar nebula models. in J.F. Kerridge and M.S. Matthews (eds.): Meteorites and the early solar system. The University of Arizona Press, Tucson, pp. 329-347, 1988

CANDIDATE SAMPLE ACQUISITION SYSTEM FOR THE ROSETTA MISSION

P. G. Magnani
C. Gerli
G. Colombina
Tecnospazio

P. Vielmo
Tecnomare

CANDIDATE SAMPLE ACQUISITION SYSTEM FOR THE ROSETTA MISSION

P.G.Magnani, C. Gerli and G. Colombina, Tecnospazio - P.Vielmo, Tecnomare

INTRODUCTION - MISSION REQUIREMENTS

The Comet Nucleus Sample Return (*CNSR*) Mission, is a cornerstone of ESA scientific program.

While Giotto, Vega I and II provided the first picture of a comet nucleus, a much improved understanding of the nucleus and processes on it will result from in situ measurements and Earth based analysis of the material samples collected on the nucleus surface.

The CNSR baseline mission foresees the landing and anchoring of a spacecraft on the comet nucleus surface (see Fig. 1.a), and the collection of the following three types of samples by means of a dedicated "Sample Acquisition System" (SAS) :

- a core sample gathered from surface down to a maximum depth of 3 meters to be cut in 0,5 m. long sections for storage;
- a volatile material sample, to be gathered at the bottom of the core sample hole;
- a surface material sample, gathered from one or more locations on the surface.

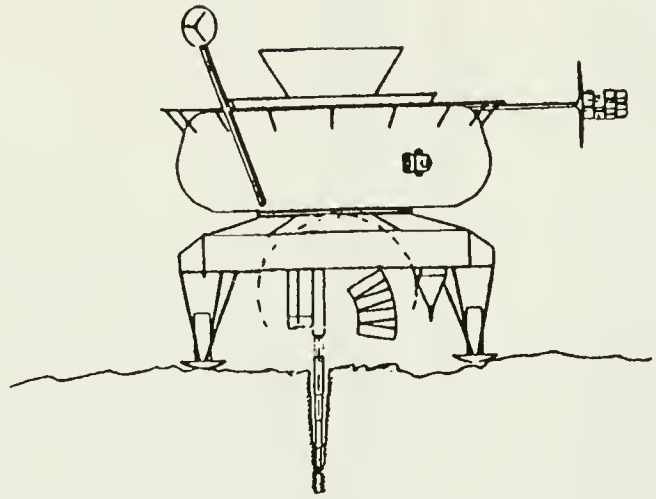
These samples will have to be placed in a storage canister in the capsule (to be returned on Earth) and preserved therein at a temperature not higher than 160° k.

If on board sensing instrumentation identified comet nucleus features not allowing a safe landing, a back-up system, based on a "harpoon" sampler, would be launched from the spacecraft hovering the comet, and recovered via a tether line; degraded sample quality would be accepted in this case (no surface and volatile samples and limited core sampling depth) (Fig. 1.b).

COMET NUCLEUS EXPECTED CHARACTERISTICS

The most likely composition of cometary nucleus, as nowadays generally accepted, is given by a finely grained structure of amorphous and/or crystalline ices (water ice or hydrates including CO_2, CO, and other gases) including micron sized dust particles (carbonauceous and/or siliceous minerals).

The expected range of physical properties of comet nucleus layers is shown in Table 1.



Comet surface

a) Main Mode

b) Degraded Mode

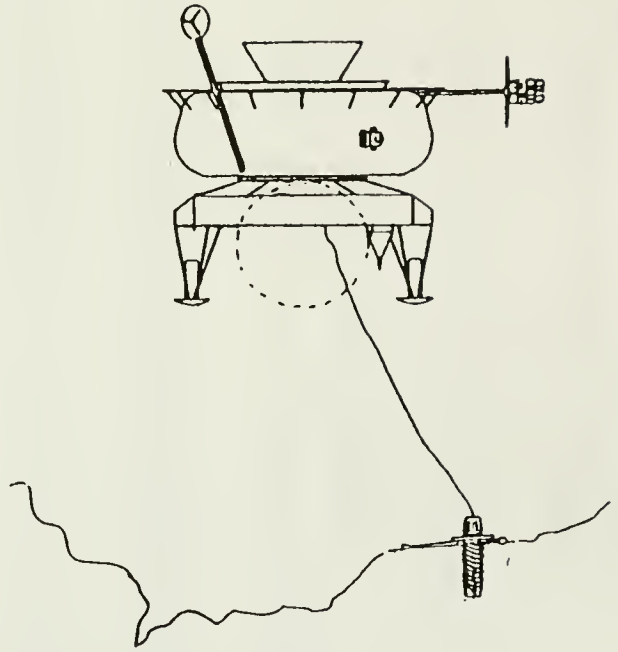


Figure 1 - S.A.S. Operative modes

TABLE 1

COMET NUCLEUS TOP LAYER
EXPECTED CHARACTERISTICS RANGE

		Minimum value	Expected value	Maximum value
Density at surface	g/cm^3	0.005	0.05	1.5
Mean density	g/cm^3	0.1	0.5	1.5
Porosity		10%	30%	80%
Thickness of mantle	m	10^{-5}	0.1	1
Tensile strength of surface	MPa	10^{-5}	10^{-3}	10
Compressive strength	MPa	10^{-4}	10^{-2}	10^{2}
Surface temperature	°K	100	130	200
Temperature at sampling depth	°K	100	130	160
Dust / ice mass ratio		0.1	0.6	1.0
Dust composition: silicates carbonaceous compounds			70% 30%	

The structure is expected to be very porous, and because of irradiation phenomena (from solar or cosmic origin) with a layering of modification of structural properties, being mainly attributed to migration and recondensation of volatile components mobilized by thermal radiation during orbital phases closer to Sun.

At nucleus mantle, the effect of sublimation of most volatile components is expected to cause an enrichment of dust components and, because of radiation, formation of (complex) organic molecular species.

The most likely stratigraphy of nucleus surface is, therefore, assumed to consist of an upper layer made of the less (or not) volatile components (dust grains) bounded together in a (highly) porous matrix overlying layers with prevailing ice content (mostly water ice).

Because of nucleus activity connected with sun irradiation, migration of nucleus parts in burst phenomena has been observed, hence a not uniform and regular surface pattern is likely to occur: some loose material such as dust, pebbles or even boulder size parts could be found, overlaying a rough, irregular surface with possible escarpements or areas in which inner layers are exposed, being the upper stratum (or "crust") blown away; a pictorial representation of comet nucleus morphology is depicted in Fig. 2 where some of the possible operational scenario features, affecting sampling process, are shown.

S.A.S. DESIGN REQUIREMENTS AND CRITERIA

The main requirements for the design of the SAS derive from the need of achieving mission scientific goals for what regards :

- sampling depth and sample quantity;
- preservation of stratigraphy pattern;
- preservation of sample microstructure;
- avoidance of contamination of sample with hetereogeneous chemical species;
- representativity of gathered samples.

Said requirements bring to the following main criteria for design :

- the system must be capable of trimming the operational parameters to encountered nucleus material features;
- all samples must be stored in the same housing in which have been gathered "in situ";
- heat generation during sample cutting process must be monitored and controlled to not disturb sample (micro) structure;
- the sampling system design has to be such as to minimize the interaction forces developed by nucleus material reactions to cutting process;
- the maximum integration of sampling system functions will have to be achieved in order to minimize their overall number (increasing functional reliability and operational flexibility).

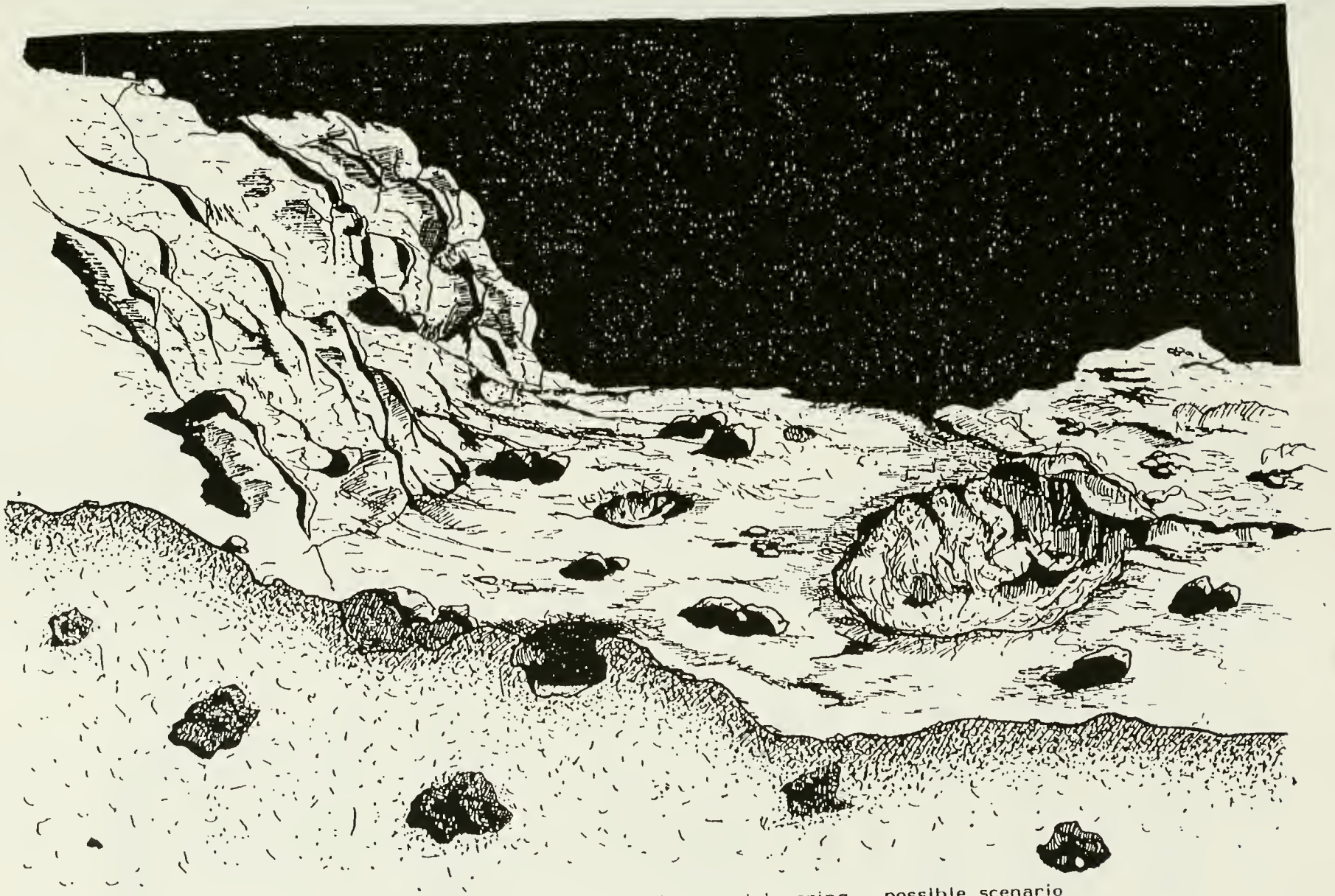


Figure 2 - Comet nucleus morphology and layering - possible scenario

IDENTIFICATION OF THE PREFERRED CONFIGURATION

On the base of the analysis of mission requirements and of trade-off between the previously described system concepts, the most suitable solution that has been identified is based on a special telescopic device supported at the end of a robotic arm (see Fig. 3).

This handling device has the possibility of being connected, by means of a standard interface at its end, with all the tools which are provided for sample gathering (core, surface, volatile samples and back-up harpoon units); this device has the possibility of extending telescopically up to a maximum of 3.6 meters length applying controlled torque to the tools it is connected with. All tools are stored in a suitable rack, at the reach of handling device.

The robotic arm can extend telescopically in order to reach possible sampling sites in a proper area below spacecraft; a rotation function allows tilting of telescopic handling device in order to perform the main SAS mission phases :

- unlatching robotic arm from storage configuration;
- grasping a sampling tool in its storage rack;
- positioning the same on sampling site;
- operating the tool together sample;
- recovering the tool from sampling site (with sample inside);
- positioning the samples (in their housing) in the return capsule.

The basic function provided by robotic arm and telescopic device is the capability to operate and activate all the sampling tools.

In the following, a brief description of the selected concepts for the sampling tools is given

Core Sampling Tools : Among the many different approaches, the core sample cutting process by rotary drill is considered the most suitable while other solutions (e.g. impact coring, vibration coring, thermal coring, etc..) are not meeting the mission scientific requirements.

In Fig. 4 the basic arrangement and operating sequence of a coring tool system is presented. The particular features of the system are :

- the hole sides are contained by an outer tube in order to avoid bore hole wall instability and missing of stratigraphy information;
- the bottom of core sample(s) is cut by a proper device, in order to avoid loss of sample material and minimize disturbance of its layering.

In the proposed concept each tool section is made of a inner sample housing tube, carrying the bottom cutting device, of an intermediate torque tube carrying the drill bit and of an outer guide tube.

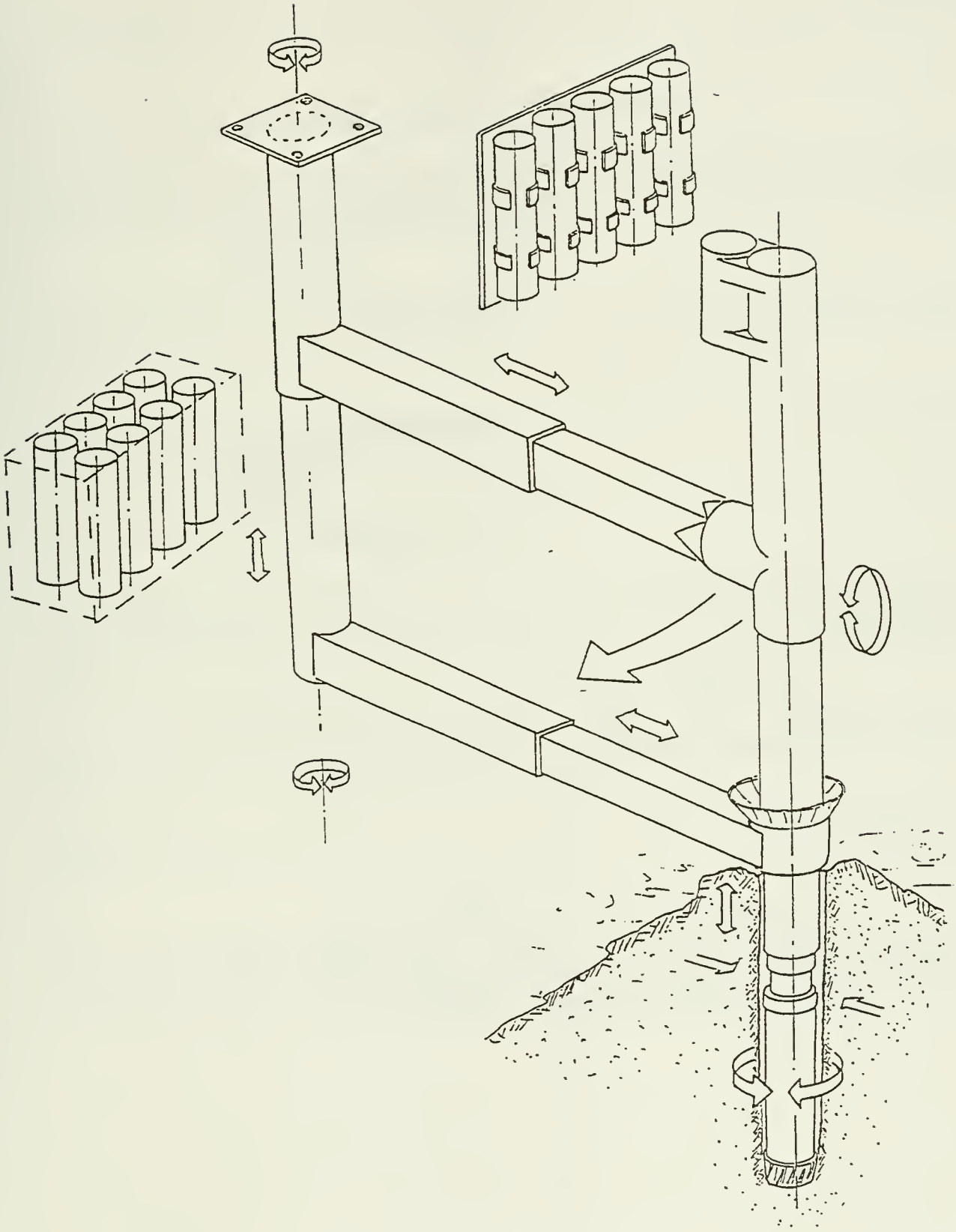


Figure 3 - Robotic arm system concept

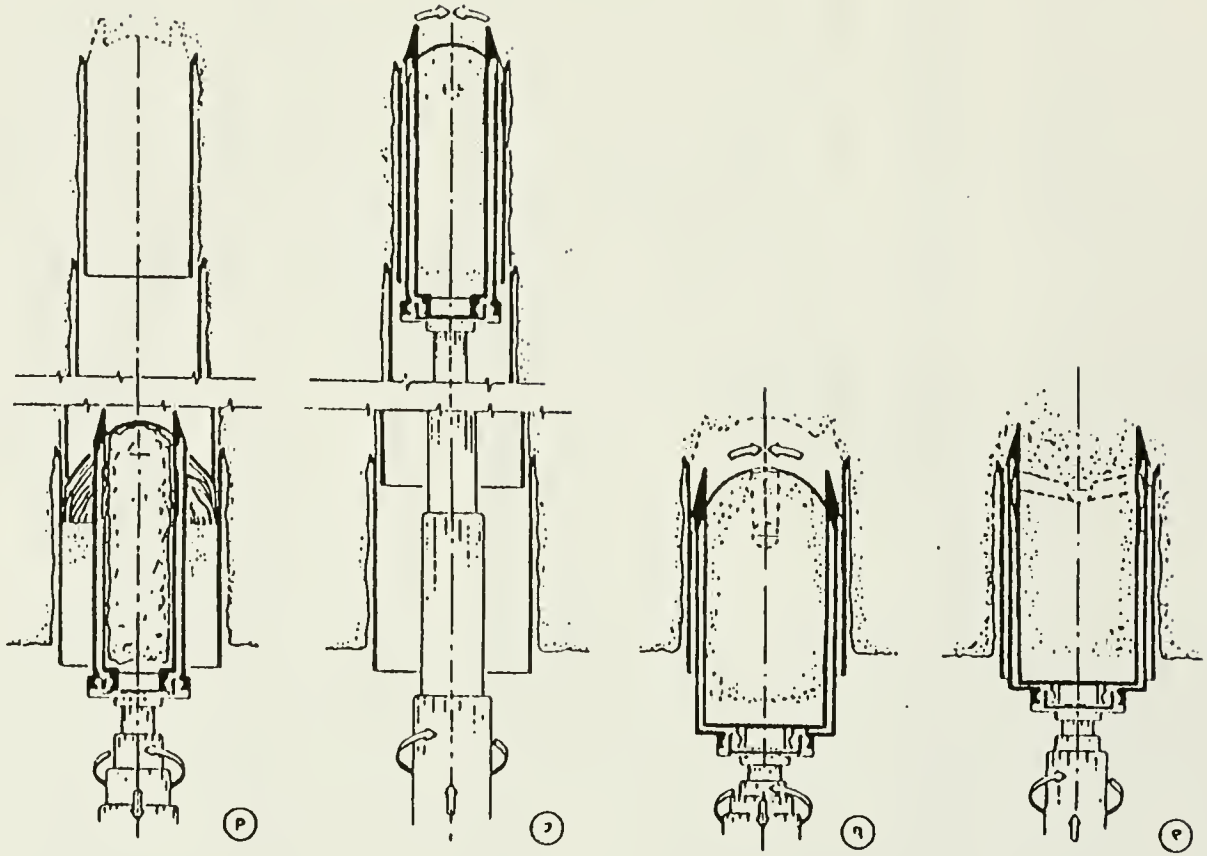


Figure 4 - Core sampling tool: operating sequence

The tool sets have diameters progressively decreasing in order to allow the drilling of each tool in the guide tube of previous one left in the hole to provide guidance and bore wall containment.

Cuttings are conveyed in the gap between torque tube and guide tube and are swept to surface by proper springs when each sample is recovered.

Volatile Sampler : The tool (see Fig. 5) collects material in the bottom of the deep core sampling hole; it allows preservations of volatile chemical species even if the tool is subject to temperature increase during handling to storage bay.

Surface Sampler : This tool concept (see Fig. 6) is based on a configuration similar to core sample tools : the surface material sampler is made of a tube having a special drill bit to disgregate nucleus "crust" and convey material to an inner sample housing pipe.

After penetration of tool into nucleus upper layer (about 0,05 m. deep) a sample bottom cutter confines the gathered material into the tool and allows its collection into the sample housing pipe which is lowered to catch it.

The main advantage of this concept is the capability to deal with every type of comet soil, due to the rotary drill action.

Harpoon : The harpoon (see Fig. 7) has to be used as a back-up sampling tool should the nominal scenario be not feasible; therefore maximum reliability must be guaranteed. For these reasons, a spinned harpoon concept has been selected for its capability to withstand different kinds of soil by varying spinning speed and for its stability during flight and impact phases.

The possibility of penetration by using the rotational speed allows a soft impact with the soil comet, with the consequent minor risks of damaging electrical and mechanical parts and to better preserve the collected material properties.

Anchoring System : The main characteristic of this device (see Fig. 8a. and b.) shall be the capability to assure a proper S/C anchoring on the comet to counteract drilling forces and torques.

Because of uncertainties on comet nucleus mechanical characteristics, a single system sizing is not likely to cover the full range of possible real operating conditions : at least two sizes of the anchoring tool will have to be foreseen, to be selected accordingly to information previously acquired on nucleus features (by the onboard sensing instrumentation).

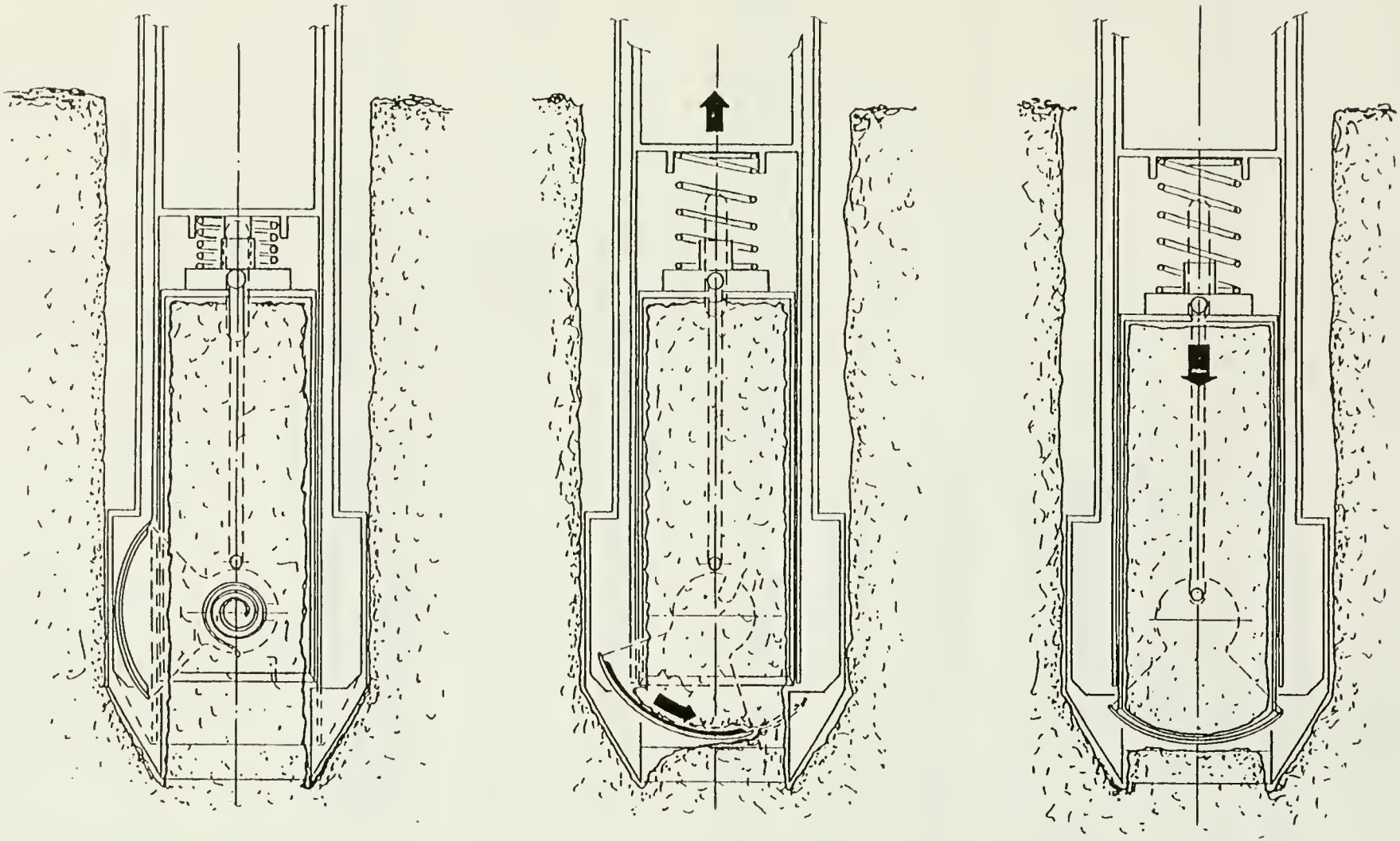


Figure 5 - Volatile sampling concept

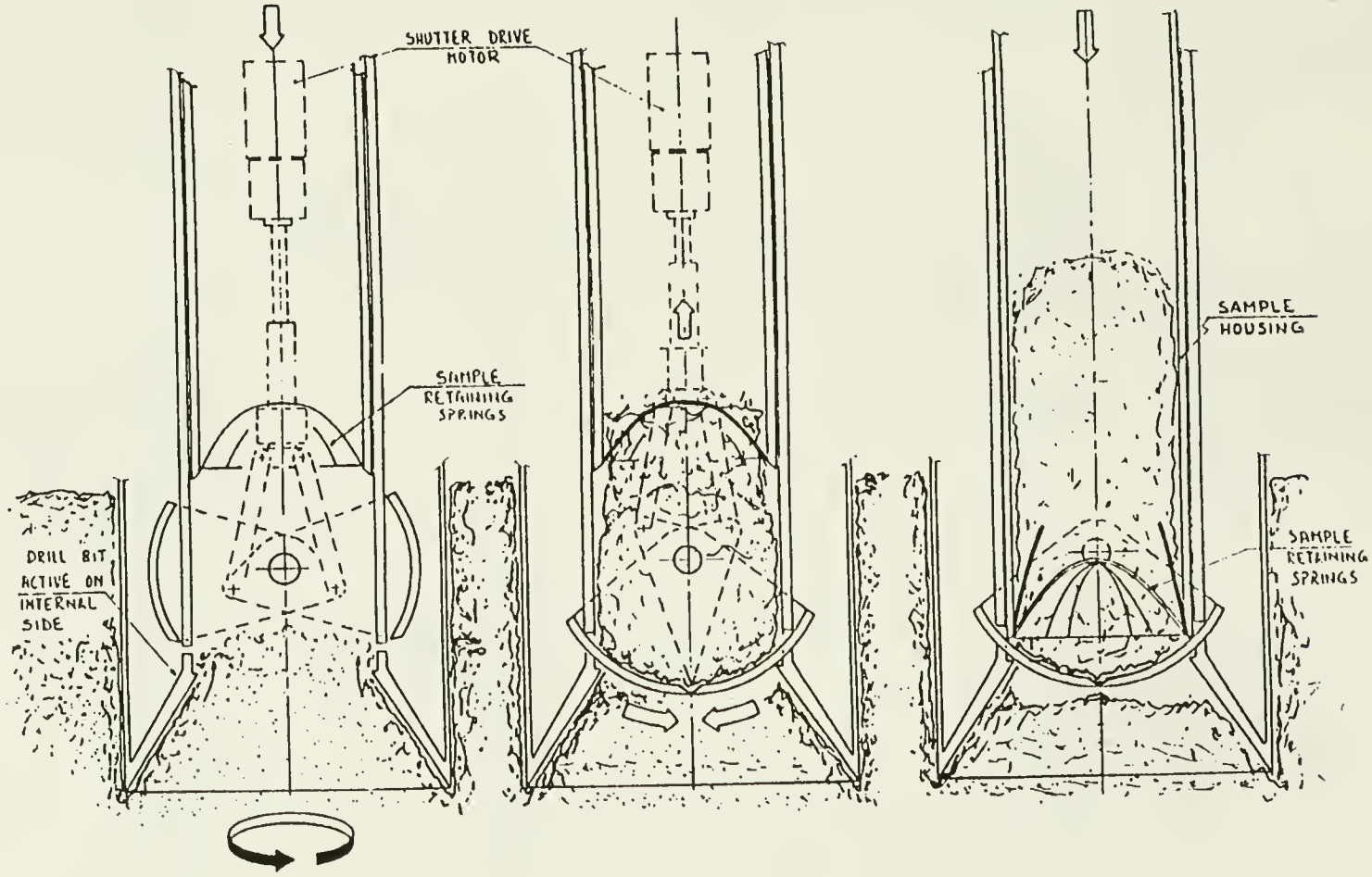


Figure 6 – S.A.S. Surface sampler concept

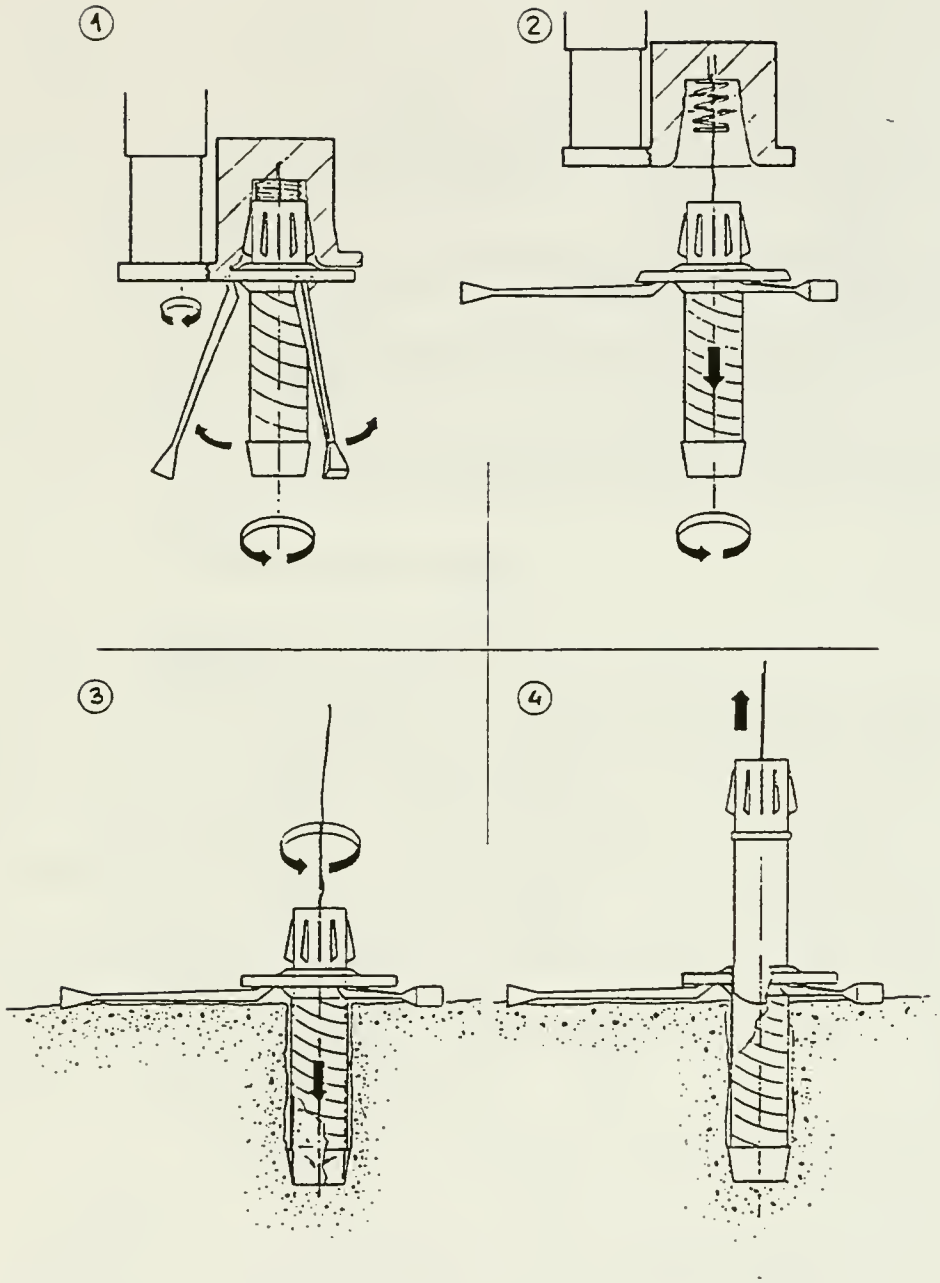


Figure 7 - Spinned harpoon operative sequence

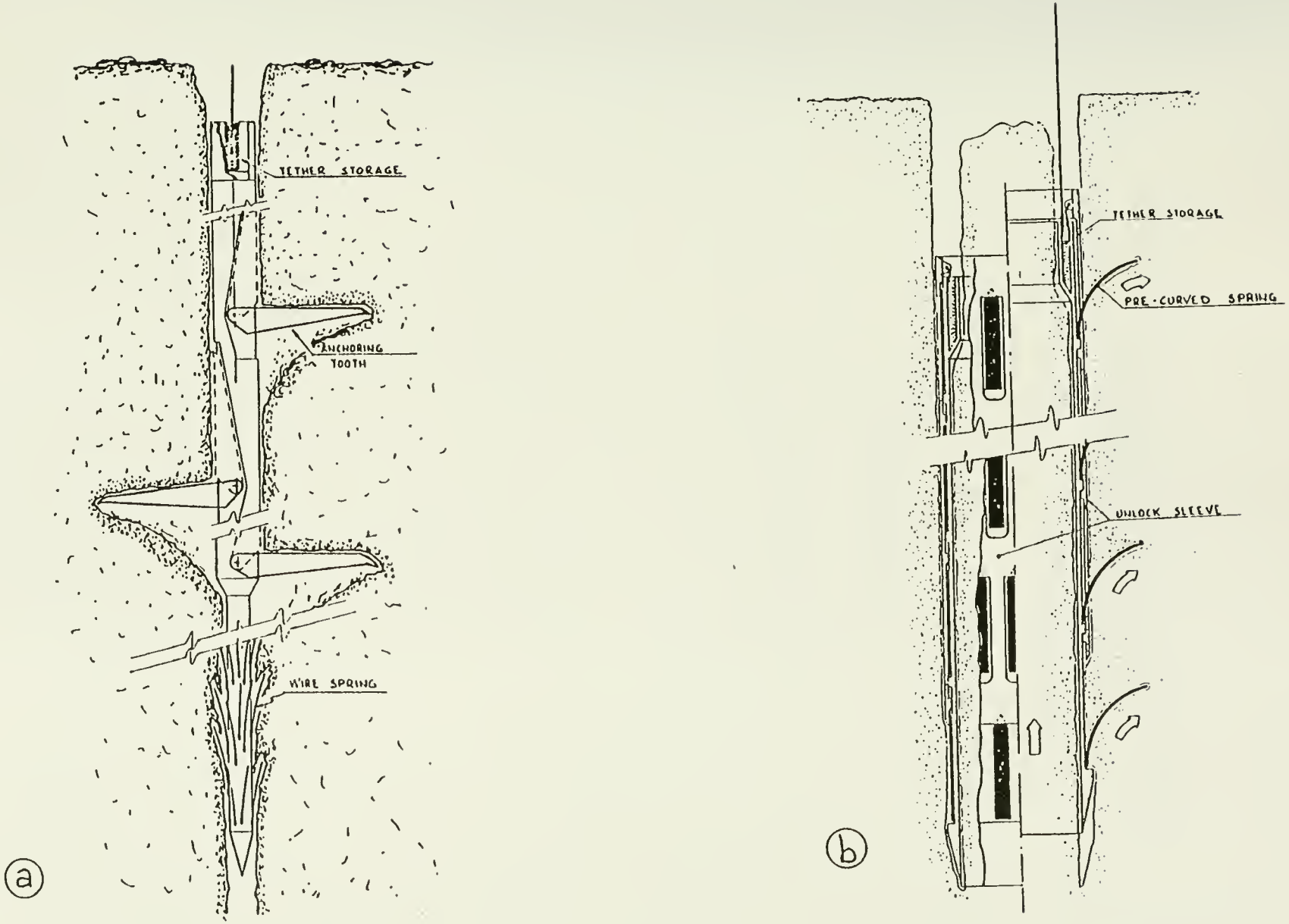


Figure 8 - Anchoring tool concepts

DESCRIPTION AND ANALYSIS OF CORE SAMPLES: THE LUNAR EXPERIENCE

David S. McKay
NASA Johnson Space Center

Judith H. Allton
Lockheed Engineering and Sciences Co.

Description and Analysis of Core Samples: The Lunar Experience

David S. McKay[1] and Judith H. Allton[2]

[1]NASA, Johnson Space Center and [2]Lockheed Engineering and Sciences Co.

INTRODUCTION

Although no samples yet have been returned from a comet, extensive experience from sampling another solar system body, the Moon, does exist. While, in overall structure, composition, and physical properties the Moon bears little resemblance to what is expected for a comet, sampling the Moon has provided some basic lessons in how to do things which may be equally applicable to cometary samples. In particular, an extensive series of core samples has been taken on the Moon, and coring is the best way to sample a comet in three dimensions.

Data from cores taken at 24 Apollo collection stations (Duke and Nagle, 1976) and 3 Luna sites have been used to provide insight into the evolution of the lunar regolith. It is now well understood that this regolith is very complex and reflects gardening (stirring of grains by micrometeorites), erosion (from impacts and solar wind sputtering), maturation (exposure on the bare lunar surface to solar winds ions and micrometeorite impacts) and comminution of coarse grains into finer grains, blanket deposition of coarse-grained layers, and other processes (fig. 1). All of these processes have been documented in cores. While a cometary regolith should not be expected to parallel in detail the lunar regolith, it is possible that the upper part of a cometary regolith may include textural, mineralogical, and chemical features which reflect the original accretion of the comet, including a form of gardening. Differences in relative velocities and gravitational attraction no doubt made this accretionary gardening qualitatively much different than the lunar version. Furthermore, at least some comets, depending on their orbits, have been subjected to impacts of the uppermost surface by small projectiles at some time in their history. Consequently, a more recent post-accretional gardening may have occurred. Finally, for comets which approach the sun, large scale erosion may have occurred driven by gas loss. The uppermost material of these comets may reflect some of the features of this erosional process, such as crust formation, and variations with depth might be expected. Overall, the upper few meters of a comet may be as complex in their own way as the upper few meters of the lunar regolith have proven to be, and by analogy, detailed studies of core samples containing this depth information will be needed to understand these processes and the details of the accretional history and the subsequent alteration history of comets.

LUNAR CORING DEVICES

Two types of coring devices were used on the Moon during the American Apollo program: drive tubes, which were manually pushed or driven with a hammer into the regolith (fig. 2), and a battery-powered, rotary-percussion drill corer, which allowed the collection of deeper cores, down to 3 meters in depth (fig. 3).

Unlike the planned comet sampling mission, the six voyages of Apollo allowed drive tube design to evolve in response to factual information about soil characteristics. Initially, the drive tubes were designed to collect a soil column 2 cm in diameter and up to 32 cm in length (two tubes screwed together doubled the column length). They were designed to be easily opened in the laboratory without disturbing the sample, a feature also desirable in comet coring devices. However, these narrow diameter tubes did not easily penetrate the denser-than-expected lunar soil (1.6 to 2.0 g/cm^3), resulting in only 50 to 60 percent recovery of soil with significant disturbance of the original stratigraphy (Carrier *et al.*, 1971). The first design change, after actually trying to core the lunar regolith, was to modify the drive tube bit from an inverted funnel shape (originally designed to collect loose, fluffy soil) to a straight wall bit (fig. 4). However, these core tube walls were relatively thick (0.5 cm) which contributed to sample distortion. Consequently, new drive tubes were designed and flown on the last three lunar missions.

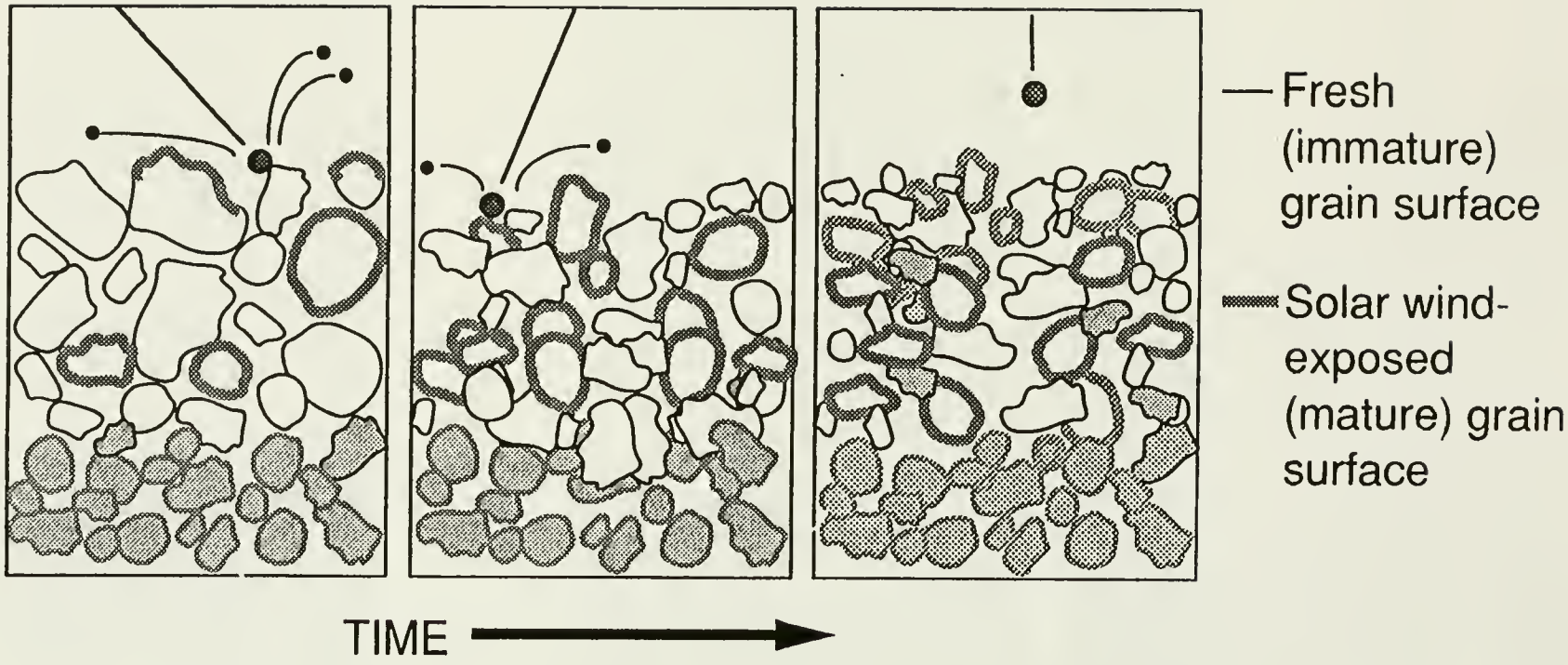


Figure 1. - Schematic diagram of three of the regolith forming processes: blanket deposition of coarse, immature grains; comminution of coarse grains into finer grains by micrometeorite bombardment; and stirring of grains, or gardening, allowing exposure to solar wind on all sides of many grains.



Figure 2. An Apollo 11 astronaut uses a hammer to drive a 2-cm diameter core tube into the lunar regolith. An extension handle is attached to the top of the core tube (NASA Photo AS11-40-5964).

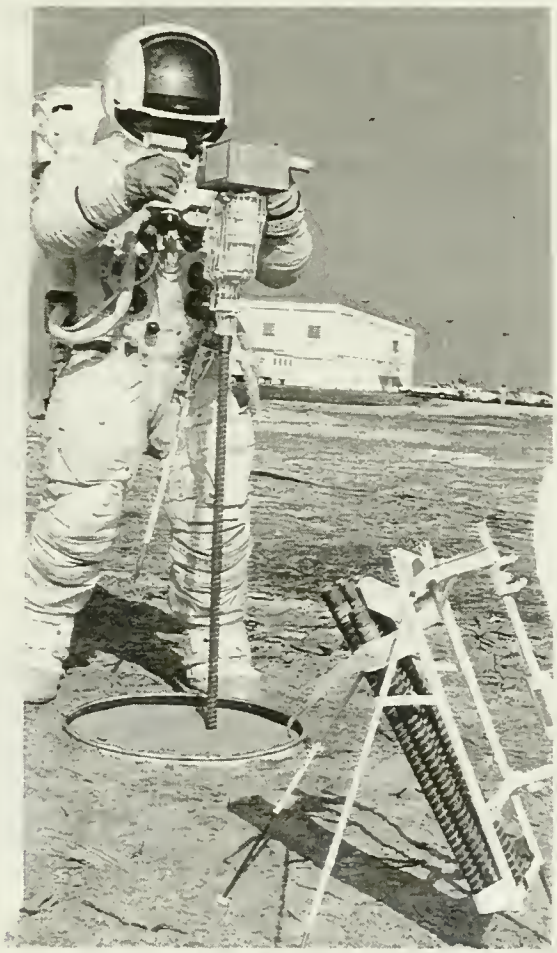


Figure 3. The Apollo Lunar Surface drill is tested prior to flight. The batteries are contained in the gray box and the motor is contained in the wire cage. Fiberglass-epoxy bore stems, used for drilling holes for heat flow probes, are shown in place of titanium drill stems in this photo; however, except for the length of individual sections, they are similar (NASA photo S-70-29673).

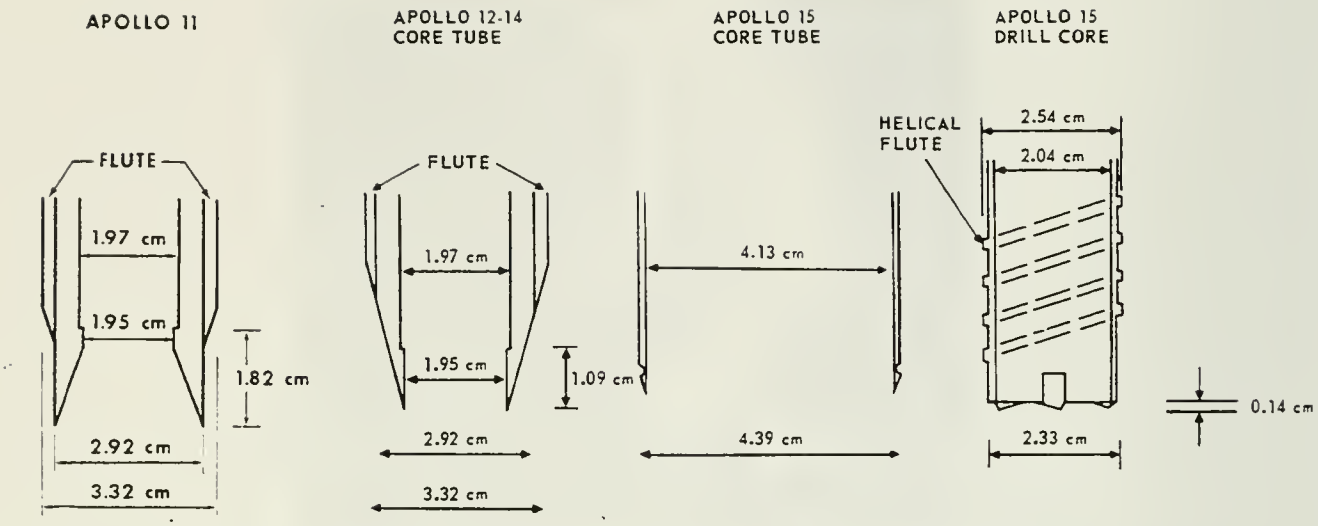


Figure 4. - The evolution of drive tube bits is illustrated by the Apollo 11, the Apollo 12 and 14, and the Apollo 15, 16, and 17 bits. The drill bit is shown for comparison (adapted from Carrier *et al.*, 1971 and Carrier *et al.*, 1972).



Figure 5. - 4-cm diameter drive tube. This tube has threads near the bottom which allow it to be screwed into another tube section. The tube on the bottom (not shown) has a steel bit formed into the aluminum tube in place of the threads (NASA photo S-71-16526).

Those new tubes (fig. 5) were able to collect a soil column 4 cm in diameter and up to 35 cm in length (two tubes screwed together doubled the column length). The wall thickness was 1 mm, the soil column collected was disturbed very little and soil recovery was nearly 100% (Carrier *et al.*, 1972). However, these tubes were designed, built and flown on very short notice; consequently, no provision was made for easily opening the tubes in the laboratory, so the ability to carefully open these tubes was not achieved until 2 years after the last Apollo mission. An additional advantage of larger diameter cores is that they provide sufficient sample at any one depth interval so that multiple analyses can be performed using a variety of techniques. For example, in the 4 cm diameter tubes, a 0.5 cm interval contained enough material (about 10 g) to allow for full grain size distribution for at least six size intervals, chemical and rare gas analyses of each size fraction, thin section grain mounts of each size fraction with enough sample left over for several other types of analyses, reserves for future analyses, and for making continuous thin sections of the core (Fruland *et al.*, 1982). The smaller diameter core tubes (2 cm) did not contain enough sample in a 0.5 cm depth interval for many of these analyses. Based on this experience, a comet sampler core should be at least 4 cm in diameter.

The battery-powered Apollo Lunar Surface Drill obtained soil columns 2 cm in diameter and up to 3 meters in length via rotary-percussive action. The 16 silver oxide-zinc batteries delivered 2270 blows per minute at 280 rpm. The length of the drill string resulted from screwing together individual tubes 42.5 cm in length (fig. 6). The bit contained 5 tungsten carbide cutting tips. Threaded flutes on the exterior of the tubes conducted the cuttings to the surface. Detailed dimensions, weights and materials of construction for both the drive tubes and the drill core can be found in Allton, 1989. Overall the drill worked well in the lunar regolith, although there was some difficulty in extracting the first stem drilled due to the very high bulk density of the soil (1.9 g/cm^3). The difficulty was resolved on later missions by running the drill in place (without further penetration) to clear the flutes of cuttings. The 3 meter deep soil columns taken by the Apollo drill were probably the most useful scientifically because the depth encompassed radiogenic profiles resulting from galactic cosmic ray bombardment. One disadvantage of the 2-cm diameter drill core, however, was lack of enough material in a narrow size interval ($\leq$ 0.5 cm) for complete size fractionation and analysis using multiple techniques on each size fraction.

Three unmanned Soviet Luna missions obtained lunar regolith cores with an impact and rotary drilling device. The drill, which operates 30^{o} from the vertical (fig. 7), automatically changed working regime in response to the density of the material being drilled. The Soviet drill differed from Apollo in that the rigid drilling tube contained an inner tube of flexible material, 260 cm long for Luna 24. The drill head interior diameter was 8 mm, while the flexible tube diameter was 12 mm. This diameter difference, the vibration during drilling or incomplete recovery of the uppermost, loose fluffy regolith may have contributed to the soil column being shorter than the drilled depth on the Luna 24 mission (Florensky *et al.*, 1977). The flexible tube, full of soil, was coiled around a drum, in spiral fashion, for return to Earth. Again, the restricted diameter of this tube, along with the disturbances of the sampling and handling technique, precluded some of the multiple analyses and detailed textural studies.

LUNAR SAMPLE RECEIVING LABORATORIES

The first three Apollo mission samples were handled under a biological quarantine protocol. Sample containers were initially brought into vacuum cabinets for opening and for preliminary volatile composition sampling. Working with samples in a vacuum cabinet with space suit gloves was chosen over electro-mechanical manipulators to allow flexibility to execute or recover from unexpected events. This approach turned out to be expensive and not practical; sudden system leaks were exciting events. Core tubes were opened, described and sampled in nitrogen atmospheres at slightly less than ambient pressure. The use of vacuum cabinetry was dropped during Apollo 14, afterwhich the biological quarantine was lifted. Samples were processed in pure nitrogen at slightly positive pressure thereafter, without significant loss of scientific information.

The canisters carrying the coiled Soviet regolith cores were opened and initially examined in a helium atmosphere (Florensky *et al.*, 1977). However, Surkov *et al.*, 1974 and 1979, reported on a chamber for receiving samples that was capable of achieving vacuum conditions. However, the chamber was filled with an inert gas before the sample canister was opened. Apparently, the Soviets too decided that sample handing in a vacuum chamber was not worth the expense and the problems. A transparent cylindrical glove box for handling lunar soil samples was described by Stakheyev *et al.*, 1974.

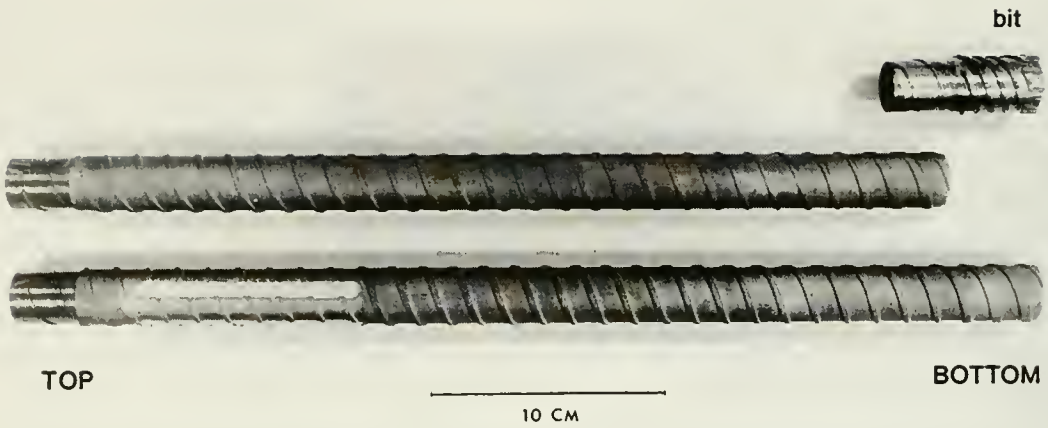


Figure 6. - Sections and bit from Apollo drill. Up to 8 sections were screwed together. All sections, except the one holding the bit, were the same length (NASA S-89-25295).

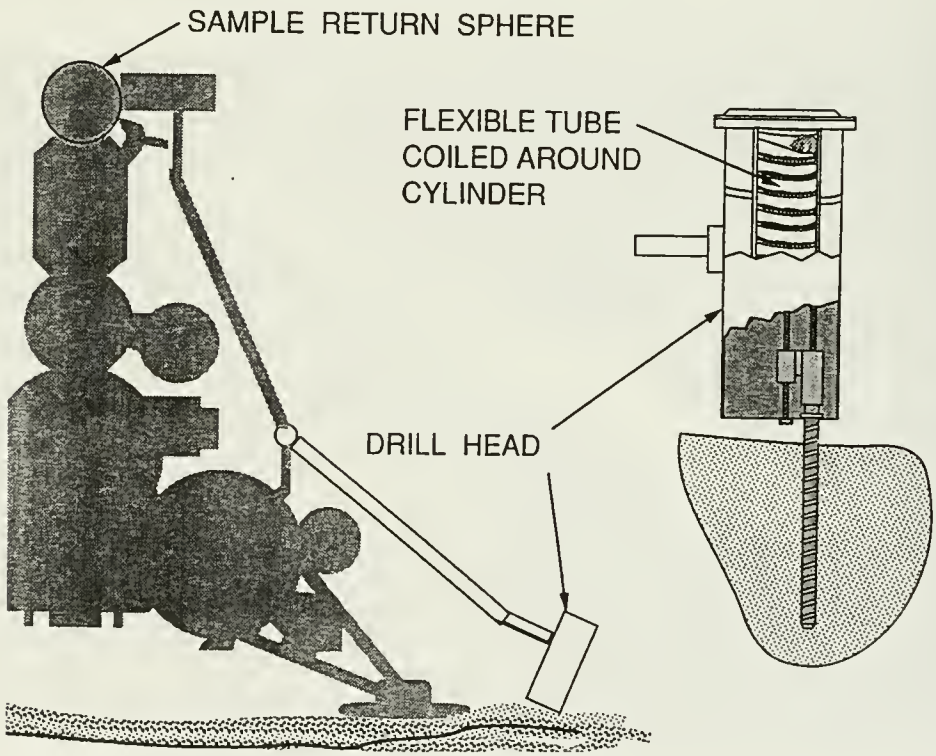


Figure 7. - Luna vehicle shown with drilling device (cylindrical shape) on arm in two positions. Drilling occurred in the lower position. The core in a flexible tube was extracted from the ground, and wound around a cylinder (enlargement) which was placed in the Earth return sphere atop the Luna vehicle (arm in upper position) (adapted from*Soviet Cosmonautics*, 1981 and Tarasov, *et al.*, 1980).

A low temperature and low pressure environment will be much more important for comet sample integrity than it was for lunar samples. However, the lunar experience with vacuum cabinets illustrates the need to have a reliable, practical system for sample handling. The sample handling system should be defined early in the mission planning. For example, totally robotic sample handling and human handling via gloves each place different requirements on the design of the sample containers.

EXTRACTION OF SCIENTIFIC INFORMATION FROM LUNAR CORES

The extraction of maximum scientific information from Apollo cores was a complex process consisting of three phases, depending on whether the information from the core was obtained before, during or after the core was opened and separated into individual samples - a process called dissection. The first phases, pre-dissection and dissection, were carried out as a curatorial function. The curatorial information was quickly and impartially distributed to all interested scientific investigators. The post-dissection phase involved work on samples requested by individual investigators or small consortia through a peer review panel, the Lunar Sample Analysis Planning Team which evolved into Lunar and Planetary Sample Team. An extensive database for all curatorial activity evolved from first-hand notes and chronological computer entries to an online accounting and tracking system for 70,000 lunar samples.

Pre-dissection

Pre-dissection included field data collected during actual coring operations on the lunar surface. This data included field relationships to other features, physical properties of the regolith (color, texture, density), and penetration depth. These data provided the geologic context for interpretation of the laboratory core analyses. Investigation of the returned core began with weighing to determine the density of the cored regolith. Next, most Apollo cores were photographed with x-rays in two orientations to provide stereo images of the contents of the tubes (fig. 8). These x-rays were used mainly to determine the degree of fill, find voids, identify major units, and locate small fragments, and they did not provide much quantifiable scientific data. Measurement of a nearly *in situ* thermal conductivity was attemped on unopened cores under vacuum (Horai *et al.*, 1980). In general the pre-dissection phase of Apollo cores provided the geologic setting, soil geotechnical properties and some basic textural information. However, recent advances in technololgy including three-dimensional x-ray computer assisted tomography (CAT scans), nuclear magnetic resonance imaging, and sophisticated digital image analysis might be used to extract more useful scientific data from future cometary cores during this pre-dissection phase. Measurements of gas pressure and composition can also be made on closed core containers.

Dissection

The dissection phase began by opening, inside of nitrogen-filled cabinets, the tubes by one of three methods, depending on the type of tube. The most convenient to open was the 2-cm diameter drive tube, in which a thin inner tube containing soil was extracted after the cap was removed. This thin inner tube was constructed of two aluminum semi-circular halves held together by teflon tubing. The teflon tube was easily cut open with a scalpel and the top aluminum tube half lifted off to reveal the soil. (This double tube construction contributed to the increased wall thickness which impeded the penetration of the tube into the dense soil and resulted in redesigning the drive tubes.) The second type core tube to be opened was the sections from the drill. These titanium alloy tubes were placed horizontally and milled open without lubricant in the nitrogen atmosphere. Without lubricants this process inflicted significant vibrations on the soil in the tube. The last method of opening cores was applied to the 4-cm diameter drive tubes. A large plunger device pushed the soil out of the drive tube and into a fixture with exactly the same sized bore. However, this fixture was constructed of layers, running the length of the core, which could be removed one by one revealing the soil.

Once opened, the exposed core soil was photographed and carefully subdivided into 0.5 cm increments (fig. 9). The 4-cm diameter drive tubes were of large enough diameter to allow for several sets of 0.5 cm increments to be



Figure 8. - X-ray photograph of 4-cm diameter Apollo drive tube showing individual fragments and regions of compacted soil. The steel bit is visible at the bottom, and a device for restraining the soil is visible at the top (NASA photo S-89-25298).

taken at the same depth. Small tools were used to remove soil, which was then sieved. Fragments larger than 1 mm were measured, photographed and color, texture, coherence, luster and cleavage were described. Preliminary gross mineral identification was sometimes made based on binocular microscope observations. The fragments and the fine soil were saved in separate vials for long term storage and allocation to investigators for further research. A portion of each increment was left untouched so than a continuous length of soil could be preserved. This undissected soil was removed from the nitrogen atmosphere in the clean room laboratory and taken to another laboratory to be preserved using both an acrylic plastic peel and impregnation by epoxy (fig. 10). Thin sections along the length of the core were produced from the epoxy impregnated portion.

Every step of the dissection was documented by written notes, extensive photography and numerous sketches. Dissection for a single core often took up to one year to complete. After the core tube was opened and before dissection began, many of the early cores had samples removed for basic petrography and chemical analysis by x-ray fluorescence in nearby laboratories. This was done as part of the preliminary examination conducted on all Apollo samples at that time. A very useful way of measuring the extent of soil exposure to the solar wind and micrometeorites, a maturity index based on ferromagnetic properties, was established in the mid-1970s (Morris, 1976). Small samples from all depth increments in cores were removed as the dissection progressed and passed on to an investigator's laboratory for measurement of this maturity index. Once established as a reliable index, ferromagnetic resonance of the sample was routinely used to survey cores during dissection, for this method requires very little sample (25 mg) and is a rapid and non-destructive measurement. Information generated during the dissection phase, including the preliminary data from the early cores and the maturity measurements, was quickly disseminated to scientific investigators via catalogs and newsletters. A similar protocol may be desirable for returned cometary core samples.

This information usually identified the major textural units within the core, described the contacts between the units, and located fragments larger than about 0.5 cm. Textural data collected during dissection were usually more detailed then the pre-dissection textural information and also included color variations and classification of rock and mineral types for larger particles. Descriptions from this dissection stage also provide the basis for accurate determinaton of true depth beneath the lunar surface of any sample. This basic sample location and textural information provides the framework for interpretation of the data from the more detailed and sophisticated post-dissection analyses which were usually performed by investigators in their own laboratories. While the amount of detailed description necessary during the dissection phase has been the subject of some debate, no one has questioned the value of basic core description and dissection data in providing a framework for subsequent analyses and interpretation. It is particularly important that the dissection phase be carefully planned because some information may be permanently lost if not acquired during this phase. Once dissected, the core cannot be reassembled to take a closer look at features such as unit boundaries.

Post-dissection

Post-dissection analyses consists of a wide variety of analyses performed by individual investigators on subsamples provided in small vials or on thin sections. While in theory, the post-dissection phase does not begin until the dissection is complete, it was practical to begin allocating and shipping samples after the first dissection unit was completed and preliminary information on the sample set was distributed. Thin sections of the nearly *in situ* soil showed the soil fragments in their lunar orientation, such as the agglutinate particle with it's glass splattered side up shown in figure 11. However, fewer scientific conclusions were drawn from particle orientation and micro-stratigraphy in these thin sections.than originally thought. Petrographic grain population studies from thin sections, did however, sometimes reveal unexpected exotic layers, such as the green glass sphere strata in an Apollo 15 core from the Apennine Front or the coarse-grained olivine layer from the Apollo 12 site.

Grains extracted from cores, sorted by size and mounted in thin sections revealed a wide variety of grain types which not only varied with depth in the core, but with grain size. Figure 12 illustrates grain size variation with depth in a core from the Apollo 15 site. Each core had its own grain size distribution pattern, and the pattern was seldom systematic or predictable. However, vertical variations in many properties were common; homogeneous cores, even short ones, were the exception. Chemical and isotopic analyses showed variation with core depth and also with grain size. Figure 13, for example, shows that the finer size fraction of this core section is enriched in rare earths compared to an intermediate size, and this pattern is somewhat different from the pattern in the lower section of this core (not shown).

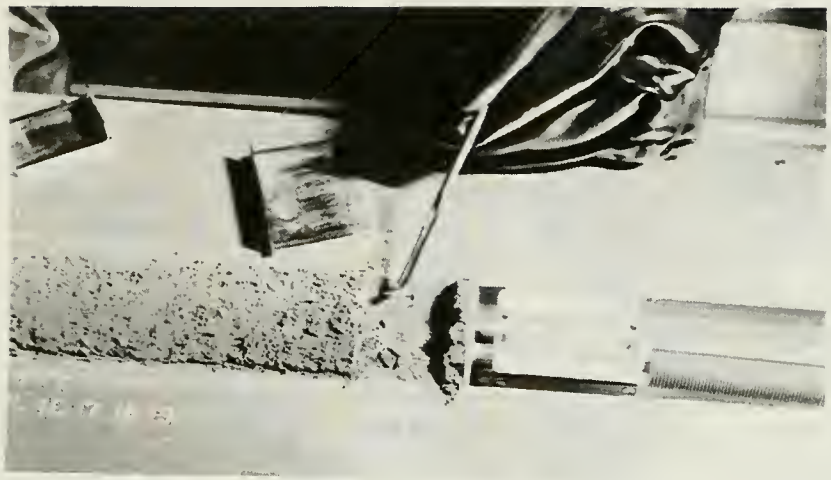


Figure 9. - Dissection of 4-cm diameter Apollo core in 0.5 cm increments using small tools inside of a nitrogen-filled cabinet.

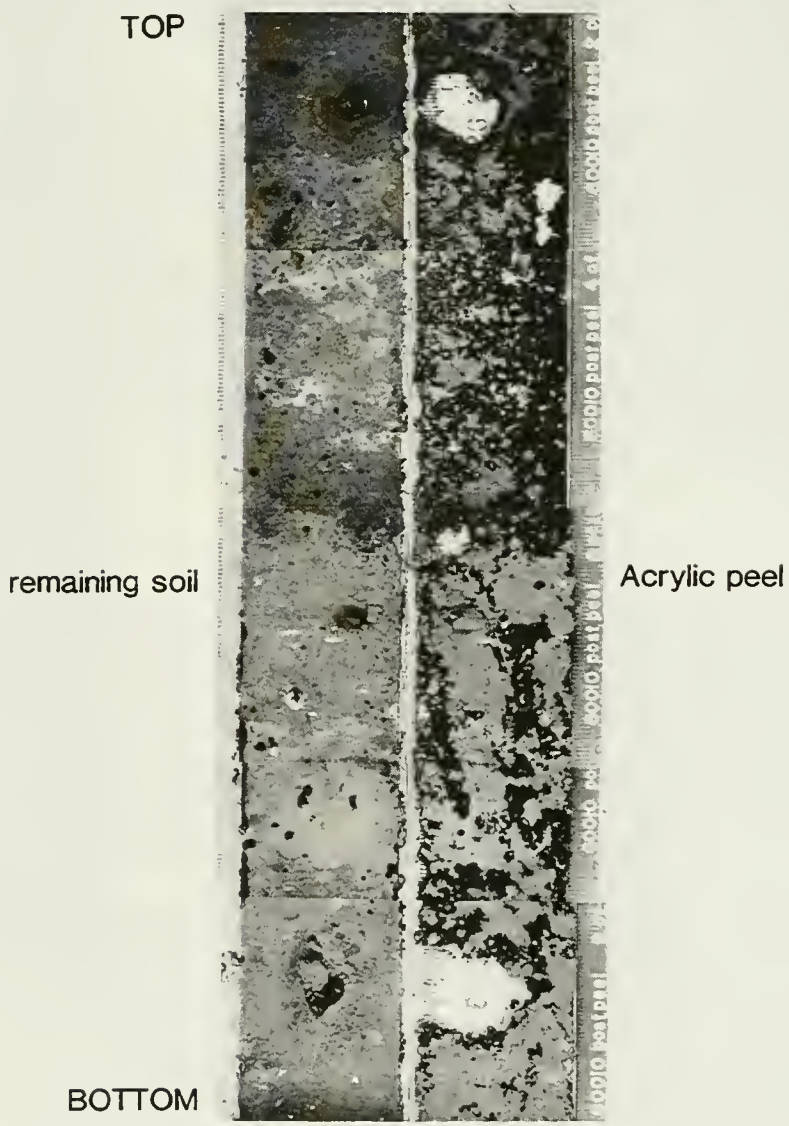


Figure 10. - Distinct color boundaries are easily observed in this 4-cm diameter core, taken from the Apollo 16 site, after a thin layer of soil has been removed with a strip of acrylic glue. The soil-ridden acrylic strip is shown on the right. The remaining soil on the left will be impregnated with epoxy which can be made into thin sections (NASA photo S-77-22213).

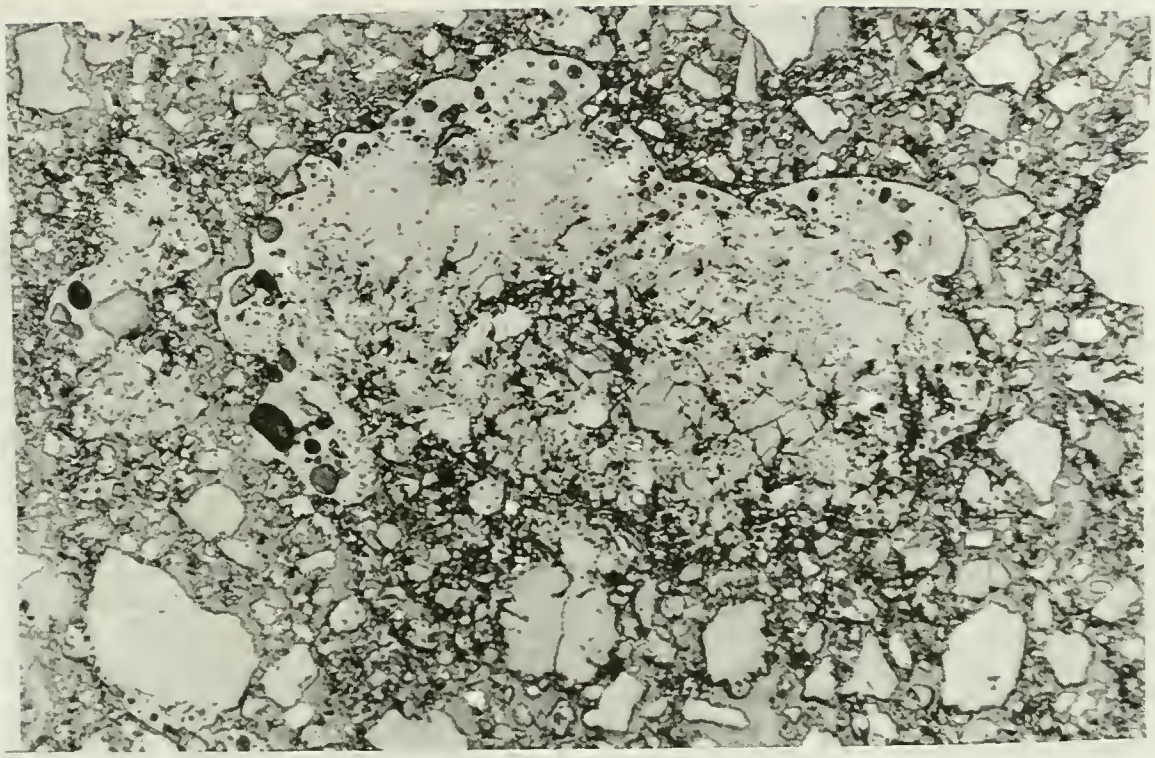


Figure 11. - Thin section of a 4-cm diameter Apollo 15 core with soil in position as collected in tube. An agglutinate is shown with its glass-coated surface facing up. The field of view is 1 mm.

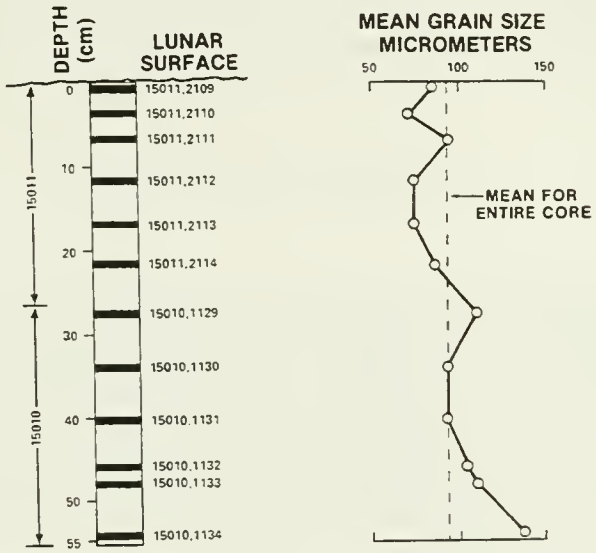


Figure 12. - Grain size variation with depth in 4-cm diameter core from Apollo 15 site (McKay *et al.*, 1980).

One of the major achievements of lunar core science was the formulation of a model for the variation of maturity properties with depth and exposure time. Trends in some vertical regolith sections could be shown to fit this model. Communition of soil fragments into smaller particles and formation of agglutinates by micrometeorite bombardment, both indicators of soil maturity, are correlated (fig. 14). Soil maturity is also evidenced by the abundance of solar flare tracks (fig. 15). The ferromagnetic resonance based index proved to correlate well with agglutinate abundance (fig. 16), mean grain size and solar flare tracks. Not only did this index vary with core depth, but also with grain size as shown in figure 17.

More and more complex scenarios had to be developed to explain the data from cores. Samples from various depths in this Apollo 16 drive tube core (fig. 18) could be related to each other only by using a combination of mixing three end members followed by a superimposed maturation evolution for only one of the mixed sets. Studies of individual grains or groups of grains from the cores has also been useful. Figure 19 shows a cluster of micrometer-size grains from an Apollo 15 core which exhibit rounding interpreted as resulting from sputter erosion. At about the same scale, figure 20 shows a cluster of mostly submicrometer grains from a porous interplanetary dust particle, the type which has been interpreted as a likely sample from a comet. If these are really comet samples, understanding of a comet would be as complete as an understanding of the Moon from a few random grains. Much understanding of the history and evolution of the lunar regolith has come from the detailed, integrated core studies set in the proper geologic framework.

Soviet Luna cores

Although each Soviet Luna core was less supported by additional samples and first-hand field data to form a framework for study, the extraction of information from these cores also occurred in pre-dissection, dissection and post-dissection phases. During the pre-dissection phase an *in situ* survey of magnetic properties was made. The flexible tube was then coiled in a flat spiral and an x-ray photograph taken. Dissection proceded by uncoiling the tube and cutting it into 25-30 cm long sections, with the position of the cut based on the magnetic and x-ray data. Each of the tube sections was placed on a special tray and then slit open. The samples were handled under a helium atmosphere. The regolith material was then visually examined, described, and photographed both in visible light and by x-ray. Small samples were removed for subsequent processing in nitrogen-filled cabinets. However, the coarsest sieve fractions were taken into an air atmosphere for hand-picking of individual fragments of rocks and minerals . Small samples of 150-200 mg were taken along the entire core at limited intervals (unspecified). In addition, larger samples of about 2 grams were taken from selected 3-4 cm intervals to carry out comprehensive studies on the separate soil zones. Half of the material at each depth was reserved for future studies (Florensky *et al.*, 1977). Post-dissection information came from more sophisticated studies conducted in research laboratories in the Soviet Union and abroad.

SUMMARY AND CONCLUSIONS

In summary, Apollo core analysis and handling experience provides a good starting point for the detailed planning of a cometary core program. Core collection and analysis is a complex task which must be carefully planned from sample collection at the comet to sample allocation in the receiving laboratory.

1. Core samples from comets are likely to have complex vertical variations and even horizontal variations, if preserved by the sampling process. These variations may reflect accretion history and accretion gardening, later impact and reworking history, and changes resulting from near-sun passage, with gas and dust disturbances. Possible endogenetic processes such as aqueous alteration or gas transport may also be reflected in cometary regoliths.

2. Collection and analysis of cores from the lunar regolith was a complex process which evolved over time so that subsequent core hardware and procedures were improved over earlier ones. This luxury will not be available for a comet mission which must be done right the first time. Very careful planning is obviously required.

3. Not only must the science requirements for the sample be integrated with the mission operation and engineering aspects, but designers of flight hardware should also be aware of the conditions under which the samples will be opened and examined upon return to Earth.

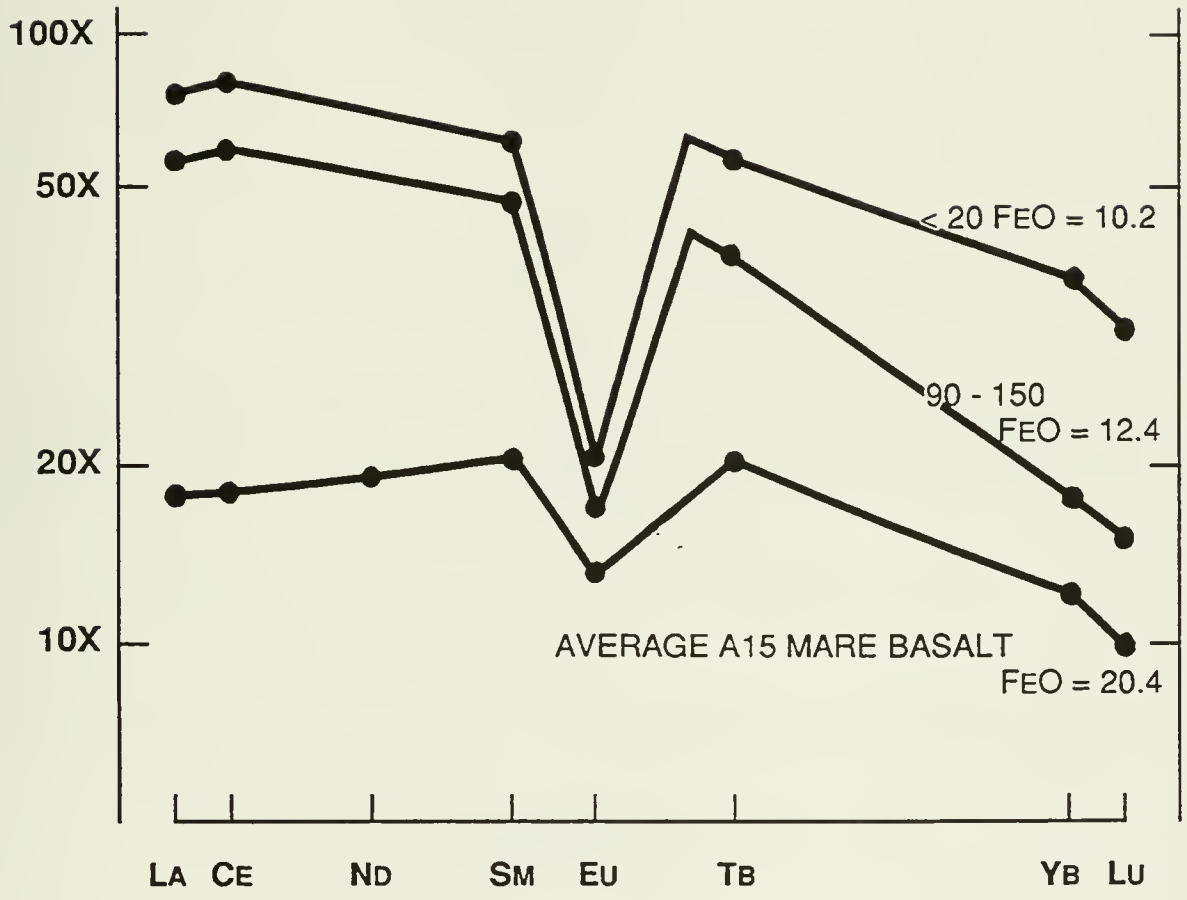


Figure 13. - The <20 μm size fraction of this Apollo 15 core is enriched in rare earths compared to the 90-150 μm fraction, illustrating differences in chemical composition with grain size. Chemical composition varies with depth in the core also; the rare earth pattern at a lower depth in this core is different (Blanchard, unpublished data).

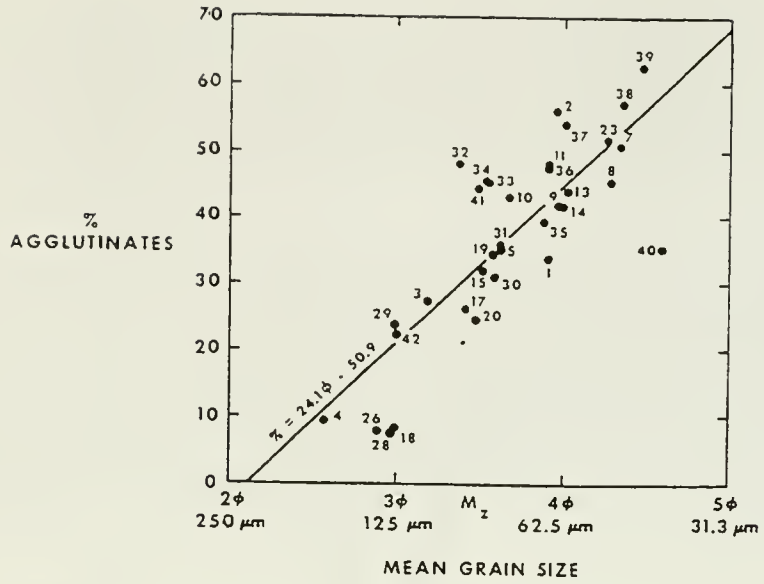


Figure 14. - Good correlation is shown for two indicators of soil maturity, the % agglutinates in the 90-150 μm size fraction and the mean grain size of the soil, in 42 Apollo 17 soils (McKay *et al.*, 1974).

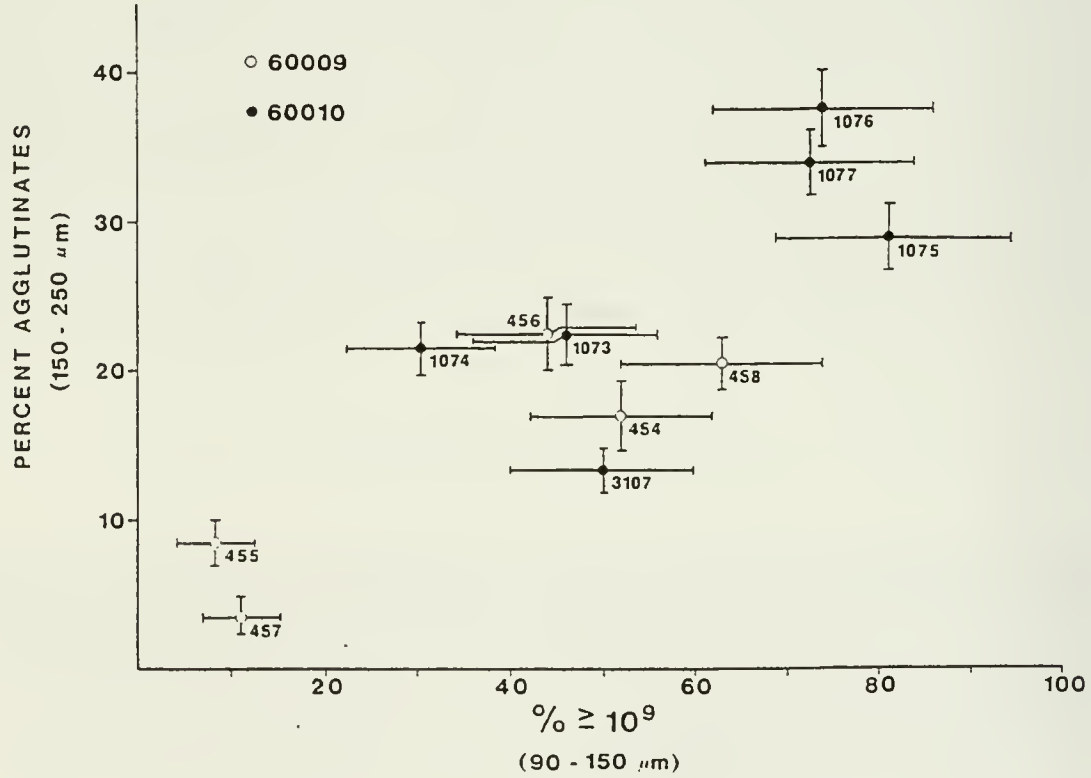


Figure 15. - Soils from a 4-cm diameter Apollo 16 core show correlation between the % agglutinates in the 150-250 μm size fraction and the solar flare particle track density in individual grains from the same soil, another indicator of soil maturity (Blanford *et al.*, 1977).

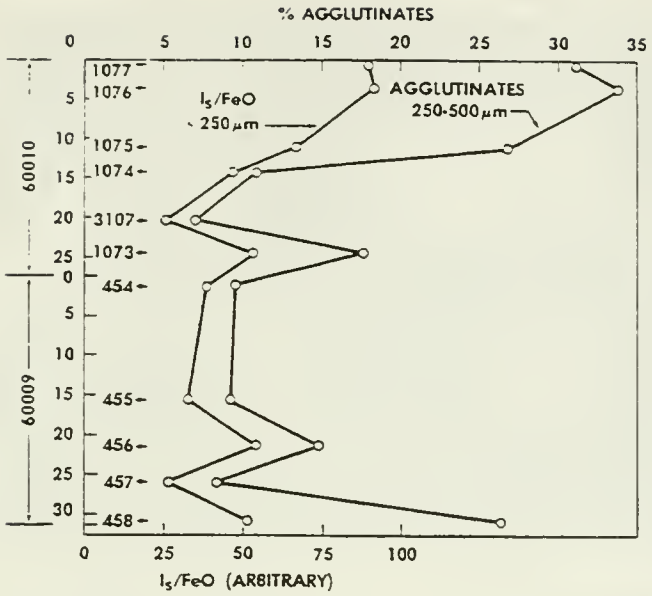


Figure 16. - Two maturity indices, I_s/FeO (a ferromagnetic based index) and percent agglutinates vary with depth in an Apollo 16 core. The soil at the surface shows the greatest maturity (McKay *et al.*, 1977).

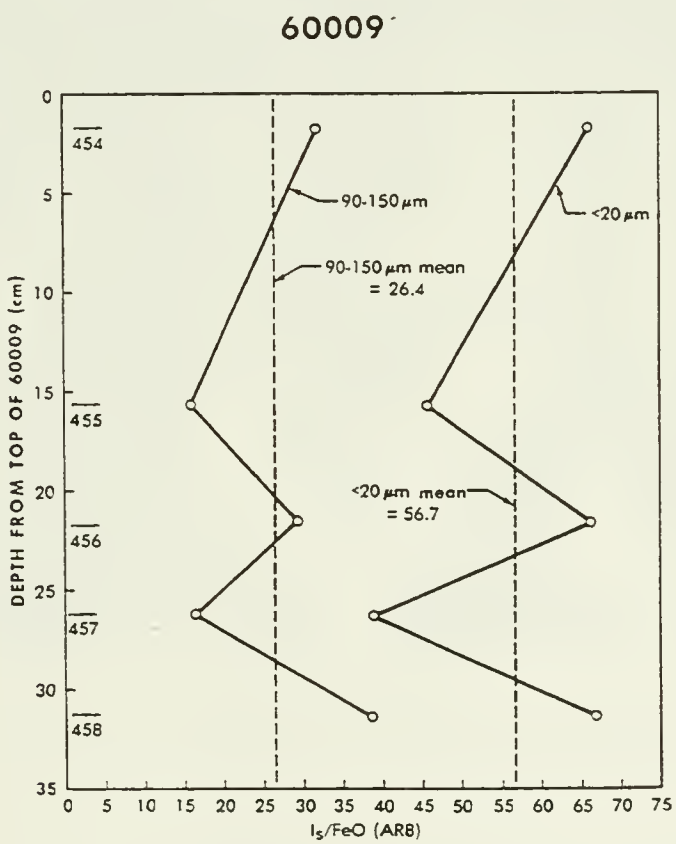


Figure 17. - The ferromagnetic index varies with depth in this Apollo 16 core and also with grain size. Increasing values of I_s/FeO indicate greater maturity (McKay *et al.*, 1976).

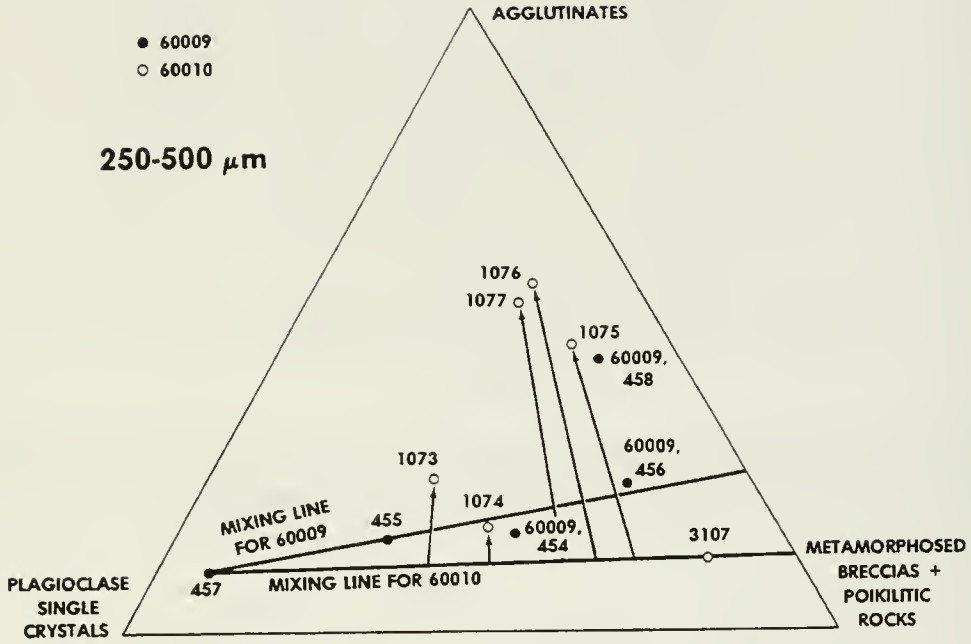


Figure 18. - Soil samples from a single Apollo 16 core can be related by superimposing a maturation evolution, evidenced by increasing agglutinates, for only one of three end-members in a soil mixture (McKay et al., 1977).

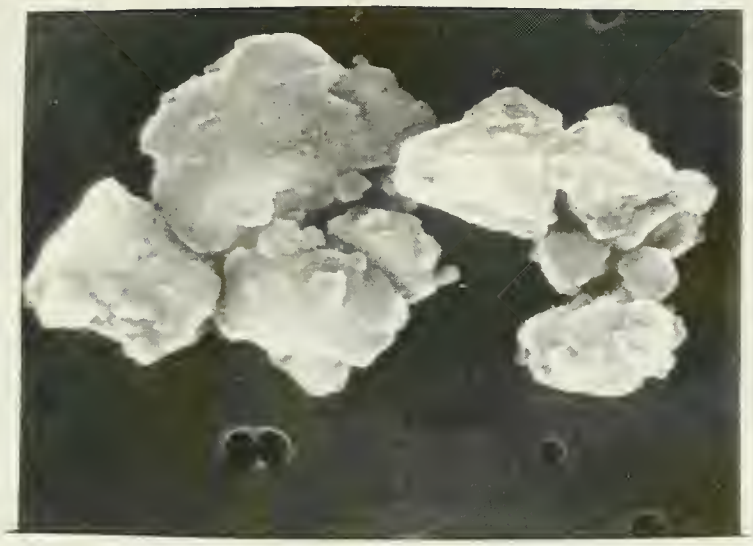


Figure 19. - Cluster of micrometer-sized grains from an Apollo 15 core which exhibit rounding interpreted as resulting from sputter erosion (NASA photo S-78-29566).



Figure 20. - Submicrometer grains from a porous interplanetary dust particle, the type which has been interpreted to be from comets.

4. Different types of information will be collected during each phase of cometary core analysis: pre-dissection, dissection, and post-dissection. Some information may be permanently lost if not collected during the appropriate phase.

5. Much of the rich experience with lunar core samples can be directly applied to cometary core handling and analysis. Examples include the three phases of data collection and analysis, the preliminary examination concept, the early and subsequent allocation of samples to outside investigators, the mechanics and bookkeeping of the curation and allocation system, and the preservation of a significant portion of the cores for future studies.

6. Cores returned from a comet can be expected to be just as complex as the lunar regolith cores, and vertical variations should be expected. Judging from the lunar experience, these vertical variations may be neither systematic nor predictable and may be highly complex. Only a wide variety of analyses interpreted in the framework provided by a geologic setting and careful dissection can begin to allow us to understand the history and evolution of a comet.

REFERENCES

_____ *Soviet Cosmonautics*, Moscow Machine Building, 1981.

Allton, Judith H.: Catalog of Apollo Lunar Surface Geological Sampling Tools and Containers. JSC 23454, LESC-26676, Johnson Space Center, Houston, TX. 1989.

Blanford, George E.; McKay, David S.; and Wood, G. C.: Particle track densities in double drive tube 60009/10. In *Proc. Lunar Sci. Conf. 8th*, pp. 3017-3025. 1977.

Carrier, W. David III; Johnson, Stewart W.; Werner, Richard A.; and Schmidt, Ralf: Disturbance in samples recovered with the Apollo core tubes. In *Proc. Lunar Sci. Conf. 2nd*, vol. 3, pp. 1959-1972. M. I. T. Press, 1971.

Carrier, W. David III; Johnson, Stewart W.; Carrasco, Lisimaco H.; and Schmidt, Ralf: Core sample depth relationships: Apollo 14 and 15. In *Proc. Lunar Sci. Conf. 3rd*, vol. 3, pp. 3213-3221. M. I. T. Press, 1972.

Duke, M. B.; and Nagle, J. S.: Lunar Core Catalog. JSC 09252. NASA, Johnson space Center, Houston, TX. 1976.

Florensky, C. P.; Basilevsky, A. V.; Ivanov, A. V.; Pronin, A. A.; and Rode, O. D: Luna 24: Geologic setting of landing site and characteristics of sample core (preliminary data). In *Proc. Lunar Sci. Conf. 8th*, pp. 3257-3279. 1977.

Fruland, R. M.; Nagle, J. S.; and Allton J. H.: Catalog of the Apollo 16 Lunar Core 60009/60010. JSC 17172, Lunar curatorial Branch Publication 61. NASA, Johnson Space Center, Houston, TX. 1982.

Horai, K.; Winkler, J. L. Jr.; Keihm, S. J.; Langseth, M. G.; Fountain, J. A.; and West, E. A.: Thermal conduction in a composite circular cylinder: A new technique for thermal conductivity measurements of lunar core samples. In *Philosophical Transactions of the Royal Society of London*, vol. 292, pp. 571-598. 1980.

McKay, D. S.; Fruland, R. M.; and Heiken, G. H.: Grain size and evolution of soils. In *Proc. Lunar Sci. Conf. 5th*, pp. 887-906. 1974.

McKay, D. S.; Morris, R. V.; Dungan, M. A.; Fruland, R. M.; and Fuhrman, R.: Comparative studies of grain size separates of 60009. In *Proc. Lunar Sci. Conf. 7th*, pp.295-313. 1976.

McKay, D. S.; Dungan, M. A.; Morris, R. V.; and Fruland, R. M.: Grain size, petrographic, and FMR studies of the double core 60009/10: A study of soil evoluton. In *Proc. Lunar Sci. Conf. 8th*, pp.2929-2952 1977.

McKay, D. S.; Basu, A.; and Nace, G.: Lunar core 15010/11: Grain size, petrology, and implications for regolith dynamics. In *Proc. Lunar Planet. Sci. Conf. 11th*, pp.1531-1550. 1980.

Morris, R. V.: Surface exposure indices of lunar soils: a comparative FMR study. In *Proc. Lunar Sci. Conf. 7th*, pp.315-335. 1976.

Stakheyev, Yu. I.; Tarasov, L. S.; Krestinina, K. K.; and Ivanov, A. V.: Box for preliminary investigation of the lunar soil in nitrogen atmosphere. In *Lunar Soil from the Sea of Fertility*, ed. Vinogradov, A. P., Publishing House "Nauka", Moscow, pp. 34-37. 1974 (Russian).

Surkov, Yu. A.; Rudnitsky, E. M.; and Glotov, V. A.: Reception and studies of lunar matter in a medium of inert gas. In *Lunar Soil from the Sea of Fertility*, ed. Vinogradov, A. P., Publishing House "Nauka", Moscow, pp. 29-33. 1974 (Russian).

Surkov, Yu. A.; Heifez, E. M.; Rudnizky, E. M.; Danilov K. D.; Glotov, V. A.; Visochkin, V. V.; and Sherstjuk, A. I.: Acceptance and investigation of lunar soil in noble gases atmosphere or/and at ultrahigh vacuum. In *Regolith from the Highland Region of the Moon*, ed. Barsukov, V. L. and Surkov, Yu. A., Publishing House "Nauka", Moscow, pp. 31-40. 1979 (Russian).

Tarasov, L. S.; Ivanov, A. V.; Vysochkin, V. V.; Rode, O. D.; Nazarov, M. A.; and Sherstyuk, A. J.: Reception and preliminary study of Luna 24 regolith core. In *Lunar Soil from Mare Crisium*, ed. Barsukov, V. L., Publishing House "Nauka", Moscow. 1980 (Russian).

THE ORIGIN, COMPOSITION, AND HISTORY OF COMETS FROM SPECTROSCOPIC STUDIES

L. J. Allamandola
NASA Ames Research Center
Moffett Field, California

THE ORIGIN, COMPOSITION AND HISTORY OF COMETS FROM SPECTROSCOPIC STUDIES

L.J. ALLAMANDOLA

NASA-Ames Research Center MS 245-6
Moffett Field, CA 94035

I. INTRODUCTION

A wealth of information essential to understanding the composition and physical structure of cometary ice and hence gain deep insight into the comet's origin and history, can be gleaned by carrying out a full range of spectroscopic studies on the returned sample. These studies ought to be among the first performed as they are generally non-destructive and will provide a broad data bank which will be crucial in planning subsequent analysis. Examples of the spectroscopic techniques discussed below, along with relative sensitivities and transitions probed, are listed in table 1. This table is by no means exhaustive and other techniques will certainly be added as more spectroscopists become aware of the unique challenges and opportunities afforded by the comet nucleus sample return mission.

Each "spectroscopy" will be summarized, with emphasis placed on the kind of information each provides. Infrared spectroscopy should be the premier method of analysis as the mid-IR absorption spectrum of a substance contains more global information about the identity and structure of that material than any other property. In fact, the greatest strides in our understanding of the composition of interstellar ices (thought by many to be the primordial material from which comets have formed) have been taken during the past ten years or so because this was when high quality infrared spectra of the interstellar medium (ISM) first became available. The interpretation of the infrared spectra of mixtures, such as expected in comets, is often (not always) ambiguous. Consequently, a full range of other non-destructive, complementary spectroscopic measurements are required to fully characterize the material, to probe for substances for which the IR is not well suited and to lay the groundwork for future analysis.

Given the likelihood that the icy component (including some of the organic and mineral phases) of the returned sample will be exceedingly complex, these techniques must be intensely developed over the next decade and then made ready to apply flawlessly to what will certainly be one of the most precious, and most challenging, samples ever analyzed.

II. THE "SPECTROSCOPIES"

A) INFRARED-ABSORPTION AND REFLECTION SPECTROSCOPY (10,000-10 cm^{-1})

Infrared spectroscopy gives great insight into a material's compostion because each chemical bond in a molecule produces a characteristic set of well defined, fundamental, vibrational frequencies. The spectrum of these frequencies, nearly all of which fall in the 4000 - 400 cm^{-1} range for molecules made up of the most abundant elements H, C, N and O, is generally very characteristic of the molecular subgroups comprising the molecule (Fig. 1). For example, every molecule which has a CH bond has at least one fundamental CH stretching mode which falls in the 3300 - 2800 cm^{-1} region, independent of how the C is further bonded (Fig 1a). The precise frequency within this region however, is determined by how that C is further bonded (Fig 1b). If the carbon is singly bonded to a C, O or N atom, the C-H stretching modes are between about 2820 and 2990 cm^{-1}, the CH bending (or deformation) modes fall in the 1400 - 1500 cm^{-1} range and the corresponding C-C, C-O, or C-N stretch lie between 1300 and 800 cm^{-1}. If it is doubly bonded the C-H stretch lies between 3000 to 3100 cm^{-1}, the CH bend in the 900-700 cm^{-1} region and the heavy atom C=C stretch (probably very weak) falls close to 1800 cm^{-1}. Finally, if it is triply bonded, the CH stretch lies close to 3300 cm^{-1}, the C≡C stretch near 2100 cm^{-1} and the C-H bend near 700 cm^{-1}. Thus obtaining the entire mid-IR spectrum allows one to place very important constraints on the types of chemical structures present.

Absorption measurements on ices in the 10,000-4000 and 400-10 cm^{-1} region are scarce, however these should prove important regions as well. The 10,000-4,000 cm^{-1} region will be rich in overtone and combination bands, and thus compounds which have modes that saturate in the mid-IR should show characteristic, unsaturated features in the near IR. (Reflection spectra of ices have been made in this region to interpret the spectra of some planets and satellites. See Nash and Nelson, 1979 and Nash and Howell, 1988 and references therein). The 400-10 cm^{-1} region is also largely unexplored for bona-fide mixed molecular ices. Here one probes very low frequency modes such as large molecule bending vibrations and lattice vibrations. The latter may well prove important in characterizing the ice structure (i.e., Are the samples crystalline or amorphous?).

A good example of how infrared spectroscopy has made an important contribution to astrophysics is provided by the analysis of the icy component of interstellar dust in molecular clouds. As recently as fifteen years ago the composition of this dust was largely speculated about, if not ignored. This situation has changed dramatically during the last decade primarily because it is now possible to directly measure the absorption spectra of interstellar ices and interpret these spectra with the aid of laboratory analog studies. Figure 2 illustrates how the direct comparison of laboratory spectra with interstellar spectra can be used to determine interstellar ice composition. Besides probing the composition each absorption band can also provide a quantitative measure of the amount of each material present, give insight into the nature of the ice, (i.e., is it amorphous, crystalline, highly polar, nonpolar etc.), and, in some cases, it can give an indication of the thermal history (Tielens and Allamandola, 1987, Allamandola, Sandford and Valero, 1988; Sandford et al, 1988; Sandford and Allamandola, 1988, Sandford and Allamandola, 1990).

The ices in comets have certainly been processed by photons and energetic particles, producing large, complex species. (Moore et. al, 1983; Lanzerotti, Brown and Johnson, 1984; Johnson, Cooper and Lanzerotti, 1986; Strazulla, Pirronello, and Foti, 1983; Khare et al., 1988; Allamandola, Sandford and Valero, 1988; Schutte,

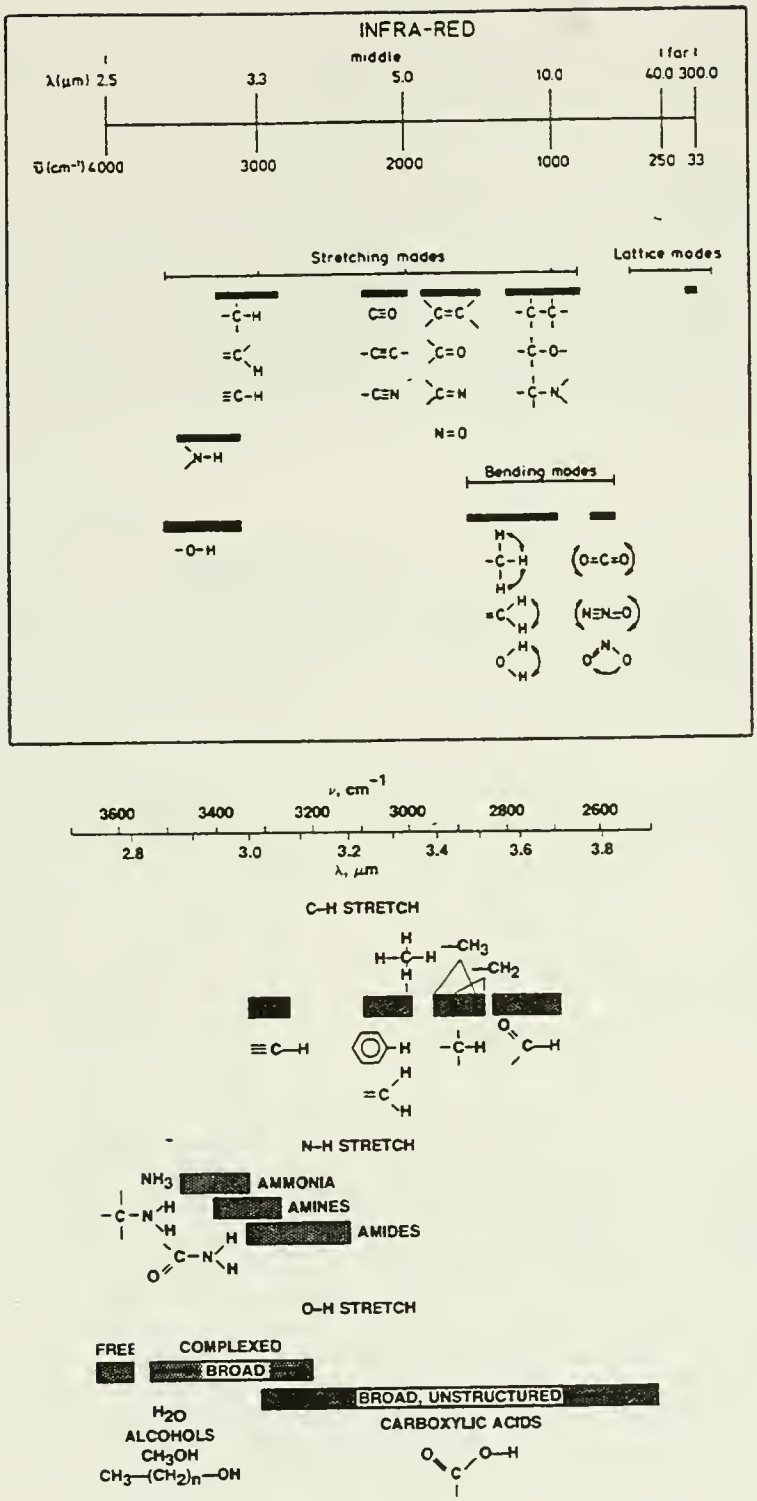


Figure 1. a) The fundamental vibrational frequency ranges for various molecular subgroups made up of the most cosmically abundant elements H, O, C, and N. b) Expansion of the 2600-3600 cm^{-1} X-H stretching range showing the precise regions in which specific types of molecules absorb. This illustrates the power of IR spectroscopy to place strong constraints on the major types of compounds present in any given sample.

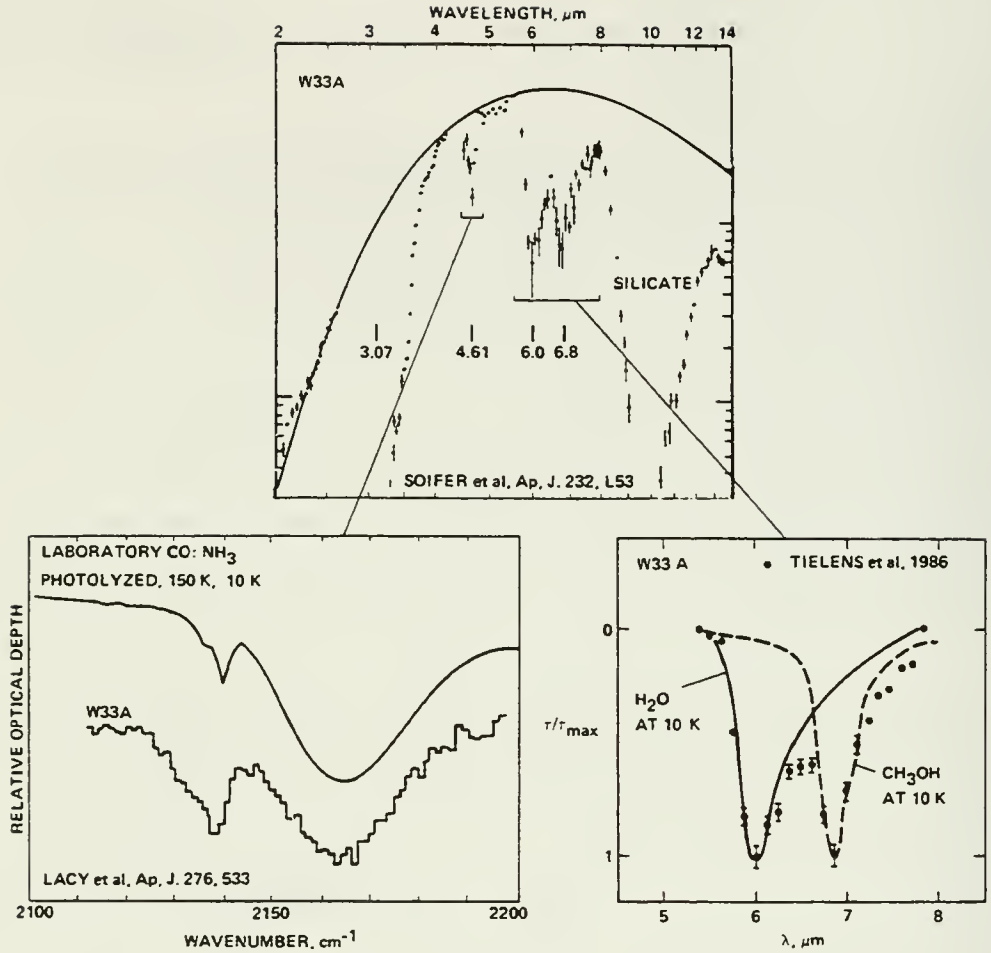


Figure 2. Top: The entire mid-infrared spectrum of an IR source (W-33A) imbedded in a dust cloud. The solid line is the presumed black body emission from the source and the dots are the spectral data measured at earth (Soifer et al., 1979). The absorption bands are due to the intervening dust and reveal its composition. The strong band at 10 microns is due to the SiO stretch in the silicates, and the strong band at 3 microns is due to the OH stretch in H_2O ice. Bottom: More recent, higher resolution observations of the interstellar ice features compared with laboratory simulations which show that CO and a cyano-(CN) containing compound are frozen in the ice (Lacy et al., 1984) and that ices made up principally of H_2O and CH_3OH account for the strong absorptions at about 6 and 7 microns (Tielens and Allamandola, 1987).

1988.) The nature of the complex species produced by these very different processes will probably differ. It is quite possible that the outer few meters is rich in material produced by energetic particle bombardment whereas deeper in, the comet may be rich in material produced in the pre-solar system interstellar cloud. Studies of these various processes which are under way in only a few laboratories must be increased to ensure that when the sample is returned, the correct interpretation can

be made. Figure 3 shows how the mid-infrared spectrum of a laboratory analog of an interstellar ice changes as the ice is UV processed, reflecting its photochemical evolution.

Figure 4 shows the spectral evolution in the CH stretching region as the photolyzed sample is warmed from 200 to 300 K. This serves to illustrate another important point concerning analysis of the returned sample. Various components (organic in the example shown in Figure 4) evaporate nearly continuously as the temperature is raised. Figure 5 shows the behavior of many IR absorption bands as a different irradiated mixture is warmed from 20 to 300°K. These results show that the comet sample must be returned at the lowest temperature possible. It is erroneous to think that above any given temperature all of the volatiles have evaporated leaving only a non-volatile residue.

B) RAMAN SPECTROSCOPY

This also measures the vibrational spectra of material and, as such, is a direct complement to the IR. It is not redundant and provides essential additional information. An example of how the infrared vibrational spectrum of a material may be different from the Raman vibrational spectum and thus yield important, different information is provided by interplanetary dust particles (IDPs). IR radiation passes

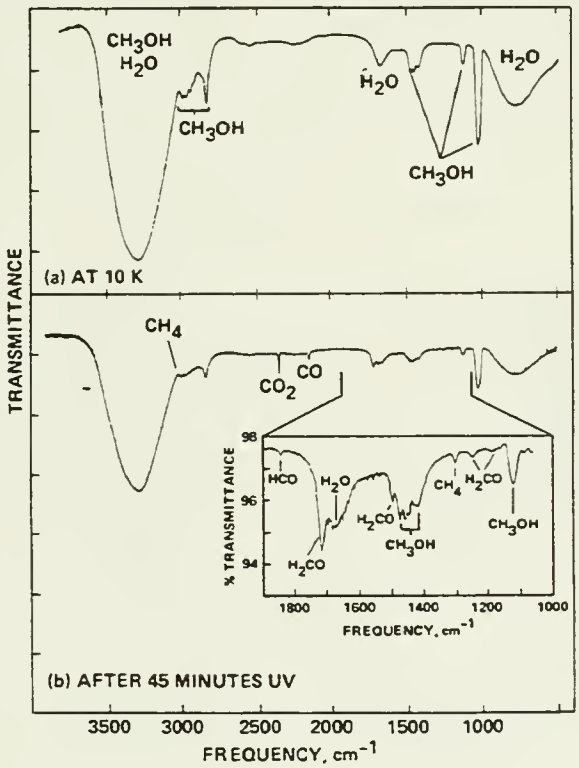


Figure 3. The infrared spectra of an H_2O: CH_3OH (2:1) ice taken at 10 K a) before and b) after 45 minutes of ultraviolet photolysis. H_2O and CH_3OH are the major constituents of many interstellar ices and presumably important precursors to cometary ices. These spectra show that HCO, H_2CO, CO, and CO_2 are important photoproducts in H_2O and CH_3OH ices (Allamandola, Sandford, and Valero, 1988).

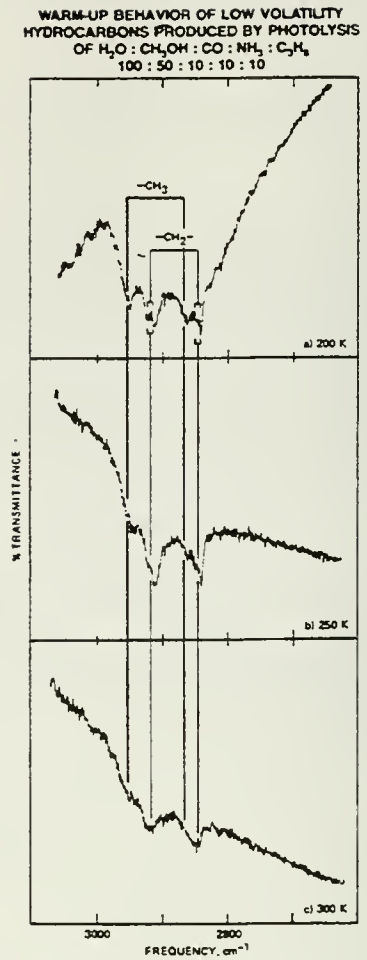


Figure 4. The infrared spectra (taken at 10 K) in the CH stretching region of the low vapor pressure materials produced by 15 hours of photolysis of an $H_2O:CH_3OH:NH_3:CO:C_3H_8$ (100:50:10:10:10) ice after temporary warm up to a) 200 K, b) 250 K, and c) 300 K. The different sublimation behavior of the various aliphatic molecular components shows that a mixture of low vapor pressure, complex, organic materials are produced upon photolysis (Allamandola, Sandford, and Valero, 1988).

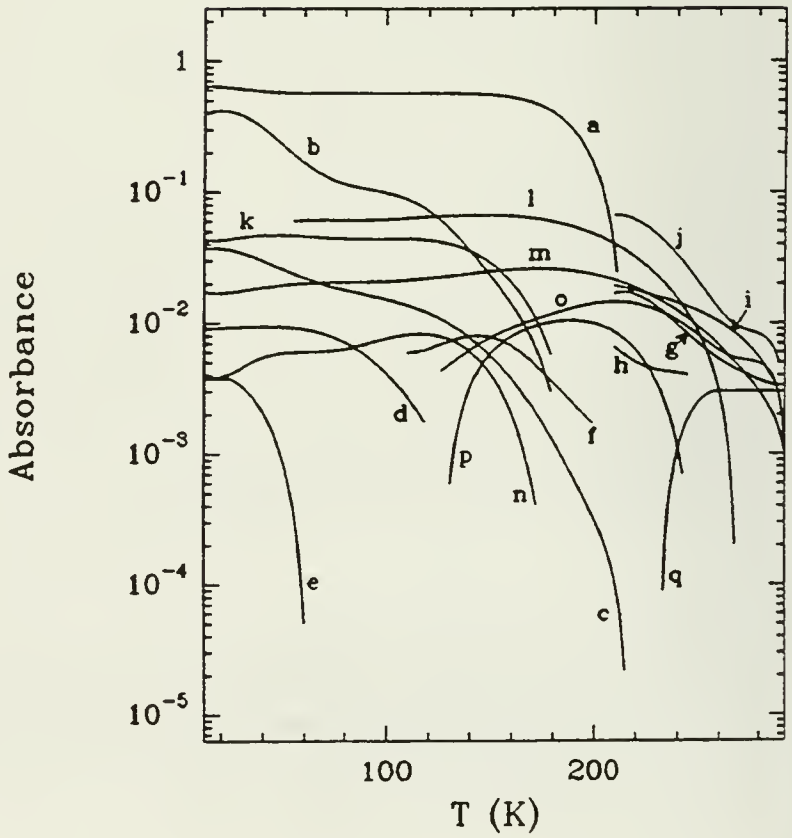


Figure 5. Infrared peak absorbance strengths as a function of temperature during warm-up for a number of infrared features present in an $H_2O:CO:NH_3$ (100:40:20) ice which was prepared by slow deposition with simultaneous photolysis at 10 K for about 20 hours. Note that the sample composition varies at all temperatures from 10 to 300 K, emphasizing how crucial it will be to return the comet nucleus sample at the lowest temperature possible (Schutte, 1988).

through the small particle and probes the bulk. Sandford and Walker (1985) have shown that the IR spectrum of an IDP can be used to characterize the dominant mineral phase. With this information they demonstrated that IDPs fall into three mineral classes, olivenes, pyroxenes and layer-lattice silicates. However, the Raman spectra of the same IDPs are very different, revealing the nature of the minor carbonaceous material present and showing no evidence of the dominant mineral phase (Allamandola, Sandford and Wopenka, 1987; Wopenka, 1988). As Raman spectra are obtained by scattering ultraviolet and visible photons, a minor amount of strongly absorbing carbonaceous material is sufficient to dominate the spectrum. The Raman spectra imply that IDPs contain an amorphous carbon phase which probably coats the minerals. In addition to the vibrational structure, some of these IDPs luminesce in the red, a common characteristic of heavily cross-conjugated carbonaceous materials. Luminescence is discussed further below.

C) ULTRAVIOLET - VISIBLE SPECTROSCOPY (1000-10,000 Å)

While the infrared is well suited to detect many of the major constituents and probe the sample's radiation and thermal history, important minor constituents and abundant species with low IR activity will remain undetected. Ultraviolet-Visible (UV-Vis) spectroscopy provides an important addition to IR spectroscopy. It may be difficult to measure resolved structure in the UV-Vis spectra of a comet nucleus sample, especially in absorption. Several strong absorptions may overlap and produce a broad, structureless band, or one strongly absorbing or luminescing material may dominate in ice poor samples. However, if the returned sample is largely icy, then the chances are high that the spectra will provide critical additional information.

Several examples will now be given which illustrate how UV-Vis spectra complement the IR and Raman spectra.

UV-VIS ABSORPTION SPECTROSCOPY

A potentially important cometary species is HCO, a radical which is readily produced by the energetic processing of ices containing CO and photolabile H atoms. Upon warm-up HCO can diffuse through the ice and react with other HCO molecules and produce $H_2C_2O_2$ (van IJzendoorn et al, 1983, 1986, 1990; d'Hendecourt et al, 1986). H addition to HCO may also produce some H_2CO and eventually perhaps CH_3OH (Tielens and Hagen, 1982). The HCO radical can be stored in water-rich ices, up to surprisingly high temperatures (120 -130 K). In an ice, HCO absorbs strongly across the visible from about 470 to 620 Å and is easily detected in absorption (van IJzendoorn et al., 1983), whereas, as shown in Figure 3, the IR absorption of HCO in a mixed ice is weak (d'Hendecourt et al, 1986; Allamandola, Sandford and Valero, 1988).

Sulfur, although minor in abundance compared to carbon, nitrogen and oxygen, is a very important interstellar element. Sulfur bearing compounds have been suggested in interstellar ices (Geballe et al, 1985) and S_2 has been detected in a cometary coma (A'Hearn, Feldman, and Schleicher, 1983). Sulfur containing compounds often absorb strongly enough in the ultraviolet and visual spectral regions to be detected, even if present in minor amounts, whereas they might go unnoticed if one only had infrared spectra.

Another potentially important reactive cometary species which may escape IR detection, but which absorbs strongly in the visible, is ozone (O_3). The visible absorption spectrum of an ice containing ozone is shown in figure 6.

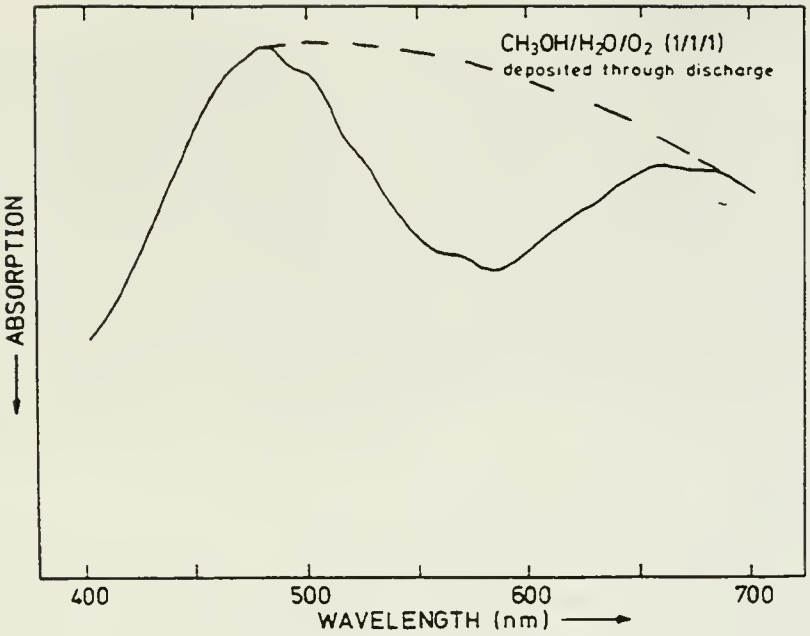


Figure 6. Single beam absorption spectrum of an $H_2O:CH_3OH:O_2$ (1:1:1) ice deposited through a discharge at 12 K. The strong, broad, absorption band under the dashed line is due to O_3 (ozone) (van der Zwet, 1986). In atomic H poor regions of dense molecular clouds O_2 is expected to be an abundant ice constituent. Energetic processing of these ices will readily produce ozone, making it a likely comet constituent as well.

UV-VIS EMISSION SPECTROSCOPY

Photoinduced Luminescence

Detection of emission induced by photon absorption is a much more sensitive technique than either Raman or IR and UV-Vis absorption spectroscopy. Furthermore it is molecule specific and does-not suffer from screening to the same extent that ultraviolet and visible absorption measurements do. By using various sources of monochromatic excitation (as from a tunable laser or dispersed light source) one can scan through the spectrum searching for frequencies which induce luminescence to the red of the excitation frequency. While the frequency which stimulates the emission gives some insight into one transition of the carrier, the emission spectra are often very characteristic of the emitter. For example, van IJzendoorn et al., 1986 gave a complete discussion of the laser induced luminescence spectroscopy of glyoxal ($H_2C_2O_2$) in various low temperature solids and used luminescence techniques to track formaldehyde (H_2CO) as well (Figure 7). Together the excitation/emission spectra can provide an unquestionable assignment.

As with the IR, this method can be used as a probe of thermal history as well. Figure 8 gives the luminescence from S_2 and figure 9 shows how the laser induced fluorescence (LIF) of S_2 in an ice varies as a function of temperature. The intensity increase of S_2 from about 100 K up to 160 K is presumably due to the diffusion of S through the ice and its preference for reacting with another sulfur atom rather than other constituents in the ice. Above 160 K, the sulfur reservoir diminishes and the S_2 apparently reacts with other ice constituents. Note that the S_2 peaks at 160 K and

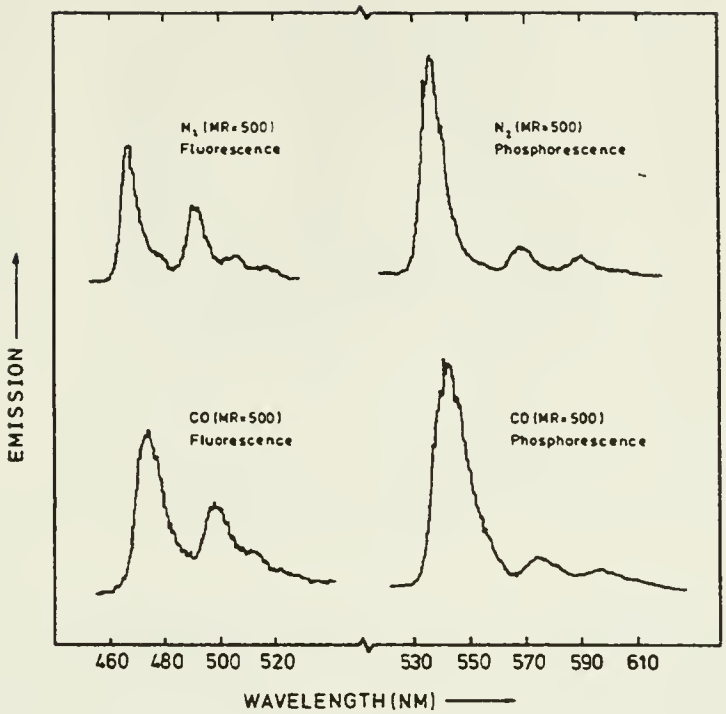


Figure 7. Laser induced fluorescence ($^1A_u \rightarrow {}^1A_g$) and phosphorescence ($^3A_u \rightarrow {}^1A_g$) spectra from glyoxal ($H_2C_2O_2$) in N_2 and CO ices. The excitation wavelength was 440 nm in both ices. The concentration of this species grows when irradiated interstellar ice analogs are warmed (van IJzendoorn et al., 1986; van IJzendoorn et al., 1990).

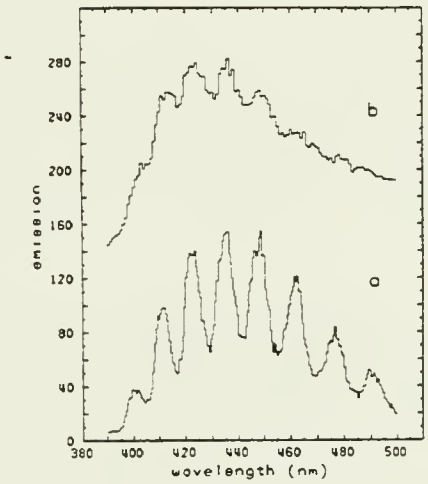


Figure 8. Laser induced fluorescence of the B-X transition of S_2 in a) H_2O:H_2S (10:1) and b) H_2O:CO:CH_4:H_2S(5:2:2:1) ices which had been photolyzed at 10 K (Grim, 1988; Grim and Greenberg, 1987).

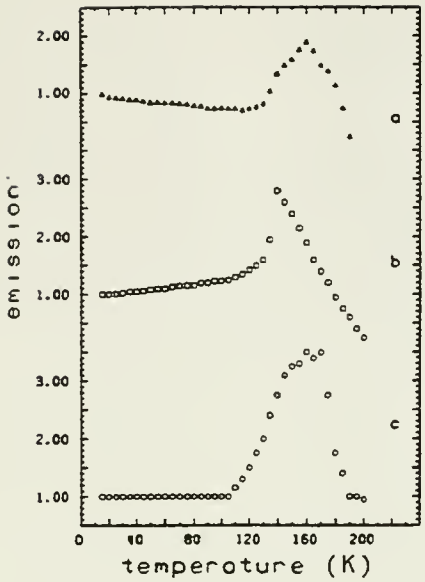


Figure 9. Intensity of the laser induced fluorescence from S_2 as a function of temperature during the warmup of the photolyzed ices: a) H_2O:H_2S(10:1); b) H_2O:CO:H_2S(10:1:1); and c) H_2O:CO:H_2S(10:2:1) showing that S atoms are trapped in these ices up to about 100 K (Grim, 1988; Grim and Greenberg, 1987). Above this temperature S can diffuse and apparently preferentially reacts with other S atoms up to about 160 K. Thus S atoms may well be trapped in the returned comet nucleus sample and luminescence from S_2 might be expected.

is not exhausted until 200 K. Thus, LIF of S_2 can potentially be used as a measure of the thermal history of the sample in the high temperature region while HCO may play this role in the low temperature regime (recall that HCO is probably depleted by 130 K, see adjacent subsections).

Chemically Induced Luminescence

All samples irradiated at 10 K which contain CO and an H atom source glow upon warm-up (Hagen, Allamandola and Greenberg, 1979; Van IJzendoorn, 1985; Van IJzendoorn, et al., 1990). The spectrum of the thermally promoted luminescence is shown in figure 10. This has been ascribed to emission form the transition state in the reaction: HCO + HCO --> $H_2C_2O_2$ (glyoxal).

The temperature range over which this particular luminescence occurs is determined by the major constituent of the ice. If it is rich in non-polar molecules such as CO and CH_4, HCO is not trapped in deep, "high temperature" sites and is depleted by the time the sample has reached 40-50K. If, on the other hand, the ice is rich in polar molecules such as H_2O, the HCO can remain trapped until the ice temperature exceeds about 120-150K (van IJzendoorn, 1985; van IJzendoorn et al., 1990).

This and other trapped radicals which can diffuse and produce luminescence during warm-up may be present in the returned sample. Thus, an attempt to monitor this sort of luminescence during the core drilling phase should be made, perhaps by placing light pipes or even filtered detecters directly in the drill bit itself. Thermally promoted luminescence should certainly be searched for during subsequent sample preparation and warm-up of parts of the returned sample.

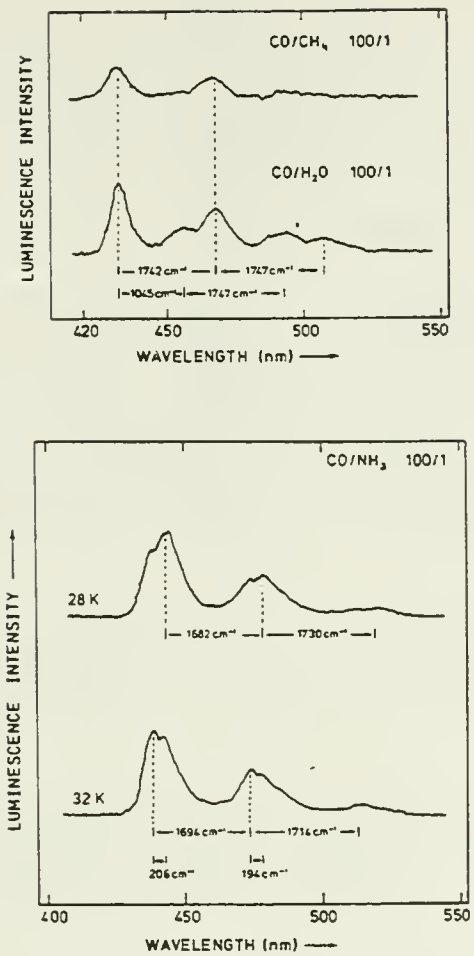


Figure 10. Chemiluminescent spectra emitted during warm up from $CO:CH_4$(100:1); $CO:H_2O$(100:1); and $CO:NH_3$(100:1) ices which had been deposited at 10 K with simultaneous deposition for two hours. In CO rich ices such as these this emission peaks in the 40-50 K range, in H_2O rich ices this emission is intermittent up to about 125 K (van IJzendoorn, 1985; van IJzendoorn et al., 1990).

D) ELECTRON SPIN RESONANCE (ESR)

A much more sensitive technique, and one which is particularly well suited to the detection of all trapped radicals because it is sensitive to all unpaired electrons, is ESR. This is especially important since, if radicals are present, some will most likely be in low concentration and probably escape detection by most of the other techniques, except perhaps luminescence. Even if luminescence from some radicals is detected, complete radical characterization of the sample will almost certainly be impossible without ESR. Tsay and coworkers have successfully applied ESR techniques to many difficult samples for several years. At this meeting they have shown the ESR spectrum of many interesting intermediates trapped in ices, many of which are reasonable to expect in cometary ices. Many of the radicals they have studied have similar chemical structures and consequently very similar UV-Vis and IR spectra. Tsay and colleagues have shown, however, that even in ices the ESR spectra of chemically similar radicals differ substantially and one can identify the individual species.

Furthermore they have shown that the ESR technique is sensitive enough to probe the radical concentration decay during warm-up to rather high temperatures. For example they have probed the HCO decay in an ice up to 150K and the CH_3CHO radical in a different ice up to 250K. Thus this technique can also be used to probe the thermal history of the sample from the low to the high temperature regimes and extends the upper temperature limit well above that discussed in the previous sections.

E) NUCLEAR MAGNETIC RESONANCE (NMR)

To the best of my knowledge, this technique has not yet been applied to mixed molecular ices but certainly should be. It can be used to probe specific nuclei such as H or ^{13}C in the sample. All of the nuclei are detectable. The "chemical shift" displayed is a measure of the local environment of the nuclei. For example, an H attached to an aliphatic carbon has a different chemical shift (i.e., resonates at a different frequency) from an H attached to an aromatic carbon or to a carbonyl carbon. In most cases, even within these chemical classes, smaller shifts are detectable which specify how much of the sample is in one subset of molecule comprising a particular class and how many are in another subset.

As all nuclei are sampled, the NMR spectrum gives a rather accurate measure of the relative amounts of all of the different kinds of molecules present, and relative amounts of each subset therein. Thus classes of molecules present to the level of a few percent which may go unnoticed with the other techniques will not escape detection.

Modern solid state NMR techniques have made a large impact on our understanding of coal, an extremely complex material (Miknis, 1988; Stock, Muntean and Botto, 1988). The analytic challenges presented by the comet sample will be similar to those encountered in coal research. A recent, elegant NMR experiment has been carried out by Cronin, Pizzarello and Frye, 1987 on the carbonaceous component of several meteorites, another very difficult material to analyze. These spectra showed, for the first time, the relative amounts of aromatic and aliphatic carbon in these materials. This information had not been possible to obtain by any of the other techniques described above, yet all have been applied extensively to meteorites.

III. CONCLUSION

The spectroscopic analysis of pristine cometary material promises to provide a very important, often non-invasive, probe of the chemical identity of the material present as well as of the physical and chemical conditions which prevailed during the comet's history. Concerning classical spectroscopy, the spectral regions which will most likely prove most useful are the infrared, the visible and ultraviolet. "Newer" spectroscopic techniques which have the potential to provide equally important information include nuclear magnetic resonance (NMR) and electron spin resonance (ESR).

The infrared should be the premier method of analysis as the mid-infrared absorption spectrum of a substance contains more global information about that substance's identity and structure than any other property. However, the interpretation of the infrared spectrum of the mixtures expected in a comet can be (not always) ambiguous. Other nondestructive, complementary spectroscopic measurements are required to characterize the material and probe for substances for which the infrared is not particularly well suited. While the mid- and far-IR span frequencies which correspond to skeletal vibrations in molecules and thus provide insight into the identity of chemical groups present, the ultraviolet, visible and

near-infrared span frequencies which correspond to electronic transitions and give insight into the molecular bonding structures present. In these regions absorption and emission studies are desirable. Absorption measurements have the potential to give an indication of the importance of conjugated bond systems, although sample porosity will almost certainly make the measurements difficult. More tractable will be luminescence studies. Measuring the luminescence spectrum excited by ultraviolet and visible photons should be straightforward. The emission spectrum, as well as the wavelength dependence of the exciting light (the excitation spectrum), give important insight into the nature of emitting materials. In addition to UV-Vis induced luminescence, thermally promoted chemiluminescence should also be searched for. Irradiation of solid materials often produces trapped ions, electrons, and radicals which can diffuse through the medium if it is warmed. Reactions involving these diffusing species often emit a spectrum which is characteristic of the reacting species. The temperature domain over which light is emitted depends on the nature of the solid. Volatile rich ices luminesce in the 10-40 K range, H_2O rich ices in the 10-150 K range and higher melting point materials luminesce at much higher temperatures. Thus the monitoring of potential luminescence during core drilling and during subsequent sample warm-up is important to consider seriously as it can provide unique information on the thermal and radiation history of the sample which cannot be obtained in any other way.

Three additional spectroscopic probes have also been briefly summarized: Raman, NMR and ESR. Raman spectroscopy is complementary to IR spectroscopy in that it measures the vibrational frequencies of the material. It is not redundant. ESR studies can directly determine the total radical content of the ice. ESR is one of the most sensitive techniques available, and the concentrations of many radicals can be probed. NMR spectra should also be measured as these reveal the fractions of various classes of all of the organic compounds present. The full potential of these last three techniques can be realized on the returned comet sample only if laboratory programs are started to learn how to apply them to realistic mixed ices. Of the three, only the ESR technique has been applied to molecular ices.

Given the likelihood that the icy component (including some of the organic and mineral phases) of the returned sample will be exceedingly complex, these techniques must be intensely developed over the next decade and then made ready to apply flawlessly to what will certainly be one of the most precious, and most challenging, samples ever analyzed.

Table 1. Summary of Spectroscopic Techniques to Apply to the Returned Comet Nucleus Sample

TECHNIQUE		SAMPLE REQUIREMENT	SENSITIVITY	TRANSITION
IR				
	Absorption	Thin Section ($\leq$ 0.5 μm)	Low	Molecular Vibrations
	Reflection	None	Low	Molecular Vibrations
UV-VIS-NIR				
	Absorption	Thin Section (0.1-0.01μm)	High	Electronic
	Emission, Laser Induced	None	Very high	Electronic
	Emission, Chemically Induced	Sample warm-up	Probably high	Electronic
RAMAN		None	Low to Moderate	Molecular Vibrations
ESR		Thin Cylinder Submicron	Extremly high	Unpaired electron spin-flip
NMR		Thin Cylinder millimeter diameter	Very low	Nucleus spin-flip

- A'Hearn, M.F. Feldman, P.D., and Schleicher, D.G., 1983, Ap. J. Letters, 274, L99
- Allamandola, L.J., Sandford, S.A., and Valero, G.J., 1988, Icarus 76, 225
- Allamandola, L.J., Sandford, S.A., and Wopenka, B., 1987, Science 237, 56
- Cronin, J.R., Pizzarello, S., and Frye, J.S., 1987, Geochim. Cosmochim. Acta, 51, 299
- d'Hendecourt, L.B., Allamandola, L.J., Grim, R.J.A., and Greenberg, J.M., 1986, Astron. Astrophys. 158, 119
- Geballe, T.R., Baas, F., Greenberg, J.M., and Schutte, W., 1985, Astron. Astrophys. 146, L6
- Grim, R.J.A., and Greenberg, J.M., 1987, Astron. Astrophys. 181, 153
- Grim, R.J.A., 1988, Ph.D. Dissertation, Leiden University, The Netherlands
- Hagen, W., Allamandola, L.J., and Greenberg, J.M., 1979, Astrophys. Sp. Sci. 65, 215
- Johnson, R.E., Cooper, J.F., Lanzerotti, L.J., 1986, in Proc. 20th ESLAB Symp. on Exploration of Halley's Comet, ESA SP-250, Vol. II, 269
- Khare, B.N., Thompson, W.R., Murray, B.G., Chyba, C., and Sagan, C., 1988, Icarus, in press
- Lacy, J.H., Baas, F., Allamandola, L.J., Persson, S.E., McGregor, P.J., Lonsdale, C.J., Geballe, T.R., and van de Bult, C.E.P., 1984, Ap. J. 276, 533
- Lanzerotti, L.J., Brown, W.L., and Johnson, R.E., 1984, in Ices in the Solar System, eds Klinger, J. et al. (Reidel, Dordrecht) 317
- Miknis, F.P., 1988, in New Trends in Coal Science, ed. Yurum, Y., (Kluwer, Dordrecht), 117
- Moore, M.H., Donn, B., Khanna, R., and A'Hearn, M.F., 1983, Icarus 54, 388
- Nash, D.B., and Howell, R.R., 1988, Science 244, 454
- Nash, D.B., and Nelson, R.M., 1979, Nature 280, 763
- Sandford, S.A., and Walker, R.M., 1985, Ap. J. 291, 838
- Sandford, S.A., and Allamandola, L.J., 1988, Icarus 76, 201
- Sandford, S.A., Allamandola, L.J., Tielens, A.G.G.M., and Valero, G.J., 1988, Ap. J. 329, 498
- Sandford, S.A., and Allamandola, L.J., 1990, Ap. J., in press
- Strazulla, G., Pironello, V., and Foti, G., 1983, Astron. Astrophys. 123, 93
- Schutte, W., 1988, Ph.D. Dissertation, Leiden University, The Netherlands

- Soifer, B.T., Puetter, R.C., Russell, R.W., Willner, S.P., Harvey, P.M., and Gillett, F.C., 1979, Ap. J. (Letters), 232, L53

- Stock, L.M., Muntean, J.V., and Botto, R.E., 1988 in New Trends in Coal Science, ed. Yurum, Y. (Kluwer, Dordrecht), 159

- Tielens, A.G.G.M., and Allamandola, L.J., 1987, in Physical Processes in Interstellar Clouds, eds. Morfill, G.E. and Scholer, M. (NATO ASI Series C210, Reidel, Dordrecht), 333

- Tielens, A.G.G.M. and Hagen, W., 1982, Astron. Astrophys, 114, 245

- van IJzendoorn, L.J., Allamandola, L.J., Baas, F., Kornig, S., and Greenberg, J.M., 1986, J. Chem. Phys. 85, 1812

- van IJzendoorn, L.J., Allamandola, L.J., Baas, F., and Greenberg, J.M., 1983, J. Chem. Phys. 78, 7019

- van IJzendoorn, L.J., 1985, Ph.D. Dissertation, Leiden University, The Netherlands

- van IJzendoorn, L.J., Allamandola, L.J., de Groot, M.S., Baas, F., van de Bult, C.E.P.M., and Greenberg, J.M., 1990, J. Phys. Chem., submitted

- van der Zwet, G.P., 1986, Ph.D. Dissertation, Leiden University, The Netherlands

- Wopenka, B., 1988, Earth and Planet. Sci. Lett. 88, 221

LABORATORY ANALYSES OF MICRON-SIZED SOLID GRAINS: EXPERIMENTAL TECHNIQUES AND RECENT RESULTS

L. Colangeli
University of Cassino
Italy

E. Bussoletti
Istituto Universitario Navale
Naples, Italy

Osservatorio Astronomico Capodimonte
Naples, Italy

LABORATORY ANALYSES OF MICRON-SIZED SOLID GRAINS: EXPERIMENTAL TECHNIQUES AND RECENT RESULTS (*)

L. Colangeli ([1]) and E. Bussoletti ([2,3])
([1]) University of Cassino, Italy;
([2]) Istituto Universitario Navale, Naples (Italy);
([3]) Osservatorio Astronomico Capodimonte, Naples (Italy)

1. INTRODUCTION

The investigation of comets has proceded for long time on remote observations from ground. In 1986 several space missions towards comet Halley have allowed, for the first time, to have a close look to a comet (Encounters with comet Halley 1986). In particular, the GIOTTO mission by the European Space Agency (ESA) has provided "in situ" observations and measurements up to a distance of about 600 Km from the nucleus. Surface morphology and physical properties have been observed; plasma, gas and dust components in the coma have been analyzed (Grewing et al. 1987). It is clear, however, that definite answers about the primordial nature of comets and their relation with interstellar material can be obtained only from direct analysis of cometary samples. Future space missions such as CRAF (NASA) and ROSETTA (ESA) have exactly this aim. In particular, the ambitious goal of Rosetta mission is to return to earth comet samples which can be analyzed carefully in laboratory.

In preparation to this event a large effort must be placed both in the improvement of existing analytical techniques and in the development of new methods which will provide as much information as possible on "returned comet samples" (hereinafter RCSs). Handling of extra-terrestrial samples will require to operate in carefully controlled and extremely "inert" ambient conditions. In addition, working on a limited amount of "unique" cometary material will also impose to use analytical techniques which should not produce alteration, contamination or destruction of the sample. Many suggestions can come from people working in laboratory on "cosmic dust"; in fact, experimental methods which are applied to analyze a) interplanetary dust particles (IDPs) collected in stratosphere, b) meteorites, and c) laboratory produced cosmic dust analog samples, can be mutuated or properly improved in the future for specific application to RCSs.

Since modern techniques used to analyze IDPs and meteorites are reviewed elsewhere in this workshop (see for instance the contributions from J. Bradley and A. Albee), we will discuss some of the most powerful techniques which are presently applied to characterize physical and chemical properties of micron and/or submicron solid grains, synthetized in laboratory with the aim of simulating cosmic dust.

2. MATERIALS

We will focus here attention mainly on carbonaceous materials, because it is commonly accepted that: a) about half of interstellar dust is in various forms of carbonaceous compounds; b) about 70 % of "small" grains detected around P/Halley's

(*) Work performed under contracts MPI 120111 (40 %) and 120257 (60 %), CNR 8800361-02, PSN 88-020, and ASI 88-060.

nucleus were carbonaceous (Jessberger et al. 1988); c) IDPs contain significant fractions of carbon. According to the results of the "working group on carbon" (Huffman 1988a) presented at the international workshop on "Experiments on cosmic dust analogues" held in Capri (Bussoletti et al. 1988), we have to bear in mind that "carbon is an extremely complicated and variable material" and in nature - as well as in space and in laboratory experiments - it can occur in various forms as, for example: disordered graphitic carbon, diamond-like carbon, cyclic and acyclic molecules, polycyclic aromatic hydrocarbons (PAHs).

Actually, a simplified way to classify different kinds of carbon is to consider two main parameters: a) the internal ordered-domain length, b) the size. The first parameter determines the largest domain length of the lattice over which order is mantained; in this scale, graphite (sp^2 hybridization) and diamond (sp^3 hybridization) represent one of the limits since they are perfectly crystalline materials and the length over which the lattice structure repeats itself is virtually infinite. On the other side of the scale, amorphous carbon represents a material with a complete internal disorder so that no regular lattice structure can be identified and the ordered domain size is virtually zero. Of course, we expect that any material formed in nature, as well as in space and in laboratory conditions, never reaches one of these two extreme configurations, except under very peculiar formation conditions (Marchand 1987). Therefore, in general, we deal with polycrystalline materials, soots and/or more or less "disordered" lattice structures. This means that the term "amorphous carbon", commonly used to identify laboratory produced carbon grains, must be rather interpreted as "internally very disordered carbon". The other parameter we have considered is just the dimension of the grains or molecules. For very small sizes ($\leq$ few Å) we fall in the field of molecules as, for example, PAHs. As soon as the size increases, we talk of submicron or micron grains but, in some cases, agglomeration of grains may produce larger "clumps". The progression from molecules to grains has assumed today a particular meaning since PAH molecules in space are probably formed by the destruction of carbonaceous grains and/or are the leftover nuclei of condensation processes to form carbon grains, for example around carbon rich stars (Allamandola et al. 1985).

The techniques most frequently used to produce "amorphous carbon" submicron and/or micron grains in laboratory are summarized in table I. In the following we will critically discuss various experimental methods used to perform physico-chemical investigation of grain samples and we will present recent results obtained on various kinds of candidate materials for cosmic dust.

3. MORPHOLOGICAL AND STRUCTURAL ANALYSIS

Dealing with powdered samples, the only way to get clear information about morphology of single micron/submicron grains is to use electron microscopy technique. Transmission electron microscopy (T.E.M.) allows to determine the size and shape of single grains, when used at high magnification (about 400,000 X), and size distribution of the samples by measuring the size of a large number (> 1000) of single particles on photographs recorded at medium magnification (about 50,000 X). Scanning electron microscopy (S.E.M.), on the contrary, is a powerful tool to determine surface properties of samples. However, we have to recall that SEM utilizes the electron beam reflected by the sample so that the intensity of the recorded signal is proportional to the atomic number, Z, of the examined material. This means that it is rather difficult to get surface details of submicron carbon grains (Z=6), while SEM is efficient for silicate particles (Z=12), and - in any case - for large particles rather than very small ones. Furthermore, TEM often requires the deposition

TABLE I. - LABORATORY TECHNIQUES USED TO PRODUCE "AMORPHOUS CARBON" GRAINS

LASER BOMBARDMENT	ARC DISCHARGE	HYDROCARBON BURNING	HYDROCARBON PLASMA DEPOSITION
LS	AC	BE/XY	QCC
Focusing of high power pulsed-laser beams on a target of bulk pure material in Ar atmosphere	Striking an arc between two amorph. carbon or graphite electrodes in Ar atmosphere	Benzene/xylene burning in Air	Quenching of an hydrocarbon plasmic gas in vacuum
Stephens 1980	Koike et al. 1980; Bussoletti et al. 1987	Day and Huffman 1973; Bussoletti et al. 1987	Sakata et al. 1983

of the sample onto special micro-grids covered with holey-carbon films. This method is clearly non destructive, but it appears rather complicate to retrive the sample after TEM analysis since the substrate-film must be removed by using fluids which may contaminate the sample. On the other hand, TEM can be performed also on thin sections (500 - 1000 Å) of grains. In this case a single grain is embedded in epoxy material and cutted by a diamond knife into submicron slices. Although destructive, this method allows to perform a 3-dimensional analysis of the physical grain structure by studying various slices of the same grain (Bradley and Brownlee 1986). In the case of SEM, the sample can be simply mounted onto a metallic substrate allowing for an easier retrival of the non-destructed sample. Both TEM and SEM investigations are performed in high vacuum conditions and the sample holder can be adapted to a cold-finger. This ensures "clean" working conditions and sample thermal control, which appear very appropriate for RCSs. On the other hand, the electron beam working conditions must be carefully selected in order to avoid the release of high energy onto the sample: structure alterations are possible for organic and polymeric substances.

In figures 1 to 3 some examples of TEM images obtained on various samples produced in laboratory are reported. In figure 1 chain-like and fluffy structures of AC amorphous carbon grains formed during condensation are evident. At high magnification the properties of single AC grains are evidenced and typical spheroidal shape appears (fig. 2). In the case of industrially produced silicon carbide (α-SiC) the grains appear mainly irregular (fig. 3). Examples of size distributions for AC and SiC grains are shown respectively in figures 4 and 5. They are obtained by measuring the maximum elongation of more than 1000 grains on various TEM photographs for each sample.

Electron microscopy allows also to investigate the internal structure of the material, when used in diffraction mode. Typical diffraction patterns of our α-SiC show the presence of isolated spots, suggesting a regular lattice structure, though their disordered arrangement in the pattern indicates that grains are mainly polycrystalline. The diffraction pattern for AC samples does not present any spot but only slightly contrasted concentric dark and light rings, according to a "nearly

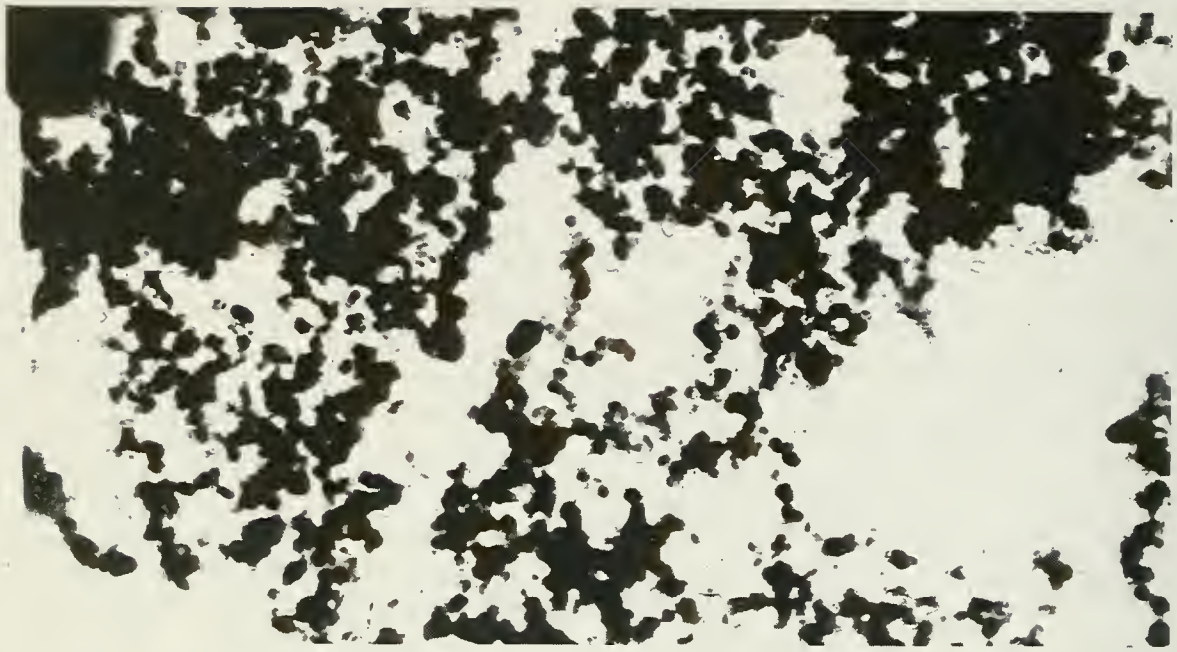


Figure 1.- TEM photograph of AC amorphous carbon sample. Chain-like and fluffy structures are evident.



Figure 2.- High magnification TEM image of a typical AC grain (maximum elongation ≈ 200 Å).



Figure 3.- TEM micrograph of an α-SiC sample; the irregular shape of the grains is evident.

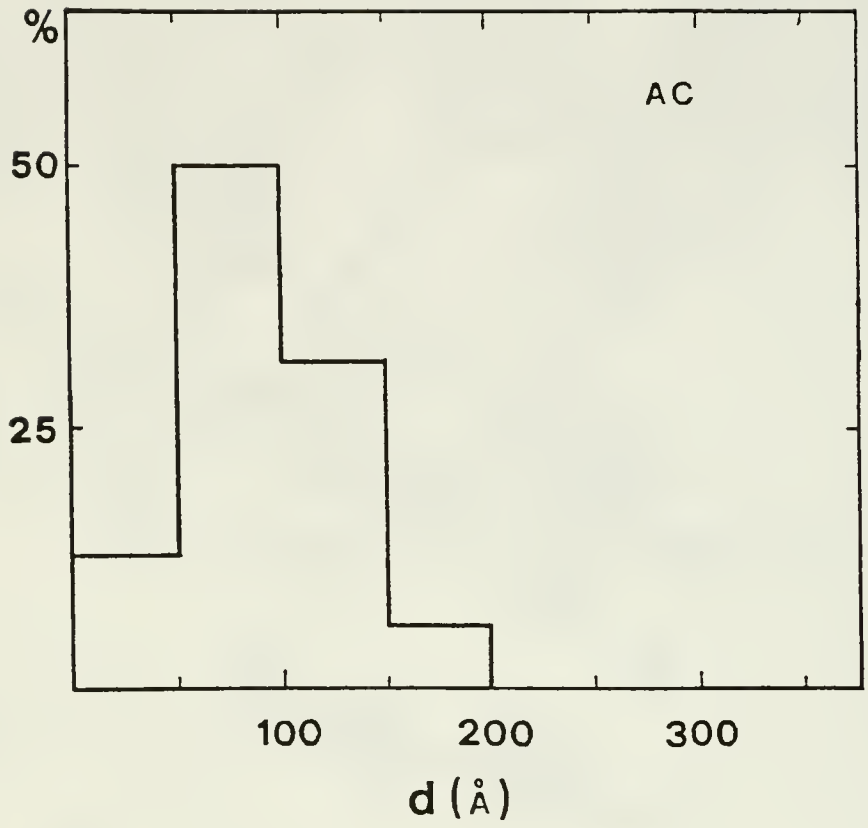


Figure 4.- Grain size distribution of AC sample obtained by measuring the maximum elongation of more than 1000 particles on TEM photographs.

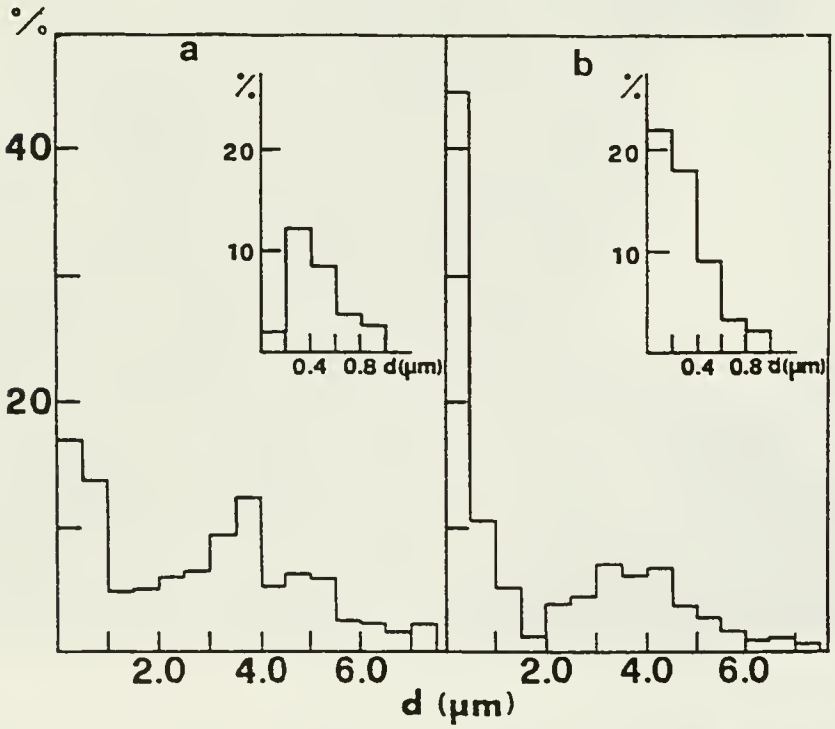


Figure 5.- Grain size distribution of SiC grains; a) raw material; b) 6 h ground grains.

amorphous" structure. We remind here that X-ray diffraction technique is an alternative method to get information similar to that obtained by electron diffraction.

4. RAMAN SPECTROSCOPY

This spectroscopic technique is generally considered complementary to IR transmission spectroscopy (see section 5), since different vibration modes may be active in the two cases. This is generally true for highly simmetric molecules characterized by an inversion centre of simmetry, meanwhile Raman and IR spectra can be very similar in the case of "disordered" non-symmetric materials. However, Raman spectroscopy is important not only to characterize optical properties but also in the clarification of internal structure of the materials. In particular, carbonaceous materials usually show two main first-order Raman scattering features at about 1600 and 1350 cm^{-1} (Tuinstra and Koenig 1970; Rosen and Novakov 1978). The first band is assigned to E_{2g} mode in single graphite crystallites (Tuinstra and Koenig 1970), while the attribution of the second feature is more controversial. In fact, this signature can be interpreted as a resonance in diamond-arranged C atoms (Tuinstra and Koenig 1970) or in rhombohedral graphitic polytype (Wieting and Verble 1979), but the possibility exists that it is associated with A_{1g} mode in disordered graphite lattice (Tuinstra and Koenig 1970; Robertson 1986). Actually, the exact position of the 1600 cm^{-1} peak seems to depend on the size of crystallites: the smaller the crystal size the larger the wavenumber. At the same time, the intensity ratio, I(1355 cm^{-1})/I(1600 cm^{-1}) increases as : i) the amount of "unorganized" carbon in the sample increases, ii) the graphite crystal size in the material decreases (Tuinstra and Koenig 1970).

Recently, Allamandola et al. (1987) have obtained Raman spectra of various IDPs, all showing the two mentioned features. Their position and relative intensity suggest that the carbonaceous component of IDPs is arranged in aromatic sub-units with ordered domains no larger that 25 Å, bridged by short aliphatic bonds. Furthermore, it has been evidenced that the IR emission spectrum of the Orion Bar nicely resembles the Raman spectrum of the examined IDPs (Allamandola et al. 1987) and that of "auto-exhaust" solid grains (Allamandola et al. 1985).

Blanco et al. (1988a, 1989) have recently performed a systematic Raman analysis of various "carbonaceous materials" produced in laboratory. In the experimental set-up an Ar^{+} laser tuned at 5145 Å has been used as a source and the power incident on the sample is about 200 mW. In figure 6 examples of Raman spectra on amorphous carbon grains show the two main features at 1355 and 1600 cm^{-1}, suggesting a structural similarity with IDPs and interstellar dust grains. In the experiments, various sample configurations have been tested. In particular, both deposition of dust on glass substrate and embedding in KBr matrix allow to obtain good signal to noise ratios in the spectra. Both these techniques seem suitable for RCS analysis. However, the deposition on clean glass substrates guaranties uncontamined preservation of the sample and prevents from risks of mechanical stresses, which are possibly produced during embedding processes in matrixes.

One relevant problem with Raman spectroscopy is the high thermal stress produced by the laser beam impinging on the sample. This effect can be partially reduced by mounting the sample on special holders which rotate during laser illumination. However, this solution presents the disadvantage that the monitored spectrum gives an information averaged over the area spanned during the laser scanning; this drawback can be critical for a non homogeneous material, as actually it is expected for RCSs.

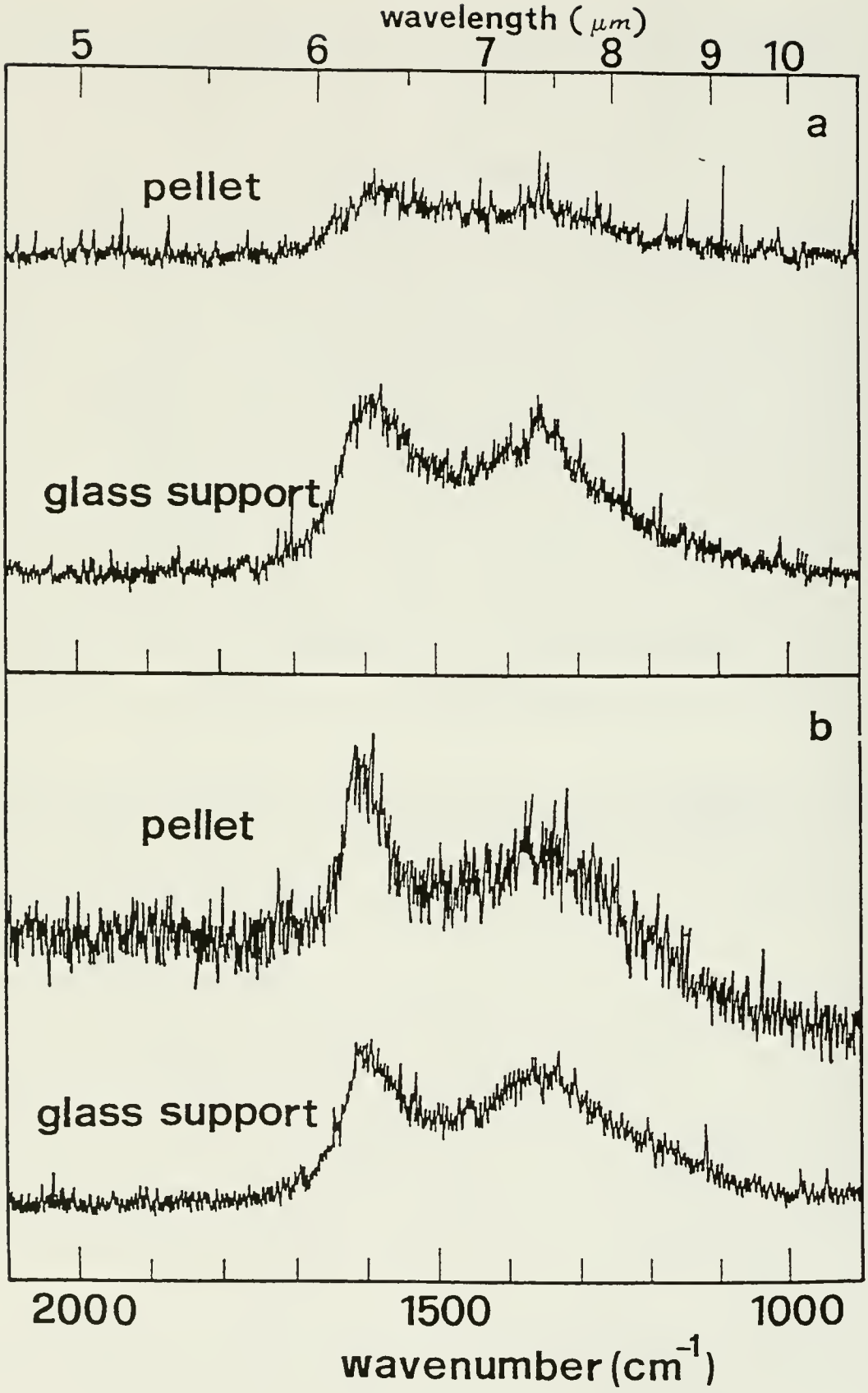


Figure 6.- Raman spectra of AC (a) and BE (b) samples embedded in KBr pellets and deposed on glass substrates.

5. OPTICAL PROPERTIES

Absorption, scattering and emission spectroscopy extended over the widest wavelength range from vacuum ultraviolet (VUV) to far infrared (FIR) is extensively used in laboratory to identify the optical properties of materials candidate to be present in space. Especially VUV and near IR portions of the spectrum appear particularly useful to diagnostics, because they contain "fingerprints" of specific chemical compounds. Their detection in laboratory and in astronomical spectra can be helpful in the classification of cosmic materials. However, when one deals with "dusty" samples in laboratory a certain number of practical problems arise; here we will mention some of the most crytical and still difficult to solve in present days.

5.1 Clustering effects

Most of the dust samples produced in laboratory occur in clumped agglomerates (see section 3). This effect may strongly affect optical measurements, especially at wavelengths where "surface modes" are active (Bohren and Huffman 1983). Therefore, the deduction of optical properties for submicron/micron grains from extinction data is not always straightforward. From a theoretical point of view, Huffman (1988b) has shown that in many cases clustering can be properly treated by considering a "shape distribution" of randomly oriented ellipsoids in the Rayleigh limit. However, clustering is expected to become significant only at wavelengths where the optical constants (n,k) of the material are sufficiently high. According to Hanner (1988), for glassy carbon this is true at $\lambda > 100$ μm. The importance of studying isolated solid grains is furtherly confirmed by the agreement existing between optical constants measured from glassy carbon films (Edoh 1983) and from single levitating grains (Pluchino et al. 1980).

5.2 Size effects

The optical properties of submicron-micron particles are also sensitive to the actual dimension of the grains. Again, this effect is more significant at wavelengths where "surface modes" are active (Bohren and Huffman 1983). A typical example is given by the behaviour of the 11.5 μm band, characteristic of SiC grains. The absorption spectra recorded for α-SiC grains after differentiated grinding, washing in ultrasonic chamber and sedimantation in acetone are compared in figure 7. The profile of the band changes according to the average size of the grains as it is also evidenced from the data collected in table II. We note that, as the size reduces, the main peak becomes sharper and more intense, while the actual peak position shifts towards shorter wavelengths. These results fit rather well with the theoretical predictions on surface resonances, confirming that optical properties of dust samples must be correlated with their morphology (Borghesi et al. 1985).

5.3 Homogeneity of data

A mandatory requirement in laboratory analysis of cosmic dust analogues is to produce homogeneous spectroscopic data of the same sample, under controlled ambient conditions and all over the widest spectroscopic wavelength range from VUV to FIR. In the case of RCSs, this requirement must be also coupled with a particular care in minimizing handling and treatment processes which may lead to a possible deterioration of the material.

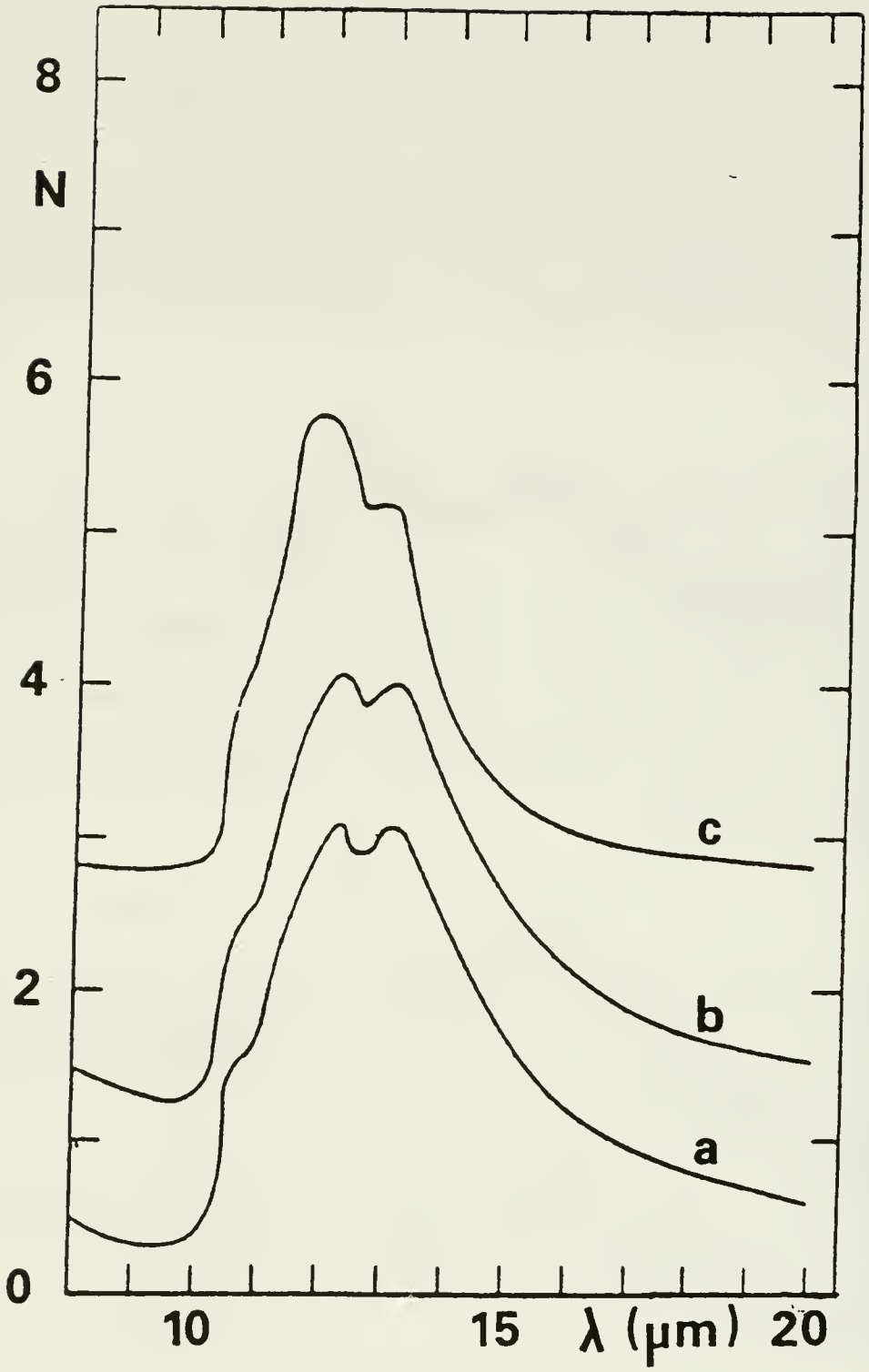


Figure 7.- Normalized extinction for α-SiC grains. The curves refer respectively to raw material (a), 6 h ground sample (b), and 6 h ground + 30 min US washed + 2 h sedimented grains (c).

TABLE II.- SPECTROSCOPIC PROPERTIES OF α-SiC GRAINS
[From Borghesi et al. 1985]

Material	<d> (μm)	LM	MP (μm)	TM	Γ_1	Γ_2	HW (μm)
α-SiC	2.3	10.7	12.2	13.2	4.8	1.0	5.5
α-SiC-G	1.9	10.7	12.0	13.0	5.2	1.2	4.1
α-SiC-GWS	0.1	10.7	11.9	12.8	8.2	1.3	2.7

G: 6h ground; GWS: 6h ground + 30 min US washed + 2h sedimented in acetone; LM: longitudinal lattice vibration mode; TM: transverse lattice vibration mode; MP : main peak; Γ_1 = I(MP) / I(continuum); Γ_2 = I(MP) / I(LM); HW: half-height band width.

In the laboratory work performed at Lecce and Naples, the full range from 1000 Å to 1 mm is covered, by using various experimental techniques and instrumentations as it is summarized in table III. In figure 8 the complete spectra of various forms of amorphous carbon grains are reported. A well pronounced peak is evident at 235 - 250 nm in all spectra. The peak for smaller AC grains (size = 80 Å) falls at shorter wavelength and appears sharper than that observed for larger BE/XY particles (size = 300 Å). In both cases the hump is attributed to a plasmon mode of surface electrons in the ground state. This is also confirmed by the absence of any absorption feature beyond 300 nm, where the extinction curves fall as $\lambda^{-\alpha}$, with $\alpha \approx 1$. Only in the 2 - 13 μm range some weak features are detected. Most of them are interpreted as due to both C=C skeletal vibrations and CH_n (n=1,2,3) radicals bound to active sites onto the grain surface. For more details about these features we refer to Borghesi et al. (1987) and Blanco et al. (1988b).

At this point we have to stress that our spectroscopic results have been obtained by using "classical" experimental techniques, which are based either on the embedding in trasparent matrix or on the deposition onto window-substrates of the material (see table III). These methods have the limitation of leaving unsolved the mentioned problem of clumping and sometimes may imply risks of contamination or alteration, especially in the view of application to RCSs.

6. NEW GENERATION OF TECHNOLOGIES

In the recent years new experimental techniques have been tested which could be succesfully applied also to RCSs, partially solving the problems found by using "classical" methods (see section 5.3). A substancial improvement could come from the suspension of "individual" isolated grains for optical analyses. Among other methods, we recall: a) laser levitation (Ashkin 1970, Ashkin and Dziedzic 1980) b) quadrupole trapping (Philip et al. 1983), c) electrostatic levitation (Marx and Mulholland 1983, Weiss-Wrana 1983, Giese et al. 1986).

An example of optical measurements performed on levitating particles is reported by Pluchino et al. (1980). In this case a carbon particle with diameter of about 1 μm is electrostatically suspended and its position monitored by detecting the scattered light from an Ar^+ laser. The signal drives a servo-system that keeps the particle levitating always in the same position. This allows scattering measurements from 10° to 170° by moving the detector around the suspension chamber. Recently, Stephens (1988) has performed extinction and scattering measurements on carbon grains

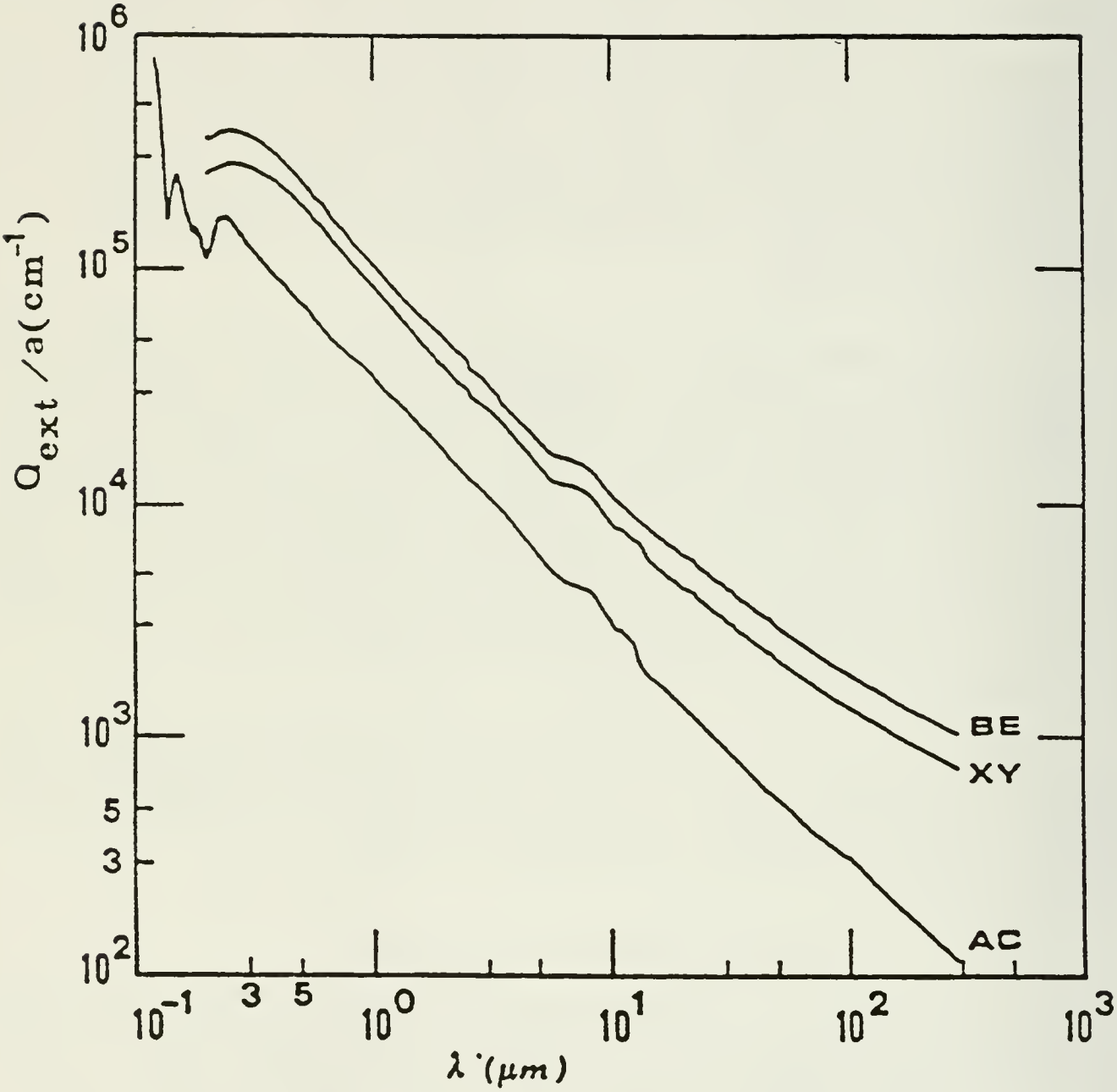


Figure 8.- The mean extinction efficiency curve for AC, BE, and XY amorphous carbon samples.

TABLE III.- INSTRUMENTATION AND EXPERIMENTAL METHODS

Spectral range	VUV 1000 Å ------ 3000 Å 2000 Å ------ 2.6 μm	UV-Vis 2.5 μm -------- 50 μm	IR 30 μm --------- 1 mm	FIR
Instrument	Synchrotron light facilities of "Adone" (Frascati) "BESSY" (Berlin)	DOUBLE-BEAM SPECTROPHOTOMETERS		INTERFEROMETER
		P.E.330	P.E.580/880	SPECAC FTIR
Sample preparation	Deposition on		Embedding in	
	LiF windows	Quartz substrates	KBr or CsI pellets	Polyethylene matrix

vaporized by laser focusing (see table I) onto bulk graphite target in a floating chamber. The submicron (100 - 500 Å) particles levitate in the chamber without any suspension system for a time lag sufficient to record the spectrum in the 200 - 1200 nm range by means of an optical multichannel detector.

Another technique which could present advantages, when applied to RCSs, is the so-called "Infrared Photothermal Beam Deflection Spectroscopy" (Low and Morterra 1983). As it is shown in their figure 2, the sample is deposited on a metallic substrate in an isolated chamber and it is heated by IR radiation coming from an interferometer. If the IR radiation flux is modulated in time, also the thermal gradient and the consequent refractive index gradient in the medium over the surface are modulated in time. When a He-Ne laser beam is passed over the surface, it is deflected and modulated, so that the detector reveals a "photothermal interferogram". This can be processed as in a conventional Fourier transform spectrometer to get the final spectrum. The main advantage of this technique is that spectroscopy can be performed avoiding any interaction of the sample with the external ambient and no particular sample preparation is required. On the other hand, the sample must be heated by the IR beam, and this effect could produce undesired chemical and strucutre alterations.

REFERENCES

Allamandola, L.J.; Tielens, A.G.G.M.; and Barker, J.R.: Polycyclic Aromatic Hydrocarbons and the Unidentified Infrared Emission Bands: Auto Exhaust along the Milky Way !, Astrophys. J. (Letters), vol. 290, 1985, pp. L25-L28.

Allamandola, L.J.; Sandford, S.A.; and Wopenka, B.: Interstellar Polycyclic Aromatic Hydrocarbons and Carbon in Interplanetary Dust Particles and Meteorites. Science, vol. 237, 1987, pp. 56-59.

Ashkin, A.: Phys. Rev. Lett., vol. 19, 1970, p. 283.

Ashkin, A.; and Dziedzic, J.M.: in "Light Scattering by Irregularly Shaped Particles", ed. D.W. Schuerman (New York: Plenum Press), 1980, p. 233.

Blanco, A.; Borghesi, A.; Bussoletti, E., Colangeli, L.; De Blasi, C.; Fonti, S.;

Fusco, C.; Orofino, V.; and Schwehm, G.: Amorphous Carbon and Carbonaceous Materials in Space; Part I: Laboratory Measurements. Nuovo Cimento, in press, 1989.

Blanco, A.; Bussoletti, E.; Colangeli, L.; Fonti, S.; and Orofino, V.: Raman Spectra of Submicron Amorphous Carbon Grains and Mixtures of Polycyclic Aromatic Hydrocarbons. Infrared Phys., vol. 28, 1988a, pp. 383-388.

Blanco, A.; Bussoletti, E.; and Colangeli, L.: A Mixture of Hydrogenated Amorphous Carbon Grains and PAH Molecules: a Candidate for the Unidentified Infrared Bands?. Astrophys. J., vol. 334, 1988b, pp. 875-882.

Bohren, C.F.; and Huffman, D.R.: Absorption and Scattering of Light by Small Particles. John Wiley & Sons, 1983.

Borghesi, A.; Bussoletti, E.; Colangeli, L.; and De Blasi, C.: Laboratory Study of SiC Submicron Particles at IR Wavelengths: a Comparative Analysis. Astron. Astrophys., vol. 153, 1985, pp. 1-8.

Borghesi, A.; Bussoletti, E.; and Colangeli, L.: Amorphous Carbon and the Unidentified Infrared Bands. Astrophys. J., vol. 314, 1987, pp. 422-428.

Bradley, J.P.; and Brownlee, D.E.: Cometary Particles: Thin Sectioning and Electron Beam Analysis. Science, vol. 231, 1986, pp. 1542-1544.

Bussoletti, E.; Colangeli, L.; Borghesi, A.; and Orofino, V.: Tabulated Extinction Efficiencies for Various Types of Submicron Amorphous Carbon Grains in the Wavelength Range 1000 Å - 300 μm. Astron. Astrophys. Suppl. Ser., vol. 70, 1987, pp. 257-268.

Bussoletti, E.; Fusco, C.; and Longo, G.: Experiments on Cosmic Dust Analogues. Astrophys. Space Sci. Library, vol. 149 (Dordrecht: Kluwer Academic Publishers), 1988.

Day, K.L.; and Huffman, D.R.: Measured Extinction Efficiency of Graphite Smokes in the Region 1200 - 6000 Å. Nature Phys. Science, vol. 243, 1973, pp. 50-51.

Edoh, O.: Optical Properties of Carbon from the Far Infrared to the Far Ultraviolet. Ph.D. dissertation, Dept. of Physics, Univ. of Arizona, 1983.

Encounters with Comet Halley, the First Results. Nature, vol. 321, 1986, pp. 259-366.

Giese, R.H.; Killinger, R.T.; Kneissel, B.; and Zerull, R.H.: Albedo and Colour of Dust Grains: Laboratory versus Cometary Results. 20th ESLAB Symposium on the Exploration of Halley's Comet, vol. II, ESA SP-250, 1986, pp. 53-57.

Grewing, M.; Praderie, F.; and Reinhard, R.: Exploration of Halley's Comet. Astron. Astrophys., vol. 187, 1987.

Hanner, M.: Grain Optical Properties. "Infrared Observations of Comets Halley and Wilson and Properties of the Grains", ed. M. Hanner, NASA CP-3004, 1988, pp. 22-49.

Huffman, D.R.: Report of the Working Group on Carbon. "Experiments on Cosmic Dust Analogues", ed. E. Bussoletti, C. Fusco, and G. Longo (Dordrecht: Kluwer

Academic Publishers), 1988a, pp. 345-347.

Huffman, D.R.: Methods and Difficulties in Laboratory Studies of Cosmic Dust Analogues. "Experiments on Cosmic Dust Analogues", ed. E. Bussoletti, C. Fusco, and G. Longo (Dordrecht: Kluwer Academic Publishers), 1988b, pp. 25-42.

Jessberger, E.K.; Christoforidis, A.; and Kissel, J.: Aspects of the Major Element Composition of Halley's Dust. Nature, vol. 332, 1988, pp. 691-695.

Koike, C.; Hasegawa, H.; and Manabe, A.: Astrophys. Space Sci., vol.67, 1980, p. 495.

Low, M.J.D.; and Morterra, C.: IR Studies of Carbons - I. Carbon, vol. 21, 1983, pp. 275-281.

Marchand, A.: Various Kinds of Solid Carbon: Structure and Optical Properties. "Polycyclic Aromatic Hydrocarbons and Astrophysics", ed. A. Leger, L. d'Hendecourt, and N. Boccara (Dordrecht: D. Reidel Publishing Company), 1987, pp. 31-54.

Marx, E.; and Mulholland, G.W.: J. Res. Nat'l. Bur. St., vol. 88, 1983, p. 321.

Philip, M.A.; Gelbard, F.; and Arnold, S.: J. Colloid and Interface Sci., vol. 91, 1983, p. 507.

Pluchino, A.B.; Goldberg, S.S.; Dowling, J.M.; and Randall, C.M.: Refractive-index Measurements of Single Micron-sized Carbon Particles. Applied Optics, vol. 19, 1980, pp. 3370-3372.

Robertson, J.: Amorphous Carbon. Advances in Phys., vol. 35, 1986, pp. 317-374.

Rosen, H.; and Novakov, T.: Identification of Primary Particulate Carbon and Sulfate Species by Raman Spectroscopy. Atmos. Environ., vol. 12, 1978, pp. 923-927.

Sakata, A.; Wada, S.; Okutsu, Y.; Shintani, H.; and Nakada, Y.: Does a 2,200 Å Hump Observed in an Artificial Carbonaceous Composite Account for UV Interstellar Extinction?. Nature, vol. 301, 1983, pp. 493-494.

Stephens, J.R.: Visible and Ultraviolet (800-130 nm) Extinction of Vapor-condensed Silicate, Carbon, and Silicon Carbide Smokes and the Interstellar Extinction Curve. Astrophys. J., vol. 237, 1980, pp. 450-461.

Stephens, J.R.: Light Scattering from Simulated Interstellar Dust. "Experiments on Cosmic Dust Analogues", ed. E. Bussoletti, C. Fusco, and G. Longo (Dordrecht: Kluwer Academic Publishers), 1988, pp. 245-252.

Tuinstra, F.; and Koenig, J.L.: Raman Spectrum of Graphite. J. Chem. Phys., vol. 53, 1970, pp. 1126-1130.

Weiss-Wrana, K.: Optical Properties of Interplanetary Dust: Comparison with Light Scattering by Larger Meteoritic and Terrestrial Grains. Astron. Astrophys., vol. 126, 1983, p. 240.

Wieting, T.J.; and Verble, J.L.: "Electrons and Phonon in Layered Crystal Strucutres", ed. T.J. Wieting and M. Schlüter (Dordrecht: D. Reidel Publishing Company), 1979, pp. 321-407.

HANDLING AND ANALYSIS OF ICES IN CRYOSTATS AND GLOVE BOXES IN VIEW OF COMETARY SAMPLES

K. Roessler
P. Hsiung
M. Heyl
Institut für Chemie 1
Kernforschungsanlage Jülich
Jülich, FRG

G. Neukum
A. Oehler
Institut für Optoelektronik
DLR-Oberpfaffenhofen
Weßling, FRG

H. Kochan
Institut für Raumsimulation
DLR-Köln
Köln, FRG

HANDLING AND ANALYSIS OF ICES IN CRYOSTATS AND GLOVE BOXES IN VIEW OF COMETARY SAMPLES*

K. Roessler[1], P. Hsiung[1], M. Heyl[1], G. Neukum[2], A. Oehler[2], and H. Kochan[3]

[1]Institut für Chemie 1, Kernforschungsanlage Jülich, D-5170 Jülich, FRG
[2]Institut für Optoelektronik, DLR-Oberpfaffenhofen, D-8031 Weßling, FRG
[3]Institut für Raumsimulation, DLR-Köln, D-5000 Köln-90, FRG

The preparation and analysis of frozen volatiles at temperatures ≤ 77 K via condensation and optical spectroscopy, resp., is traditionally performed in cryostats in situ such as described in (Pross L. et al., 1976; Biel E. et al., 1988). The study of larger ice samples, in particular to simulate processes in icy material of the solar system such as comets necessitated a somewhat different approach, cf. e.g. (Dobrovolsky O.V. et al., 1977; Ibadinov K.I. et al., 1987; Saunders R.S. et al., 1986; Storrs A.D. et al., 1988). Preparation, the proper study in a cooled sample holder, and analysis of the states before and after the experiment have often to be performed at different sites, thus, necessitating cryotransport and handling of the samples under protective conditions, i.e. inert and cold atmosphere or vacuum. This became even more stringent for the comet simulation experiments performed since 1987 by a team of scientists from different disciplines in the Big Space Simulator in the German Aerospace Research Establishment DLR-Köln (Bischoff A. et al., 1988; Grün E. et al., 1987, 1988, 1989; Klinger J. et al., 1989; Kochan H. et al., 1989; Roessler K. et al., 1988, 1989; Spohn T. et al., 1989; Thiel K. et al., 1989). Three experiments have been performed with water ice and water-CO_2-ice mineral dust mixtures in April 1987 (KOSI-I), April 1988 (KOSI-II), and November 1988 (KOSI-III). A fourth experiment is prepared for May 1989 (KOSI-IV). These experiments deal with icy material of approx. 10 l volume and 4 to 5 kg weight, each for a standard and the proper sample to be irradiated several ten hours with an artificial sun of approx. 1-3 SC. Techniques applied for cryohandling, -transport, -storage and -analysis will be reported here. They may be considered as first tentative steps in view of the development of methods for treatment of icy samples from space brought to earth via return missions such as ROSETTA.

TEMPERATURE DEMANDS

The temperature of comets may range from 80 to 250 K and more at the surface. Thus, liquid nitrogen can be considered as a convenient cooling agent for sample preparation and handling. Only for special examinations, such as high resolution spectroscopy or condensation of CO, CH_4 and N_2, temperatures lower than 77 K are needed. Table 1 gives a list of temperatures for some critical processes. From Table 1 it can be seen that dry ice-methanol cooling baths will not be sufficient for studies with volatile components such as CO_2. Besides cooling liquids also electrical methods (Peltier-effect) can be applied. However, their heat capacity is in general low, and samples cannot be easily transported.

CRYOSTATS WITH REMOVABLE PLUGS

Conventional bath cryostats with cold fingers (5 or 77 K) such as used for low temperature spectroscopy in general do not allow manipulations at the chilled sample nor is it possible to introduce an already preexisting ice sample. This can be achieved

*This work is financially supported by Deutsche Forschungsgemeinschaft DFG

Table 1: Temperatures in K (rounded values) for processes in ices

4	liquid helium evaporation
10-14	migration of H starts in H_2O ice
< 72	evaporation of CO at 1 bar
77	evaporation of nitrogen at 1 bar
80-120	amorphous to cubic transition in NH_3 ice
100-110	migration of OH starts in H_2O ice
110-130	migration of O_2H starts in H_2O ice
135±10	amorphous to cubic transition in H_2O ice
130-150	sublimation of CO_2 in vacuum
165±10	cubic to hexagonal transition in H_2O ice
195	sublimation of CO_2 at 1 bar
195	dry ice/methanol cooling
196	melting of NH_3
240	evaporation of NH_3 at 1 bar
< 273	melting of H_2O with impurities
273	melting of pure H_2O at 1 bar

by a removable plug system positioned around the cold finger and connected tightly to the cryostat body via two rubber-O-rings (Pross L. et al., 1976). In the version shown in Fig. 1a it is provided with optical windows for spectroscopy. It can be removed from the cryostat after mounting onto an evacuated cross tube by means of a push-pull fead through. The plug can even be separated from the rest by a valve system, and can be exchanged for another plug (e.g. change from quartz to KBr windows when going from VIS to IR spectroscopy). The sample hangs free on the cold finger and is accessible to manipulation. After processing the plug is remounted and the cryostat can be transported to another site. In order to load samples from the outside, a glove box system with N_2 purging gas allowed to open the cold cryostat without giving atmospheric moisture or CO_2 a chance to condense onto sample and walls, Fig. 1b. Special window plugs containing gas nozzles were developed for simultaneous condensation of ices on KBr cold plates and optical spectroscopy in transmission (Biel E. et al., 1988; Roessler K., Eich G. et al., 1989).

LIQUID NITROGEN DEWARS AND BATHS

For transport and storage of closed samples liquid nitrogen containing dewars are best suited. The material of the sample containers should be relatively thick. It should possess high heat capacity in order to allow short removal of the samples from the bath. For the same reason all tools by which samples are touched should be made out of metal and chilled before use by immersion into liquid nitrogen. They should be provided with insulating handles in order to prevent heat flow from the hands of the operator. Furthermore, thermally insulating gloves should be worn.

For transport and handling of open samples cold N_2 gas evaporating from liquid N_2 baths can be used as a protective medium. Fig. 2a shows the tank used in KOSI experiments. It is made out of stainless steel (2 mm) and it is deliberately not a dewar in order to induce vigorous evaporation of N_2 gas. The KOSI samples (30 cm diameter and 15 cm high) are stored in the cylindrical recipient which is surrounded by liquid nitrogen. The cold N_2 gas (130-150 K) protects the surface of the sample from thermal effects (e.g. sublimation of CO_2) and condensation of atmospheric H_2O or CO_2. This effect is improved by a steel cover, which is kept cold by heat conductivity. The irradiated KOSI samples and the standards are stored and transported in this tank into the central glove box for further analysis.

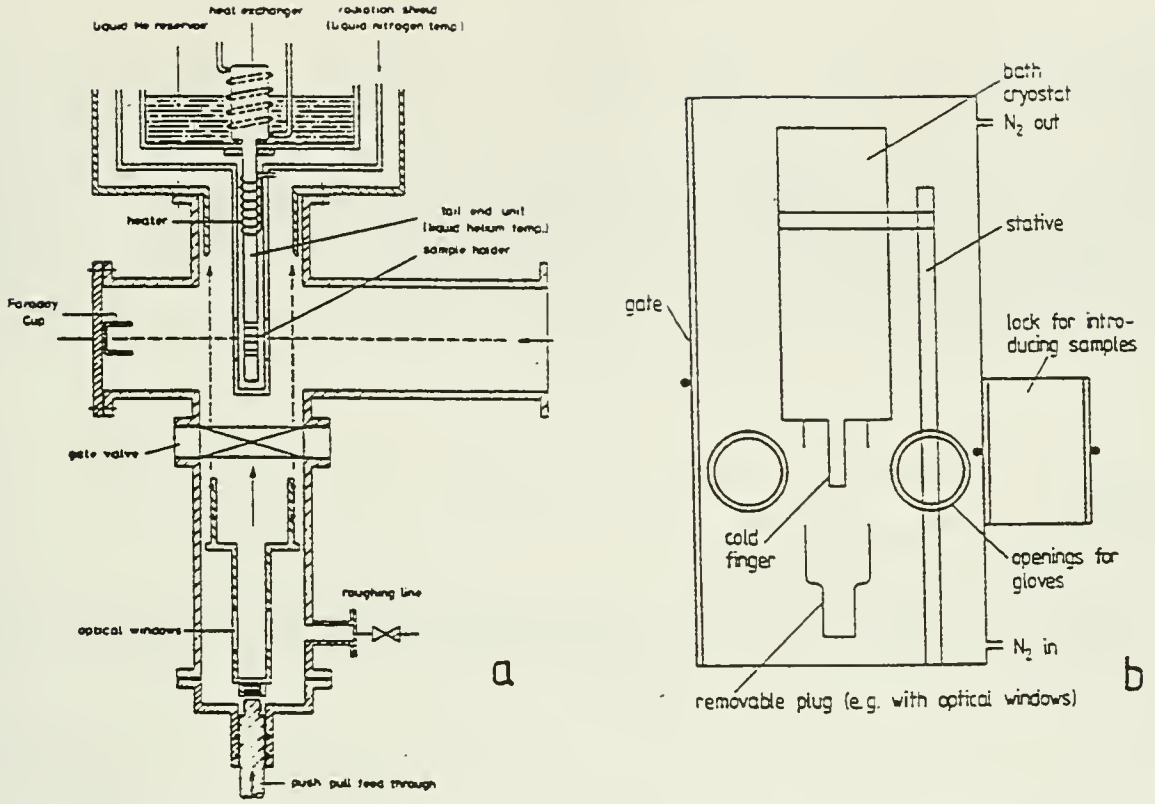


Fig. 1: Bath cryostat with removable (window) plug mounted on an evacuated cross tube (a) and glove box system to load icy samples onto the cold finger of the cryostat (b)

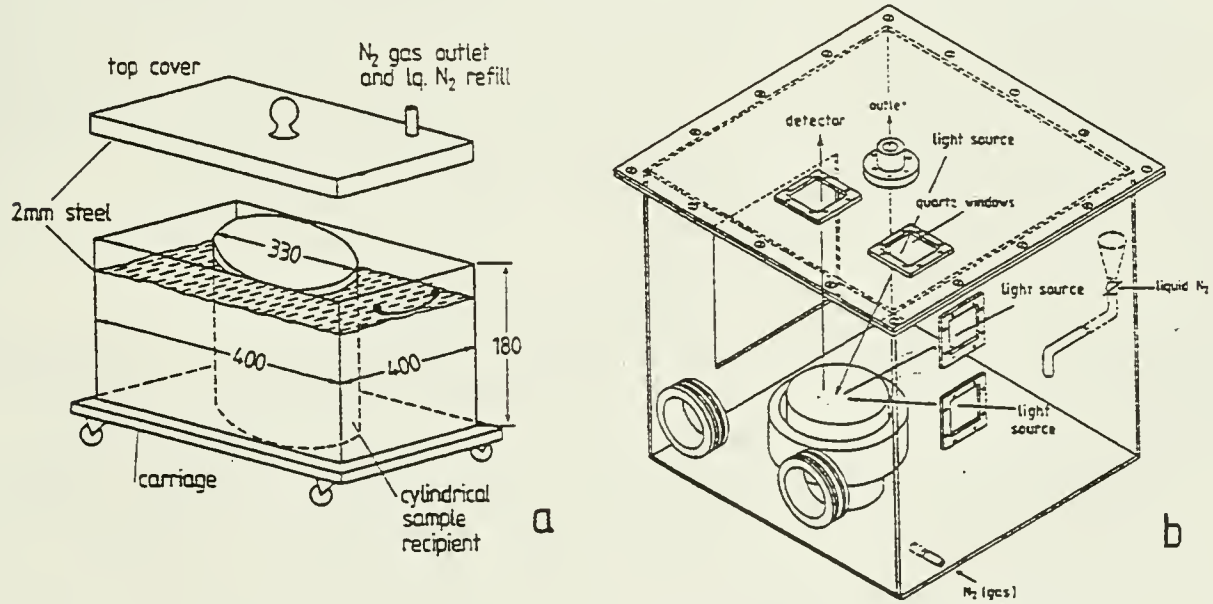


Fig. 2: Stainless steel tank with liquid nitrogen and the KOSI sample recipient (a) and central glove box (80x80x80 cm) with lq. N_2 bath and windows for optical reflexion spectroscopy at three angles (b)

GLOVE BOX WITH LIQUID NITROGEN TANK

Fig. 2b shows the 80x80x80 cm glove box used for KOSI experiments.It is made out of 1 cm thick plexiglass and contains several holes for gloves (made out of rubber with insulating layers), quartz windows for optical spectroscopy from the outside (remote sensing), a lock system for samples and tools (not shown in Fig. 2b), and many electric connections. More effective than purging the box by dry N_2 gas (5.0) is to use the N_2 evaporating from the bath itself. An overpressure of 1.1 bar has to be maintained to hinder penetration of atmospheric gases. The relatively steep temperature gradient to the walls prevents freezing from the outside, except for the lower regions of the glove box where temperatures of 200 to 220 K were measured at the outer walls. This, however, has the advantage that sample containers, tools, etc. which were stored here, were already precooled.

IN SITU ANALYSIS

The analysis of the non-irradiated standard and the irradiated KOSI samples consists of five steps:

1) General visual inspection of surface and morphology during sample taking and deepening of pits (Fig. 3, for KOSI-III).
2) Mesurement of temperature. Fig. 4 shows the temperatures of KOSI-III sample after insertion into the liquid N_2 tank measured by three thermocouples (1 cm, 6 cm and 11 cm below the actual surface) during the operations in the glove box. Temperatures are reasonably low to prevent sublimation of CO_2.
3) Optical reflexion spectroscopy in VIS and IR (450 to 2500 nm) in remote sensing, in particular to determine the Albedo, with Barnes field and similar spectrometers. Fig. 5 shows the general arrangement around the glove box. Fig. 6a shows the sample before irradiation, Fig. 6b the irradiated sample, both with the blank standard. Fig. 7 exhibits the spectra obtained for KOSI-III (average over three angles). It can be see that the sample under irradiation became slightly darker and that H_2O and CO_2 peaks disappeared at least partly.
4) Test of material strength by drilling boreholes with a penetrator provided with a Newtonmeter (ESA/ESTEC, Dr. G. Schwehm). The most important result is the detection of crusts formed under the loose dust layer. The steep rise and fall of the force indicates the thickness of the layers. Fig. 8a,b are from KOSI-II. The results for KOSI-III are reported in (Thiel K. et al. 1989).
5) Measurement of electrical conductivity of surface and bulk (ESA/ESTEC, Dr. G. Schwehm), planned for KOSI-IV.

EXTERNAL SAMPLE ANALYSIS

Samples were taken from non-irradiated standard and KOSI material for following analyses. The first 6 methods require very cold sample taking in order to maintain their specific properties.

1) CO_2 content via collecting gases evolving upon heating of samples to ambient temperature and gas chromatography. Fig. 9 gives the CO_2 profiles for KOSI-III; further details in (Roessler K., Hsiung P. et al. 1989). The starting material contained 13.8 wt. % CO_2, the non-irradiated standard did not show severe losses upon filling, except for the surface layer. After 41 h irradiation at 1.3-2.7 SC artificial sunlight, CO_2 was almost totally lost from the upper and middle layers. Only nea the cooling back plate some CO_2 remained. A very CO_2 rich white layer (1-2 mm) was observed on the back plate itself indicating inward diffusion of CO_2.
2) Investigation of crystal structure via X-ray diffraction (in cooperation with Prof. E. Mayer, Univ. Innsbruck, Austria).

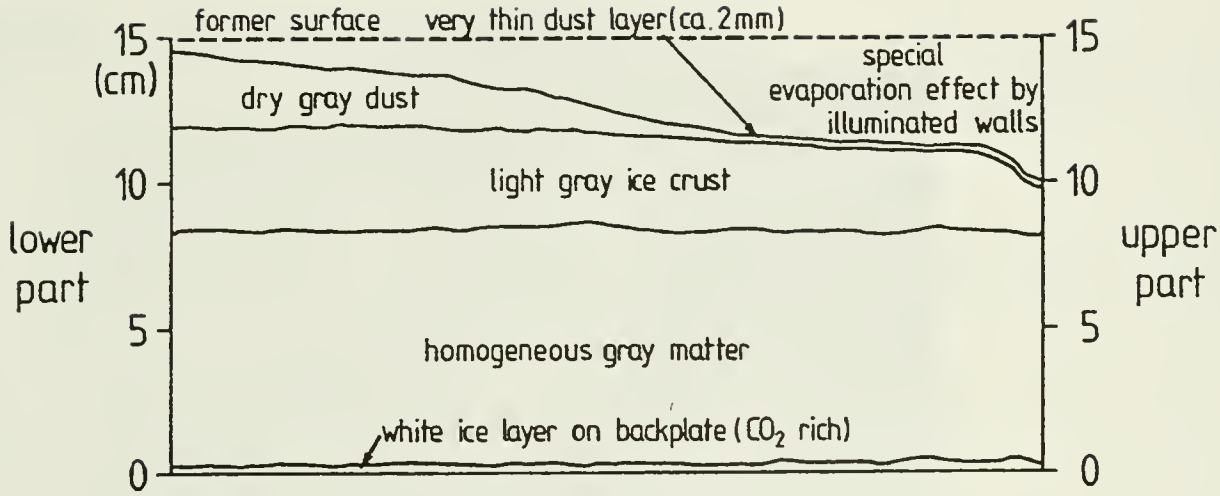


Fig. 3: Results of visual inspection of KOSI-III sample after irradiation for 41 h with 1.3 to 2.7 SC artificial sunlight.

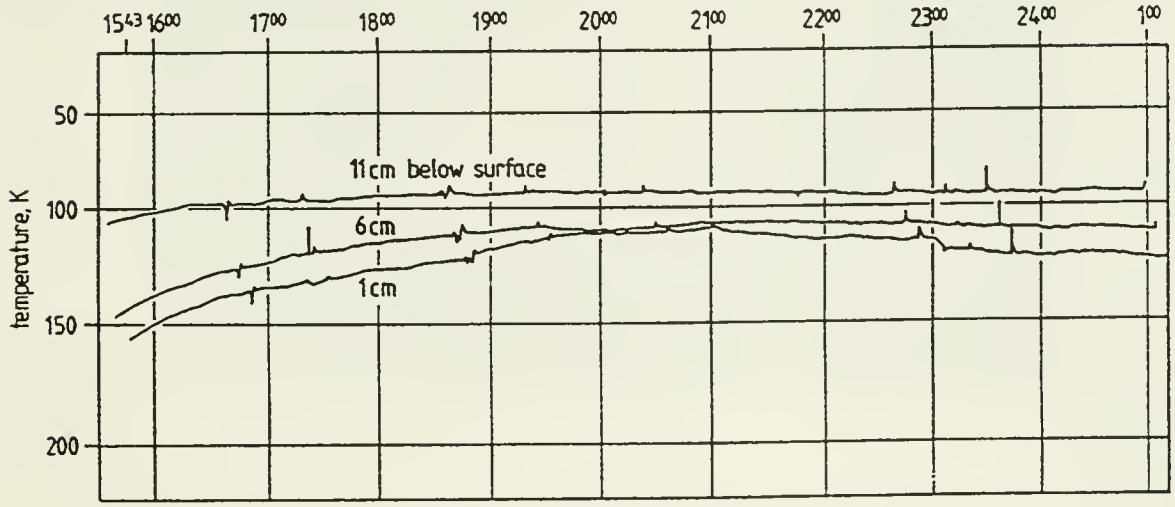


Fig. 4: Temperatures of KOSI-III sample in liquid N_2 bath inside the glove box during operations for in situ analysis and sample taking

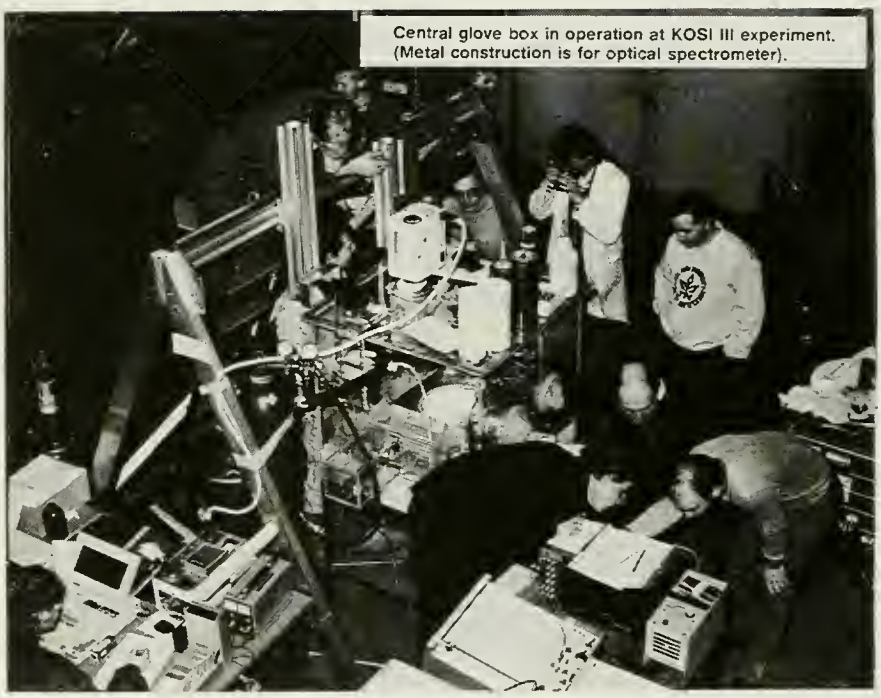


Fig. 5: Central glove box in operation at KOSI-III experiment, with support for optical spectrometer

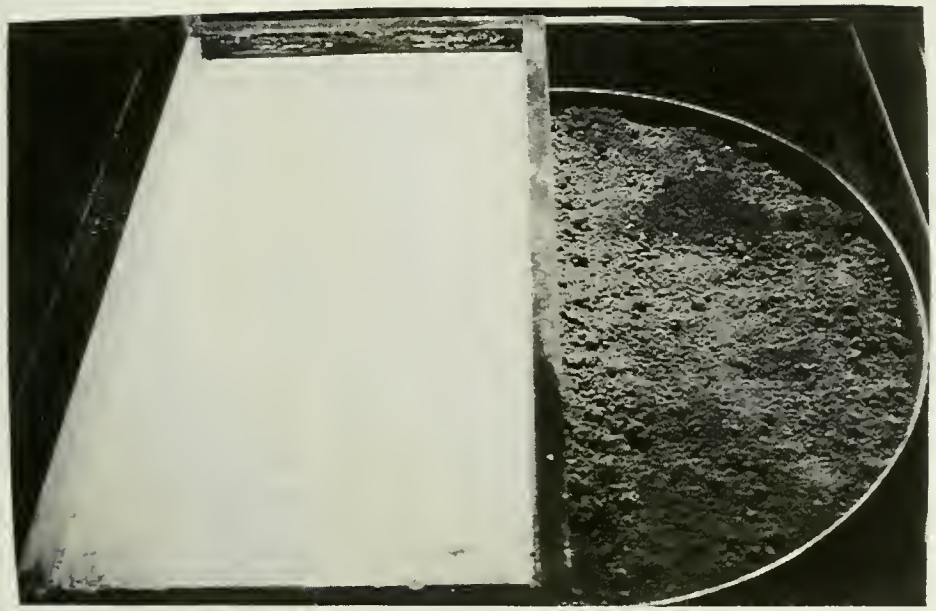


Fig. 6: Non-irradiated reference standard

(a) and irradiated KOSI-III sample



(b) with blank

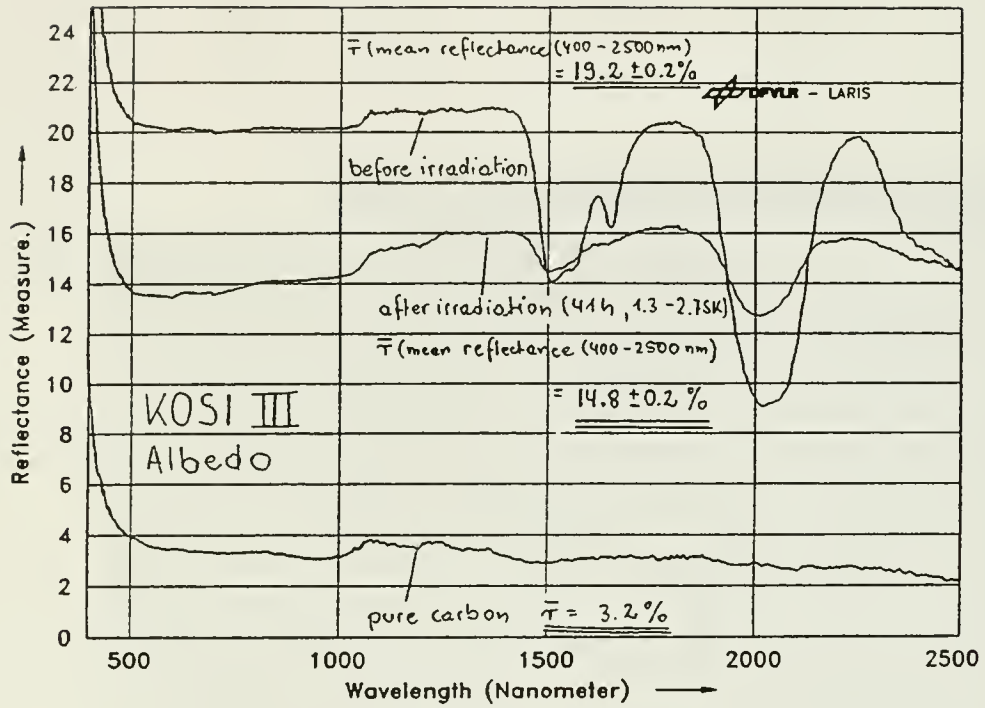


Fig. 7: Reflexion spectra and Albedo values for KOSI-III before and after artificial sun irradiation

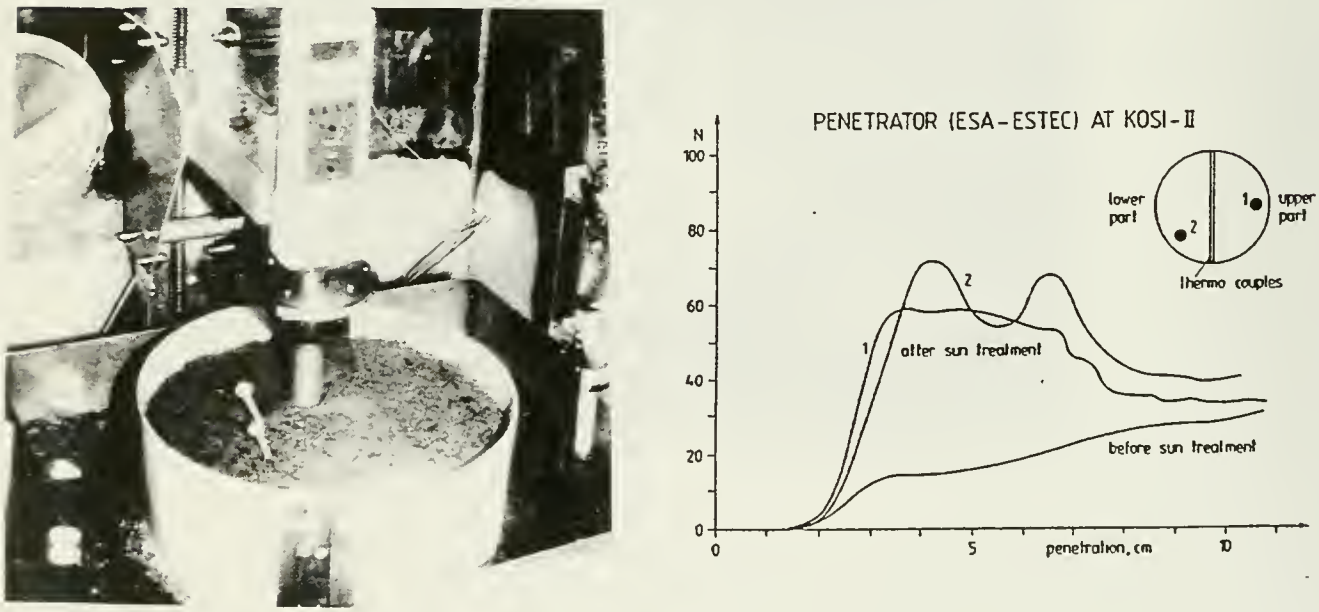


Fig. 8: Material strength test and attempts to draw borekernels with ESA/ESTEC Penetrator at KOSI-II. a) the penetrator, b) material strength before and after irradiation with approx. 26 h 1-2 SC artificial sunlight.

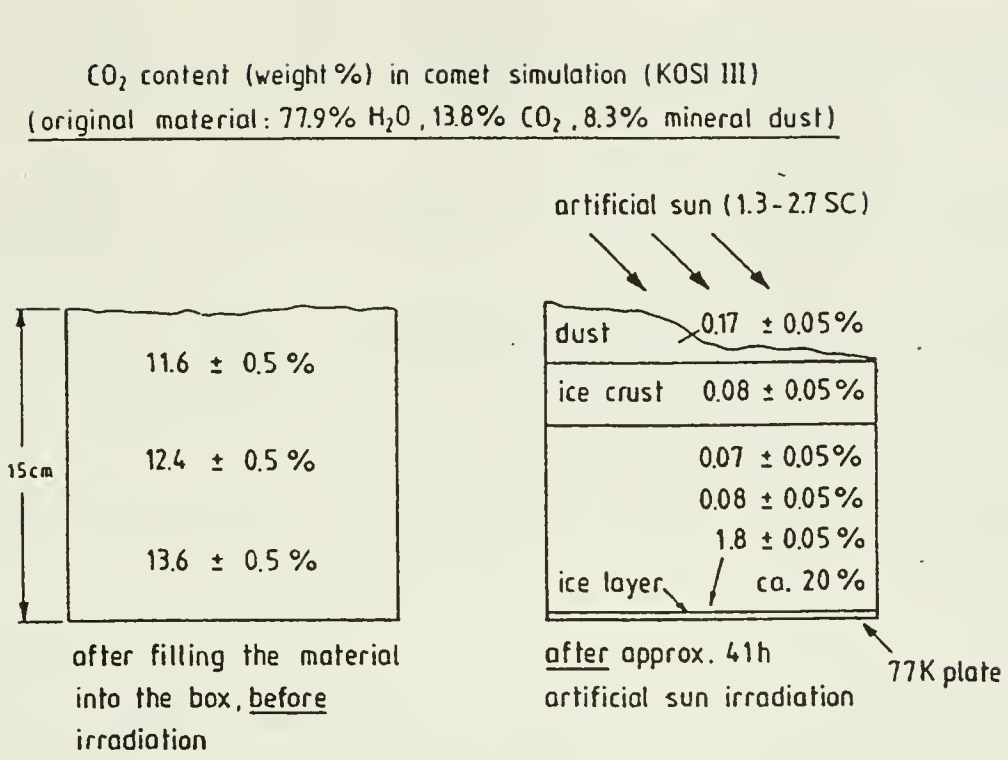


Fig. 9: CO_2 content in KOSI-III sample before and after artificial sun irradiation

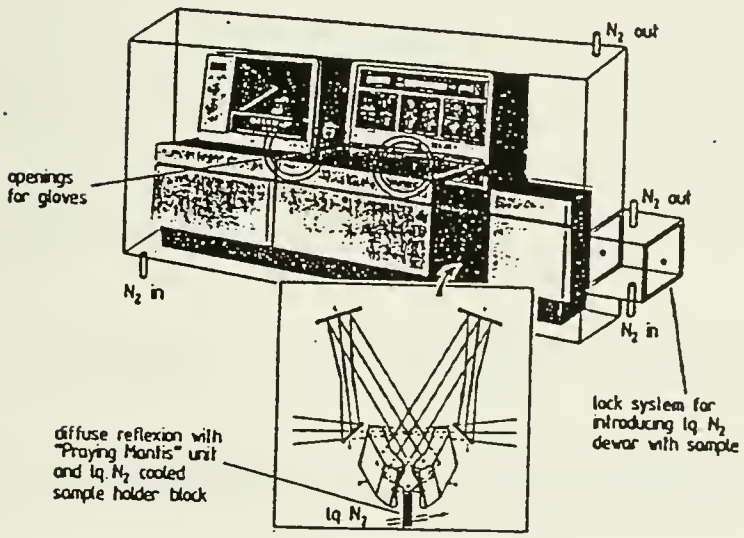


Fig. 10: Satellite glove box with IR-spectrometer and liquid N_2 cooled sample holder for diffuse reflexion

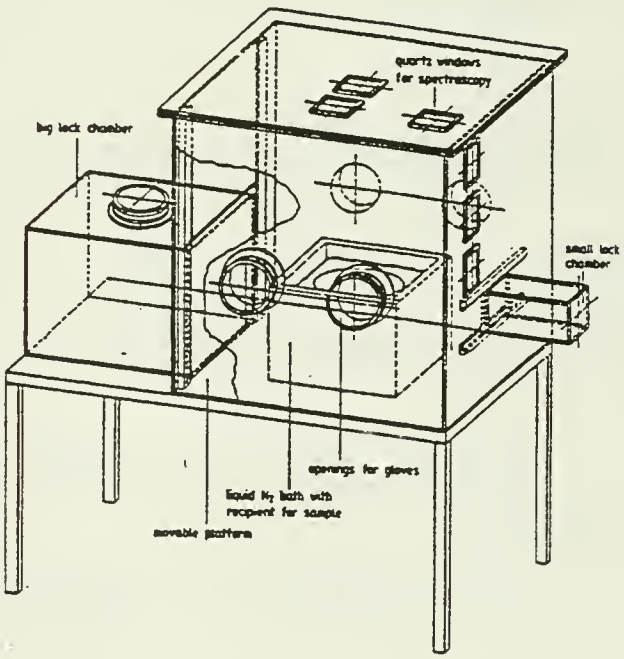


Fig. 11: New concept of central glove box (for KOSI-IV and following)

3) Measurement of microporosity (in preparation by Prof. J. Klinger and Dr. B. Schmitt, Glaciologie, CNRS, Grenoble).
4) Determination of density and overall porosity (Dr. H. Hellmann, DLR-Köln).
5) IR-diffuse reflexion spectroscopy in satellite glove box (Fig. 10, Dr. E. Langenscheidt, KFA-Jülich).
6) Differential thermal analysis DTA and differential scanning calorimetry DSC (in preparation, KFA-Jülich)

The following methods do not require very low temperatures and samples can be taken or stored with less precaution:

7) Mineralogy and petrography (texture and structure) via drilling boreholes and removing borekernels of material (2 and 4 cm in diameter), fixation with gels and analysis after thin sectioning in a cold laboratory (233 to 269 K) (in preparation by H. Düren, Prof. D. Stöffler, Univ. Münster).
8) High performance liquid chromatography HPLC for chemical compounds such as e.g. CH_3OH, CH_2O, HCOOH, etc. newly formed by the interaction of heat, UV light and catalytic processes on the mineral dust (clay) grains (KFA-Jülich).
9) Isotope ratios $^{16}O/^{18}O$ and H/D via mass spectrometry (Dr. H. Stichler, GSF-Neuherberg and Dr. H. Förstel, KFA-Jülich). If $^{12}C/^{13}C$ ratio of CO_2 has to be checked, the samples must be taken and stored at low temperatures (< 195 K).
10) SEM of dry residue (Prof. K. Thiel, Universität Köln).

In future experiments, KOSI-IV etc., a new somewhat larger glove box (1x1x1 m) is conceived containing a turnable platform for the sample container which can be moved up and down in order to yield best access to the sample surface in view of in situ analysis (Fig. 11). An important improvement is the addition of a large lock chamber for introduction of the samples into the glove box under protective gas and for storage and bringing out small samples in larger dewars.

If further developed and refined some of the methods described above may be considered in the planning of a return sample receiving station.

REFERENCES

Biel E., Patnaik A., and Roessler K. (1988) Herstellung binärer Eisschichten durch Kondensation aus der Gasphase, Rpt. Jül-2248, Kernforschungsanlage Jülich, FRG, pp. 1-60.

Bischoff A. and Stöffler D. (1988) Comet nucleus simulation experiments: mineralogical aspects of sample preparation and analysis (abstract), Lunar and Planetary Science XIX, pp. 90-91, Lunar and Planetary Institute, Houston.

Dobrovolsky O.V. and Kajmakov E. (1977) Surface phenomena in simulated cometary nuclei, In Comets, Asteroids, Meteorites (Delsemme A.H. ed.) pp. 37-46, University of Toledo, Ohio.

Grün E., Kochan H., Roessler K., and Stöffler D. (1987) Simulation of cometary nuclei, In Diversity and Similarity of Comets (Rolfe E.J. and Battrick B. eds.) ESA-SP-278, pp. 501-508.

Grün E., Kochan H., Roessler K., and Stöffler D. (1988) Initial comet simulation experiments at DFVLR, In Experiments on Cosmic Dust Analogues (Bussoletti E. et al. eds.) pp. 17-23, Kluwer Acad. Publ., Dordrecht.

Grün E. and KOSI-team (1989) Modifications of comet material by the sublimation process, this issue (abstract in Workshop on Analysis of Returned Comet Nucleus Samples, 1989, Milpitas, Cal., pp. 24-25, Lunar and Planetary Institute, Houston).

Ibadinov K.I. and Aliev S. (1987) Sublimation characteristics of H_2O comet nucleus with CO_2 impurities, In Diversity and Similarity of Comets (Rolfe E.J. and Battrick B. eds.) ESA-SP-278, pp. 710-719.

Klinger J., Benckhoff J., Espinasse S., Grün E., Ip W., Joõ F., Keller H.U., Kochan H., Kohl H., Roessler K., Seboldt W., Spohn T., and Thiel K. (1989) How far do results of recent simulation experiments fit current models of cometary nuclei?, Proc. Lunar Planet. Sci. Conf. 19th, pp. 493-497.

Kochan H., Benckhoff J., Bischoff A., Fechtig H., Feuerbacher B., Grün E., Joõ F., Klinger J., Kohl H., Krankowsky D., Roessler K., Seboldt W., Thiel K., Schwehm G., and Weishaupt U. (1989) Laboratory simulation of a cometary nucleus: experimental setup and first results, Proc. Lunar Planet. Sci. Conf. 19th, pp. 487-492.

Kochan H., Feuerbacher B., Joõ F., Klinger J., Seboldt W., Bischoff A., Düren H., Stöffler D., Spohn T., Fechtig H., Grün E., Kohl H., Krankowsky D., Roessler K., Thiel K., Schwehm G., and Weishaupt U. (1989) Comet simulation experiments in the DFVLR Space Simulators, Adv. Space Res., in press.

Pross L., Hemmerich J., and Roessler K. (1976) Transportable cryostat for charged particle irradiation and optical spectroscopy, Rev. Sci. Instrum. 47, 353-355.

Roessler K., Bischoff A., Eich G., Grün E., Fechtig H., Joõ F., Klinger J., Kochan H., Stöffler D., and Thiel K. (1988) Cometary matter in observation and simulation experiments (abstract) Lunar and Planetary Science XIX, pp. 996-997, Lunar and Planetary Institute, Houston.

Roessler K., Eich G., Heyl M., Kochan H., Oehler A., Patnaik A., Schlosser W., and Schulz R. (1989) Handling and analysis of ices in cryostats and glove boxes in view of cometary samples (abstract) In Workshop on Analysis of Returned Comet Nucleus Samples, 1989, Milpitas, Cal., pp. 62-63.

Roessler K., Hsiung P., Kochan H., Hellmann H., Düren H., Thiel K., and Kölzer G. (1989) A model comet made from mineral dust and H_2O-CO_2 ice: sample preparation development (abstract) In Lunar and Planetary Science XX, pp. 920-921, Lunar and Planetary Institut, Houston.

Saunders R.S., Fanale F.P., Parker T.J., Stephens J.B., and Sutton S. (1986) Properties of filamentary sublimation residues from dispersion of clay in ice, Icarus 66, 94-104.

Spohn T., Benckhoff J., Klinger J., Grün E., and Kochan H. (1989) Thermal modeling of two KOSI comet nucleus simulation experiments, Adv. Space Res., in press.

Storrs A.D., Fanale F.P., Saunders R.S., and Stephens J.B. (1988) The formation of filamentary sublimate residues (FSR) from mineral grains, Icarus 76, 493-512.

Thiel K., Kochan H., Roessler K., Grün E., Schwehm G., Hellmann H., Hsiung P., and Kölzer G. (1989) Mechanical and SEM analysis of artificial comet nucleus samples, this issue (abstract in Workshop on Analysis of Returned Comet Nucleus Samples, 1989, Milpitas, Cal., pp. 75-76, Lunar and Planetary Institute, Houston).

Thiel K., Kölzer G., Kochan H., Grün E., and Kohl H. (1989) Crustal evolution and dust emission of artificial cometary nuclei (abstract) In Lunar Planet Sci. Conf. XX, pp. 1113-1114, Lunar and Planetary Institute, Houston.

ELECTRON SPIN RESONANCE (ESR) STUDIES OF RETURNED COMET NUCLEUS SAMPLES

Fun-Dow Tsay
Soon Sam Kim
Ranty H. Liang
Jet Propulsion Laboratory
California Institute of Technology
Pasadena, California

ELECTRON SPIN RESONANCE (ESR) STUDIES OF RETURNED COMET NUCLEUS SAMPLES*

Fun-Dow Tsay, Soon Sam Kim and Ranty H. Liang
JET PROPULSION LABORATORY, CALIFORNIA INSTITUTE OF TECHNOLOGY
PASADENA, CA 91109

ABSTRACT

Electron Spin Resonance (ESR) studies have been carried out on organic and inorganic free radicals generated by gamma-ray and/or UV-irradiation and trapped in ice matrices. It is suggested that the concentration of these free radicals together with their thermal stability can be used as an accurate built-in geothermometer and radiation probe for returned comet nucleus sample studies. ESR studies have also been carried out on paramagnetic (Mn^{2+}, Ti^{3+} and Fe^{3+}) and ferromagnetic (ferric oxide and metallic iron) centers known to be present in terrestrial and extraterrestrial samples. The presence or absence of these magnetic centers coupled with their characteristic ESR lineshape can be used to investigate the shock effects, quenching/cooling rate and oxidation-reduction conditions in the formation and subsequent evolution of returned comet nucleus samples.

INTRODUCTION

The most important scientific objective of the planned Comet Nucleus Sample Return Mission is to return to Earth the least altered, pristine samples which could reflect formation conditions and evolutionary processes in the early solar nebula. The returned cometary samples are expected to consist of fine-grained silicate materials mixed to some extent with ices. The cometary ices may imbed in them such simple molecules as CO, CO_2, H_2O, NH_3 and CH_4 as well as organics (H_2CO, CH_3OH, HCOOH and $HCONH_2$) and/or more complex compounds (Kissel et. al., 1987: Allamandola et. al., 1988). Because of the exposure to ionizing radiation from cosmic-ray, gamma-ray and solar wind protons at low temperature, free radicals in the form of $\bullet H$, $\bullet OH$, $\bullet CH_3$ and $-\dot{C}H_2$ are expected to be formed and trapped in the solid ice matrices. The kind of trapped radical species together with their concentration and thermal stability can be used as a dosimeter as well as a geothermometer to determine thermal and radiation histories as well as outgassing and other possible alteration effects since the nucleus material was formed. The free radicals that are known to contain unpaired electrons are all paramagnetic in nature. Thus, they can be readily detected and characterized in their native form by the Electron Spin Resonance (ESR) method. In fact, ESR has been shown to be a non-destructive, highly sensitive tool for the detection and characterization of paramagnetic (Fe^{3+}, Ti^{3+} and Mn^{2+}), ferromagnetic (magnetite, hematite, maghemite and metallic iron), and radiation damage centers in terrestrial and extraterrestrial geological samples (Tsay et. al., 1971, 1972a, 1973; Ahrens et. al., 1976; Vizgirda et. al., 1980; Beckett et. al., 1988). The purpose of this paper is to point out the potential use of ESR as an effective method in the study of returned comet nucleus samples, in particular, in the analysis of fine-grained, solid state icy samples.

* Work Supported by NASA.

EXPERIMENTAL

ESR Spectroscopy: ESR measures the absorption of microwaves by a paramagnetic or ferromagnetic center in the presence of an applied external magnetic field. Conventional ESR experiments are carried out with varying magnetic fields on samples in a tuned resonant cavity operated at a certain frequency. The magnetic field position (g-value) at which resonance occurs, together with the number of resonance lines (fine and hyperfine structure) and the separation between them (zero-field splitting and hyperfine coupling constant), provides a direct identification of magnetic species, their oxidation state and chemical environment. Detailed analyses of ESR signals and their response to physical and chemical treatments can furnish further information on the nature, origin, thermal stability and formation condition of the magnetic species examined. The sensitivity of ESR is such that it can detect 3×10^{12} standard spin (or molecules assuming one spin per molecule). Thus, milligram-size cometary samples can be examined non-destructively as a function of temperature by ESR. In many instances, ESR has the advantage of detailed submicroscopic identification of transient species and/or reaction intermediates generated in UV and/or gamma-ray radiation. We intend to use the unique capability of ESR to investigate the thermal cycling, radiation exposure, shock effects and oxidation/reduction conditions in the formation and evolution of comet nucleus samples.

ESR Experiments: The ESR measurements were carried out on samples sealed in 2-3 mm o.d. quartz tubes. An ESR spectrometer (Varian E-Line Century Series with 15" magnet) operating at X-band (9.2 GHz) was used with 100 KHz field modulation. The spectrometer was equipped with variable temperature accessories for low temperature measurements. A ^{60}Co gamma-ray source and an UV-enhanced Xenon lamp (ILC Technology, LX 300 UV) with a water filter (4 cm path length) were used for irradiation experiments.

RESULTS AND DISCUSSION

Thermal and Radiation Histories: Free radicals in the form of •OH and $\dot{H}O_2$ have been detected in γ-irradiated ice at 77°K (see Fig. 1). These free radicals

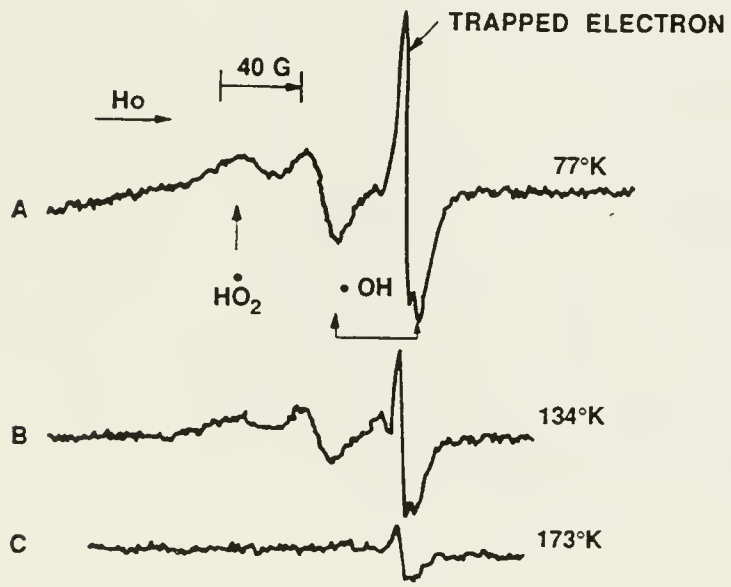


Fig. 1. ESR spectra observed for the γ-irradiated ice at various temperatures. Note the decaying of ESR signal amplitude and the relative intensity ratio at high temperature.

are found to be unstable and to decay rapidly above 110°K as reported (Siegel et. al., 1961). No ESR signals of the free radicals can be detected above 160°K. The characteristic ESR signals of •H having a hyperfine coupling constant of 500 gauss and present in γ-irradiated ice can only be detected below 60°K.

ESR studies have also been carried out on free radicals generated in gamma-ray and/or UV-irradiated simple organic compounds and trapped in ice matrices. Various organic free radical species are formed in γ-irradiated formaldehyde (H_2CO) as a function of temperature (See Fig. 2). The characteristic ESR signals of •CHO doublet are found to be unstable above 160°K, and no ESR signals can be detected at 223°K.

ESR signals attributable to $-\dot{C}H_2$ organic free radicals are detected in the UV-irradiated polycrystalline samples of simple nitrogen containing organic compounds such as glycine (NH_2CH_2COOH) at room temperature (See Fig. 3). The triplet ESR signals of $-\dot{C}H_2$ are also detected in UV-irradiated frozen aqueous solutions containing glycine at 77°K (Fig. 3). The ESR signals detected in ice matrices at low temperature are found to be unstable at elevated temperature and to disappear at 273°K.

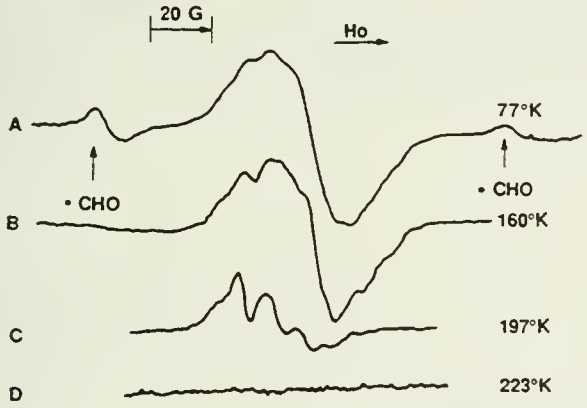


Fig. 2 Temperature-dependent ESR spectra observed for γ-irradiated formaldehyde (H_2CO). The broadened center peaks detected at 77°K and 160°K are the composite spectrum of the ESR signals arising from multiple radical species (•CH_3, $-O\dot{C}HO-$ and •OCHO). The dominant spectral features are the quartet of •CH_3 at 197°K.

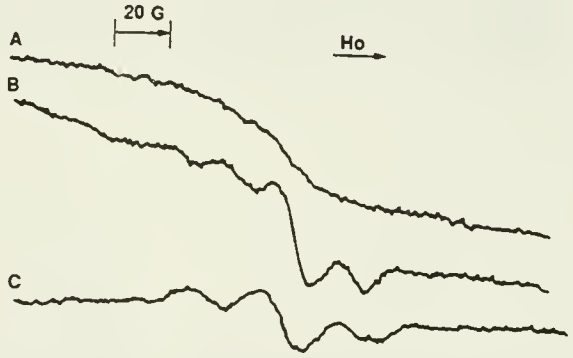


Fig. 3 ESR spectra of $-\dot{C}H_2$ in UV-irradiated glycine (NH_2CH_2COOH).

A. Before irradiation.

B. UV-irradiated polycrystalline sample of glycine at 296°K.

C. UV-irradiated ice containing 0.2M glycine at 77°K.

By ESR definition, the least altered, pristine comet nucleus sample should contain all the organic and inorganic free radicals produced and stabilized in its environment since the formation of the sample. The total free radical concentration a pristine sample should have can be recreated by re-irradiation of the returned sample at its prevailing temperature since the sample was formed.

Any deviation in free radical concentration from its original value is a good indicator in determining the extent of alteration that a returned cometary sample has undergone. The ESR detection of a variety of organic and inorganic free radicals together with the concentration and thermal stability measurements can reveal further information on the thermal and radiation histories of returned cometary samples.

Shock Effects and Cooling/Quenching Rate: The ESR methodology has been developed to determine shock-induced effects on carbonate minerals (Vizgirda et. al., 1980). By studying the ESR spectrum of Mn^{2+} present as impurity in calcite, it is possible to establish the distortion in the crystal structure as a function of shock loading and determine the shock loading history of a sample of unknown history. The lattice distortion caused by shock-induced effects can be effectively quantified through the ESR measurements of zero-field splitting parameters in Mn^{2+}. The characteristic ESR signals of Mn^{2+} in calcite are shown in Fig. 4.

ESR studies have been carried out on C-1, C-2, and C-3 carbonaceous meteorites. These meteorites are known to contain large amounts of high molecular weight organic compounds and the C-2 chondrites show evidence of extraterrestrial aqueous alteration as indicated by the presence of calcite in this group. ESR signals attributable to organic free radicals along with the characteristic ESR signals of calcite are detected in the C-2 group (Mighei, Murchison, Murray, Nogoya and Cold Bokkeveld) as shown in Fig. 4.

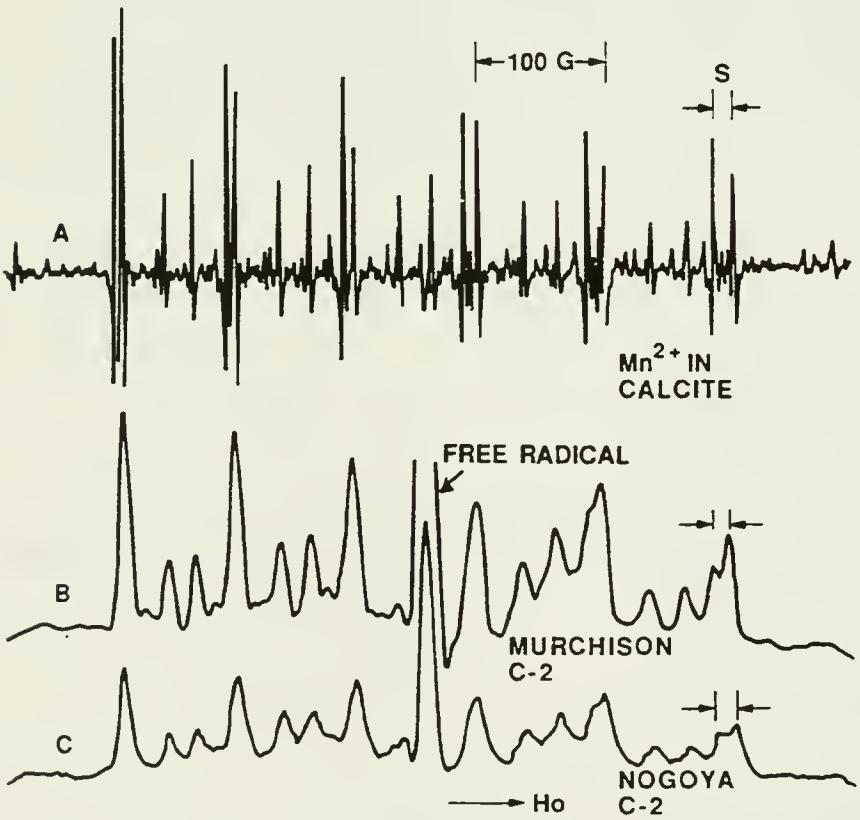


Fig. 4

Second-derivative ESR spectra of Mn^{2+} in calcite as detected in a terrestrial sample (A) and in C-2 carbonaceous meteorites (B and C). Note the intense ESR signals of organic free radicals observed for meteorites. The zero-field splitting parameter D which can be measured from the high-field peak separation S has been shown to decrease with increasing shock effects (Vizgirda et. al., 1980)

In addition to the ESR detection of shock effects, the ESR lineshape of Mn^{2+} can also serve as an indicator on how fast a frozen sample has been cooled or quenched from high temperature. The broadened, asymmetric lineshape of Mn^{2+} in a frozen glassy sample has been shown to be caused by the aggregation and inhomogeneous distribution of randomly oriented and unevenly distorted magnetic sites in a glassy environment (Tsay et. al., 1972b).

The extent of aggregation, inhomogeneity and anisotropy in random orientation will depend on the cooling and quenching rate of the sample. As a result, the cooling and thermal cycling effects will ultimately dictate the outcome of the ESR lineshape observed for Mn^{2+} in a frozen glassy sample. As seen in Fig. 5, the ESR spectrum shows the characteristic lineshape of Mn^{2+} with a single zero-field splitting parameter of 81.0 G for a polycrystalline sample of calcite with a well-defined site symmetry. In contrast, the grossly asymmetric lineshape of Mn^{2+} in frozen methanol results from an assembly of inhomogeneous distorted sites with a zero-field splitting parameter spread over a range of 80 - 150 G (Fig. 5). A much more symmetric ESR lineshape is observed for Mn^{2+} in water at 23°C (Fig. 5). This is because the rapid molecular motion of Mn^{2+} has effectively averaged out the anisotropy in the random orientation of magnetic centers relative to the applied external magnetic field. However, only a broad, featureless ESR spectrum is observed for a slowly cooled frozen aqueous solution of Mn^{2+} (Fig. 5). A detailed ESR lineshape analysis of magnetic centers such as Mn^{2+} in a fine-grained, icy sample can provide information on the outgassing, thermal cycling and other possible alteration processes that may have occurred in the returned comet nucleus samples.

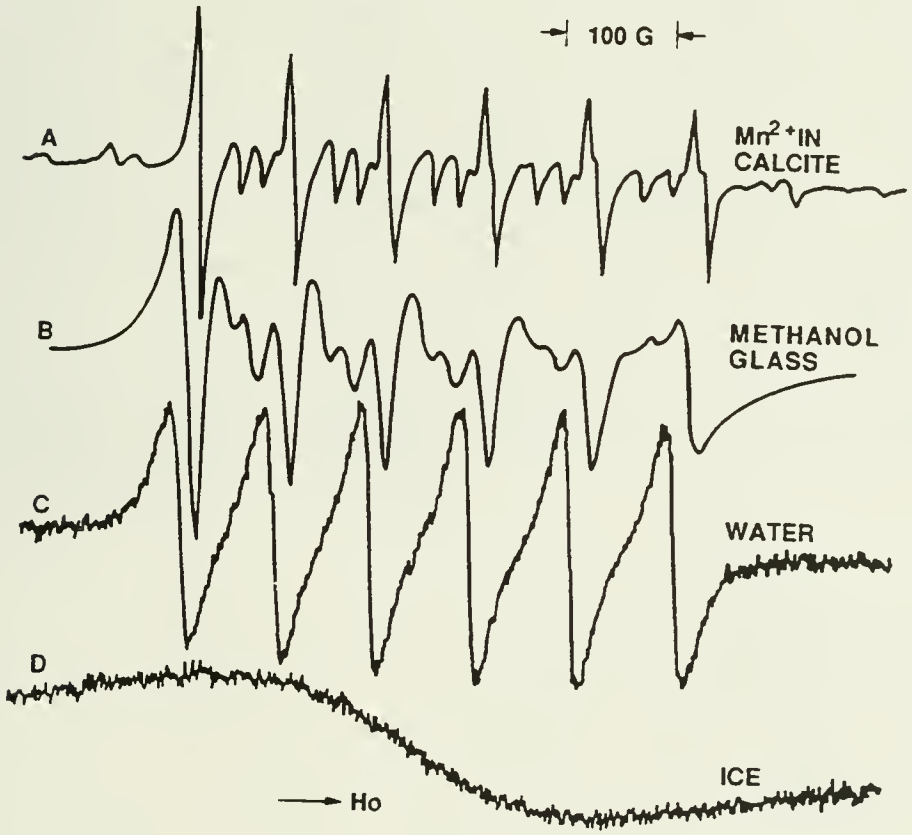


Fig. 5

A comparison of first-derivative ESR spectra observed for Mn^{2+} in different environments.

A. In a polycrystalline sample of calcite at 77°K.

B. In a frozen glassy sample of Methanol at 77°K.

C. In water at 296°K.

D. In ice at 77°K.

Reduction-Oxidation Conditions: Previous ESR studies have successfully related the annealing temperature and surface exposure parameter to the magnetic properties of very fine lunar metallic Fe phases ubiquitously present (Tsay et. al., 1971, 1972b, 1973; Tsay and Live, 1974). In addition no significant amount of Fe^{3+} has been detected in the returned lunar surface samples, indicating highly reducing conditions prevail on the surface of moon (See Fig. 6). In order to detect the minute amount of Fe^{3+} and Ti^{3+} that may be present in the returned lunar sample in the presence of strongly interfering signals arising from ferromagnetic metallic Fe, the second-derivative ESR detection method is employed (See Fig. 6). In general, the second-derivative detection method can be used effectively in determining the weak, narrow spectral features which are concealed in the strong, broad component of paramagnetic and ferromagnetic centers. This coupled with lineshape analyses, intensity measurements and temperature dependence studies makes ESR particularly useful in distinguishing between various paramagnetic and ferromagnetic centers as well as between distinct ferromagnetic centers (See Fig. 7) that are likely to be present in the returned cometary samples.

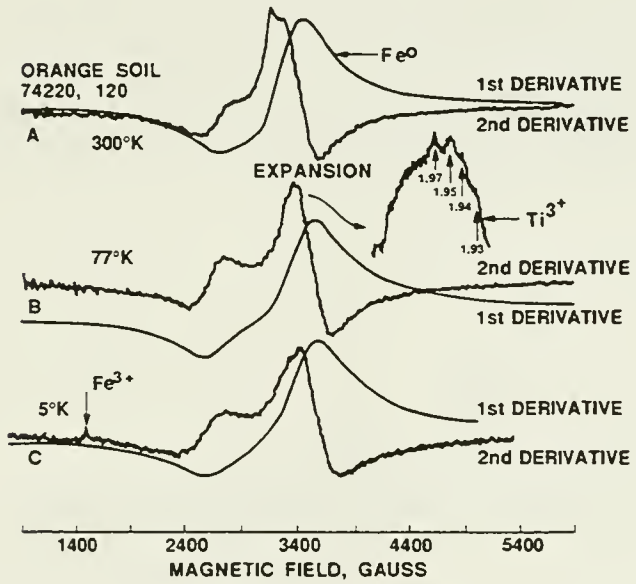


Fig. 6 First- and second-derivative ESR detection of ferromagnetic Fe^0, paramagnetic Fe^{3+} and Ti^{3+} in a lunar sample (orange soil). The intense ESR signals (centered at 3400 G) are due to superparamagnetic and single-domain Fe^0 formed by the solar-wind reduction of Fe^{2+} on the surface of the moon. Note the ESR detection of paramagnetic Fe^{3+} at 4°K. (spectrum C)

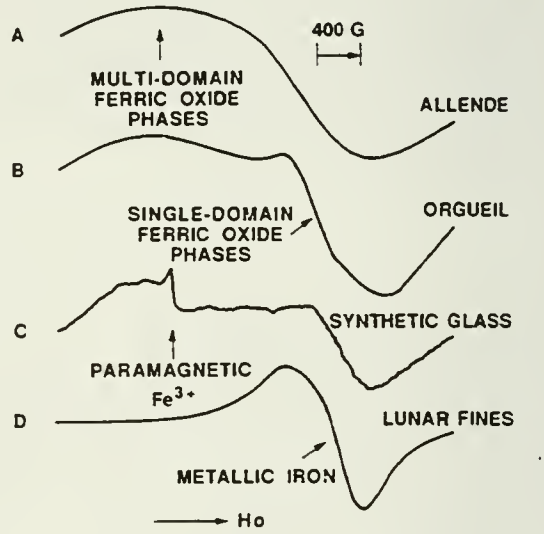


Fig. 7 A comparison of ESR spectra observed for various magnetic phases in terrestrial and extraterrestrial samples.

Recently, ESR has been used to make the first direct measurement of Ti^{3+} in meteoritic and synthetic hibonite (Beckett et. al., 1988). The ESR study has further established the use of Ti^{3+}/Ti^{4+} ratios as indicators of oxygen fugacity in probing redox conditions in the early solar nebula (Beckett et. al., 1988). The ESR detection of the presence or absence of paramagnetic (Fe^{3+} and Ti^{3+}) and ferromagnetic (metallic Fe and ferric oxide phases) in the returned cometary samples should provide information about the formation conditions of comets and their subsequent evolutionary processes.

Nuclear Magnetic Resonance (NMR) Studies: Solid-state NMR was first employed at JPL in the detection of solar-wind proton and other hydrogen-containing molecules likely to occur in the returned lunar samples. Unfortunately, the unexpected high concentration of metallic Fe present as ferromagnetic centers renders the NMR method relatively ineffective in detecting magnetic nuclear species for the returned lunar samples. In general, because of the presence of paramagnetic and ferromagnetic centers in geological samples, in-situ NMR studies are restricted in those terrestrial and extraterrestrial samples that are devoid of such paramagnetic and ferromagnetic centers as Fe^{3+}, magnetite, hematite and metallic Fe. However, the multiple pulse NMR method developed at JPL which has been successfully applied to the study of single-crystalline and polycrystalline ice (Burum and Rhim, 1979; Rhim et. al., 1979) can be used in the investigation of the returned cometary icy samples, provided that the samples are free of paramagnetic and ferromagnetic contamination.

CONCLUSIONS

A series of organic and inorganic free radicals that are likely to be preserved in the returned cometary icy samples have been generated and studied in their native form by ESR. The potential use of ESR free radical concentration and thermal stability measurements as a means of probing the thermal and radiation histories of the returned cometary samples has been demonstrated in the present study. ESR studies have also been carried out on paramagnetic (Fe^{3+}, Mn^{2+} and Ti^{3+}) and ferromagnetic (metallic Fe and ferric oxides) centers in terrestrial and extraterrestrial samples. It has been shown that by analogy, the ESR detection of the magnetic centers if present in the returned cometary samples should furnish further information on the physical and chemical conditions in the formation and evolution of the returned cometary samples. At present, technology is available for the development of a miniaturized ESR spectrometer system for future planetary landing missions. Other than to perform sample selection and in-situ sample analysis task, a miniaturized ESR system will undoubtedly help to search and locate the least altered, pristine samples for a Comet Nucleus Sample Return Mission.

REFERENCES

Ahrens T. J., Tsay F. D. and Live D. H. (1976). Shock-induced fine-grained recrystallization of olivine: Evidence against subsolidus reduction of Fe^{2+}. Proc. 7th Lunar Sci. Conf. pp. 1143-1156.

Allamandola L. J., Sandford S. A., and Valero G. J. (1988). Photochemical and thermal evolution of interstellar/precometary ice analogs. Icarus 76, pp. 225-252.

Beckett J. R., Live D., Tsay F. D., Grossman L., and Stolper E. (1988) Ti^{3+} in meteoritic and synthetic hibonite. Geochim. Cosmochim. Acta, 52, pp. 1479-1495.

Burum D. P. and Rhim W. K. (1979). An improved NMR technique for homonuclear dipolar decoupling in solids: Application to polycrystalline ice. J. Chem. Phys., 70(7), pp. 3553-3554.

Kissel J. and Kruger F. R. (1987). The organic component in dust from Comet Halley as measured by the PUMA mass spectrometor on board Vega 1. Nature, 326, pp. 755-760.

Rhim W. K., Burum D. P. and Elleman D. D. (1979). Proton anisotropic chemical shift spectra in a single crystal of hexagonal ice. J. Chem. Phys., 71(7), pp. 3139-3141.

Siegel S., Flournoy J. M. and Baum L. H. (1961). Irradiation Yields of Radicals in gamma-irradiated ice at 4.2°K and 77°K. J. Chem. Phys., 34(5), pp. 1782-1788.

Tsay F. D., Chan S. I. and Manatt S. L. (1971). Ferromagnetic resonance of lunar samples. Geochim. Cosmoshim. Acta, 35, pp. 865-875.

Tsay F. D., Chan S. I. and Manatt S. L. (1972a). Electron paramagnetic resonance of radiation damage in a lunar rock. Nature, 237(77), pp. 121-122.

Tsay F. D., Manatt S. L. and Chan S. I. (1972b). Electron spin resonance of manganous ions if frozen methanol solution. Chem. Phys. Letters, 17(2), pp. 223-226.

Tsay F. D., Manatt S. L. and Chan S. I. (1973). Magnetic phases in lunar fines: metallic Fe or ferric oxides?, Geochim. Cosmochim. Acta, 37, pp. 1201-1211.

Tsay F. D. and Live D. (1974). Ferromagnetic resonance studies of thermal effects on lunar metallic Fe phases. Proc. 5th Lunar Sci. Conf., pp. 2737-2747.

Vizgirda J., Ahrens T. and Tsay F. D. (1980). Shock-induced effects in calcite from Cactus Crater. Geochim. Cosmochim. Acta, 44, pp. 1059-1069.

DATE DUE

REPORT DOCU

Form Approved
OMB No. 0704-0188

Public reporting burden for this collection of information is
gathering and maintaining the data needed, and completing
collection of information, including suggestions for reducing
Davis Highway, Suite 1204, Arlington, VA 22202-4302, and

tructions, searching existing data sources,
urden estimate or any other aspect of this
n Operations and Reports, 1215 Jefferson
4-0188), Washington, DC 20503.

1. AGENCY USE ONLY *(Leave blank)*

2. ES COVERED
ion

4. TITLE AND SUBTITLE
Analysis of Returned Comet Nucl

NDING NUMBERS
35-52-22

6. AUTHOR(S)
Sherwood Chang, Compiler

7. PERFORMING ORGANIZATION NAME(S) A
Ames Research Center
Moffett Field, CA 94035-1000

RFORMING ORGANIZATION
PORT NUMBER
-950093

9. SPONSORING/MONITORING AGENCY NA
National Aeronautics and Space A
Washington, DC 20546-0001

PONSORING/MONITORING
GENCY REPORT NUMBER
NASA CP-10152

11. SUPPLEMENTARY NOTES

GAYLORD PRINTED IN U.S.A.

Point of Contact: Sherwood Chang, Ames Research Center, MS 239-4, Moffett Field, CA 94035-1000;
(415) 604-5733

12a. DISTRIBUTION/AVAILABILITY STATEMENT

Unclassified — Unlimited
Subject Category 91

12b. DISTRIBUTION CODE

13. ABSTRACT *(Maximum 200 words)*

This volume contains abstracts that have been accepted by the Program Committee for presentation at the Workshop on Analysis of Returned Comet Nucleus Samples, held in Milpitas, California, January 16–18, 1989. Conveners are Sherwood Chang (NASA Ames Research Center) and Larry Nyquist (NASA Johnson Space Center). Program Committee members are Thomas Ahrens (ex-officio; California Institute of Technology), Lou Allamandola (NASA Ames Research Center), David Blake (NASA Ames Research Center), Donald Brownlee (University of Washington, Seattle), Theodore E. Bunch (NASA Ames Research Center), Humberto Campins (Planetary Science Institute), Jeff Cuzzi (NASA Ames Research Center), Eberhard Grün (Max-Plank-Institut für Kernphysik), Martha Hanner (Jet Propulsion Laboratory), Alan Harris (Jet Propulsion Laboratory), John Kerridge (University of California, Los Angeles), Yves Langevin (University of Paris), Gerhard Schwehm (ESTEC), and Paul Weissman (Jet Propulsion Laboratory).

Logistics and administrative support for the workshop were provided by the Lunar and Planetary Institute Projects Office.

14. SUBJECT TERMS
Comets, Comet nucleus, Sample return missions

15. NUMBER OF PAGES
530

16. PRICE CODE
A23

17. SECURITY CLASSIFICATION OF REPORT	18. SECURITY CLASSIFICATION OF THIS PAGE	19. SECURITY CLASSIFICATION OF ABSTRACT	20. LIMITATION OF ABSTRACT
Unclassified	Unclassified		

WELLESLEY COLLEGE LIBRARY
3 5002 03295 0151

Astro q0B 721 .A52 1997

Analysis of returned comet nucleus samples

Astro q0B 721 .A52 1997

Analysis of returned comet nucleus samples